An assessment of the impact of climate change on the efficiency and feasibility of four run-of-the-river hydropower schemes in UK catchments

PhD Thesis

Submitted in fulfilment for the degree of Doctor of Philosophy

Ernesto Pastén Zapata

Department of Geography

University of Sheffield

September 2017

Table of Contents

Abstract

Globally, climate change is projected to affect the hydrological cycle. Nevertheless, the projected changes vary per region. Global Climate Models (GCMs) are the main tool used to project the changes in the future climate. Nevertheless, their spatial scale is large compared to the scale required for the assessment of local impacts. Therefore, Regional Climate Models (RCMs) have been developed to project climate change in specific regions. Often, the simulation biases of the RCMs are large and require bias correction before being used in the assessment of climate change impacts. From the water users, run-of-the-river (ROR) hydropower is expected to be altered by the future changes in water availability as it relies on the available flow for the generation of energy. This research assesses the impacts of climate change on four ROR hydropower schemes within the UK using the climate projections from the state-of-the-art Euro-CORDEX RCMs driven by RCP 2.6, 4.5 and 8.5. The study evaluates the simulation skill of the RCMs by comparing their outputs with present observations of temperature, precipitation and river flow (generated using the RCM outputs to drive a HEC-HMS hydrological model). Furthermore, two quantile mapping bias correction approaches are employed to evaluate possible differences in their outputs. One approach corrects the RCM biases whereas the other corrects the GCM and RCM biases. The results project an increase in future hydropower generation for two of the sites, little change for another and an uncertain projection for the last one. Furthermore, results show that the selection of the bias correction approaches is an important source of uncertainty as it can lead to opposite direction of change when considering the multi-model ensemble mean. The study highlights the importance of developing site-specific analyses, as the large-scale projections cannot be generalized, and provides a methodology to develop such analyses.

List of Figures

Chapter 1

Chapter 2

Chapter 3

Chapter 4

Chapter 5

Chapter 6

Annex A

List of Tables

Chapter 1

Chapter 2

Chapter 3

Chapter 4

Chapter 5

Chapter 6

Annex B

Abbreviations and acronyms

BC-Eval	Bias correction of the RCM bias
BC-Histo	Bias correction of the GCM and RCM bias
BFI	Base Flow Index, ratio of the flow observed 95% of the time to the mean flow
BGS	British Geological Survey
CEH	Centre of Ecology and Hydrology
CHESS	Climate, Hydrology and Ecology research Support System
CMIP3	Coupled Model Intercomparison Project Phase 3
CMIP5	Coupled Model Intercomparison Project Phase 5
DPSBAR	Mean drainage path slope
GCM	Global Climate Model
HOF (or Qmin)	Hands Off Flow, when the flow is equal of below this value, the scheme stops
MORECS	Met Office Rainfall and Evaporation Calculation System
MEM	Multi-Model Ensemble Mean
NERC	Natural Environment Research Council
NSE	Nash Sutcliffe Index
PET	Potential Evapotranspiration
PROPWET	Proportion of time soils are wet
Q10	Measure of high flows: flow that is equalled or exceeded 10% of the time
Q95	Measure of low flows: flow that is equalled or exceeded 95% of the time
Qd	Maximum flow of water diverted to the hydropower scheme
Qmax	High flow at which the hydropower scheme is stopped to avoid damages
RCM	Regional Climate Model
RCP	Representative Concentration Pathway
ROR	Run-Of-the-River
UH	Unit Hydrograph

Acknowledgements

I would like to thank everybody that shared time with me during my stay at Sheffield. I am grateful for the experience of studying abroad and living in such a welcoming community.

Gracias a mis padres por que a ellos les debo todo. Gracias a mis abuelos por prestarme a sus hijos.

Gracias a Oana por los bonitos momentos que hemos vivido juntos y por los que siguen, pero sobretodo gracias por Javi.

Gracias a Javier por ser maravilloso y no dejar de sorprenderme.

I would also like to thank hugely Dr. Julie Jones and Dr. Helen Moggridge for their support and guidance during my PhD studies. I am also thankful to Dr. Martin Widmann for sharing his time and valuable ideas for the development of this research.

Finally, thanks to Conacyt for funding my PhD studies.

1. Introduction

There is a general agreement indicating that climate change will affect the Earth's current climatology due to greenhouse gas emissions, regardless of future attempts to decrease them (IPCC, 2007; Carless and Whitehead, 2013). Global changes are likely to be observed as increasing precipitation and temperature with an increasing difference between the dry and wet regions of most of the Earth but with different impacts for each region (Stocker et al., 2013; Schneider et al., 2013; Giorgi et al., 2014). The hydrological cycle will also suffer changes as precipitation directly influences river-runoff, groundwater recharge and water availability. Additionally, temperature affects the evapotranspiration magnitude, an important component of the water cycle. Moreover, catchments are projected to experience variations in the intensity, frequency and length of extreme events, such as droughts and floods (Maurer et al., 2009). Therefore, agriculture, drinking water supply, industry, and hydropower generation will be affected by changes in hydrology, among other sectors. Hydropower schemes are valuable for power generation and water resource management (Hamududu & Killingtveit, 2012). From the different types of hydropower scheme, run-of-the-river (RoR) schemes mainly depend on river flow as the main input for power generation and a slight change in the river regime will directly affect the hydropower operation. Due to potential differences of the impacts of climate change for the different regions of the world, it is important to evaluate the impacts for each specific case.

The main aim of this thesis is to assess the climate change impacts on the efficiency and feasibility of potential and operating RoR hydropower schemes located in four catchments across the UK. In order to reach the objective, projections of the Euro-CORDEX (Jacob et al., 2014) Regional Climate Models (RCMs) driven by Global Climate Models (GCMs) of the fifth phase of the Coupled Model Intercomparison Project (CMIP5) (Taylor et al., 2012) are used to simulate each catchment's temperature and precipitation. The projections from three Representative Concentration Pathways (RCPs) (Moss et al. 2010) are analysed. Bias correction using the parametric quantile mapping method is applied to the climate model's outputs. Afterwards, both the uncorrected and bias-corrected climate outputs are coupled with a previously calibrated hydrological model to simulate the river flow from each catchment. The simulated river flow is then used to estimate the hydropower generation from the potential and installed hydropower schemes. The study compares each catchment's projected changes in the mean and extremes of temperature, precipitation, river flow and hydropower generation against the observed values of a reference period.

This chapter briefly introduces the main subjects related to this research. Thus, the chapter gives background information related to climate change and its links to hydrology, GCMs, GCM downscaling approaches, bias correction of climate models, hydrological models, coupling climate and hydrological models, the hydropower theory and its current status and the projected impacts of climate change on hydropower. The chapter ends by stating the research's main objective, specific objectives and research questions.

1.1. Climate change and hydrology

The main input for the generation of RoR hydropower is the volume of water available in the rivers. Therefore, the impacts of climate change on river regimes is an important part of this research. A brief description of climate change and its links and impacts on the river regime is given next. Radiative forcing gives an estimation of the changes introduced to the Earth's energy budget by natural, external and anthropogenic forces (VijayaVenkataRaman et al., 2012). The radiative forcing magnitude is estimated using observations, greenhouse gases properties and numerical models (IPCC, 2014). There is evidence from observations that the concentrations of greenhouse gases in the atmosphere have increased as well as the sea surface, land surface, subsurface ocean and atmospheric temperatures (Cubasch et al., 2013). Anthropogenic greenhouse emissions have increased from 1970 to 2010 and 40% percent of the total CO_2 emissions from 1750 to 2010 have been produced from 1970 to 2010 (IPCC, 2014). There is a general agreement that climate change is and will continue affecting the Earth's current climatology due to greenhouse gas emission, regardless of future attempts to decrease them (Carless and Whitehead, 2013). More than half of the increase in the mean annual temperature from 1951 to 2010 is an effect of human activities (Bindoff et al., 2013). These changes along with the expected increase in extreme precipitation intensity (Smith et al., 2014; Watts et al., 2015) will impact human and natural systems, including the hydrological cycle. Changes in river regimes and their consequent water availability will affect different water users (agriculture, industry, domestic supply, etc.). Climate change impact analyses provide an insight of the impact of future climate changes under projected emissions scenarios, and provide a framework to evaluate mitigation and adaptation measures.

In the UK, the observed annual precipitation has experienced little change and from 1961 to 2009 the frequency of extreme events has increased with increases in winter rainfall and decreases during summer (Murphy et al., 2009; Jones et al., 2012). Nevertheless, these changes are not significantly linked to climate change (Watts et al., 2015). The observed mean annual temperature trend in the UK from 1961 to 2012 shows an increase of 0.2°C per decade (Robinson et al., 2017). From 1961 to 2010, streamflow has increased during all seasons in the UK, except for spring in Wales and England, and during summer for England. Streamflow has increased in winter during the last 40 years with no change in the observed low flows or droughts. Finally, the intensity of high flows has increased for all the UK with a decrease in the low flows only observed in England (Hannaford, 2015).

Climate change is projected to produce runoff increases for 47% of the world's land by 2050 and decreases for 36% of the land with no significant change for the rest of the world. For the UK, projections include decreases in runoff and flood frequency with increases in flood magnitude and changes in the month of maximum river runoff (Arnell and Gosling, 2013). Such changes are a consequence of the projected variations in mean and extreme precipitation as well as its temporal distribution (Solomon et al. 2007). The dry spell frequency is projected to increase slightly across the country, with higher increases in the south and east (Jones et al., 2010). The IPCC (2014) projects an increase in the mean annual precipitation for

high latitudes at the end of the century. In contrast, a decrease in the mid-latitudes is projected. Extreme precipitation is more likely to be observed in the mid-latitudes.

1.2. Global climate models

GCMs are the main tool to simulate future projections of climate change (Wilby and Harris, 2006; IPCC, 2013). GCMs are based on physical laws addressing large-scale climatic features and regional climate variables through the use of mathematical equations that are solved using 3D grids (Rummukainen, 2010; Prudhomme & Davies, 2009). Nowadays, a range of different GCMs have been developed by climate modeling groups. At the moment, the most advanced GCM simulations publically available are those developed by CMIP5 (Taylor et al., 2012). Simulations using CMIP5 GCMs were undertaken for four different climate scenarios from 1850 to 2100 based on projections considering population growth, social responses and technical development. The scenarios are a result from a review of scenario literature done by the research community. Each scenario is termed as a Representative Concentration Pathway (RCP) (Moss et al., 2010; van Vuuren et al., 2011). These are representative because they are only one possible scenario from a range of possibilities resulting in the specific radiative forcing (Fig. 1.1). Pathway means that the concentration trajectory through the simulation is of interest (Moss et al., 2010). RCP 2.6 projects a radiative forcing peak of 3 W/m^2 before 2100 and then it declines. RCP 4.5 and RCP 6 project and stabilization of the radiative forcing by 2100 of 4.5 W/m^2 and 6 W/m^2, respectively. Finally, RCP 8.5 projects a radiative forcing larger than 8.5 W/m^2 by 2100 (Moss et al., 2010; van Vuuren et al., 2011).

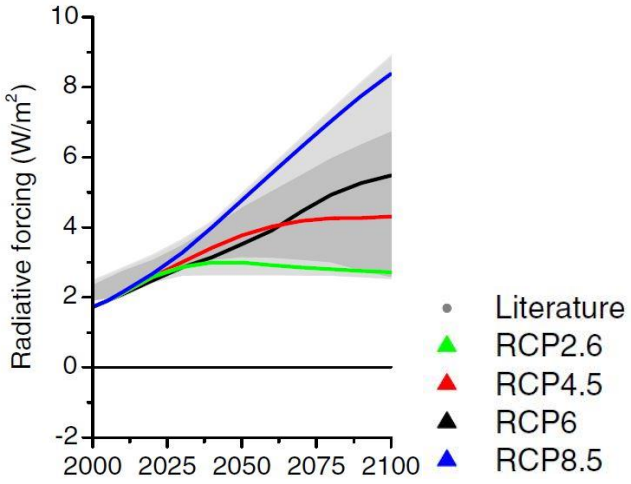

Figure 1.1 Radiative forcing from the Representative Concentration Pathways 2.6, 4.5, 6 and 8.5. Light shaded area represents the 98th percentile of the available literature and the dark shaded area represents the 90th percentile of the available literature from van Vuuren et al. (2011)

It is difficult to compare the simulation skill of the CMIP5 models against the skill from their predecessor GCMs from the third phase of the Coupled Model Intercomparison Project (CMIP3) because they don't share a common scenario (Knutti and Sedlacek, 2013). Nevertheless, efforts to compare them have been done. For temperature the main improvement of the CMIP5 models is their simulation of extremes (Koutroulis et al., 2016). Furthermore, the skill of the CMIP5 models to simulate extreme precipitation and

temperature is better than the skill from the CMIP3 models. Additionally, the spread of the extreme temperature simulation decreases for the CMIP5 models (Sillmann et al., 2013). The mean precipitation is simulated better than the extreme precipitation in the CMIP5 models (Koutroulis et al., 2016).

GCMs present four main sources of uncertainty (Ledbetter et al., 2012). First is the parameterisation used by GCMs to represent physical processes that are not satisfactorily simulated. Second is the different approaches and formulae used by each GCM to simulate processes from the atmosphere, ocean and land surface. Third is the natural variability from each climate model. The last uncertainty source is the difference between the GCM resolution and the scale required for local impact studies.

Regarding the last source of uncertainty described above, the typical horizontal GCM resolution is not smaller than 100km (Teutschbein & Seibert, 2012; Rummukainen, 2016). Therefore, GCMs cannot be used for fine-scale impact analyses (Ahmed et al., 2013). Using GCM outputs for local impact analysis would provide biased results because of the difference in resolutions (Parry et al., 2007; Prudhomme & Davies, 2009). In order to overcome this problem, two downscaling approaches have been developed: dynamical downscaling (DD) and statistical downscaling (SD). These downscaling methods complement each other as they are independent (Benestad, 2007).

1.2.1. Statistical downscaling

SD establishes statistical links between local and large scale weather (Frias et al.,2006; Maraun et al., 2010). Several statistical methods have been developed to downscale large-scale variables into finer resolution scales using transfer functions (see Fig. 1.2). SD approaches can be applied to relate the outputs from both GCMs and RCMs with the local weather. Compared to DD, SD has better skill to reproduce extremes (Vrac et al., 2012). Nevertheless, the main disadvantage of the method is that it doesn't consider the climate system feedbacks, nor corrects wrong model physics. There are three main SD approaches: 1) Perfect Prognosis (PP), 2) Model Output Statistics (MOS), and 3) Weather Generators (WG) (Maraun et al., 2010). From these, MOS has been more frequently used in the assessment of climate changes on hydrology (e.g. Wetterhal et al, 2012; Teutschbein and Seibert, 2012; Teng et al., 2015; Rojas et al., 2011; Prudhomme et al., 2013).

MOS considers the outputs from GCMs and RCMs, and downscales them to estimate the value of the local-scale variable. MOS is calibrated using RCMs or GCM outputs whereas PP is calibrated using large-scale observations. Unconditional WG are only calibrated to local observations, not considering modelled outputs from previous RCMs or GCMs. Additionally, MOS corrects the bias that the larger-scale models could carry. The most used MOS methods are the simplest method, scaling method and quantile mapping (Maraun et al., 2010) (see section 1.3.1).

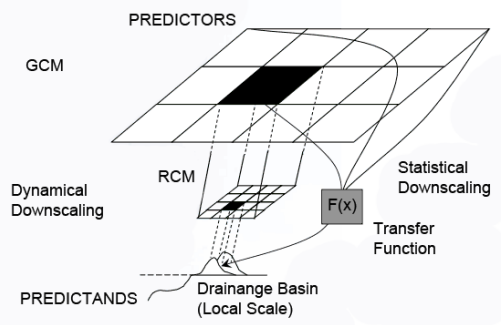

Figure 1.2 Graphical representation of statistical and dynamical downscaling (Wetterhall, 2014)

Figure 1.3 Grid size difference for ECHAM5 GCM (larger) and RegCM3 RCM (smaller) in the Apulia Region (line delimited), Italy. Points indicate gauging stations (from Guyennon et al., 2013)

1.2.2. Dynamical Downscaling: Regional Climate Models

DD nests an RCM with a higher grid box resolution into a driving GCM to reproduce the climatic features of the area (Frias et al., 2006) (see Figures 1.2 and 1.3). The resulting RCM focuses on a specific region of the world (Rummukainen, 2016). The computer power required to perform DD is the main disadvantage of this approach as increasing the climate model resolution requires costly additional computational power (Casanueva et al., 2016). However, the development of new RCMs has increased in the last decades along with the increasing availability of computer power (Muerth et al., 2013). Furthermore, increasing the resolution of RCMs is one of the main research paths that many climate modeling groups are focusing on (Wetterhall et al., 2012). At the moment, RCM resolution generally varies from 50km to even less than 10km (Rummukainen, 2016; Kay et al., 2015; Rockel, 2015).

RCMs have been found to successfully improve the representation of regional (subcontinental to subnational) climatic characteristics compared to the GCM from which they are driven (Frei at al., 2003; Fowler et al., 2005; Frei et al., 2006; Leung et al., 2003; Rummukainen et al., 2016). Nevertheless, the

RCM skill depends on the GCM from which it was downscaled, carrying its associated bias (Fowler et al., 2007). Also, the RCM skill is not always accurate as some biases are still present in their outputs, for example inaccuracies in simulating precipitation in regions of complex orography (Herrera et al., 2010; Prein et al., 2015). The added value of employing a RCM rather than a GCM depends on the study site characteristics. For instance, an advantage of using RCMs could be expected when analysing a local site with complex orography that is not well represented by the GCM. In contrast, there might not be any added-value from using RCMs for large and homogeneous areas (Rummukainen et al., 2016).

For Europe, a set of RCM simulations at two different resolutions (12.5 km or 0.11° and 50 km or 0.44°) have been undertaken as part of the Euro-CORDEX initiative (Jacob et al., 2014). These RCMs downscale CMIP5 GCM simulations (Taylor et al., 2012) using the different RCPs (Moss et al., 2010; van Vuuren et al., 2011). The RCMs from the Euro-CORDEX project are expected to be suitable for use for the analysis of the regional impacts of climate change (Giorgi et al., 2009).

1.2.3. Statistical and dynamical downscaling skill comparison

A direct comparison of the skill from the downscaling methods is complex due to the different spatial regions, predictors and predictands used. Consequently, each has an associated uncertainty that is complex to quantify (Fowler et al., 2007). Nonetheless, the main advantages and disadvantages for each downscaling approach can be identified (Table 1.1).

Table 1.1 Advantages and disadvantages of SD and DD (based on Wilby & Wigley, 1997; Fowler et al., 2007; Wetterhall, 2014)

Method	Advantages	Disadvantages
Statistical Downscaling	- Computationally cheap and efficient compared to DD - Easily transferable to other regions - Generates very fine resolution data (point data) - Based on accepted statistical methods - Integrates observations to the downscaling process - Effective at describing extreme events - Easily creates ensembles of future scenarios - Normally, extremes frequency is better reproduced than intensity	- Performance depends on the selected predictors - Depends on the driving climate model boundaries - Requires good and long observational records - Regional and seasonal characteristics might affect its skill - The stationary relationship between predictors and predictands is not always fulfilled - Climate system feedbacks are not considered - Mean is better simulated than extremes
Dynamical Downscaling	- Produces fine resolution data, being able to successfully simulate regional characteristics/processes - Generates information based in physical consistent processes - Includes feedbacks from the climate system - Skillful at simulating the occurrence of extremes	- Computationally expensive compared to SD - Skill depends on boundaries from the driving GCM - Restricted simulation periods (generally 30 years) - Variability in internal parameterization (use of ensembles is recommended) - Misrepresents orographic precipitation - Fails to simulate the intensity of extremes

Generally, the differences between the observations and SD outputs are smaller than the differences between the observations and the DD outputs (Vrac et al., 2102). RCMs have the ability to reproduce the interannual variability of the GCMs and local feedbacks, while SD seem to require an acceptable resolution RCM to provide better results (Guyennon et al., 2013). Teutschbein & Seibert (2012) noted that RCMs underestimate the variance of the observed daily precipitation and had lower skill in reproducing the variables in cold climates (e.g. the subarctic). Also, results from the different downscaling methods depend on the season, elevation and region of application (Yoon et al., 2012).

Downscaling of extreme precipitation events has proven to be difficult and the use of different thresholds to define extreme events has complicated the comparison between downscaling approaches (Fowler et al., 2007). The intensity, duration and frequency of rainfall are more important statistics for the analysis of extremes instead of the seasonal or monthly precipitation accumulation (Smith et al., 2014). Furthermore, sub-daily precipitation is more accurate than daily time scales when analysing extreme events as daily precipitation records could miss important rainfall occurrence (Wetterhall et al., 2011). Overall, SD is better to represent extremes in impacts studies as one of the main limitations of RCMs is their failure to represent convective precipitation (Rockel, 2015).

1.3. Bias correction

When the GCM or RCM resolution matches the required scale for impact analyses but the climate model skill is not good enough to reproduce past observations, then bias correction might be required to improve the model's skill (Christensen et al., 2008). Bias correction techniques relate statistical characteristics from the observations and simulations considering an observed baseline period (Lafon et al., 2013). The main assumption behind bias correction is that the statistical relationship between observations and simulations obtained during the baseline period will remain unchanged during the future (Teutschbein & Seibert, 2012). Diverse bias correction methods have been developed to overcome biases in the mean, variance and/or the entire distribution. Some of the bias correction methods are linear scaling, local intensity scaling, power transformation, variance scaling, quantile mapping and delta change correction. Bias correction of RCM outputs is a now common practice in climate change impact analyses (e.g. Prudhomme et al., 2013; Cloke et al., 2013; Prudhomme et al., 2012; Rojas et al., 2011; Huang et al., 2014; Graham et al., 2007; Kleinn et al., 2005).

1.3.1. Skill comparison of the bias correction methods

The performance of the different bias correction methods depends on the climate characteristics of the study site and on the observation period and observational dataset used to train the method. Previous studies have compared the performance of different bias correction methods. In general, previous studies found that the best performing bias correction methods are those focusing on correcting the complete distribution of the RCM simulation, such as quantile mapping (Wetterhal et al, 2012; Teutschbein and Seibert, 2012; Lafon et al., 2013). A quantile mapping method using a double gamma distribution approach to correct the precipitation outputs also gives good results (Teng et al., 2015). Additionally, the studies

concluded that the bias-corrected RCM outputs were closer to the observations than the uncorrected outputs. The main quantile mapping methods that are used to bias-correct the outputs from climate models are parametric quantile mapping, its variation using a double distribution to bias correct precipitation and empirical quantile mapping. However, the complexity and amount of data required by the empirical quantile mapping method are its main limitations (Lafon et al., 2013). Therefore, this study uses both parametric quantile mapping bias correction methods which are described next.

1.3.2.Quantile mapping

Quantile mapping modifies the distribution of the temperature and precipitation simulated by the RCM so that it coincides with the distribution of the observations. This is performed by applying a function correcting the occurrence distribution of the RCM (Maraun et al, 2010; Dettinger et al., 2004; Ines and Hanse, 2006; Piani et al., 2010; Déqué, 2007). For precipitation, the Gamma distribution (Thom, 1958) usually provides a good statistical estimate (Piani et al., 2010; Block et al., 2009). Gamma distribution's shape parameter α refers to its profile. If α is less than 1, the distribution is exponential with asymptotes on the axes. If α is one, the distribution is exponential. Finally, the distribution is skewed when α is greater than 1. The scale parameter β defines the dispersal of the Gamma distribution. A small β implies a compact dispersion and, therefore, low probability of extreme event occurrence. In contrast, a large β signifies a wider dispersion and higher probability of extreme precipitation For each month, the Gamma (g) distribution (with shape (α) and scale (β) parameters) is fitted to the daily precipitation and the normal (n) distribution (with mean (μ) and standard deviation (σ)) to the daily temperature. As RCMs generally simulate too many days with very low precipitation (Chen et al., 2013), an initial step adjusts the number of simulated dry days, matching them with the number of observed dry days using a wet day threshold below which all simulated values are changed to zero.

After the wet day adjustment, the quantile mapping method matches the distributions of the simulations and of the observations using their cumulative distribution functions (CDF):

$$P_c(d) = F_g^{-1}\left(F_g(P_R(d), \alpha_R, \beta_R), \alpha_O, \beta_O\right) \quad \text{Eq. 1.1}$$

$$T_c(d) = F_n^{-1}(F_n(T_R(d), \mu_R, \sigma_R^2), \mu_O, \sigma_O^2) \quad \text{Eq. 1.2}$$

Where $P_c(d)$ and $P_R(d)$ are the bias-corrected and uncorrected RCM daily precipitation, respectively. Likewise, $T_c(d)$ and $T_R(d)$ represent the bias-corrected and uncorrected RCM daily temperature. The raw RCM CDF is symbolized with F, and F^{-1} stands for the inverse CDF of the observations. The 'g' and 'n' subscripts represent the Gamma and normal distributions, respectively. Finally, the 'R' and 'O' subscripts are used to symbolize the distribution parameters from the raw RCM and observations, respectively.

1.3.3. Quantile mapping using double Gamma distribution for precipitation

A side effect of the Gamma distribution quantile mapping is the inflation of extreme precipitation events (Wetterhal et al., 2012; Chen et al., 2013; Cannon et al., 2015) affecting the analysis of climate change

impacts to hydrology, specifically floods (Cloke et al., 2013). This side effect is a result from fitting a single gamma distribution to the complete precipitation distribution as the correction parameters will focus on the more frequent values, ignoring the extremes, which might be largely different (Yang et al., 2010; Teng et al., 2015). In order to avoid this problem, precipitation is also bias corrected using the double Gamma quantile mapping bias correction which divides the precipitation distribution in two separate segments and corrects each one using a Gamma distribution. The segmentation of the precipitation distribution for bias correction has been performed before, overall decreasing the biases in the extremes (e.g. Grillakis et al., 2013; Guthjar and Heinemann, 2013; Yang et al., 2010)

1.3.4. Bias correction limitations

Bias correction methods have inherent assumptions and limitations. However, bias correction is often used in climate change impact studies because of the biases from the climate models' outputs. The limitations of the bias correction methods are their dependence on the training period (Ehret et al., 2012; Lafon et al., 2013), the assumption of temporal stability of the correction function in the future (Smith et al. 2014; Velázquez et al., 2015; Chen et al., 2015), the possible alteration of the RCM climate signal and its appropriateness for impact analysis (Maraun, 2013; Velázquez et al., 2015), the inter-variable consistency (Wilcke et al., 2013), the sub-grid variability and inflation of variance (Maraun, 2013), and the spatial representation of the RCM grid boxes over complex terrain (Maraun and Widmann, 2015) Furthermore, bias correction is just a statistical adjustment of the climate model simulations and cannot remove the model's fundamental errors (Maraun, 2016). Also, it has been argued that the climate model outputs are significantly modified after bias correction and affect the output of the impact models (Ehret et al., 2012). In hydrological impacts, bias correction can lead to unreal flood magnitudes (Wetterhal et al., 2012, Huang et al., 2014). Nevertheless, as currently the climate models are biased, bias correction can be applied to multi-model ensembles to increase the simulation skill, but effort should focus in improving the skill of the uncorrected climate models (Ehret et al., 2012) by means of better parameterisations or improving the representation of the physical processes.

1.4. Hydrological modelling

Globally, future climate variability is expected to modify river flow regimes (Arnell & Gosling, 2013). This will depend on the catchment's location and characteristics. For instance, at the moment more regions experience an increase in extreme precipitation events than regions experiencing a decrease (IPCC, 2014). These changes could impact regions unprepared to face extreme precipitation events of higher intensity and frequency leading to flooding events. Additionally, the mean surface temperature is projected to rise with more frequent heat waves during the 21st century (IPCC, 2014). Thus, evapotranspiration is likely to increase, decreasing the volume of water available for runoff.

The relationships and interactions between a catchment's physical properties, climate and their associated runoff are complex. Hydrological models are the main instruments used to assess and explain these natural complexities. These models describe different hydrological processes and variables such as rainfall,

evapotranspiration, infiltration, groundwater, and surface water runoff, among others (Singh and Frevert, 2006). Furthermore, hydrological models help to analyse environment and water resource problems as well as future scenarios. These models can be used in a wide variety of applications, including: future climate change impacts on water availability, water resources planning, flood prediction, water demand and supply management, and future changes on river regimes, among others (Pechlivanidis et al., 2011). By assessing future issues, models provide the opportunity to evaluate the implementation of prospective strategies and policies (Singh and Frevert, 2006).

The first attempt to simulate a catchment's hydrology was performed using the Standford Watershed Model (SWM) (Crawford and Lingley, 1966). The number and complexity of the hydrological models has grown since then. Nowadays, hydrological models are capable of simulating a catchment's water flow, sediment and chemical transport as well as nutrient and microbial processes and anthropogenic impacts. Practical applications of hydrological models include the assessment of climate change and management strategies impacts. Therefore, the models are important for decision making. Nevertheless, disadvantages of modern hydrological models include large data requirements, not being user friendly and lacking a clear definition of their limitations or guidance on their applicability. Some of the hydrological models that are currently being used in hydrological analyses include (but are not limited to): ARNO (Todini, 1996), GR4J (Perrin et al., 2003), HBV (Lindstrom et al., 1997); HYPE (Lindstrom et al., 2010), HEC-HMS (Scharffenberg, 2003), LISFLOOD (De Roo et al., 2000), PDM (Moore, 2007), RORB (Minns and Hall, 1996), TOPKAPI (Todini and Ciarapica, 2002), TOPMODEL (Beven and Kirby, 1984) and WEAP (Danner et al., 2006).

Model calibration and validation intend to improve and test the model performance by comparing the observed and simulated values. Calibration involves a scientifically based adjustment of some model parameters in order to obtain a better fit between model outputs and observed data. Two calibration approaches are used: manual and automatic calibration. Manual calibration depends on the expertise of the modeller to define parameter values that improve the model fit. Automatic calibration is a computer-based method that speeds up the calibration. It involves the integration of objective functions, optimization algorithms and a termination criterion (Sorooshian and Gupta, 1995). Objective functions are commonly used to numerically determine the difference between the model outputs and the observed values (Schaefli and Gupta, 2007). Additionally, multi-objective analysis can be employed to integrate several objective functions into a single objective criterion. This is used because a set of parameters values providing the best fit according to a certain objective function might not provide the best fit when they are used for another objective function (Beven, 2001). Nowadays, automatic calibration is not sufficiently developed to replace manual calibration. Therefore, most successful calibrations involve a mixture of manual and automated methodologies (Pechlivanidis et al., 2011). Nevertheless, in some cases over-parameterisation, data limitation and deficiencies in the model structure can negatively affect the calibration process (Lee and Moon, 2007).

When the calibration is completed, validation is used to test the performance of the calibrated model for a different period from which it was calibrated (Pechlivanidis et al., 2011). It is common that the model performs better during the calibration period. This characteristic is known as model divergence (Sorooshian and Gupta, 1995). The modeller should evaluate the model divergence magnitude and decide to accept or modify the model (Pechlivanidis et al., 2011).

One important consideration is the difficulty to assess the model's reliability outside its calibration and validation limits. This is relevant when future climate change scenarios are being evaluated as these scenarios generally involve the application of rainfall magnitudes above the calibration and validation observed values (Van Steenbergen and Willems, 2012).

1.5. Coupling climate and hydrological models

Globally, the future of water resources is projected to be impacted by climate and non-climate driven factors with negative impacts being more important than the benefits (Jiménez Cisneros et al., 2014). The hydrological community is aware of this threat and has developed climate change impact analyses for different regions of the world (see section 1.7 for a description of selected examples). The typical chain used to assess the impacts of climate change in hydrology is as follows: outputs (normally precipitation and temperature) from GCMs or RCMs are coupled with a calibrated hydrological model to simulate the catchment's streamflow. Normally, the skill of the coupled models is assessed by evaluating their capability to reproduce historical streamflow observations. Afterwards, future streamflow simulations based on RCP projections are used to estimate the potential impacts of climate change towards future flood frequency, groundwater recharge, low flows estimation, hydropower potential, among others. This analysis chain might have slight variations that are described next.

Hydrological impact analysis can use one or an ensemble of climate models. The number of models depends on their availability for the study catchment and the available computer power. By using only one model, a slight idea of the possible future streamflow can be gained. In contrast, using an ensemble of climate models provides a range of possible scenarios that could be unperceived when using only one climate model. Furthermore, the use of an ensemble of climate models decreases the uncertainty from the difference in methods and parameterizations used by the different climate models (Ledbetter et al., 2012).

As GCM and RCM outputs have bias restricting their direct application in hydrological impact analyses for some catchments (Prudhomme & Davies, 2009; Fowler et al., 2007), bias correction methods are often applied (e.g. Wetterhall et al., 2012; Teng et al., 2015; Rojas et al., 2011; Prudhomme et al., 2013). The selection of the bias correction method will depend on the needs and availability of data and computational power. Additionally, only one or two emission scenarios are normally used based on their importance to the analysis and study site.

Normally, one hydrological model is used to generate future streamflow scenarios. However, some studies have used more than one hydrological model to account for the uncertainty generated by the use of different

hydrological models and therefore different parameterizations (e.g. Teng et al., 2015; Kay et al., 2009; Kay and Jones, 2012; Dibike and Coulibaly (2005).

An important number of studies have been developed worldwide, mainly focusing on flood and drought frequency and on the availability of water resources. Section 1.7 provides a description of selected studies focused in Europe and in the UK.

1.6. Uncertainties in the analysis of climate change impacts on hydrology

The analysis of climate change impacts on hydrology is accompanied with uncertainty sources such as: 1) GCM uncertainty, 2) downscaling uncertainty, 3) uncertainties in the magnitude of future scenarios, 4) hydrological modelling uncertainty and 5) uncertainty from the bias correction method (Prudhomme & Davies, 2009).

GCM uncertainty refers to the fact that diverse global models give diverse outputs for the same region. Downscaling uncertainty arises from the use of different downscaling procedures as each method gives different outputs. The same is true for the emission scenario and hydrological model uncertainty. GCM uncertainty is larger than emission scenario uncertainty and downscaling uncertainty (Graham et al., 2007). Hydrological model uncertainty was previously seen as insignificant for impact studies. However, nowadays it has been acknowledged that hydrological uncertainty can be as large as the GCM uncertainty (Prudhomme et al., 2014). Therefore, a robust analysis should include the outputs from several GCMs or RCMs, bias correction techniques and hydrological models to account for the uncertainties from each source (Haylock et al., 2006). However, this is time demanding and the computational requirements often restrict the development of a complete analysis. Whereas multi climate model and emission scenario analysis are frequent in the hydrological impacts scientific literature (e.g. Cloke et al., 2013; Wetterhall et al., 2012; Arnell, 2011; Ledbetter et al., 2012), they normally use one impact model (Arnell and Lloyd-Hughes, 2014) and few studies have started to assess multiple impact models at a global scale (e.g. Prudhomme et al., 2014, Dankers et al., 2014). Furthermore, the uncertainty level should be considered for decision making planning and implementation (Smith et al., 2014). As the uncertainty of the analysis is high, it negatively influences decision making (Chen et al., 2006; Wilby et al., 2006).

1.7. Previous studies assessing the impacts of climate change on hydrology

The analysis of the potential impacts of climate change on hydrological regimes has been widely analysed for different regions of the world (Arnell, 2011). Globally, it is projected that by the 2050's the annual runoff will increase for 47% of the land surface and reduce for 36%. The remaining percentage is projected to have no significant change. Additionally, floods and droughts are projected to increase for 50% and 44% of the Earth, respectively (Arnell & Gosling, 2013). This section focuses in studies developed for Europe and the UK.

1.7.1.Europe

The following studies have analysed the impacts of climate change on hydrology in Europe in a continental and local basis. This selection represents only a percentage of the available literature related to the topic but serves as a background of the status of the research for the region. In a pan-European context, uncorrected RCMs have biases that result in unreliable future flood projections that remain after bias correction for some cases (Rojas et al., 2011). Climate change simulations project larger impacts in the river flow regime of the Mediterranean, boreal and temperate continental regions of Europe, whereas impacts are smaller for the temperate oceanic zone (which includes the UK) (Schneider et al., 2013). In general, water availability is projected to increase in the north of Europe and decrease in the south (van Vliet et al., 2015; Schneider et al., 2013) with hydrological extremes increasing all over Europe (van Vliet et al., 2015). However, it has also been observed that the flood hazard is projected to decrease in northern and eastern Europe (Dankers et al., 2014). Considering the frequency of droughts, this is projected to increase by 20% in central and western Europe (Prudhomme et al., 2014).

The performance of an ensemble of the Euro-CORDEX RCMs to simulate observed precipitation within Europe was analysed by Prein et al. (2015) and Casanueva et al. (2016). They found that the state-of-the-art RCMs had biases when simulating precipitation for some regions of the continent. These biases could be in part reduced by improving the parameterization from the different RCMs. In general, biases were larger for regions with complex orography such as the Alps, Carpathians and regions from France and Spain, among others. Nevertheless, higher resolution RCMs simulate extreme orographic precipitation better in comparison to the coarser resolution RCMs. Casanueva et al. (2016) bias corrected RCM outputs concluding that the method increased the accuracy of the RCMs. However, they stated that progress should focus in improving RCM parameterization to provide accurate simulations without the need of post-processing methods.

1.7.2.UK

The projected changes in climate and their effect towards the hydrological cycle is an important research topic of the UK's scientific community (Hannaford, 2015). During the past decades there has been an increased interest in evaluating how the impacts of climate change will affect the water resources and the reliability of the future projections. A considerable number of studies have assessed the impacts of climate change in the hydrology of the UK using different methodologies. Table 1.2 provides a list of the main characteristics of selected studies performed in the UK.

Most studies focused on the development of methodologies to analyse the impacts of climate change on water resources with several studies including an analysis of the sources of uncertainty. Also, hydrological models have been validated following a climate change impacts framework (e.g. Bell et al., 2007) and daily bias-corrected streamflow projections have been made available for the public for 281 catchments within the UK (e.g. Prudhomme et al., 2013).

Table 1.2 Previous studies analysing the impacts of climate change on UK's hydrology

Reference	Objective	Study site(s)	Post-processing	GCM/RCMs	Hydrological Model	Conclusion
Prudhomme et al., 2003	Proposes a methodology to assess the uncertainty of climate change impacts to flood regimes and compares it with the natural variability	5 catchments (ranging from 10 to 280 km^2)	Proportional downscaling	7 GCMs using 14 different runs	Probability Distributed Model	GCM uncertainty is higher than the emission scenario uncertainty. Therefore the decrease of climate change impact uncertainty depends on GCM improvement
Wilby et al., 2006	Methodology for climate change impact assessment at catchment scale and to explore the uncertainty in future river flow and water quality indicators	River Kennet (1200 km^2)	Statistical downscaling model	3 GCMs: HadCM3, CGCM2, CSIRO	CATCHMOD (water balance) and INCA (quality)	Larger uncertainty is due to the choice of GCM compared to the hydrological model uncertainty. The climate change signal might be opposite for the different GCMs
Prudhomme and Davies, 2009	Suggests how to assess uncertainties within a climate change impact study. Evaluates the skill to simulate the baseline climate, understanding downscaling uncertainty and comparing it with the hydrological model uncertainty	4 catchments ranging from 255 to 751 km^2	Dynamical downscaling (RCM) and statistical downscaling model	3 GCMs and 1 RCM: HadCM3, CGCM2, CSIRO-Mk2 and HadRM3 (dynamically downscaled from HadCM3)	Two models based on the Probability distributed moisture model (PDM)	GCM uncertainty is larger than downscaling uncertainty and both are greater than the hydrological model uncertainty or natural variability. No GCM or downscaling technique outperform the others
Kay et al., 2015	Test the performance of very high resolution climate model outputs for streamflow simulation and investigate the effect of RCM resolution on projections of change in peak river flows	32 study catchments in southern Britain	None	RCMs: HadGEM3 (12 km); UKV (1.5 km) (ERA & HadGEM3 GCM-driven)	CLASSIC-GB	The 1.5km convection-permitting RCM performs worse than a 12km RCM to simulate river flow. Main cause: convection-permitting models simulate too intense heavy rainfall
Prudhomme et al., 2013	Provide datasets that facilitate the assessment of climate change impacts on water-related issues across GB using a daily scale for river flow and monthly for groundwater levels	281 Great Britain catchments	BC: Parametric QM	RCM: HadRM3-PPE, 11 member ensemble (25 km)	CLASSIC, CERF, PDM	Largest departures during dry conditions and regions. It is recommended to use all 11 simulation results to incorporate uncertainty and the largest variability of signal change
Cloke et al., 2013	Evaluate impacts on projected high flows from different ensemble approaches and bias correction techniques to improve the simulation of precipitation	Upper Severn Catchment (4,062 km^2)	BC: Double-Gamma distribution	19 GCM-RCM members and 11 HADRM3 RCM projections with different sensitivities from UKCP09 (25 km)	HBV-light	There are large uncertainties in the results. Specially, bias correction has a clear effect on the results. Uncorrected RCMs don't produce reliable precipitation simulation, therefore their use in impact studies is not practical
Wetterhall et al., 2012	Investigate the performance of 3 bias correction methods to simulate precipitation and assess the performance of conditioning bias correction to months and weather patterns	Upper Severn river (2,000 km2)	BC: Quantile mapping, distribution-based scaling, direct method	16 ENSEMBLES' RCMs (25km) driven by ER40	HBV	More sophisticated (distribution-based) bias correction techniques are more beneficial than simpler techniques. Uncorrected RCMs cannot capture flood events that are captured by the corrected RCMs

Table 1.2. Continuation

Reference	Objective	Study site(s)	Post-processing	GCM/RCMs	Hydrological Model	Conclusion
Arnell, 2011	Examine relationships between climate forcing and hydrological response using six catchments with different hydrological characteristics in the UK and multiple climate scenarios from the IPCC Fourth Assessment Report	6 catchments ranging from 74 to 1134 km^2	N/A	21 GCMs	Cat-PDM	Large spread in hydrologic simulations due to the simulated precipitation from different GCMs. Summer PET affects low flows. GCM uncertainty is larger than hydrological uncertainty. Impact studies should use the full range of climate models available considering the diversity of their hydrological response
Diaz-Nieto and Wilby, 2005	Explore the merits of employing Change Factor (CF) and Statistical Downscaling (SD) post-processing with respect to low flow scenarios highlighting the conditions where the use of the more complex SD is beneficial over the use of the simpler CF	River Thames at Kingston	Change Factor and Statistical Downscaling for Precip and PET	GCM: HadCM3	CATCHMOD	Low flows until autumn and an increase in flows for late winter and early spring. Increased risk of low flows and droughts in summer and autumn. For the downscaled B2 scenario an increase in low flows and winter precipitation. A major advantage of CF and SD over RCMs is that scenarios can be generated quickly as GCMs become available
Wilby and Harris, 2006	Present a probabilistic framework combining projections from different GCMs, emission scenarios, downscaling techniques and impact model uncertainty to generate probabilistic information of low flows	River Thames at Kingston	Change Factor and Statitical Downscaling for Precip and PET	4 GCMs: CGCM2, CSIROMk2, ECHAM4, HadCM3	CATCHMOD	Using a single GCM or impact model could be questionable for climate change impact assessments. Two different GCMs provided contrasting results for the river flow scenarios. The paper proposes a method to objectively weight the uncertainty components
Bell et al., 2007	A spatially-distributed hydrological model is directly coupled with RCMs to provide regional estimations of river flow and flood frequency	25 British catchments	N/A	25km RCM driven by the ERA reanalysis	GridtoGrid	The model performs best in topographically-driven catchments compared to baseflow dominated catchments. The simulated FDC are close to the observations. In general, the model performs well but worse than the PDM model
Fowler and Kilsby, 2007	Determine how well RCM simulates the daily distribution of annual and seasonal flows. Also analyses the mean annual runoff, seasonality of flows and Q5 and Q95 frequency	8 catchments ranging from 35 to 1300 km^2	BC by monthly factors	RCM: HadRM3H (50km)	ADM model (a simplified version of the Arno model)	RCMs need bias-correction to be used for hydrological impact assessment. Corrected RCMs provide some confidence to assess the future climate changes. SRES A2: increase of annual runoff at high elevation catchments but a decrease for low elevation sites. Summer flow decreases but winter flow increases. Q95 decreases in summer and Q5 increases, especially at high elevation catchments

Table 1.2. Continuation

Reference	Objective	Study site(s)	Post-processing	GCM/RCMs	Hydrological Model	Conclusion
Kay et al., 2009	Investigates the uncertainty from six different sources towards the simulation of flood frequency under climate change	Boult at Stile Bridge (277 km^2), Duddon at Duddon Hall (86 km^2)	Three variations of the delta change method	8 RCMs nested on HadAM3H GCM	PDM and GridtoGrid	GCM uncertainty is the largest source of uncertainty. Large biases from a specific GCM highly influences the overall GCM uncertainty. If that GCM was omitted, the GCM uncertainty would be largely reduced
Christierson et al., 2012	Development of a method to use probabilistic climate projections in a national scale and identify and quantify the uncertainties from river flow changes	70 study catchments	N/A	UKCP09 probabilistic data, 11 variants from HadRM3 and projections from previous national assessment	PDM and CATCHMOD	For the 2020s under a medium emissions scenario: warmer winters and wetter summers. Large climate model uncertainties especially in winter. Increase of winter river flow in the northwestern region of the UK with decreases in the other regions during the whole year
Kay and Jones, 2012	Uses three transient climate projections (1950-2099) to investigate changes in flood frequency and timing for 2 British catchments	Boult at Stile Bridge (277 km^2) and Duddon at Duddon Hall (86 km^2)	N/A	HadRM3 RCM (25km) nested on HadCM3. 3 ensemble runs: high, low and moderate climate sensibility	PDM and GridtoGrid	Flood frequency is unlikely to change linearly in the future because of the natural variability and the non-linear relationship between rainfall and streamflow. Results suggest an increase in flood risk for the whole country
Ledbetter et al., 2012	Introduce a method for the development of climate change scenarios including climate variability by resampling the climate model outputs and generating new precipitation projections	Eden catchment (307 km^2) in Scotland	N/A	13 GCMs from CMIP3	PDM	Climate variability is significant for the assessment of precipitation changes. Due to the non-linear hydrological response, the use of a range of climate models is beneficial to assess possible projections
Prudhomme et al., 2012	Provide an assessment of the seasonal variation in river flow for the 2050s in the UK using 11 climate scenarios from UKCP09	Whole UK	Quantile mapping (Precip.), linear correction (Temp.)	11 realisations of HadRM3	CERF	Under A1B Scenario: Almost all models project a decrease in summer flow. For the other seasons the variability is higher between scenarios and the different parts of Britain.
Charlton and Arnell, 2014	Evaluate potential changes in next century's hydrology and derive relationships between climate and hydrological indicators of change to identify the key drivers of change	6 catchments ranging from 74 to 1134 km^2	N/A	10000 scenarios based on UKCP09	Cat-PDM	There is a large hydrological impact spread. A considerable number of scenarios are required to derive a robust distribution of changes. Catchments respond different based on their geological conditions and differences in the baseline water balance. High flows are affected by winter precipitation and low flows by summer precipitation and temperature

The catchments used as study sites for the analyses vary from 35 km^2 to approximately 4,000 km^2. There is also heterogeneity regarding the post-processing techniques that have been used. Alternatively, some studies have used the uncorrected RCM outputs to perform their analyses. However, most of the studies used some sort of post-processing ranging from the simplest downscaling methods (e.g. Prudhomme et al., 2003; Wilby et al., 2006; Prudhomme & Davies, 2009) to complex forms of distribution-based bias correction (e.g. Prudhomme et al., 2013; Cloke et al., 2013; Wetterhall et al., 2013).

Different GCMs and RCMs have been used to assess the impact of climate change. These have been used to account for the uncertainty in the selection of the climate model. However, there is a tendency to use the Met Office Hadley Center HadCM3 GCM and HadRM3 over the other climate models as these have provided good results when simulating the UK climate. The UKCP09 probabilistic projections of future climate have been used by some of the most recent studies (e.g. Christierson et al., 2012; Charlton & Arnell, 2014).

A large number of hydrological models have been employed to simulate streamflow using the RCM outputs as driving data. These models vary from lumped models (e.g. PDM) to semi-distributed models (e.g. CLASSIC), to grid to grid models (e.g. GridtoGrid). Some have been especially designed to simulate streamflow within the UK (e.g. CLASSIC-GB). Most of the studies have used only one model to simulate streamflow with only few cases including more than one.

The general conclusions indicate that bias correcting RCM precipitation and temperature increases the agreement between RCM precipitation and temperature outputs and the observations. Additionally, coupling bias-corrected RCM outputs with hydrological models result in streamflow simulations that are closer to the observations. However, as discussed on section 1.3, bias correction is used under certain assumptions that should be considered when analysing their results. Most of the studies focusing on the uncertainty from the different aspects of the chain analysis conclude that the largest uncertainty comes from the used GCM or RCM, followed by the uncertainty from the bias correction method and the hydrological model contributes with the smallest source of uncertainty (Wilby et al., 2006; Prudhomme et al., 2003; Prudhomme & Davies, 2009; Arnell, 2011; Kay et al., 2009).

1.8. Hydropower theory and current status

Hydropower is defined as the production of energy derived from the fall of water from an upper to a lower level, taking advantage of gravity (Kumar et al., 2011). The energy from falling water is transformed into mechanical energy by a turbine. The resulting mechanical energy can either produce work or be transformed into electric energy. The sources of water input can be classified as natural (spring, waterfall, stream, reach, natural lake) or manmade (dams, canal drop, wastewater discharges) (US Department of Energy, 1983).

The main objective of a hydropower scheme is to make the most of the potential energy of flowing water. The water flow and head (elevation difference) define the potential amount of energy that can be produced

by a particular system. The actual energy output depends in the efficiency of the scheme's turbine (US Department of Energy, 1983; CEC, 1998). Thus, the hydropower equation is defined as:

$$P = \eta_H g h \rho q$$

P is the power (W), η_H is the turbine efficiency (%), g is the gravity (9.81 m/s^2), ρ is the density of water (1000 kg/m^3), h is the head defined as the altitude difference between the scheme's inlet and discharge (m) and q is the volume of water flowing through the scheme (m^3/s). The efficiency of the scheme depends on the site, equipment and installation characteristics (US Department of Energy, 1983; Woods et al., 2010).

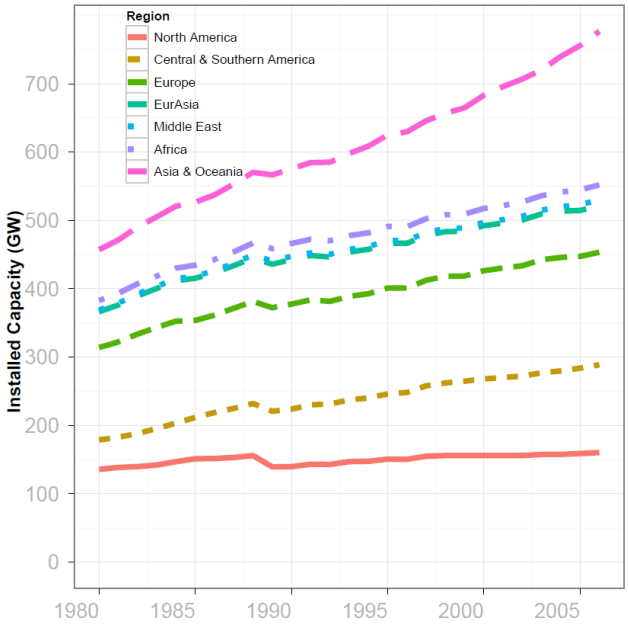

Figure 1.4 Trends in the installed hydropower capacity per region (1980-2006) (Hamududu & Killingtveit, 2012)

Global hydropower generation is estimated to be increasing at a pace of 2.3% per year (Fig. 1.4). Following the current global trends, the hydropower installed capacity will increase by 75% by 2050, considering 2008 as base year (Hamududu & Killingtveit, 2012). In 2008, hydropower generation represented 16% of the global energy supply and in 2011, the global technical hydropower potential was 14,756 TWh/yr with only 25% of it installed (IJHD, 2010; Kumar et al., 2011). Africa, Asia and Latin America are the regions with the largest undeveloped potential. America and Europe can increase their actual technical potential by 50%, but Kumar et al. (2011) suggest that an economical evaluation should be developed to determine its feasibility

For Europe, 27% of the total energy generation is expected to be generated by renewable sources by 2030 (European Council, 2014; European Council, 2017). From the renewable sources, wind and solar energy are directly influenced by the weather variation (von Bremen, 2010). Therefore, hydropower is perceived as an important supplementary source when the generation from other renewable energy sources decreases (Francois et al., 2014). Projections for England show that the hydropower share could reach

65% when considering the optimal generation mix among hydropower, wind and solar energy (Francois et al., 2016).

In the UK, the latest Government target envisages an 80% CO_2 reduction by 2050 compared to the 1990 baseline (Act. C.C., 2008). An increase in power generated by renewable resources is key to reach such target and new small-scale hydropower schemes are expected to be part of the energy generation share (Woods et al., 2010; Carless and Whitehead, 2013). From 2012 to 2016 the renewable energy generation in the UK has doubled from 36,967 GWh to 76,106 GWh and the small-scale hydropower installed capacity has also grown from 216 MW to 358 MW (DECC, 2017). The installed capacity of large-scale hydropower has remained unchanged during the same period as new sites are unavailable as all the economic and environmental feasible locations are already used.

1.8.1. Classification of hydropower schemes

Hydropower schemes are mainly composed of a weir, a flow diversion system, a turbine and a depleted reach. Normally, hydropower schemes are non-consumptive (water entering and exiting the generation station will have the same volume) and can be classified according to their different properties. Common classifications are related to its size, head and facility type. Head categorization refers to the difference between the upstream and downstream elevations from which water flows (Kumar et al., 2011). According to its head, hydropower schemes can be classified as high (100 meters or more), medium (from 30 to 100 meters) or low (from 2 to 30 meters) (CEC, 1998). Different turbine types can be used depending on the scheme's head. Pelton turbines are generally associated with high heads, Francis turbines with medium heads and Kaplan, Archimedes screws and Bulb turbines with low heads (Kumar et al., 2011).

The size categorization of hydropower schemes refers to the installed capacity of the site. However, the classification is arbitrary as there is no global agreement on the definition of each category. Schwartz et al. (2005), classified the schemes into large (higher than 30 MW), small (500KW – 30 MW), mini (100KW-500KW) and micro (10KW-100KW) schemes. Globally, only 5% of the total small hydropower potential has been exploited (EIA, 2010).

Based on their facility, hydropower schemes can be classified as run-of-the-river (RoR), reservoir, pumped storage or in-stream at existing sites. RoR schemes have their main energy source from the river flow. Therefore, these schemes depend on the seasonality of local precipitation and runoff. Compared to other schemes, RoRs are relatively inexpensive and have lower environmental impacts. Storage schemes accumulate water for posterior use. By creating a water reserve, these schemes avoid depending on precipitation seasonality, to a certain degree. These schemes are able to alleviate the effects of floods and droughts, and provide water for other users. A storage plant can be connected to several reservoirs with pipelines. Pumped storage refers to schemes were water from the downstream is pumped towards an upstream reservoir and then used to generate hydropower. The pumps used in these schemes employ energy generated by the same scheme. Finally, the in-stream technology application at existing sites

encompasses the installation of turbines in previous hydropower sites where they can improve the performance (Kumar et al., 2011).

1.8.2. Run-of-the-river hydropower

In the UK, the potential for development of RoR schemes is highly linked to micro and small hydropower schemes (see Tables 1.3 and 1.4). The importance of micro-hydropower is linked to increases in the cost of fossil fuels as well as environmental standards (US Department of Energy, 1983). Additionally, small hydropower schemes have advantages over large schemes such as a short payback time, low investments and minor maintenance requirements. These schemes are a decentralized source of power generation and are frequently individually owned. Challenges associated with small schemes are related to flow variation instability affecting the constant energy generation and possible floods (Schwartz et al., 2005). New or planned RoR schemes are currently spread across Europe (Francois et al., 2016). The flow duration curve (FDC) is commonly used to design micro-hydropower schemes (US Department of Energy, 1983). This curve is based on past observations and provides an estimate of the amount of the time when a certain river flow is equalled or exceeded.

Table 1.3 Number of barriers per power category (adapted from EA, 2010)

	0-10 kW	10-20 kW	20-50 kW	50-100 kW	100-500 kW	500-1500 kW	> 1500kW	Total	Percentage
Southern Region	1,225	117	108	35	10	0	0	1,495	6%
Anglian Region	1,126	145	150	51	46	0	0	1,518	6%
Thames Region	1,390	188	159	100	94	49	0	1,980	8%
South West Region	1,968	339	324	132	116	15	1	2,895	11%
Midlands Region	2,720	409	353	151	158	38	14	3,843	15%
Wales	1,639	713	923	360	363	74	43	4,115	16%
North West Region	2,510	698	729	385	385	60	5	4,772	18%
North East Region	3,075	809	638	283	376	124	12	5,317	21%
Total	15,653	3,418	3,384	1,497	1,548	360	75	25,935	
Percentage	60%	13%	13%	6%	6%	1%	0%		

Table 1.4 Total power potential per power category (kW) (adapted from EA, 2010)

	0-10 kW	10-20 kW	20-50 kW	50-100 kW	100-500 kW	500-1500 kW	> 1500kW	Total	Percentage
Southern Region	2,473	1,640	3,436	2,447	1,109	0	0	11,105	1%
Anglian Region	2,711	2,000	4,817	3,627	6,346	0	0	19,501	2%
Thames Region	5,918	4,914	10,089	9,245	22,859	9,326	4,286	66,637	6%
South West Region	3,396	2,685	4,864	7,328	19,117	41,954	0	79,344	7%
Midlands Region	6,377	5,758	11,261	10,593	32,857	36,163	27,796	130,805	11%
Wales	9,953	9,888	23,457	26,930	80,000	44,818	10,895	205,941	17%
North West Region	10,496	11,440	19,789	20,350	83,314	98,459	25,224	269,072	23%
North East Region	6,767	10,354	29,415	24,383	79,077	63,408	182,019	395,423	34%
Total	48,091	48,679	107,128	104,903	324,679	294,128	250,220	1,177,828	
Percentage	4%	4%	9%	9%	28%	25%	21%		

1.8.3. Hydropower good practices guideline

In 2009, the UK's Environment Agency (EA) produced the most recent good practice guidelines for hydropower schemes. The guidelines suggest an initial environmental assessment before construction including an evaluation of the scheme's potential impacts to 1) the river flow, 2) areas of scientific, natural or conservation importance, 3) chemical and physical water quality, 4) biological water quality, 5) fisheries and protected species, 6) flood risk management, and 7) river navigation (EA, 2009).

In general, a hydropower scheme situated within or immediately adjacent to a main channel would not affect the main flow and therefore would be environmentally acceptable compared to schemes with depleted reaches which are likely to negatively affect fish migration. The depleted volume should not affect the minimum river flow required by fish communities. Additionally, hydropower schemes should incorporate a proper fish passage to allow the downstream or upstream movement of fish (EA, 2009).

Important parameters for hydropower schemes are the annual hydrograph, FDC, mean flow, depleted reach, base flow index (BFI, ratio of the flow observed 95% of the time to the mean flow), residual flow, hands-off flow (HOF), design flow and turbine start-up flow. The annual hydrograph provides daily flow information including the daily variation. The FDC describes the statistical availability of a particular flow volume by giving the percentage of time that it is equalled or exceeded. The mean flow is the average flow of the river during a defined period. The depleted reach refers to the river section between the water abstraction (upstream) and the return point after the hydropower scheme (downstream). The HOF is established for environmental reasons. Abstraction will not begin until the flow is above the HOF by at least a volume equal to the turbine start flow and stop if the flow is below the HOF plus the start-up flow. The BFI shows how a particular site is influenced by its geology and soil water storing capacity. A high baseflow has a ratio bigger than 0.2, a medium baseflow has a ratio between 0.2 and 0.1 and a low baseflow has a ratio smaller than 0.1. Finally, the maximum design flow is the maximum flow that the scheme can abstract from the river and it is commonly defined as the mean average flow. (EA, 2009).

1.8.4. Current status of RoR hydropower research in the UK

The assessment of low head hydropower potential in the UK is currently an area of interest in the UK (EA, 2011). In 2010, the EA concluded a study aiming to map hydropower opportunities and sensitivities for England and Wales (EA, 2010). The analysis involves the estimation of head, flow and fish sensitivity for the different existing barriers within the area. Results indicate that the best hydropower opportunities are located on the North East, North West, Wales and Midlands. Power potential from these four regions accounts for 85% of the estimated power potential (Table 1.4).

Following the EA initial study (EA, 2010), an analysis focusing on the Middle Severn catchment was performed by JBA consulting group (EA, 2011) using higher resolution to estimate the site's parameters and including only sites with potential higher than 50kW. From 627 sites, 36 have potential to generate more than 50kW and only 18 have attractive potential for a profitable investment. The 36 sites are classified as highly sensitive and therefore require mitigation actions before developing the scheme. The study

estimates 90% less energy potential than the initial estimation (e.g. 20.3 MW in EA (2010) compared to 1.9 MW in EA (2011)). The study concludes that the main limitations of the initial estimations are due to the employed resolution which gave wrong flow volumes and counted the same barrier twice. Noteworthy, none of these studies have included a climate change impact analysis.

1.8.5. Hydropower and climate change

Climate change may modify the hydropower production and its temporal variability (Francois et al., 2014). Projected effects of climate change are alterations in local precipitation and temperature affecting river flow timing, river flow volumes, snowmelt timing, evapotranspiration, sediment load and other ecosystem processes (Kumar et al., 2011; Madani, 2011). The future size and efficiency of current hydropower schemes are generally determined based on current water availability. Also, droughts and floods affect hydropower operation. Nevertheless, most of the actual hydropower plants were designed and built with no consideration of climate change. Therefore, extreme events are likely to affect actual infrastructure in addition to changes in water availability. Scheme design should also consider the effects of climate change prior to the constructions of future hydropower plants (Mideska and Kallbekken, 2010; Renofalt, et al., 2010). For schemes to operate most efficiently over the year, analysis of both the mean flow and its variation is necessary to determine their optimum size and design. Preparation of adaptation strategies towards climate change is essential (Noreña et al., 2009). Plans ignoring the effects of climate change are associated with high risks (Brown et al., 2011).

In general, few studies have quantitatively analysed the effects of climate change on technical hydropower potential (Kumar et al., 2011). Future changes in river regime could generate variability of hydropower potential (Lehner et al., 2005). Schemes with less or no storage capacity, such as RoR schemes, will be more vulnerable to such alterations as they depend on the river flow (Tamm et al., 2016). Furthermore, climate change could affect future water demand and supply, jeopardizing hydropower generation where more users are involved (Hamududu & Killingtveit, 2012; Kumar et al., 2011). In such cases, it will be complicated to assess if flow variations are produced by water abstractions, cyclic fluctuations or climate change (Lehner et al., 2005). Changes in the magnitude and frequency of extreme events (droughts and floods) are likely to impact hydropower schemes. Increases in sediment load could damage turbines, decreasing their efficiency (Kumar et al., 2011). Considering the above, mitigation and adaptation measures should be considered for current and potential schemes, based on detailed assessments (Hamududu & Killingtveit, 2012).

Overall decreases in the hydropower potential are projected by RCPs 2.6 and 8.5 for Europe with slight increases for the north of Europe and in the UK (Van Vliet et al., 2015). Similar results were obtained in previous studies using previous generations of RCMs (eg. Hamududu and Killingtveit, 2012; Lehner et al. 2005). Even in regions where a marked annual behaviour is observed, different seasonal trends could occur having distinct impacts towards the periodical hydropower generation. This emphasizes the need to analyse the changes in the flow annual average and seasonal distributions (Kumar et al., 2011).

1.8.6. The impact of climate change on RoR hydropower

The analysis of climate change impacts on RoR hydropower schemes is a new area of research that has attracted attention recently. In the UK, a proposed scheme in the Severn catchment based on UKCP09 climate projections is projected to increase production in winter and decrease in summer with no change over the annual generation by 2050 (Carless and Whitehead, 2013). In contrast, seasonal and annual increases in power produced by RoR schemes in Estonia are projected by 2100 based on two RCMs bias corrected by the monthly additive correction for temperature and the local intensity scaling for precipitation (Tamm et al., 2016). These studies represent a first approach for the development of a climate change analysis in RoR schemes. Nevertheless, the studies could be complemented by integrating more than one study site, using better bias correction methods and including a larger combination of climate models to decrease the uncertainty of the projections. The present study addresses the mentioned gaps to get a better understanding of the impacts of climate change to RoR hydropower schemes.

1.9. Main objective, specific objectives and research questions

The main objective of this research is to assess how climate change will affect RoR hydropower efficiency and feasibility within UK study catchments. In this thesis the following research questions will be addressed:

i) Is the relative performance of the 0.11° Euro-CORDEX RCMs better than their 0.44° version to simulate climate and river flow? (Chapter 4)

ii) Is the current skill of the Euro-CORDEX RCMs able to generate useful inputs for the analysis of climate change impacts to hydrology? (Chapter 4)

iii) To what extent are the projected changes in climate (Chapter 5), flow regime and hydropower generation (Chapter 6) robust when considering two different bias correction approaches (namely using RCMs driven by perfect boundary conditions or RCMs driven by GCMs to train the bias correction method)?

Research question iii) looks into the results obtained by two different bias correction approaches. Bias correction of the RCM simulations driven by perfect boundary conditions corrects the RCM bias only whereas bias correction of the RCM simulations driven by a GCM corrects the bias from both the GCM and the RCM. Normally the first approach is used to evaluate the simulation skill of different RCMs or from one RCM at two different resolutions. The latter approach is frequently used in impact studies where the uncertainty in the climate change projection is intended to be reduced. Nevertheless, after applying both approaches the results might be contrasting, even with opposite climate change signal signs. Therefore, the research question looks into the robustness of using both approaches by analysing if the direction of the climate change signal is similar after applying both correction approaches.

Furthermore, to achieve the aim of the project and answer the research questions the following specific objectives are defined: a) Select suitable study catchments and collect historic precipitation, temperature, river flow and hydropower data for these study catchments, b) Collect RCM data (namely evaluation. historical and RCP simulations), c) Bias-correct the precipitation and temperature of RCMs to the study

catchment-scale, d) compare among, develop and calibrate hydrologic model(s) for the demonstration catchments, e) couple the hydrological model with the RCMs to simulate future river flow, f) calculate the energy generation produced by the hydropower plants and their generation considering the projected future river flows, and g) assess the impacts on efficiency and feasibility for the selected hydropower schemes based in the future scenarios.

The development of a study integrating the climate change effects on hydropower efficiency and feasibility will expand the knowledge of the hydropower industry as well as the availability of data for water and hydropower managers in order to adapt to future impacts in water availability and power generation. Furthermore, this study will evaluate the skill of current state-of-the-art RCMs that are currently used in impact studies and at the same time the potential benefits and limitations of using bias-corrected RCM outputs. As far as the author is aware, to date few studies have explicitly considered the influence of bias correcting against GCM-driven RCMs (historical simulations) or RCMs driven by perfect boundary conditions (evaluation simulations).

This thesis consists of seven chapters. This introduction is the first chapter of the thesis. In chapter two the criteria used to select the study catchments is shown along with the precipitation, temperature and river flow characteristics of each catchment. Chapter three displays the methodology followed for the development of the hydrological model for each catchment and the results from their calibration and validation. The evaluation of the climate and hydrological simulation skill of uncorrected and bias-corrected RCMs is described in chapter four. The future climate projections from each catchment are shown in chapter five, considering two different bias correction approaches. Chapter six continues the analysis from chapter five by integrating the hydrology and hydropower generation projections. Finally, chapter seven integrates the main conclusions of the thesis.

2. Study catchments

2.1. Introduction

This chapter describes the criteria used for the selection of the study catchments and describes the main characteristics of the selected catchments. The aim of this study is to better understand the impacts of climate change on catchment hydrology and its consequences for the feasibility and sustainability of run of the river (ROR) hydropower schemes within the UK. For this purpose, four study catchments with potential or installed ROR hydropower schemes of a comparable size are analysed. The selected study catchments represent different regional climates and physical features within the UK, also incorporating both high and low head hydropower schemes. The selected study catchments define the area where the study will be performed.

The chapter begins by defining the criteria used for the study site selection. Afterwards the main characteristics of each study catchment are described including their elevation and watercourses, land cover, soil type, climate, hydrology, links between the catchment's climate and hydrology, and information related to the proposed or installed hydropower scheme.

2.2. Criteria for the selection of the study catchments

The following criteria are used for the selection of the study catchments:

a) *Catchments where installed or feasible ROR hydropower schemes are or could be located.* Different databases provide information about installed schemes such as the Office of Gas and Electricity Markets (Ofgem), community based schemes and plants licenced by the Environment Agency. Feasible ROR schemes are listed in the Environment Agency's mapping of hydropower opportunities in England and Wales study (EA, 2010).

b) *Catchments where the hydropower scheme's maximum generation is at least 100 kW.* Potential ROR hydropower schemes within England and Wales include schemes generating less than 1kW to 10,000kW (EA, 2010). The climate change impact to the schemes with low energy generation is expected to be less important due to their potential generation. Nevertheless, ROR schemes with a high power generation are scarce. Therefore, a threshold of 100kW is defined for the selection of the study sites.

c) *Catchments geographically spread across England and Wales.* As the change signal and magnitude might be distinct for different latitudes and regions within the UK (Lehner et al., (2005); Arnell & Gosling (2013)), it is relevant to include study catchments with a geographical spread. Additionally, this study considers the Environment Agency's mapping of hydropower opportunities in England and Wales study (EA, 2010) as reference, therefore only study catchments within England and Wales are selected.

d) *Natural catchments are preferred but human-influenced catchments are also selected.* Catchments that are heavily affected by anthropogenic activities such as water extraction and discharge modify the natural river flow of the catchment, increasing the hydrological modelling uncertainty. Therefore,

natural catchments where there is low or no anthropogenic impact are preferred over heavily impacted catchments. However, most of the UK catchments are modified. Thus, potential and installed hydropower schemes might be affected by this factor. Therefore, for the selection, catchments with some level of anthropogenic influence are also considered.

e) *Availability and length of daily streamflow data.* The accessibility to this data is essential for the development of the catchments' hydrological models and for the analysis of river flow regimes. A minimum length of 30 years of daily data is set as limit in order to have enough data to analyse each catchment.

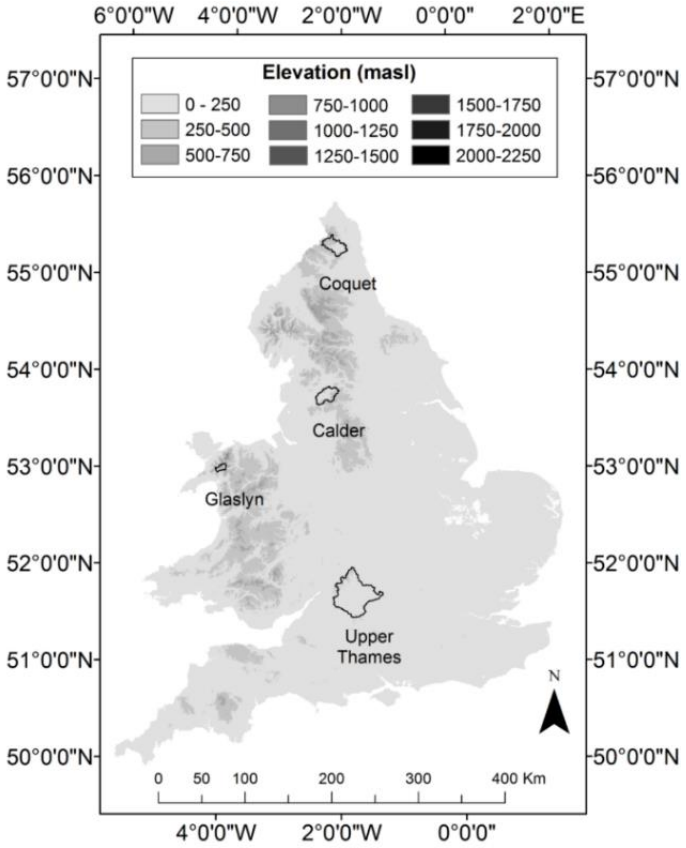

Figure 2. 1 Orography and location of the study catchments within England and Wales (with data from ©GeoPerspectives supplied by Bluesky 2014 and ©NERC (CEH) 2012. For Great Britain: Contains Ordnance Survey data ©Crown copyright and database right 2012)

The selection criteria aim to include study sites with different characteristics, representative of the diverse conditions that can be found for a ROR hydropower scheme within England and Wales. As a result, four study sites with contrasting location, area, elevation, land cover, soil type, precipitation, temperature, potential evapotranspiration, river flow regime and hydropower scheme characteristics are chosen. The selected catchments are the Coquet catchment in Northumberland, northern England; the Calder catchment in Lancashire; the Glaslyn catchment in upland Gwynedd, northern Wales; and the Upper Thames catchment covering parts of Swindon, Oxfordshire and Gloucestershire in southern England (Fig. 2.1). A summary of the characteristics of each study catchment is shown in Table 2.1. These study catchments are expected to be suitable for the analysis of different climate change impacts towards the

river regime and hydropower operation and are also representative of the different catchment characteristics found in England and Wales. The following sections describe the physical, climate, hydrological and hydropower characteristics of each study site.

Table 2. 1 Summary of the characteristics of the study sites

		Upper Thames	Glaslyn	Calder	Coquet
Extent	Area (km^2)	1616	69	316	346
Elevation	Maximum elevation (masl)	330	1080	556	775
	Minimum elevation (masl)	52	30	40	71
	DPSBAR (m/km)[1]	39	309	94	140
Land cover	Grassland (%)	36.6	53.1	58.6	45.9
	Urban (%)	5.3	0.1	16.8	0.5
	Mountain (%)	0.6	29.8	15.0	33.5
	Water (%)	1.2	2.2	0.7	0.1
	Woodland (%)	6.7	14.3	6.9	13.2
	Arable (%)	49.7	0.4	2.0	6.9
Soil type	Loamy sand (%)	9.0	17.9	6.5	41.3
	Clay loam (%)	57.1	38.4	80.5	28.7
	Loam (%)	13.8	34.8	3.5	11.6
	Loamy clay (%)	11.4	0.0	0.0	2.4
	Not available (%)	0.0	0.9	0.0	0.0
	Mixture (%)	8.6	8.0	9.5	16.1
	PROPWET[2]	0.32	0.62	0.55	0.45
Precipitation	90th percentile (mm/day)	6.7	24.4	10.3	7.7
	95th percentile (mm/day)	10.2	34.2	14.8	11.9
	Annual mean (mm/year)	762	2957	1251	968
	Wettest - driest month difference (mm)	30	184	69	40
Temperature	Annual mean (°C)	9.7	8.1	8.4	7.4
	Warmest - coldest month difference (°C)	12.2	10.6	11.9	11.5
Potential evapotranspiration	Annual mean (mm/yr)	522	477	486	473
River flow	Daily mean (m^3/s)	15.3	5.8	8.8	6.1
	Q10 (m^3/s)[3]	34.8	13.5	19.9	12.4
	Q95 (m^3/s)[4]	1.90	0.55	1.99	0.84
	BFI[5]	0.70	0.32	0.42	0.47
Hydropower[6]	Status	Feasible	In operation	In operation	Feasible
	Turbine	Archimedes screw	Pelton	Archimedes screw	Archimedes screw
	Head (m)	1.7	176.0	2.2	2.0
	Maximum generation (kW)	225	640	100	118
	Hands off flow (m^3/s)	1.90	0.09	1.28	0.84
	Maximum extraction (m^3/s)	17.52	0.45	7.31	7.81

[1]The mean drainage path slope (DPSBAR) index gives an estimation of the catchment's steepness: above 300m/km for mountainous terrain and below 25m/km for flat zones (Marsh and Hannaford, 2008)
[2]The proportion of time soils are wet (PROPWET) index estimates the catchment flooding tendency: above 0.8 for wet areas and below 0.2 for dry zones (Marsh and Hannaford, 2008)
[3]The Q10 is a measure of the high flows observed within the catchment. It is defined as the river flow equalled or exceeded the 10% of the time
[4]The Q10 is a measure of the low flows observed within the catchment. It is defined as the river flow equalled or exceeded the 95% of the time
[5]The base flow index (BFI) estimates the groundwater contribution to the surface flow: high values indicate an important groundwater contribution and low values represent little groundwater contribution (Marsh and Hannaford, 2008)
[6]For the feasible sites, data is based on estimations from the Environment Agency (EA, 2010)

2.3. Physical description

The physical characteristics of each study catchment are described next. Such characteristics include the elevation, watercourses, land cover and soil type. Additionally, their importance towards this study is highlighted in each section.

2.3.1. Elevation and watercourses

Differentiating high-elevation and low-elevation catchments is important because runoff from catchments at high elevations is greater as a result of the larger precipitation volumes they receive and the slope of particular zones of the catchment might affect the precipitation spatial distribution (Davie, 2008) and the hydrological pathways. The watercourses provide an insight of the flow direction and the paths from the principal and tributary streams. The following section describes the elevation, area and water courses of the study catchments. Additionally, the mean drainage path slope (DPSBAR) index is provided. The DPSBAR gives an estimation of the catchment steepness. For mountainous terrain it reaches values above 300 m/km and below 25 m/km for flat areas.

2.3.1.1. Upper Thames

The Upper Thames catchment has an area of 1,616 km^2 and it is located on southern England between latitudes 51°30’23”N and 52°1’33”N, and longitudes 1°18’6”W and 2°8’37”W (Fig. 2.1). The catchment is mostly flat with elevation ranging from 52 to 330 meters above sea level (masl) and highest elevations in the north and northwest. The Upper Thames DSPBAR is 39 m/km (Marsh and Hannaford, 2008), typical of a flat catchment. The River Thames is the main river of the catchment flowing from west to east with several tributaries such as the Swill Brook, Ampney Brook, Churn, Coln, Ray and Windrush Rivers (Fig. 2.2a). Streamflow originates in the west, north and south, flowing towards the main river at the centre of the catchment. The main river flows from west to east, leaving the catchment at the Eynsham gauging station.

2.3.1.2. Glaslyn

The Glaslyn catchment has an area of 68.6 km^2 and it is located on the Gwynedd Welsh County between latitudes 52°59’41”N and 53°5’1”N, and longitudes 4°10’29”W and 3°58’33”W (Fig. 2.1). The catchment has a complex topography with elevation varying from 30 to 1,080 masl and a DSPBAR of 309 m/km (Marsh and Hannaford, 2008). The highest elevation is located in the north of the catchment with high altitudes also located on the east and west. Elevation decreases from these peaks towards the central and southern areas of the catchment (Fig. 2.2b). The River Glaslyn has an approximate length of 14.3km and receives inflow from tributary streams such as Cynnyd, Merch, Cwm Llan, Gorsen, Llynendno and Colwyn. Surface water follows two main directions: 1) flows generated in the north and northeast have a southwest direction, and 2) flow generated in the northwest flows to the south. The main river leaves the catchment at the Beddgelert gauging station, located in the southwest.

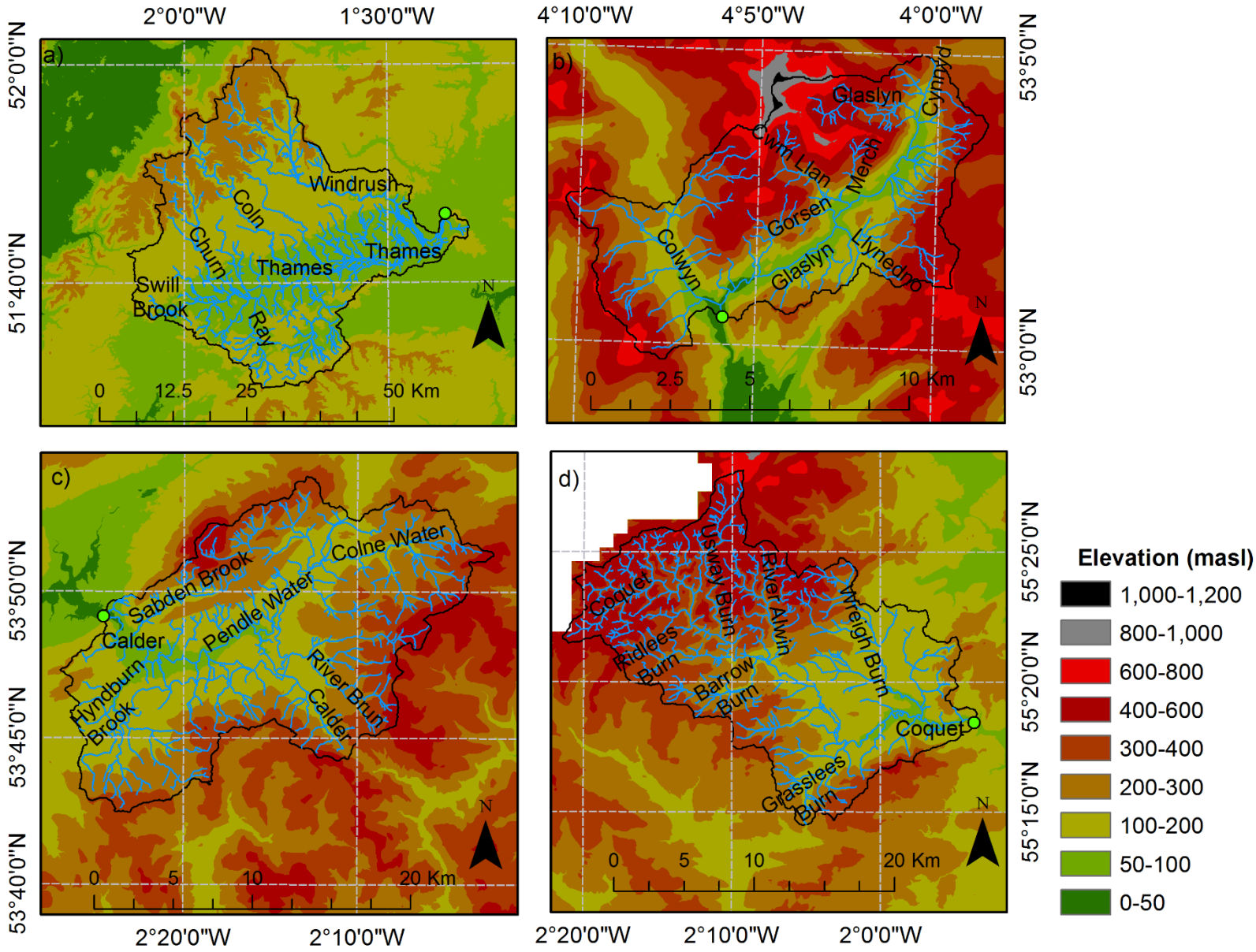

Figure 2. 2 Elevation and watercourses: a) Upper Thames, b) Glaslyn, c) Calder, d) Coquet. The streamflow gauging stations are represented with a green circle and areas with no data are shown in white (with data from ©GeoPerspectives supplied by Bluesky 2014 and © Database Right/Copyright NERC – Centre for Ecology & Hydrology. All rights reserved. Contains Ordnance Survey data © Crown copyright and database right 2014)

2.3.1.3. Calder

The River Calder drains a 316 km^2 catchment located in eastern Lancashire between latitudes 53°42'23"N and 53°54'3"N, and longitudes 2°27'0"W and 2°1'51"W (Fig. 2.1). The elevation of the catchment varies from 40 to 556 masl with higher elevations in the north, east and south. Elevation decreases towards the central valley with the lower elevations located on the west and northwest (Fig. 2.2c). The DPSBAR is 94 m/km indicating that the catchment is mostly flat (Marsh and Hannaford, 2008). The River Calder has an approximate length of 34 kms and drains flows from tributaries such as Colne water, River Brun, River Don, Pendle water, Sabden Brook and Hyndburn Brook. In general, surface water flows from the north, south and east towards the central valley and finally leaves the catchment in the northwest through the Whalley weir gauging station.

2.3.1.4. Coquet

The Coquet catchment has an area of 346 km^2 and it is located in Northumberland between latitudes 55°14'25"N and 55°28'20"N, and longitudes 1°53'12"W and 2°21'33"W (Fig. 2.1). The elevation of the catchment varies from 71 to 775 masl. Higher elevations are found in the north and northeast, decreasing towards the southwest where the lower elevations are located (Fig. 2.2d). The DPSBAR index is 140 m/km (Marsh and Hannaford, 2008), representative of a catchment with mixed steepness. The River Coquet is the main river of the catchment with tributaries including the Usway burn, Ridlees burn, Barrow burn, River Alwin, Grasslees burn and Wreigh burn. Surface water flows from north and west towards the southeast of the catchment, leaving it at the Rothbury gauging station.

2.3.2. Land cover

Land cover provides an initial insight of the vegetation canopy cover. Canopy intercepts and retains rainfall before it reaches the catchment's ground making it available for evaporation. For example, large forests will store rainfall in the trees, preventing it from reaching the catchment's ground and from generating runoff. Additionally, land cover provides information about the extent of urban and agricultural areas that could potentially influence the catchment's natural water cycle due, for example, to water abstractions and discharges. Urban areas additionally drain runoff faster than the natural rate (Davie, 2008). Finally, land cover data combined with the reference evapotranspiration (see section 3.3.1.3.2) gives an estimation of the potential evapotranspiration based on the vegetation cover. In this study land cover is separated into woodland, arable or agriculture, grassland, mountain, water and urban areas. The extent of each land cover category for each catchment is shown in Figure 2.3 and described next.

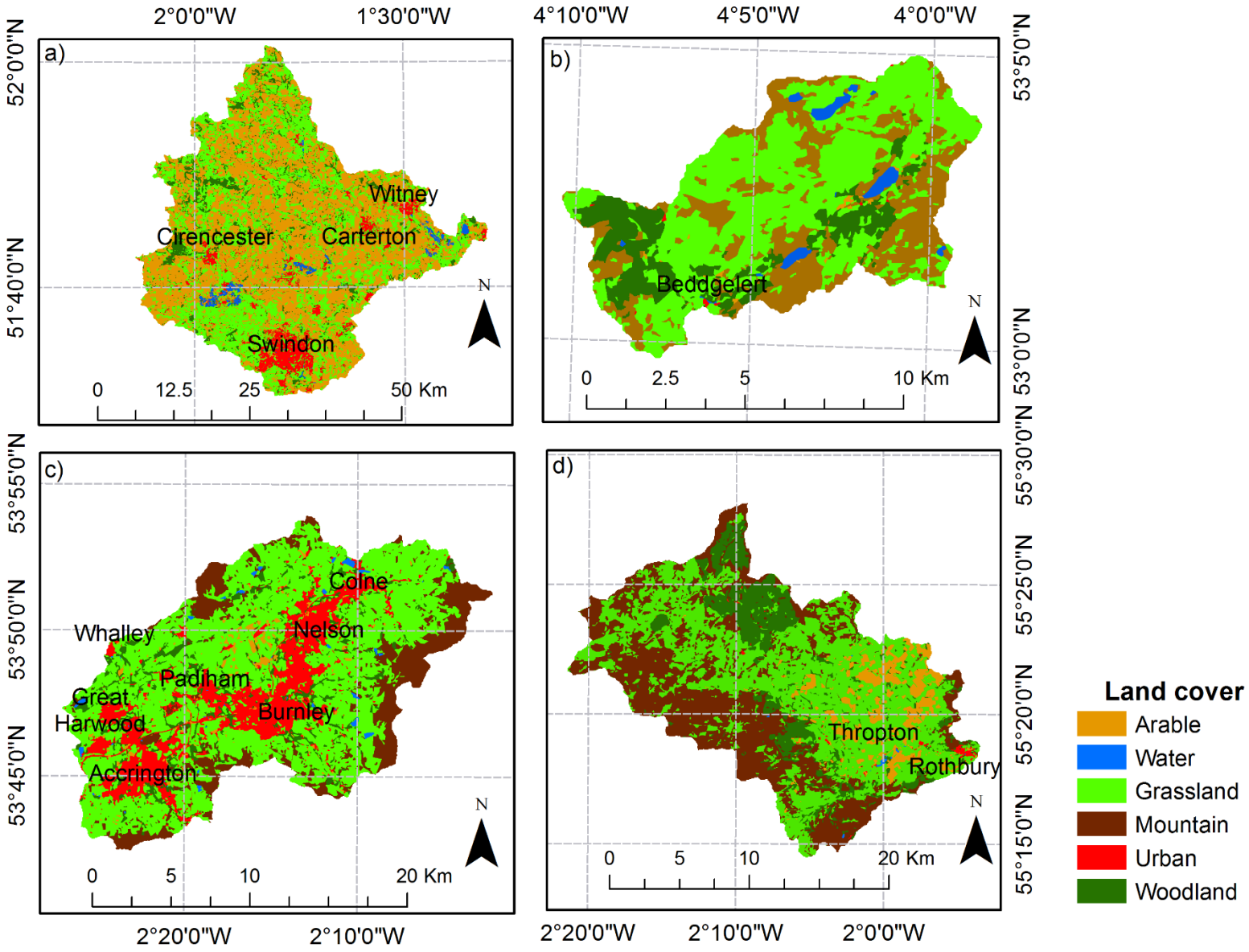

Figure 2. 3 Land cover and main urban areas: a) Upper Thames, b) Glaslyn, c) Calder, d) Coquet (based on Morton et al., 2011; with data from © Crown Copyright/database right 2016. A British Geological Survey/EDINA supplied service)

2.3.2.1. Upper Thames

Agriculture is present in almost 50% of the catchment along with large extensions of grassland (37%) (Fig. 2.3a). In contrast, woodlands (6.7%) and mountain (0.6%) habitats are found in small portions of the catchment and urban areas cover 5% of the catchment. Swindon is the catchment's largest urban area and Witney, Carterton and Cirencester are also located within the catchment.

2.3.2.2. Glaslyn

The catchment is mostly covered by grasslands (53.1%), mountains (29.8%) and woodlands (14.3%). Agriculture and urban areas cover a minimal extension of the catchment, 0.4% and 0.1% respectively. The Beddgelert village is the most important human settlement within the catchment (Fig. 2.3b).

2.3.2.3. Calder

Grassland covers more than half of the catchment (58.6%) (Fig. 2.3c). Urban areas such as Colne, Nelson, Burnley, Accrington, Padiham, Great Harwood and Whalley represent the second largest land cover category with almost 17%. This is the largest urban cover percentage from all study catchments. Mountain and woodland together cover approximately 20% of the catchment and the agriculture cover is minimal with 2%.

2.3.2.4. Coquet

Grassland and mountain together cover approximately 75% of the catchment (Fig. 2.3d). Woodland is the third largest land cover category within the catchment (13.2%). Additionally, agriculture covers 7% and urban areas 0.5% of the catchment. The most important human settlements within the catchment are Rothbury and Thropton.

2.3.3. Soil type

Soil type provides an insight of the permeability of each catchment and the amount of water that it can store. These characteristics determine the amount of rainfall that is infiltrated to the groundwater and the volume available for runoff. For example, sand tends to be more permeable than clay loam and loam is capable of storing more water than sand. Additionally, the soil type also helps to estimate the rate at which rainfall infiltrates through the soil, known as hydraulic conductivity. This is relevant when successive storms are present in the catchment and the initial wetness of the soil, or in other words its degree of saturation, plays a major role for runoff generation (Raghunath, 2006; Davie, 2008). In this study the different soil types are divided into sand, loam, loamy sand, clay loam, loamy clay and a mixture of all. The percentages of each catchment's soil types are shown next. Additionally, the proportion of time when soils are wet (PROPWET) is provided for each catchment. PROPWET estimates the catchment's flooding tendency, varying from more than 0.80 in the wettest areas of the UK to less than 0.20 in the driest zones (Marsh and Hannaford, 2008).

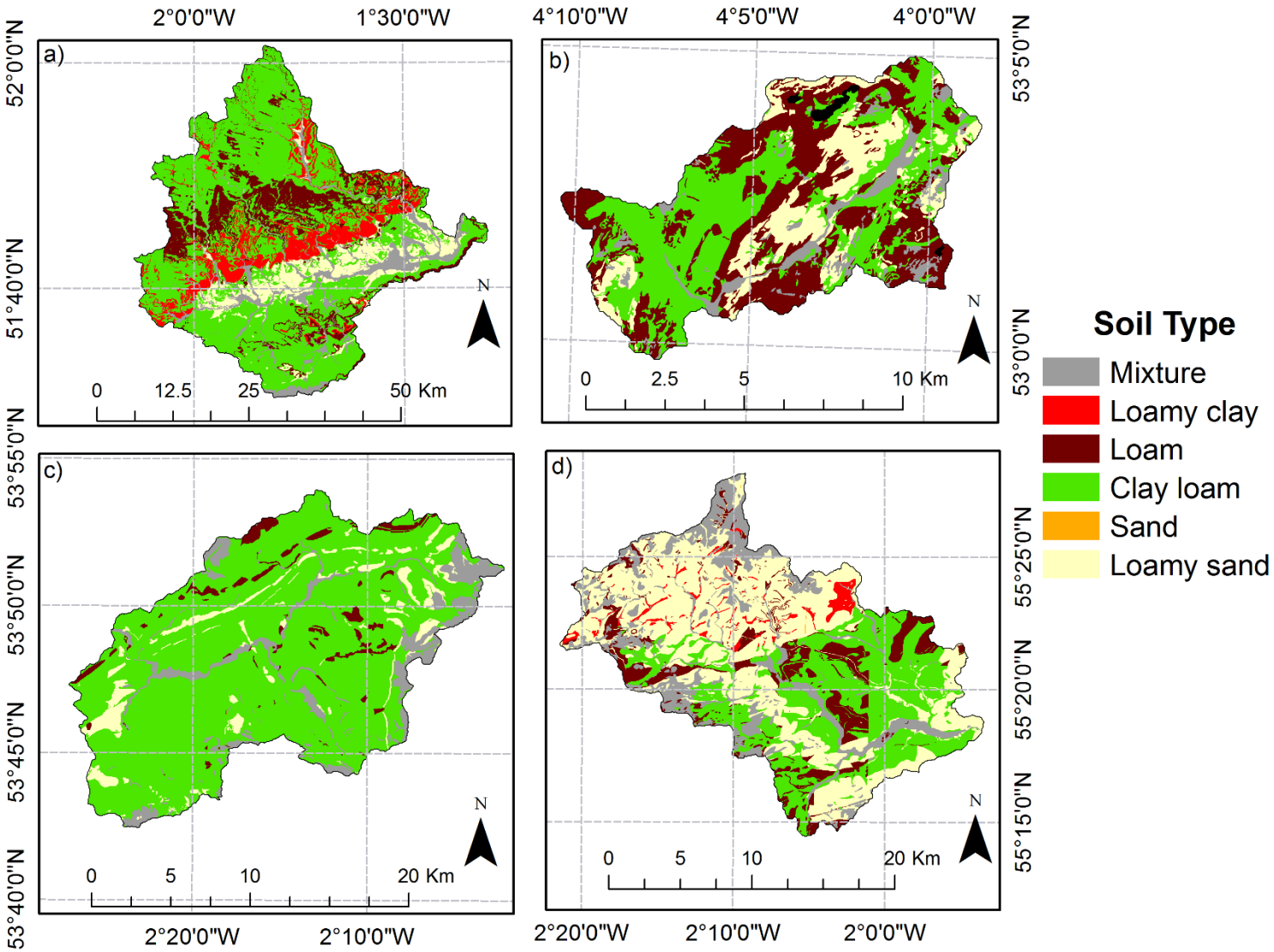

Figure 2. 4 Soil type: a) Upper Thames, b) Glaslyn, c) Calder, d) Coquet. Areas with no data are shown in black. © Crown Copyright/database right 2016. A British Geological Survey/EDINA supplied service

2.3.3.1. Upper Thames

The geology of the catchment is mixed, with permeable zones in the parts where streamflow originates and clay on the lower regions of the catchment (Marsh and Hannaford, 2008). More than half of the catchment is formed of clay loam (Fig. 2.4a). Additionally, loam and loamy clay are present in 14% and 11% respectively. Finally, loamy sand and a mixture of all soils, each cover 9% of the catchment. The PROPWET index for the catchment is 0.32 (Marsh and Hannaford, 2008).

2.3.3.2. Glaslyn

In general, the catchment is made of impermeable volcanic rocks (Marsh and Hannaford, 2008). The catchment is mainly dominated by loam and clay loam, which almost cover 75% of the entire catchment (Fig. 2.4b). Loamy sand is also present in 18% of the catchment, and a mixture of all in 8% of the catchment. The PROPWET index for the catchment is 0.62.

2.3.3.3. Calder

The catchment's geology is mainly formed of moderate permeability bedrocks with mixed permeability soils. Boulder Clay covers most of the catchment (Marsh and Hannaford, 2008). Clay loam is present in 80% of the catchment (Fig. 2.4c). Additionally, a mixture of all soils covers approximately 10% of the catchment followed by loamy sand (6.5%) and loam (3.5%). The catchment's PROPWET index is 0.55.

2.3.3.4. Coquet

The permeability of the catchment is low. The catchment's uplands are covered by peat and the valley's surface is made up of Boulder Clay and alluvium (Marsh and Hannaford, 2008). Loamy sand (41%) is the catchment's dominant soil type, with a high presence of clay loam (29%). A mixture of all soil types covers 16% of the catchment. Loam and loamy clay are also found on the catchment, with 11.6% and 2.4% respectively (Fig. 2.4d). PROPWET is 0.45 for this catchment.

2.4. Climate

The following section gives information about the climate of each catchment. It focuses on the three most important climate variables for hydrology: precipitation, temperature and evapotranspiration. For these variables, monthly and annual means are shown along with their spatial distribution and other statistics relevant for this study.

2.4.1.Precipitation

Precipitation is the main input of water to the catchment. It includes all forms of water entering from the atmosphere into the catchment, e.g. rainfall, drizzle, snow, hail and sleet. Within a catchment, precipitation occurrence and magnitude vary spatially and temporally due to static (e.g. altitude and slope) and dynamic (varying weather system) influences (Davie, 2008). In this section statistics of the observed precipitation are shown, such as the mean annual and monthly accumulated precipitation, the spatial distribution of the mean annual accumulated precipitation, high precipitation percentiles, the monthly mean dry days and the monthly mean days with precipitation above the 90th percentile. The monthly dry days are estimated by

adding the number of days in a month with precipitation lower than 1 mm/day (as used in Zhang et al., 2011). The number of days in a month with precipitation above the 90th percentile is used to represent monthly extreme precipitation events. Also, the annual precipitation linear trend is analysed using a linear regression and its statistical significance assessed using a t-test.

The observed precipitation records used in this study are based on the Centre for Ecology and Hydrology (CEH) Gridded Estimates of Areal Rainfall (CEH-GEAR) dataset (Tanguy et al., 2014; Keller et al., 2015). CEH-GEAR provides 1-km gridded monthly and daily precipitation observations for the UK from 1890 to 2012 using data from the Met Office's raingauges. CEH-GEAR uses the natural neighbour interpolation method, followed by a normalization step and a monthly correction. The natural neighbour interpolation method implies the definition of Thiessen polygons (polygon where no other raingauge is closer than the analysed gauge) for each raingauge at each time step. Additionally, Thiessen polygons are delineated for each grid point, considering the grid point as another raingauge. Gauges with polygons overlapping the grid point polygon are used to estimate the grid point rainfall considering the area of overlap as weight factor. Subsequently, the Spackman (Spackman, 1993) Standard period Average Annual Rainfall (SAAR) is used as normalisation method due to the uniform distribution of the raingauge network. Finally, a monthly correction factor is applied to each daily estimate. This assures an agreement between the monthly estimate and the monthly estimate derived from the accumulated daily estimates.

For consistency in the remainder of this chapter, CEH-GEAR data from 1976 to 2012 will be used as this is the maximum available observation length from all catchments and variables (e.g. the Calder observed river flow record begins in 1976). CEH-GEAR estimates no rainfall value when the nearest raingauge is not within a distance of 100 km from the gridbox. Nevertheless, this is not an issue for the selected period.

2.4.1.1. Upper Thames

The mean annual accumulated precipitation is 762 mm/year. The linear trend shows a statistically non-significant annual increase of 1.9 mm per year in the accumulated precipitation (19 mm per decade) (Table 2.2). Also, variability increases for the second half of the time series as indicated by the standard deviation, which varies from 84 mm/year between 1976 and 1994 to 162 mm/year between 1995 and 2012. Years with annual accumulated precipitation above the average +1 standard deviation are more frequent after 1992. Nevertheless, years with accumulated precipitation below the average -1 standard deviation are seen during the complete period (Fig. 2.5). Spatially, the highest precipitation occurs in the northwest, where the higher elevations of the catchment are located (Fig. 2.6a). The precipitation volume gradually decreases towards the southeast where the catchment's outlet is found. There is a difference of 315 mm/year between the points of highest and lowest precipitation.

Table 2. 2 Linear regression trend coefficients (from 1976 to 2012) for the mean annual precipitation, temperature and river flow in each catchment along with their t-test p-value (significant trends are shown in bold)

	Precipitation (mm/yr)				Temperature (°C/yr)				River flow (cumecs/yr)			
Catchment	Upper Thames	Glaslyn	Calder	Coquet	Upper Thames	Glaslyn	Calder	Coquet	Upper Thames	Glaslyn	Calder	Coquet
Coefficient	1.9	4.7	0.8	3.4	**0.03**	**0.02**	**0.03**	**0.02**	0.05	0.00	0.01	0.01
p-value	0.34	0.41	0.78	0.10	**0.00**	**0.00**	**0.00**	**0.00**	0.51	0.75	0.85	0.55

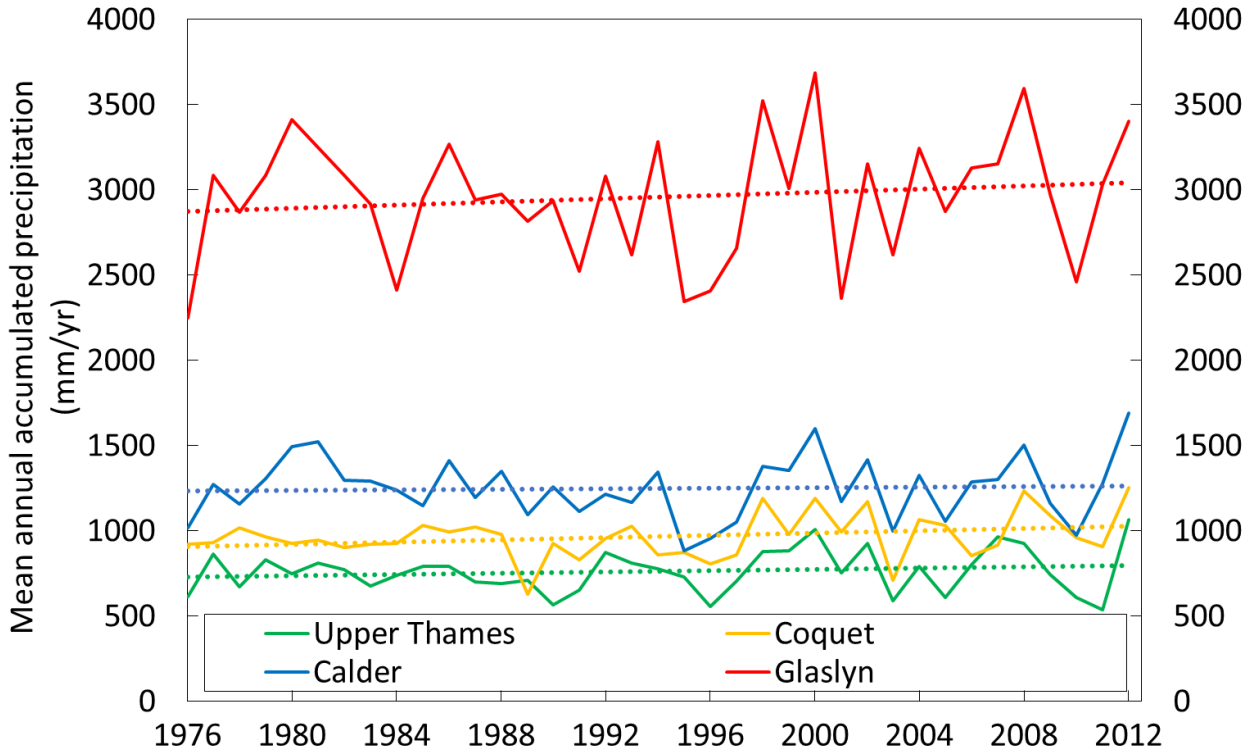

Figure 2. 5. Mean annual accumulated precipitation (1976-2010). Dashed lines represent the linear trend

The monthly accumulated precipitation varies from 82 mm in December to 52 mm in February and April. The highest accumulated monthly precipitation is observed from August to January and the lowest from February to July (Fig. 2.7a). The difference between the wettest and driest months is 30 mm. The monthly mean of the dry days is smaller during winter (December, January, February) and larger for summer (June, July, August) with all months having at least an average of 17 dry days. The Upper Thames catchment is drier every month compared to the other study catchments (Fig. 2.8).

High and very high extremes of daily precipitation are represented by the 90th and 95th percentiles, 6.7 mm/day and 10.2 mm/day respectively. The mean number of monthly days with precipitation above the 90th percentile is larger from October to January and smaller in spring and summer. All months have at least two days with precipitation above the 90th percentile. For May and June, the monthly mean number of days with precipitation above the 90th percentile is larger for the Upper Thames catchment than for any other study catchment (Fig. 2.9).

2.4.1.2. Glaslyn

The catchment's mean annual accumulated precipitation is 2,957 mm/year, the largest annual accumulated precipitation observed in all study catchments. The linear trend is also the largest from all catchments with a statistically non-significant increase of 4.7 mm per year (47 mm per decade) (Table 2.2.). The variability in the second half of the time series increases with a standard deviation of 306 mm/year from 1976 to 1994 and 429 mm/year from 1995 to 2012 (Fig. 2.5). The largest precipitation values are observed in the north where the annual accumulated precipitation is above 4,000 mm/year. The lowest precipitation values are above 2,000 mm/year in the south and southwest (Fig. 2.6b).

The accumulated precipitation is above 150 mm for all months. Higher monthly precipitation values are observed from October to January, each month accumulating over 300 mm/month. April, May and June are the months with lower accumulated precipitation (Fig. 2.7b). The difference between the wettest and driest months is 184 mm. The monthly mean of dry days is larger in late spring and summer (Fig. 2.8). The catchment has the lowest monthly mean of dry days compared to the other catchment.

The 90th precipitation percentile is 24.4 mm/day, whilst the 95th precipitation percentile is 34.2 mm/day. The monthly mean days above the 90th precipitation percentile is greatest in late autumn and winter (Fig. 2.9). In general, this is the largest mean compared to the other study catchments except for late spring and summer.

2.4.1.3. Calder

The catchment's mean annual accumulated precipitation is 1,251 mm/year. The linear trend is the smallest of all the study catchments with a statistically non-significant annual increase of 0.8 mm (8 mm per decade) (Table 2.2). The precipitation variability has increased in the more recent period when comparing the standard deviation of 132 mm/year from 1976 to 1994 with the 230 mm/year from 1995 to 2012 (Fig. 2.5). The highest accumulated precipitation is observed in the north with approximately 1,500 mm/year. In contrast, the central valley has the lowest precipitation of the catchment with approximately 1,070 mm/year (Fig. 2.6c). Additionally, other regions of high precipitation are observed in the south of the catchment.

The monthly precipitation is larger during winter and smaller in late spring and summer (Fig.2.7c). From October to January the monthly precipitation is above 127 mm/month. In contrast, precipitation is below 91 mm/month from April to July. The precipitation difference between the wettest and driest month is 69 mm. The monthly mean of dry days is larger in summer than in the other months (Fig. 2.8).

The 90th and 95th precipitation percentiles are 10.3 mm/day and 14.8 mm/day, respectively. Days with precipitation exceeding the 90th precipitation percentile are more frequent from September to January with at least 3.7 days exceeding the threshold. Contrastingly, the 90th precipitation percentile is exceeded in spring and summer with less frequency (Fig. 2.9).

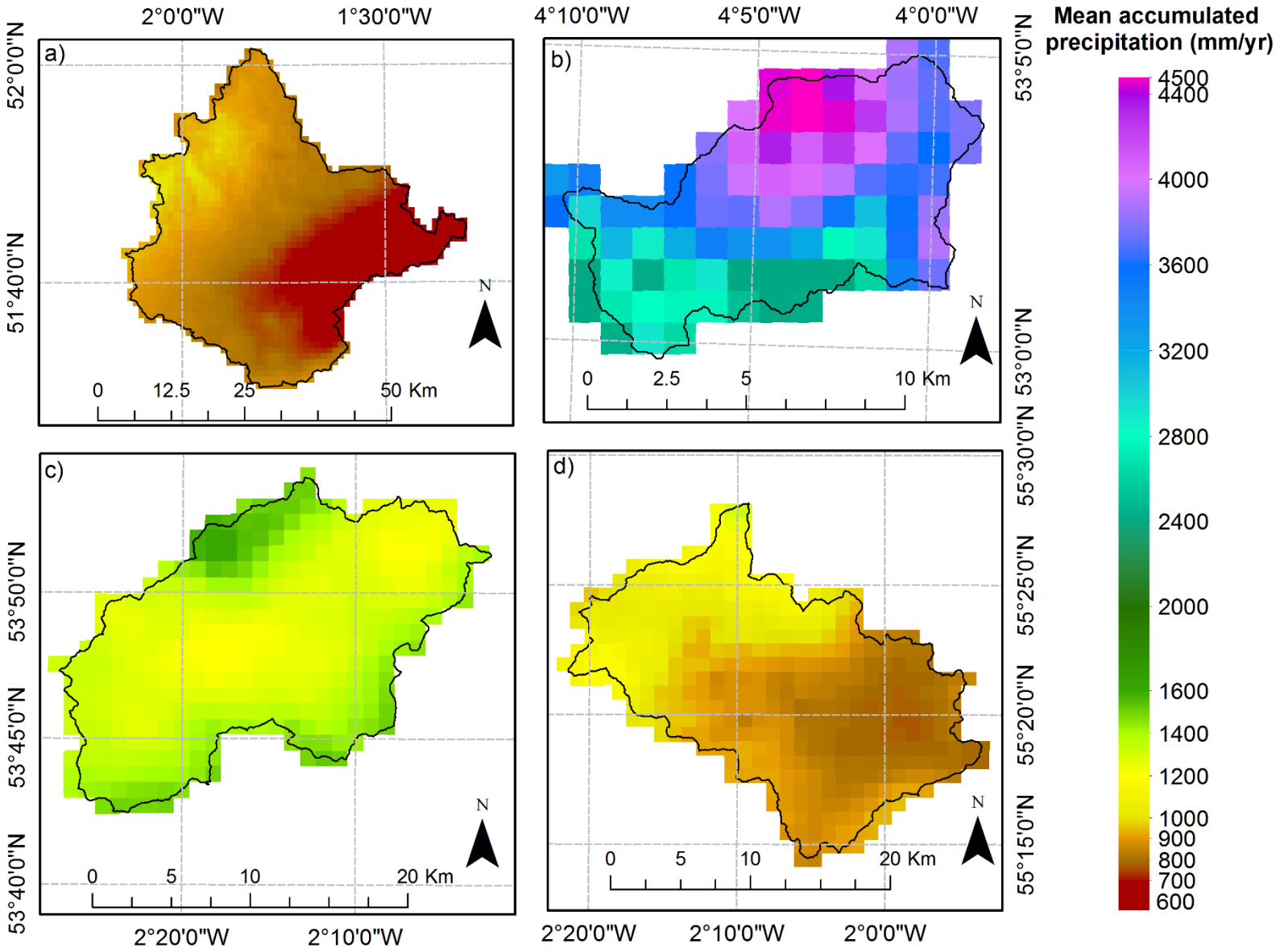

Figure 2. 6 Spatial distribution of the mean annual accumulated precipitation (1976-2012): a) Upper Thames, b) Glaslyn, c) Calder, d) Coquet

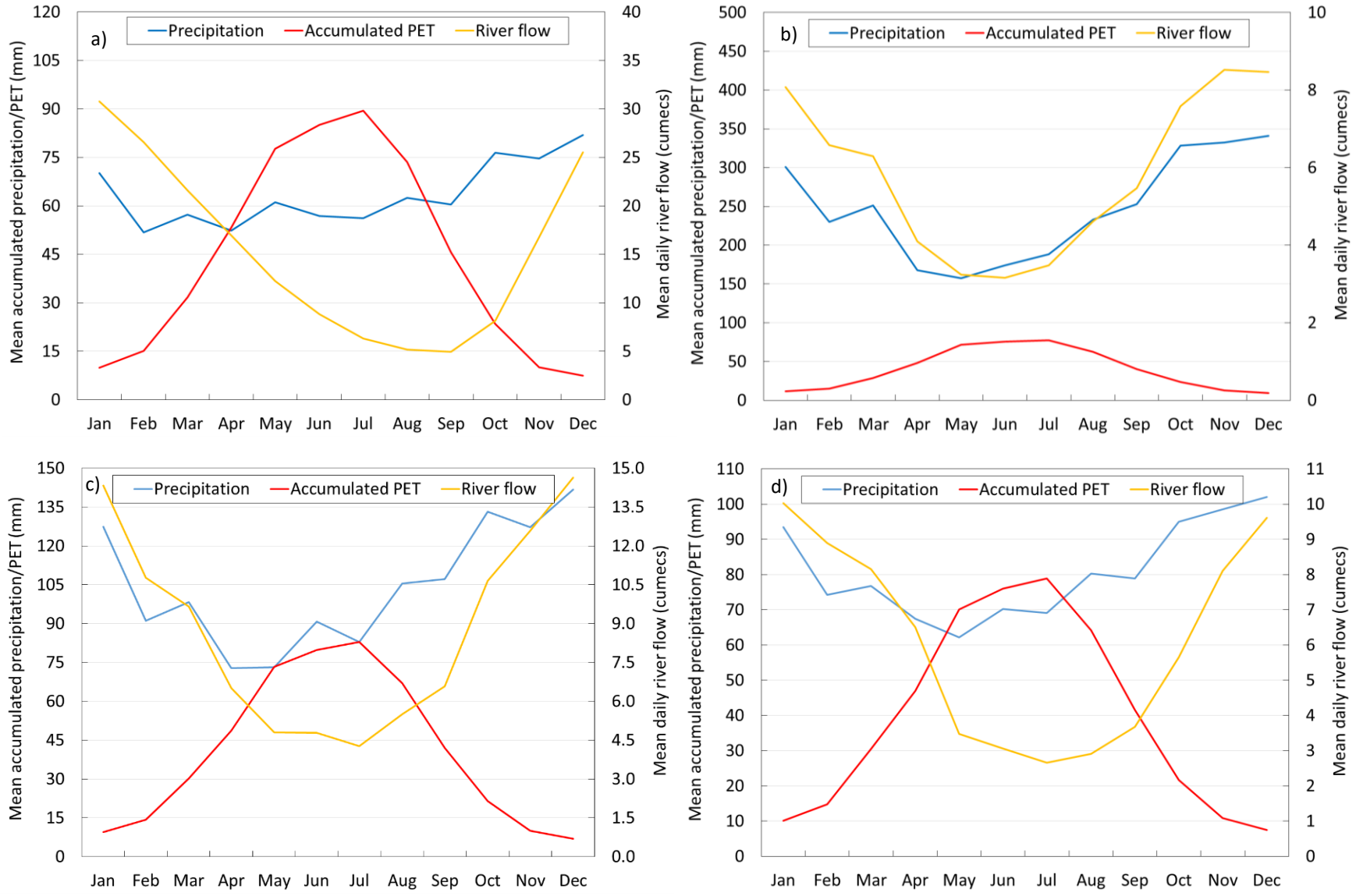

Figure 2. 7 Monthly mean accumulated precipitation and potential evapotranspiration (mm/month) and monthly mean daily river flow (m^3/s) for a) Upper Thames, b) Glaslyn, c) Calder, d) Coquet. Please note the difference in the scales

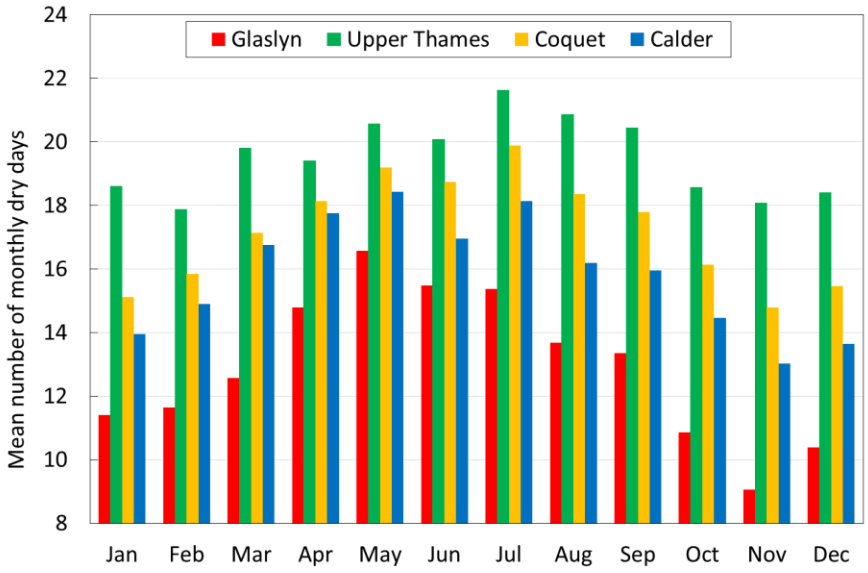

Figure 2. 8 Mean monthly dry days (precipitation <1 mm, as used in Zhang et al., 2011)

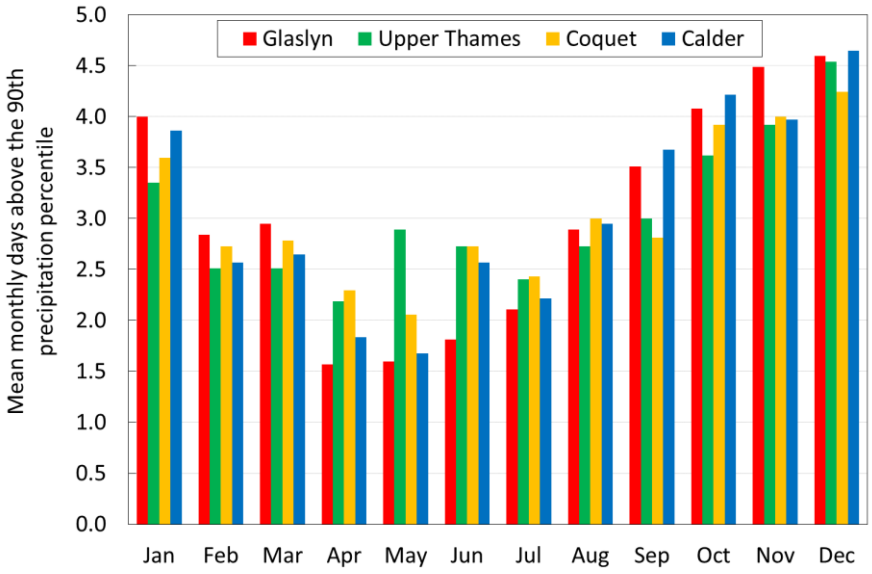

Figure 2. 9 Mean monthly days with precipitation higher than the 90th precipitation percentile

2.4.1.4. Coquet

The mean annual accumulated precipitation is 968 mm/year. The linear trend shows an annual precipitation increase of 3.4 mm (34 mm per decade). The variability of the mean annual accumulated precipitation increases for the second half of the time series: standard deviation of 159 mm/year from 1995 to 2012, compared to 92 mm/year from 1976 to 1994 (Fig. 2.5). Precipitation is higher in the north and northeast of the catchment where precipitation is larger than 1,100 mm/year. The precipitation amount decreases towards the south and southwest where it reaches values lower than 800 mm/year (Fig. 2.6d).

Monthly precipitation is larger than 90 mm/month from October to January and below 70 mm/month from April to July (Fig. 2.7d). The difference between the wettest and driest months is 40 mm. Drier months are observed from April to September with at least 17 dry days per month. November and January have the shortest number of dry days, not exceeding 15 days per month (Fig. 2.8).

The 90th and 95th precipitation percentiles are 7.7 mm/day and 11.9 mm/day, respectively. Days exceeding the 90th precipitation percentile are above 3.6 days/month from October to January. In contrast, the percentile is at most exceeded for 3 days/month from February to September (Fig. 2.9).

2.4.2. Temperature

Temperature functions as control of the volume of water vapour that is present in the air (Davie, 2008). Additionally, it is one of the main variables determining the evapotranspiration volume. This section provides information about the observed temperature in the study catchments including their annual and monthly mean temperature, the temperature spatial distribution and mean monthly days with average temperature lower than 0°C. Snowmelt is not a dominant element of the UK's climate affecting river flow (Bell and Moore, 1999). However, the days with mean temperature below 0°C are shown to give an estimate of the days where conditions favour snow cover. Additionally, the annual temperature trend is analysed by a linear regression along with its statistical significance using a t-test.

This study uses observed temperature data from the Natural Environment Research Council (NERC) Climate, Hydrology and Ecology research Support System (CHESS) (Robinson et al., 2015). The CHESS dataset consists of daily 1-km gridded observed temperature for the UK from 1961 to 2012. The CHESS dataset uses mean daily temperature observations from the Met Office Rainfall and Evaporation Calculation System (MORECS) (Hough and Jones, 1997) as input data. CHESS interpolated these input data using a bi-cubic spline and adjusted using the 50-m resolution Integrated Hydrological Digital Terrain Model from Morris and Flavin (Morris and Flavin, 1990). In this chapter, the mean daily temperature analysis covers from 1976 to 2012.

2.4.2.1. Upper Thames

The Upper Thames catchment is the warmer of the study catchments with a mean annual temperature of 9.7°C. A statistically significant increasing temperature trend of 0.03 °C per year (0.3 °C per decade) is observed (Table 2.2). Most years from the second half of the time series are above the mean annual temperature average (Fig. 2.10). The monthly mean temperature ranges from 4°C in January to 16.3°C in July. For all months, the mean temperature is higher in the Upper Thames catchment than in the rest of the study catchments (Fig. 2.11). Spatially, colder mean annual temperatures are observed in the higher elevation areas in the north where they reach 8.5°C. Temperature increases towards the central valley where the highest mean annual temperature is 10°C (Fig. 2.12a). Days below 0°C are observed in winter, early spring and late autumn (Fig. 2.13). These are always less than 4 days per month. The Upper Thames catchment has the lowest number of days below 0°C for all months compared to the rest of the catchments.

2.4.2.2. Glaslyn

The catchment's mean annual temperature is 8.1°C. There is a statistically significant increasing temperature trend of 0.02 °C per year (0.2 °C per decade) (Table 2.2). Years from the last section of the mean annual temperature time series are frequently above the time series' average (Fig. 2.10). The coldest temperatures are observed in January and February (3.1°C) and the warmest in July (13.8°C) (Fig. 2.11). Spatially, colder mean annual temperatures are associated with the higher elevations which are found at the north of the catchment (5.2°C). Warmer temperatures can reach 9.6°C in the central valley where elevation is lower (Fig. 2.12b). Days where temperature decreases below 0°C are observed from November to March and are always below 5.5 days per month (Fig. 2.13).

2.4.2.3. Calder

The catchment's mean annual temperature is 8.4°C. There is a statistically significant increasing annual temperature trend of 0.03°C per year (0.3 °C per decade) (Table 2.2). Temperatures from the second half of the mean annual temperature time series are frequently above the average (Fig. 2.10). July is the warmest month (14.9°C) and January the coldest (3.0°C) (Fig. 2.11). Colder temperatures are observed in the north and east of the catchment where the higher elevations are located. In these zones the mean annual temperature reaches 6.7°C. Temperature tends to increase towards the central valley where mean annual temperatures of 9.4°C are observed (Fig. 2.12c). Days where the temperature is below 0°C are observed from November to March, but these are more frequent from December to February with at least 4.5 days/month (Fig. 2.13).

2.4.2.4. Coquet

The catchment's mean annual temperature is 7.4°C. The time series of the mean annual temperatures shows a statistically significant increasing linear trend of 0.02°C per year (0.2 °C per decade) (Table 2.2). Years from the second half of the time series are above the whole time series average (Fig. 2.10). For all months, the mean monthly temperature of the Coquet catchment is colder than the other study catchments (Fig. 2.11). January is the coldest month with a mean of 2.2°C and July the warmest with 13.6°C. Colder temperatures are observed at the north of the catchment with temperatures of 4.7°C. Temperature gradually increases from the north and northwest towards the south and southeast. The warmer temperatures are located on the southeast (8.6°C) (Fig. 2.12d). The catchment has the largest number of days with temperature below 0°C compared to the rest of the study catchments. Days with temperatures below 0°C are observed from November to April, but these are more frequent from December to February with at least 6 days per month (Fig. 2.13).

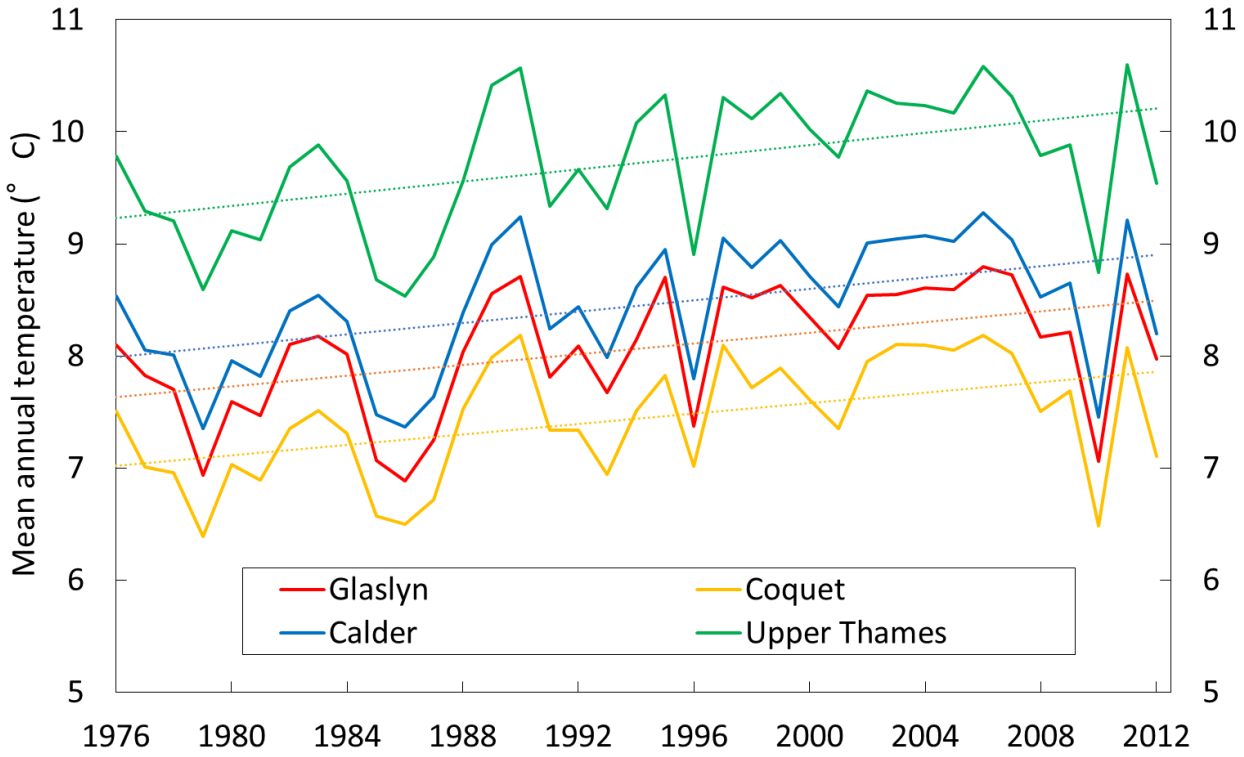

Figure 2. 10 Mean annual temperature (1976 – 2010). Dashed lines represent the linear trend line from the observed period

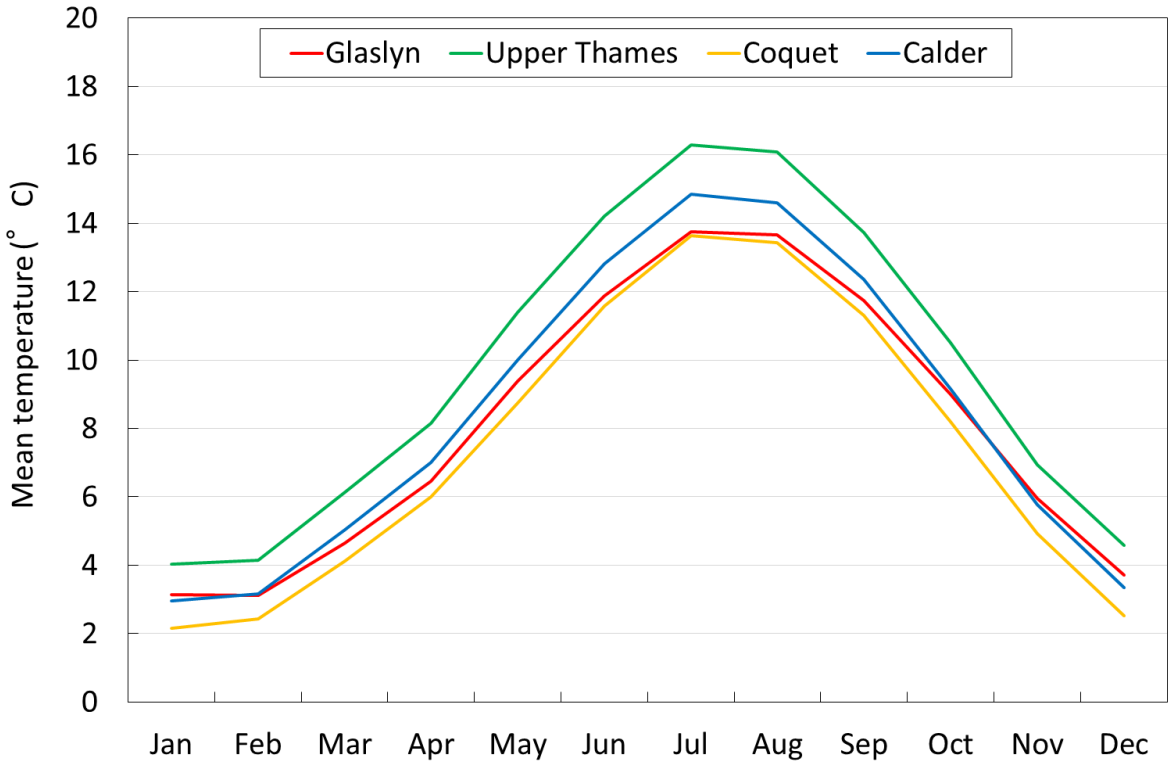

Figure 2. 11 Mean monthly temperature of the study catchments

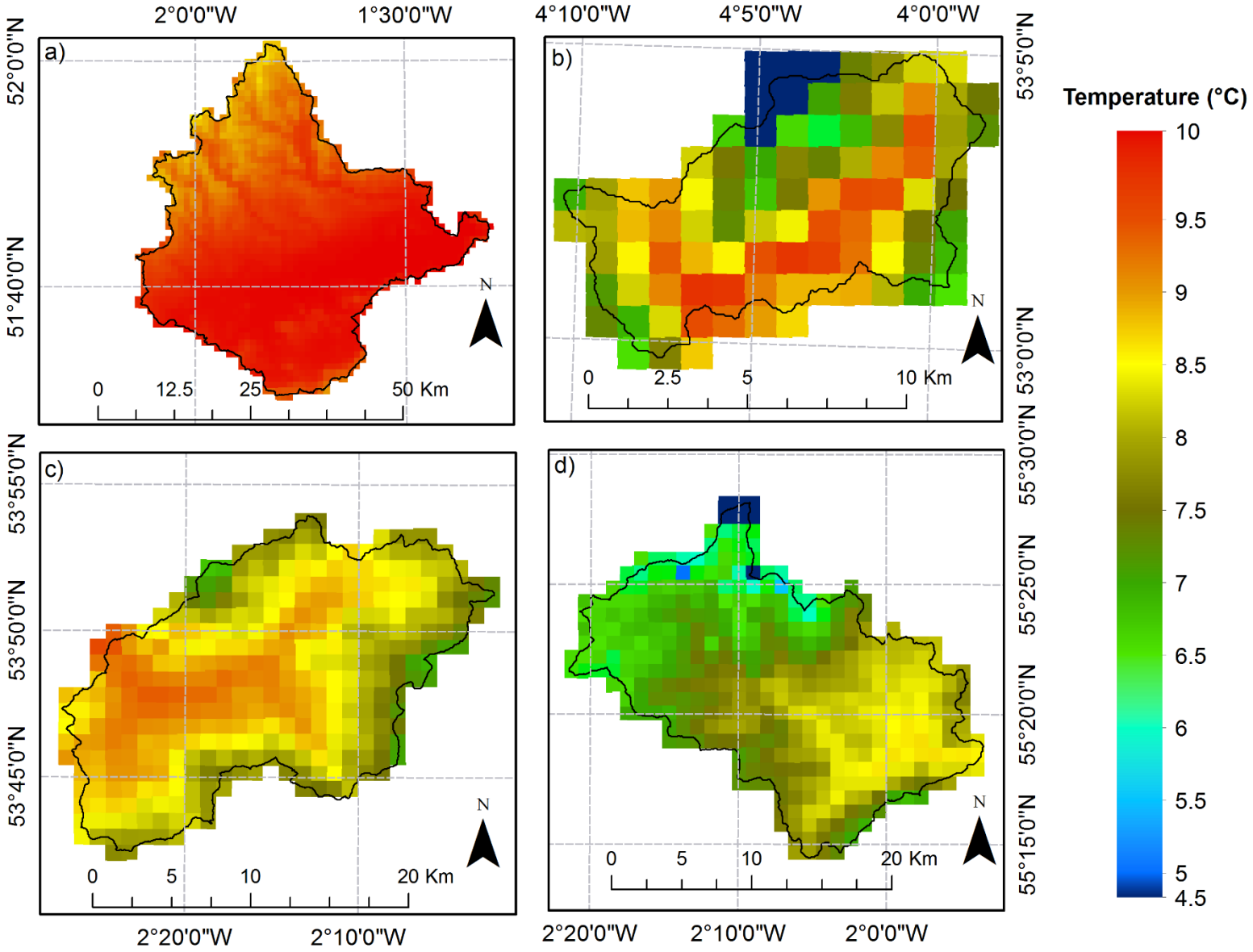

Figure 2. 12 Spatial distribution of the mean annual temperature (1976-2010): a) Upper Thames, b) Glaslyn, c) Calder, d) Coquet

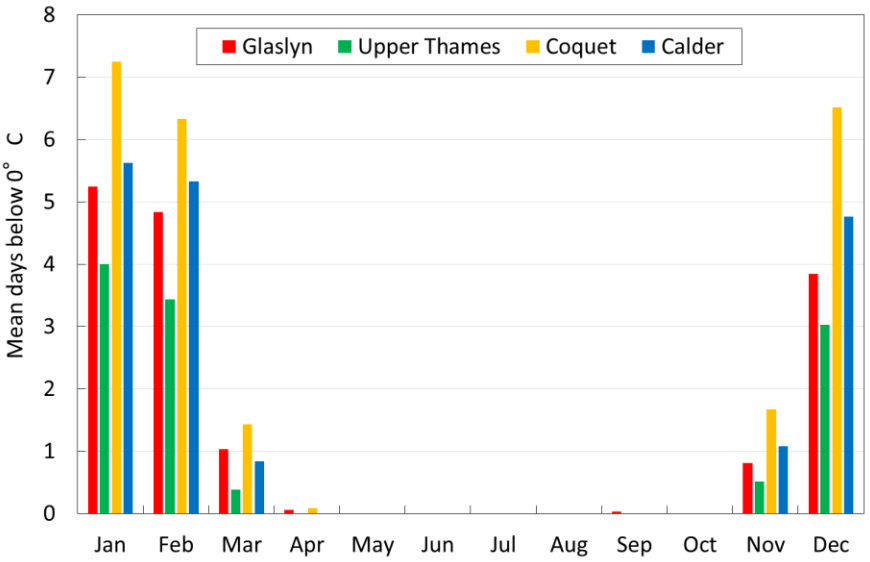

Figure 2. 13 Mean monthly days with mean temperature below 0°C

2.4.3. Potential evapotranspiration

Potential evapotranspiration (PET) estimates the amount of water lost from the catchment through evapotranspiration when water availability is not limited. Therefore, PET can be an important river flow control. Data from the daily 1-km gridded NERC´s CHESS-PET (Robinson et al., 2017) estimates are used as PET observations in this study. The CHESS-PET dataset covers from 1961 to 2012 and it is based in the Penman-Monteith equation (Allen et al., 1998). This equation is a function of the mean air temperature, wind speed, surface air pressure, specific humidity and the downward short and longwave radiation. CHESS-PET obtains the values of these variables from MORECS (Hough and Jones, 1997), interpolates them to the 1km resolution and finally adjusts them considering elevation differences based on the 50-m resolution Integrated Hydrological Digital Terrain Model (Morris and Flavin, 1990). The PET data shown in this chapter covers from 1976 to 2012.

2.4.3.1. Upper Thames

The catchment's mean annual accumulated PET, 522 mm/year, is the largest of all study catchments. The monthly accumulated PET has higher values during summer and lower in winter (Fig. 2.7a). PET behaviour shows a similarity with temperature. However, the actual evapotranspiration will depend on the availability of water. The monthly accumulated PET varies from 7 mm/month in December to 90 mm/month in July. Spatially, most of the catchment has annual PET values around 530 mm/year with low and high extreme values more frequently observed at the north (Fig. 2.14a).

2.4.3.2. Glaslyn

The mean annual accumulated PET is 477 mm/year. The monthly accumulated PET has lower values in December and January and larger values from May to July (Fig. 2.7b). Higher PET is found on the low-elevation central zone of the catchment and lower PET values are more commonly observed on the high elevations found on the north of the catchment (Fig. 2.14b).

2.4.3.3. Calder

The mean accumulated PET is 486 mm/year. January and February have the lower PET with values below 10 mm/year. In contrast, higher PET is observed from May to July (Fig. 2.7c). Lower PET is normally found in the central region of the catchment which is also associated with the lower elevations. In contrast, higher PET values are commonly observed on the high elevations located at the north of the catchment (Fig. 2.14c).

2.4.3.4. Coquet

The annual accumulated PET in the Coquet catchment is the lowest of all the study catchments with 473 mm/day. The monthly accumulated PET has lower values in January and December. Higher PET is observed from May to July with values above 70 mm/month (Fig. 2.7d). Spatially, most of the catchment has PET estimations of approximately 470 mm/year or above, except for a few zones where PET is smaller (Fig. 2.14d).

2.5. River flow

The river flow from each catchment represents the main energy input for the hydropower schemes, and therefore their power generation depends on the volume of water flowing through the river. This section gives information related to the observed river flow of each catchment. Annual and monthly means are shown and the statistical significance of the annual river flow trend derived from a linear regression analysis is assessed using a t-test. Additionally, other statistics related to the river regime and low and high flows are provided. In this section the high flows are represented by the Q10 statistic. This value indicates the flow that is observed or exceeded 10% of the time. The Q10 value is selected as high flows statistic because it has been used before in studies that analyse changes in high flows within the UK and Europe (e.g. Hannaford and March, 2008; Prudhomme et al., 2011; Hannaford and Buys, 2012). In addition, the Q95 is used to estimate the low flows in each catchment. The value indicates the flow that is observed or exceeded 95% of the time. This value is used because it is widely used to analyse low flows (e.g. Arnell, 2011; Chen et al., 2013) and it is also used as default value for the Hands Off Flow (generation stops if the river flow reaches this value) of proposed hydropower schemes (EA, 2009). Another relevant statistic for the ROR hydropower schemes is the Q2 (flow observed or exceeded 2% of the time) as this is related to flooding conditions that force the scheme to stop operating. An analysis of the Q2 statistic is provided in section 6.3.3.

In the UK, the CEH's National River Flow Archive (NRFA) records daily river flow data using a network of over 1,500 gauging stations. The length of the river flow records varies for each gauging station and mainly depends on the opening date and interruptions in the daily measurement. This chapter uses river flow data from 1976 to 2012 as this is the period of time where continuous records for all the catchments are available.

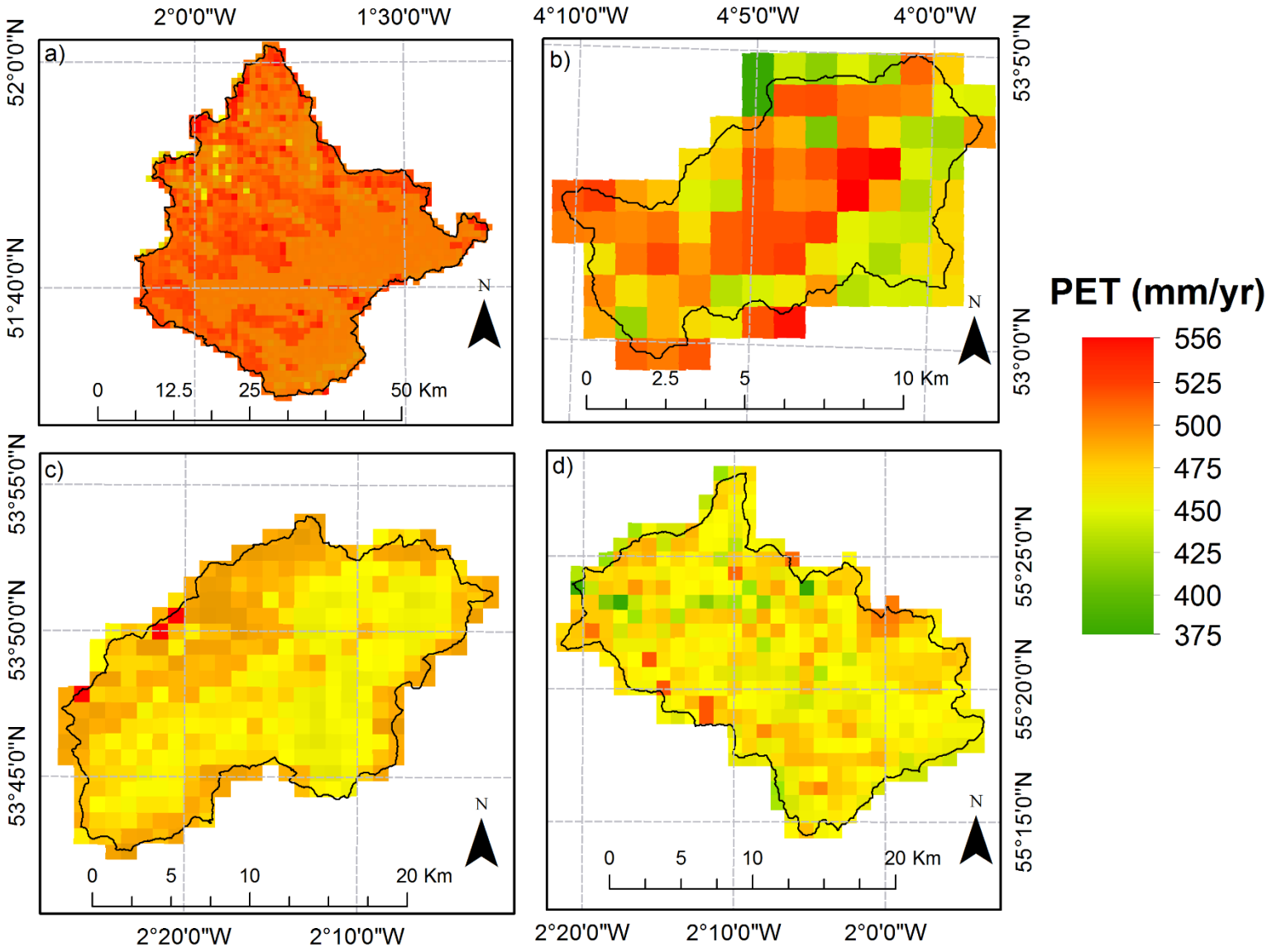

Figure 2. 14 Spatial distribution of the mean annual accumulated PET in mm/year: a) Upper Thames, b) Glaslyn, c) Calder, d) Coquet

2.5.1. Upper Thames

River flow from the Upper Thames is recorded at the Eynsham gauging station (ID 39008). The station is a 30-meter wide complex structure including gates, locks and a weir located at coordinates 1°46'31"N, 1°21'23"W (Fig. 2.2a). The operation of the gates and locks affect the measurement and high flows are bypassed by an unmeasured side channel. Furthermore, the catchment's runoff is affected by public supply abstractions, effluent returns and reservoirs (Marsh and Hannaford, 2008). The CEH has developed a daily naturalised river flow time series to tackle such problems by adjusting the observed flow considering upstream abstractions and discharges (Marsh and Hannaford, 2008). However, the accuracy of this naturalised flow is influenced by the abstraction and discharge estimations in which it is based. For this catchment, the naturalised river flow time series are used for the analysis.

The mean annual daily river flow for the Upper Thames catchment, 15.3 m^3/s, is larger than for the rest of the study catchments. The linear trend shows a statistically non-significant annual increase of 0.05 m^3/s (Table 2.2) with a larger spread in the year to year variability during second half of the time series (standard deviation of 5.9 m^3/s from 1995 to 2012) compared to the first half (standard deviation of 3.5 m^3/s from 1976 to 1994) (Fig. 2.15).

The monthly mean daily flow from December to March is above 20 m^3/s and below 9 m^3/s from June to October (Fig. 2.7a). The Base Flow Index (BFI) provides an estimation of the groundwater contribution towards the river flow: higher BFI indicates a higher groundwater contribution and in contrast a low BFI is representative of low groundwater contribution (Gustard et al., 1992). For the Upper Thames, the BFI is 0.70, indicating an important contribution from groundwater sources.

The flow duration curve (FDC) indicates the amount of the time that a certain flow volume is equalled or exceeded (Davie, 2008). For the Upper Thames, the FDC shows that river flow is normally larger than that in the rest of the catchments except for the low flows where the FDC decreases abruptly (~ from the Q95) (Fig. 2.16). The Q10 (the flow that is observed or exceeded 10% of the time) is used as indicator of the catchment's high flows and the Q95 (the flow that is observed or exceeded 95% of the time) as an indicator of the low flows. For this catchment, the Q10 is 34.8 m^3/s and the Q95 is 1.90 m^3/s.

High flows are more commonly observed during winter as the Q10 is exceeded more frequently during this season. In contrast, high flows are rare from May to October when the mean of days above the Q10 is always below one (Fig. 2.17). Low flow conditions are normally observed from July to October when the mean of days below the Q95 is above three, whilst this statistic is zero from December to March (Fig. 2.18).

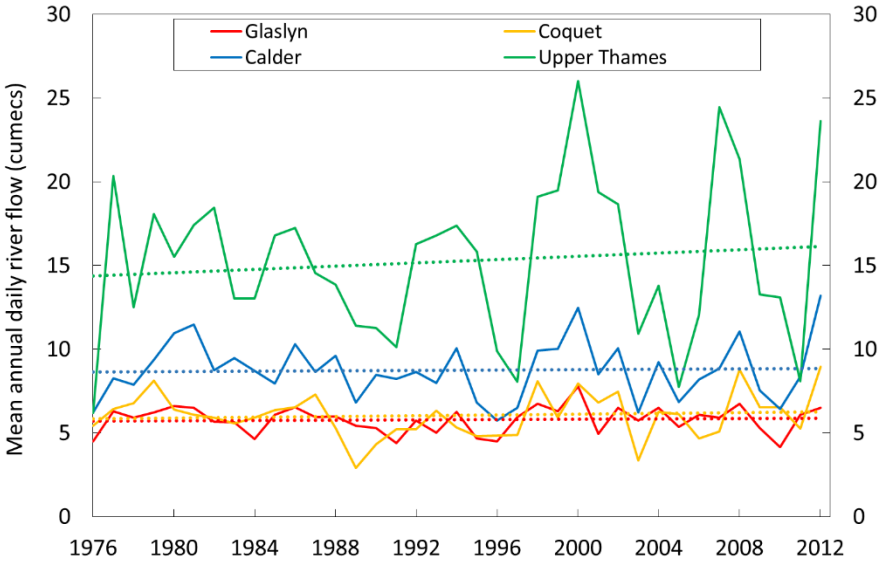

Figure 2. 15 Annual mean daily river flow (1976 – 2010). Dashed lines represent the linear trend

2.5.2.Glaslyn

The River Glaslyn streamflow is gauged at the Beddgelert station (ID 65001) located at coordinates 53°0'29"N and 4°6'5"W (Fig. 2.2b). The gauging station is a 20-m wide river cross section with an unstable bed and it is bypassed at high flows. Runoff in the catchment is marginally affected by reservoirs and hydropower operation (Marsh and Hannaford, 2008).

The mean annual daily river flow is 5.8 m^3/s. The catchment has the largest amount of annual precipitation compared to all study catchments, but it also has the lowest daily river flow mean. This is mainly due to the size of the catchment. There is no increase or decrease in the annual river flow trend. The standard deviation from the first half of the time series (1976-1994) is 0.7 m^3/s and 0.9 m^3/s for the second half (1995-2012) (Fig. 2.15). This is linked to the increase of precipitation variability which also increases in the second segment of the observed period. The mean monthly river flow is higher from November to January when the flow is above 8 m^3/s for each month. River flows below 3.5 m^3/s are present from May to July (Fig. 2.7b).

The BFI for the catchment is 0.32, denoting a low contribution from groundwater to the river flow. The FDC for the Glaslyn catchment is similar to the FDC from the Coquet catchment, except for the low flows (approximately from Q75 to Q100) where the Glaslyn catchment has the lowest flows of all the study catchments (Fig. 2.16). The catchment's Q10 is 13.5 m^3/s and the Q95 is 0.55 m^3/s. The Q10 is more frequently exceeded from October to January, when at least four days per month have flows above the Q10. In contrast, the Q10 is exceeded less than two days per month from April to July (Fig. 2.17). The low flow period is from May to August when flows are below the Q95 at least three days per month (Fig. 2.18).

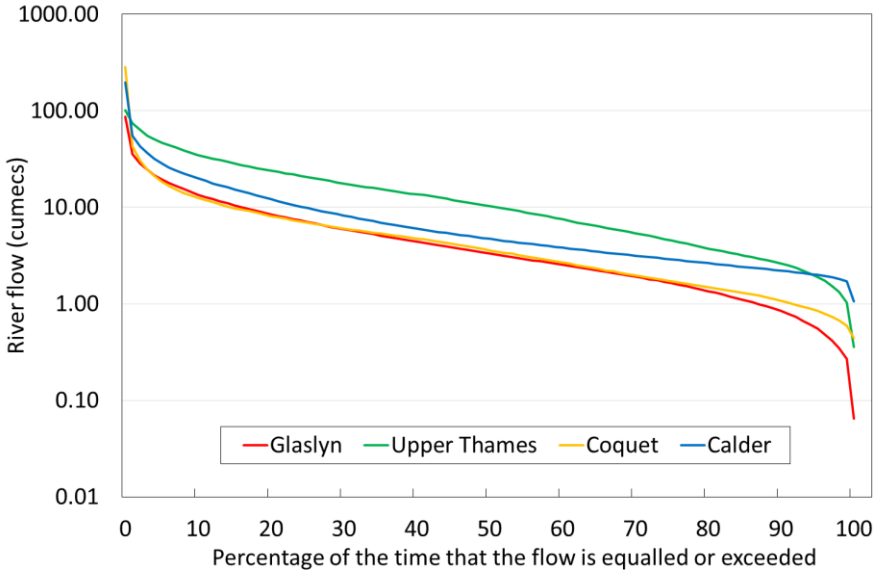

Figure 2. 16 Flow duration curves in logarithmic scale (with daily data from 1976-2010)

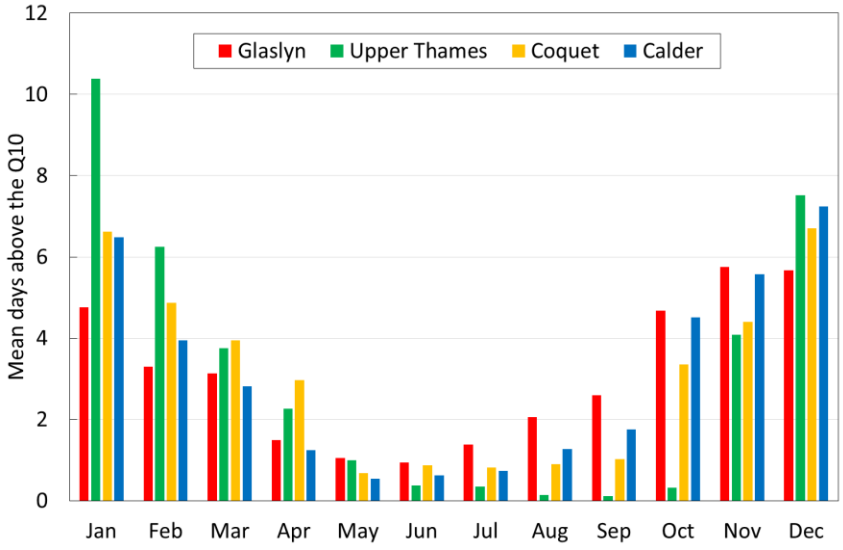

Figure 2. 17 Mean number of days above the Q10 per month

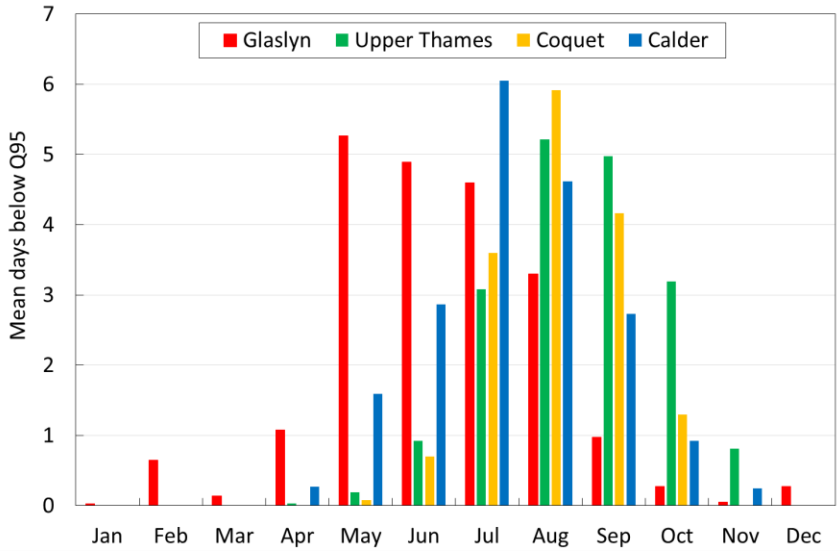

Figure 2. 18 Mean number of days below the Q95 per month

2.5.3.Calder

The Calder catchment river flow is gauged at coordinates 53°49'10"N and 2°24'47"W, where the Whalley Weir station (ID 71004) is located (Fig. 2.2c). The gauging station is a 24.4 m wide weir that drowns at high flows and has weed growth problems. Runoff is mainly affected by industrial discharges and marginally affected by industrial abstractions (Marsh and Hannaford, 2008).

The gauged mean annual daily river flow is 8.8 m^3/s. There is a statistically non-significant annual river flow trend increase of 0.01 m^3/s (Fig. 2.15 and Table 2.2). The standard deviation from 1976 to 1994 is 1.3 m^3/s and 2.2 m^3/s from 1995 to 2012. Higher river flow volumes are observed from October to February when streamflow is above 10 m^3/s (Fig. 2.7c). In contrast, the months with lower river flow are from May to July with observations below 5 m^3/s.

The catchment's BFI is 0.42, reflecting a moderate groundwater contribution towards surface water. The FDC shows a steadier river flow in comparison to the other study catchments, which might be a result of the effluent discharge within the catchment (Fig.2.16). The catchment's Q10 is 19.9 m^3/s and the Q95 is 1.99 m^3/s. The Q10 is more frequently exceeded from October to January when at least 4.5 days per month have flows above the Q10 (Fig. 2.17). Low flows are commonly observed from June to September when the monthly flow is below the Q95 at least for 2.7 days per month (Fig. 2.18).

2.5.4. Coquet

River flow from the Coquet catchment is gauged at the Rothbury station (ID 22009), located at coordinates 55°18'30"N and 1°53'46"W (Fig. 2.2d). The Rothbury station is a velocity area station with good control for most flows, except high flows that might be underestimated. The catchment has small groundwater extractions which do not greatly affect the natural river flow (Marsh and Hannaford, 2008).

The catchment's mean annual daily river flow is 6.0 m^3/s with a statistically non-significant annual increasing trend of 0.01 m^3/s. The standard deviation from the first half of the data (1976-1994) is 1.1 m^3/s and 1.6 m^3/s during the second half (1995-2012) (Fig. 2.15). The mean monthly river flow is larger from November to March with values above 8.1 m^3/s. The monthly river flow is below 3.5 m^3/s from May to August (Fig. 2.7d).

The BFI is 0.47, indicating a moderate contribution of groundwater to the catchment's river flow. The FDC shows extremely high events and the groundwater contribution for the low flows (Fig. 2.16). The Q10 is 12.4 m^3/s and the Q95 is 0.84 m^3/s. Events where the Q10 is exceeded are more frequent from November to February (Fig. 2.17). In contrast, events where flow is below the Q95 are more commonly observed from July to October (Fig. 2.18).

2.6. Precipitation-PET-streamflow relationship

This section gives an insight of the relationship between the catchment's precipitation, PET and streamflow.

2.6.1. Upper Thames

The monthly accumulated precipitation varies slightly during the year with the highest value observed during late autumn and winter (Fig. 2.7a). In contrast, the monthly accumulated PET varies from less than 10 mm/month to 90 mm/month with the peak during summer and the lowest during winter. The monthly accumulated precipitation is larger than the monthly accumulated PET from September to April (Fig. 2.7a). During the remaining months, the accumulated PET exceeds the accumulated precipitation. When the monthly PET increases the river flow decreases, and when PET decreases the river flow increases. The months with the highest accumulated PET are also the months with the lowest river flow and when PET is the lowest the river flow is the highest. The Spearman correlation coefficients between precipitation and river flow vary from 0.14 to 0.28 for all months and are statistically significant for all months (p-value < 0.001) (Fig. 2.19).

2.6.2. Glaslyn

The seasonal precipitation difference is evident for this catchment as the difference between the wettest and driest month is 184 mm (Fig.2.7b). Additionally, the catchment's precipitation is high compared to the other study catchments, with a monthly mean of 157 mm for the driest month (May). In contrast, the highest monthly PET is 78 mm in July. Therefore, the amount of monthly precipitation is always larger than the amount of monthly PET. As a result, the catchment's monthly river flow closely follows the precipitation monthly regime. The Spearman correlation coefficient shows a moderate to strong correlation between the monthly precipitation and river flow. Correlation is lower from May to August with coefficients below 0.52, and above 0.56 for the rest of the months. The correlation between precipitation and river flow is significant for all months (p-value < 0.001) (Fig. 2.19).

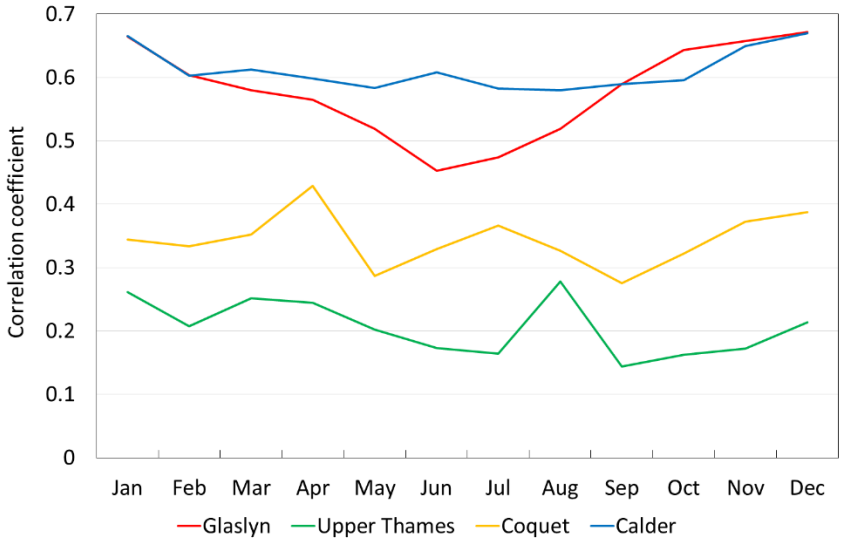

Figure 2. 19 Monthly Spearman correlation coefficient between precipitation and river flow. The p-values for all months for each catchment are <0.001, indicating a significant positive correlation between precipitation and river flow

2.6.3. Calder

The monthly PET is below 15 mm/month from November to February and above 70 mm/month from May to July (Fig. 2.7c). In contrast, precipitation is larger from October to January. The driest months are April and May with precipitation less than 75 mm/month. The monthly accumulated PET magnitude is similar to the monthly accumulated precipitation during May and July. For the rest of the months, precipitation is larger than PET. Even if the monthly PET is never larger than the monthly precipitation, it impacts river flow during the months where the PET is large. For the months when the PET is low, river flow follows a regime similar to the monthly precipitation. The Spearman correlation coefficients show statistically significant correlations (p-value < 0.001) between precipitation and river flow throughout the year with coefficients above 0.58 (Fig. 2.19).

2.6.4. Coquet

The monthly precipitation difference from the wettest and driest month is 40 mm (Fig. 2.7d). The driest month is below 65 mm. Similar to the rest of the study catchments, the monthly PET has larger values during summer and lower for winter. The largest PET estimations are above 70 mm/month from May to July. For this catchment, the river flow regime follows the precipitation regime when the monthly PET is low. As PET increases, the river flow does not follow the precipitation regime, indicating a seasonal behaviour that varies according to the PET volume. This is true for months when PET exceeds 10 mm and most evident for the months when the PET exceeds the precipitation amount (May, June and July). The precipitation and river flow Spearman correlation coefficients range from 0.28 (September) to 0.43 (April) (Fig. 2.19) and are statistically significant for each month (p-values < 0.001).

2.7. Hydropower schemes

The following section describes the main characteristics of the analysed ROR hydropower schemes. In this study, from the analysed schemes, two are installed and currently generating energy (Glaslyn and Calder) and two are proposed sites (Upper Thames and Coquet) according to the Environment Agency (EA, 2010). This section describes the schemes' location, operation, head, turbine, turbine efficiency, peak abstraction and Hands-Off flow (HOF). The location indicates whether the scheme is found upstream or downstream within the catchment and its distance from the river flow gauge. The head refers to the elevation difference between the scheme's water abstraction point and the discharge at the turbine's outlet. The scheme's turbine is important as every turbine operates differently and each type has a particular efficiency which is important to determine power output. The peak abstraction, or the maximum volume of water that can be abstracted from the river is related to the scheme's installed capacity. Finally, the schemes stop operating if the water flowing through the river reaches or falls below the HOF.

2.7.1. Upper Thames at Eynsham lock

The Eynsham Lock scheme is proposed by the Environment Agency's mapping hydropower opportunities study with an estimated maximum generation of 225 kW (EA, 2010). The proposed location of the scheme (51° 45' 30"N, 1° 21' 18"W) lies on the River Thames, near the Eynsham streamflow gauging station that can be used to determine the water volumes flowing through the scheme (Fig. 2.2a). The proposed low-head scheme uses inflow diverted from the main river through a short-length channel presently managed by locks and gates, discharging the flow at the end of the channel (Fig. 2.20a). The scheme's head, estimated by the Environment Agency using the Light Detection and Ranging (LIDAR) dataset, is 1.68 meters (EA, 2010). As this is a proposed hydropower scheme some of its operational characteristics are assumed and explained next. The Eynsham Lock is a low-head scheme. Therefore, the turbine efficiency of the operating low-head Whalley weir scheme is supposed to be plausible for this scheme. Considering the scheme's characteristics, the peak abstraction is calculated at 17.52 m^3/s. Finally, as this is a non-consumptive water use, a HOF equivalent to the Q95 is used (following EA, 2009). Therefore, the HOF is 1.9m^3/s for this study site.

2.7.2. Glaslyn at Hafod y Llan scheme

The Hafod y Llan hydropower scheme is a 640 kW Pelton turbine system. This scheme has the largest hydropower generation of all study sites. The scheme abstracts water from the Cwm Llan stream, a four-km tributary of the River Glaslyn, at coordinates 53°2'51"N, 4°3'30"W. The abstraction point is connected to the turbine by a 1-km underground pipe. After being used, water is discharged at the confluence of the Cwm Llan and Merch streams at coordinates 53°2'31"N, 4°2'46"W (Fig. 2.20b), later joining the River Glaslyn. The HOF threshold is 90 litres per second (0.09 m^3/s), and the peak abstraction is 450 litres per second (0.45 m^3/s). The head of the scheme is 176 meters, the largest of all the hydropower schemes under analysis. This head is the main factor for the large generation of the hydropower scheme. The distance between the scheme's abstraction point and the river flow gauge is approximately 7.3 km through the river pathway.

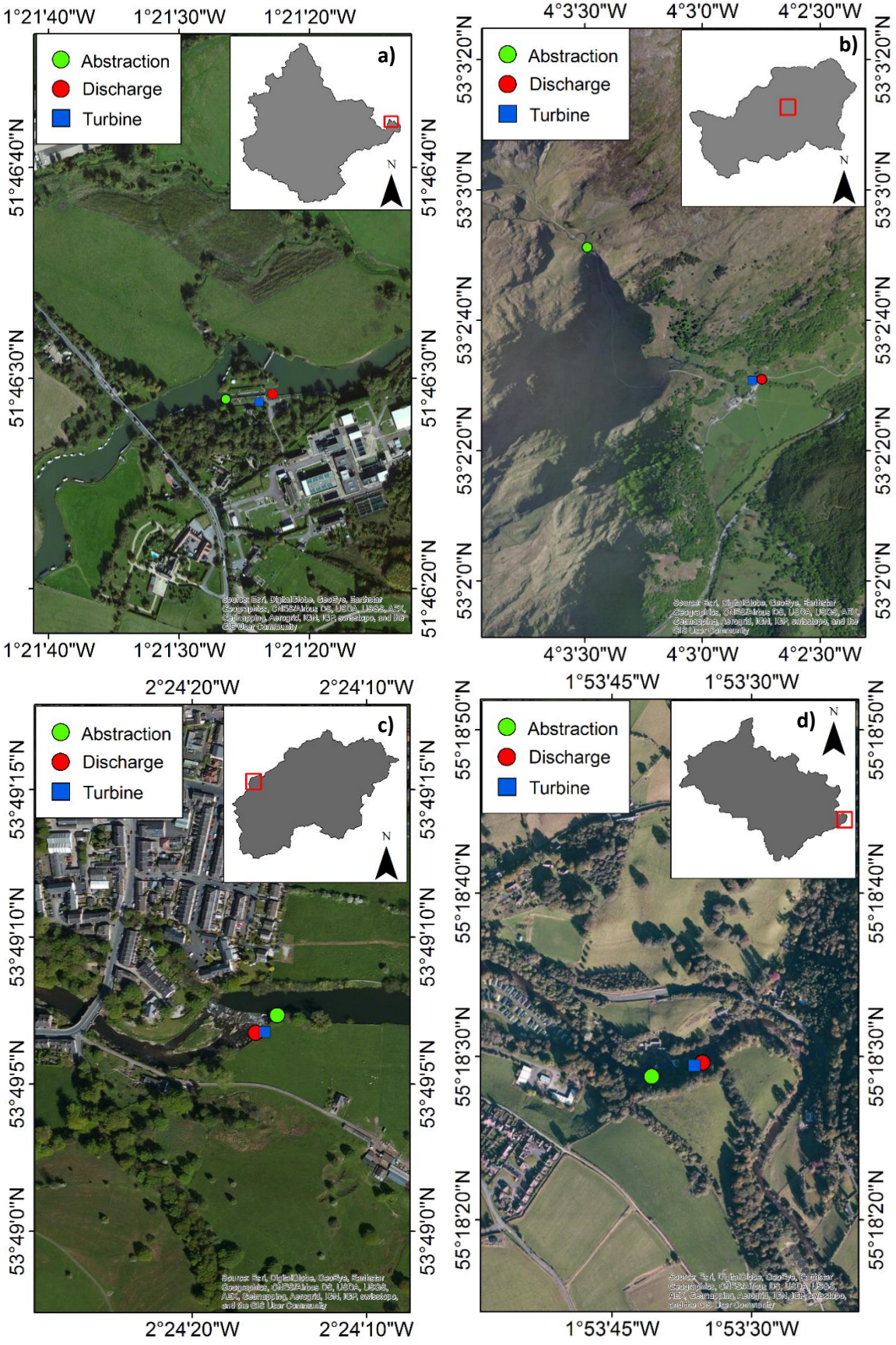

Figure 2. 20 Location of the hydropower schemes and their abstraction and discharge points: a) Upper Thames, b) Glaslyn, c) Calder, d) Coquet

2.7.3.Calder at Whalley weir scheme

The hydropower scheme near Whalley weir uses a 100 kW Archimedes screw (Fig. 2.20c). This low-head ROR scheme abstracts water from the River Calder at coordinates 53°49'7"N, 2°24'15"W. The water intake is located just upstream of the Whalley weir and flows to the Archimedes screw that is located parallel to the weir. The discharge is downstream of the weir. The scheme abstracts only a small percentage of the total river flow as most of the flow passes through the weir. The HOF threshold is 1,280 litres per second (1.28 m^3/s) and the peak abstraction is 7,310 litres per second (7.31 m^3/s). The scheme's head is 2.2 meters with a turbine efficiency of 77%. The Whalley weir streamflow gauging station, located 400 m downstream, can be used as reference for the river flow available for generation.

2.7.4. Coquet at Rothbury weir

The Rothbury weir hydropower scheme was proposed by the Environment Agency's mapping hydropower opportunities study with a maximum generation of 118 kW (EA, 2010). The proposed low-head scheme would abstract water from the River Coquet at coordinates 55°18'29"N, 1°53'41"W (Fig. 2.20d), near the Rothbury streamflow gauging station that can be used to measure the available river flow. The proposed scheme would be located near the Rothbury weir taking advantage of the difference between the weir's upstream and downstream elevation using an Archimedes screw as turbine. Therefore, the scheme is suggested to abstract water upstream of the weir and discharge it immediately downstream The scheme's head of 2 metres was estimated using LIDAR data (EA, 2010). The scheme's HOF is supposed to be equivalent to the river's observed Q95, 0.84 m^3/s. A turbine efficiency similar to the Calder catchment scheme is supposed for this scheme as the conditions are similar. Finally, a peak abstraction of 7.81 m^3/s is estimated based on the scheme's characteristics.

2.8. Summary

This chapter presents the process followed for the selection of the study catchments. The sites are selected according to a set of criteria and the selected study catchments represent the area where the research is developed. The chosen study catchments have installed RoR schemes or sites that have been proposed by the Environmental Agency (EA, 2010) as potential sites for the development of a RoR scheme. In addition, the sites have an installed or proposed capacity of at least 100 kW as the impacts of climate change are expected to have smaller effects in the energy generation of schemes with lower installed capacities. This research uses the Environmental Agency's mapping of hydropower opportunities study (EA, 2010) as reference, this study was performed for England and Wales. Therefore, only sites within England and Wales are considered for the selection of the study sites from this research. Also, to analyse the historical river regime characteristics, observed river flow records of at least 30 years are available for each study catchment. Furthermore, the river flow gauges are located near the hydropower schemes in three of the sites to decrease the uncertainty of estimating the flow available for the generation of hydropower. Finally, for the development of a model that simulates the energy generation, records of the daily generation are available for the selected schemes that are currently in operation. The range of sites that satisfy the characteristics mentioned above is small compared to the total number of RoR schemes

currently operating within the UK or the number of potential sites that are proposed by the Environment Agency. Nevertheless, the selected study catchments cover the diversity of physical, climate, hydrological and hydropower generation characteristics that can be found in England and Wales. The criteria used here has the purpose of selecting the sites that are more appropriate for the development of the study and at the same time decreasing possible extra uncertainty (e.g. sites with enough river flow data to calibrate the hydrological models, sites where the hydropower scheme's inlet is located near the river flow gauge, among others). Thus, the criteria eliminates a large number of potential sites. However, except for the upper Thames catchment, the selected study sites are located within the regions (Wales, north west and north east) that have the larger power potential within England and Wales (Table 1.4). Finally, given the different characteristics of the study sites, the results of this analysis are expected to be representative of the impacts of climate change on the different RoR schemes located across the UK and be useful for the planning of future RoR schemes and the definition of policies related to their construction and operation. The chapter provides a description of the physical characteristics, climate, river regime and hydropower schemes found in each of the selected study catchments.

All the catchment characteristics shown in this chapter are used during the development of the study. Some are used for the configuration of the hydrological model, others as output from the regional climate models (RCMs), as mean of evaluating the performance of the hydrological model and RCMs and/or to estimate the hydropower schemes' power generation. For instance, the land cover and soil type variables are solely used during the configuration of the hydrological model. Precipitation, temperature and potential evapotranspiration are used as input to generate the river flow simulations, but are also used to evaluate the performance of the climate models. River flow is used to evaluate the performance of the coupled hydrological and climate models and as input for the estimation of hydropower generation. Additionally, the different characteristics from each hydropower scheme are important to determine the main variables that could affect their performance in a changing climate.

As mentioned above, the complete set of catchment characteristic shown in this chapter is important for the study. Nevertheless, the study evaluates the performance of the current state-of-the-art RCMs to simulate the present climate and assesses their utility to simulate present hydrology when coupled with a hydrological model. Furthermore, the main objective of the study is to evaluate the impacts of climate change on hydropower generation by assessing climate changes under the current Representative Concentration Pathways (RCPs) scenarios. For river regime and hydropower generation, it is expected that climate change will have different impacts depending on the catchments and schemes' characteristics. Therefore, to include the diversity of the possible changes it is important to include a set of study catchments with a wide diversity in their characteristics, such as those selected in this study.

Some conclusions can be obtained from the observed climate and river flow time series. Initially, it can be seen that the variability of the mean annual precipitation increases in the second half of the time series for all catchments (section 2.4.1) and impacts the variability of the river flow in all catchments, which also

increases in the last period of observations (section 2.5). This is a robust change as it occurs in all the study catchments. Considering the significance of the annual trend of the variables, it is observed that only the temperature trends are statistically significant for all catchments (section 2.4.2). The trends observed here are consistent with what other studies have found. For temperature, the trend indicates an increase between 0.2°C and 0.3°C per decade, consistent with the findings from Robinson et al. (2017). The changes in precipitation observed here are not statistically significant, supported by the findings from Watts et al. (2015). For river flow, an increasing or no change trend for all catchments is observed (similar to Hannaford et al., 2015).

In the following chapters climate and hydrological simulations are evaluated and analysed for each of the study catchments.

3. Hydrological simulation

3.1. Introduction

In order to assess the changes in hydrology caused by climate change, a hydrological model for each of the study catchments is developed. Hydrological models mainly describe a catchment's physical interactions between the climate and river flow at the catchment's outlet (Prudhomme and Davies, 2009). This is an intermediate and fundamental step to reach the main aim of this thesis as the hydrological model provides a tool to evaluate the changes in river flow based in climate inputs and allows the subsequent assessment of the changes in hydropower generation. Thus, the process described in this chapter is relevant for the main aim of this research.

During the recent decades, hydrological models have developed and improved to analyse the water resources at the catchment scale. Hydrological models are one of the main tools used to evaluate water resources and environmental problems, scenarios and strategies (Singh and Frevert, 2006) and are fundamental for the analysis of catchment-scale impacts of climate change (e. g. Wilby and Harris, 2006; Cloke et al., 2013).

Given the large offer of hydrological modeling software, choosing a hydrological model for a specific analysis is an important step. Besides the collection of the required data and the estimation of the model parameters, the evaluation of the simulation skill of the hydrological model through performance measures is also relevant.

This chapter describes the analysis performed for the selection of the hydrological model and the methodology used for the estimation of the parameters required by the model. Additionally, a set of evaluation metrics and graphs used for the calibration and validation of the hydrological model is described. Furthermore, a comparison of the skill of the models is performed by analysing the results from other studies performed within the UK. A summary of the main findings is provided at the end of the chapter.

3.2. Selection of the hydrological model

The fast growth and development of the hydrological modelling sector has resulted in an increase of the number of available modelling software. Each modelling software has its particular structure, parameterization and conceptualization of the system. Therefore, even with similar inputs the results of each model could differ. Additionally, the data requirements vary for each hydrological model, this being one of the main decisive factors when choosing which hydrological model to use. Normally, a hydrological model is selected for a study if it fulfils the research goal by describing the catchment processes in an appropriate manner, using data requirements that are readily available or not difficult to obtain or estimate and providing results that are useful for the user needs.

The current availability of hydrological modelling software is large, ranging from free to priced models, user-friendly to plain code models and from simple to very complex simulation of the catchment's physical relationships, among other characteristics. Section 1.4 mentions some of the hydrological modelling

software that have been developed by research groups and that are commonly used for research purposes. A summary of the data requirements, temporal and spatial characteristic from each of those models is shown in Table 3.1. The main climate data requirements included in the comparison are precipitation, temperature and potential evapotranspiration time series. The required physical properties compared are the catchment's topography, aquifer and soil properties, topographic index and land use. The spatial scale of the models ranges from lumped models that simulate the whole catchment as a single unit, semi-distributed models that simulate the catchment using several representative units and distributed models that simulate the catchment by commonly dividing it into grids. The temporal scale considered here ranges from a continuous simulation to time steps of one minute and daily time steps.

Table 3. 1 Main characteristics of selected hydrological models

Model	Precipitation	Temperature	Potential Evapotranspiration	Topography	Aquifer properties	Soil properties	Topographic index	Land use	Spatial Scale	Shortest Temporal Scale
ARNO	o	o	o	+/-	+/-	o	+/-	o	SD	cont
GR4J	o	x	o	x	o	o	x	x	L	day
HBV	o	o	+/-	o	+/-	o	+/-	o	SD	min
HYPE	o	o	+/-	o	o	o	+/-	o	SD	day
HEC-HMS	o	+/-	O	x	x	o	x	o	L/D	min
LISFLOOD	o	o	o	o	+/-	o	+/-	o	D	min
PDM	o	+/-	o	+/-	+/-	+/-	+/-	+/-	L	min
RORB	o	+/-	+/-	+/-	+/-	+/-	+/-	+/-	D	cont
TOPKAPI	o	+/-	+/-	o	x	o	o	o	L/SD	cont
TOPMODEL	o	+/-	+/-	+/-	+/-	+/-	o	+/-	D	cont
WEAP	o	x	o	x	o	o	x	o	D	day

Note: SD: Semi-distributed; D: distributed; L: lumped; cont: continuous; day: daily; min: sub-daily; o: required or included; x: not required or included; +/-: may be used as input or might be included as output.

The methodology of this research is expected to be easily reproduced elsewhere. Therefore, priced models and models requiring special permissions to be used (e.g. WEAP is priced, except for developing countries; HBV requires permission to be used) are removed from the selection process. One of the main problems regarding the analysis of climate change impacts using climate models is the spatial differences between the catchment area and the climate model grid box. This is well illustrated in the Glaslyn catchment. The area of the Glaslyn catchment is smaller than the area covered by one Regional Climate Model (RCM) grid box, meaning that only a lumped model could be used for this catchment when assessing the impacts of climate change as the RCM outputs cover the entire catchment. Thus, for consistency among the catchment, only lumped models are used (although, it is acknowledged that for large catchments, as the upper Thames, a distributed model could generate more accurate simulations). The final criterion is the availability of guidelines for the estimation of the required parameters because this reduces the uncertainty that could be generated by estimating parameters using approaches different to the ones used by the model developers.

As a result, the Hydrologic Modelling System from the Hydrologic Engineering Center (HEC-HMS) is selected from the list of models in Table 3.1, as it satisfies the research requirements specified above.

3.3. The Hydrologic Modelling System from the Hydrologic Engineering Center (HEC-HMS)

The HEC-HMS hydrologic modelling software is developed by the US Army Corps of Engineers. The main objective of the program is to simulate rainfall-runoff processes within study catchments using three components, namely: 1) catchment model, 2) meteorological model, and 3) control specifications.

The catchment model includes different components that are used to represent the study catchment. These components are: canopy characteristics, surface storage, water losses, transform and baseflow (see Figure 3.1), and each will be explained throughout this section. The software provides different calculation methods for each component. For this research, canopy is simulated using the dynamic canopy method which requires the definition of the initial and maximum storage, a crop coefficient time series and the selection of a soil uptake method. Surface water is simulated using the simple surface method that needs the initial and maximum storage values. Losses are estimated using the soil moisture accounting method that needs the estimation of the impervious area, maximum infiltration rate, soil storage, groundwater storage and their storages at the beginning of the simulation. The transform method used in this research is the Snyder unit hydrograph for which the lag time and peaking coefficient must be estimated. Finally, baseflow is simulated using the recession method that requires the estimation of the initial discharge, recession constant and ratio to peak threshold.

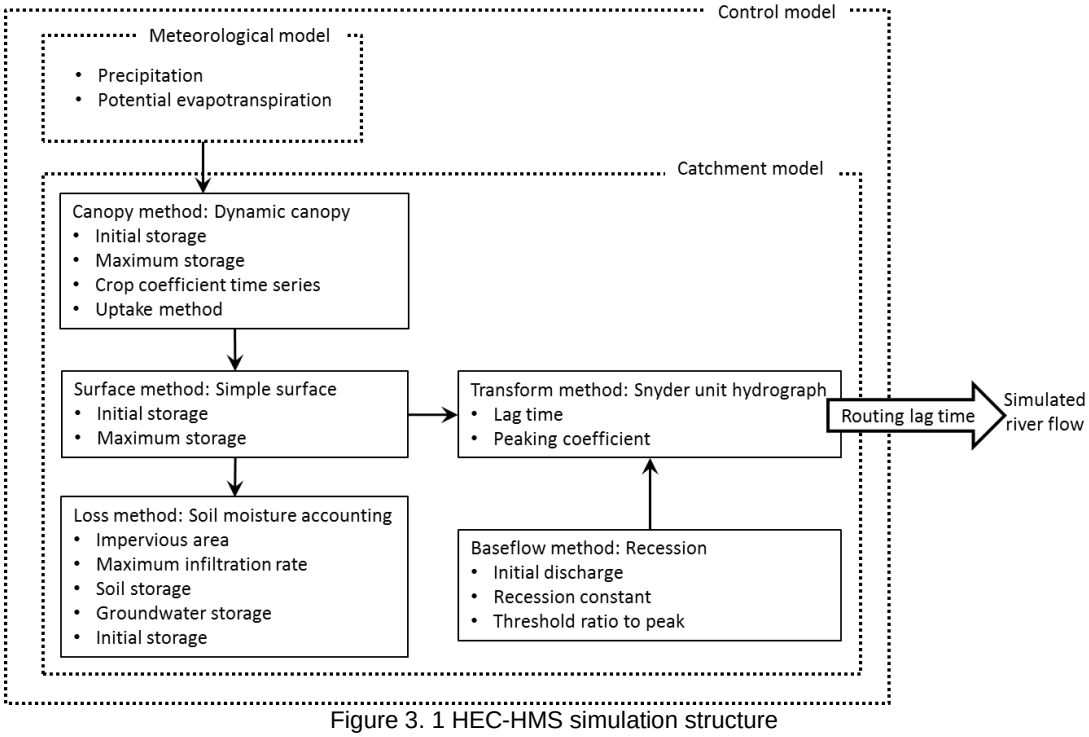

Figure 3. 1 HEC-HMS simulation structure

The meteorological model includes the climate variables that the model uses as drivers for the simulation. For this research daily precipitation and potential evapotranspiration time series for each catchment are used as input for the meteorological model.

The control model is used to define the period in which the model will be run. It basically requires the simulation starting and finishing dates. These dates vary for each catchment based on the availability of river flow data and the periods selected for model calibration and validation (see section 3.5).

HEC-HMS has been used in studies analysing climate change impacts in water resources (e.g. Babel et al., 2014; Azmat et al., 2015), simulating river flow in ungauged catchments (e.g. Ibrahim-Bathis and Ahmed, 2016; Gumindoga et al., 2016) and arid regions (e.g. El Alfy, 2016; Derdour et al., 2017; Wang et al., 2016) with good results. Additionally, research has focused on improving the model capabilities (e.g. Dariane et al., 2016; Zema et al., 2016). Presently, the HEC-HMS model has increased its presence in Europe by carrying out workshops and integrating the community that is currently applying the model in European catchments.

3.3.1. Setup of the HEC-HMS model

This section provides a detailed explanation of the methodology used to integrate the hydrological model. The initial configuration of the model and the required observed data sets are detailed. Also, each parameter's definition and estimation procedure is explained. The parameter values used to drive the HEC-HMS model are shown in Table 3.2 along with any changes in the calibration step.

Table 3.2 Estimated parameters and changes during the calibration (shown in bold) of the HEC-HMS model

		Upper Thames		Glaslyn		Calder		Coquet	
Element	**Parameter**	Initial	Calibration	Initial	Calibration	Initial	Calibration	Initial	Calibration
	Area(Km^2)	1616.2	1616.2	67.1	67.1	316	316	346	346
Dynamic Canopy	Initial Storage (%)	50	50	50	50	50	50	50	50
	Max Storage (mm)	2.89	2.89	2.55	2.55	3.28	3.28	2.57	2.57
Simple Surface	Initial Storage (%)	0	0	0	0	0	0	0	0
	Max Storage (mm)	**10**	**95**	**10**	**7**	**10**	**105**	**10**	**100**
Soil Moisture Accounting	Soil (%)	90	90	90	90	90	90	90	90
	GW1 (%)	40	40	40	40	40	40	40	40
	GW2 (%)	0	0	0	0	0	0	0	0
	Max Infiltration (mm/hr)	**0.68**	**0.97**	16.9	16.9	**9.1**	**11.8**	**32.33**	**0.34**
	Impervious (%)	5.3	5.3	0.14	0.14	16.8	16.8	0.5	0.5
	Soil Storage (mm)	**40.5**	**15**	20	20	162.7	162.7	**8.7**	**1**
	Tension Storage (mm)	**10.5**	**5**	**19.7**	**16.7**	**160**	**161.8**	**8.5**	**0.9**
	Soil Percolation (mm/hr)	**0.08**	**0.05**	0.5	0.5	0.5	0.5	**0.5**	**0.04**
	GW1 Storage (mm)	80	80	80	80	80	80	80	80
	GW1 Percolation (mm/hr)	1	1	1	1	1	1	1	1
Snyder Unit Hydrograph	Standard Lag (hr)	37.03	37.03	8.4	8.4	17.65	17.65	20.35	20.35
	Peaking Coefficient	0.513	0.513	0.56	0.56	0.44	0.44	0.877	0.877
Recession	Initial Discharge (cumecs)	14.1	14.1	2.8	2.8	7	7	12	12
	Recession Constant	**0.87**	**0.97**	**0.85**	**0.96**	**0.82**	**0.997**	**0.93**	**0.99**
	Ratio	0.7	0.7	0.15	0.15	**0.59**	**0.05**	**0.62**	**0.16**
Routing	Lag	**2900**	**1300**	0	0	0	0	**1400**	**300**

GW: Groundwater

3.3.1.1. Temporal and spatial resolution

The first step to construct the hydrological model is to define its temporal and spatial resolutions. A daily time step is used as temporal resolution for every calculation as this is the time step from the climate and hydrological observations that are used as model input and for evaluation. Additionally, data from the climate models is also available in daily time steps.

A lumped model is used as spatial resolution. As explained in section 3.2, the size of the Glaslyn catchment is smaller than the area of a RCM grid box and is therefore not suitable for the direct application of a semi-distributed or distributed hydrological model. Using a lumped model allows an identical methodology to be used for all catchments. This means that the inputs to the model will be catchment-sized averaged values (e.g. the mean daily precipitation or potential evapotranspiration (PET) over the entire catchment).

3.3.1.2. Precipitation, river flow and potential evapotranspiration time series

Daily precipitation and PET are part of HEC-HMS's meteorological model and also its main driving climate variables. Daily observed precipitation time series are obtained from the CEH-GEAR dataset, described in section 2.3.1. Similarly, estimations of the daily PET are obtained from the CHESS-PET dataset described in section 2.3.3. The CEH-GEAR and CHESS-PET datasets provide gridded observations or estimations. All the grids within each catchment are used to generate daily time series of the catchment's mean precipitation and PET. Such time series are used as input for the hydrological model.

Additionally, daily river flow is used to evaluate the performance of the model by comparing the simulated river flow with the observations. For each catchment, observed daily river flow time series from the Centre of Ecology and Hydrology's (CEH) National River Flow Archive gauging stations are used for comparison. Information from each gauging station and their observed records are provided in section 2.5.

3.3.1.3. Canopy method: Dynamic canopy

In HEC-HMS, canopy storage is related to the amount of rainfall that is intercepted by the vegetation before reaching the soil surface (Scharffenberg and Fleming, 2013). Thus, streamflow is reduced as a result of the canopy interception (Kozak et al., 2007; Bulcock & Jewitt, 2010) as the intercepted precipitation cannot be part of the runoff and subsequent subsurface processes (Savenije, 2004) and it is loss as evapotranspiration (Scharffenberg and Fleming, 2013).

3.3.1.3.1. Maximum and initial canopy storage

The Leaf Area Index (LAI), defined as the area of leaf surface per unit area of soil surface (Campbell, 2007), is used to estimate the maximum canopy storage (S^c_{max}) (in mm) by applying equation 3.1 (Von Hoyningen-Huene, 1981). This equation has given good results when compared to field measurements (Kozak at al., 2007; Bulcock & Jewitt, 2010):

$$S^c_{max} = 0.935 + 0.498(LAI) - 0.00575(LAI^2) \quad \text{Eq. 3.1}$$

The maximum canopy storage capacity is estimated using LAI satellite images from the Moderate-resolution Imaging Spectroradiometer (MODIS). The MODIS satellite image approximates LAI at 1-km

resolutions with a frequency of 8 days. For each catchment, monthly images from 2000 to 2014 are obtained by selecting the images closer to the 15th day of each month. An example of the images used to estimate the catchments' LAI distribution is shown in Figure 3.2 for January and July 2010. LAI depends on the season because it is influenced by the growing conditions of the vegetation. Therefore, the LAI images were used to estimate the monthly maximum canopy storage using equation 3.1. An example of the resulting maximum canopy estimates is shown in Figure 3.3 for January and July 2010. An average of all the processed images is used as estimate of the maximum canopy storage and used as input for the hydrological model. Satellite images that could not capture the entire catchment characteristics (for instance, due to cloud interference) (e.g. Fig. 3.3d for January) are not included in the average estimation. The canopy value at the beginning of the simulations (initial canopy) is set at 50% of the maximum canopy.

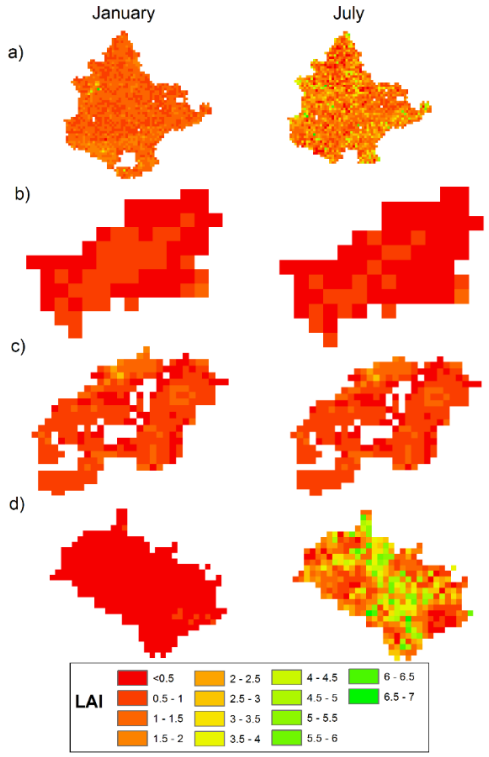

Figure 3. 2 Leaf Area Index (LAI) image from MODIS in January and July 2010 for the a) upper Thames, b) Glaslyn, c) Calder and d) Coquet catchments

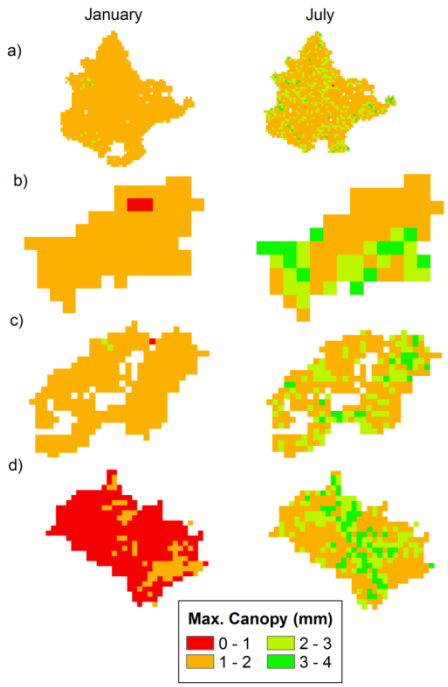

Figure 3. 3 Estimated maximum canopy for January and July 2010 for the a) upper Thames, b) Glaslyn, c) Calder and d) Coquet catchments

3.3.1.3.2. Crop coefficient time series

Evaporation and transpiration losses depend on the catchment's vegetation and its PET rates. Vegetation data for each catchment is obtained from the Land Cover Map of Great Britain 2007 (Morton et al., 2011). The main land cover classifications used by the CEH are employed: grassland, mountain/heath/bog, woodland, freshwater, urban and arable (shown in Figure 2.3 and reported in Table 2.1). The arable area is divided into the different crops grown within each catchment: wheat, barley, potato, maize and oil seed rape (Defra, 2011). The approximate area used for each crop is estimated using reported historical time series.

The crop coefficient (Kc) relates the effects of evaporation and transpiration from a particular vegetation type. The coefficient integrates the characteristics of the crop and the soil evaporation effects and it is used following the procedure recommended by Allen et al. (1998) which is explained below. The actual evapotranspiration rate from a crop (or land cover) (ETc) is estimated by relating its Kc to the reference evapotranspiration (ETo), using equation 3.2:

$$ET_c = k_c ET_o \qquad \text{Eq. 3.2}$$

Table 3. 3 Lengths of the development stages (days) (from Allen et al., 1998)

Cover	Initial	Development	Mid	Late
Mountain	180	60	90	35
Grassland	10	20		
Oil seed rape	25	35	55	30
Wheat	40	30	40	20
Barley	40	30	40	20
Potato	30	35	50	30
Maize	30	40	50	30
Woodland	Same value all year			
Urban	Same value all year			

Kc time series are developed by associating the length of the vegetation development stages with their corresponding coefficient. The used growing stage lengths and their associated coefficients are shown in Table 3.3 and Table 3.4, respectively. The missing initial coefficients are estimated by interpolating the late and middle stages coefficients. The initial stage of all land covers is defined to start in April, based on information found in the literature (Allen et al., 1998). For each catchment, a one-year long daily crop coefficient time series is generated for each land cover. Afterwards, an average daily coefficient time series is developed for each catchment using equation 3.3:

$$Kc_t = \frac{\sum A_i Kc_{i,t}}{\sum A_i} \qquad \text{Eq. 3.3}$$

Where Kc_t stands for the average daily catchment coefficient, A is the area and $Kc_{i,t}$ the daily coefficient of land cover i. The resulting time series is used for all the simulated years and introduced to HEC-HMS.

Table 3. 4 Crop coefficients (Kc) for the different growing stages and land covers (from Allen et al., 1998)

Land cover	Kc ini	Kc mid	Kc late
Freshwater		0.65	1.25
Mountain	1.05	1.10	1.10
Urban	0.20	0.20	0.20
Grassland	0.30	0.75	0.75
Woodland	1.00	1.00	1.00
Oil seed rape	0.35	1.15	0.35
Wheat	0.55	1.15	0.33
Barley		1.15	0.25
Potato		1.15	0.75
Maize		1.18	0.76

Different crop coefficient time series are obtained for each catchment (Figure 3.4). Overall the year, the coefficients are larger for the catchments with fewer urban and agricultural areas. In contrast, the upper Thames catchment has an extensive agricultural area and its crop coefficient curve strongly follows the growing stages of the cultivated vegetation.

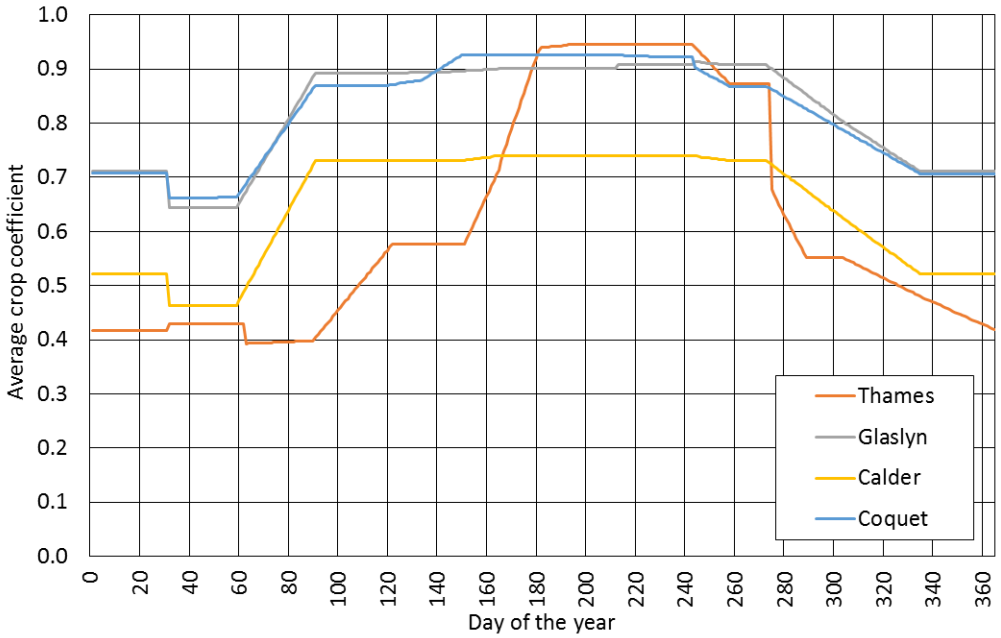

Figure 3.4 Annual time series of the daily average crop coefficient for each catchment

3.3.1.3.3. Uptake from the soil

The canopy method includes a routine to simulate the extraction of water from the soil. In this analysis, the tension reduction method is used. For this methodology, water is extracted from the soil zone and the tension zone storages (both defined in the soil moisture accounting loss rate method). The difference is that water is always abstracted from the soil zone at the PET rate and in the tension zone the extraction rate decreases (Scharffenberg and Fleming, 2013).

3.3.1.4. Surface method: simple surface

In HEC-HMS, the surface method represents the volume of water that could accumulate in the catchment's surface. The surface storage is filled at the precipitation rate and the amount of water accumulated in this storage is subject to infiltration or evapotranspiration. If the precipitation volume is higher than the infiltration rate and the maximum surface storage is filled, then the excess precipitation is converted into runoff. For this method, the surface storage at the beginning of the simulation and the maximum surface storage must be estimated (Scharffenberg and Fleming, 2013).

3.3.1.4.1. Initial and maximum surface storage

For this research, the simple surface method was mainly used for model calibration purposes. Thus, this value is adjusted during the calibration of the model to improve the model's simulation skill.

3.3.1.5. Loss method: soil moisture accounting

The loss method is used to estimate the catchment's infiltration volume. In HEC-HMS, the only routine capable of simulating continuous events is the soil moisture accounting method. This method uses three layers (soil, upper groundwater and the optional lower groundwater) to simulate the water movement in the

soil. Furthermore, the soil storage zone is divided into tension and gravity storage regions (Scharffenberg and Fleming, 2013). The parameters required for the loss method simulation are explained next.

3.3.1.5.1. Impervious area

The model assumes that all the precipitation falling in the impervious area (here considered as the urban land cover) becomes direct runoff (Scharffenberg and Fleming, 2013). The impervious area of the catchment is estimated from the Land Cover Map of Great Britain 2007 (Morton et al., 2011), shown in Figure 2.3 and Table 2.1. This area is introduced into the model as a percentage of the total area of the catchment.

3.3.1.5.2. Maximum infiltration rate

The maximum infiltration rate is defined as the upper limit at which water infiltrates from the surface into the soil storage layers. The actual infiltration rate of a time step depends on the water availability and the potential infiltration, which is estimated by a linear relationship involving the maximum infiltration (MI), the maximum soil storage and the soil storage at the beginning of the time step (Scharffenberg and Fleming, 2013):

$$Potential\ infiltration\ (mm/hr) = MI - \left(\frac{Current\ soil\ storage}{Max.soil\ storage}\right) MI \qquad \text{Eq. 3.4}$$

The MI rate is calculated as a weighted average of the saturated hydraulic conductivity (SHC) from the soils within the catchment (shown in Figure 2.4 and given in Table 3.5) and the area they cover (A):

$$MI\ (mm/hr) = \frac{\sum A_i SHC_i}{\sum A_i} \qquad \text{Eq. 3.5}$$

Table 3. 5 Soil type parameter estimates (from Rawls & Brakensiek, 1982, as published in Feldman, 2000)

Soil class	Porosity (cm^3/cm)	Sat. Hydraulic conductivity (cm/hr)
Loamy sand	0.437	6.11
Loam	0.463	1.32
Clay loam	0.464	0.23
Average	0.455	2.55

3.3.1.5.3. Soil storage

Soil storage is the amount of water that can be stored in the soil layer before being lost to deep groundwater. The soil layer is divided into tension storage and upper soil storage. The upper soil storage can be lost to evapotranspiration and/or percolation. On the other hand, the tension storage volume is only lost to evapotranspiration. Evapotranspiration will first take water from the upper zone storage and, if it dries, it will take water from the tension storage. Furthermore, the evapotranspiration rate is reduced when water is abstracted from the tension storage (Feldman, 2000; Scharffenberg and Fleming, 2013).

The available soil storage is estimated considering the soil porosity and the thickness of the soil layer. The average porosity of the catchment's different soil types is shown in Table 3.5. The thickness of the soil layer is estimated using the Basic Superficial Thickness Model (BSTM) (Lawley and Garcia-Bajo, 2010)

developed by the British Geological Survey (BGS) (Figure 3.5). This model is based on the DiGMapGB-50 Version 5 geological map and borehole records from the BGS dated before August 2008. As the model uses existing borehole data, its accuracy depends on the availability of this data which is scarce in rural settlements and abundant in urban areas and main roads (Lawley and Garcia-Bajo, 2010). The soil thickness for each catchment is defined as the average thickness estimated by the BSTM. The porosity of each soil type is multiplied by the average thickness of the soil layer and then divided by the area of the soil type within the catchment. The total soil storage is estimated by adding the available storage of all the soil types.

Once the total soil storage is estimated, it is distributed into the tension and upper soil zones. As there is no data to estimate such distribution, each zone is assigned 50% from the total soil storage. These values can be modified during the calibration of the model.

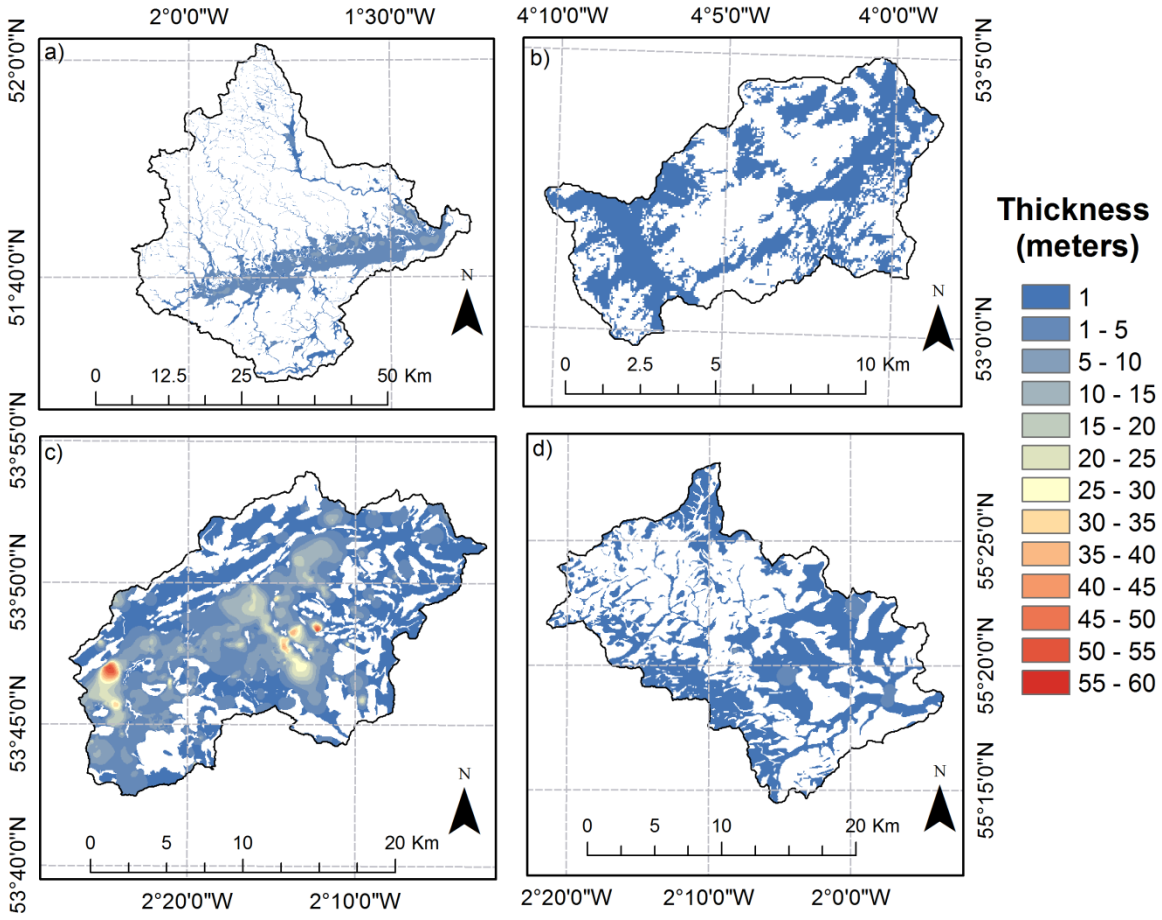

Figure 3. 5 Thickness variation of the superficial deposits according to the Basic Superficial Thickness Model (Lawley and Garcia-Bajo, 2010) for the a) upper Thames, b) Glaslyn, c) Calder and d) Coquet catchments. The white areas represent regions where no data is available

3.3.1.5.4. Groundwater

The model provides two groundwater layers to represent shallow processes (Scharffenberg and Fleming, 2013). The groundwater processes (e.g. groundwater recharge) are not relevant for this research. Therefore, only one layer is used to simulate the water infiltrated to groundwater. Based on the above, a value of 80 mm is assigned to the groundwater storage volume and a value of 1 mm/hr used as groundwater percolation rate (infiltration to deep groundwater).

3.3.1.5.5. Initial storages

Initial values for the soil and groundwater storages have to be defined for the simulation. These values are only used as start-up values for beginning the simulation (Scharffenberg and Fleming, 2013). In other words, for a long term simulation the relevance of this parameters is low as the simulation climate input will adjust them to the correct value in the subsequent time steps. Nevertheless, here the initial soil storage is fixed at 90% and the groundwater storage at 40%, which is representative of wet conditions following a precipitation event.

3.3.1.6. Transform method: Snyder unit hydrograph

The transform method estimates the surface runoff in the model according to the different rainfall volumes (Scharffenberg and Fleming, 2013). For this research, the synthetic Snyder unit hydrograph (UH) is used as transform method. The Snyder UH uses the lag time, peak flow and total time as parameters to characterize each catchment's response to rainfall (Feldman, 2000).

3.3.1.6.1. Lag time

The UH lag time (t_p), in hours, is estimated by equation 3.6:

$$t_p = 0.75 C_t (L L_c)^{0.3} \qquad \text{Eq. 3.6}$$

C_t is a catchment coefficient, L stands for the length of the main stream and L_c is the stream length measured from the closest point to the catchment centroid and the outlet. The catchment coefficient ranges between 0.4 for mountainous areas and and 8 for flat catchments (Bedient & Huber, 1992; Feldman, 2000). The coefficient is estimated using the main stream slope (S) according to the Taylor-Schwarz formula (Taylor and Schwarz, 1952):

$$C_t = \frac{1.65}{(\sqrt{S})^{0.38}} \qquad \text{Eq. 3.7}$$

The catchment's outlet and head flow elevations are used to estimate the slope of the main stream with data from the 50x50 meter Integrated Hydrological Digital Terrain Model (IHDTM) (Morris & Flavin, 1990; Morris & Flavin, 1994).

3.3.1.6.2. Peaking coefficient

The UH peaking coefficient (C_p) is determined by equation 3.8:

$$C_p = \frac{t_p U_p}{2.75 A} \qquad \text{Eq. 3.8}$$

A stands for the catchment's area (km^2), t_p is the lag time (hr) and U_p (m^3/s) is the peak of the standard UH. The 2.75 value is a conversion constant for the SI units (Feldman, 2000).

3.3.1.7. Baseflow method: Recession

In HEC-HMS, the baseflow method is used to simulate the subsurface processes and the observed baseflow behavior. The method estimates an exponential recession of the baseflow after a rainfall event. The parameters required by the method are the initial discharge (m^3/s), the recession constant and the ratio to peak threshold.

3.3.1.7.1. Initial discharge

The initial discharge is the baseflow at the start of the simulation (Scharffenberg and Fleming, 2013). In this case, as observations are available, the river flow observed in each catchment during the first time step of the simulation is used as initial discharge.

3.3.1.7.2. Recession constant

The recession constant is the rate at which baseflow decreases when no rainfall is present. It is estimated as the ratio of the baseflow from the current time step and the baseflow from the previous time step (Scharffenberg and Fleming, 2013). Nevertheless, the recession constant varies according to the prior river flow volume, the magnitude of the precipitation event and the catchment conditions before the precipitation event (see Fig. 3.6). Therefore, the recession constant from diverse observed precipitation events is estimated along with their mean (used as model input) and standard deviation (Table 3.6).

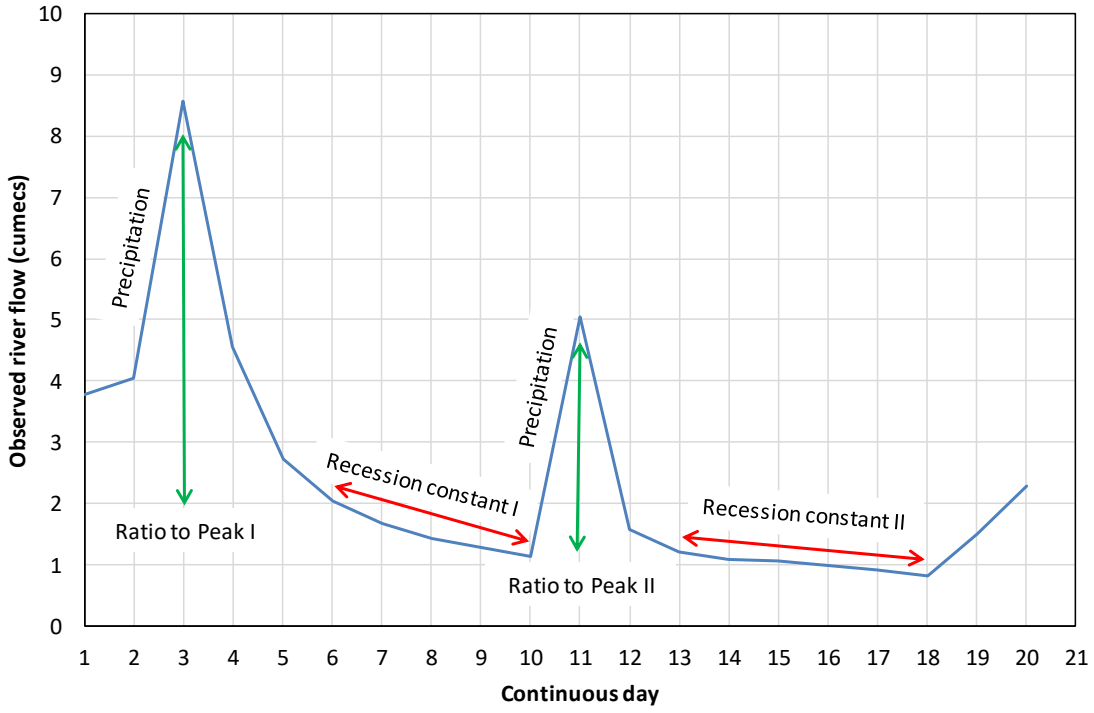

Figure 3. 6 River flow response to two precipitation events in the Glaslyn catchment. The graph shows the recession constant in red and the ratio to peak thresholds in green for both events. It can be seen that both parameters are different for each event

Table 3. 6 Mean and standard deviation from each catchment's recession constant

	Upper Thames	Glaslyn	Calder	Coquet
Mean	0.87	0.85	0.82	0.93
St. Dev	0.12	0.09	0.18	0.07

3.3.1.7.3. Threshold ratio to peak

The ratio to peak threshold initiates the recession constant when the flow of the current time step divided by the peak flow is lower than the threshold ratio (Scharffenberg and Fleming, 2013). Similar to the recession constant, the ratio to peak threshold varies according to the precipitation event magnitude and the catchment's conditions prior to the precipitation event (see Fig. 3.6). Therefore, the same precipitation events from section 3.3.1.7.2 are used to estimate the mean and standard deviation statistics for this parameter (shown in Table 3.7).

Table 3. 7 Mean and standard deviation from each catchment's ratio to peak threshold

	Upper Thames	Glaslyn	Calder	Coquet
Mean	0.71	0.15	0.59	0.62
St. Dev	0.18	0.10	0.42	0.17

3.3.1.8. Routing lag time

This parameter represents the river flow travel time within the catchment until it reaches the outlet (Scharffenberg and Fleming, 2013). Each catchment has a different time length to respond to precipitation according to the catchment's size, slope and urban area, among other characteristics. The lag time is estimated by calculating the correlation coefficient between the time series of the observed daily precipitation and the time series of the daily river flow observed the same and each subsequent day for five days after the precipitation event. The interval with the river flow with the highest correlation coefficient is interpreted to be the catchment's mean routing lag time (shown in Table 3.8).

Table 3. 8 Correlation coefficient of between the daily observed precipitation and the daily river flow observed the same and subsequent days (highest coefficient shown in bold)

Catchment	Same day	1	2	3	4	5
Upper Thames	0.11	0.24	**0.29**	0.27	0.25	0.24
Glaslyn	**0.69**	0.65	0.36	0.28	0.26	0.27
Calder	**0.67**	0.61	0.35	0.28	0.24	0.19
Coquet	0.40	**0.67**	0.49	0.22	0.15	0.13

3.4. Model Evaluation

There is no standard protocol to test the skill from hydrological models (Hrachowitz et al., 2013). Here, to evaluate the simulation skill of the hydrological model, the available observation records are divided in two same-length periods, where possible. One of the periods is used to calibrate the model parameters and the other is used to evaluate the calibrated model outside the calibration period. Here, the most recent period is used for calibration and the oldest period for validation.

Table 3. 9 Periods used for calibration and validation for each catchment according to the available observations record

Catchment	Observations record	Calibration	Validation
Upper Thames	1961-2012	1987-2012	1961-1986
Glaslyn	1962-2012	1987-2012	1962-1986
Coquet	1973-2012	1993-2012	1973-1992
Calder	1976-2012	1994-2012	1976-1993

3.4.1.Evaluation graphs and indices

Graphs and indices are used to evaluate the simulation skill of the hydrological models. The graphs used in this analysis show differences between the observed and simulated river flows at the daily and monthly time step, the differences between the observed and simulated river regime and flow duration curves (FDC), the observed and simulated average number of days in a month when the river flow exceeds the Q10 and when it is below the Q95, monthly river flow boxplots and finally a seasonal comparison between the simulation biases and the observed river flow. Additionally, five statistical indices are used to complement the graphs. The Nash-Sutcliffe coefficient of efficiency (NSE) is the most common indicator used in hydrological studies, but using different indicators provides an advantage toward the evaluation of the model's skill (Ahmed, 2012). The calculation of each evaluation index is explained next.

3.4.1.1. Mean absolute errors (MAE)

This index computes the difference between the observed and simulated hydrographs. The difference could be positive or negative and compensate each other. Thus, the index considers the absolute values of the differences. The desired value of this index is zero (Feldman, 2000).

$$MAE = \frac{\sum_{t=1}^{n}\left|Q_t^{obs} - Q_t^{sim}\right|}{n} \qquad \text{Eq. 3.9}$$

Q_t^{obs} stands for the observed river flow for time step t and Q_t^{sim} represents the simulated river flow for time step t and n is the total number of time steps.

3.4.1.2. Residual volume (RV)

The residual volume refers to the difference between the simulated and observed volumes. This index can be negative or positive and mainly relates to the ability of the model to reproduce the total volumes of the observed records. The expected result of this model is a value closer to zero.

$$Vol.Residual = \sum_{t=1}^{n}\left(Q_t^{sim} - Q_t^{obs}\right) \qquad \text{Eq. 3.10}$$

Q_t^{obs} stands for the observed river flow for time step t and Q_t^{sim} represents the simulated river flow for time step t.

3.4.1.3. Root mean square error (RMSE)

The index evaluates the scatter of the residuals. A model performs better if this index is closer to zero (Ahmed, 2012).

$$RMSE = \left[\frac{\sum_{t=1}^{n}\left(Q_t^{obs} - Q_t^{sim}\right)^2}{n}\right]^{1/2} \quad \text{Eq. 3.11}$$

Q_t^{obs} stands or the observed river flow for time step t and Q_t^{sim} represents the simulated river flow for time step t and n is the total number of time steps

3.4.1.4. Ratio of the RMSE to the observations' standard deviation (RSR)

This ratio standardizes the RMSE by using the standard deviation of the observations. The index was developed by Moriasi et al. (2007) to classify the model performance by normalizing the RMSE statistic. The index varies from zero, the optimal value, to a large positive number. The following criterion is recommended to evaluate the model's performance in a monthly time step (Moriasi et al., 2007).

Very good	$0 \leq$ RSR ≤ 0.5
Good	$0.5 <$ RSR ≤ 0.6
Satisfactory	$0.6 <$ RSR ≤ 0.7
Unsatisfactory	RSR > 0.7

3.4.1.5. Nash Sutcliffe efficiency index (NSE)

The NSE evaluates the model's magnitude of residual variance and compares it to the data variance, in other words it is the ratio of the "noise" and "information". The NSE estimates the model ability to produce simulated flows that fit a 1:1 curve when compared to the observations. The NSE ranges from one to negative infinite with a perfect model having a value equal to one. Negative values indicate a model with no skill and positive decimals represent an acceptable model (Nash & Sutcliffe, 1970; Moriasi et al., 2007).

$$NSE = 1 - \left[\frac{\sum_{t=1}^{n}\left(Q_t^{obs} - Q_t^{sim}\right)^2}{\sum_{t=1}^{n}\left(Q_t^{obs} - Q^{mean}\right)^2}\right] \quad \text{Eq. 3.12}$$

Q_t^{obs} stands for the observed river flow for time step t, Q_t^{sim} represents the simulated river flow for time step t and Q_t^{mean} is the average of the observed river flows during the analyzed time period. For a monthly time step, Moriasi et al. (2007) recommended the following performance classification:

Very good	$0.75 <$ NSE ≤ 1
Good	$0.65 <$ NSE ≤ 0.75
Satisfactory	$0.50 <$ NSE ≤ 0.65
Unsatisfactory	NSE ≤ 0.5

3.5. Model calibration

Calibration takes place once the initial parameters of the model are estimated and used to drive the initial simulations. The calibration of the model is an iterative process with the goal of improving the model's skill by modifying selected parameters within control limits. Here, calibration is performed using the automatic calibration procedure included in the HEC-HMS model along with expertise from the modeller to control the changes of the parameters within physically consistent limits. Initially, the calibration is performed considering the reduction of the RMSE as objective function. For each catchment, eight parameters can be modified to improve the objective function. The BSTM database has important limitations (data is scarce to generate estimations of the parameters for the entire catchment). Therefore, the maximum infiltration, soil storage, tension storage and soil percolation are used for the calibration. As the recession constant and baseflow threshold ratios vary according to the precipitation event, and the catchment's preceding conditions, these parameters are also available for calibration. The model requires the routing lag time in minutes, but, due to data limitations, the lag time could only be estimated in a daily step. Therefore, this parameter is also available for modification. Finally, the surface maximum storage serves as control for the generation of runoff once the maximum storage is reached and is also used to calibrate the model. Other parameters were not modified during the calibration because their values are more certain or they are not relevant for the purposes of this analysis. For instance, parameters related to the groundwater storage and its percolation are not used during the calibration as the groundwater processes are not important for the study compared to the surface runoff generation processes that relate to the availability of water for hydropower generation.

Given the level of uncertainty and simulation importance of each parameter, these are grouped in the order in which they are used during calibration. The first group includes the maximum surface storage and routing lag time. The maximum infiltration, soil storage, tension storage and soil percolation are included in the second group. Finally, the third group is composed by the baseflow recession constant and the baseflow threshold. Once the first objective function is improved to its maximum degree, a second objective function is used focusing on reducing the residual volume using the group of parameters in the same order that they were used to satisfy the first objective function. However, after calibration using the second objective function, the parameter values rarely change.

During calibration, seven parameters are modified for the upper Thames, three parameters for the Glaslyn, five for the Calder, and eight for the Coquet catchment. The parameter values after calibration are shown in Table 3.2. The performance indices described in section 3.4.1 are used to evaluate whether the calibration process improves the model performance. The results for the calibration period are shown next.

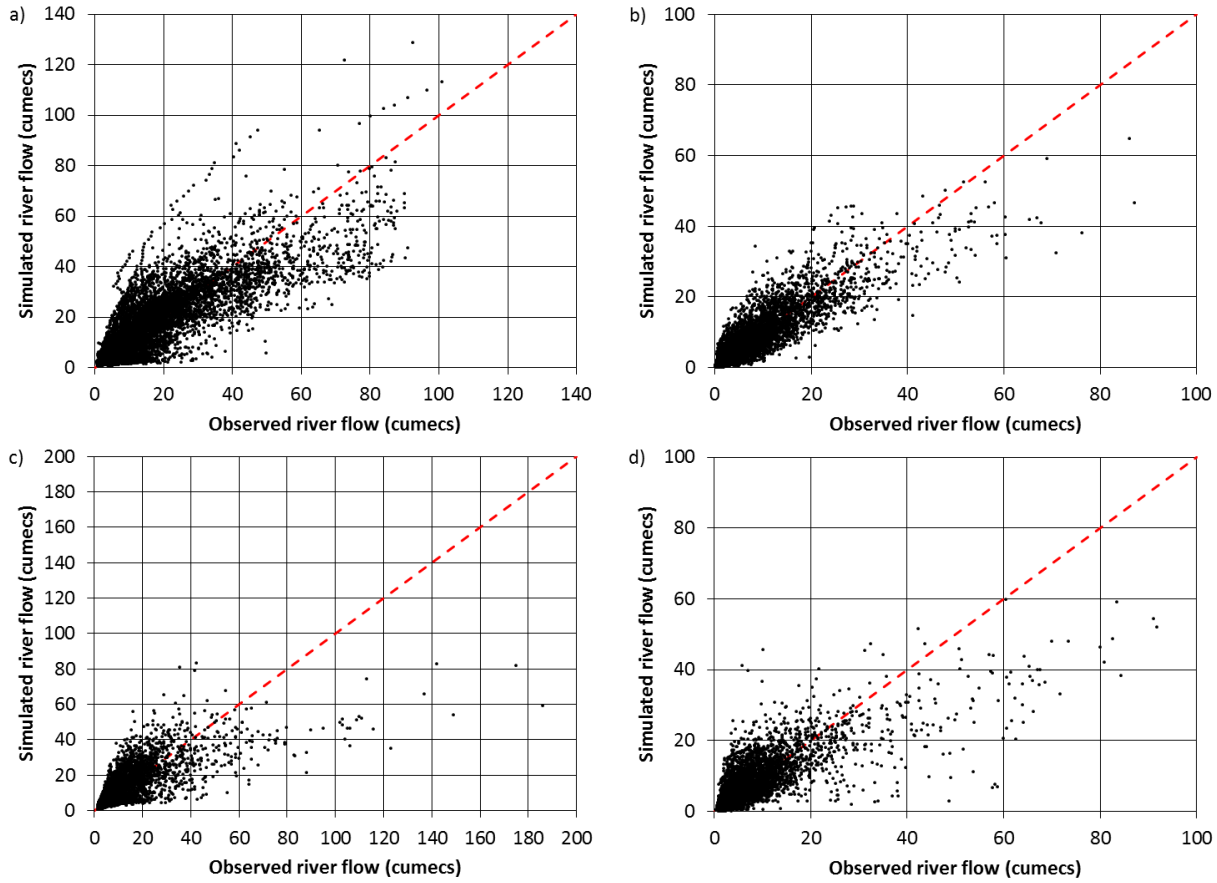

Figure 3. 7 Daily observed vs. simulated river flow during the calibration periods for a) Upper Thames, b) Glaslyn, c) Calder, and d) Coquet catchments. The red dotted line represents the 1:1 curve

The comparison plot of the simulated and observed river flows provides an insight of the model's skill. Considering a daily time step, the models from all catchments seem to reproduce the river flow accurately as the plots tend follow a 1:1 curve (Fig. 3.7). The hydrological models from the Glaslyn and Calder catchments seem to be more accurate compared to the upper Thames and Coquet catchments. For all catchments, the difference between observations and simulations is greater when larger river flow volumes are observed. Considering a monthly time step, the models from all catchments simulate river flow accurately (Fig. 3.8). There are few cases in the upper Thames and Coquet catchments when the simulated flow largely differs from the observed flow.

The models' skill to simulate the mean monthly river flow behaviour is assessed by comparing the observed and simulated river flow regime curves (Fig. 3.9). In general, for the calibration period the models from all catchments reproduce the observed monthly curve pattern accurately. The models from the Glaslyn and Calder catchments are more accurate than the upper Thames and Coquet catchments. Nevertheless, there are differences between the observed and simulated monthly river flows. The monthly mean absolute error is 26% for the upper Thames, 5% for the Glaslyn, 11% for the Calder and 17% for the Coquet catchment.

The largest differences for each catchment are observed during August for the upper Thames (61% error) and Calder (25% error) and July for the Glaslyn (12% error) and Coquet (38% error).

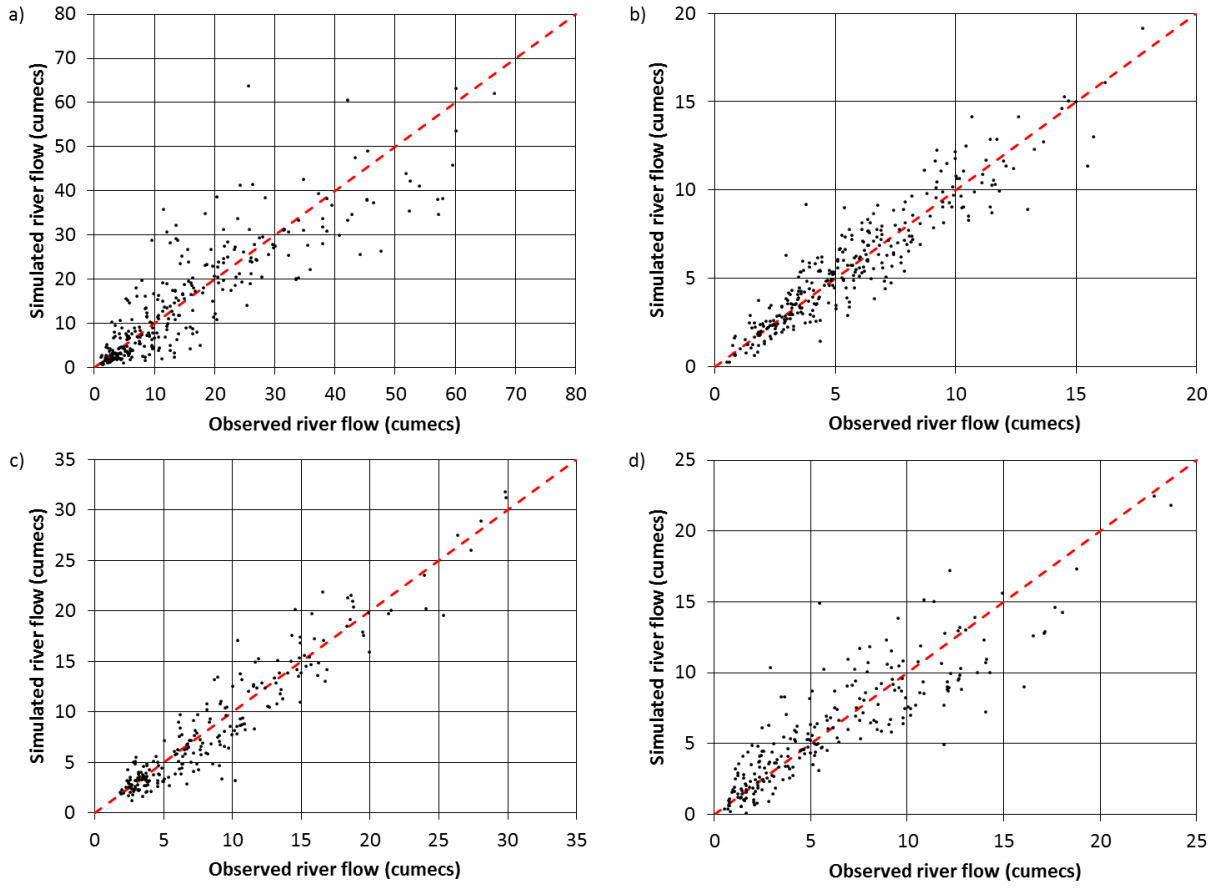

Figure 3. 8 Monthly mean observed vs. simulated river flow during the calibration periods for a) Upper Thames, b) Glaslyn, c) Calder, and d) Coquet catchments. The red dotted line represents the 1:1 curve

Some of the model error might be an effect of the natural variability of the river flow observations. Thus, boxplots of the monthly river flow are useful to evaluate the observed and simulated variability. For all catchments, the winter months have the larger observed river flow variability, whereas variability is smaller during summer. In the upper Thames catchment, the simulation variability is similar to the observed variability during autumn and winter and larger for the remaining months (Fig. 3.10). The hydrological model of the Glaslyn catchment simulates the observed river flow variability accurately (Fig. 3.11). For the Calder catchment, the hydrological model reproduces the observed river flow variability accurately with larger differences during January, May and November (Fig. 3.12). Finally, compared to the observed river flow variability, the Coquet model simulates larger variability during summer and autumn and smaller during winter (Fig. 3.13).

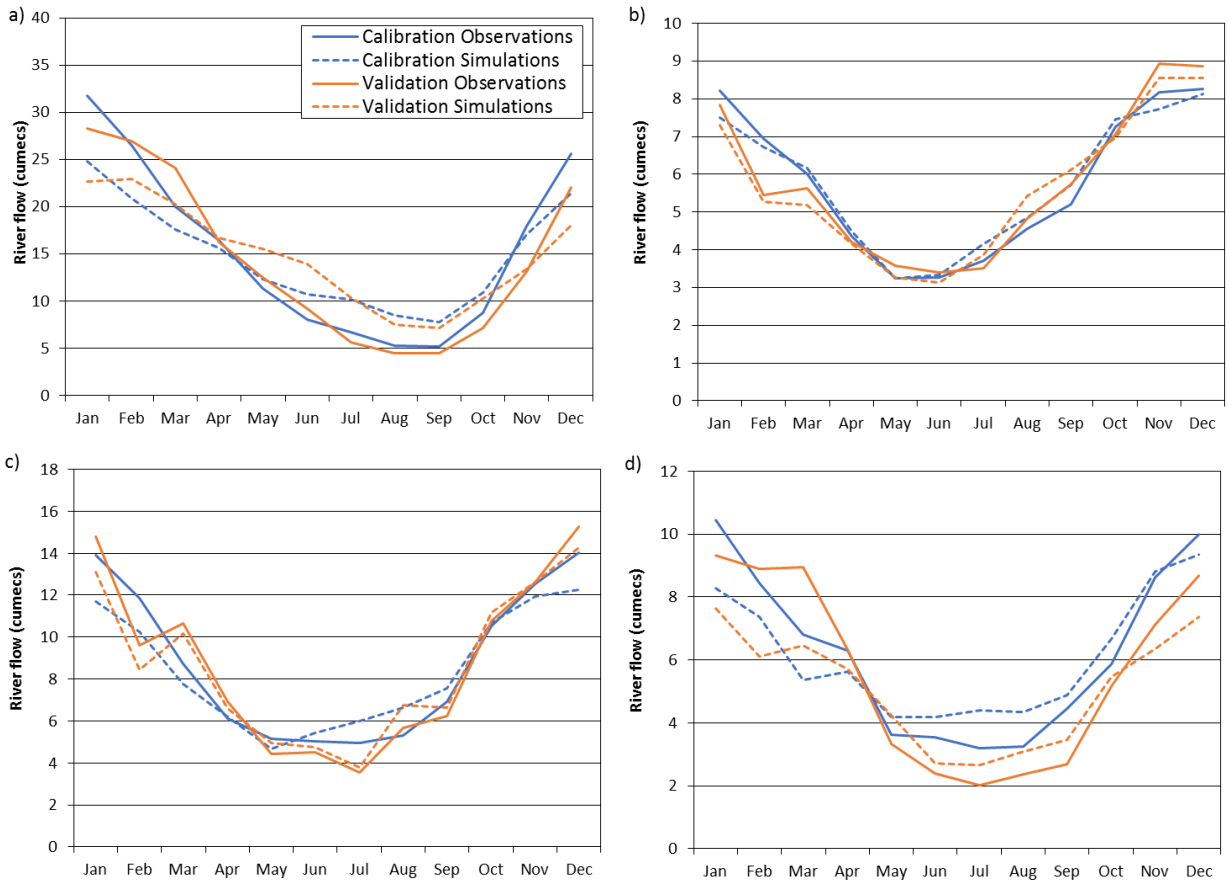

Figure 3. 9 Simulated and observed river flow regimes during the calibration and validation periods for a) Upper Thames, b) Glaslyn, c) Calder and d) Coquet catchments

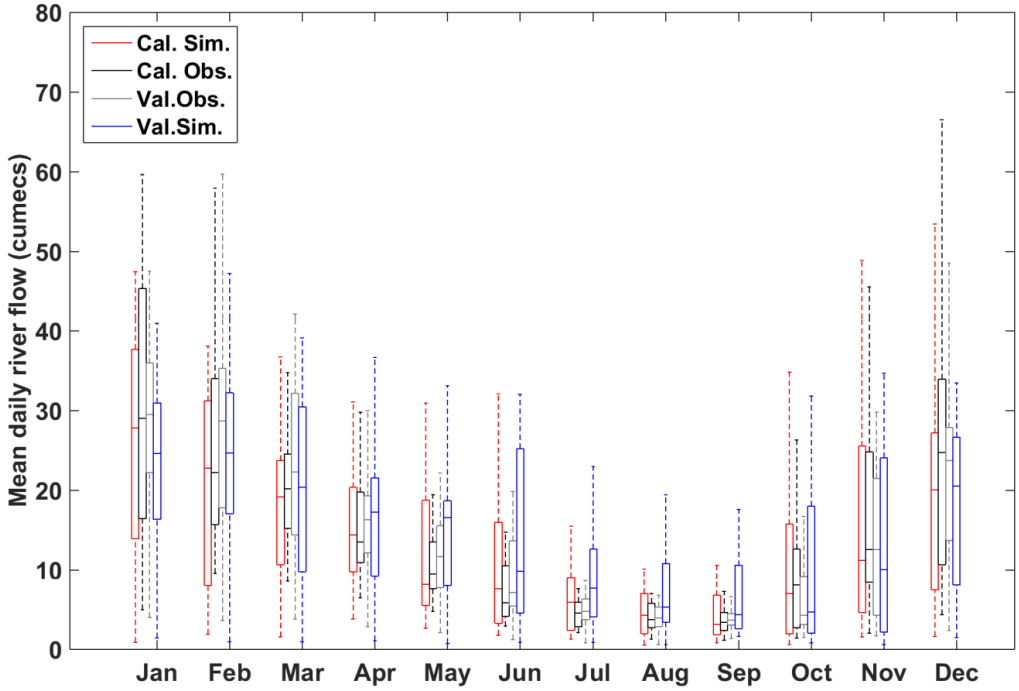

Figure 3. 10 Observed (obs) and simulated (sim) monthly river flow boxplots during the calibration (cal) and validation (val) periods for the upper Thames catchment

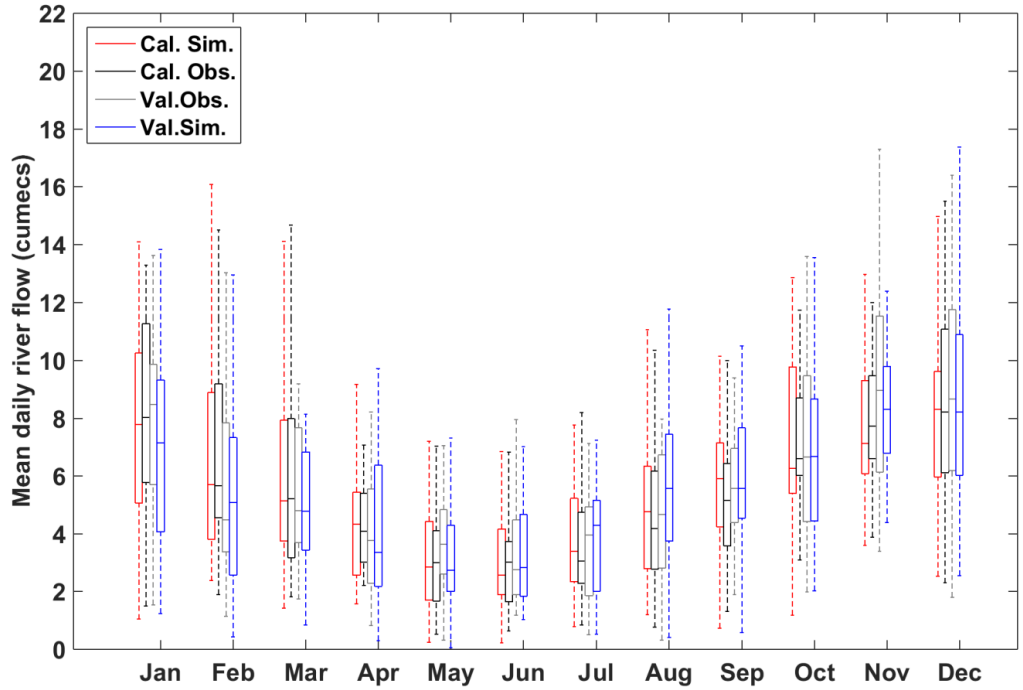

Figure 3. 11 Observed (obs) and simulated (sim) monthly river flow boxplots during the calibration (cal) and validation (val) periods for the Glaslyn catchment

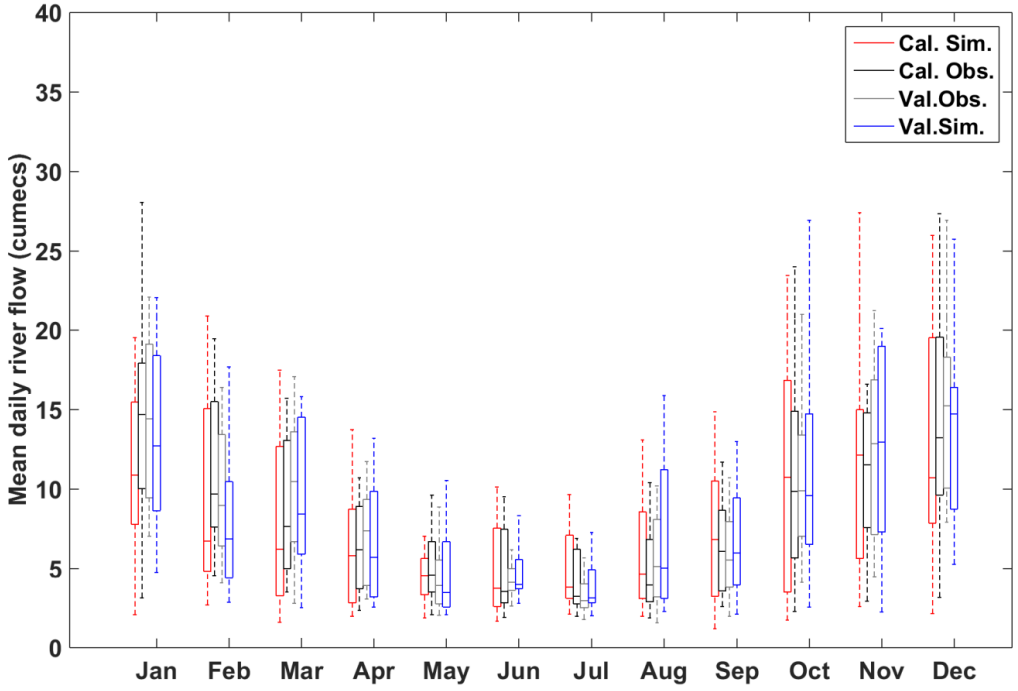

Figure 3. 12 Observed (obs) and simulated (sim) monthly river flow boxplots during the calibration (cal) and validation (val) periods for the Calder catchment

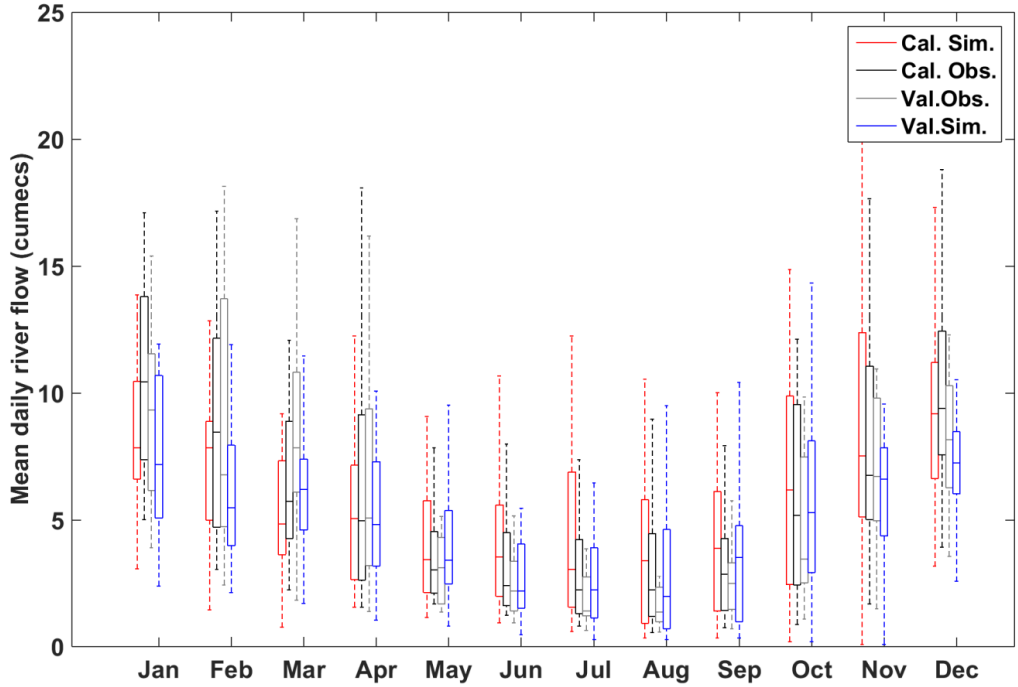

Figure 3. 13 Observed (obs) and simulated (sim) monthly river flow boxplots during the calibration (cal) and validation (val) periods for the Coquet catchment

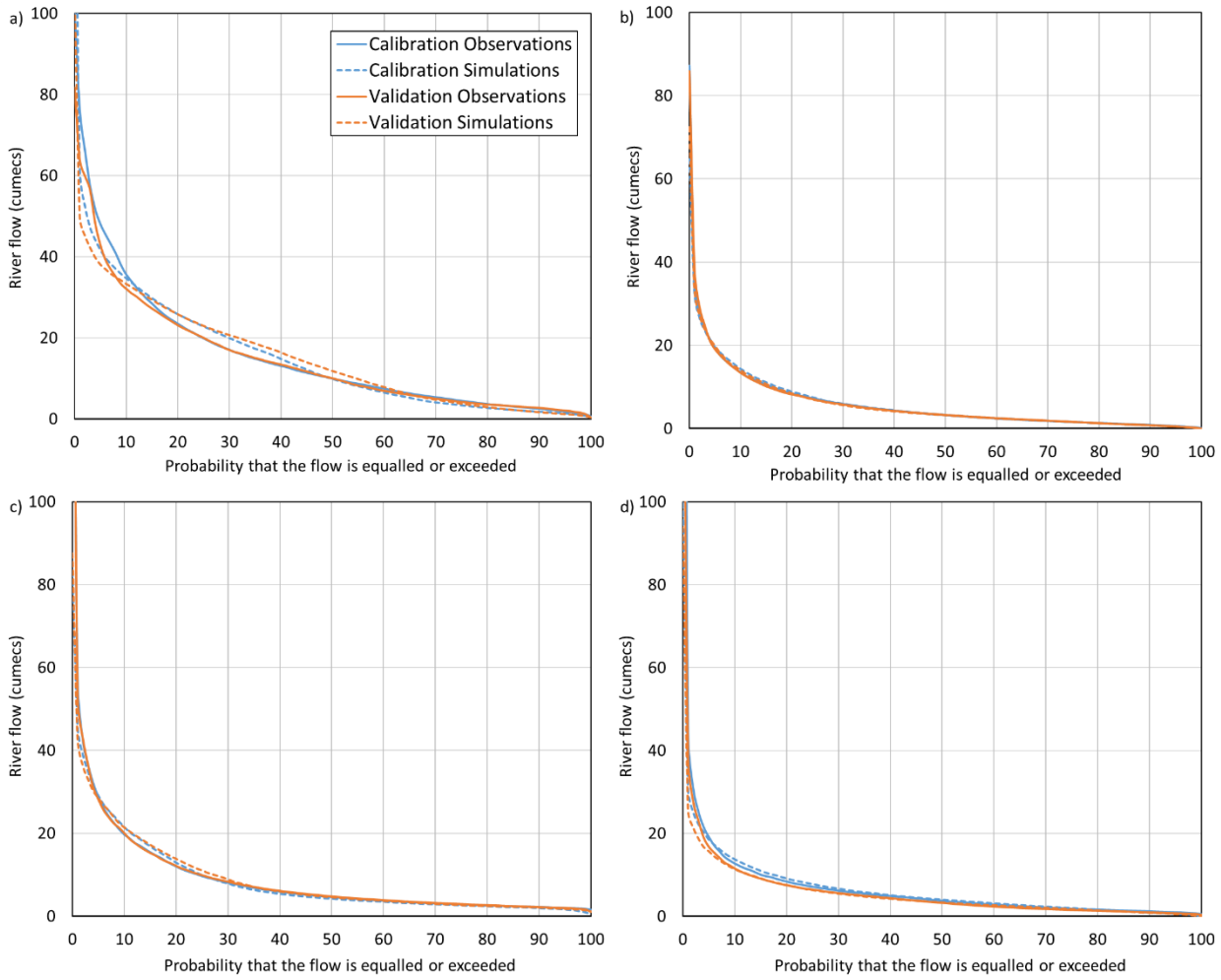

Figure 3.14 Simulated and observed flow duration curves during the calibration and validation periods for a) Upper Thames, b) Glaslyn, c) Calder and d) Coquet catchments

Except for the upper Thames catchment, the models reproduce each catchment's FDC accurately (Fig. 3.14). In the upper Thames, the model simulates the FDC accurately from approximately Q45 to Q100. Nevertheless, it has problems simulating the higher end of the river flows except between the Q10 and the Q15 where the model simulates the observed values accurately. The model from the Glaslyn catchment accurately simulates the entire FDC. For the Calder catchment, the model slightly overestimates the FDC between Q5 and Q20 but accurately simulates the rest of the FDC. Finally, for the Coquet catchment the model only underestimates the very high flows, above Q5.

The models' ability to reproduce the monthly frequency of high flows is evaluated by plotting the average number of days in a month that the catchment's Q10 is exceeded (Fig. 3.15). Compared to the observations, the models simulate more days exceeding the Q10 from June to October for the upper Thames, in March and from July to November for the Calder and from June to December for the Coquet catchment. In contrast, compared to the observations, the models simulate fewer days exceeding the Q10 from January to April and in December for the upper Thames and in January for the Coquet catchment. In the Glaslyn catchment

the model performs accurately for all months. For all catchments, the difference between the observed and simulated annual mean number of days in a month exceeding the Q10 is not larger than one day.

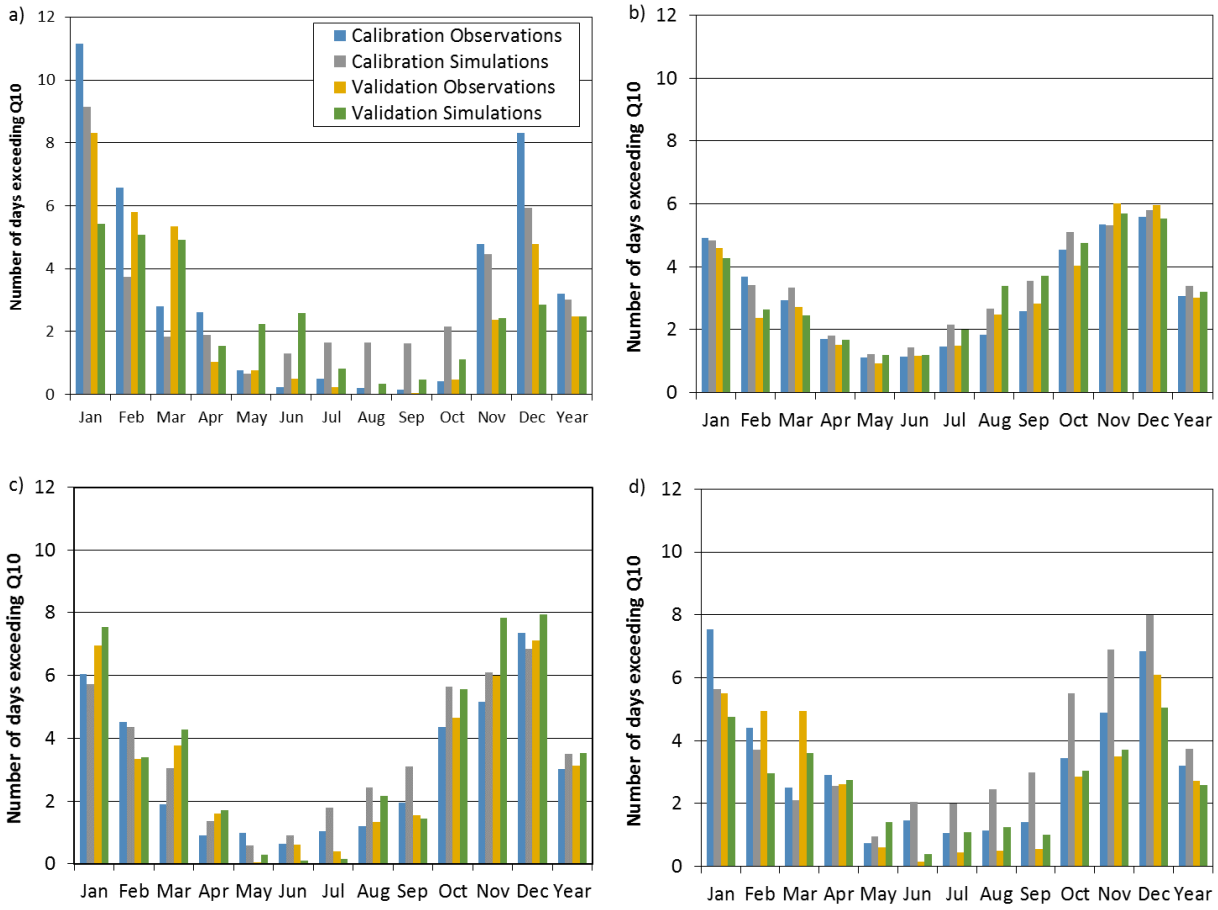

Figure 3. 15 Average number of days within the month when the Q10 of the catchment is exceeded during the calibration and validation periods for a) Upper Thames, b) Glaslyn, c) Calder and d) Coquet catchments

Additionally, the models' ability to reproduce the monthly frequency of low flows is evaluated by plotting the average number of days in a month when the river flow is below the catchment's Q95 (Fig. 3.16). For all catchments, the simulated monthly frequency of low flows is larger than the observations for most months. This can be an effect of the hydrological model inability to describe the seasonality of low flows. In other words, days below the Q95 generally occur during summer and autumn and are less frequent or non-existent during the other seasons. The simulation is not able to reproduce this seasonality. The overestimation from the annual monthly frequency is 2 days for the upper Thames, 0.1 days for the Glaslyn, 1.2 days for the Calder and 1.3 days for the Coquet.

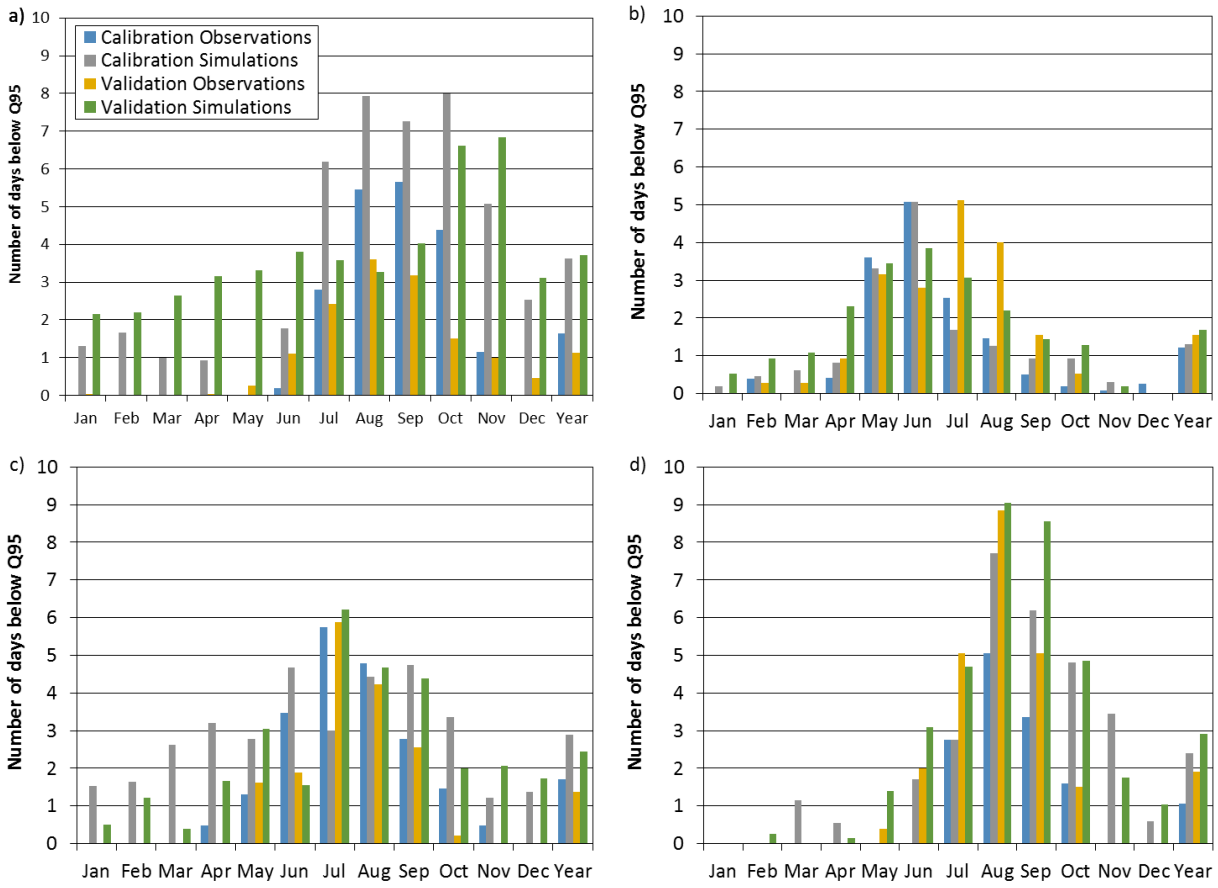

Figure 3. 16 Average number of days within the month when the river flow is below the Q95 of the catchment during the calibration and validation periods for a) Upper Thames, b) Glaslyn, c) Calder and d) Coquet catchments

Visual inspection shows that the simulation biases increase as the observed river flow increases in all seasons (Fig. 3.17). For all catchments, the magnitude of the biases is larger during winter and normally smaller during summer but few cases where the biases are large in such season are observed. The largest biases are observed in the Calder catchment. Furthermore, there is an apparent underestimation of winter and spring river flow in the upper Thames catchment. For all the catchments and seasons, the largest observed flows are underestimated in general.

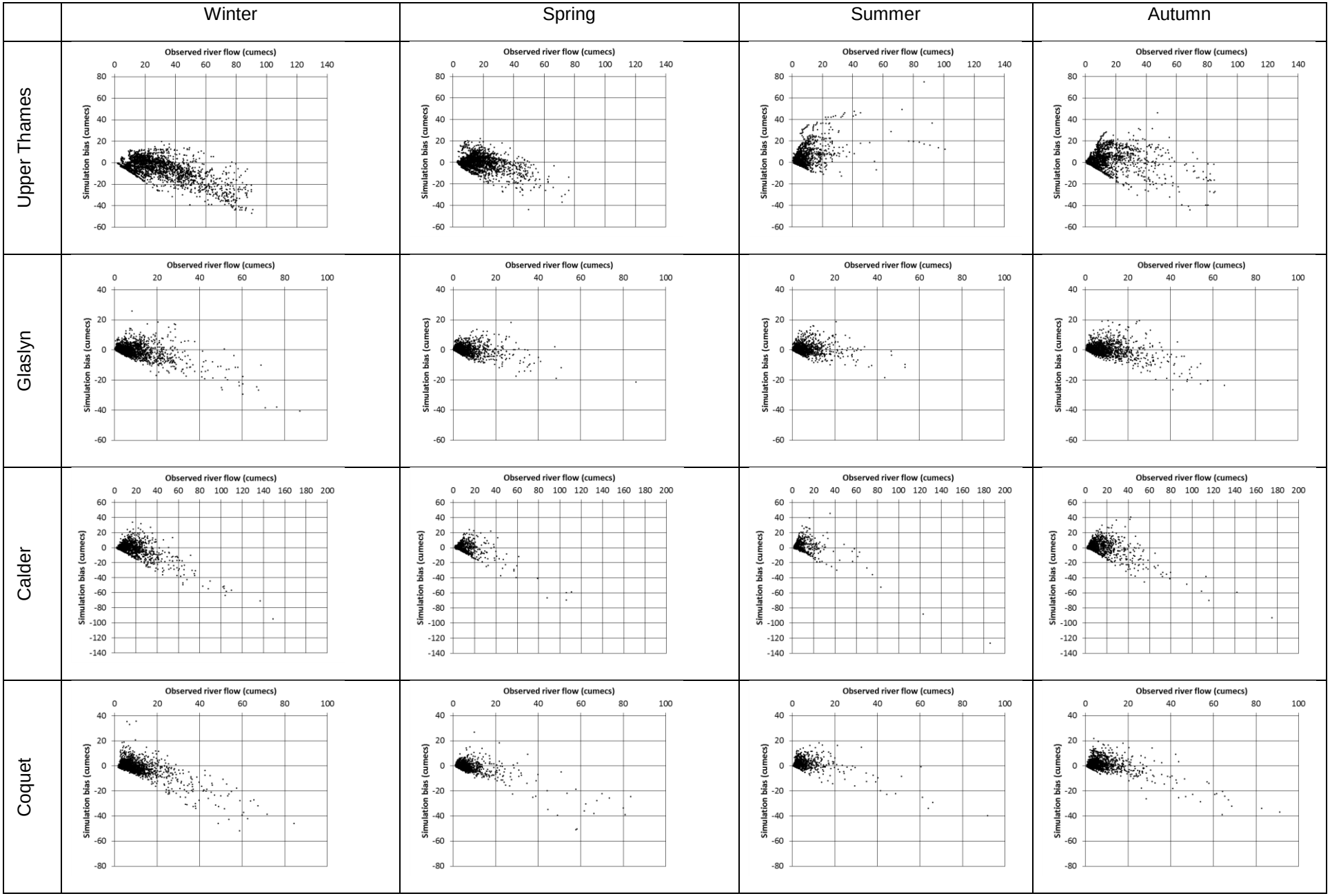

Figure 3. 17 Daily simulation biases vs. observed river flow per season for the four catchments during the calibration

Considering the normalized daily time step indices, the Glaslyn model outperforms the models from the other catchments and the upper Thames is the model with the lowest skill. The MAE and RMSE are larger for the upper Thames and Calder catchments than for the Glaslyn and Coquet (see Table 3.10). The residual volume indicates that the models tend to underestimate the total river flow for all catchments except for the Glaslyn catchment. For this index, the upper Thames has the largest error followed by the Calder, Coquet and Glaslyn catchments, in that order. Nevertheless, for the prior indices larger errors from the upper Thames and Calder are expected as the mean river flow from these catchments is larger than the river flow from the other catchments and therefore prone to larger errors. In contrast, the RSR and NSE indices include a normalization parameter. The NSE values for all catchments are above 0.6 and the RSR values below 0.6 except for the upper Thames where the RSR is 1. According to the NSE results, the model from the Glaslyn catchment has the best skill followed by the upper Thames, Coquet and Calder catchments, in that order. In contrast, the RSR shows that the differences between simulations and observations are smaller for the Glaslyn catchment and larger for the upper Thames, with the Calder and Coquet catchments' error in-between. Considering the monthly time step results, the MAE, RMSE, and RV indices show that the smallest simulation errors are from the Glaslyn catchment and the largest from the upper Thames (See Table 3.10). For the Coquet and Calder catchments the indices denote errors of similar magnitude. Based on the Moriasi et al. (2007) criterion, the NSE results imply a very good skill of the models from the Glaslyn, Calder and Coquet catchments, and a good performance for the model from the upper Thames. The RSR results indicate a very good skill of the models in all the catchments.

Table 3. 10 Performance indices for the calibration and validation periods in a daily time step

	Upper Thames					Glaslyn					Calder					Coquet				
	MAE	NSE	RV	RMSE	RSR	MAE	NSE	RV	RMSE	RSR	MAE	NSE	RV	RMSE	RSR	MAE	NSE	RV	RMSE	RSR
Calibration	5.4	0.70	-4407	8.5	1.0	2.0	0.78	218	3.4	0.5	3.5	0.61	-2255	7.2	0.6	2.6	0.63	-612	5.6	0.6
Validation	6.0	0.58	3661	9.0	0.6	2.2	0.75	-974	3.6	0.5	3.4	0.60	-937	6.8	0.6	2.5	0.54	-3577	5.6	0.7

Table 3. 11 Performance indices for the calibration and validation periods in a monthly time step. For the normalized indices, green denotes a very good simulation, blue denotes good skill, orange satisfactory skill and red no skill

	Upper Thames					Glaslyn					Calder					Coquet				
	MAE	NSE	RV	RMSE	RSR	MAE	NSE	RV	RMSE	RSR	MAE	NSE	RV	RMSE	RSR	MAE	NSE	RV	RMSE	RSR
Calibration	4.6	0.74	-153	6.9	0.5	0.9	0.86	7	1.2	0.4	1.5	0.89	-75	2.0	0.3	1.6	0.77	-21	2.2	0.5
Validation	5.1	0.63	115	7.1	0.6	1.1	0.79	-32	1.5	0.5	1.3	0.90	-32	1.8	0.3	1.6	0.71	-120	2.4	0.5

3.6. Model validation

During validation, the calibrated hydrological models are evaluated outside the period in which it was calibrated. It is expected that the calibrated model suitably simulates the observed river flow from periods outside the calibration period, but its skill is also expected to decrease during validation (Sorooshian and Gupta, 1995). This section shows the results from each catchment's validation period.

The observed versus simulated daily river flow plots show a good performance from the models. The plots from all catchments follow the 1:1 curve (Fig. 3.18). When comparing among the catchments, the Glaslyn and Calder models reproduce the observations more accurately than the upper Thames and Coquet catchments. For the upper Thames and Coquet there are several cases when the simulation bias is large and the points are plotted from the 1:1 curve. When plotting the simulated versus observed monthly river

flow values, the graph from all catchments clearly follows the 1:1 curve (Fig. 3.19). For the Coquet catchment, some of the large observed values plot distant from the 1:1.

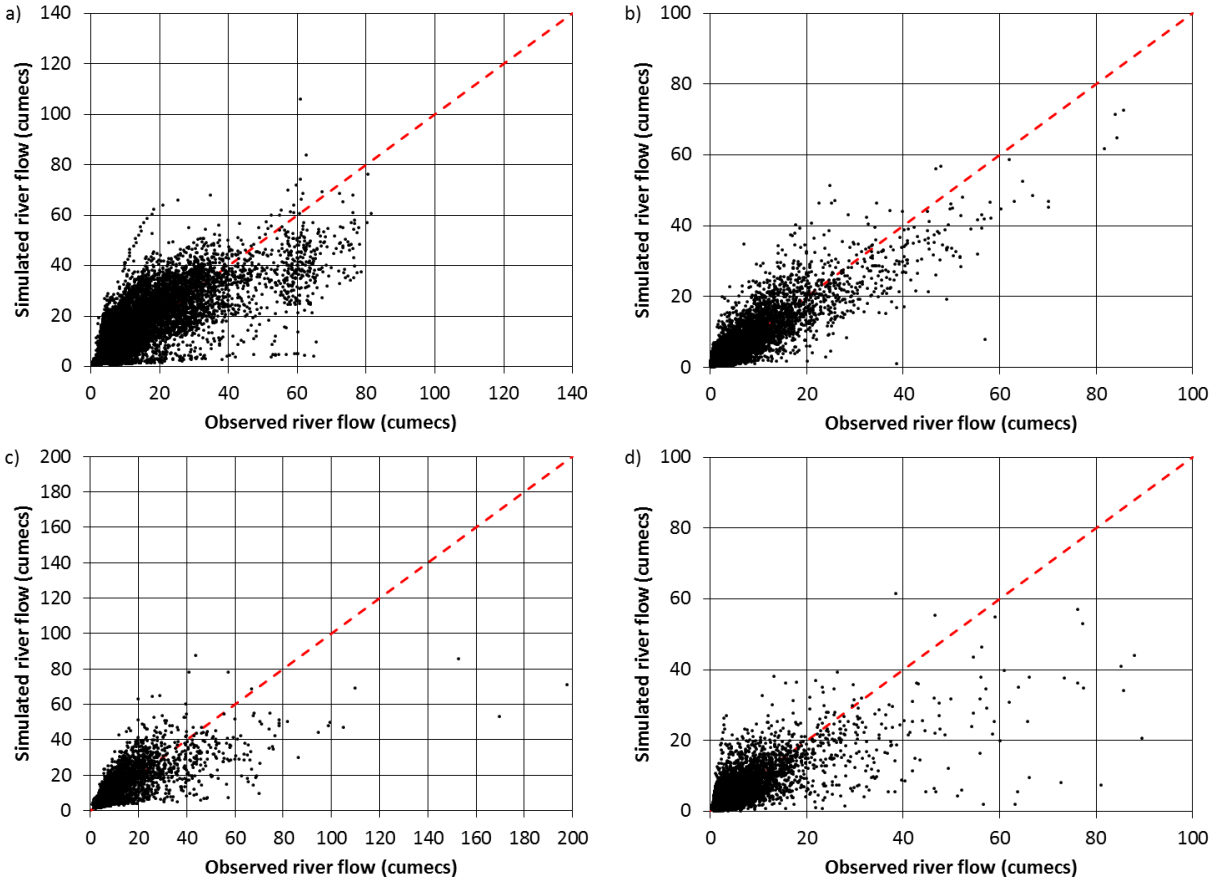

Figure 3. 18 Daily observed vs. simulated river flow during the validation periods for a) Upper Thames, b) Glaslyn, c) Calder, and d) Coquet catchments. The red dotted line represents the 1:1 curve

The models simulate the observed river regime curve accurately during the validation period (Fig. 3.9). Nevertheless, compared to the calibration, the overall error for all catchments increased except for the Calder catchment. The monthly mean absolute error is 34% for the upper Thames, 6% for the Glaslyn, 8% for the Calder and 21% for the Coquet catchment. The largest differences between the simulations and observations for each catchment are in July for the upper Thames (84% error) and Coquet (33% error), and August for the Glaslyn (13% error) and Calder (19% error).

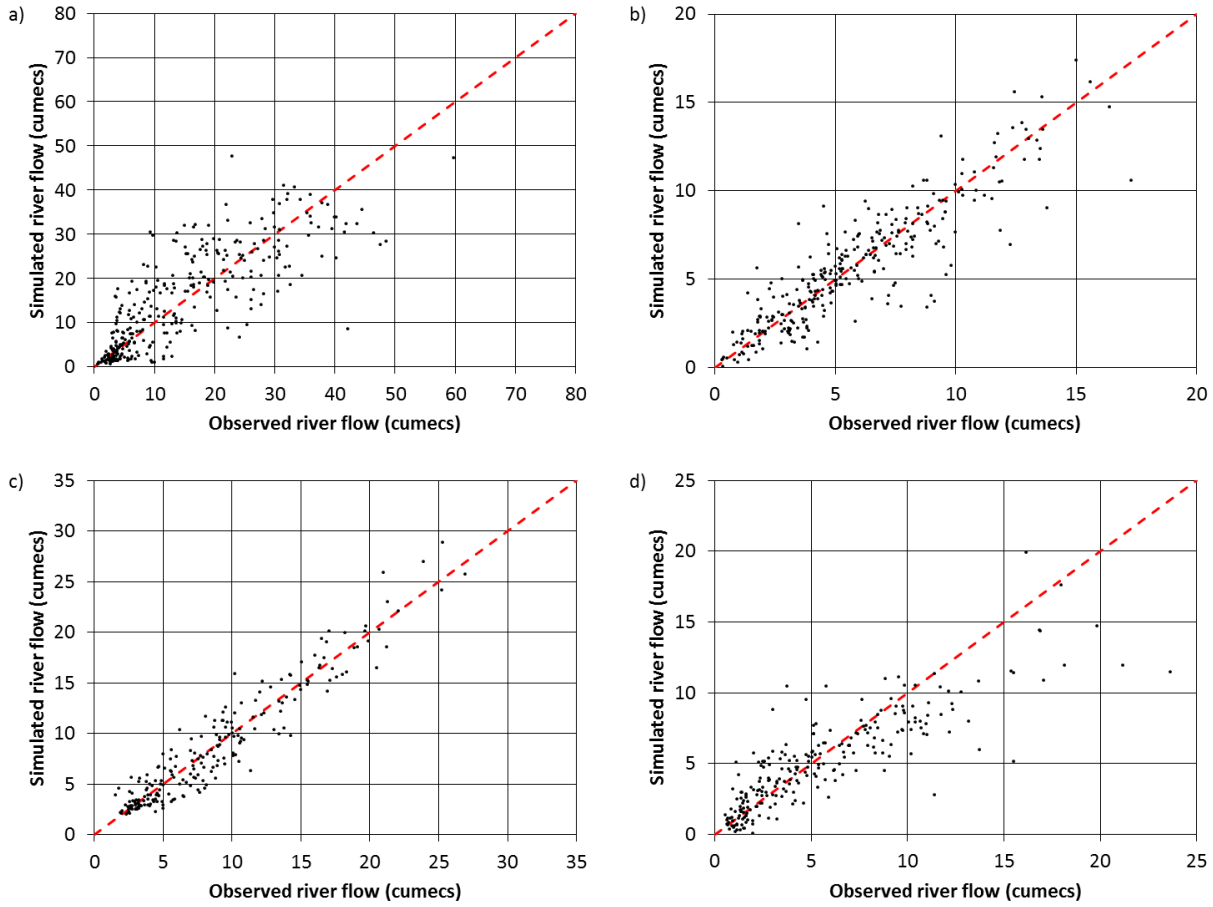

Figure 3. 19 Monthly mean observed vs. simulated river flow during the validation periods for a) Upper Thames, b) Glaslyn, c) Calder, and d) Coquet catchments. The red dotted line represents the 1:1 curve

Overall, the models simulate the observed river flow variability adequately, except for the upper Thames catchment during summer and for the Coquet catchment during winter. The model for the upper Thames catchment reproduces the river flow accurately except from May to October when the model variability is larger than the observed variability. This is stressed during the summer months (Fig. 3.10). For the Glaslyn catchment, there are no major differences between the observed and simulated river flow variability (Fig. 3.11). The main differences occur during August, when the simulated variability is larger, and November, when the observed variability is larger. In the Calder catchment the main differences are from June to August when the simulated variability is larger (Fig. 3.12). Nevertheless, differences in the observations' variability between the calibration and the validation periods are also evident for June and July. Differences between the observed and simulated variability are present in February, May, July, August, November and December for the Coquet catchment (Fig. 3.13). However, changes between the observed variability from the calibration and validation periods are also noticeable during July, August, November and December.

The skill of the models to simulate the FDC from each catchment during the validation is similar to their skill during the calibration period (Fig. 3.14). As in the calibration period, during the validation the upper Thames

catchment model overestimates the observations from the Q10 to Q60 and underestimates the high flows above the Q5. For the Glaslyn catchment, the model simulates the complete FDC accurately. The Calder catchment model slightly overestimates the river flows from Q5 to Q30. Finally, the simulated FDC from the Coquet catchment overestimates the extremely high river flow observations (above the Q5).

During the validation period, the models kept their ability to simulate the frequency of monthly days when the Q10 is exceeded (Fig. 3.15). The models underestimate the frequency of days exceeding the Q10 in December, January, February and March for the upper Thames, in June for the Calder and in January, February, March and December for the Coquet catchment. In contrast, the models overestimate the frequency of days exceeding the Q10 from April to August for the upper Thames, from July to October for the Glaslyn, in January, August, October, November and December for the Calder and in May, July and August for the Coquet catchment. The difference between the observed and simulated annual mean number of days in a month exceeding the Q10 is not more than one day in all of the catchments.

In general, the models' skill to simulate the monthly number of days when the river flow is below the Q95 remains similar during the validation and calibration periods for the Glaslyn and Calder catchments, whereas it deteriorates for the upper Thames and improves for the Coquet (Fig. 3.16). The models overestimate the number of days when the river flow is below the Q95 for all months except August in the upper Thames, during April and June for the Glaslyn, during February, April, May and from September to December for the Calder and during May, June and from September to December for the Coquet catchment. The annual mean monthly days when river flow is below the Q95 is overestimated by 2.6 days for the upper Thames, 0.1 days for the Glaslyn, by 1.1 day for the Calder and by 1 day for the Coquet catchment.

Most daily time step indices show a slight decrease in the hydrological models' skill during validation (see Table 3.10). For the upper Thames catchment, the MAE, NSE and RMSE show a decrease in the model performance. Similarly, for the Glaslyn catchment the MAE, NSE, RV and RMSE indicate a decrease in the model's skill and for the Coquet catchment the NSE, RV and RSR also imply a reduction in the skill of the model. In contrast, for the Calder catchment only the NSE denotes a slight deterioration in the skill of the model. Several monthly time step indices have the same values as in the calibration period (see Table 3.10). Only the RV for the upper Thames and all metrics for the Calder catchment show an improvement of the hydrological model during validation. Based on the criterion from Moriasi et al. (2007) the NSE values imply a very good performance for the Glaslyn and Calder catchments and a good performance for the upper Thames and Coquet catchments. Additionally, using the same criterion, the RSR values denote a very good skill from the model for the Glaslyn, Calder and Coquet catchments and a good skill for the upper Thames catchment model.

In general, for all catchments, larger and more frequent seasonal simulation biases are observed during winter (Fig. 3.20). Nevertheless, for the upper Thames and Coquet catchments, spring simulation biases are also large, but not as frequent as during winter. During summer and autumn, the simulation biases are smaller compared to the other seasons.

3.7. Model skill comparison with other studies in the UK

There is an extensive literature regarding the application of hydrological analyses within the UK. The use of hydrological models to assess the water resources situation from different catchments within Britain has increased in the last decades along with the need to evaluate the impacts of climate change. A comprehensive summary of the studies using hydrological models within the UK is shown in Table 3.11. The table shows the wide range of hydrological models that have been used to simulate catchment-scale river flow within the UK, ranging from lumped, semi-distributed and fully distributed models. There are examples of huge efforts from research groups that have generated hydrological models for a considerably large number of catchments (e.g. Christierson et al., 2012 and Crooks et al., 2009). The Thames catchment is frequently analysed in different studies (e.g. Bell et al., 2012; Walsh et al., 2016; Wilby, 2005) because of its importance for the city of London. All the studies use the NSE as common evaluation index for the skill of the hydrological model. This index is normally estimated in a daily time step, but there are cases where the sub-daily (e.g. Bell et al., 2012; Crooks et al., 2009) or monthly (e.g. Diaz-Nieto and Wilby, 2005) NSE are used as evaluation metrics based on the study requirements and data availability. There is no standard minimum NSE threshold to accept a model and in practice the acceptance threshold varies for each study. Wilby (2005) only selected a set of Monte Carlo simulations with daily NSE values above 0.8 whereas Christierson et al. (2012) accepted models with the daily NSE higher than 0.5 from a set of hydrological models from 70 catchments and Crooks et al. (2009) accepted models exceeding 0.6 for a daily time step NSE and 0.8 for a monthly time step NSE. Furthermore, as discussed in section 3.4.1.5, Moriasi et al. (2007) suggested that a model is satisfactory if the monthly NSE is above 0.5.

The models from this study satisfy most of the criteria that was used in previous studies. Therefore, the model's skill can be defined as moderate or good. Crooks et al. (2009) developed 120 lumped models using the PDM model for different catchments in the UK. Then, they divided the UK in regions and the NSE from the catchments located within such region were averaged to provide a region mean skill. The upper Thames catchment is in a region with a mean NSE of 0.52. Likewise, the Glaslyn and Calder catchments are in a region with mean NSE of 0.66 and in the Coquet catchment region the mean NSE is 0.52. Additionally, Bell et al. (2012) provided the mean NSE values for human-influenced and natural catchments within the Thames catchment. For the disturbed catchments, such as the Eynsham catchment, the NSE value ranged from 0.55 during the calibration and 0.33 during validation. Given the NSE values found in literature, the skill from the hydrological models developed in this research can be categorized as good and reliable when generating river flow simulations.

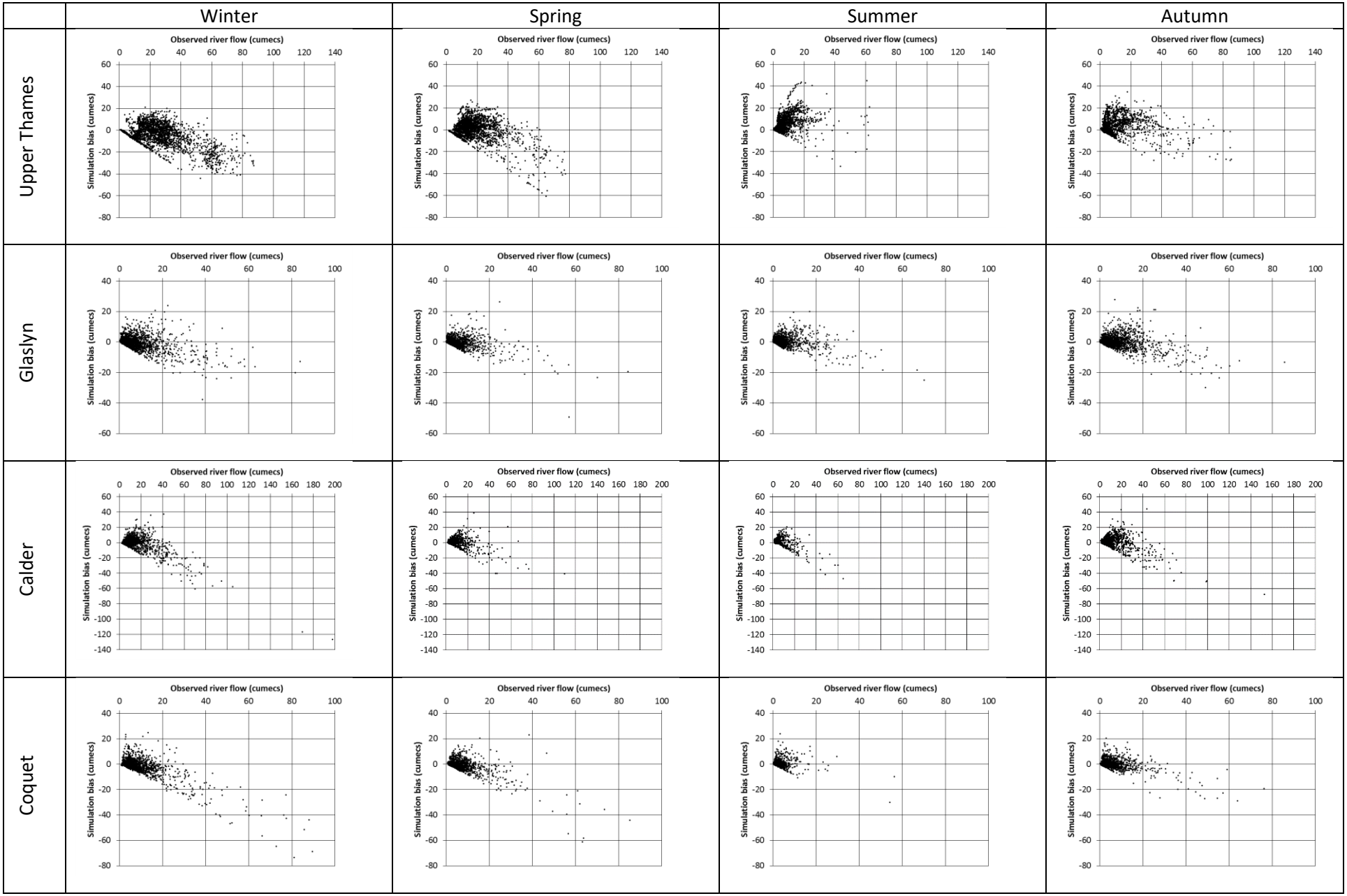

Figure 3. 20 Daily simulation biases vs. observed river flow per season for the four catchments during the validation

Table 3. 12 Performance indices from other hydrological models used in the UK

Reference	Catchment and/or Gauge(s)	Model	Period		NSE	
			Calibration	Validation	Calibration	Validation
Walsh et al. (2016)	Thames catchment	CATCHMOD (lumped)				
	@ Teddington Weir		1961-1978	1979-2002	0.88	0.86
	@ Feildes Weir		1961-1975	1979-2002	0.68	0.69
	@ Days Weir		1961-1978	1979-2002	0.86	0.9
Carless and Whitehead (2013)	Plynlimon flume	IHACRES	1986-2009		0.79	
Chistierson et al. (2012)	70 locations in the UK	PDM-Lumped CATCHMOD (semi-distributed)	Varies		selected only > 0.5	
Bell et al. (2012)	34 locations in the Thames	Grid to Grid (distributed)	Done on a 15-min time step		Free from anthropogenic incluences	
			01Jan1999 - 18Jun2001	01Jan1997-18Jun1999	0.5-0.84 (mean 0.77)	0.4-0.77 (mean 0.75)
					Disturbed	
					- to 0.85 (mean 0.55)	- to 0.84 (mean 0.33)
Prudhomme and Davies (2009)	South Tyme @ Haydon Bridge	Mod A (Lumped)	1980-1990	Varies from 25 to 17 yrs	0.7	0.64
	Thet @ Melford Bridge				0.63	0.76
	Medway @ Chaffor Weir				0.62	0.65
	Ithon @ Dissert				0.82	0.76
Prudhomme and Davies (2009)	South Tyme @ Haydon Bridge	Mod B (Lumped)	1980-1990	Varies from 25 to 17 yrs	0.7	0.67
	Thet @ Melford Bridge				0.7	0.77
	Medway @ Chaffor Weir				0.63	0.61
	Ithon @ Dissert				0.79	0.78
Diaz-Nieto and Wilby (2005)	Thames @ Kingston	CATCHMOD (lumped)	1961-1990		0.96 (Monthy)	
Crooks et al. (2009)	120 catchments in the UK	PDM (Lumped)	Varies		0.63 (average)	
Crooks et al. (2009)	35 catchments in the UK	CLASSIC (semi-distributed)	Varies		0.82 (average)	
Ledbetter et al. (2012)	Eden catchment	PDM (Lumped)	1967-2001		0.66 (Daily) 0.96 (Monthly)	
Arnell (2011)	6 catchments	CatPDM (Lumped)	1980-1983	1983-1989	Range from 0.44 to 0.82	Range from 0.45 to 0.75
Wilby et al. (2006)	River Kennet @ Knighton	CATCHMOD (lumped)	1961-1990		0.86	
	River Kennet @ Theale				0.78	
Cloke et al. (2013)	Upper Severn	HBV-Light	1986-2006		0.9	
Wetterhall et al. (2012)	Upper Severn	HBV (lumped)	1986-2006		> 0.85	
Crookes et al., (2014)	41 catchments in th eUK	CLASSIC-GB	1991-2000		wide range based on spatial resolution and catchment; most results above 0.6	

3.8. Summary and discussion

This chapter shows the methodology used for selecting the hydrological model, constructing the model for the different catchments, evaluating the models' simulation skill during the calibration and validation periods and finally compares their skill with hydrological models from other studies. Thus, the information shown in this chapter represents an important step towards the fulfilment of the thesis objectives as the hydrological model is an important tool to link the climate with the river flow.

The methodology used in this study is expected to be replicable for other catchments. Therefore, in addition to the model's simulation structure, criteria related to its availability and application simplicity are included in the selection of the model. Based on the comparison with other available models, the HEC-HMS is used in the study. The selection of the model is based on its availability as open source (free) software that could be easily used elsewhere. In addition, the parameters/data required by the model are not very complex to obtain or estimate. This is important for the reproducibility of the method developed in this study for data-scarce regions. Furthermore, a detailed user's manual focusing on technical aspects related to the estimation of the required parameters is available. This represents an important tool in order to be consistent with the model's background theory that was used and followed by its developers. Finally, the extent of a RCM cell (12 x 12 km) covers the entire Glaslyn catchment (69 km^2). As a consequence, the use of a semi-distributed or distributed model would not be advantageous. Thus, to be consistent, a lumped model is used to simulate the river flow in all catchments and the HEC-HMS model has the option to perform lumped simulations. It is acknowledged that for the larger size catchments, a semi-distributed or distributed model could be advantageous. However, the models developed in this research have been found to have similar simulation skill compared to semi-distributed or distributed models generated for similar catchments in other studies (Table 3.12).

Different hydrological models might use contrasting approaches, formulae and parameterizations to relate the climate, physics and river flow of a catchment. Thus, the simulation from different models can provide a diverse range of results (Dankers et al., 2014). Here, only one hydrological model is used. Therefore, the uncertainty from the hydrological model is not considered in this study. This is important as it has been demonstrated that the hydrological model uncertainty can be as large as the GCM uncertainty (Prudhomme et al., 2014). Nevertheless, for each catchment, the hydrological model developed here is expected to provide reliable projections to evaluate the impacts of climate change as the simulation skill is good (sections 3.5 and 3.6).

Model limitations and uncertainty sources must be acknowledged. Initially, the parameters from the hydrological models generated in this analysis remain unchanged throughout the entire simulation. Therefore, models do not simulate any seasonal variation in the hydrological parameters as all months are simulated using the same parameters. This represents a limitation as the interactions between the surface and subsurface processes vary for each season and even for each precipitation event (Shaw et al., 2010). Specific parameters that remain unchanged and restrain the models' simulation skill have also been

identified in previous studies using different hydrological models. These parameters include changes in land use (Crooks et al., 2009; Walsh et al., 2016), soil properties (Crooks et al., 2009) and impervious areas (Walsh et al., 2016). Additionally, the natural river flow can be altered by human influences, such as agricultural management, urbanization and river management, among others (Shaw et al., 2010). These human alterations are too complex to be included in the hydrological models and increase the simulation complexity. Here, only changes due to climate change are included in the simulation.

Furthermore, the estimation of the parameters required by hydrological models can be problematic (Pappenberger and Beven, 2006). Important limitations relate to the model uncertainty derived from the lack of local measurements of required parameters, which are then obtained from global estimates. Clark et al. (2016, pg. 60) have summarized this deficiency by stating that "we do not even know the saturated hydraulic conductivity of the soil to within an order of magnitude, much less the vertical rooting profiles, soil thickness, interception capacity, and so forth. While we can estimate these parameters globally, they are very crude estimates…". In support of the previous statement, this study encountered that the soil thickness from the upper Thames catchment has not been measured for most of the catchment (section 3.3.1.5.3). This is not a minor issue as the Thames catchment is one of the most studied catchments in the world (e.g. Walsh et al., 2016; Bell et al., 2012; Diaz-Nieto and Wilby, 2005; Wilby and Harris, 2006). Therefore, it is evident that these research gaps negatively impact on the accurate simulation of the hydrological processes. Nevertheless, with the model's conceptualization of the hydrological processes and the available data, skilful simulations of river flow are generated for each catchment in this study.

It is shown that the model evaluation process is in part subjective. This might be a consequence of the fact that there is no standard protocol to test the hydrological model skill (Hrachowitz et al., 2013). The NSE is commonly used to assess the simulation skill from the hydrological models (e.g. Walsh et al., 2016; Carless and Whitehead, 2013; Crooks et al., 2009; Prudhomme and Davies, 2009). Nevertheless, as shown in section 3.7, different studies use different NSE thresholds to define if a model has an acceptable simulation skill. Here, other evaluation statistics are used to assess the models' skill to simulate the river flow characteristics that are relevant for the study. These evaluation statistics include the ratio of the RMSE to the observations standard deviation, volume residual, mean absolute error and root mean square error. The simulation skill from the models developed in this study ranges from good (upper Thames catchment) to very good (Glaslyn, Calder and Coquet catchments) (sections 3.5 and 3.6). These results support the reliability of the subsequent analysis. Nevertheless, following the issues mentioned at the beginning of this paragraph, it is highlighted that an international protocol to assess the skill of hydrological models is a research gap that, if fulfilled, could benefit the hydrological community by decreasing the hydrological modelling uncertainty and allowing a fair comparison between model simulations. Satisfying this gap is out of the reach of the current study. Furthermore, it is acknowledged that this might be an intensive and complex task as it would require the development of a protocol considering global catchment characteristics (e.g. applicable in artic, wet, arid or semi-arid catchments) and also possible limitations due to the

availability of river flow observations. However, the set of performance measures and graphs used here can be a component of the protocol along with other complementary measures (e.g. metrics related to the FDC shown in Crooks et al. (2014) and Kay et al. (2015)).

It is necessary to highlight that the hydrological model from the upper Thames catchment underperforms compared to the models from the other catchments. There are some factors that could influence the accuracy of the model from this specific catchment. For instance, due to its importance as a water source for the city of London, management policies to mitigate the impacts of droughts and floods have modified the catchment's natural river flow through history (Bell et al., 2012). Also, when using lumped models, area averaged data (such as the catchment's mean precipitation or PET) contributes to the modelling uncertainty (Diaz-Nieto and Wilby, 2005), particularly for large catchments where some precipitation events might occur only in one region of the catchment with low contribution to the river flow generation, but impact on the precipitation area average estimation. Wet day thresholds have been previously used to remove the effect of small precipitation amounts (e.g. Diaz-Nieto and Wilby, 2005), but this was not used in this research to keep consistency between the catchments. Finally, distributed or semi-distributed models could have better skill than lumped models when simulating large-area catchments with non-natural river flows, as lumped models use area-average inputs. Some research projects have used lumped models for small to moderate size catchments and semi-distributed models for larger catchments (e.g. Crooks et al., 2009) with good results. Nevertheless, here a lumped model is used in all catchments for consistency and because this methodology is expected to be replicable in other regions where the input data for a semi-distributed model might not be available (e.g. exact location of abstractions and discharges along the river, distributed parameter values, among others).

It is important to understand that the results from hydrological models will carry the uncertainty from the input data along with uncertainties related to the representation of the physical hydrological processes (Shaw et al., 2010). Nevertheless, even if not perfect, reliable models have proven to be useful for the analysis of future strategies and climate change impacts (e.g. Prudhomme and Davies, 2009; Christierson et al., 2012). Therefore, based on their evaluation, the models developed in this study are expected to be a useful tool to assess the impacts of climate change, shown in the following chapters.

4. Evaluation of the regional climate models and downscaling/bias correction methods

4.1. Introduction

This chapter summarizes the methodology used to evaluate the performance of the Regional Climate Models (RCMs). The main objective of the thesis is to assess the climate change impacts on hydropower generation. In order to do so, climate projections from RCMs are used as drivers of the hydrological models developed in chapter 3. However, prior to the analysis of future projections, a preliminary step evaluates the simulation skill of the RCMs. Furthermore, RCMs are commonly biased, there is a need to bias correct them before their application in the assessment of impacts (Christensen et al., 2008). Also, higher-resolution RCMs might have an added value over the lower-resolution RCMs for the simulation of the climate variables (Di Luca et al., 2015). Therefore, the simulation skill evaluation shown in this chapter also includes the outputs from RCMs at two different simulation resolutions as well as their bias-corrected simulation at both resolutions, addressing the research question **i) Is the relative performance of the 0.11° Euro-CORDEX RCMs better than their 0.44° version to simulate climate and river flow?** Furthermore, as the simulated river flow driven by the RCM climate outputs is also evaluated, the second research question is also addressed in this chapter: **ii) Is the current skill of the Euro-CORDEX RCMs able to generate useful inputs for the analysis of climate change impacts on hydrology?** Useful input means river flow projections with biases small enough to be used by the planners and end users. This question is analysed both for the uncorrected and bias-corrected simulations.

The chapter begins by describing the evaluation approach, including the analysed RCMs and bias correction methods. Also, the formulae employed to estimate the potential evapotranspiration (PET) are shown along with the process followed to simulate the study catchments' river flow. Subsequently, the observation datasets, cross-validation methodology and performance measures are explained. The results section shows an analysis of the PET estimations compared to the observations, a sensitivity analysis regarding the selection of RCM grid boxes for the simulation of catchment processes, bias correction results and the temperature, precipitation and river flow metrics.

The evaluation of the climate model simulation skill, i.e. comparison of model outputs with observations, is important for the development of the models (Kotlarsky et al., 2014). Additionally, the evaluation of the models provides information about the accuracy of their outputs considering the simulated variable, location and the application for which they will be used (Maraun et al., 2015). The evaluation is also important because the simulation skill of the climate models and downscaling methods might be location dependent (Chen et al., 2013). Therefore, the evaluation serves two main purposes: 1) provide feedback about model performance, and 2) test of the model performance for their application in impact analyses.

Climate model evaluation is generally performed by testing the skill of a particular model to simulate the recent past. Therefore, statistics from the model simulations are compared with observed statistics and the simulation skill is quantified as the distance between both statistics (Di Luca et al., 2015). Analysing the climate's whole range of aspects is not possible; hence a selection of the characteristics of interest is used

for evaluation (Maraun et al., 2015). Consequently, the evaluation employs performance measures that are relevant for the analysis or application of interest (Di Luca et al., 2015).

4.2. Evaluation approach

In this research, for each catchment the evaluation focuses in the Euro-CORDEX RCM's precipitation and temperature outputs at their two available resolutions: 0.11° and 0.44°. The outputs are bias corrected using statistical methods. Both the uncorrected and bias-corrected (explained in section 4.2.2) outputs are compared with temperature and precipitation observations using a set of performance measures (section 4.2.7). Temperature is also used to estimate the PET (explained in section 4.2.3). Subsequently, the estimated potential evapotranspiration and precipitation time series are used to drive the HEC-HMs hydrological model to estimate the river flow. Afterwards, the simulated river flow is compared with the observations through a set of performance measures. The process is schematically summarized in Figure 4.1.

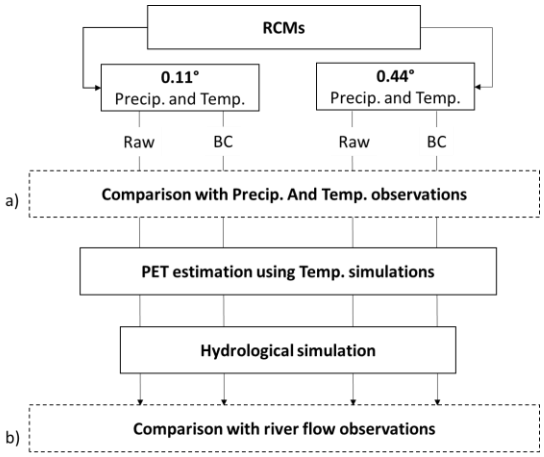

Figure 4. 1 Evaluation approach scheme: a) temperature and precipitation evaluation, b) river flow evaluation

4.2.1.Regional Climate Models (RCMs)

In this chapter, different RCMs are assessed as their simulation skill might vary depending on the season or region (Maraun et al., 2010). Furthermore, using several RCMs is beneficial for obtaining robust results. This study tests five state-of-the-art RCMs from the Euro-CORDEX project (Giorgi et al., 2009; Jacob et al., 2014). For their evaluation, RCMs simulations are driven by the ERA-Interim observation reanalysis (Dee et al., 2011) as lateral boundary conditions. The use of the reanalysis data as boundary conditions is the standard procedure for RCM validation as it reflects the regional climate observed variability avoiding biases caused by GCM large-scale forcing (Kotlarski et al., 2014). The five RCMs used in the study are listed in Table 4.1. These RCMs are selected based on their skill to reproduce observations in Britain according to Kotlarski et al. (2014).

Table 4. 1 Information from the RCMs used in this study

RCM	Institute	Reference
CCLM-CLMCOM	Brandenburg University of Technology (BTU)	Böhm et al., 2006; Rockel et al., 2008
HIRHAM 5	Danish Meteorological Institute (DMI)	Christensen et al., 1998
RACMO22E	Royal Netherlands Meteorological Institute (KNMI)	Van Meijgaard et al., 2012
RCA4	Swedish Meteorological and Hydrological Institute (SMHI)	Samuelsson et al., 2011
WRF 3.3.1	Institute Pierre Simon Laplace (IPSL) and Institute National de l'Environment Industriel et des Risques (INERIS)	Skamarock et al., 2008

4.2.1.1. RCM spatial resolution

The Euro-CORDEX project provides RCMs at two spatial resolutions: 0.44° (50km) and 0.11° (12.5km). In this chapter, both resolutions are evaluated for each of the five RCMs that are used. Figure 4.2 shows the location of the study catchments along with the grid boxes from each RCM resolution that are used for the simulation of the catchment. The RCM cells are selected with the aim of fully covering the complete extension of the catchment.

4.2.1.2. Simulation sensitivity to grid box selection

The area covered by the RCM grid boxes is arbitrarily defined without consideration of the natural landscape. Therefore, there is a difference between the catchment's natural boundaries and the area covered by the RCM grid boxes. Given this coverage difference, the selection of the RCM grid boxes used to simulate catchment processes might not be completely straightforward. An issue that has been analysed in previous studies is the skill from different domain sizes containing the area of interest. Eden et al. (2014) compared the simulation performance from domains of 3x3 and 5x5 grid cells centred to precipitation stations. Similarly, Wong et al. (2014) used a 3x3 grid box domain and Maraun and Widmann (2015) employed an 11x11 domain in their analyses. Additionally, the representativeness of the grid box containing the study area might be influenced by the RCM's systematic displacements, resulting in better correlations between the observations and grid cells neighbouring the grid box containing the study area (Maraun and Widmann, 2015). In this study, RCMs grid boxes are selected intending to cover the complete study catchments as shown in Figure 4.2. Nevertheless, an analysis of the correlation between the observations and different RCM grid cells and domains is performed to evaluate the concepts commented above.

4.2.2. Bias correction

Generally, RCM simulations have biases and therefore require bias correction techniques (Christensen et al., 2008). Recent studies have found that the Euro-CORDEX RCMs have biases when simulating local climate even at the 0.11° resolution (Prein et al., 2015; Casanueva et al., 2016; Kotlarsky et al., 2011). Therefore, RCM outputs need post-processing techniques to reduce such biases. A detailed discussion about bias correction is shown in section 1.3. Considering the skill from the different bias correction

techniques (section 1.3.1), in this study the parametric quantile mapping method is used to correct the precipitation and temperature simulations based on the observation's distribution parameters (Piani et al., 2010). A description of the approach and formula followed to bias correct both variables is shown in sections 1.3.2 to 1.3.4. For the double Gamma distribution quantile mapping of precipitation, the precipitation distribution is divided in two at the 90th precipitation percentile as it is systematically observed to be the point where the biases in extremes increase exponentially (See section 4.3.5, Fig. 4.34). Whereas the objective of this thesis is not to produce the perfect bias-correction method, the method with best potential is used here. The grid boxes from the 0.11° RCMs cover almost the same area as the catchment observations. Therefore, for this resolution the method con be considered as pure bias correction. In contrast, for the 0.44° RCMs, in some cases the grid boxes are considerably larger than the catchment and therefore the bias correction method also includes a downscaling attribute.

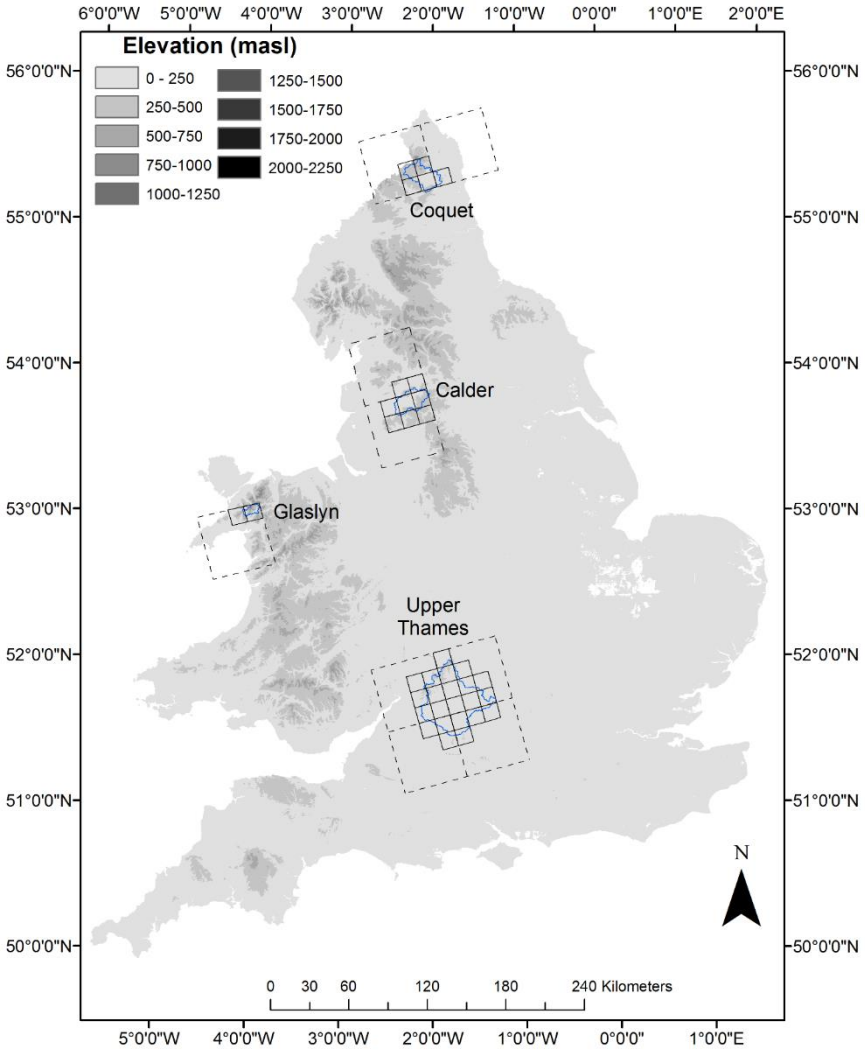

Figure 4. 2 Location of the study catchments and the RCM grid boxes used for their simulation. Grid boxes from the 0.11° RCMs are shown with solid lines and grid boxes from the 0.44° RCMs with dashed lines.

4.2.3.Potential evapotranspiration estimation

The main climatological inputs required by the HEC-HMS hydrological model are daily precipitation and PET. Daily precipitation is a direct RCM output. However, PET is not simulated by all climate models and it is generally estimated using empirical formulae (Rudd and Kay, 2016). Such formulae vary from physically-based formulae, including the primary variables influencing the evaporative process: temperature, radiation, wind speed and atmospheric humidity (e.g. Penman-Monteith) or formulae that are function of one climatic variable (e.g. temperature-based formulae). There is no consensus on which formula represents the best approach to estimate PET in a climate change context (Kay et al., 2013). The importance of using all variables has been advocated and demonstrated previously (McVicar et al., 2012; Donohue et al., 2010; Rudd and Kay, 2016; Clark et al., 2016). However, in a climate change context, the data required by the physically-based formulae are uncertain compared to the input from one variable formulae (Kingston et al., 2009). In previous analyses, physically based PET formulae have been outperformed by temperature-based formulae mainly due to the uncertainty of the extra variables required by the physical formulae (e.g. Kay and Davies, 2008; Oudin et al., 2005). Additionally, during the calibration of the hydrological model its parameters are modified to provide maximum simulation efficiency regardless of the PET formula, but the formula impacts on the future projections (Seiller and Anctil, 2016; Bartholomeu et al., 2015).

Here, considering the above, PET is estimated using two temperature-based formulae: the Oudin (Oudin et al., 2005) and Hamon (Hamon, 1961) equations. These formulae are used because temperature has a large agreement between the climate models (Johnson and Sharma, 2009) and it is "better constrained by climate observations than almost any other variable" (Allen and Ingram, 2002). Furthermore, temperature is commonly bias-corrected in climate change impact studies, aiding in the estimation of bias-corrected PET. PET is estimated using temperature observations as input and compared with the CHESS-PET dataset to assess the skill of each formula. In the following equations, the daylight hours (based on the latitude and day of the year) are symbolized by D and ϕ_T stands for the saturated water vapour density (g/m^3) at the daily mean temperature (T, in °C). The extraterrestrial solar radiation (Re) is the solar radiation received at the top of the Earth's atmosphere which can be estimated by the latitude and day of the year. The density of water is symbolized by ρ and the latent heat flux by λ (2.45 MJ/kg) (Allen et al., 1998).

Hamon (Hamon, 1961, as reported in Xu and Singh, 2001)

$$PET\ (mm\ day^{-1}) = (0.55D^2\varphi_T)25.4 \qquad \text{Eq. 4.1}$$

$$\varphi_T = \frac{4.95e^{(0.062T)}}{100} \qquad \text{Eq. 4.2}$$

Oudin (Oudin et al., 2005)

$$\begin{cases} PET\ (mm\ day^{-1}) = \frac{R_e}{\lambda\rho}\left(\frac{T+5}{100}\right) & if\ T+5>0 \\ PET\ (mm\ day^{-1}) = 0 & otherwise \end{cases} \qquad \text{Eq. 4.3}$$

4.2.4. River flow simulation

In this study, river flow is simulated using the HEC-HMS hydrological model that was previously calibrated and validated for each catchment (explained in Chapter 3). Runoff is also simulated by climate models. However, due to the spatial inconsistencies between the boundaries of the climate model simulation cells and the natural catchment limits, hydrological models are commonly employed to simulate river flow using RCM precipitation and temperature as input (for example Teischbein and Seibert, 2012; Wetterhall et al., 2012; Prudhomme et al., 2013; Rojas et al., 2011; Cloke et al., 2013; Teng et al., 2015; Kay et al., 2015).

The HEC-HMS hydrological model uses daily precipitation and PET time series as input. The precipitation output from each RCM is input to the HEC-HMS model while daily PET is estimated using the formulae discussed in section 4.2.3, using the daily temperature simulation from each RCM as input. Additionally, bias-corrected time series of precipitation and PET (using the bias-corrected temperature as input) are used to estimate a "bias-corrected" river flow. Therefore, for each RCM at each resolution, three streamflow time series are simulated: 1) driven by uncorrected precipitation and uncorrected temperature, 2) driven by bias-corrected precipitation using the gamma distribution and bias-corrected temperature using the normal distribution, and 3) driven by bias-corrected precipitation using the double gamma distribution and bias-corrected temperature using the normal distribution.

4.2.5. Observation datasets

In order to validate RCM performance, observations from the analysed variables are compared with the RCM simulations. This process requires high quality observations (Maraun et al., 2015). Additionally, observations are used to calibrate the precipitation and temperature bias correction methods. In this study, daily precipitation observations are obtained from the CEH-GEAR dataset (Tanguy et al., 2014; Keller et al., 2015), daily observed mean temperature from the CHESS dataset (Robinson et al., 2015), and daily river flow data from the CEH's NRFA. Detailed information about CEH-GEAR is provided in Chapter 2, section 2.4.1, the CHESS dataset is explained in Chapter 2, section 2.4.2., and details regarding the NRFA are described in Chapter 2, section 2.5.

4.2.6. Cross-validation for the bias correction methods

In this study, the five-fold cross-validation approach (Maraun et al., 2015; Maraun, 2016) is used to evaluate the bias correction methods. The approach consists of the following steps: (a) divide the study period in five non-overlapping blocks of the same length, (b) calibrate the model parameters using four of the blocks, (c) use the calibrated model parameters to predict the remaining block, and (d) repeat the procedure until the cross-validated time series of the complete study period is generated (See Fig. 4.3). The availability of data from each RCM driven by the ERA-Interim simulation (evaluation run) varies for each RCM and represents a limitation for the selection of the study period. Considering the requirements of the cross-validation approach and the available time series from each RCM, 1979 to 2008 is used as study period for RACMO, 1984 to 2008 for RCA and 1989 to 2008 for CCLM, RACMO and WRF.

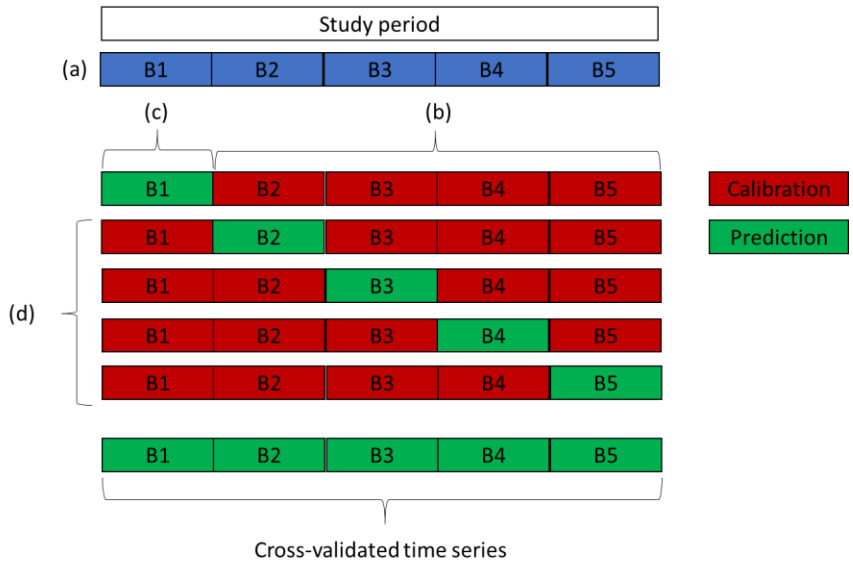

Figure 4. 3 Five-fold cross-validation scheme

4.2.7.Performance measures

For the evaluation of the RCM simulation skill, a set of performance measures are defined. Each performance measure focuses on specific aspects of the variable such as its distribution, time series, mean or extremes. The performance measures are defined following the VALUE framework recommendations (Maraun et al., 2015). It is important to consider that only using wet days for the estimation of percentile performance measures has proven to be misleading particularly for the analysis of heavy precipitation (Schär et al., 2016). Thus, here the percentile performance measures are estimated considering the complete precipitation time series. For the analysis of extreme precipitation, the performance measures derived by the CCl/CLIVAR/JCOMM Expert Team on Climate Change Detection and Indices are used (Zhang et al., 2011). The suite of performance measures used to evaluate RCM performance is shown in Table 4.2 along with their description and category.

Table 4. 2 Description of the precipitation, temperature and river flow performance measures, mpe = mean percentage error

Index	Category	Description
Precipitation		
95th percentile	Distribution-based	95th precipitation percentile considering all days (mm/day)
90th percentile	Distribution-based	90th precipitation percentile considering all days (mm/day)
50th percentile	Distribution-based	50th precipitation percentile considering all days (mm/day)
25th percentile	Distribution-based	25th precipitation percentile considering all days (mm/day)
Mean length of the monthly wet spell	Distribution-based	Average monthly mean wet spell length (days)
Mean length of the monthly dry spell	Distribution-based	Average monthly mean dry spell length (days)
Mean annual accumulated precipitation	Distribution-based	Mean accumulated precipitation per year (mean percentage error, mpe)
Mean monthly accumulated precipitation	Distribution-based	Absolute average difference between the simulated and observed mean accumulated precipitation per month (mpe)
Monthly MSE	Time series-based	Estimation of the monthly mean square error (mm^2)
Spearman correlation	Time series-based	Spearman correlation coefficients between the RCM and observation time series(no units)
Maximum one day precipitation (RX1day)	Distribution-based	Monthly maximum one day precipitation (mm)
Simple Daily Intensity Index (SDII)	Distribution-based	Ratio of the annual total precipitation to the number of wet days ($\geq$1 mm)
Number of heavy precipitation days (R10)	Distribution-based	Number of days with precipitation $\geq$ 10mm within a year
Number of very heavy precipitation days (R20)	Distribution-based	Number of days with precipitation $\geq$ 20mm within a year
Very wet days (R95p)	Distribution-based	Annual total precipitation from days > 95th percentile
Temperature		
Mean annual temperature	Distribution-based	Mean annual temperature (mpe)
Monthly mean temperature	Distribution-based	Absolute average difference between the simulated and observed mean monthly temperature (mpe)
99th percentile of the mean temperature	Distribution-based	99th mean temperature percentile (°C/day)
1st percentile of the mean temperature	Distribution-based	1st mean temperature percentiles (°C/day)
Pearson correlation	Time series-based	Pearson correlation coefficients between the RCM and observation time series (no units)
River Flow		
Q10	Distribution-based	Measure of high flows, river flow that is exceeded for 10% of the time series (m^3/s)
Q95	Distribution-based	Measure of low flows, river flow that is exceeded for 95% of the time series (m^3/s)
Annual frequency of Q10	Distribution-based	Annual mean number of days that the observed Q10 is exceeded (days)
Mean annual river flow	Distribution-based	Annual mean daily river flow (mpe)
Mean winter (DJF) river flow	Distribution-based	Winter mean daily river flow (mpe)
Mean spring (MAM) river flow	Distribution-based	Spring mean daily river flow (mpe)
Mean summer (JJA) river flow	Distribution-based	Summer mean daily river flow (mpe)
Mean autumn (SON) river flow	Distribution-based	Autumn mean daily river flow (mpe)
Monthly NSE	Time series-based	Monthly Nash Sutcliffe Efficiency index (no units) (defined in section 3.4.1.5)
Monthly MSE	Time series-based	Monthly mean square error [(m^3/s)^2]
Spearman correlation	Time series-based	Spearman correlation coefficients between the RCM and observation time series(no units)

4.3. Results

The following section shows the results of the evaluation of the uncorrected and bias-corrected RCM outputs at the two spatial resolutions under analysis. Additionally, the section provides results from steps prior to the evaluation of the RCM simulation skill. Initially, results from the PET estimation are given followed by results from the simulation impact due to the grid box selection and the bias correction methods. Afterwards, the temperature, precipitation and river flow simulation metrics are shown.

4.3.1. Observed and simulated PET

The Hamon formula underestimates the daily observed PET from October to March in all catchments (Figs. 4.4, and Figs in Annex A, A1, A2 and A3; frames a, b, c, j, k, l). In contrast, the formula overestimates the daily observed PET during summer in all the study catchments (Figs. 4.4, and Figs in Annex A, A1, A2 and A3; frames f, g, h). Throughout the year the formula estimates several days of low PET that are not in compliance with the observations. This is more evident from April to September when the PET estimation for several days is close to zero. The Hamon formula underestimates the monthly accumulated PET from November to March and overestimates it from April to October (Figure 4.6 and Table 4.3). The highest mean percentage errors (mpe) are found during summer and can be as high as 131% (Coquet catchment during July). February, March, October and November have the smaller mpe. Overall, the formula performs better for the Upper Thames catchment (averaged absolute mpe of 40%) and worse for the Coquet catchment (averaged absolute mpe of 53%).

In contrast, the Oudin formula underestimates the PET from days with large observed PET from November to February (Figs. 4.5, A4, A5 and A6; frames a, b, k, l). Additionally, the method fails to estimate days with low PET from July to September (Figs. 4.5, A4, A5 and A6; frames a, b, k, l). For all catchments, the formula underestimates the monthly accumulated PET from January to April and overestimates it from June to October (Fig. 4.6 and Table 4.3). For the remaining months, the formula overestimates or underestimates the observed PET depending on the catchment. The highest mpe also varies for each catchment: from June to November for the Upper Thames catchment and during winter for the rest of the catchments. In general, the formula's performance is better for the Upper Thames catchment (average absolute mpe of 15%) and worse for the Coquet catchment (averaged absolute mpe of 21%).

By comparing the results from both formulae, the Oudin formula consistently outperforms the Hamon method to reproduce the observed PET for all the study catchments. Moreover, the Hamon method can have large biases (mpe > 100%) for the accumulated monthly PET and also provide low PET estimations for days when the observed PET is large. Overall, both methods perform better for the upper Thames catchment and worse for the Coquet catchment. However, the lowest mpe for the Hamon formula (upper Thames catchment, 40%) is high compared to the highest mpe from the Oudin formula (Coquet catchment, 21%). It has been shown that, compared to the Oudin method, the Hamon formula has large biases. Therefore, for the rest of this study, the Oudin formula is used to estimate daily PET.

Table 4. 3 Mean percentage error (mpe) for the simulated monthly PET using the Hamon and Oudin formulae

Method	Catchment	Jan	Feb	Mar	Apr	May	Jun	Jul	Aug	Sep	Oct	Nov	Dec	Abs. Av.
Hamon	Upper Thames	-33%	-15%	-11%	14%	49%	98%	110%	70%	32%	17%	-6%	-26%	40%
	Glaslyn	-53%	-26%	-12%	16%	51%	107%	121%	77%	32%	1%	-36%	-55%	49%
	Calder	-45%	-21%	-13%	19%	53%	108%	122%	77%	33%	12%	-21%	-42%	47%
	Coquet	-57%	-31%	-18%	20%	57%	117%	131%	80%	29%	3%	-37%	-59%	53%
Oudin	Upper Thames	-4%	-7%	-5%	-4%	3%	13%	21%	23%	26%	34%	27%	7%	15%
	Glaslyn	-33%	-23%	-13%	-10%	-2%	12%	22%	24%	22%	12%	-16%	-33%	18%
	Calder	-27%	-21%	-14%	-7%	0%	12%	20%	22%	21%	21%	-2%	-23%	16%
	Coquet	-45%	-36%	-25%	-14%	-5%	9%	18%	18%	12%	4%	-25%	-46%	21%

4.3.2.Simulation sensitivity to the selection of RCM grid boxes

The grid box representativeness and larger domain size (discussed in section 4.2.1.2) are analysed using the 0.44° RCMs. For this resolution, a domain of 3x3 grid cells centred in the study catchment is used. Correlations are calculated for the domain average, each individual grid box and the grid boxes selected to simulate the catchment's climate in this study. Figs. 4.7e-h illustrate the distribution of the domain and cells used for each catchment. The 0.11° RCMs are used to evaluate the correlation of different size domains. For this resolution, correlations are estimated for domains of 12x12 and 6x6 grid cells and for the catchments extension (see Figs. 4.7a-d). Correlations are only shown for the precipitation time series as, for all study catchments, the temperature Pearson correlation coefficients are higher than 0.9 for all RCMs at both resolutions. Precipitation doesn't follow a normal distribution. Therefore the Spearman correlation coefficient is estimated. Results are shown in Tables 4.4 to 4.11. For each catchment, a ranking considering the correlation between the grid box and observations from the analysed RCMs is shown in the last row where 1 represents the highest correlation.

Correlation for the 0.44° resolution RCMs varies from 0.44 to 0.645 for the upper Thames, from 0.47 to 0.62 for the Glaslyn, from 0.42 to 0.64 for the Calder and from 0.34 to 0.59 for the Coquet catchment. In general, for all catchments the correlation from CCLM grid cells is higher than for the other RCMs, except for the Glaslyn catchment where the correlation from RACMO grid cells is as high as the CCLM correlation. In contrast, the WRF grid cells have the lowest correlation in all catchments. The 3x3 grid cell domain has a high rank for all catchments: the highest rank for the Glaslyn and Coquet catchments (Tables 4.5 and 4.7) and the second highest for the Calder and upper Thames catchments (Tables 4.4 and 4.6). This demonstrates that using a larger domain than the area of interest can provide higher correlation between observations and simulations. Eden et al. (2014) had similar findings correlating rainfall station records with RACMO and CCLM grid boxes in the UK. The grid cells that cover the catchment's area have the higher ranking for the upper Thames and Calder catchments (Tables 4.4 and 4.6). Nevertheless, for the Glaslyn and Coquet catchments their ranking is low (Tables 4.5 and 4.7). Therefore, in this study the representativeness issue stated by Maraun and Widmann (2015) is catchment-dependent and, in these cases, occurring at catchments with complex orography.

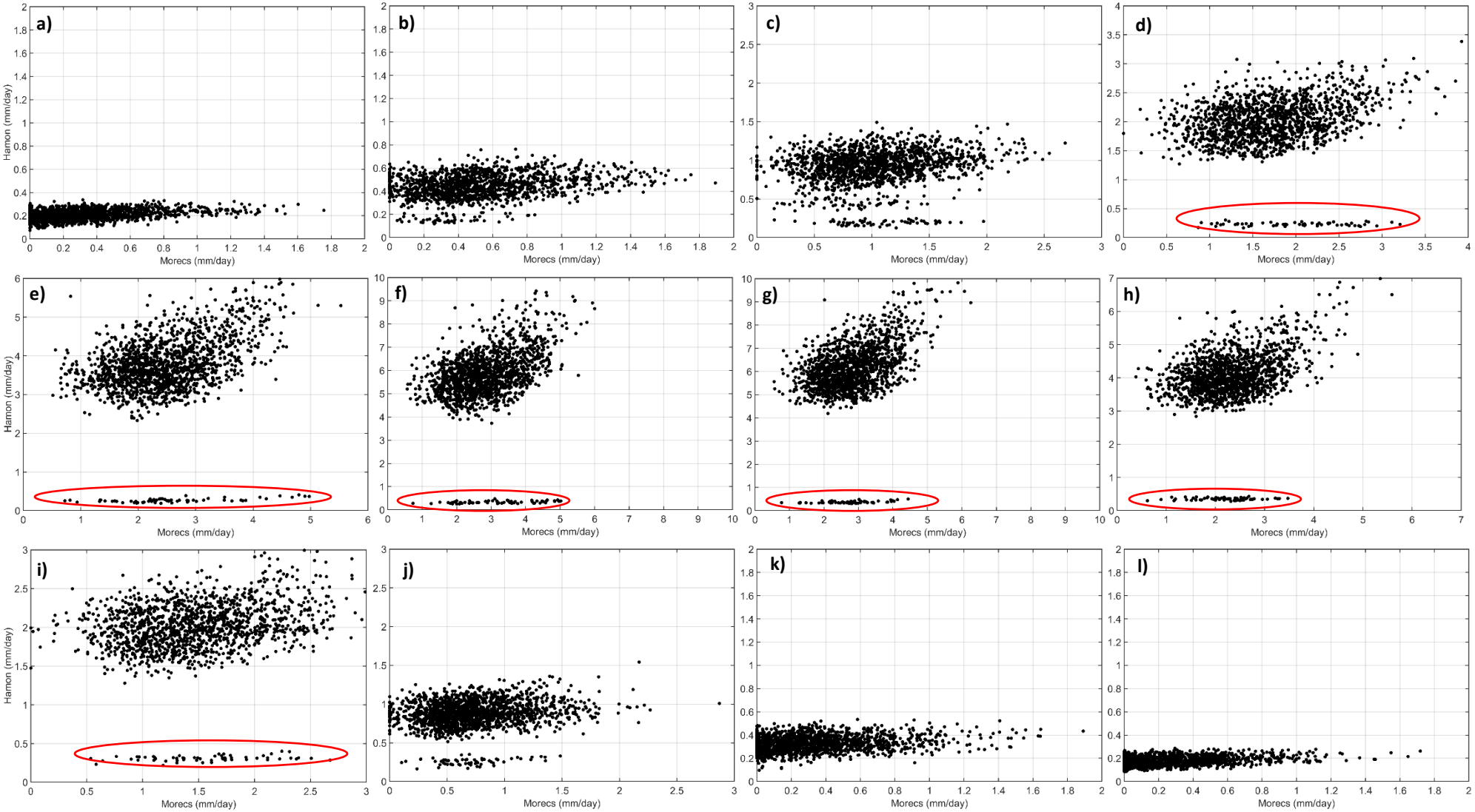

Figure 4. 4. Scatter plots between daily observed (Morecs) and simulated PET using the Hamon formula for the upper Thames catchment: a) January, b) February, c) March, d) April, e) May, f) June, g) July, h) August, i) September, j) October, k) November, and l) December. Please note the difference in the axis. Frequent underestimated days are circled in red

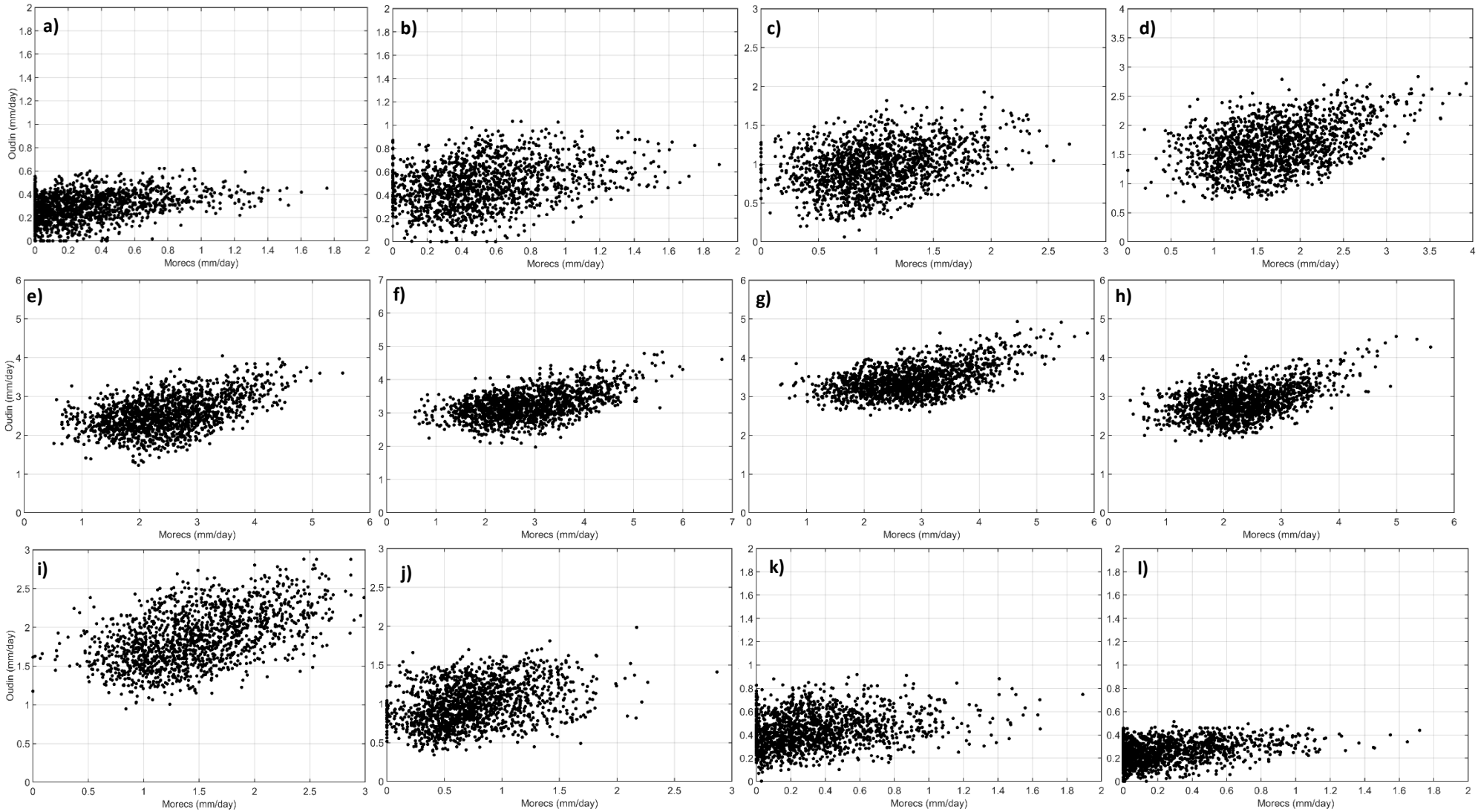

Figure 4. 5 Scatter plots between daily observed (Morecs) and simulated PET using the Oudin formula for the upper Thames catchment: a) January, b) February, c) March, d) April, e) May, f) June, g) July, h) August, i) September, j) October, k) November, and l) December. Please note the difference in the axis

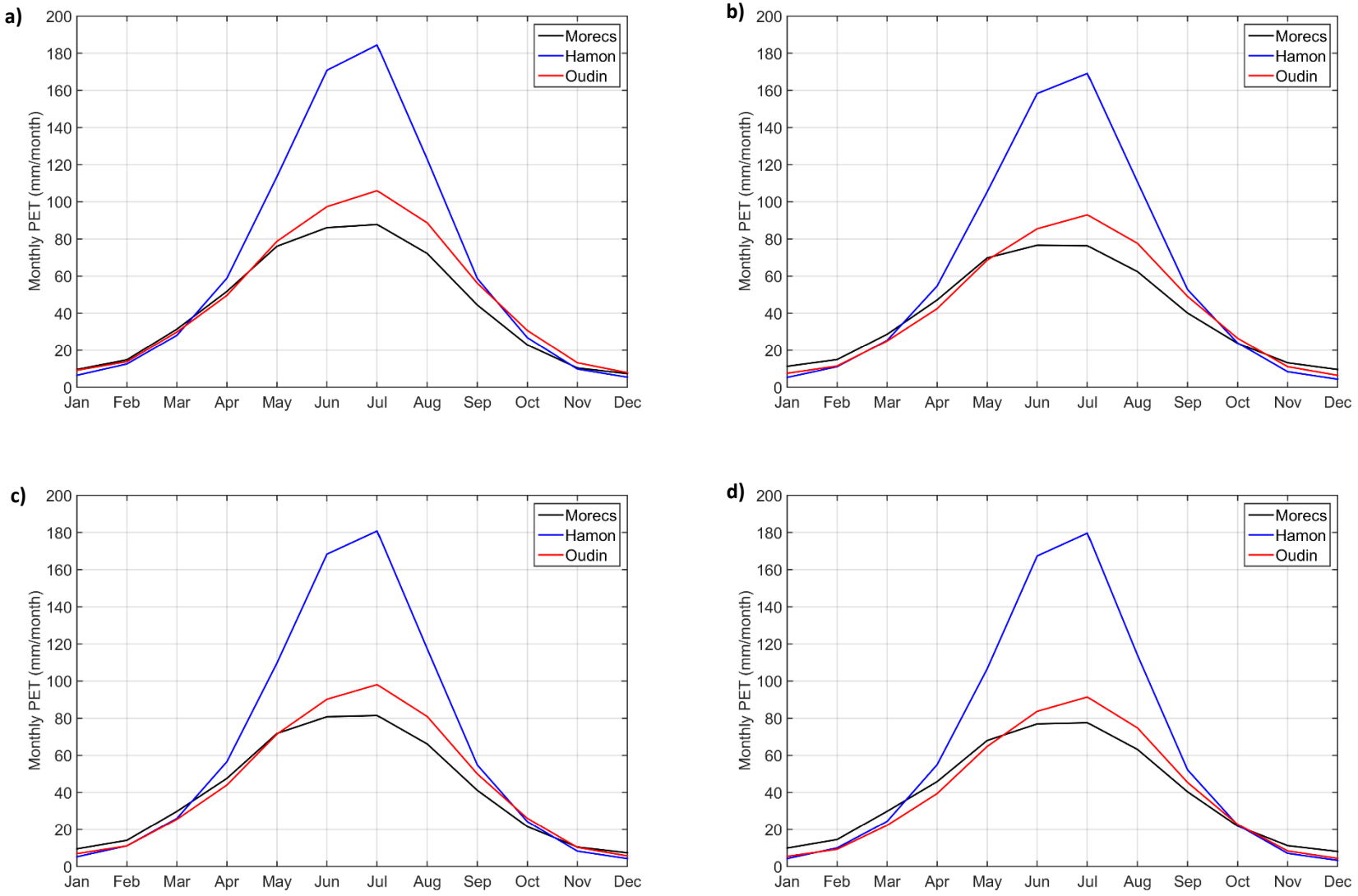

Figure 4. 6 Observed and simulated monthly accumulated PET using the Hamon and Oudin formulae for: a) upper Thames, b) Glaslyn, c) Calder, d) Coquet

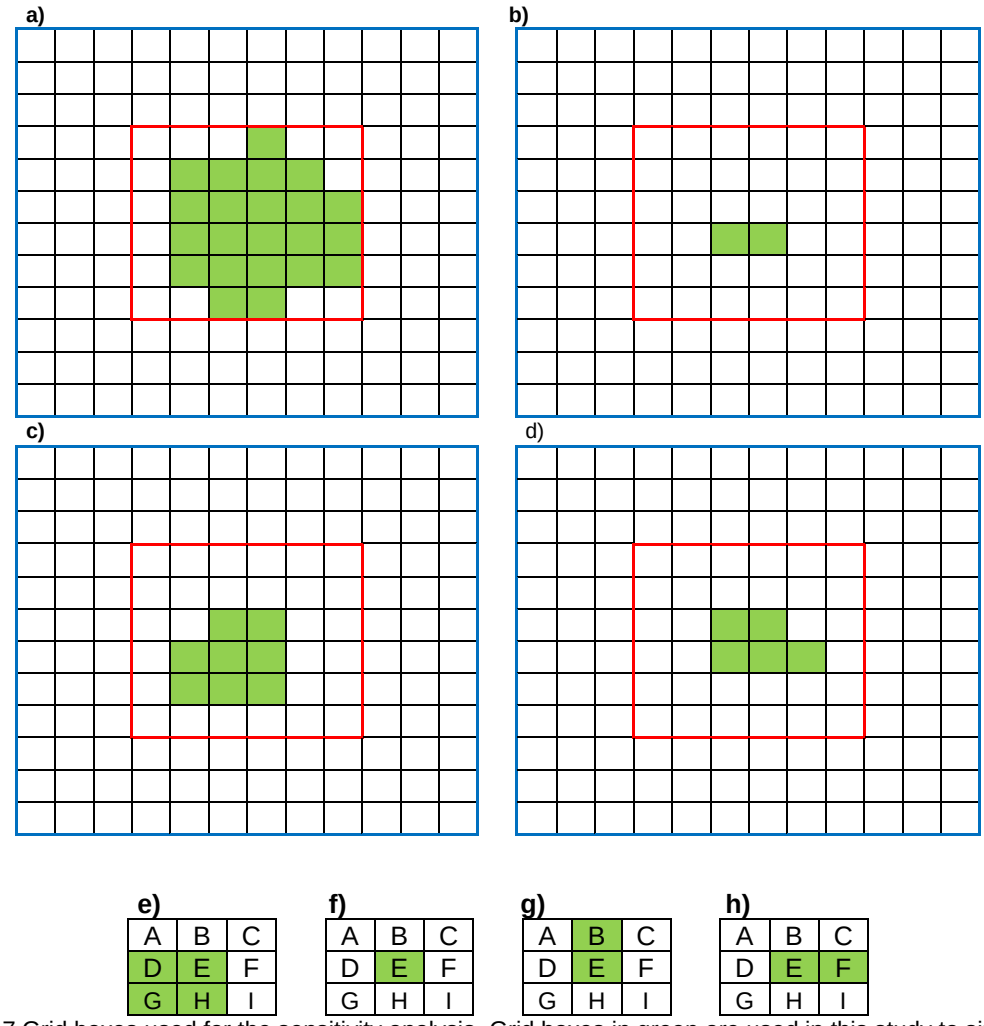

Figure 4. 7 Grid boxes used for the sensitivity analysis. Grid boxes in green are used in this study to simulate the catchment's climate as the catchment is located within that region. The red line indicates the 6x6 grid box domain and the blue line 12x12 grid box domain

Correlation for the 0.11° RCMs varies from 0.51 to 0.69 for the upper Thames, from 0.56 to 0.65 for the Glaslyn, from 0.53 to 0.68 for the Calder and from 0.42 to 0.63 for the Coquet catchment. For all catchments the CCLM domains have a higher correlation than the other RCMs grid boxes. In contrast, the RCA and WRF domains have the lower correlation coefficients. For all catchments, the 6x6 and 12x12 grid cell domains have higher rankings than the grid cells covering the catchment. This supports the results from Eden et al. (2014). Compared to the 0.44° RCMs, the 0.11° RCMs grid cells have higher correlation with the catchment observations. However, these results should be carefully interpreted as only the correlation between observed and simulated time series is assessed, omitting other performance measures that evaluate other aspects of RCM performance such as means, extremes and thresholds. Results considering these measures are shown in sections 4.3.4 and 4.3.5.

Table 4. 4 Grid box rank and Spearman correlation between observed and simulated precipitation for the upper Thames catchment using the 0.44° RCMs

RCM/CELL	A	B	C	D	E	F	G	H	I	3x3	DEGH
CCLM	0.64	0.62	0.60	0.64	0.62	0.60	0.63	0.61	0.59	0.65	0.64
HIRHAM	0.49	0.47	0.46	0.50	0.49	0.47	0.51	0.50	0.47	0.51	0.51
RACMO	0.58	0.55	0.53	0.58	0.56	0.54	0.59	0.57	0.55	0.58	0.59
RCA	0.48	0.48	0.47	0.50	0.50	0.47	0.53	0.51	0.48	0.52	0.52
WRF	0.47	0.46	0.44	0.48	0.46	0.44	0.49	0.48	0.46	0.50	0.50
Ranking	6	8	11	4	7	10	3	5	9	2	1

Table 4. 5 Grid box rank and Spearman correlation between observed and simulated precipitation for the Glaslyn catchment using the 0.44° RCMs

RCM/CELL	A	B	C	D	E	F	G	H	I	3x3
CCLM	0.61	0.61	0.60	0.61	0.60	0.58	0.59	0.58	0.55	0.62
HIRHAM	0.53	0.55	0.53	0.55	0.55	0.52	0.56	0.55	0.52	0.57
RACMO	0.60	0.60	0.58	0.62	0.61	0.57	0.61	0.61	0.55	0.62
RCA	0.53	0.54	0.53	0.55	0.54	0.52	0.55	0.53	0.50	0.55
WRF	0.48	0.47	0.48	0.50	0.53	0.49	0.54	0.52	0.49	0.55
Ranking	7	5	8	3	4	9	2	6	10	1

Table 4. 6 Grid box rank and Spearman correlation between observed and simulated precipitation for the Calder catchment using the 0.44° RCMs

RCM/CELL	A	B	C	D	E	F	G	H	I	3x3	BE
CCLM	0.64	0.64	0.61	0.63	0.62	0.59	0.60	0.59	0.56	0.64	0.64
HIRHAM	0.53	0.54	0.50	0.53	0.52	0.48	0.51	0.50	0.46	0.54	0.54
RACMO	0.60	0.61	0.57	0.60	0.59	0.55	0.56	0.53	0.51	0.60	0.61
RCA	0.51	0.52	0.48	0.51	0.50	0.47	0.50	0.48	0.46	0.52	0.52
WRF	0.52	0.51	0.45	0.50	0.50	0.44	0.48	0.48	0.42	0.53	0.52
Ranking	4	3	8	5	6	10	7	9	11	2	1

Table 4. 7 Grid box rank and Spearman correlation between observed and simulated precipitation for the Coquet catchment using the 0.44° RCMs

RCM/CELL	A	B	C	D	E	F	G	H	I	3x3	EF
CCLM	0.55	0.56	0.54	0.56	0.56	0.54	0.56	0.56	0.54	0.59	0.56
HIRHAM	0.45	0.43	0.36	0.47	0.46	0.36	0.44	0.47	0.34	0.47	0.44
RACMO	0.50	0.49	0.45	0.51	0.52	0.46	0.49	0.53	0.45	0.54	0.51
RCA	0.43	0.42	0.40	0.45	0.44	0.41	0.44	0.45	0.40	0.46	0.44
WRF	0.39	0.39	0.34	0.39	0.40	0.36	0.39	0.41	0.35	0.46	0.41
Ranking	6	8	1	4	3	9	7	2	10	1	5

Table 4. 8 Domain rank and Spearman correlation between observed and simulated precipitation for the upper Thames catchment using the 0.11° RCMs

RCM/CELL	12x12	6x6	Catchment
CCLM	0.69	0.67	0.67
HIRHAM	0.59	0.58	0.57
RACMO	0.60	0.59	0.58
RCA	0.53	0.51	0.51
WRF	0.55	0.52	0.52
Ranking	1	2	3

Table 4. 9 Domain rank and Spearman correlation between observed and simulated precipitation for the Glaslyn catchment using the 0.11° RCMs

RCM/CELL	12x12	6x6	Catchment
CCLM	0.65	0.65	0.64
HIRHAM	0.61	0.61	0.61
RACMO	0.61	0.62	0.62
RCA	0.57	0.57	0.56
WRF	0.57	0.58	0.57
Ranking	1	2	3

Table 4. 10 Domain rank and Spearman correlation between observed and simulated precipitation for the Calder catchment using the 0.11° RCMs

RCM/CELL	12x12	6x6	Catchment
CCLM	0.68	0.67	0.65
HIRHAM	0.60	0.60	0.60
RACMO	0.61	0.61	0.60
RCA	0.55	0.54	0.53
WRF	0.55	0.55	0.54
Ranking	1	2	3

Table 4. 11 Domain rank and Spearman correlation between observed and simulated precipitation for the Coquet catchment using the 0.11° RCMs

RCM/CELL	12x12	6x6	Catchment
CCLM	0.62	0.63	0.61
HIRHAM	0.49	0.52	0.48
RACMO	0.52	0.54	0.50
RCA	0.42	0.44	0.42
WRF	0.46	0.48	0.45
Ranking	2	1	3

4.3.3.Bias correction

One of the main questions that arises when comparing the outputs from a climate model and the observations is whether the outputs require post-processing techniques to reduce their biases. This is important as the biases might be part of the variable's natural variability. Therefore, to assess whether RCM biases are part of the natural variability, the procedure proposed by Kim et al. (2016) is partially used. The method is performed for each month. It mainly consists of five steps: 1) estimating the mean and standard deviation values for the temperature observations (shape and scale parameters for the precipitation observations), 2) generate a random 30 year time series using the observation parameters and estimate the new parameters from this random time series, 3) repeat the previous step until 100,000 random time series and their distribution parameters are obtained, 4) estimate the distribution parameters from the RCM time series, 5) graph all the parameters that were estimated (from observations, random time series and RCMs). In this procedure, the parameters from the random time series represent the temperature or precipitation natural variability. Any RCM with parameters outside the natural variability limits is interpreted to have biases larger than the natural variability and therefore appropriate for post-processing.

Graphs are generated following the procedure described above for temperature and precipitation from all the study catchments. For temperature, the distribution parameters of the RCMs are closer or within the

boundaries of the estimated natural variability for most of the months in the upper Thames catchment (Fig. 4.8). This indicates a good simulation of temperature from most of the RCMs for this catchment. In contrast, for the Glaslyn catchment the RCMs have distribution parameters that lie outside the natural variability boundaries for all months (Fig. 4.9), clearly indicating the presence of biases unaccounted in the natural variability. For the Calder catchment, the distribution parameters of the RCMs are close, but not within the natural variability boundaries for most of the months (Fig. 4.10). Finally, the RCMs temperature distribution parameters lie outside the natural variability of the Coquet catchment (Fig. 4.11). Comparing all the study catchments, the temperature distribution parameters of the RCMs are closer to the natural variability boundaries for the Thames and Calder catchment, in that order. In contrast, for the Glaslyn and Coquet catchments the RCM distribution parameters lie away from the natural variability. These results indicate a higher simulation skill for the RCMs when applied to catchments with low elevation ranges and problems to simulate temperature in catchments with complex orography. Additionally, there is not a clear result indicating a better skill from the higher resolution RCMs compared to their coarser version. These results imply the benefit from using a bias-correction method in order to reduce biases that are unaccounted within the natural variability of temperature.

A monthly quantile mapping bias correction method using the normal distribution is applied to the RCM simulated temperature. The probability distribution functions (PDF) from all uncorrected RCMs demonstrate a deviation from the observations PDF (Fig. 4.12a, c, e, g). The impact of the bias correction method is observed when the PDFs from the bias-corrected RCMs are plotted with the observations PDF (Figs. 4.b, d, f, h). The plot shows an almost perfect fit between the PDFs from the observations and from the post-processed RCMs for all catchments. Additionally, for all catchments and months the distribution parameters from bias-corrected RCMs are situated within the observation's natural variability boundaries (Figs. 4.8 to 4.11).

Results are similar for precipitation. Uncorrected RCMs have distribution parameters outside the natural variability of the observations for all catchments and months (Figs. 4.13, 4.14, 4.15, 4.16). Only 0.11° WRF and 0.11° RACMO lie within the natural variation limits in few cases (e.g. June and October in the upper Thames, April, May, September, October, November and December in the Calder, and most months in the Coquet). In contrast with temperature, the analysis doesn't show a better performance in a particular catchment. Results show that RCM skill could benefit from bias correcting precipitation.

Precipitation simulations are bias corrected using two methodologies: quantile mapping using a gamma distribution and quantile mapping using a double gamma distribution. For all catchments and months the gamma distribution method corrects the distribution parameters from all RCMs as the distribution parameters are located within the natural variability boundaries after the correction (Figs. 4.13, 4.14, 4.15, 4.16). As shown in section 4.3.5, quantile mapping using the gamma distribution reduces most of the distribution biases, except the higher end of the distribution. Therefore, a double gamma quantile mapping correction is applied. The bias correction method is applied to two sections of the distribution, the first one to the values below the 90^{th} percentile and the second one to values above the 90^{th} percentile. This

threshold is selected as the gamma distribution method reduces the biases until the 90th percentile, after which the biases increased exponentially (see section 4.3.5).

The effect of the double gamma bias correction method is assessed by plotting the distribution parameters from the higher tail of the distribution (values above the 90th percentile). The graphs show that the simulated distribution of the uncorrected parameters are closer to the observed distribution parameters for the upper Thames catchment than the others (Fig. 4.17). For the Glaslyn catchment, the distribution parameters generally lie outside the natural variability for all months (Fig. 4.18). For the Calder catchment, the distribution parameters lie outside the observation's natural variability for February, March, June, July, August, November and December (Fig. 4.19). Finally, for the Coquet catchment the distribution parameter from March, April, September and November lie outside the natural variability boundaries (Fig. 4.20). These results denote the bias between observed and simulated extremes and support the approach of employing a double gamma distribution to reduce the bias in extremes.

The cumulative distribution functions (CDF) for the uncorrected RCMs show a deviation from the observations (Figs. 4.21a, c, e, g). The deviation is greater for the Glaslyn catchment (Fig. 4.21c) than for the other catchments. The CDFs after RCMs are bias-corrected using the double gamma distribution show a reduction of their deviation from observations for all catchments (Figs. 4.21b, d, f, h). Nevertheless, after bias correction, a deviation from the observations is still evident. Additionally, after bias correction using the double gamma distribution, the distribution parameters of the RCM simulations lie within the natural variability of the observations for the majority of the RCMs for all months and catchments (Figs. 4.17 to 4.20).

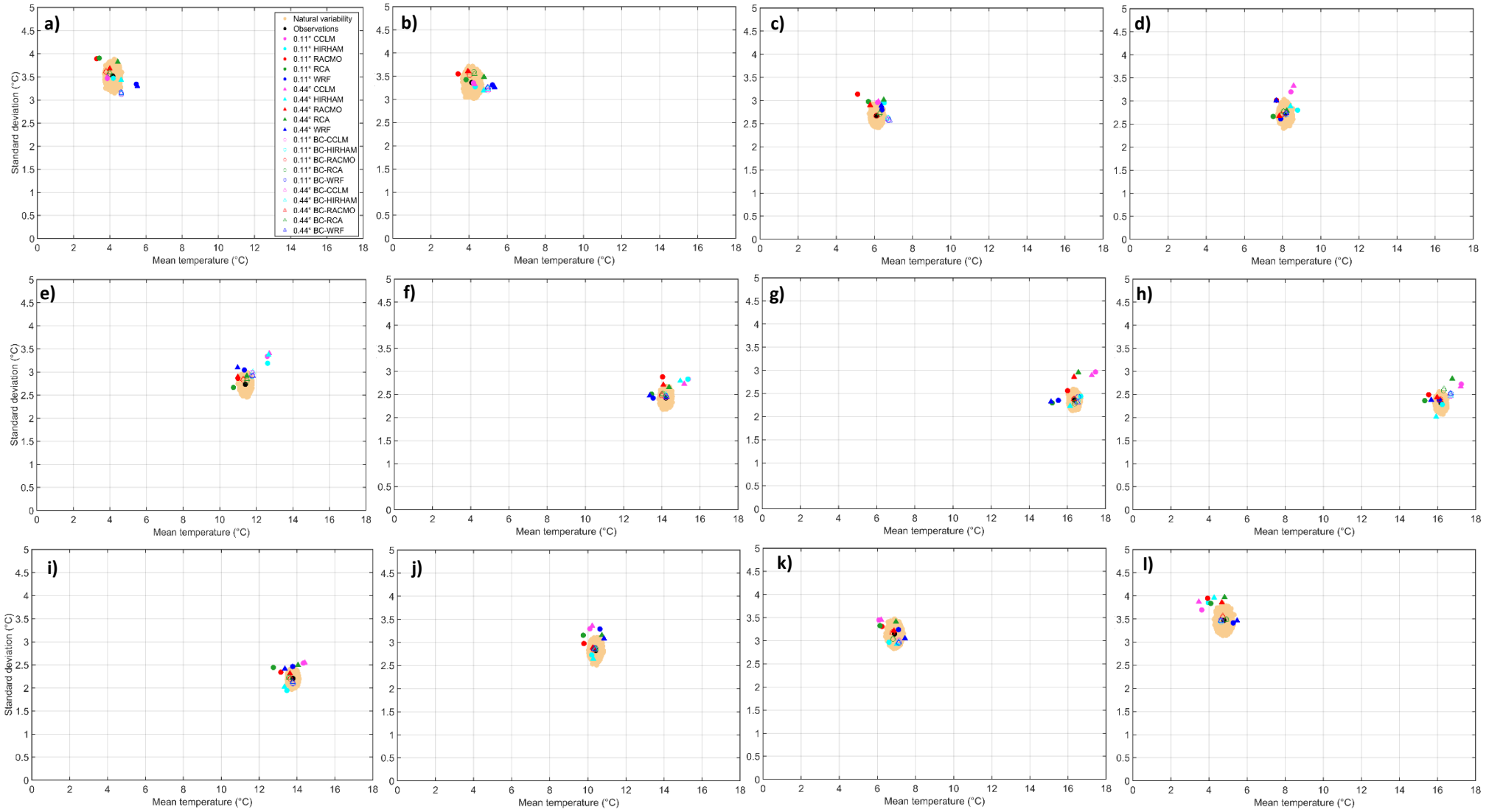

Figure 4. 8 Temperature natural variability and observations and RCM temperature distribution parameters: a) January, b) February, c) March, d) April, e) May, f) June, g) July, h) August, i) September, j) October, k) November, and l) December. Upper Thames catchment

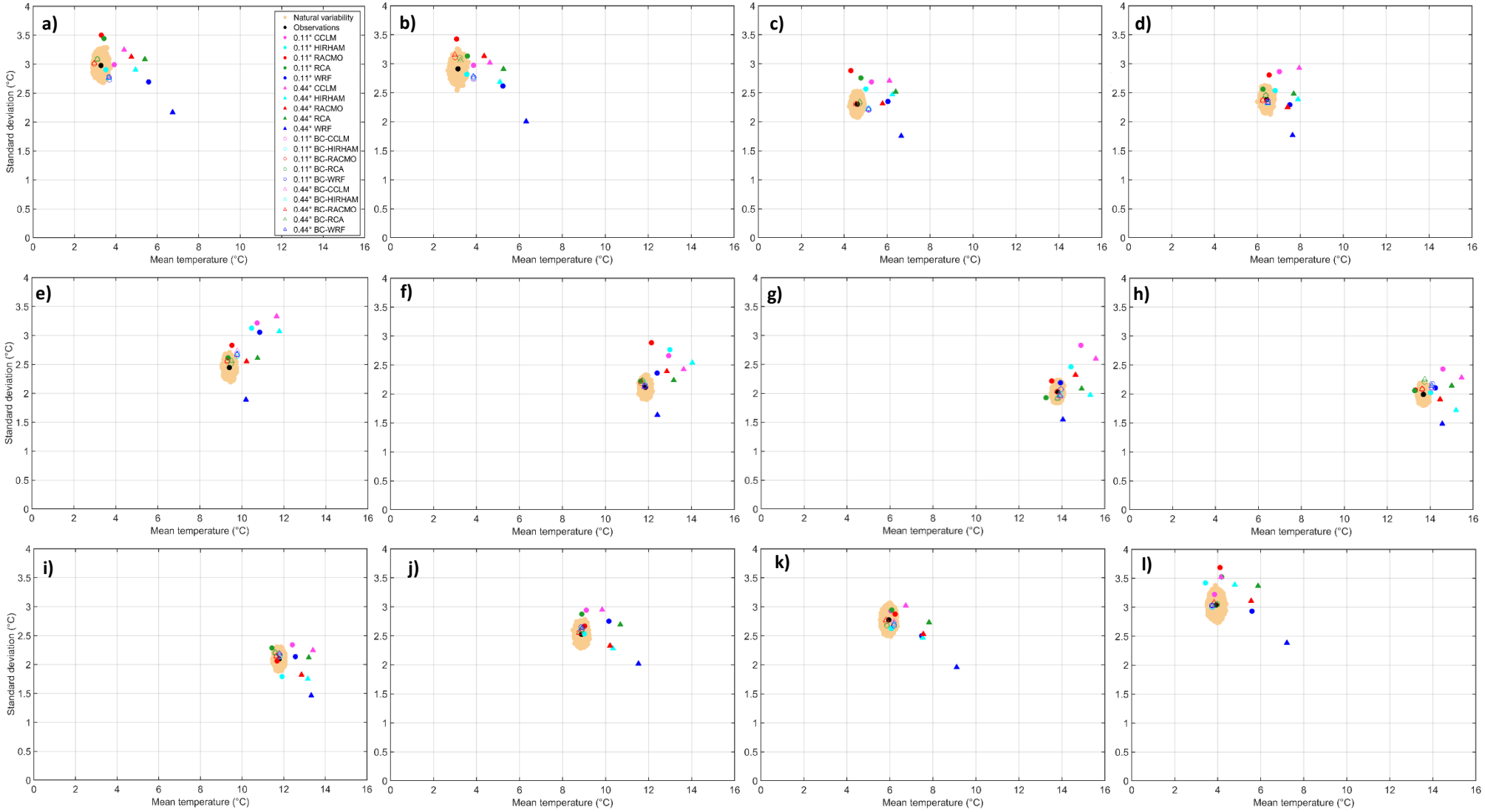

Figure 4. 9 Temperature natural variability and observations and RCM temperature distribution parameters: a) January, b) February, c) March, d) April, e) May, f) June, g) July, h) August, i) September, j) October, k) November, and l) December. Glaslyn catchment

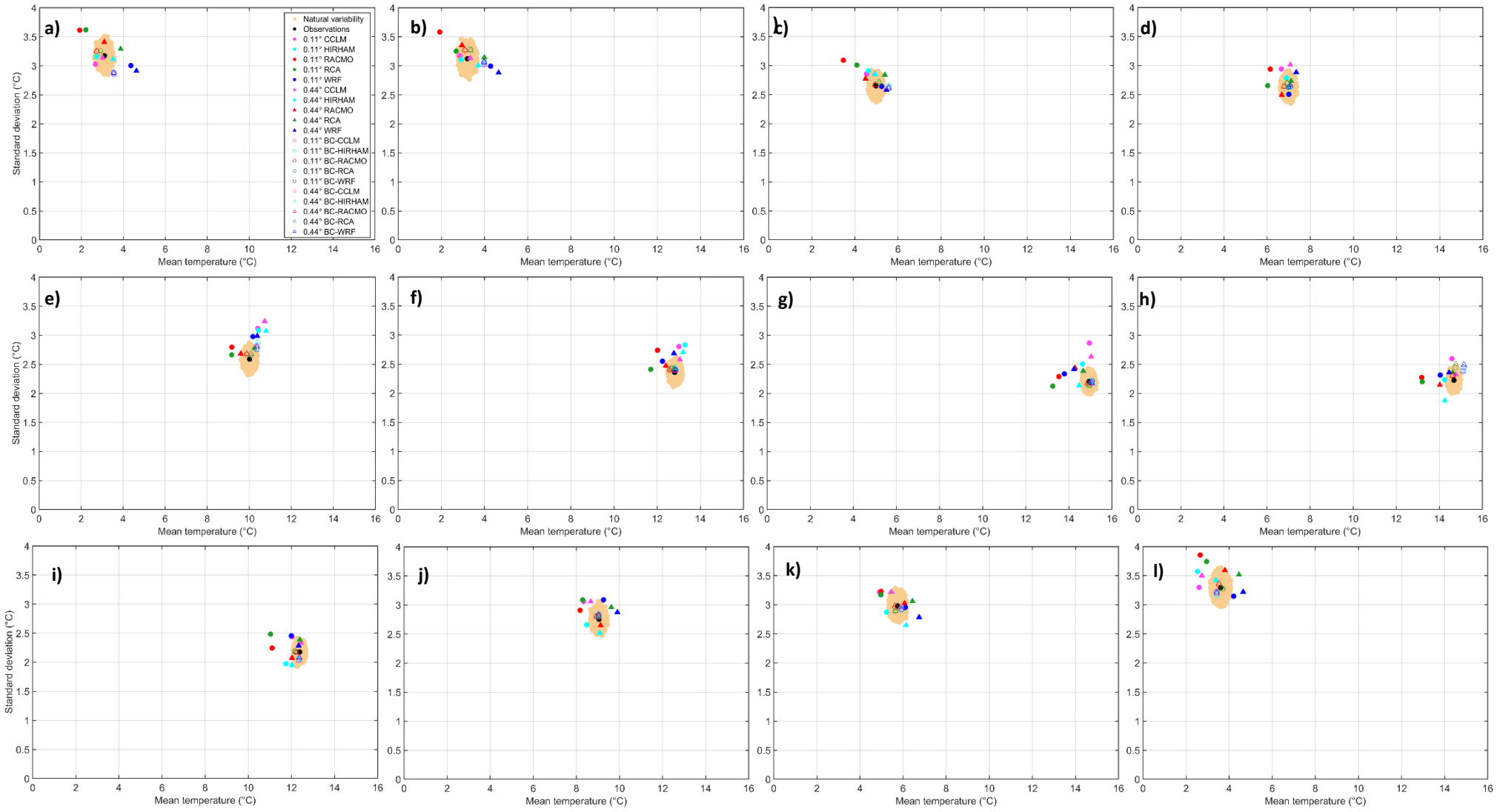

Figure 4. 10 Temperature natural variability and observations and RCM temperature distribution parameters: a) January, b) February, c) March, d) April, e) May, f) June, g) July, h) August, i) September, j) October, k) November, and l) December. Calder catchment

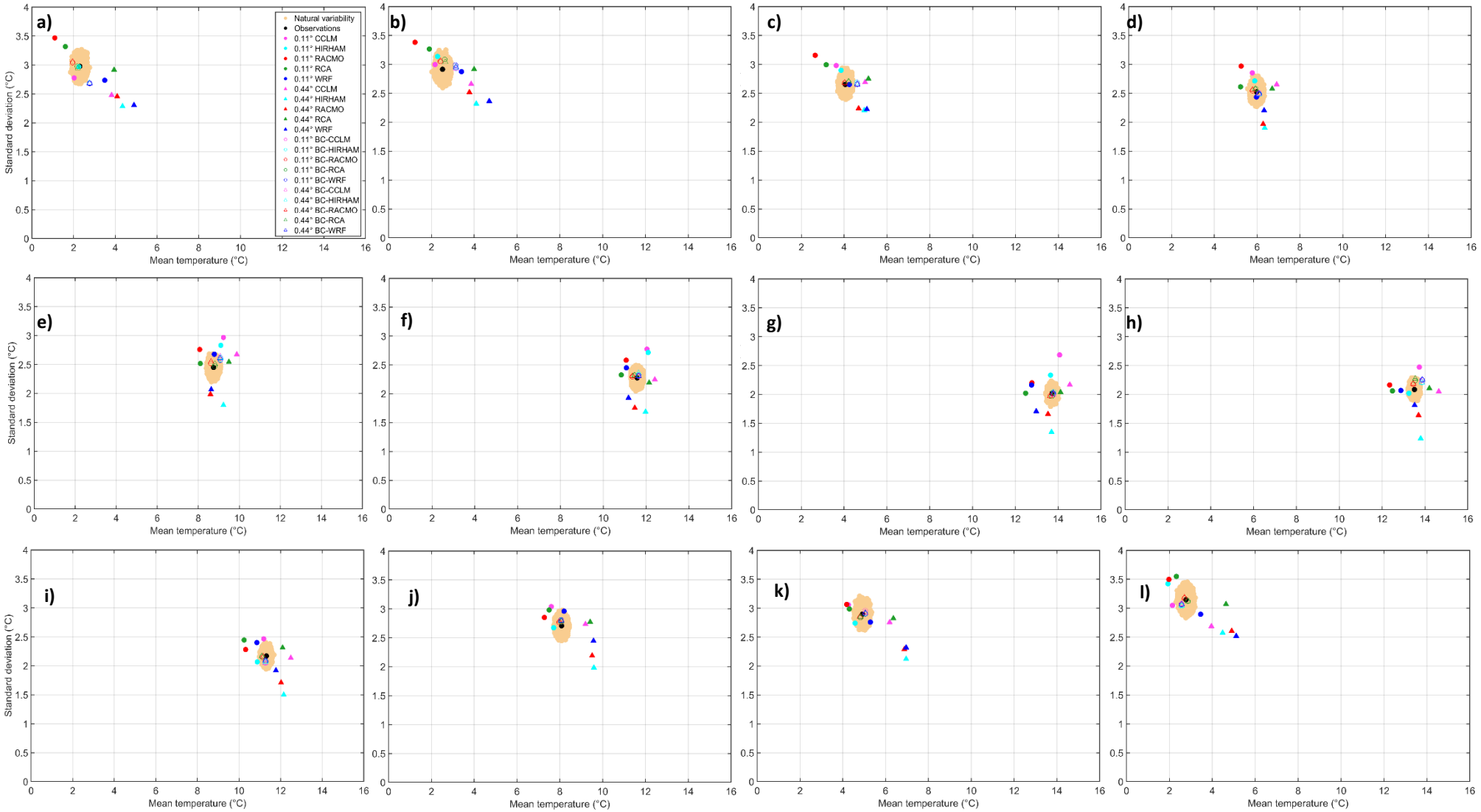

Figure 4. 11 Temperature natural variability and observations and RCM temperature distribution parameters: a) January, b) February, c) March, d) April, e) May, f) June, g) July, h) August, i) September, j) October, k) November, and l) December. Coquet catchment

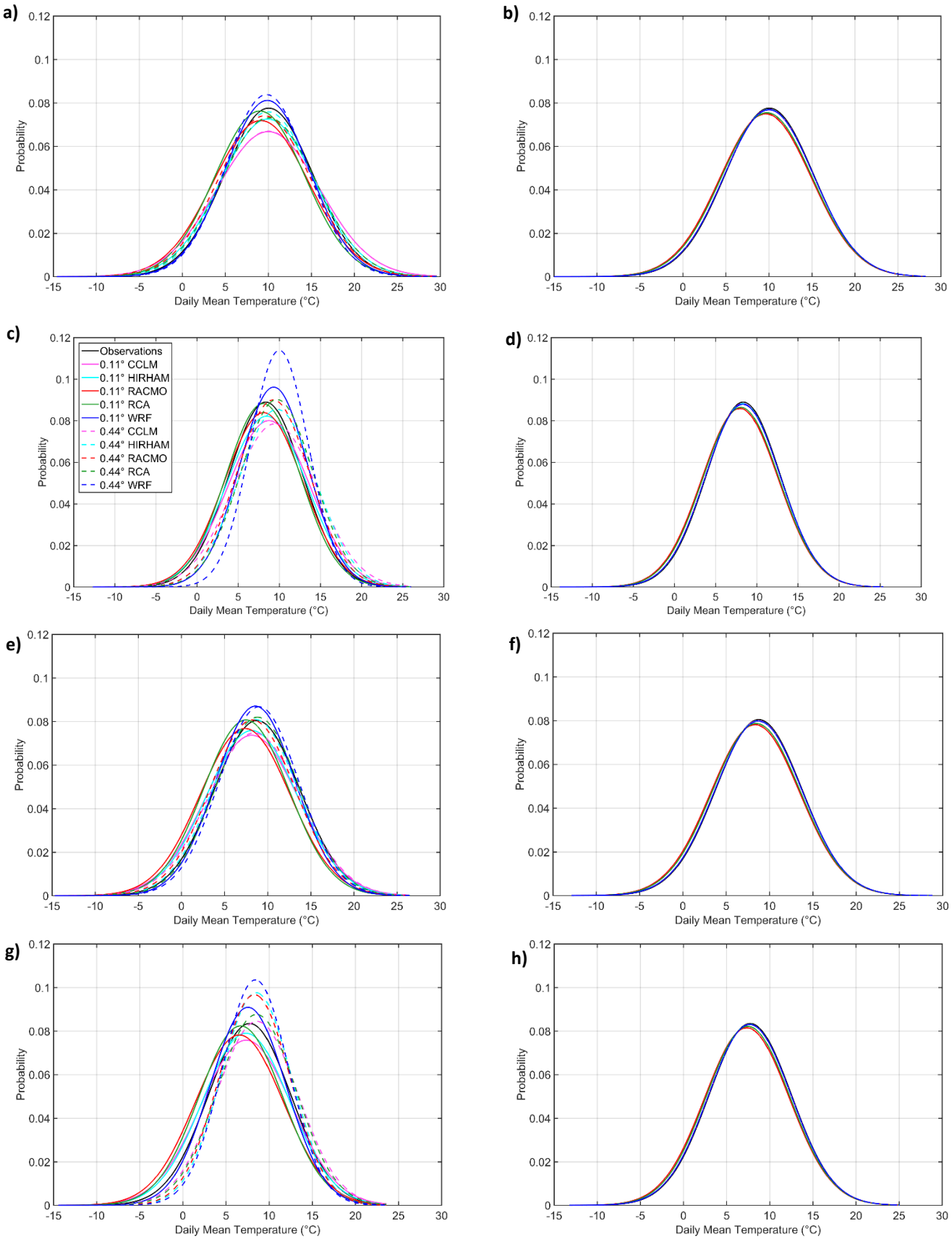

Figure 4. 12 Temperature probability distribution functions: a) Upper Thames uncorrected RCMs, b) Upper Thames bias-corrected RCMs, c) Glaslyn uncorrected RCMs, d) Glaslyn bias-corrected RCMs, e) Calder uncorrected RCMs, f) Calder bias-corrected RCMs, g) Coquet uncorrected RCMs, h) Coquet bias-corrected RCMs

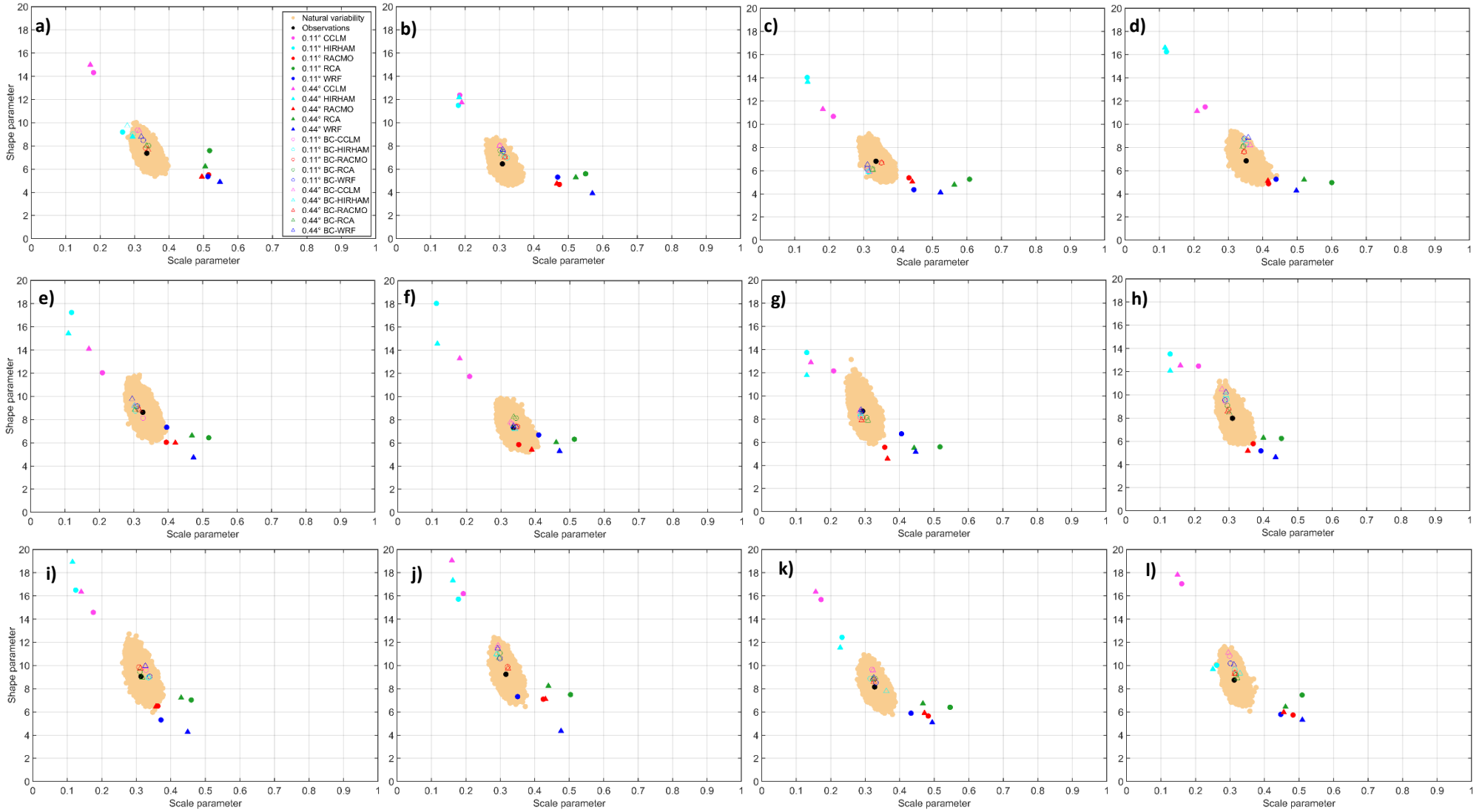

Figure 4. 13 Precipitation estimated natural variability and observations and RCM precipitation distribution parameters: a) January, b) February, c) March, d) April, e) May, f) June, g) July, h) August, i) September, j) October, k) November, and l) December. Upper Thames catchment

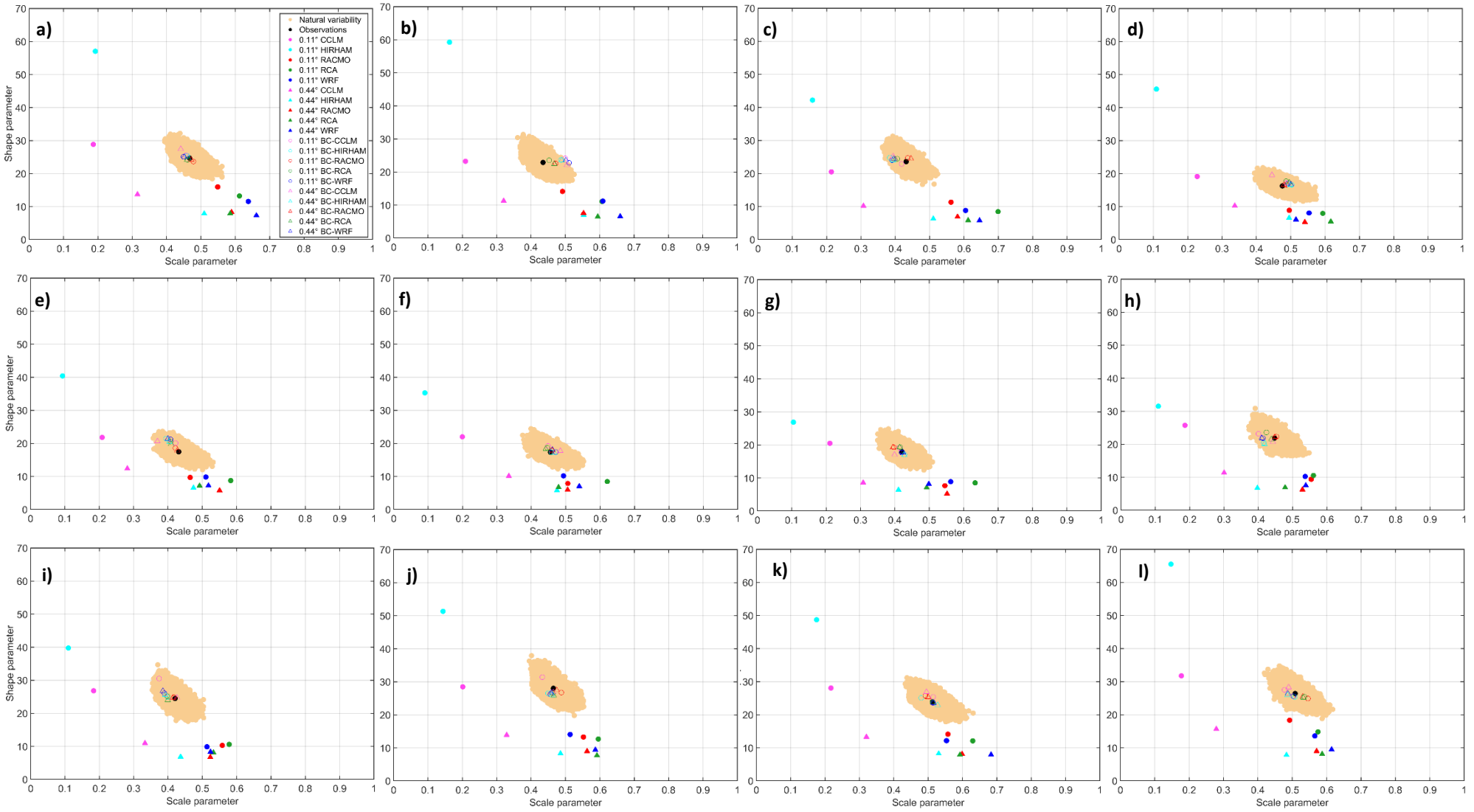

Figure 4. 14 Precipitation estimated natural variability and observations and RCM precipitation distribution parameters: a) January, b) February, c) March, d) April, e) May, f) June, g) July, h) August, i) September, j) October, k) November, and l) December. Glaslyn catchment

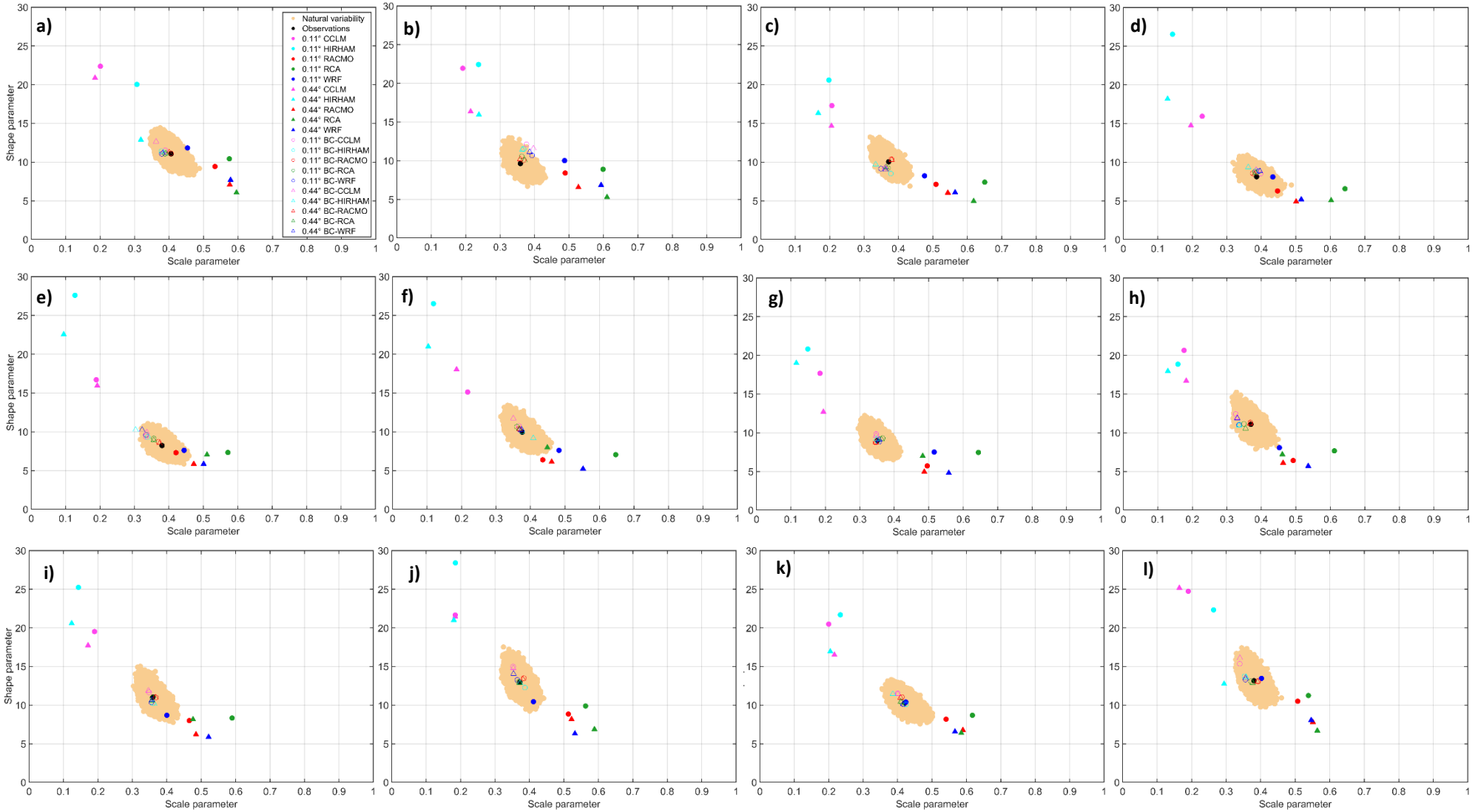

Figure 4. 15 Precipitation estimated natural variability and observations and RCM precipitation distribution parameters: a) January, b) February, c) March, d) April, e) May, f) June, g) July, h) August, i) September, j) October, k) November, and l) December. Calder catchment

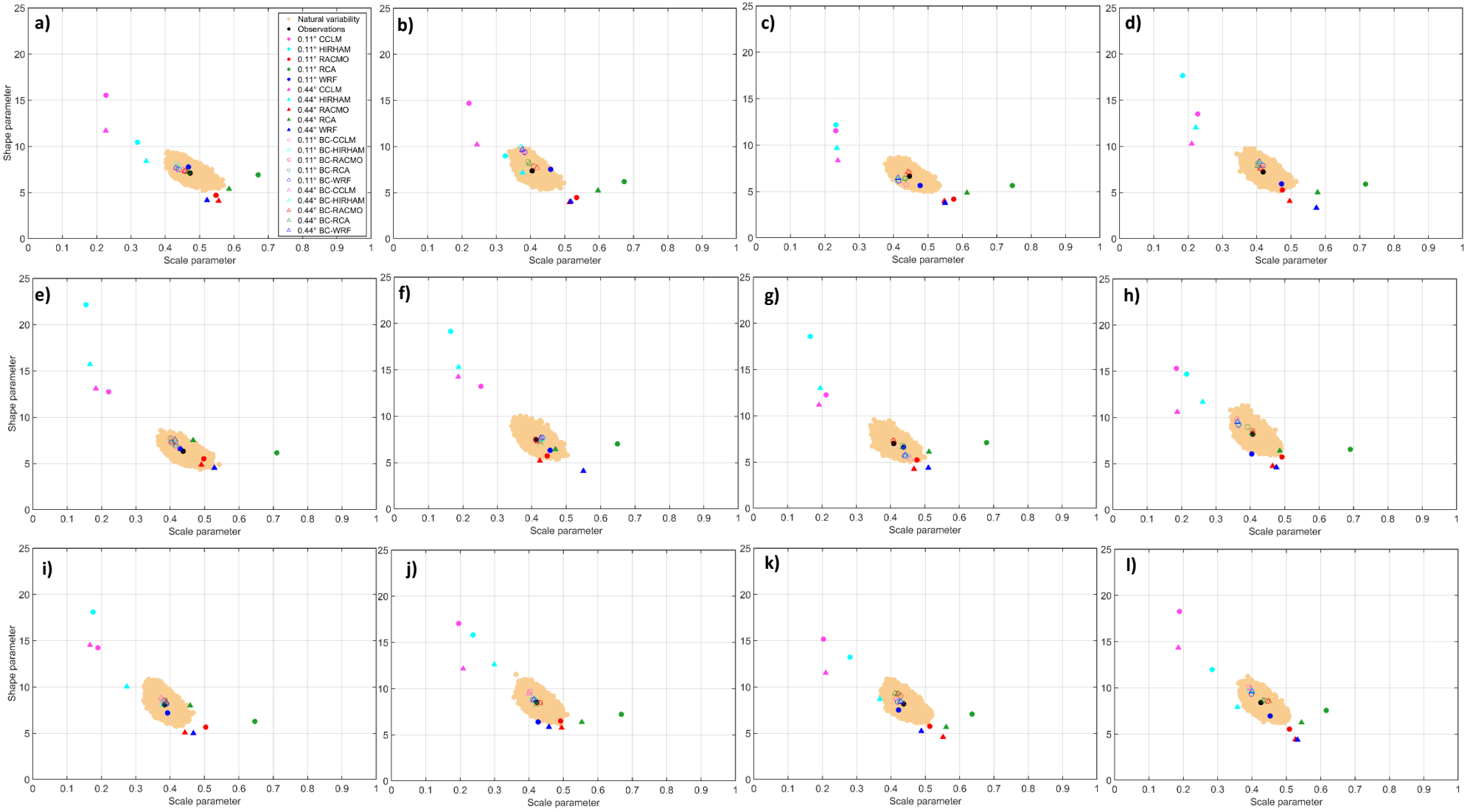

Figure 4. 16 Precipitation estimated natural variability and observations and RCM precipitation distribution parameters: a) January, b) February, c) March, d) April, e) May, f) June, g) July, h) August, i) September, j) October, k) November, and l) December. Coquet catchment

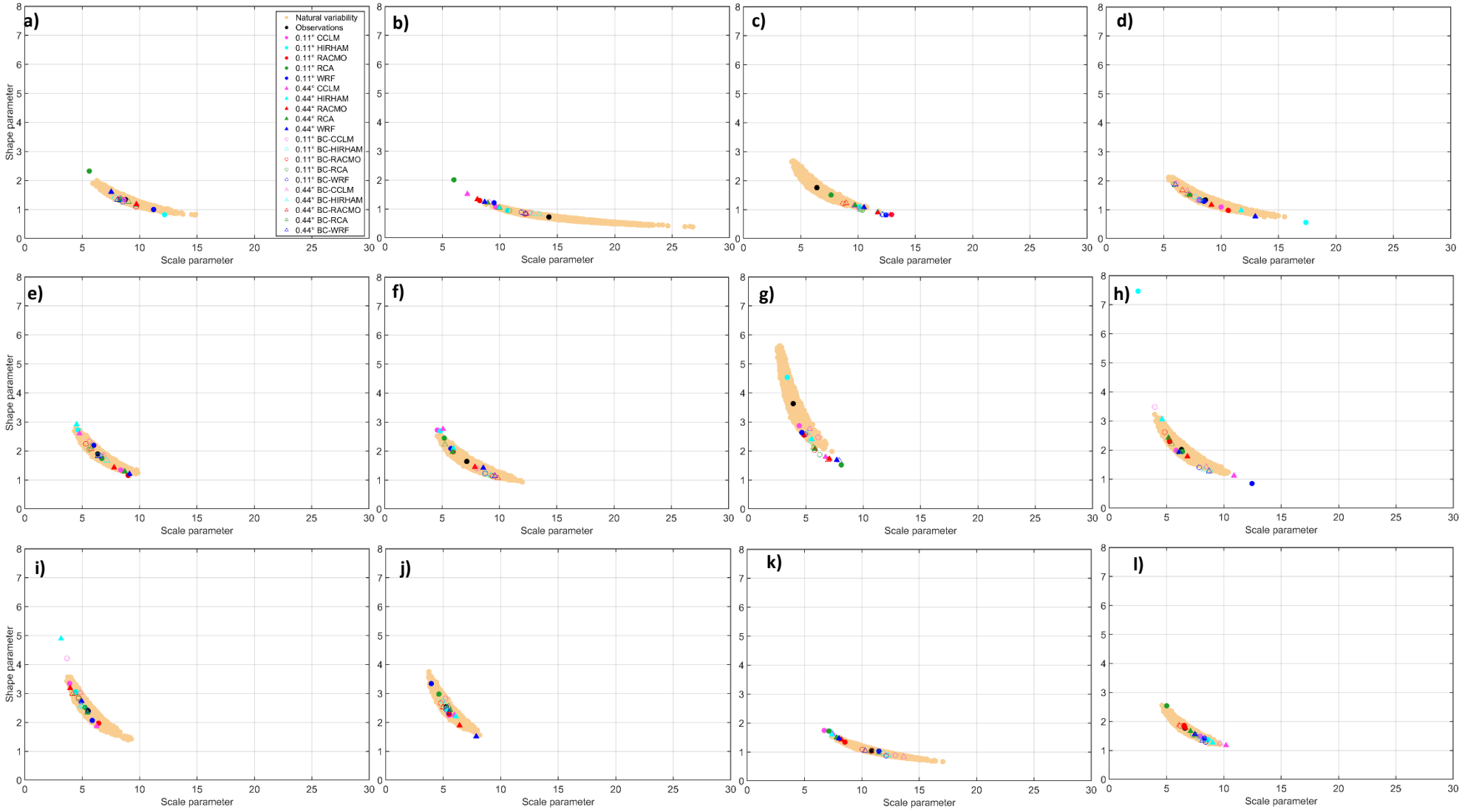

Figure 4. 17 Extreme precipitation estimated natural variability and observations and RCM extreme precipitation distribution parameters: a) January, b) February, c) March, d) April, e) May, f) June, g) July, h) August, i) September, j) October, k) November, and l) December. Upper Thames catchment

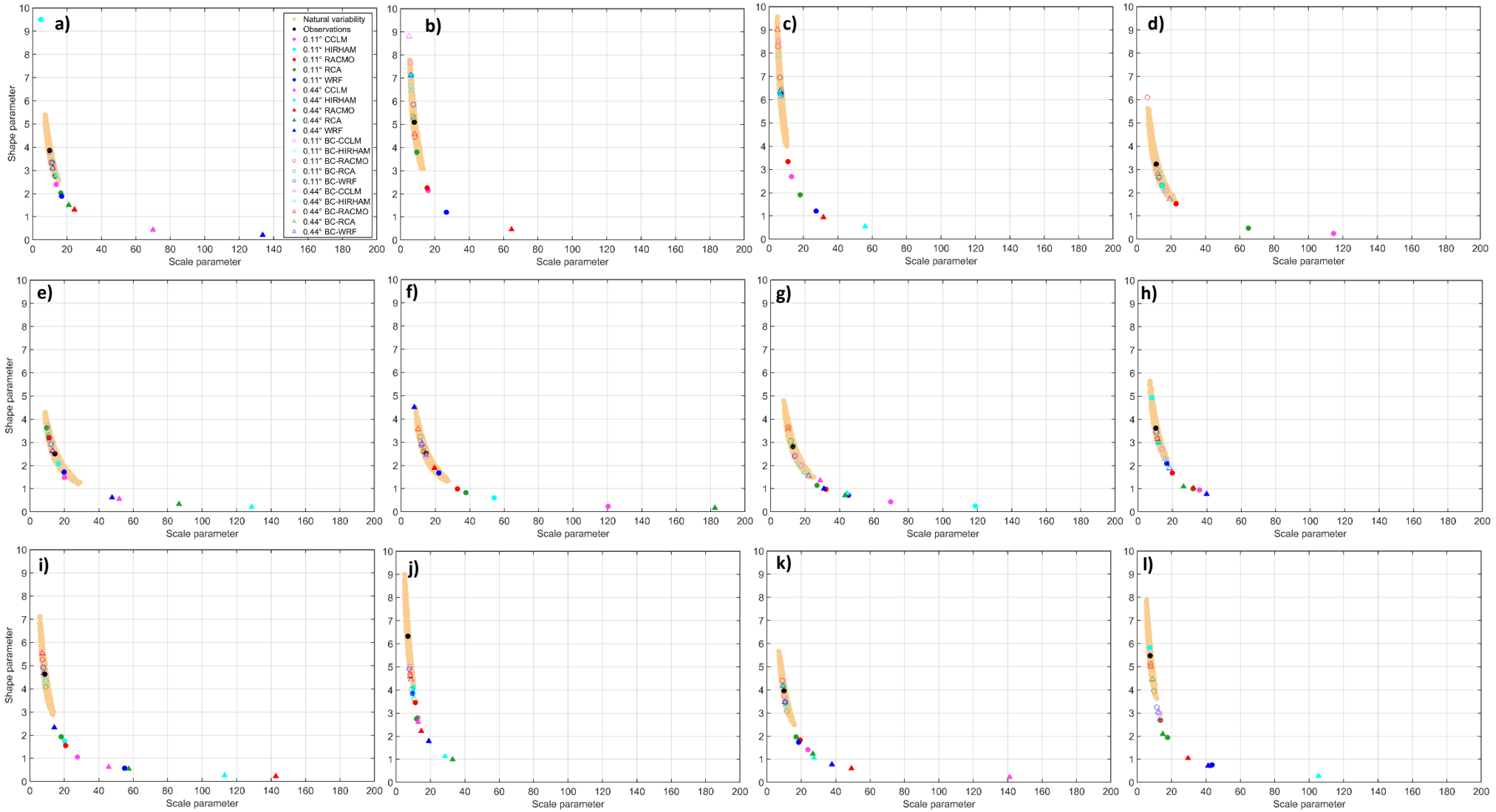

Figure 4. 18 Extreme precipitation estimated natural variability and observations and RCM extreme precipitation distribution parameters: a) January, b) February, c) March, d) April, e) May, f) June, g) July, h) August, i) September, j) October, k) November, and l) December. Glaslyn catchment

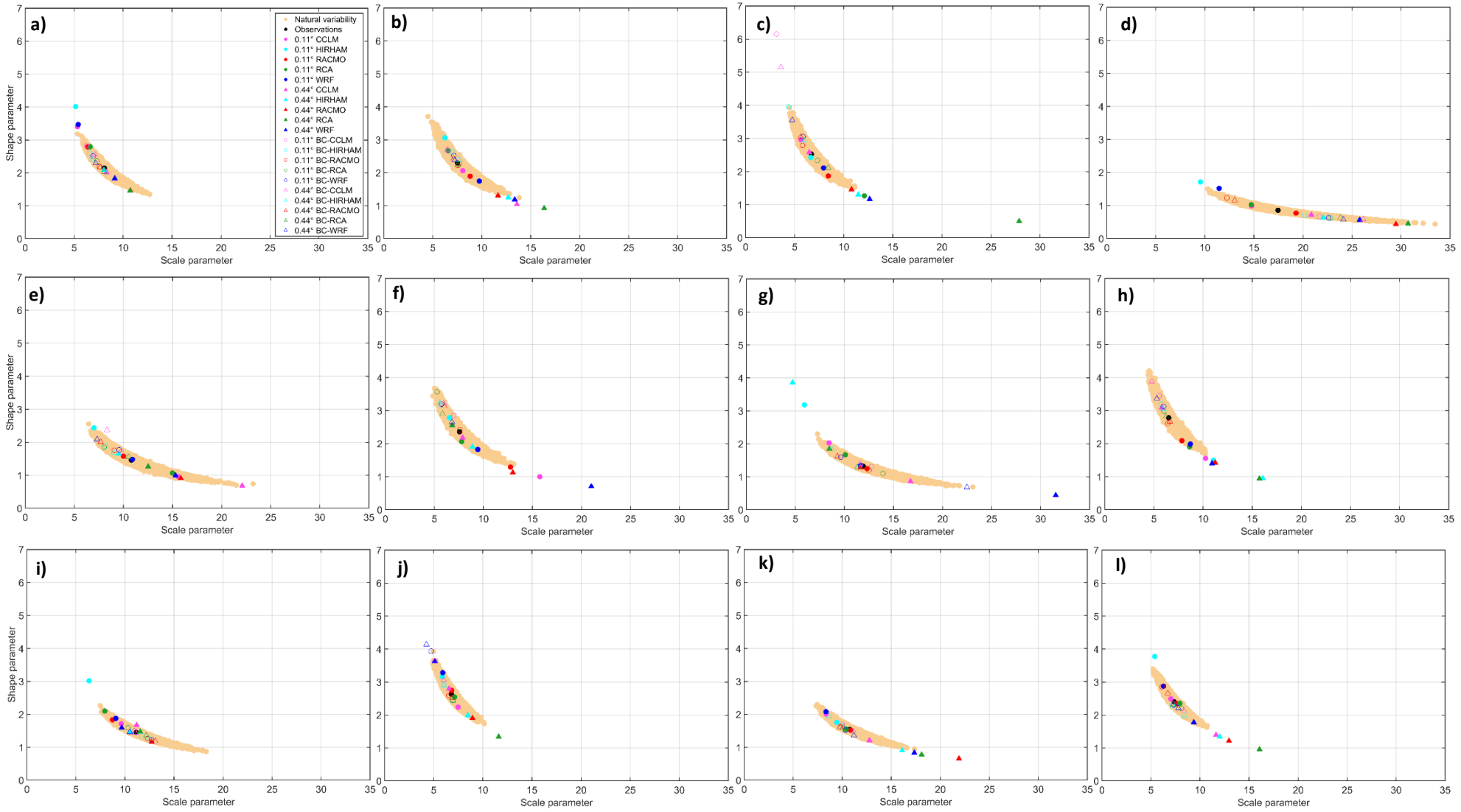

Figure 4. 19Extreme precipitation estimated natural variability and observations and RCM extreme precipitation distribution parameters: a) January, b) February, c) March, d) April, e) May, f) June, g) July, h) August, i) September, j) October, k) November, and l) December. Calder catchment

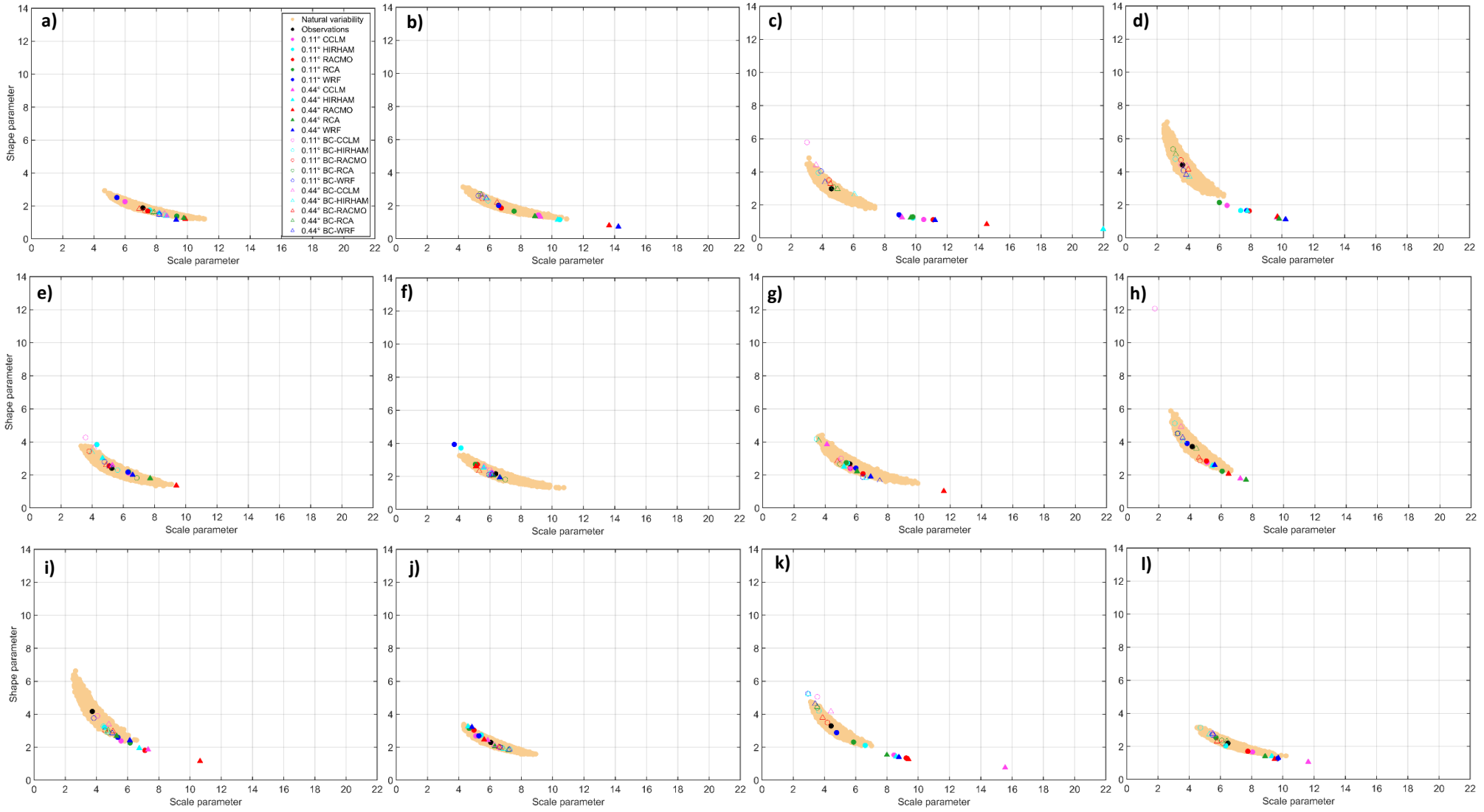

Figure 4. 20 Extreme precipitation estimated natural variability and observations and RCM extreme precipitation distribution parameters: a) January, b) February, c) March, d) April, e) May, f) June, g) July, h) August, i) September, j) October, k) November, and l) December. Coquet catchment

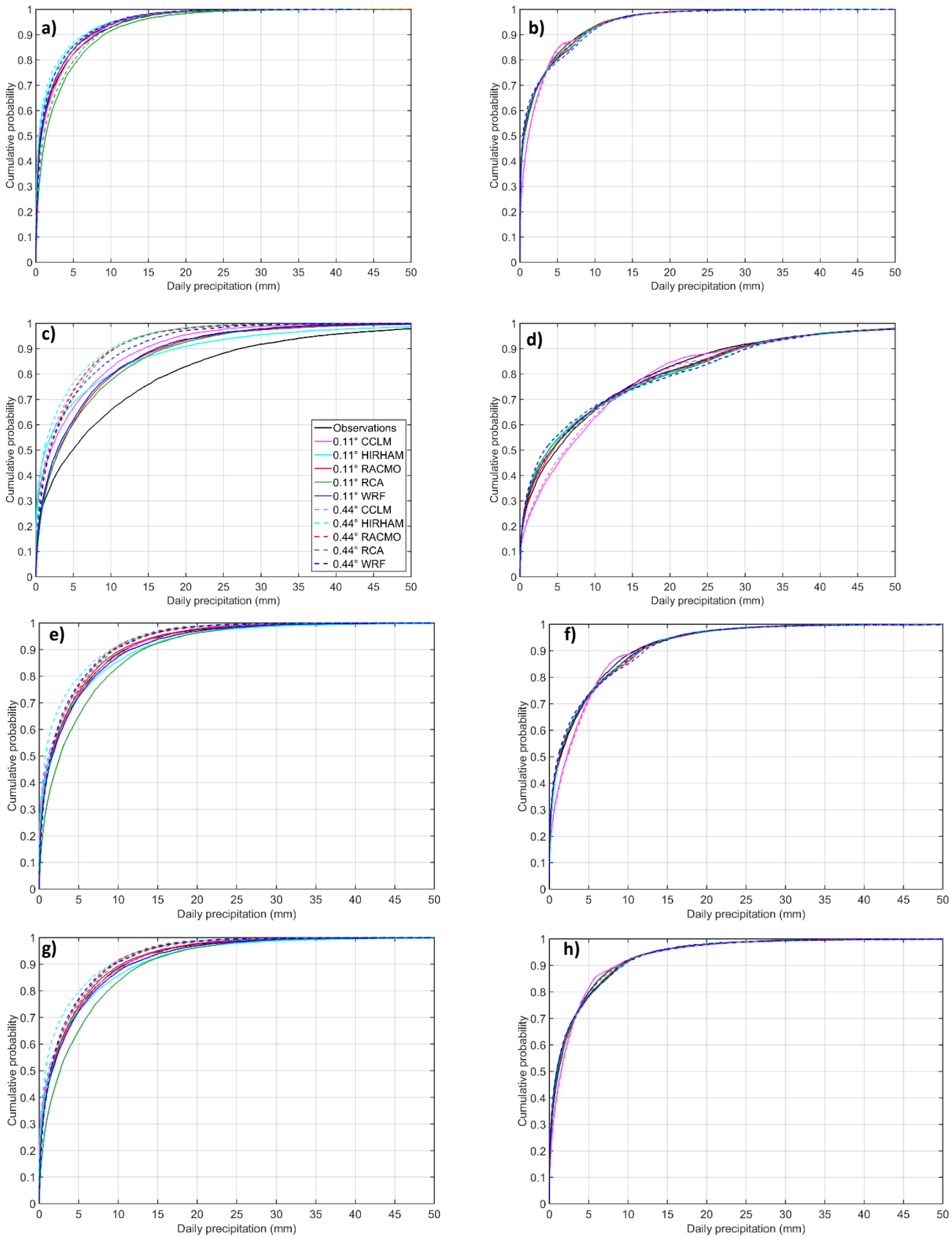

Figure 4. 21 Precipitation cumulative distribution function: a) Upper Thames uncorrected RCMs, b) Upper Thames bias-corrected (double gamma) RCMs, c) Glaslyn uncorrected RCMs, d) Glaslyn bias-corrected (double gamma) RCMs, e) Calder uncorrected RCMs, f) Calder bias-corrected (double gamma) RCMs, g) Coquet uncorrected RCMs, h) Coquet bias-corrected (double gamma) RCMs

4.3.4. Temperature metrics

In section 4.3.3, the effects of bias correction for the temperature distribution are shown using the PDF from the uncorrected and bias-corrected RCMs and comparing them with the PDF of the observations. In this section the effect of bias correction is shown using the multi-model bias spread from both RCM resolutions along the percentiles of the distribution for both the uncorrected and bias-corrected time series (Fig. 4.22). For the upper Thames and Calder catchments, the spread from the uncorrected RCMs at both resolutions is similar. Both catchments are flat and therefore there is no large difference among the temperature along the catchment. In contrast, the Glaslyn and Coquet catchments have a complex topography that is linked to large temperature differences within the catchments. Consequently, for these two catchments the 0.44° RCMs overestimate the observed temperature as they miss the differences in topography and therefore in temperature. The 0.11° RCMs simulate such changes resulting in a better performance in general. Based on the percentile biases, the upper Thames is simulated best by the RCMs, followed by the Calder, Coquet and Glaslyn catchments, in that order, showing a dependency on the topographic complexity of the catchment.

After bias correction, the bias spread from both resolutions decreases. Biases from both resolutions for all the catchments are small except for the extreme low and high percentiles. A difference among the spreads from both resolutions is no longer observed as the correction method reduces the percentile bias equally.

In general, for all RCMs at both resolutions the bias correction method reduces the biases for all of the performance measures, except for the correlation coefficient which slightly increases in most cases. The small change in the correlation coefficient is expected as the correction method modifies the distribution of the simulations but does not focus on modifying the day to day simulation. The extreme percentile biases from the uncorrected RCMs are similar for both resolutions, in other words, there is no evidence showing that a particular resolution outperforms the other for these performance measures. This is also true for the mean annual and mean monthly temperature metrics for the upper Thames catchment (Fig. 4.23). However, generally for the Glaslyn and Coquet catchments the 0.11° RCMs outperform their coarser version when evaluating the mean annual temperature bias (Figs. 4.24 and 4.26). In contrast, the coarser RCMs normally outperform the high-resolution RCMs for this performance measure in the Calder catchment (Fig. 4.25). Similarly, for the mean monthly absolute biases, the high-resolution RCMs outperform their coarser resolution version for the Glaslyn and Coquet catchments (Figs. 4.24 and 4.26), but the opposite happens for the Calder catchment (Fig. 4.25). After bias correction, the performance from all RCMs at both resolutions becomes similar without any clear indication that a particular resolution outperforms the other.

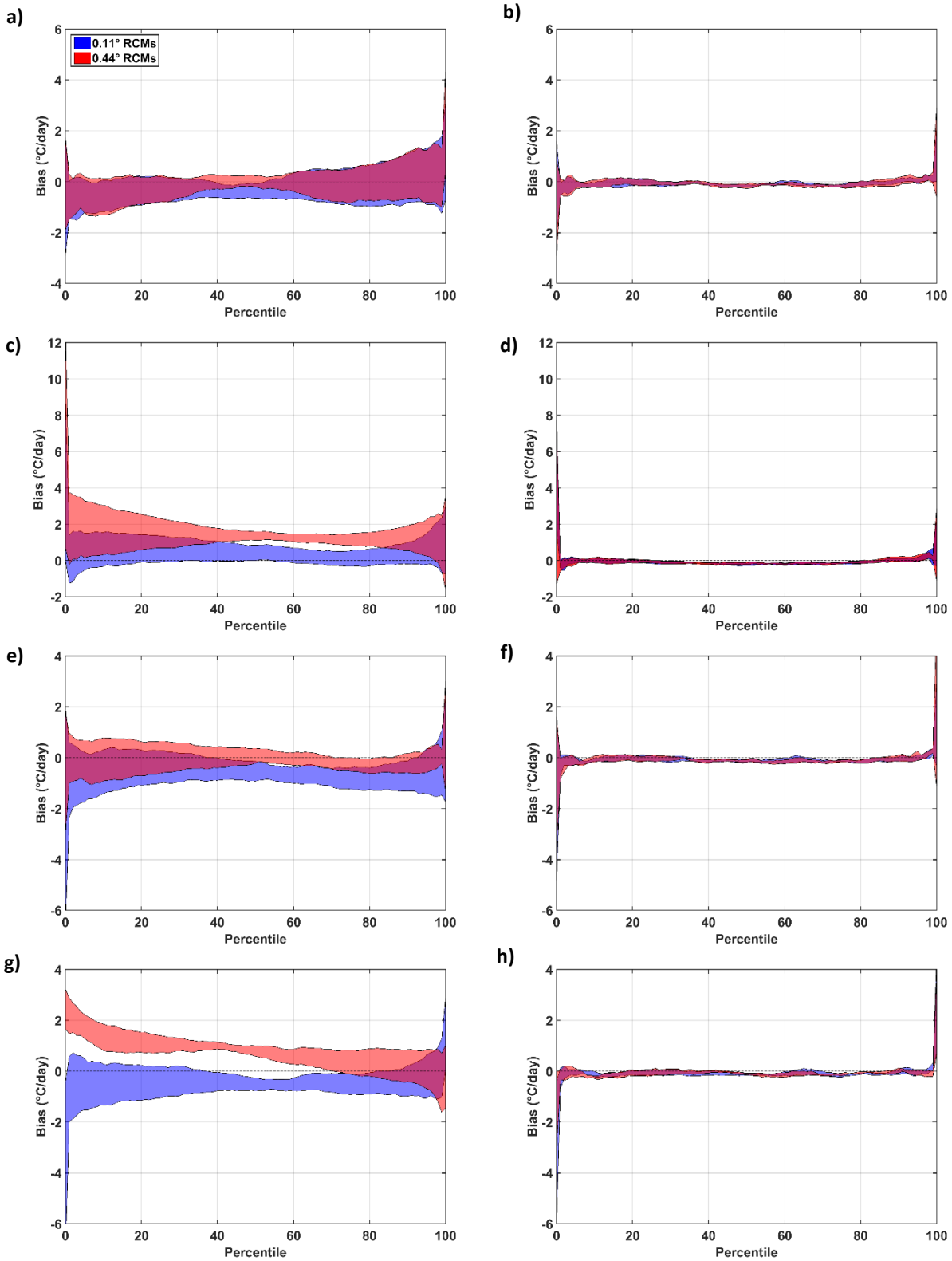

Figure 4. 22 Temperature percentile biases. The red area represents the spread form the 0.44° RCMs and the blue area the spread from the 0.11° RCMs: a) Upper Thames uncorrected RCMs, b) Upper Thames bias-corrected RCMs, c) Glaslyn uncorrected RCMs, d) Glaslyn bias-corrected RCMs, e) Calder uncorrected RCMs, f) Calder bias-corrected RCMs, g) Coquet uncorrected RCMs, h) Coquet bias-corrected RCMs

As expected, biases are smaller for all performance measures after the RCMs are bias corrected. However, exceptions are noted such as: smaller biases for the Calder catchment 99th temperature percentile metric when using the uncorrected 0.44° RACMO, 0.44° WRF and 0.44° HIRHAM (Fig. 4.25), and smaller biases for the upper Thames 1st temperature percentile when using the uncorrected 0.11° WRF (Fig. 4.23). Additionally, for the correlation coefficient some uncorrected RCMs show higher performance than their bias-corrected alternative version, indicating that bias correction does not impact this performance measure importantly.

Finally, the simulation skill of each uncorrected RCM at both resolutions is compared (see Table 4.12). A rank is given to each RCM based on their performance considering all performance measures. This provides an insight of the added value of higher resolutions RCMs compared to their coarser resolution considering the performance measures that are used. For the uncorrected RCM, two 0.11° RCMs ranked higher than their 0.44° version for the upper Thames catchment, five for the Glaslyn catchment, one for the Calder catchment and five for the Coquet catchment. Results show the added value of higher resolution uncorrected RCMs for catchments with complex topography. However, this is not valid for flat catchments in which temperature might be simulated similarly by the coarser scale simulation. The area of the catchment seems to play a minor role as the Calder and Coquet catchments have a similar extent, but the added value of high-resolution RCMs is only observed in the topographically-complex Coquet catchment. A ranking is not done for the bias-corrected simulations as the correction method implies the removal of biases and therefore the simulation skill is similar among the bias-corrected RCMs.

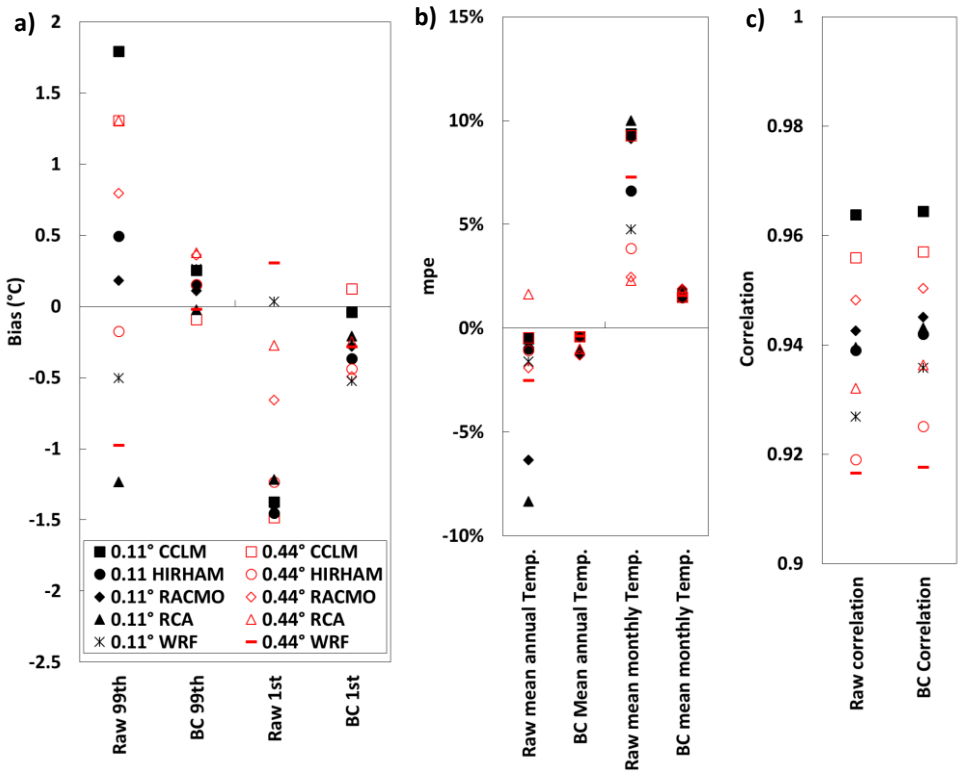

Figure 4. 23 Results for the temperature performance measures in the upper Thames catchment: a) 99th and 1st percentiles bias, b) mean annual and mean monthly (absolute) temperature bias, c) correlation coefficient

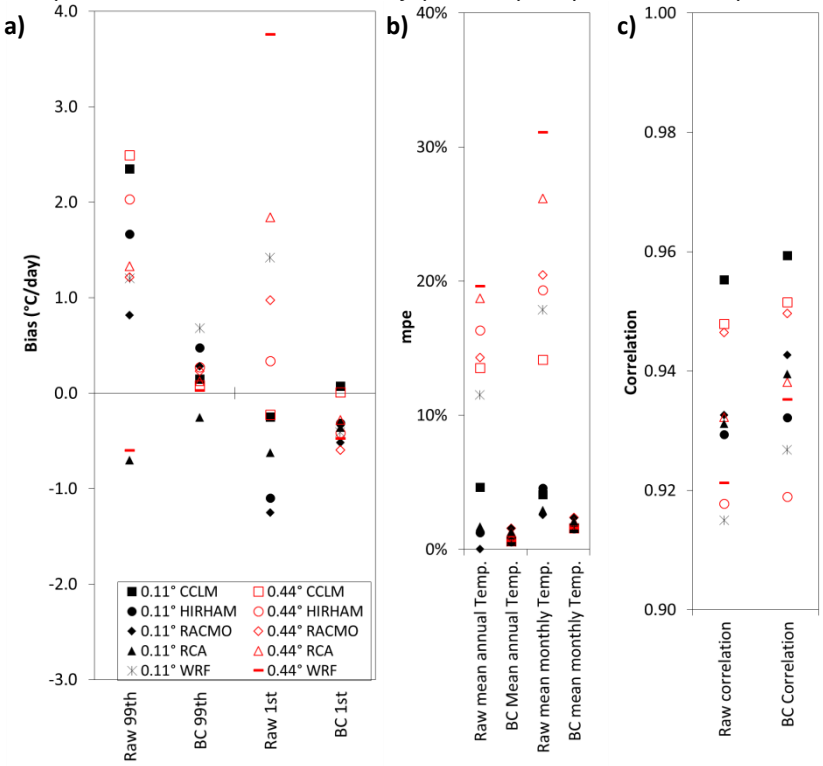

Figure 4. 24 Results for the temperature performance measures in the Glaslyn catchment: a) 99th and 1st percentiles bias, b) mean annual and mean monthly (absolute) temperature bias, c) correlation coefficient

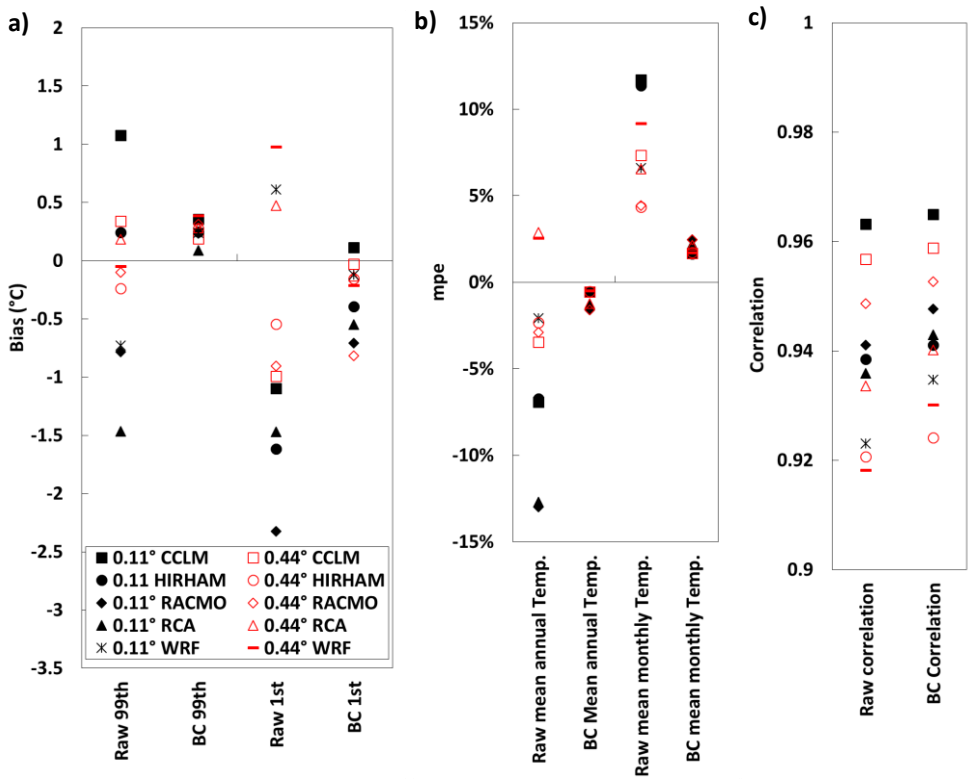

Figure 4. 25 Results for the temperature performance measures in the Calder catchment: a) 99th and 1st percentiles bias, b) mean annual and mean monthly (absolute) temperatures bias, c) correlation coefficient

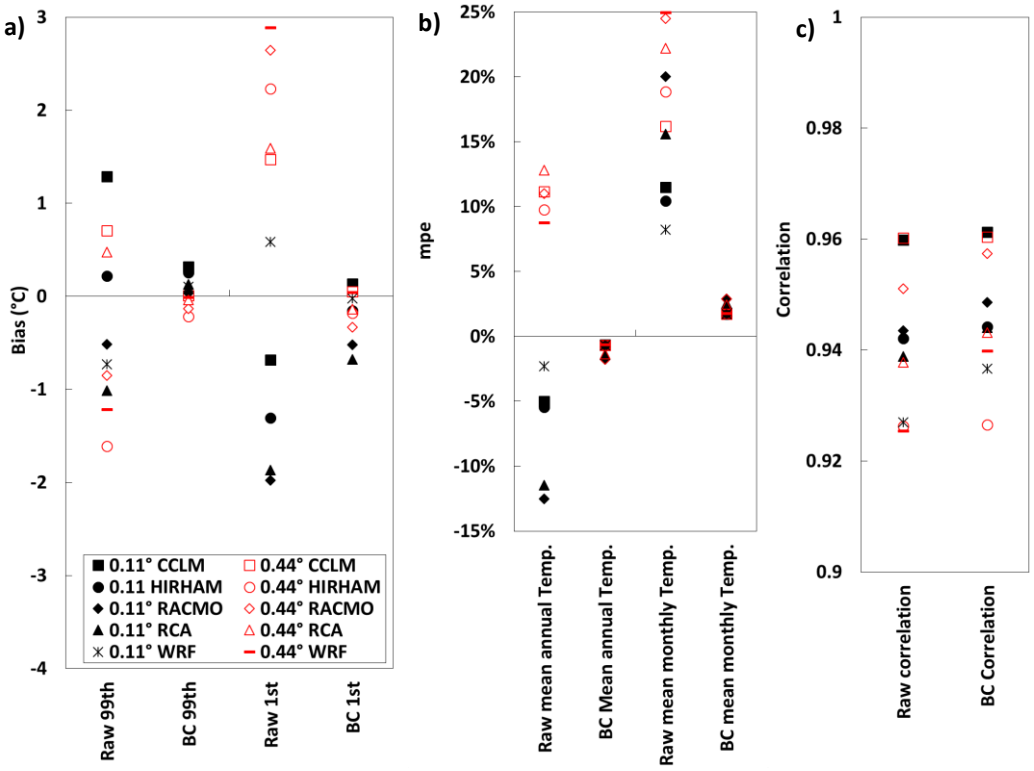

Figure 4. 26 Results for the temperature performance measures in the Coquet catchment: a) 99th and 1st percentiles bias, b) mean annual and mean monthly (absolute) temperature bias, c) correlation coefficient

Table 4. 12 Temperature performance ranking of the different uncorrected RCMs at 0.11° (11) and 0.44° (44) (1 = best, 10 = worst)

	RCM	99th percentile	1st percentile	Mean annual Temp.	Mean monthly Temp.	Correlation	Average score	Ranking
Upper Thames	0.11°CCLM	10	7	2	9	1	5.8	6
	0.11°HIRHAM	3	9	3	5	6	5.2	5
	0.11°RACMO	2	8	9	7	4	6	7
	0.11°RCA	7	5	10	10	5	7.4	10
	0.11°WRF	4	1	5	4	8	4.4	2
	0.44°CCLM	9	10	1	8	2	6	7
	0.44°HIRHAM	1	6	4	3	9	4.6	3
	0.44°RACMO	5	4	7	2	3	4.2	1
	0.44°RCA	8	2	6	1	7	4.8	4
	0.44°WRF	6	3	8	6	10	6.6	9
Glaslyn	0.11°CCLM	9	2	4	3	1	3.8	3
	0.11°HIRHAM	7	6	2	4	7	5.2	5
	0.11°RACMO	3	7	1	1	4	3.2	1
	0.11°RCA	2	4	3	2	6	3.4	2
	0.11°WRF	4	8	5	6	10	6.6	7
	0.44°CCLM	10	1	6	5	2	4.8	4
	0.44°HIRHAM	8	3	8	7	9	7	8
	0.44°RACMO	5	5	7	8	3	5.6	6
	0.44°RCA	6	9	9	9	5	7.6	9
	0.44°WRF	1	10	10	10	8	7.8	10
Calder	0.11°CCLM	9	7	8	8	1	6.6	7
	0.11°HIRHAM	5	9	7	7	5	6.6	7
	0.11°RACMO	8	10	10	10	4	8.4	9
	0.11°RCA	10	8	9	9	6	8.4	9
	0.11°WRF	7	3	1	4	8	4.6	4
	0.44°CCLM	6	6	6	5	2	5	5
	0.44°HIRHAM	4	2	2	1	9	3.6	2
	0.44°RACMO	2	4	5	2	3	3.2	1
	0.44°RCA	3	1	4	3	7	3.6	2
	0.44°WRF	1	5	3	6	10	5	5
Coquet	0.11°CCLM	9	2	2	3	2	3.6	3
	0.11°HIRHAM	1	3	3	2	5	2.8	1
	0.11°RACMO	3	7	9	7	4	6	5
	0.11°RCA	7	6	8	4	6	6.2	6
	0.11°WRF	5	1	1	1	8	3.2	2
	0.44°CCLM	4	4	7	5	1	4.2	4
	0.44°HIRHAM	10	8	5	6	9	7.6	9
	0.44°RACMO	6	9	6	9	3	6.6	8
	0.44°RCA	2	5	10	8	7	6.4	7
	0.44°WRF	8	10	4	10	10	8.4	10

4.3.5.Precipitation metrics

Historically, RCMs tend to have larger biases when simulating precipitation compared to their simulation of temperature. This is more evident in regions of complex topography. The Euro-CORDEX RCMs continue having this issue as it has been demonstrated by Torma et al. (2015) and Prein et al. (2015). Figure 4.27 shows the multi-model bias spread from all precipitation percentiles for both RCM resolutions. For the uncorrected RCMs, biases are larger for the Glaslyn catchment, which has the more complex topography, supporting the findings from Torma et al. (2015) and Prein et al. (2015). In general, biases at all catchments increase approximately after the 50th percentile. For the upper Thames catchment, the percentile biases are smaller than for the rest of the catchments. After the gamma-distribution bias correction the percentile biases decrease for all catchments until approximately the 90th percentile (Fig. 4.27, frames e, f, g, h). Below the 90th percentile biases are generally lower than 1 mm/day for most of the catchments, and reduced importantly for the Glaslyn catchment. Nevertheless, after the 90th percentile, the percentile biases increase exponentially for all catchments. Therefore, the double gamma bias correction is applied by dividing the distribution in two at the 90th percentile. For all catchments, after applying the double gamma bias correction the percentile biases after the 90th percentile decrease compared to the gamma bias correction (Fig. 4.27, frames i, j, k, l). However, a pattern in all catchment is observed: at the 90th percentile there is a maximum bias for all catchments. This maximum is not present in the gamma bias correction. Therefore, it can be stated that, compared to the gamma bias correction, the double gamma bias correction decreases the overall percentile biases, but generates a systematic bias in the percentile at which the distribution is divided. Also, the double gamma correction has large biases for the very extreme precipitation percentiles (approximately the 99th percentile).

In general, both bias correction methods reduce the biases for all metrics and catchments (Figs. 4.28 to 4.31). For the 95th percentile metric, bias correction reduces the bias from all catchments with the double gamma providing the lowest biases. For the 90th percentile biases are generally larger for the double gamma correction method compared to the gamma method because of the reason explained in the previous paragraph. For the 50th and 25th percentile metrics, the biases from both correction methods are similar. For the SDII, in general the uncorrected RCMs have the smaller biases in the upper Thames and Coquet catchments (Figs 4.28 and 4.31). For all catchments the mean annual and monthly biases are reduced similarly by both correction methods. The monthly MSE is only reduced by the correction methods for the Glaslyn catchment (Fig. 4.29). The R95p is only reduced by the double gamma method and the correlation does not change greatly after bias correction. For some RCMs the mean dry and wet spells performance improved after bias correction, but not for all RCMs. In general, the biases in the R10 and R20 metrics decreased more with the double gamma method, but this varies according to the analysed catchment.

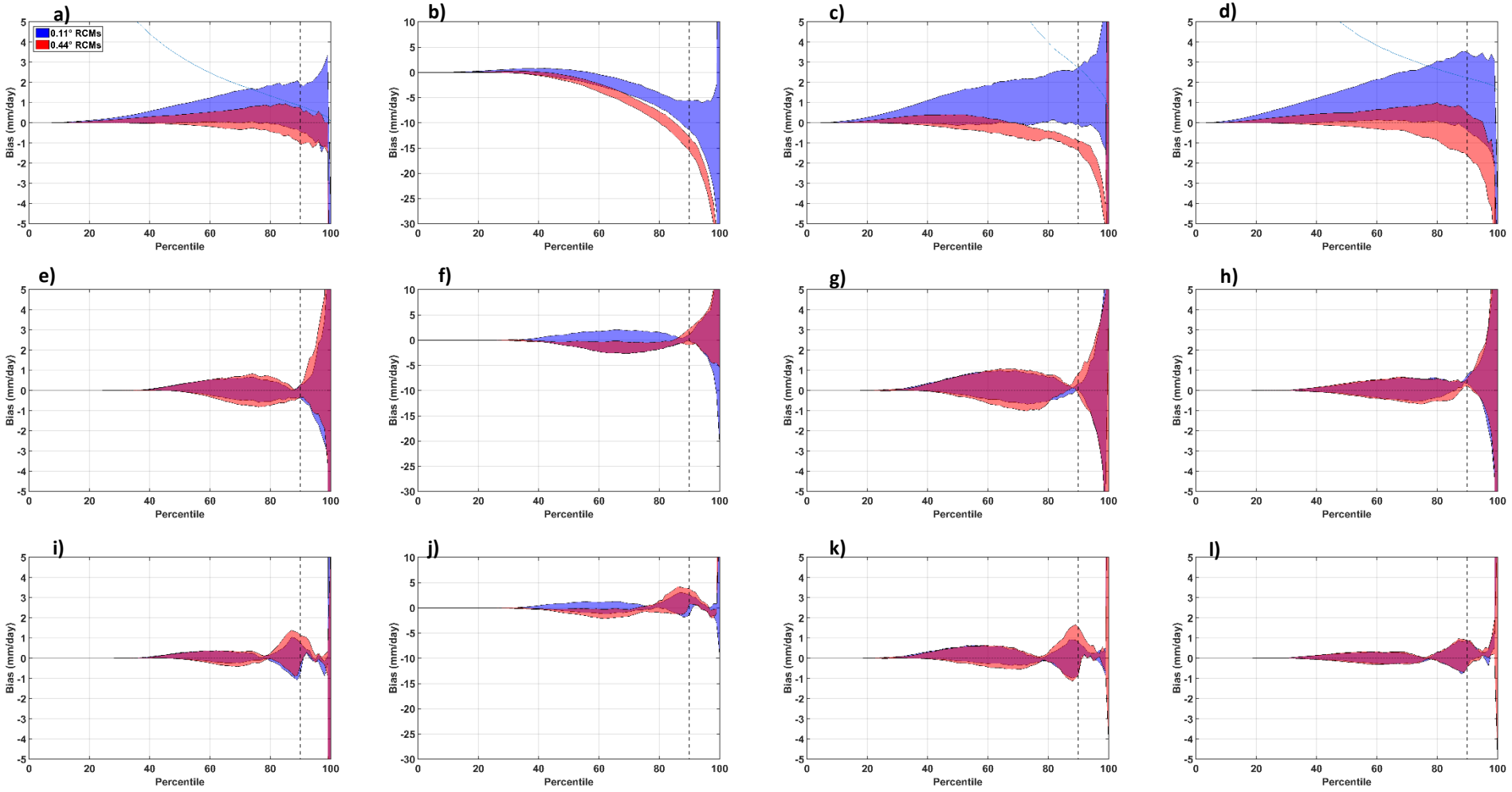

Figure 4. 27 Precipitation percentile biases. The blue area represents the spread form the 0.44° RCMs and the red area the spread from the 0.11° RCMs: uncorrected RCMs for a) Upper Thames, b) Glaslyn, c) Calder, d) Coquet; bias-corrected RCMs using the gamma distribution for e) upper Thames, f) Glaslyn, g) Calder, h) Coquet; bias-corrected RCMs using the double-gamma distribution for i) upper Thames, j) Glaslyn, k) Calder, l) Coquet. The dotted vertical line represents the precipitation 90th percentile

The application of the double gamma bias correction includes the determination of more distribution parameters, increasing the uncertainty in the correction process. Therefore, it is important to assess whether the results from applying a double gamma bias correction support the increased uncertainty. In general, both bias correction approaches reduce the biases for most of the performance measures at all catchments and for every RCM. Nevertheless, some exceptions are observed. The mean wet spell length is frequently better simulated by the uncorrected RCMs. There are also cases where the SDII biases are smaller for the uncorrected RCMs (in the upper Thames for most RCMs –Fig. 4.28- and in the Calder and Coquet –Figs. 4.30 and 4.31- for some RCMs). For the Glaslyn catchment, the uncorrected RCMs have the larger biases because of the difficulty to reproduce its complex topography in a small area (Fig. 4.29). For the rest of the catchments, uncorrected RCMs have the smaller biases for a few performance measures, but no other pattern is observed. The uncorrected RCA model normally has the largest biases for all catchments and most of the performance measures.

Comparing the results from both correction methods, performance depends on the RCM, but the double gamma bias correction has smaller biases for most catchments and performance measures. Nevertheless, for the 90th percentile metric the double gamma correction method has larger bias than the gamma method (Fig. 4.27, frames i, j, k, l) as a result of the problem discussed in the first paragraph of this section. For the Glaslyn catchment, the double gamma correction has larger biases for the R20 metric for all RCMs (Fig. 4.29). Similarly, in the Calder catchment the double gamma correction has larger biases for the R10 metric when applied to the HIRHAM, RACMO and RCA models (Fig. 4.30). Also, when applied to the CCLM model it results in larger biases for the 50th percentile in the upper Thames, Calder and Coquet. In the Coquet catchment, the method results in larger biases for the monthly MSE metric when using the WRF, CCLM and HIRHAM RCMs and for the RX1day metric when using the HIRHAM and RCA models (Fig. 4.31). Finally, the method has larger biases for the annual mean precipitation in the Calder when correcting the CCLM and HIRHAM RCMs (Fig. 4.30) and in the Coquet when applied to the CCLM RCM (Fig. 4.31). The double gamma method doesn't always reduce the biases as the results depend on the catchment, RCM and performance measure analysed. However, in general for most of the performance measures results show a decrease in the biases for all catchments after correcting the precipitation using the double gamma method, except for the cases mentioned above.

The performance from each uncorrected RCM is compared to identify a benefit from using a particular model resolution (see Table 4.13). Results show that only the use of high-resolution in the Glaslyn catchment provides a clear added value compared to their coarser resolution as the final rank of all high-resolution models is better. In contrast, for the rest of the catchments there is no clear benefit from using the high-resolution models as it varies between RCMs. In the upper Thames two uncorrected 0.11° RCMs outperforms their coarser versions, three in the Calder catchment and three in the Coquet catchment. After applying bias correction, the performance of all RCMs and resolutions becomes similar due to the construction of the correction method. Therefore, a ranking of skill simulation would not give significant results.

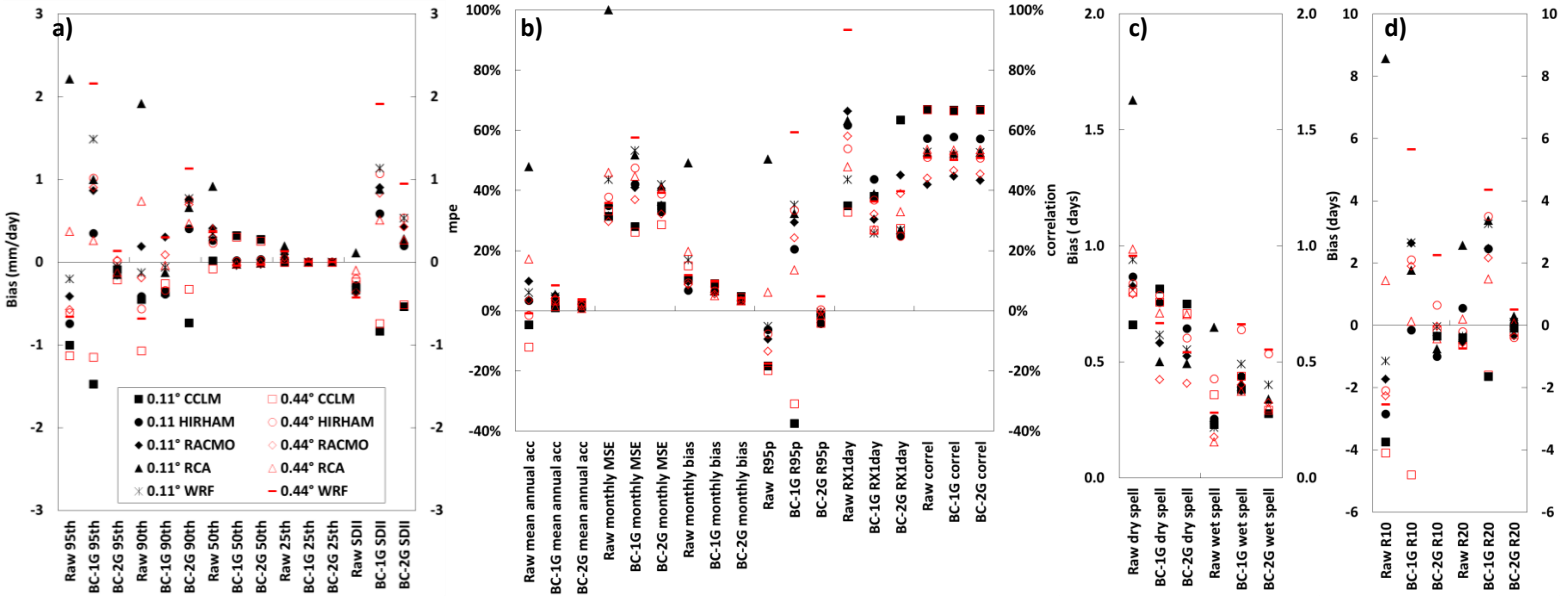

Figure 4. 28 Results for the precipitation performance measures in the upper Thames catchment: a) 95th , 90th , 50th , 25th percentiles and SDII bias, b) mean annual and monthly (absolute) precipitation bias, monthly MSE, R95p, RX1day and correlation, c) dry and wet spell length, d) R10 and R20

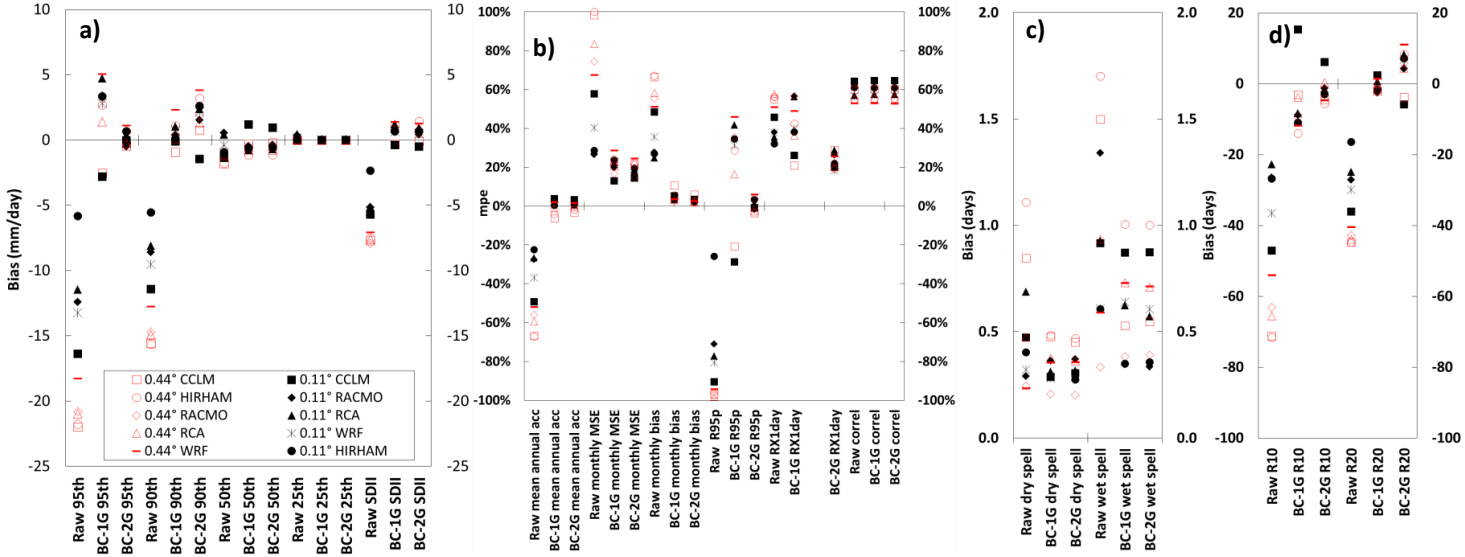

Figure 4. 29 Results for the precipitation performance measures in the Glaslyn catchment: a) 95th , 90th , 50th , 25th percentiles and SDII bias, b) mean annual and monthly (absolute) precipitation bias, monthly MSE, R95p, RX1day and correlation, c) dry and wet spell length, d) R10 and R20

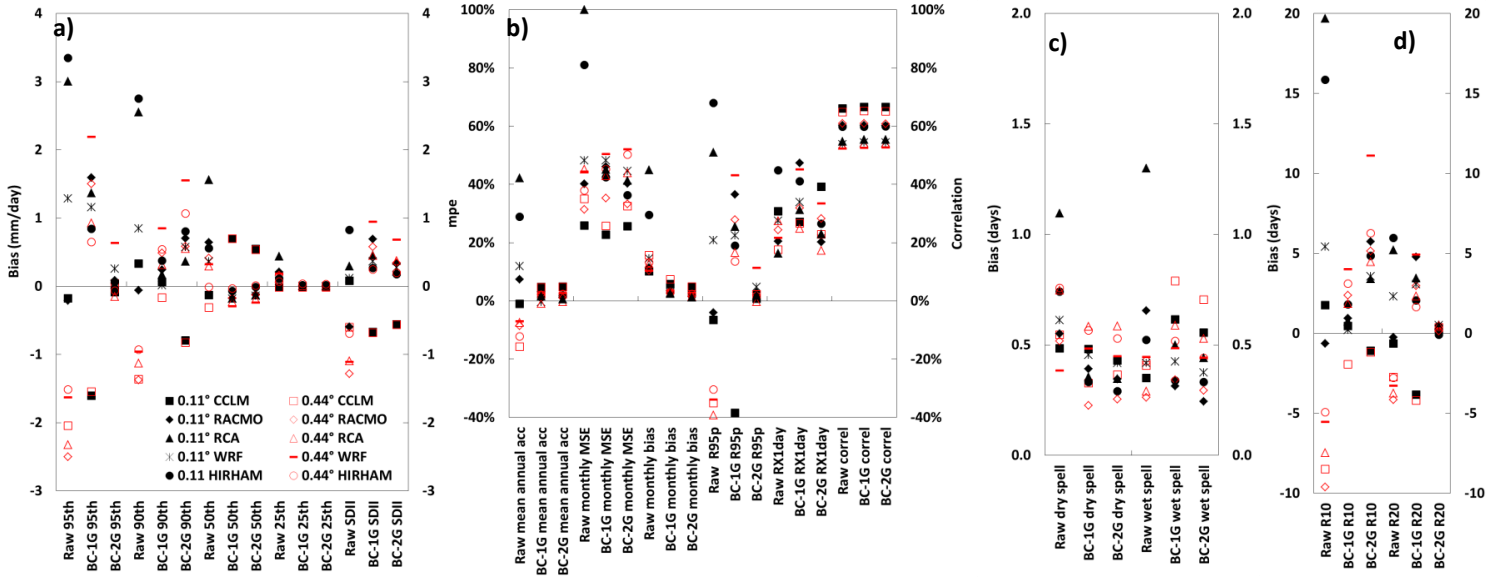

Figure 4. 30 Results for the precipitation performance measures in the Calder catchment: a) 95th , 90th , 50th , 25th percentiles and SDII bias, b) mean annual and monthly (absolute) precipitation bias, monthly MSE, R95p, RX1day and correlation, c) dry and wet spell length, d) R10 and R20

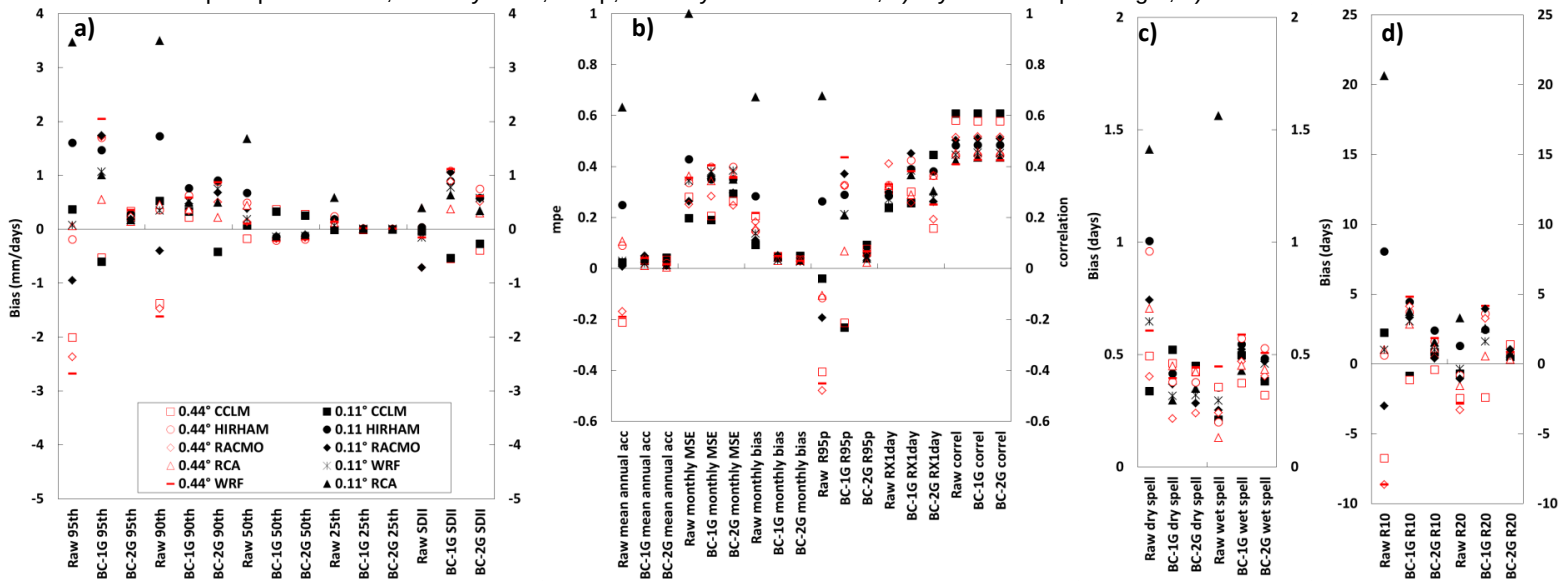

Figure 4. 31 Results for the precipitation performance measures in the Coquet catchment: a) 95th , 90th , 50th , 25th percentiles and SDII bias, b) mean annual and monthly (absolute) precipitation bias, monthly MSE, R95p, RX1day and correlation, c) dry and wet spell length, d) R10 and R20

Table 4. 13 Precipitation performance ranking of the different RCMs at 0.11° (11) and 0.44°(44), before and after bias correction (1 = best, 10 = worst)

	RCM	95th Pctl	90th Pctl	50th Pctl	25th Pctl	Mean Annual Precip	Monthly MSE	Dry Spell Mean Length	Wet Spell Mean Length	Monthly Bias	Correlation	SDII	R10	R20	R95p	RX1day	Average score	Ranking
Upper Thames	11CCLM	8	5	1	2	5	2	1	4	5	1	6	8	4	8	2	4.13	1
	11HIRHAM	7	4	4	3	3	5	6	6	1	3	5	7	6	3	7	4.67	4
	11RACMO	3	2	9	8	7	3	4	5	4	10	9	3	5	5	9	5.73	8
	11RCA	10	10	10	10	10	10	10	10	10	6	2	10	10	10	8	9.07	10
	11WRF	1	1	6	7	6	8	7	3	8	5	7	1	3	1	3	4.47	2
	44CCLM	9	9	2	1	8	4	3	8	7	2	4	9	8	9	1	5.6	7
	44HIRHAM	5	6	3	5	2	7	5	9	3	7	3	4	1	4	5	4.6	3
	44RACMO	4	3	5	6	4	1	2	2	2	9	8	5	7	6	6	4.67	4
	44RCA	2	8	8	4	9	9	9	1	9	4	1	2	1	2	4	4.87	6
	44WRF	6	7	7	9	1	6	8	7	6	8	10	6	9	7	10	7.13	9
Glaslyn	11CCLM	5	5	8	2	5	5	6	5	5	1	5	5	5	5	5	4.8	5
	11HIRHAM	1	1	6	5	1	3	5	3	2	3	1	3	1	1	1	2.47	1
	11RACMO	3	3	3	9	3	1	3	8	3	2	3	2	3	2	4	3.47	3
	11RCA	2	2	2	10	2	2	8	6	1	6	2	1	2	3	2	3.4	2
	11WRF	4	4	1	6	4	4	4	4	4	7	4	4	4	4	3	4.07	4
	44CCLM	10	9	10	3	9	9	9	9	9	5	9	9	9	8	7	8.27	9
	44HIRHAM	9	10	9	1	10	10	10	10	10	9	7	10	10	9	9	8.87	10
	44RACMO	7	7	4	7	7	7	2	1	7	4	10	7	7	7	8	6.13	7
	44RCA	8	8	7	4	8	8	7	7	8	8	8	8	8	10	10	7.8	8
	44WRF	6	6	5	8	6	6	1	2	6	10	6	6	6	6	6	5.73	6
Calder	11CCLM	1	2	2	1	1	1	2	3	1	1	1	2	2	2	9	2.07	1
	11HIRHAM	10	10	8	5	9	9	7	8	9	5	7	9	10	10	10	8.4	9
	11RACMO	2	1	9	9	3	5	5	9	4	4	4	1	1	1	3	4.07	2
	11RCA	9	9	10	10	10	10	10	10	10	6	3	10	9	9	1	8.4	9
	11WRF	3	3	6	4	6	8	6	5	7	8	2	4	3	3	8	5.07	5
	44CCLM	6	7	4	2	8	3	4	4	8	2	5	7	4	6	2	4.8	3
	44HIRHAM	4	4	1	3	7	4	9	6	6	7	6	3	5	4	5	4.93	4
	44RACMO	8	8	7	7	5	2	3	1	3	3	10	8	8	8	6	5.8	7
	44RCA	7	6	3	6	4	7	8	2	5	9	8	6	7	7	7	6.13	8
	44WRF	5	5	5	8	2	6	1	7	2	10	9	5	6	5	4	5.33	6
Coquet	11CCLM	4	5	1	1	2	1	1	3	1	1	3	4	2	1	2	2.1	1
	11HIRHAM	6	9	9	7	9	9	9	7	9	5	1	7	5	6	4	6.8	8
	11RACMO	5	3	6	8	1	3	7	5	2	4	9	5	4	5	5	4.8	4
	11RCA	10	10	10	10	10	10	10	10	10	9	7	10	9	10	1	9.1	10
	11WRF	2	1	5	3	3	6	5	6	3	7	5	2	1	2	3	3.6	2
	44CCLM	7	6	4	2	8	4	3	8	7	2	3	6	7	7	6	5.3	6
	44HIRHAM	3	2	8	9	4	5	8	2	4	8	1	1	3	4	8	4.7	3
	44RACMO	8	7	3	4	6	2	2	4	6	3	9	8	10	9	10	6.1	7
	44RCA	1	4	7	5	5	8	6	1	5	6	7	3	6	3	7	4.9	5
	44WRF	9	8	2	6	7	7	4	9	8	10	5	9	8	8	9	7.3	9

4.3.6. River flow metrics

The effect of bias correction towards the spread simulation of river flow is illustrated in Figure 4.32. The top row shows the simulated flow duration curve using the uncorrected RCM outputs. Except for the Glaslyn catchment, the RCMs spread range covers the observations for all catchments. In contrast, both resolutions underestimate the river flow for the Glaslyn catchment. Using the bias-corrected temperature and precipitation (Gamma distribution), in all catchments the spread of the simulation is reduced and most of the observations are covered by the simulation spread (middle row). The observations from the Glaslyn catchment are covered after this bias correction. Finally, after using the precipitation outputs corrected using the double Gamma distribution, the spread reduces even more for all catchments (bottom row). Most of the observed flow duration curves are covered by the simulation spread, but there are some sections that lie outside the simulation spread, which could also be an effect of the hydrological model uncertainty.

In general, the bias spread considering all RCMs reduces after bias correction. For most of the performance measures, the bias spread reduction is greater after applying the double Gamma bias correction method. Nevertheless, in some cases the spread suffers no great change when applying the double Gamma bias correction compared to the Gamma method, for example the mean winter flow in the Calder catchment (Fig. 4.35) or mean autumn flow in the Glaslyn catchment (Fig. 4.34). In general, for all catchments the mean annual and seasonal flows are simulated better by the bias corrected RCMs. However, the bias magnitude also depends of the skill of the hydrological model. In other words, the biases from a bias-corrected RCM might be large because of the skill of the hydrological model that is used, for example mean summer flow in the upper Thames catchment (Fig. 4.33), for which the hydrological model has problems simulating low flows (section 3.6). The monthly MSE change after bias correction varies depending on the RCM, but as a group, the biases in all RCMs decrease. The Spearman correlation coefficient after bias correction also varies according to the RCM, but in general varies more for river flow than for precipitation. The monthly NSE improves by bias correction, generating only positive values after applying the method. In general, the Q10, Q95, and mean annual Q10 frequency bias spread decreases when bias corrected, and RCMs are normally more accurate for these metrics after the double Gamma bias correction method. The accuracy of the double Gamma bias-corrected RCMs is adequate for all metrics and catchments, except for the mean summer river flow that has large bias for all catchments except for the Glaslyn catchment.

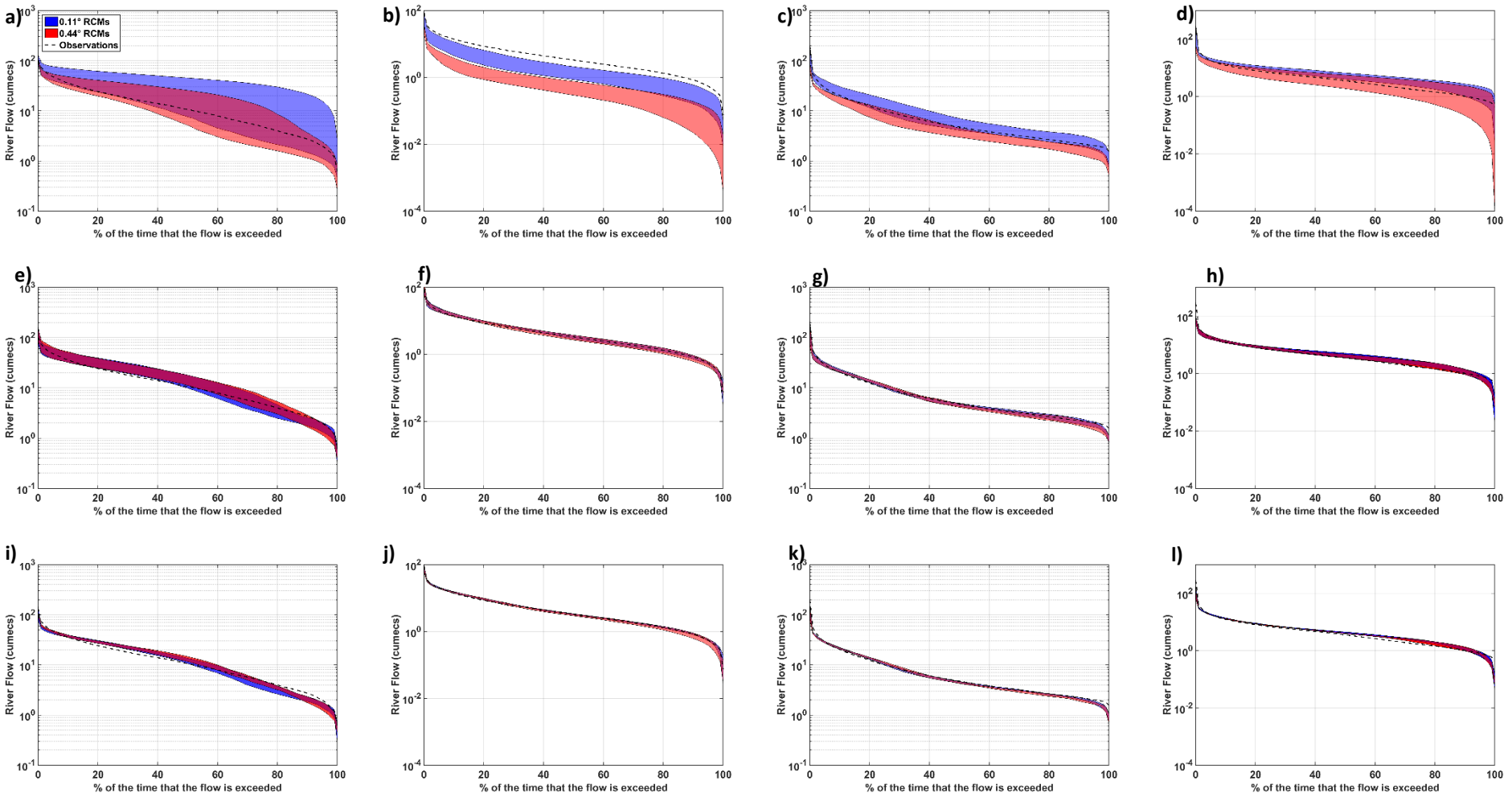

Figure 4. 32 River flow duration curves. The blue area represents the spread form the 0.44° RCMs and the red area the spread from the 0.11° RCMs: uncorrected RCMs for a) Upper Thames, b) Glaslyn, c) Calder, d) Coquet; bias-corrected RCMs using the gamma distribution for e) upper Thames, f) Glaslyn, g) Calder, h) Coquet; bias-corrected RCMs using the double-gamma distribution for i) upper Thames, j) Glaslyn, k) Calder, l) Coquet. The dotted vertical line represents the precipitation 90th percentile

A comparison between the river flow biases for all performance measures and RCMs at each catchment is useful to evaluate whether the uncorrected RCMs provide satisfactory simulations or if they would benefit from the application of simple or more complex bias-correction techniques. In general, for all catchments the uncorrected RCMs at both resolutions have the larger biases. However, there are some exceptions, such as the uncorrected 0.11° CCLM at the Coquet catchment (Fig. 4.36) and the uncorrected 0.44° RACMO and WRF at the Calder catchment (Fig. 4.35). A comparison between the Gamma distribution and double Gamma distribution bias correction techniques becomes complex as the reduction in bias from the correction depends on the RCM, resolution and the catchment where it is applied. For example, for the upper Thames, the double Gamma bias correction applied to the 0.11° HIRHAM, RCA and WRF have the smaller bias. However, for RACMO, the double Gamma bias corrected 0.44° RACMO has the smaller bias. In general, the results show that the correction method with smaller bias depends on the catchment and used RCM, which might be an effect of the uncorrected simulation that is better corrected by one method than the other for specific evaluation measures (also seen by Casanueva et al., 2016). However, in the majority of the cases the double Gamma distribution bias correction outperforms the Gamma distributions bias correction.

Table 4.14 compares the performance from each RCM at both resolutions. A rank integrates the results from all performance measures for each RCM. This provides an insight on the benefit of higher resolutions RCMs compared to their coarser resolution. It is only in the Glaslyn catchment that all the uncorrected high-resolution RCMs outperform their low resolution version. In contrast, only two uncorrected high-resolution RCMs outperform their low resolution version for the upper Thames and Coquet catchments, and only one for the Calder catchment. These results show that it is only for the Glaslyn catchment that there is a clear improvement in model skill from using the 0.11° RCMs over the 0.44° RCMs. However, as shown above, the biases from the uncorrected high-resolution RCMs are generally large and inadequate for impact assessments in this catchment. As discussed in the previous sections, a ranking of the simulation skill after bias correction would not give robust results as the correction improves the skill of the models to a similar extent.

In order to determine whether a particular uncorrected RCM outperforms the others, the results from Table 4.14 are used. From the uncorrected RCMs the 0.11° HIRHAM outperforms the other RCMs for the upper Thames and Glaslyn catchments, whereas for the Calder and Coquet catchments, the 0.11°CCLM RCM has the smaller bias in general. The location of the catchments might play a role in the results, as the southernmost catchments are simulated better by 0.11° HIRHAM and the northernmost by 0.11° CCLM, but this needs further research which is out of the scope of this thesis. Both RCMs have a 0.11° resolution, which indicates a benefit from using high-resolution RCMs. However, as shown above, this is not always true as the benefit from the 0.11° resolution over the 0.44° resolution is RCM-dependent.

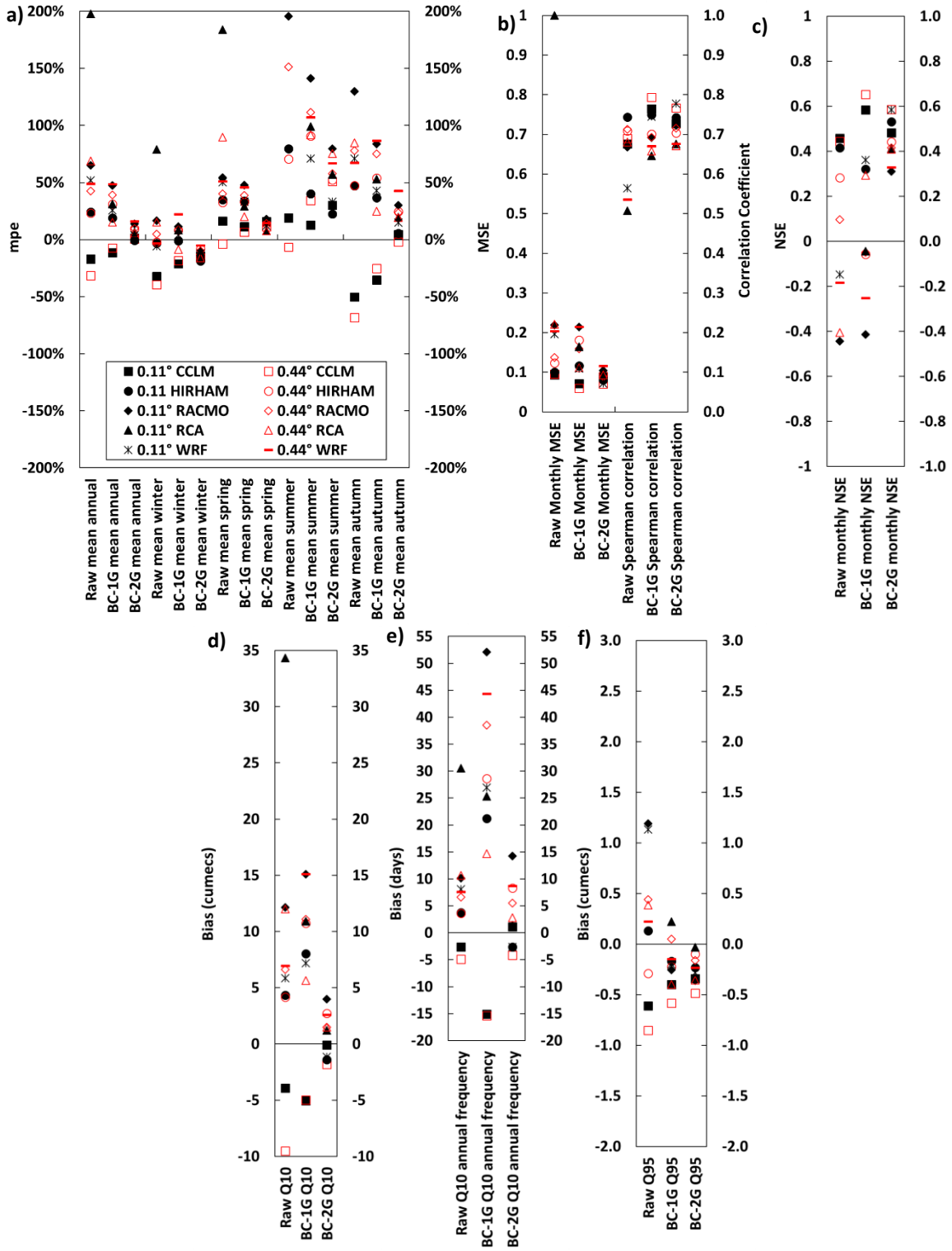

Figure 4. 33 Results for the river flow performance measures in the upper Thames catchment: a) annual and seasonal mean bias, b) mean square error and Spearman correlation coefficient, c) NSE, d) Q10 bias, e) Q10 annual frequency bias, f) Q95 bias, please note the different scale in the y-xis

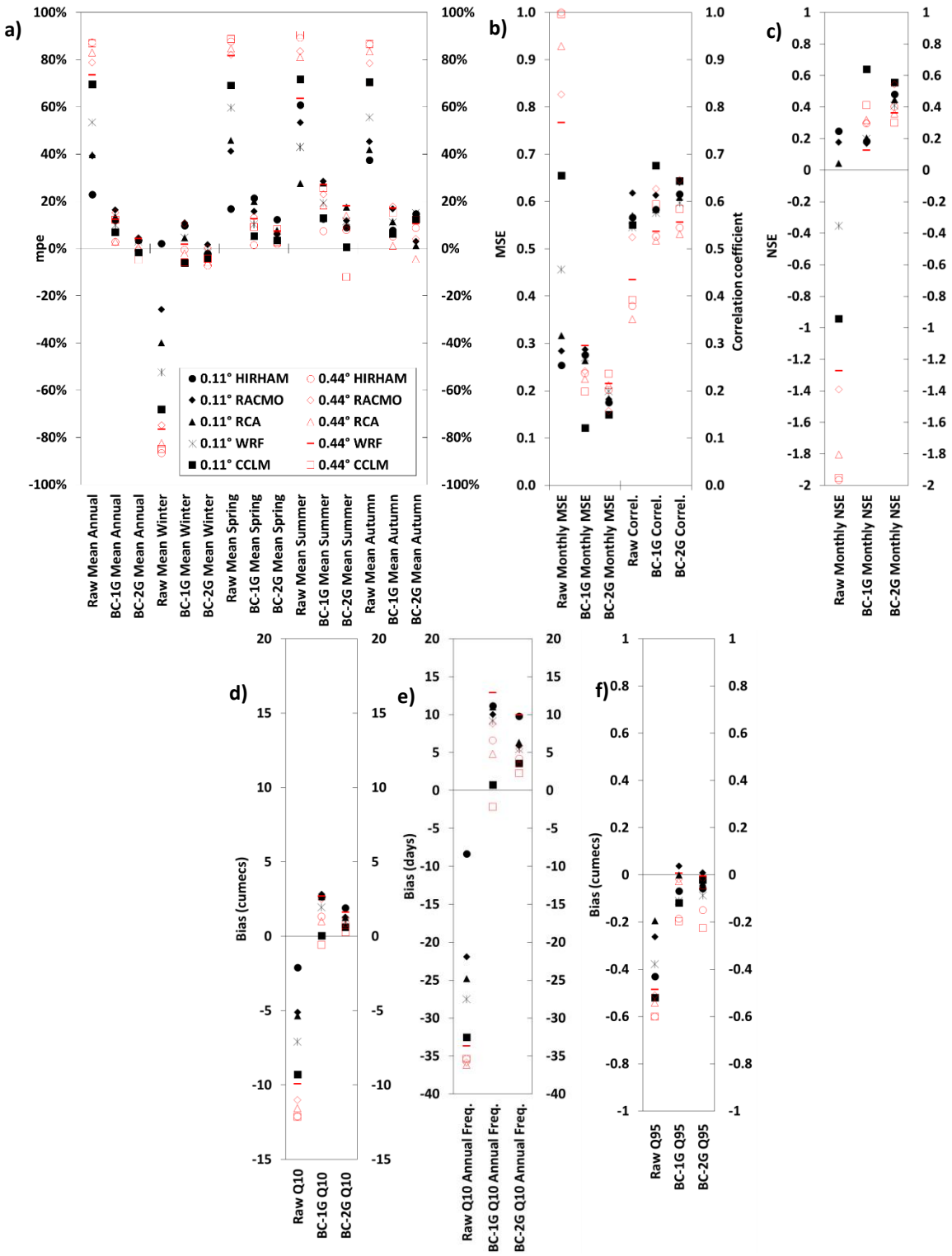

Figure 4. 34 Results for the river flow performance measures in the Glaslyn catchment: a) annual and seasonal mean bias, b) mean square error and Spearman correlation coefficient, c) NSE, d) Q10 bias, e) Q10 annual frequency bias, f) Q95 bias, please note the different scale in the y-xis

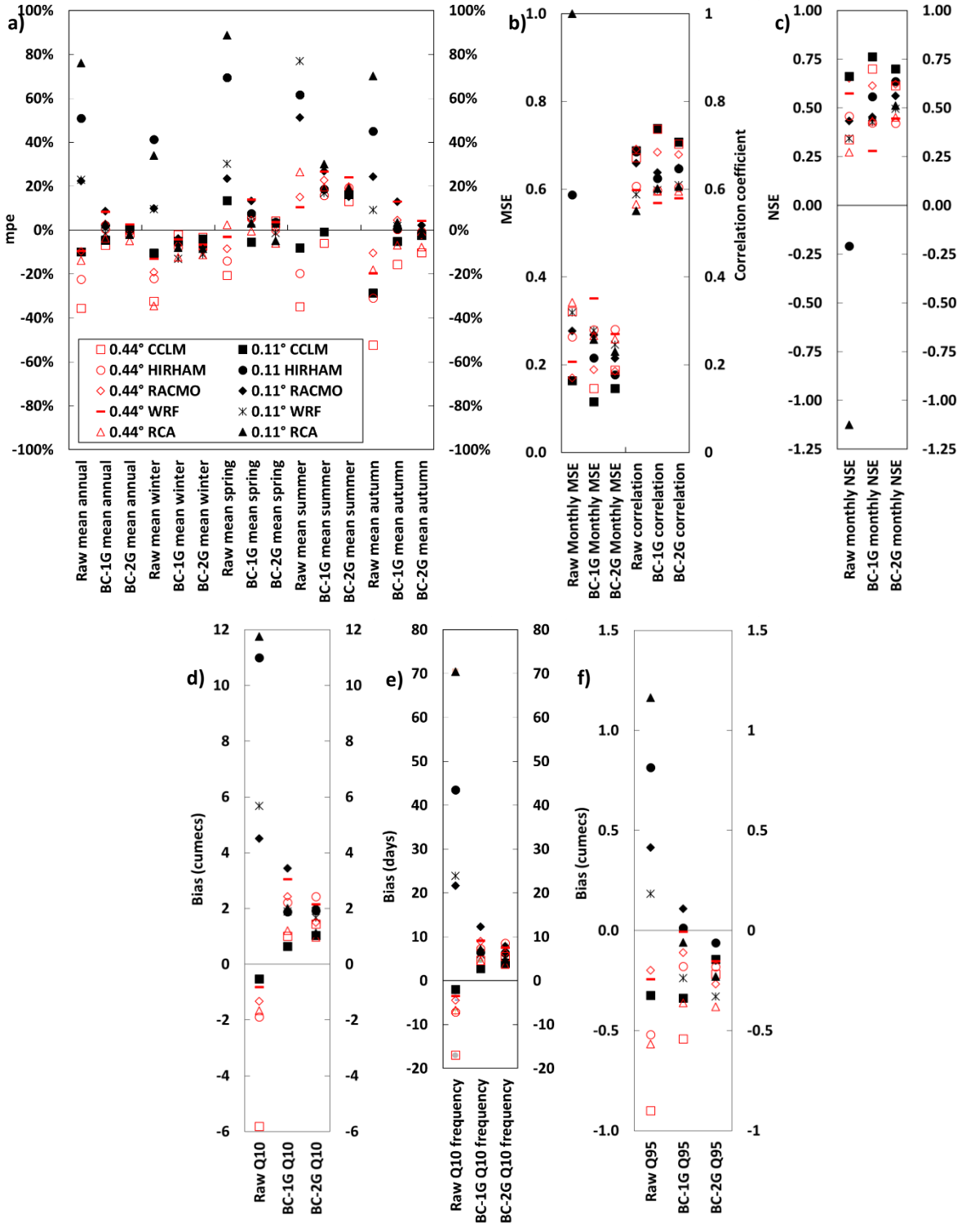

Figure 4. 35 Results for the river flow performance measures in the Calder catchment: a) annual and seasonal mean bias, b) mean square error and Spearman correlation coefficient, c) NSE, d) Q10 bias, e) Q10 annual frequency bias, f) Q95 bias, please note the different scale in the y-xis

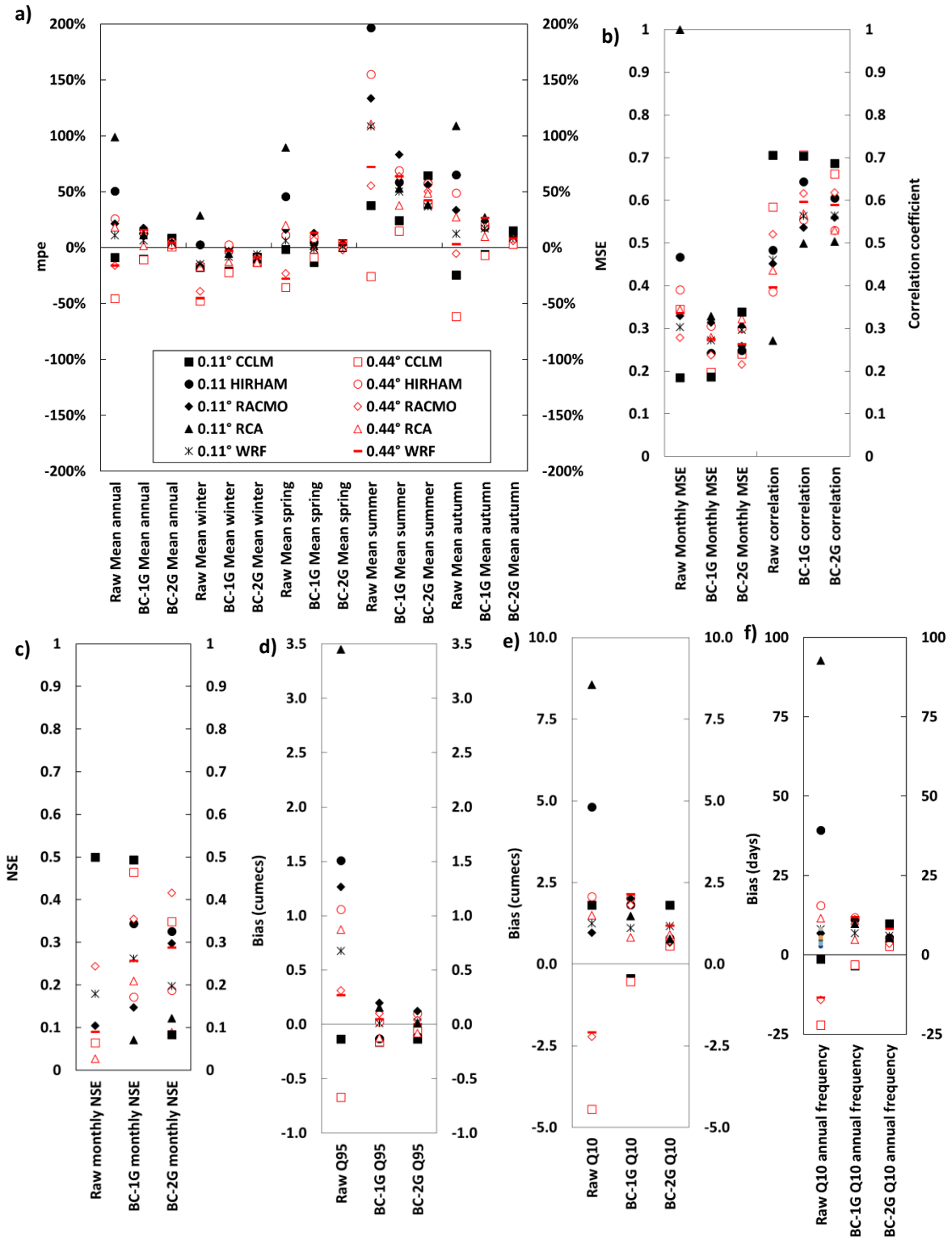

Figure 4. 36 Results for the river flow performance measures in the Coquet catchment: a) annual and seasonal mean bias, b) mean square error and Spearman correlation coefficient, c) NSE, d) Q10 bias, e) Q10 annual frequency bias, f) Q95 bias, please note the different scale in the y-xis

Table 4. 14 River flow performance ranking of the different RCMs at 0.11° (11) and 0.44°(44), before and after bias correction (1 = best, 10 = worst)

	RCM	Q10	Q10 Annual Freq.	Q95	Mean annual river flow	Monthly NSE	Monthly MSE	Mean winter river flow	Mean spring river flow	Mean Summer river flow	Mean autumn river flow	Spearman correlation	Average Performance	Ranking
Upper Thames	11CCLM	1	1	6	1	1	1	8	2	2	3	6	2.9	3
	11HIRHAM	3	3	1	3	3	3	2	4	4	1	1	2.5	1
	11RACMO	9	8	9	8	9	8	7	8	6	9	7	8.0	9
	11RCA	10	10	10	10	10	10	10	10	10	10	10	10	10
	11WRF	4	7	8	7	6	6	5	6	9	6	8	6.5	7
	44CCLM	7	4	7	4	2	2	9	1	1	5	4	4.2	4
	44HIRHAM	2	2	3	2	4	4	1	3	3	2	3	2.6	2
	44RACMO	5	5	5	5	5	5	4	5	5	7	2	4.8	5
	44RCA	8	9	4	9	8	9	6	9	7	8	5	7.5	8
	44WRF	6	6	2	6	7	7	3	7	8	4	9	5.9	6
Glaslyn	11CCLM	5	5	7	5	5	5	5	5	6	6	4	5.3	5
	11HIRHAM	1	1	4	1	3	1	1	1	4	1	3	1.9	1
	11RACMO	2	2	2	2	2	2	2	2	3	3	1	2.1	2
	11RCA	3	3	1	3	1	3	3	3	1	2	2	2.3	3
	11WRF	4	4	3	4	4	4	4	4	2	4	5	3.8	4
	44CCLM	10	7	9	9	9	9	9	10	10	10	8	9.1	9
	44HIRHAM	9	7	10	10	10	10	10	9	9	9	9	9.3	10
	44RACMO	7	9	6	7	7	7	6	7	8	7	6	7.0	7
	44RCA	8	10	8	8	8	8	8	8	7	8	10	8.3	8
	44WRF	6	6	5	6	6	6	7	6	5	5	7	5.9	6
Calder	11CCLM	1	1	4	3	1	1	3	4	1	6	2	2.5	1
	11HIRHAM	9	9	8	9	9	9	10	9	8	8	3	8.3	9
	11RACMO	6	7	5	6	5	5	2	7	7	5	5	5.5	5
	11RCA	10	10	10	10	10	10	8	10	10	10	10	9.8	10
	11WRF	7	8	1	7	6	6	1	8	9	1	8	5.6	6
	44CCLM	8	6	9	8	7	7	7	6	6	9	4	7.0	8
	44HIRHAM	5	5	6	5	4	4	6	5	4	7	6	5.2	4
	44RACMO	3	3	2	2	2	2	5	3	3	2	1	2.5	2
	44RCA	4	4	7	4	8	8	9	1	5	3	9	5.6	6
	44WRF	2	2	3	1	3	3	4	2	2	4	7	3.0	3
Coquet	11CCLM	4	1	1	1	1	1	5	1	2	4	1	2.0	1
	11HIRHAM	9	9	9	9	9	9	1	9	9	9	4	7.8	9
	11RACMO	1	2	8	6	4	4	4	4	7	6	6	4.7	4
	11RCA	10	10	10	10	10	10	7	10	10	10	10	9.7	10
	11WRF	2	3	5	2	3	3	2	2	5	3	5	3.2	2
	44CCLM	8	8	4	8	6	7	10	8	1	8	2	6.4	7
	44HIRHAM	5	7	7	7	8	8	3	3	8	7	9	6.5	8
	44RACMO	7	6	3	3	2	2	8	6	3	2	3	4.1	3
	44RCA	3	4	6	5	7	6	6	5	6	5	7	5.5	6
	44WRF	6	5	2	4	5	5	9	7	4	1	8	5.1	5

4.4. Summary and discussion

This chapter shows the evaluation of the skill in simulating the observed precipitation and temperature of five Euro-CORDEX RCMs at two different simulation resolutions (50 km or 0.44° and 12.5 km or 0.11°).

The RCM climate outputs are coupled with a hydrological model to simulate river flow which is also evaluated against observations. Bias correction using quantile mapping is used to reduce RCM precipitation and temperature biases. The bias corrected RCM temperature and precipitation outputs are also validated along with their "bias-corrected" simulated river flow. RCM validation gives information about the climate model skill that can be used as feedback information for their developers or as an evaluation tool to assess their accuracy to simulate recent past climate as a background for impact studies. The results from this procedure allow the following research questions to be addressed:

i) Is the relative performance of the 0.11° Euro-CORDEX RCMs better than their 0.44° version to simulate climate and river flow?

It is important to address this research question as there is great effort and resources from the climate modeling community focused on increasing the resolution of RCM simulations (e.g. Kendon et al., 2012; Casanueva et al., 2016; Prein et al., 2015; Kotlarski et al., 2014). The Euro-CORDEX initiative provides an opportunity to robustly evaluate the added value of increasing the resolution of the simulations as it includes a set of RCMs run at two resolutions driven by perfect boundary conditions which makes their skill comparable. Furthermore, assessing the added value of the resolution increase is relevant for the hydrological impact community to gain an insight of the possible benefits and disadvantages of using high-resolution simulations compared to the low-resolution simulations. As far as the author is aware, studies of this type have been done before for specific RCMs (e.g. Dankers et al., 2007; Graham et al., 2007; Kay et al., 2015), but there is not a state-of-the-art multi-model robust assessment of these characteristics.

For temperature there is added value of the uncorrected higher resolution RCMs only for catchments with complex topography as the 0.44° RCMs do not capture the temperature that is a result of the complex elevation differences. In contrast, for flat catchments temperature is accurately simulated at the coarser resolution. Bias correction reduces the biases from both simulations at both resolutions, as expected. However, the correlation is not greatly modified as bias correction adjusts the distribution of the variable and not the day to day sequence. Biases are larger at both tails of the distribution but these are lower than 1°C for all catchments, RCMs and resolutions.

The precipitation biases for the uncorrected RCMs are larger for the Glaslyn catchment due to its complex topography. In contrast, the upper Thames catchment has smaller biases because of its flat nature. This accentuates the importance of validating RCM ouputs particularly in regions with complex topography (Huang et al., 2014). Concerning the precipitation simulation skill for the Glaslyn catchment from the RCM simulations at both resolutions, it has been shown that the 0.11° simulations outperform the 0.44° simulations. These results are consistent with previous studies (e.g. Fowler et al., 2007; Önol, 2012; Torma et al., 2015; Prein et al., 2016). However, biases are large for both resolutions and bias correction is required to provide accurate simulations, similar to the findings from Casanueva et al. (2016). However, bias correction is a mere statistical technique that does not improve fundamental model errors (Maraun, 2016). This is further discussed at the end of this section.

Bias correction decreases most of the RCM precipitation biases as expected. The gamma distribution - quantile mapping method systematically reduces the biases below the 90th percentile of the distribution, but increases the biases exponentially after that point. In contrast, the double gamma distribution quantile mapping decreases the biases before and after the 90th percentile, however a bias increase occurs at the 90th percentile. Compared to the gamma bias correction, the double gamma bias correction decreases the overall percentile biases, but generates larger bias in the percentile in which the distribution is divided. Improvements in the simulation of the precipitation distribution using a double distribution bias correction compared to the single distribution approach have also been reported by Yang et al. (2010), Gutjahr and Heinemann (2013) and Teng et al. (2015).

Overall, both bias correction methods decrease the precipitation biases from the uncorrected RCMs. Of both methods, the double gamma bias correction has smaller biases for most catchments and performance measures. However, there are cases when the double gamma quantile mapping bias correction does not provide the lowest bias. For instance, biases from the uncorrected RCMs are frequently smaller for the mean wet spell length and SDII. Also, other performance measures have smaller biases when using the gamma quantile mapping bias correction, but this varies according to the analysed catchment, season and RCM. Casanueva et al. (2016) reached a similar conclusion.

Comparing the river flow simulation skill of the uncorrected RCMs, only the use of high-resolution RCMs in the Glaslyn catchment provides a clear added value compared to their coarser resolution. However, biases are large for most of the performance measures in this catchment even for the high-resolution RCMs. In the rest of the catchments there is no clear benefit from using the high resolution RCMs.

The uncorrected 0.11° RCMs consistently outperformed their 0.44° version for the Glaslyn catchment only. Nevertheless, for this catchment the biases from the 0.11° RCMs were large for the analysis of river flow. For the rest of the catchments there is no clear benefit from using the higher resolution models because both resolution RCMs performed similarly. The reason behind the benefit from the 0.11° RCMs in the Glaslyn catchment might be its complex topography and small extension for which precipitation is better represented by the high-resolution RCMs, which then feeds forward into river flow.

In summary, it can be stated that a clear added value from the high-resolution simulations is only observed for the complex-topography catchments for temperature and only for the Glaslyn catchment for precipitation. Nevertheless, for this catchment biases in the high-resolution precipitation simulation are large impacting in the river flow simulation by giving biased results.

ii) Is the current skill of the Euro-CORDEX RCMs able to generate useful inputs for the analysis of climate change impacts on hydrology?

In this contexts, “useful” refers to climate outputs that provide supporting grounds for the analysis of hydrological impacts by the planners and end users. In other words, could the hydrological model driven by RCM outputs simulate the observed hydrology sufficiently enough to be faithfully used in future projections?

The final decision will be one by the end user, but the performance metrics used here allow a fair comparison of the simulation skill of the models. In this research both the uncorrected and bias-corrected outputs were analysed.

The spread of the simulated river flow from the uncorrected RCMs cover the observed FDC from all catchments except for the Glaslyn catchment in which the simulations are largely biased. Nevertheless, the simulation spread in each of the catchments is large.

Bias correction is an important approach that improves the simulation skill providing reliable simulations of the observed river flow (Muerth et al., 2013; Maraun, 2016). Here, bias-corrected RCM outputs generally reduce the bias of the river flow. Considering all the analysed RCMs as a group, the simulation spread is reduced when using the Gamma distribution bias correction but it is reduced even more after applying the double Gamma correction (see section 4.3.6).

The results shown here demonstrate that bias correction normally reduces the bias of the RCM simulation providing outputs suitable for impact analyses. However, there are cases where the skill of the hydrological model is also relevant and might increase the bias. For instance, the simulation bias of the summer flow in the upper Thames is linked to deficiencies in the hydrological model (see sections 3.5 and 3.6). Additionally, previous studies have indicated that bias corrected outputs are not reliable to reproduce floods (Huang et al., 2014; Cloke et al., 2013). This could be linked to the fact that the gamma distribution quantile mapping systematically increases the precipitation bias exponentially after the 90th precipitation percentile for all study catchments (see section 4.3.5). In this study, the application of a double gamma distribution bias correction reduces the bias above the 90th precipitation percentile approximately until the 99th precipitation percentile. As a consequence, the bias in the high flows performance measure is reduced when using the double gamma bias correction (see section 4.3.6). Therefore, more sophisticated bias correction methods provide a larger benefit than simpler techniques (Wetterhal et al., 2012). However, comparing among both precipitation correction techniques, the best method depends on the catchment, RCM and performance measure.

Based on the information shown above, the research question is answered by stating that only for the topographically-complex Glaslyn catchment the uncorrected RCMs cannot provide useful river flow simulations. For the other catchments, the simulation spread is large and therefore the bias correction represents an option for decreasing the spread.

Previously, it has been noted that increasing the RCM resolution does not in general give a clear added value in the river flow simulation skill for both the uncorrected (Dankers et al., 2007; Graham et al., 2007) and bias-corrected (Huang et al., 2014; Graham et al., 2007) RCM simulations. Furthermore, there are cases when the coarser-resolution have a better simulation skill than the high-resolution models (Kay et al., 2015). Nevertheless, studies often analyse only one RCM. Here a multi-model approach is used, giving robust results.

Other relevant results are obtained from the methodology followed in this chapter. Such results include the estimation of PET, selection of grid boxes for the simulation of the catchments' climate and theoretical concepts regarding the RCM evaluation process.

The best approach to estimate PET is currently a subject of debate (e.g. McVicar et al., 2012; Donohue et al., 2010; Rudd and Kay, 2016; Clark et al., 2016). Nevertheless, in a climate change study the uncertainty of extra variables that are largely biased by the current state-of-the-art climate models might be troublesome for the estimation of PET using a physically-based formula and even for analysis of present PET, temperature-based approaches have outperformed physically-based formulae mainly due to the uncertainty of including extra variables in the PET estimation (e.g. Kay and Davies, 2008; Oudin et al., 2005). Therefore, temperature-based formulae are used in this study. Here, the Oudin formula consistently outperforms the Hamon method for all catchments when compared to the reference PET. The Hamon formula has large biases in the accumulated PET for summer months, sometimes with a mean percentage error above 100%, and frequently underestimates the PET from April to September. In contrast, the Oudin formula PET estimates are closer to the observations. Results are consistent with those from Shaw and Riha (2011) who also identified the high sensitivity of the Hamon formula.

Regarding the selection of RCM gridboxes for the simulation of the catchment's climate, the correlation between precipitation from the catchment observations and from the RCM simulations is higher for larger RCM gridbox domains than for the gridboxes covering the study catchments (except for the upper Thames and Calder catchments considering the 0.44° simulation resolution). Similar results were obtained by Eden et al. (2014) for station observations compared 3x3 and 5x5 RCM gridboxes. Here, observations for the entire catchment are compared with domains of 3x3 grid boxes for the 0.44° RCMs and domains of 6x6 and 12x12 grid boxes for the 0.11° RCMs. The result can be an effect of the link between the catchment's climate and the regional climate that is simulated better by the larger domain. However, the catchment extremes are expected to be better simulated by the grid boxes covering it. Furthermore, the gridbox representativeness issue that questions the simulation skill of the gridboxes covering the study catchments due to RCM's systematic displacements (Maraun and Widmann, 2015) occurs at the catchments with complex orography, Glaslyn and Coquet. For these catchments, the observations have a higher correlation with the simulations of a neighbouring grid box than those from the grid box covering the catchment. However, to assess the consistency of this finding similar analyses should be performed in other catchments with complex orography to assess if this is a regular error in RCM simulations.

The evaluation of the RCM simulation skill performed here implicitly also evaluates the reanalysis data the drives the climate models (Brands et al., 2012). Nevertheless, for England and Wales ERA-Interim has been found to represent precipitation accurately (Leeuw et al., 2015) reducing this source of uncertainty.

The validation process described in this chapter serves as base for the analysis of climate change impacts from this study. As it was shown, there is no clear added value from using the high-resolution RCMs in the study catchments, except for the Glaslyn catchment, and for that catchment biases are large when using

the high-resolution RCMs. For the rest of the analysis, only the 0.11° RCMs will be used to estimate the impacts of climate change in the study catchments. From the results shown here, the need for bias correction is evident. In general, the normal distribution and double gamma distribution quantile mapping bias correction methods provided the lowest biases for temperature and precipitation, respectively. In the rest of the study these methods will be used to bias correct the RCM projections. Based on the results from this chapter and the large biases from the uncorrected RCM simulations, the following chapters will show the uncorrected and bias-corrected results but will only discuss the bias-corrected results in detail as their biases are smaller. However, it should be considered that the correction methods do not correct the fundamental errors from the climate models (Maraun, 2016) and their application in impact analysis should be done with caution (Cloke et al., 2013). This is mainly because the physics behind the GCMs and RCMs are lost after bias correction and change the simulated output significantly (Ehret et al., 2012). Nevertheless, as the GCMs and RCMs normally have errors in the simulation of key processes for the simulation of precipitation, bias correction is often used in the assessment of climate change impacts to get results that are closer to the observations. In other words, the limitations of the method are acknowledged but there is no better option to get projections with small biases and reduced uncertainty. This seems that will continue until the GCMs and RCMs develop to a level where this post-processing is not required to get the desired quality in the information.

5. Climate projections

5.1. Introduction

In chapter 4, an analysis of the uncorrected and bias-corrected RCM skill to simulate current climate (1979-2008) is shown. The analysis is performed on the Euro-CORDEX RCMs driven by perfect boundary conditions (Era-Interim reanalysis). Additionally, the river flow simulation skill is evaluated using the RCM outputs as drivers of a HEC-HMS hydrological model for each catchment for the same time period. This chapter shows the next step of the analysis, namely the assessment of the climate change impacts on climate based on the Euro-CORDEX simulations forced by the Representative Concentration Pathways (RCPs) 2.6, 4.5 and 8.5 (Van Vuuren et al., 2011).

The analysis of this chapter is performed for a set of RCMs driven by GCMs considering its uncorrected and bias-corrected outputs. This chapter evaluates the effect in the climate change signal from employing two different bias correction approaches: 1) bias correction using the evaluation simulations (ERA-Interim-driven) to obtain the distribution parameters (further on referred as BC-Eval), and 2) bias correction using the historical simulations (driven by GCMs) to get the distribution parameters (further on referred as BC-Histo). The Multi-model Ensemble Mean (MEM) is used to assess the impacts of climate change in the future climate from each bias correction approach. Here, the climate change signal is considered to be robust if it is in the same direction for both bias correction approaches. Following this procedure, the chapter intends to answer research question iii) **to what extent are the projected changes in climate robust, considering both bias correction approaches?**

Initially, this chapter outlines the currently available GCM-RCM projections from the Euro-CORDEX project. Subsequently, considerations regarding the bias correction of GCM-RCM projections are discussed followed by the description of the process used to select the GCM-RCM combinations employed for the analysis. Then, the temperature and precipitation results for each catchment are shown. Results from each variable include the analysis of their annual time series, their monthly distribution and the frequency of exceedance of certain thresholds of particular interest for this study.

5.2. Strategy for the selection of the GCM-RCM combinations

As discussed in chapter 1, current computer power makes the running and simulation of RCMs possible. It is expected that in the coming years, with increasing computer power, the resolution of climate models will increase even more and will cover larger geographical regions. For example, a 1.5-km resolution RCM has been developed and used to simulate climate and river flow for the south of the UK (Kendon et al., 2012; Chan et al., 2013; Kay et al., 2015). The geographical extent of the model domain is mainly influenced by the amount of resources required to perform the simulation. Such resources are mainly computer power and time. Also, these are the main limitations that prevent simulations from all available RCMs driven by all available GCMs being undertaken (Jury et al., 2015). In the case of the Euro-CORDEX project, the RCP projections are driven by GCMs from the Fifth Phase of the Coupled Model Intercomparison Project (CMIP5). At the time of this analysis, the available GCM-RCM combinations from Euro-CORDEX are shown in Figure 5.1. It is worth stating that Euro-CORDEX is still being developed. Thus, new model combinations will become available in the future.

In this study, an analysis of the available GCM-RCM combinations is performed for each study catchment aiming to select the combinations with the best skill in simulating the present climate. The selection approach is explained in the following section.

		GCM				
		MOHC-HadGEM2-ES	**ICHEC**-EC-EARTH	**MPI**-ESM-LR	**IPSL**-CM5A-MR	**CERFACS**-CNRM-CM5-LR
RCM	**CCLM**4-8-17	Historical	Historical	Historical	Historical	Historical
		RCP 2.6	RCP 2.6	RCP 2.6	RCP 2.6	RCP 2.6
		RCP 4.5	RCP 4.5	RCP 4.5	RCP 4.5	RCP 4.5
		RCP 8.5	RCP 8.5	RCP 8.5	RCP 8.5	RCP 8.5
	HIRHAM5	Historical	Historical	Historical	Historical	Historical
		RCP 2.6	RCP 2.6	RCP 2.6	RCP 2.6	RCP 2.6
		RCP 4.5	RCP 4.5	RCP 4.5	RCP 4.5	RCP 4.5
		RCP 8.5	RCP 8.5	RCP 8.5	RCP 8.5	RCP 8.5
	RACMO22E	Historical	Historical	Historical	Historical	Historical
		RCP 2.6	RCP 2.6	RCP 2.6	RCP 2.6	RCP 2.6
		RCP 4.5	RCP 4.5	RCP 4.5	RCP 4.5	RCP 4.5
		RCP 8.5	RCP 8.5	RCP 8.5	RCP 8.5	RCP 8.5
	RCA4	Historical	Historical	Historical	Historical	Historical
		RCP 2.6	RCP 2.6	RCP 2.6	RCP 2.6	RCP 2.6
		RCP 4.5	RCP 4.5	RCP 4.5	RCP 4.5	RCP 4.5
		RCP 8.5	RCP 8.5	RCP 8.5	RCP 8.5	RCP 8.5
	WRF331F	Historical	Historical	Historical	Historical	Historical
		RCP 2.6	RCP 2.6	RCP 2.6	RCP 2.6	RCP 2.6
		RCP 4.5	RCP 4.5	RCP 4.5	RCP 4.5	RCP 4.5
		RCP 8.5	RCP 8.5	RCP 8.5	RCP 8.5	RCP 8.5

Figure 5. 1 Available Euro-CORDEX GCM-RCM combinations (shown in green) at the time of this analysis. Identifiers used for each model in this study are shown in bold

5.2.1. Bias correction using historical or evaluation simulations

In the literature there are two different approaches to calibrate the distribution parameters of the bias correction method. One approach uses the historical simulations (BC-Histo) whereas the other uses the evaluation simulations (BC-Eval). In the evaluation simulations, RCMs are driven by perfect boundary conditions, or in other words, driven by observation reanalysis data. In contrast, RCMs in the historical simulations are driven by GCMs.

Nevertheless, future RCP projections are only generated by RCMs driven by GCMs. Furthermore, the RCP projections from a specific GCM-RCM combination begins where the historical time series from that same GCM-RCM projection concluded. If the historical time series is biased compared to the observations, the future projections will also be biased. For example, Figure 5.2 shows the mean annual temperature time series for the Coquet catchment simulated by the ICHEC-RACMO combination. In this graph the time series of the evaluation, historical and RCP simulations are plotted along with the observed mean annual temperature. In this particular case the evaluation simulation is closer to the observations than the historical time series. For most of the time series, the historical simulation underestimates the observed temperature by approximately 2°C. Furthermore, the RCP projections begin where the historical simulation ends, keeping the 2°C bias. Thus, this highlights the need to carefully select GCM-RCM combinations with small biases or the need to bias correct the GCM-RCM simulations to reduce their biases (as recommended by Christensen et al., 2008 and Chen et al., 2015).

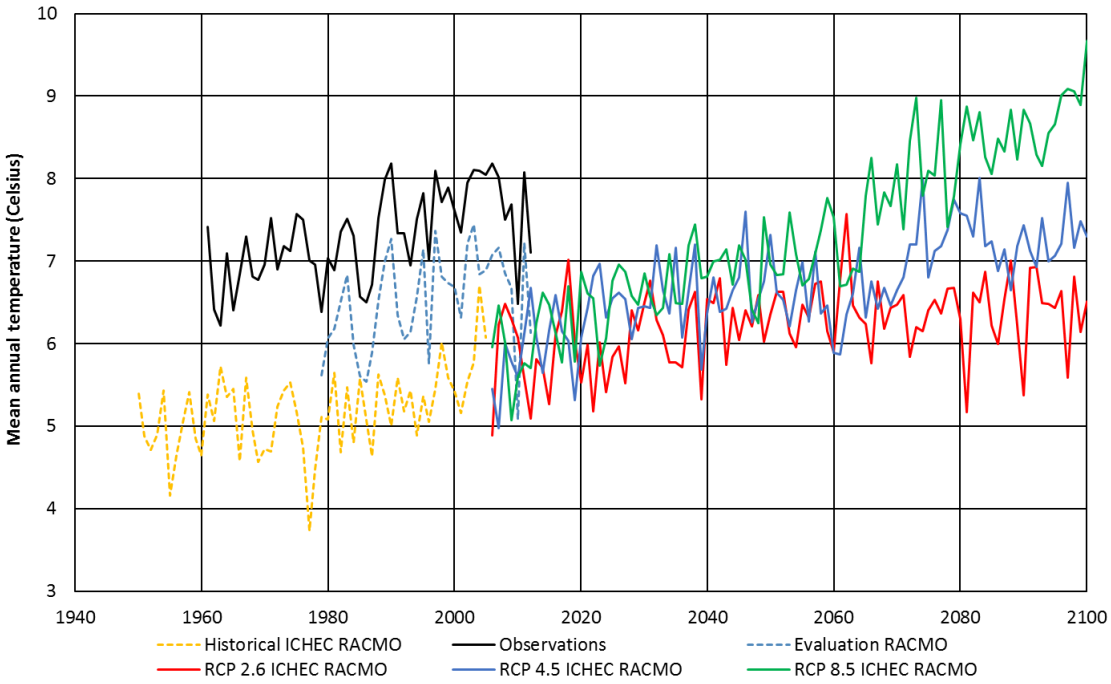

Figure 5. 2 Historical, evaluation and RCP time series for the mean annual temperature in the Coquet catchment using the ICHEC-RACMO combination

As the BC-Eval approach is trained using RCMs driven by perfect boundary conditions, when used to bias correct a RCP projection, the resulting simulation will only correct the RCM biases keeping the GCM biases. In contrast, the BC-Histo approach is trained using RCMs driven by GCMs. Thus, when using the BC-Histo approach the biases from both the RCM and GCM will be removed in the corrected projection. The selected approach mainly depends on the objective of the analysis undertaken. The BC-Eval method is commonly used by the climate community because it is useful to compare the uncertainty of different RCMs (e.g. Casanueva et al., 2016). On the other hand, the BC-Histo approach is generally used in climate change impact analysis where the objective is to decrease the overall uncertainty of the projection (e.g. Mbaye et al., 2016).

Additionally, when using the BC-Histo approach, as the historical simulation is long (longest historical simulations cover from 1950 to 2005) some of the current climatic characteristics might be suppressed. For instance, in the previous example, Figure 5.2 shows that in the historical simulation there is an increasing trend that is more perceptible in the second half of the simulation. If the complete time series are used to obtain the bias correction parameters, then such current behaviour would not be replicated. This issue has been addressed in previous studies by using the last 30 years of the historical simulations to estimate the bias correction parameters instead of the complete time series (e.g. Arnell, 2011).

When using the BC-Eval approach the complexity of the selection of the RCM-GCM combination increases. This is due to the fact that in the evaluation simulations RCMs are driven by perfect boundary conditions. When using the BC-Eval approach four main cases are observed. These are discussed next.

Case 1: The historical time series of a GCM-RCM simulation is closer to the observations than the RCM evaluation simulation. For example, figure 5.3 shows the mean annual temperature simulation for the

Coquet catchment using the MOHC-RCA combination for the historical, evaluation, RCP 2.6 and bias-corrected RCP 2.6 simulations.

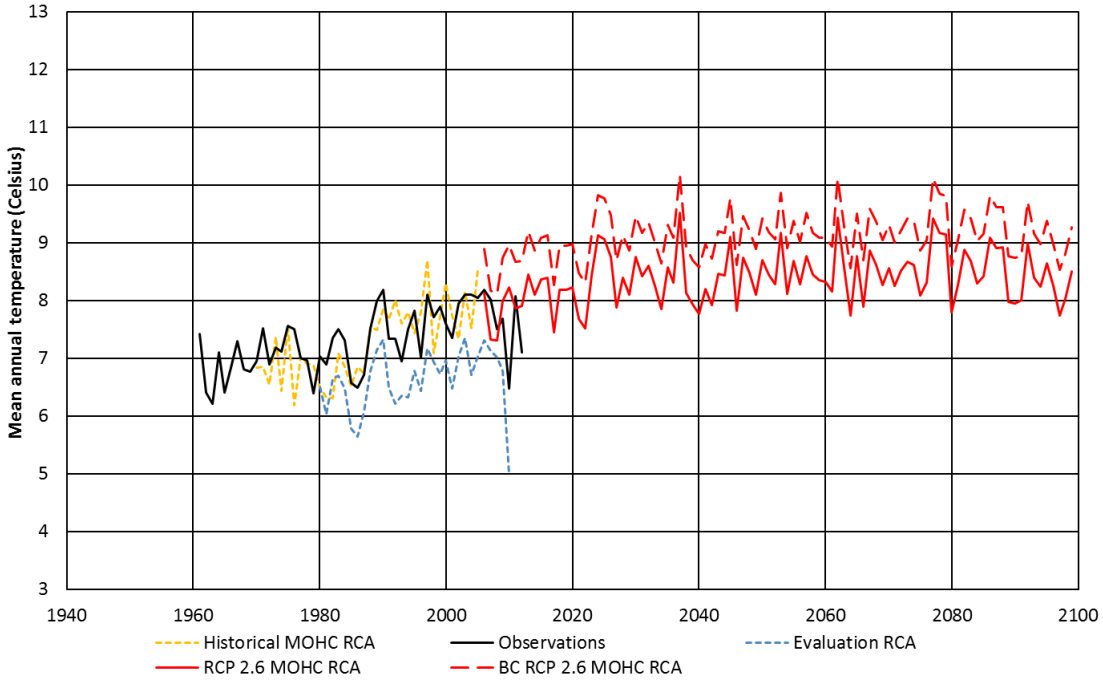

Figure 5. 3 Case 1 for the BC-Eval approach: Historical simulation is closer to the observations than the evaluation simulation, example of the mean annual temperature in the Coquet catchment using the MOHC-RCA combination (BC = bias corrected)

Case 2: The evaluation simulation is closer to the observations compared to the historical simulation. For example, figure 5.4 shows the mean annual temperature simulations for the Glaslyn catchment using the ICHEC-RACMO combination for the historical, evaluation, and uncorrected and bias-corrected RCP 4.5 and 8.5 projections.

Case 3: The evaluation and historical simulations have similar biases. For example, figure 5.5 shows the annual accumulated precipitation simulation for the Coquet catchment using the MPI-RCA combination for the historical, evaluation and uncorrected and bias-corrected RCP 2.6.

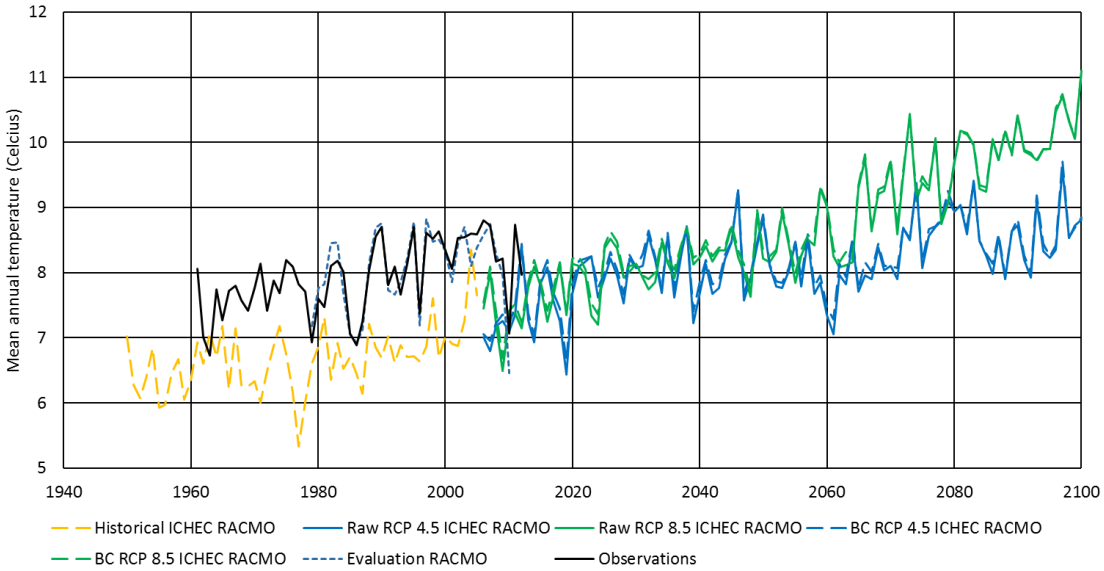

Figure 5. 4 Case 2 for the BC-Eval approach: Evaluation simulation is closer to the observations than the historical simulation, example of the mean annual temperature in the Glaslyn catchment using the ICHEC-RACMO combination (BC = bias corrected)

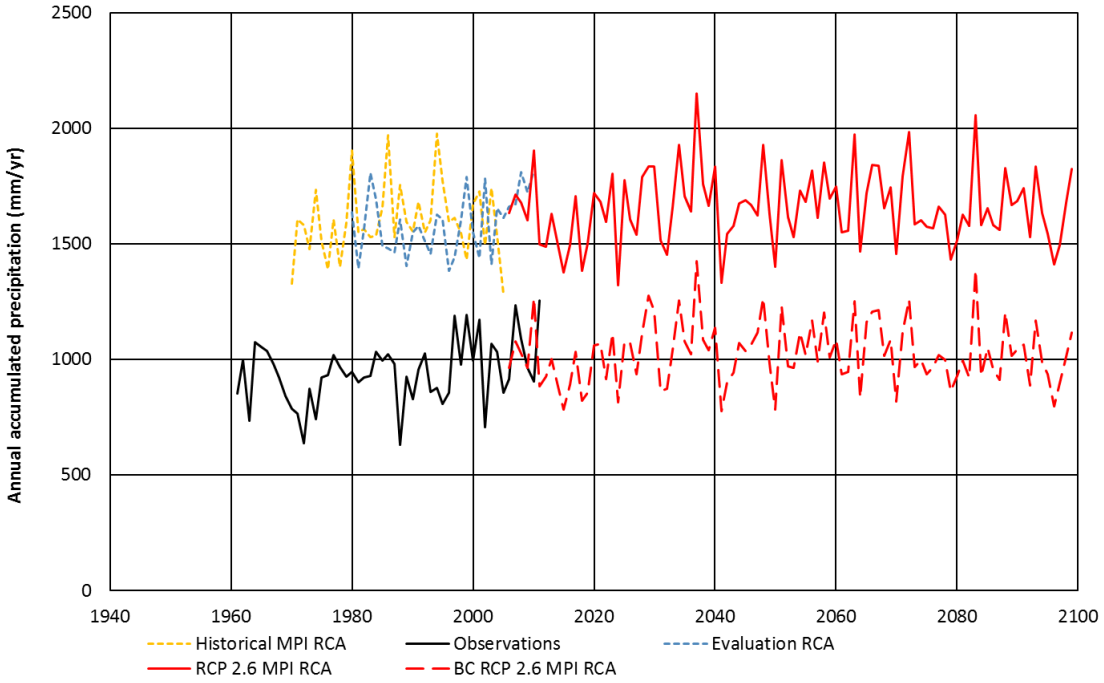

Figure 5. 5 Case 3 for the BC-Eval approach: Both the evaluation and historical simulations have similar biases, example of the annual accumulated precipitation in the Coquet catchment using the MPI-RCA combination (BC = bias corrected)

Case 4: Ideally, the skill level of both the historical and the evaluation simulations skill is similar and close to the observations. For example, figure 5.6 shows the mean annual temperature simulation for the Glaslyn catchment using the MPI-RCA combination for the historical, evaluation and uncorrected and bias-corrected RCP 4.5 and 8.5 projections.

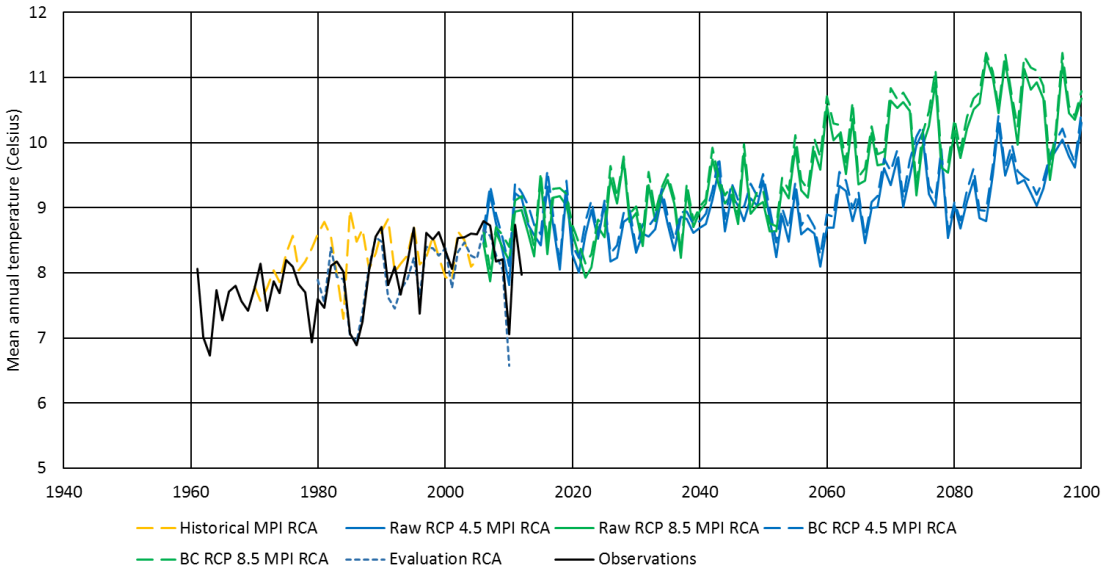

Figure 5. 6 Case 4 for the BC-Eval approach: Both the evaluation and historical simulations have similar skill and both are close to the observations, example of the mean annual temperature for the Glaslyn catchment using the MPI-RCA combination (BC = bias corrected)

In case 1, the historical simulation closely agrees with the observations whereas the evaluation simulation is biased. As the simulation skill of the historical time series is good, the uncorrected future projection has no large bias at the beginning of the simulation. However, after bias correction using the BC-Eval approach, the biases in the corrected projection increase at the beginning of the simulation.

In case 2, the evaluation simulation biases are small compared to the historical simulation. As the historical run is biased, the beginning of the uncorrected RCP projections is also biased with respect to the observations. When using the BC-Eval approach there is almost no difference between the uncorrected and the bias-corrected projections. As a result, the bias at the beginning of the projection remains even after applying bias correction.

In cases 3 and 4, as the evaluation and historical biases are similar, their distribution parameters are likely to be similar and therefore the bias correction will perform as expected. For case 3, the biases from both the historical and evaluation simulations are similar and the uncorrected projection has a similar bias at the beginning of its simulation. Nevertheless, this bias is removed after applying bias correction. For case 4, both the historical and evaluation time series have a good simulation skill and the uncorrected future projections follow the observations trend. In this particular case, the bias correction effect could be minimal (for the mean parameter of the distribution, but might correct the variability parameter).

From the previous analysis, it is obvious that using the BC-Eval approach requires a previous analysis of the different simulation time series in order to select the GCM-RCM combinations that would benefit from bias correction. In contrast, the BC-Histo approach can be applied to any RCP with the security that it will give results agreeing with the parameters from the observations' distribution. Nevertheless, the historical simulations do not capture the timing of internal variability as the evaluation simulations do.

In this study both bias correction approaches are compared. This aims to solve the question: in an analysis of the impacts of climate change, does it matter which approach to use? This is important as the results obtained from each approach might or not be contradictory. Also, a comparison of the results from each approach has not been done before in this context. A recent 30-year period (1976-2005) is used to train the bias correction methods. Both approaches are applied to six GCM-RCM combinations per catchment (section 5.2.3) that are selected based on the methods described in section 5.2.2.

5.2.2.Criteria for the selection of GCM-RCM combinations

The selection of GCM-RCM combinations intends to remove combinations with low simulation skill from the analysis with the objective of tackling the discrepancy issues described in section 5.2.1. Some combinations might have large biases. For the analysis of regional impacts, employing a subset of the best performing models can provide better information than using the full set of available combinations (Ramesh and Goswami, 2014). The selection analysis is done for each month and catchment as the simulation skill from each combination depends on the catchment, season and climate variable. Thus, for each catchment the 13 GCM-RCM available combinations (Fig. 5.1) are analysed in order to select which ones to use in the assessment of climate change impacts considering both bias correction approaches. The analysis aims to remove the possible gaps between the observations and projections as described in section 5.2.1.

For the selection of the model combinations based on the BC-Histo approach, a two-step process is followed:

1) The model combinations are ranked based on their skill in reproducing the observed mean and scale parameters for temperature and precipitation, respectively. Based on the ranking, the worst three combinations are removed from the analysis and the remaining ten combinations are used in the second step.
2) The combinations that passed through step 1 are ranked based on their skill to reproduce the observed standard deviation and shape parameters for temperature and precipitation, respectively. The ranking is used for the final selection explained below.

In contrast, for the BC-Eval approach the following selection method is used:

1) Initially, the temperature mean and precipitation scale parameters are considered. The models are ranked based on how similar the evaluation simulation parameters are to the historical simulation parameters. The bottom three model combinations are removed from the analysis based on the ranking, whilst the remaining ten combinations pass to step 2.
2) The remaining ten model combinations are ranked based on the similarity between their temperature standard deviation and precipitation shape parameters with the historical simulation parameters. This ranking is used for the final selection explained next.

The final selection considers both bias correction approaches. Therefore, the top six models appearing on both step 2 rankings are selected. The selection is done by averaging the similarity of the monthly parameters from 1989 to 2005 (the period of overlap between the evaluation and historical simulations). The process described above was applied in each catchment. Results are shown in the next section.

5.2.3.Selected GCM-RCM combinations

This section shows the chosen GCM-RCM combinations for each catchment when using the selection process described in the previous section. A comparison between the monthly observed and simulated temperature and precipitation parameters is shown for the Upper Thames (Figs. 5.7 and 5.8), Glaslyn (Figs. A7 and A8), Calder (Figs. A9 and A10) and Coquet (Figs. A11 and A12). As stated in the previous section, the distribution parameters from each combination are catchment-dependent.

Some special behaviour can be observed in the parameters' graphs. The scale parameter from the observations of the Glaslyn catchment is higher than 15 for all months (Fig. A8), but from all combinations only the MOHC-CCLM combination equals or exceed this value for some of the months. Nevertheless, the shape parameter of this combination is largely biased for most of the months compared to the rest of the combinations. This shows the large precipitation biases of all simulations compared to the observations in this catchment, also detected in section 4.3.5. In all catchments, for most of the months there is a clustering from the driving GCMs in the temperature parameters graphs (e.g. shown as clustering of same coloured shapes) (Figs. 5.7, A7, A9 and A11). In contrast, for most of the months the precipitation parameters are clustered based on the RCM used (e.g. shown as clustering of same shape types). This is observed for all catchments (Figs. 5.8, A10 and A12) except for the Glaslyn catchment where this is not evident (Fig. A8). This supports the fact that temperature is influenced by the large scale climatology, and therefore the GCMs have more weight in the simulation of temperature than the RCMs. On the other hand, the simulation of precipitation depends more in the RCM as the physical interactions involving the precipitation process are resolved at the RCM scale and as consequence there is a clustering in the precipitation parameters according to the RCM used (previously mentioned in Rummukainen, 2016).

After performing the selection analysis, the selected combinations are shown in Table 5.1. As a result of the selection procedure, the selected ensemble of climate model combinations is not the same for all of the catchments. This is a consequence of the simulation skill of each combination which varies depending on the catchment that is analysed. Nevertheless, the MOHC-RACMO and MOHC-RCA combinations are part of the selected ensemble in all catchments and there are some other combinations that passed the selection process for three out of the four catchments. Also, some model combinations were not selected for any of the catchments: ICHEC-CCLM, MPI-CCLM, IPSL-WRF and CERFACS-CCLM. This gives an insight of the large weight of the GCMs in the simulation. For instance, CCLM only passed the selection process when driven by the MOHC GCM. Nevertheless, the MOHC-CCLM combination is selected for three catchments while the remaining MOHC-driven combinations are selected in all of the catchments.

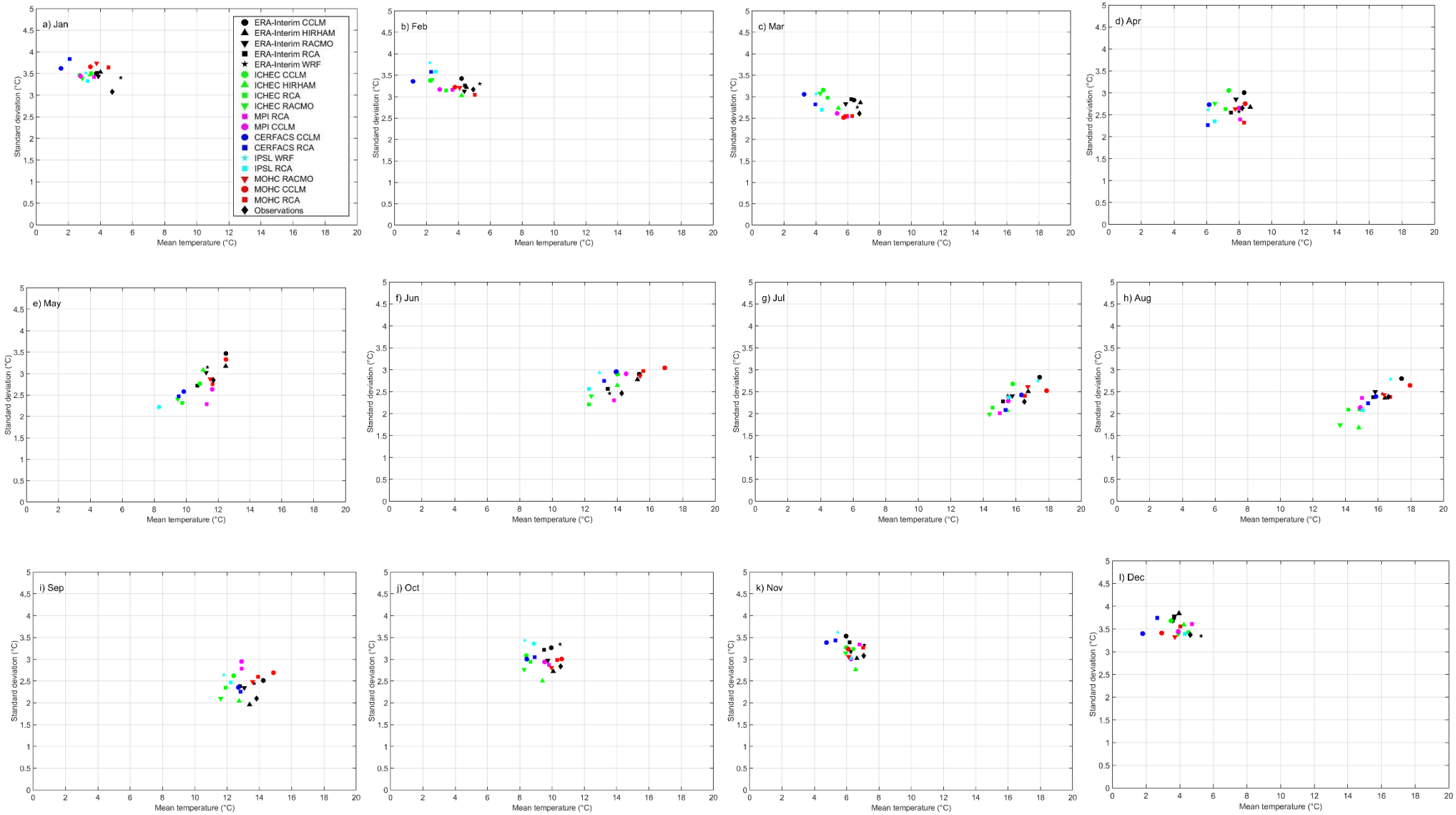

Figure 5. 7 Temperature distribution parameters for the observations, evaluation and historical simulations for the upper Thames catchment

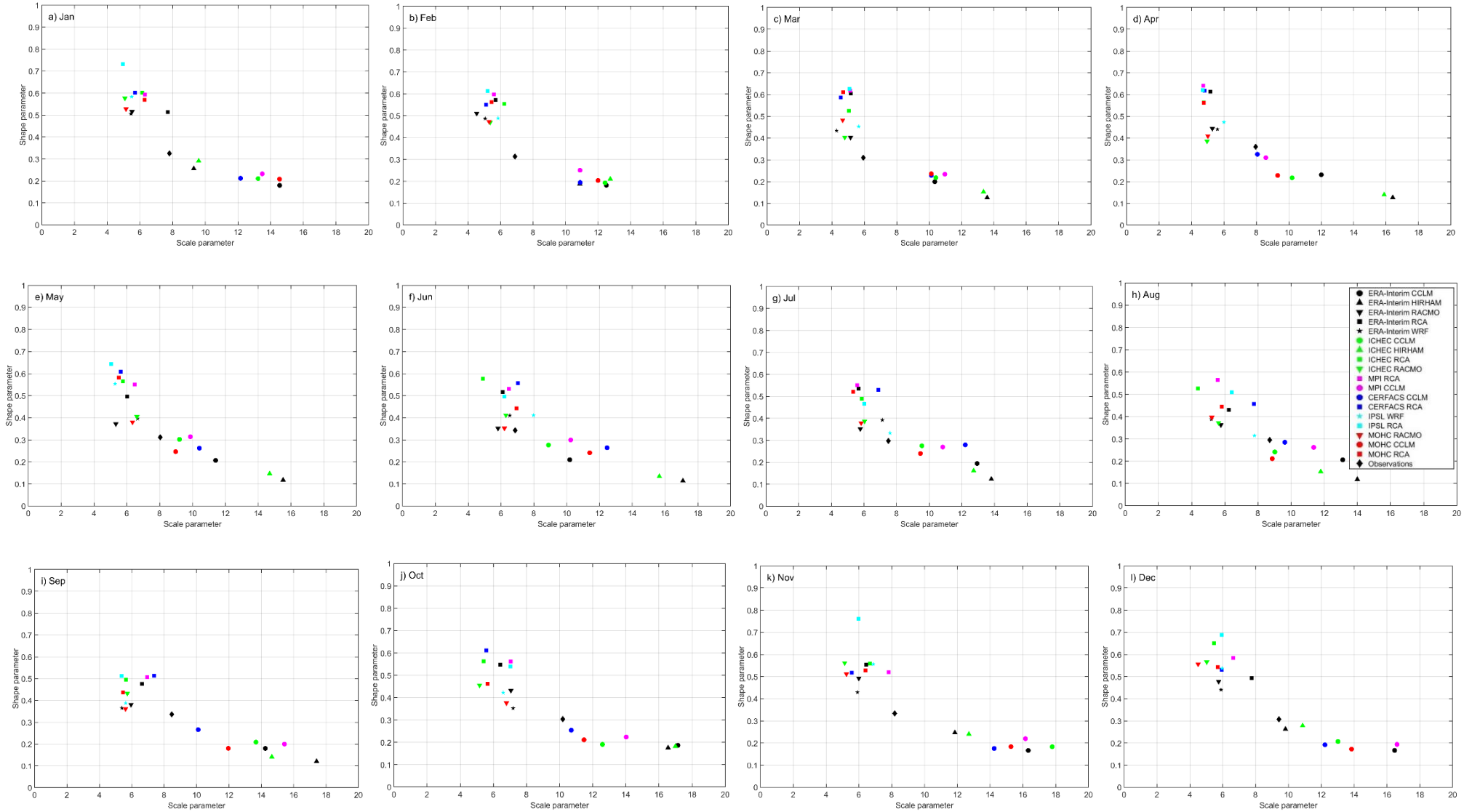

Figure 5. 8 Precipitation distribution parameters for the observations, evaluation and historical simulations for the upper Thames catchment

Table 5. 1 Selected GCM-RCM combinations for each catchment

Upper Thames	Glaslyn	Calder	Coquet
ICHEC HIRHAM	ICHEC HIRHAM	ICHEC RACMO	CERFACS RCA
ICHEC RCA	ICHEC RACMO	ICHEC RCA	ICHEC HIRHAM
MOHC CCLM	IPSL RCA	MOHC CCLM	ICHEC RACMO
MOHC RACMO	MOHC RACMO	MOHC RACMO	MOHC CCLM
MOHC RCA	MOHC RCA	MOHC RCA	MOHC RACMO
MPI RCA	MPI RCA	MPI RCA	MOHC RCA

There is some consistency if the results from this selection process are compared to the RCM rankings generated in chapter 4 (Tables 4.12 and 4.13). CCLM ranks high for precipitation for all catchments, except for the Glaslyn, and intermediate for temperature. In the selection used in this chapter, CCLM is selected in all catchments except in the Glaslyn catchment. Also, for the Glaslyn catchment the selected combinations include the top three best performing RCMs based on the ranking from chapter 4. Except for the Glaslyn catchment, WRF is often ranked high for precipitation and temperature. Nevertheless, projections from this RCM are only available driven by IPSL and such combination is not selected for any of the catchments. This could represent a poor simulation skill from the GCM which is only selected in the Glaslyn catchment when driving RCA. For this specific catchment, based on the rankings from chapter 4, RCA outperformed WRF. Thus, these results are consistent. For the Calder catchment, the HIRHAM and WRF RCMs are left outside by the selection criteria. This is consistent as for this catchment, HIRHAM had the lowest precipitation rank and because of the reason explained above for WRF. Finally, for the upper Thames and Coquet catchments it is difficult to do a fair comparison as four out of the five RCMs were selected in each catchment. Only WRF was left out from the selection, which can be an effect of the driving GCM skill as stated above.

Previous studies have analysed the performance of the CMIP5 GCMs both globally and regionally by comparing their simulated outputs against different observation datasets by means of performance measures. Relevant findings related to the GCMs used in this study are described next. The simulation skill to reproduce the global precipitation is best from MOHC, CERFACS and MPI (Mehran et al., 2014), whereas for the global temperature and precipitation extremes, MOHC and MPI have the best simulation skill (Sillmann et al, 2013). In Europe, the mean temperature is simulated better by MOHC, CERFACS, MPI and IPSL in that order (Jury et al., 2015), whereas in the lateral boundary of the Euro-CORDEX domain MPI has the best simulation skill for temperature (Brands et al., 2012). Considering a seasonal basis, temperature in winter is better simulated by MOHC and MPI and in summer by MPI and IPSL (Cattiaux et al., 2015). The mean precipitation in Europe is better simulated by IPSL, MOHC, CERFACS and MPI, in that order (Jury et al., 2015), whereas specifically for northern Europe MPI has the best skill in simulating the mean and extreme precipitation and temperature, evaluated using the 95th percentile for precipitation and the 95th and 5th percentile for temperature (Koutroulis et al., 2016)

Additionally, the simulation of storm tracks is relevant as their location and activity influence the regional climate, and the cyclones embedded in the storm tracks determine the day to day weather (Chang et al., 2012). Zappa et al. (2013) found that most of the CMIP5 models have good skill simulating the

cyclone behaviour in the North Atlantic. From the GCMs used in this analysis, ICHEC outperformed the rest when simulating the position, frequency and intensity of cyclones.

The simulation skill of the GCMs considerably varies seasonally (Wojcik, 2015) and also depending on the performance measure analysed and the observational dataset used as reference. It is also noted that the simulation skill from ICHEC has been seldom analysed. Nevertheless, MOHC and MPI consistently outperformed the rest of the models for the simulation of precipitation and temperature, whereas ICHEC had the best skill in simulating storm tracks.

There is agreement between the results described above and the GCMs selected following the criteria established in this chapter. Specifically, in this study MOHC and ICHEC are repeatedly selected in all catchments, whereas MPI is selected in three out of the four catchments. The results from the projected scenarios of the selected combinations are explained in the following sections.

5.3. Results

Results for the RCP 2.6, 4.5 and 8.5 projected scenarios for the analysed variables are shown in this section. First, temperature results are shown (section 5.3.1), followed by precipitation (section 5.3.2). The results shown in these sections are based on the MEM, except when otherwise stated. For most of the results, projections are divided in three 30-year periods: 2011-2040, 2041-2070, 2071-2100. Changes are analysed in comparison with the reference period (1976-2005). Given that two different bias correction approaches are analysed, a common independent reference data is used for the comparison of future changes and the evaluation of the robustness of the changes. Therefore, the observations are used as reference. This is supported by a t-test for temperature and a Mann-Whitney test for precipitation that evaluate the difference in means and variance between the observations and the average of the bias-corrected historical and evaluation simulations (common approach for the comparison of projected changes) in the reference period. Results from the tests indicate that the means and variances of both time series are equal (p-values > 0.05) (Table 5.2).

Table 5.2 p-values from the difference in means and variances tests between the observations and the averaged (BC-Eval and BC-Histo) bias-corrected time series of temperature and precipitation, a p-value > 0.05 indicates that there is no difference between the means and variances from both time series.

	Temperature	Precipitation
Upper Thames	0.57	0.97
Glaslyn	0.76	1.00
Calder	0.98	0.89
Coquet	0.98	0.97

5.3.1. Temperature

The assessment of each variable includes an evaluation of the uncorrected and bias corrected time series for the mean annual temperature as well as the monthly mean temperature over the period of analysis. Additionally, the frequency of cases when a particular threshold is exceeded is included in the analysis. The temperature threshold used here is relevant for river flow as it represents a decrease of 10% in the mean annual river flow that would impact the sectors that depend on the availability of water.

5.3.1.1. Mean annual temperature

The mean annual temperature in the uncorrected projections has perceptible biases compared to the observations' trend for all catchments (Fig. 5.9), except for the Glaslyn catchment (Fig. 5.9b). The bias extent varies depending on the catchment, but it is approximately 1°C in each of the catchments, except the Glaslyn. Bias correction, using both the evaluation and historical runs, removes the offset at the beginning of the projections. As a consequence, the time series of the bias-corrected simulation agrees with the last period of observations for all catchments and RCPs. Differences between the two bias-corrected simulations are perceptible towards the end of the time series with differences generally largest for RCP 8.5 and smallest for RCP 2.6. An assessment of the trend from 2006 to 2100 in the projected temperature is performed using a linear regression analysis. The trends from all RCP projections in all catchments are statistically significant using a t-test analysis (p-value < 0.05) (Table B1). Also, the bias correction methods do not (or slightly) modify the trend of the uncorrected projections. The decadal temperature trend varies from 0 °C to 0.1°C for RCP 2.6, from 0.1 °C to 0.2 °C for RCP 4.5 and from 0.3 °C to 0.4 °C for RCP 8.5. The RCP 8.5 trend has major similarity to the observed trend (1976-2005) than the other RCP trends.

The analysis of the mean annual temperature change in 30-year time slices compared to the 1976-2005 reference period gives an insight of the projected changes during the whole century, dividing it in same length periods. Results show that the uncorrected models simulate a smaller change compared to the bias-corrected models (Fig. 5.10). The MEM of the uncorrected GCM-RCM combinations indicates an increase in the mean annual temperature for all RCPs and time slices, except for the RCP 2.6 in the Calder catchment and the 2011-2040 time slice under the RCP 4.5 projection for the Coquet and Calder catchments. In contrast, after bias correction the changes in all emission scenarios, catchments and time slices are positive. The BC-Histo approach results in larger temperature changes compared to BC-Eval. In general, each bias corrected simulation projects changes of similar magnitude for each RCP in all of the study catchments. The statistical significance of the changes is evaluated by means of the standard deviation of the ensemble projections compared to the mean of the reference period. Changes are statistically significant for the bias-corrected mean annual temperature projections for all catchments, RCPs and time periods. Considering the RCP 2.6 scenario, BC-Eval projects an increase in the mean annual temperature of 0.9°C by the end of the century, whereas the BC-Histo projection projects an increase that varies from 1°C to 1.1°C by the end of the century. Similarly, for RCP 4.5 BC-Eval projects an increase in the mean annual temperature ranging from 1.6°C to 1.9°C by the end of the century, whereas BC-Histo projects an increase ranging from 1.9°C to 2.2°C. Finally, for RCP 8.5 the projections for the end of the century range from 2.6°C to 3.1°C for BC-Eval and from 3.2°C to 3.6°C for BC-Histo. In terms of percentage change considering the observations from 1976 to 2005 as reference period, the differences between the BC-Eval and BC-Histo projections range in all catchments from 1% to 3% for RCP 2.6, from 1% to 5% for RCP 4.5 and from 1% to 7% for RCP 8.5 (Table B2).

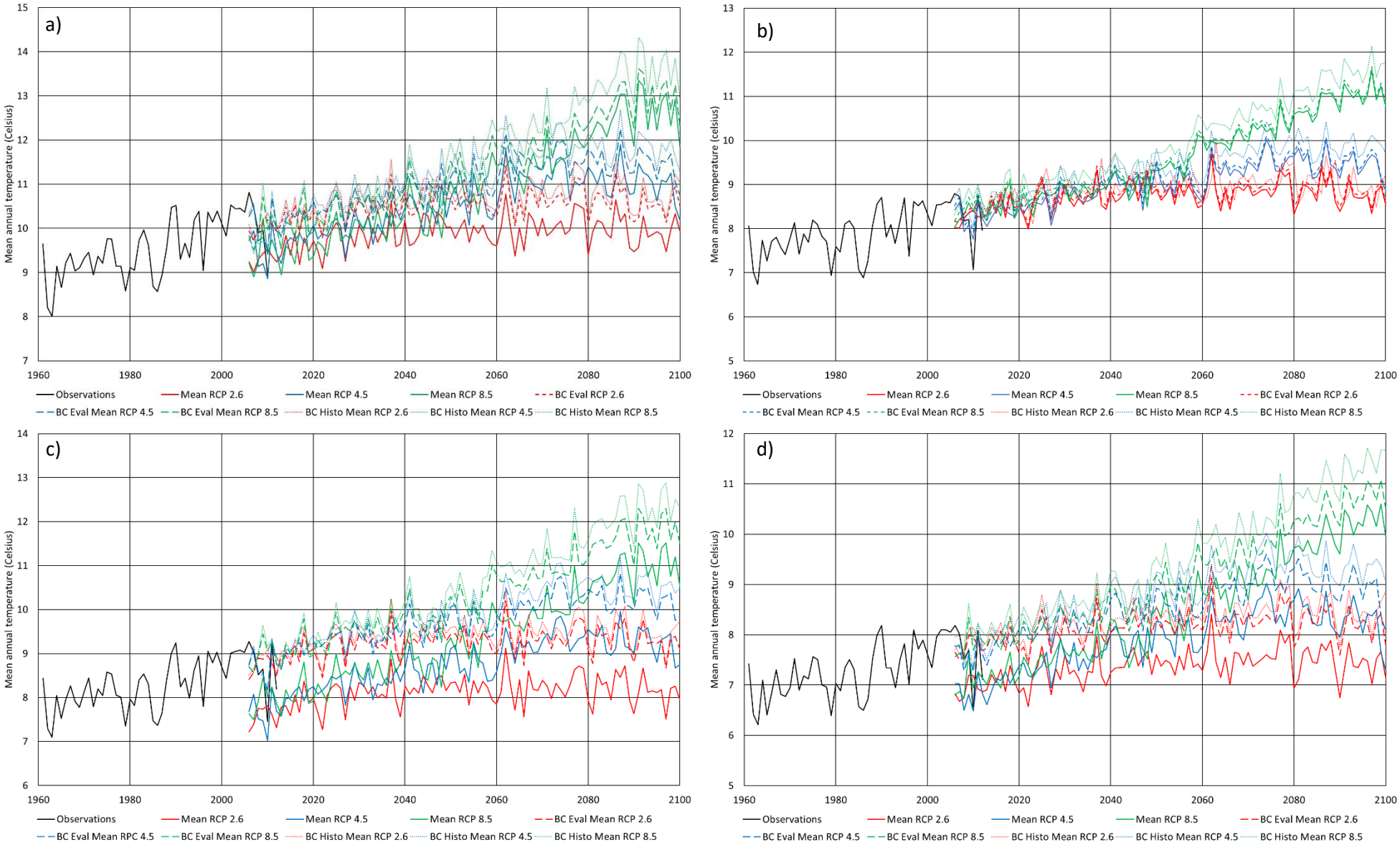

Figure 5. 9 Mean annual temperature time series for the uncorrected and bias corrected RCP projections for: a) upper Thames, b) Glaslyn, c) Calder and d) Coquet catchments

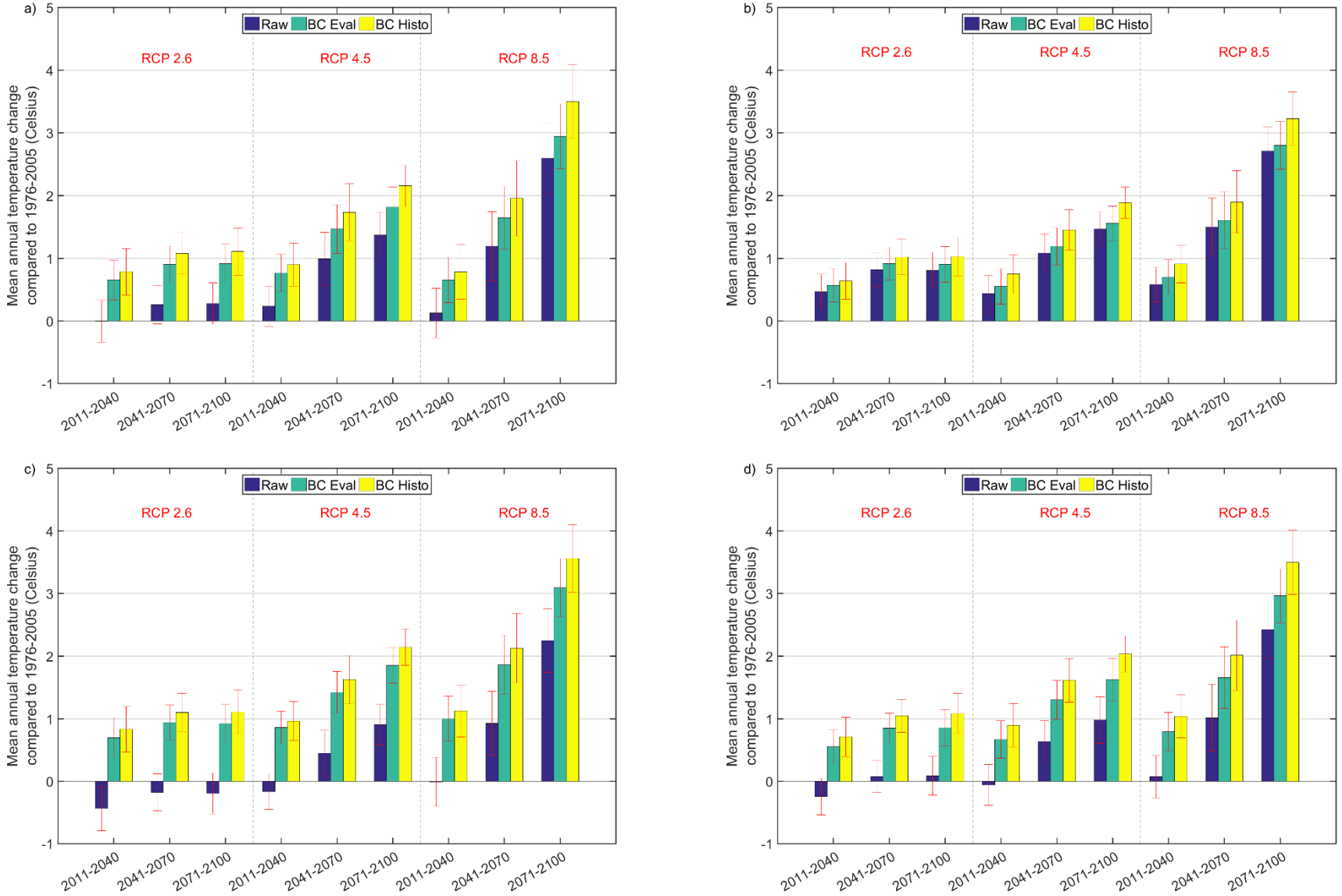

Figure 5. 10 Temperature change compared to 1976-2005 under RCP 2.6, 4.5 and 8.5 using uncorrected and bias corrected outputs for the a) Upper Thames, b) Glaslyn, c) Calder and d) Coquet catchments. The standard deviation from the ensemble simulation is represented by the red bars

The variation in the simulations is assessed next considering the individual simulations of all combinations. This gives an insight of the uncertainty in the simulation given the different GCM-RCM combinations used. The standard deviation from all uncorrected and bias-corrected scenarios is similar with the higher value being 0.6°C (Table B2), which is only observed for RCP 8.5. Both bias correction methods do not affect the standard deviation as the standard deviation from the raw simulations remains almost unchanged. The range from the uncorrected simulations is kept after using the BC-Eval approach. In contrast, after using BC-Histo, the range from the simulations decreases (Fig. 5.11 and Table B2). This is linked to the findings related to the temperature distribution parameters shown in section 5.2.3. Specifically, GCMs have more influence in the simulation of temperature. In all catchments, when employing the BC-Eval approach, the RCM biases are corrected but the GCM biases kept. Thus after using BC-Eval the simulation spread suffers no major change. In contrast, when correcting the GCM biases (using the BC-Histo approach) the simulation spread is reduced by even more than 50% in some cases.

5.3.1.2. Mean monthly temperature

The mean monthly temperature time series show that, except for some cases, the uncorrected projections have no gap with the observations time series for all catchments and most months (Figs. A13 to A16). This could be a direct consequence of the models' selection criteria that discards combinations with the lowest parameter similarity when compared to the distribution parameters of the observations. As a result, the difference between the uncorrected and bias-corrected time series is not large. Nevertheless, there are some cases where the uncorrected RCMs are biased compared to the observations and bias correction removes such biases. This is an indication that the applied selection criteria targets the models with smaller biases and therefore with best simulation skill for the evaluated parameters. However, this method can fall short for some months in certain catchments where biases are observed (e.g. June and August in the Calder catchment and February in the Coquet catchment).

Considering the projected changes in the monthly temperature compared to the 1976-2005 reference period, almost all RCPs and bias correction methods project an increase of temperature for all months (Figs. A17 to A20). Nevertheless, results vary in the magnitude and distribution of the changes for each catchment and RCP projection. For the upper Thames catchment (Fig. A17), considering RCPs 2.6 and 4.5 the BC-Histo method projects larger increases from January to June whereas the BC-Eval has the largest temperature increase projections from July to December. In contrast, for RCP 8.5 BC-Histo projects the largest increases from January to May with similar projections to BC-Eval for the remaining months. The BC-Histo method projects larger increases from January to June whereas the uncorrected and BC-Eval method project a uniform increase throughout all months. Largest increases for all RCPs are projected for April using the BC-Histo method, reaching increases by the end of the century of approximately 2.5°C, 3.7°C and 4.7°C for RCP 2.6, 4.5 and 8.5, respectively.

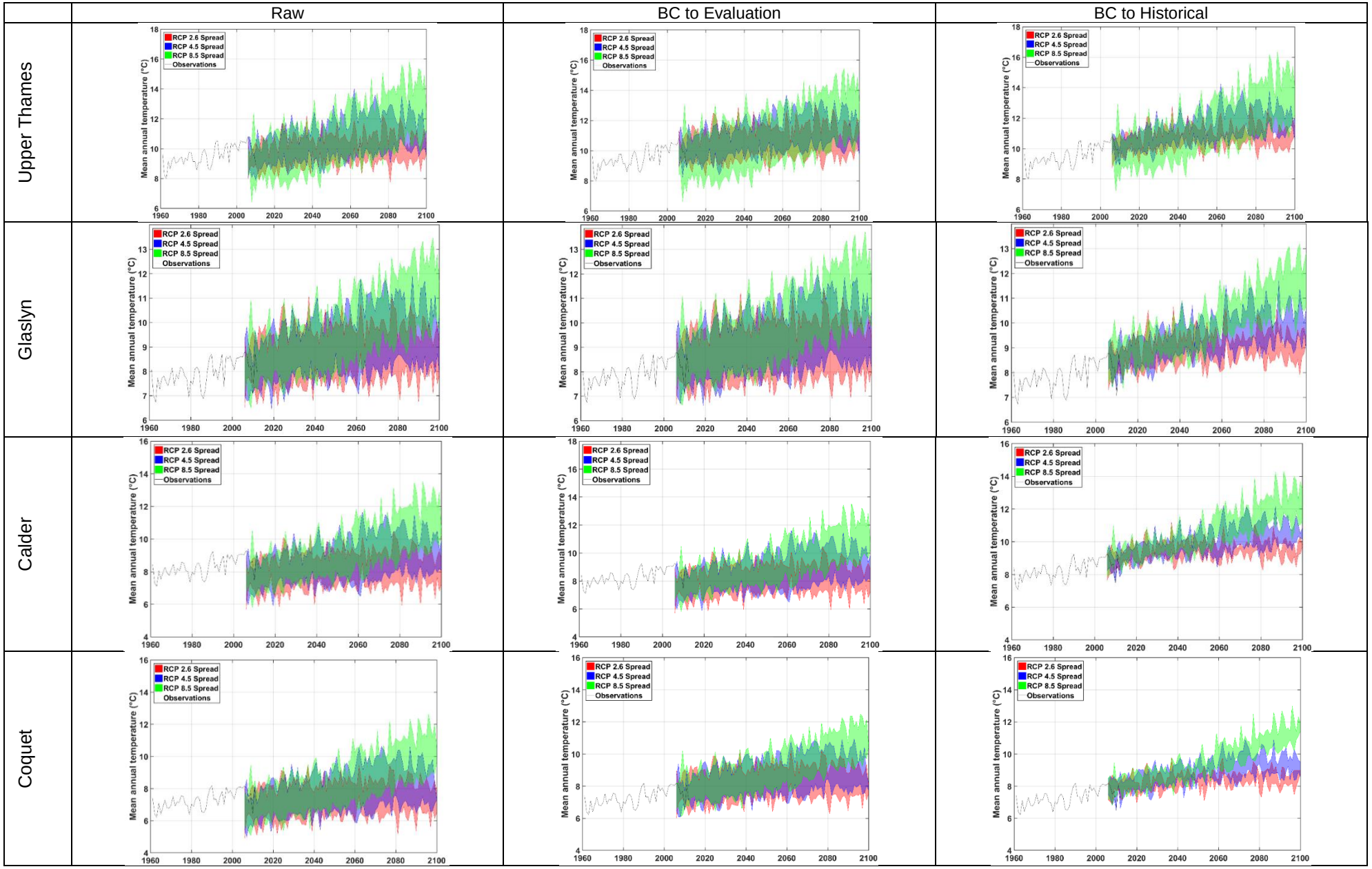

Figure 5. 11 Mean annual temperature simulation spread for each RCP using uncorrected and bias corrected projections for each catchment

For the Glaslyn catchment, for all RCPs the BC-Histo method projects the largest temperature increase compared to the uncorrected and BC-Eval projections (Fig. A18). The uncorrected and bias-corrected simulations and all RCPs project larger increases for winter and autumn as well as for April and June. The largest increases for RCP 2.6 are simulated by the BC-Eval method in December (1.3°C), for RCP 4.5 by the BC-Histo method in February (1.3°C), and for RCP 8.5 by the BC-Histo method in August (1.4°C). The expected temperature increase for this catchment is not as large as in the other catchments.

For the Calder catchment, the uncorrected RCP 2.6 projections decrease in the mean monthly temperature (Fig. A19). Both bias-correction methods change the sign of the climate change signal, projecting an increase in the mean monthly temperature of all months. Furthermore, the projection from both correction methods gives similar results for most months in all RCP scenarios. Only from February to April the BC-Histo projects larger temperature increases than BC-Eval and by the end of the century for RCP 8.5 from August to October. The projected increase is uniform for all months based on the RCP 2.6 and 4.5 projections, except for February that has the largest projected increase. For RCP 8.5, the distribution of the temperature increase is irregular with larger increases in autumn, February and August. Largest temperature increases are projected in February by the BC-Histo method for RCP 2.6 (1.8°C) and 4.5 (2.7°C) whereas for RCP 8.5 has the largest temperature increase projections in August and September (4.5°C).

Uncorrected projections for the Coquet catchment simulate temperature decreases for the beginning of the century (2011-2040) from January to March in all RCP scenarios and also in summer for RCP 2.6 (Fig. A20). Nevertheless, both bias correction methods change the direction of the climate change signal, projecting an increase in the mean monthly temperature for all months and RCPs. Both bias correction methods project similar temperature increases for all seasons, except for spring when the projected increase is smaller. In most of the cases the projection from the BC-Histo method is higher than the BC-Eval method projection. The largest projected temperature for RCP 2.6 is 1.5°C in November, for RCP 4.5 is 2.8°C in December and for RCP 8.5, 4.3°C in October and November.

5.3.1.3. Threshold exceedance

In addition to the annual and monthly temperature time series analysis, a physically-based threshold is estimated to evaluate possible impacts on river flow if such threshold is reached. With this in mind, the threshold is defined as the increase in the mean annual temperature that generates an annual PET volume that would reduce the annual river flow by 10%. A 10% reduction is set as threshold as it would represent an important impact to the water users that depend on the availability of water, affecting the water management strategies and priorities. This rough estimate is calculated using a simple water balance relationship without considering further complexities in the atmospheric and hydrologic systems (e.g. changes to the circulation of cloud formation processes, changes in the atmosphere's moisture holding capacity, water storage into the system, flow routing lag, extractions, etc.). The water balance defines the mean annual river flow as the difference between the observed mean annual precipitation and the estimated annual PET. The results from this analysis are summarized in Fig. 5.12. As explanation of this plot, consider the upper Thames catchment where it is estimated that with an increase of 0.8°C in the mean annual temperature (x-axis) the actual mean annual PET will increase

by 27 mm/yr (red dotted line). Additionally, with such PET increase, the annual river flow is expected to decrease by 10% (solid red line). For the rest of the catchments, river flow will decrease by 10% compared to the actual observed river flow when the annual temperature increases by 1.7°C in the Coquet catchment and 2.6°C in the Calder catchment. It is worth noting that for the Glaslyn catchment, river flow is not expected to decrease by 10% even with an annual temperature increase of 3°C. Nevertheless, for this catchment a threshold of 1°C is defined as this is an upland catchment whose vegetation could be significantly impacted by a 1°C increment in the mean annual temperature.

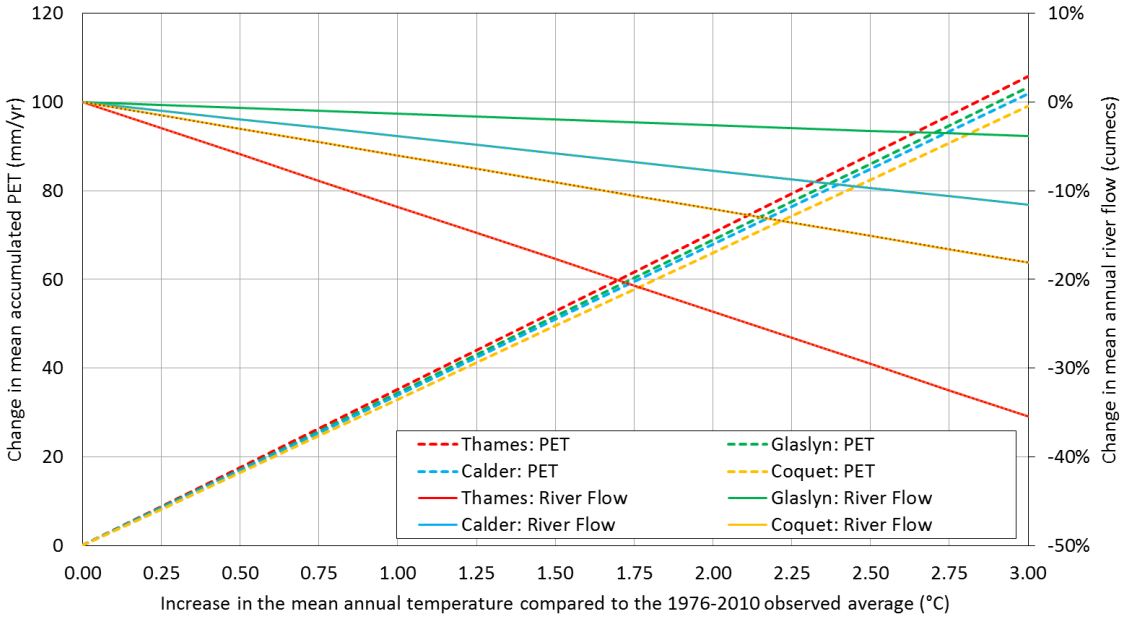

Figure 5. 12 Changes in the annual PET and mean annual river flow as function of an increase in the mean annual temperature observed from 1976 to 2005

Considering the thresholds described above, based in a linear regression analysis of the annual frequency in which the threshold is reached, the annual trends are significant (using a t-test) for all projections in all catchments with few exceptions (Table B3). For the upper Thames, the trends in the uncorrected RCP 2.6 and 4.5 projections are not significant. In the Glaslyn catchment only the uncorrected RCP 2.6 projection is not significant. Finally, for the Calder and Coquet catchments all uncorrected projections are not statistically significant.

An analysis of the number of years in a 5-year moving window when the threshold is exceeded aids in the visualization of the changes as it reduces the impact of the annual variability (Fig. 5.13). Results are shown as a percentage of the five years in the window. Therefore, a 100% is equivalent to five years exceeding the threshold and similarly, 40% represents two years exceeding the threshold.

Only the upper Thames catchment had years when the defined threshold was reached in the past (Fig. 5.13a). For the rest of the catchments, the threshold was not reached in the observations. In all catchments, the uncorrected RCP projections tend to give a lower frequency than in the bias-corrected projections. In most of the cases, the BC-Histo method gives a higher frequency than the BC-Eval method, but there are few cases where this varies per catchment and per RCP scenario. For instance, in some cases both methods give similar results (e.g. RCP 4.5 in the Calder catchment, Fig. 5.13c), or

BC-Eval gives a higher frequency than BC-Histo (e.g. RCP 2.6 in the Coquet catchment, Fig. 5.13d). Also, there are other cases when the uncorrected projection frequency is similar to the bias-corrected frequency (e.g. RCP 4.5 in the Glaslyn catchment, Fig. 5.13b, and RCP 2.6 in the Calder catchment, Fig. 5.13c). Additionally, when using the BC-Histo approach, the frequency from the RCP 4.5 projection reaches similar values to the ones obtained from the RCP 8.5 that is bias-corrected using the BC-Eval approach.

Considering now the frequency observed by the end of the century (2070-2100), this period has contrasting results among the different RCPs. The upper Thames catchment has the largest frequency from all study catchments with frequency percentages ranging from 20% to 80% for RCP 2.6, from 60% to 100% for RCP 4.5 and from 75% to 100% for RCP 8.5 (Fig. 5.13a). In the Glaslyn catchment the frequency ranges from the 30% to 50% for RCP 2.6, from 50% to 90% for RCP 4.5 and from 90% to 100% for RCP 8.5 (Fig. 5.13b). The Calder catchment has the lowest threshold exceedance frequency (Fig. 5.13c). In this catchment, the frequency ranges from 0% to 10% for RCP 2.6, from 0% to 40% for RCP 4.5 and from 10% to almost 100% for RCP 8.5. Finally, for the Coquet catchment the threshold exceedance frequency varies from 0% to 40% for RCP 26, from 20% to 90% for RCP 4.5 and from 40% to 100% for RCP 8.5 (Fig. 5.13d). It is observed that the RCP 8.5 projections reach a 100% of frequency for all catchments denoting the possibility of a constant reduction of 10% in river flow by the end of the century.

5.3.2.Precipitation

This section analyses the other climate variable of relevance for this study. The analysis of precipitation starts with an assessment of the mean annual accumulated precipitation time series simulated by the uncorrected and bias-corrected RCP projections. This includes an evaluation of the variability and of the annual projected future change compared to the reference period (1976-2005). Subsequently, an evaluation of the projected monthly precipitation changes is shown. Finally, an analysis of frequency exceedance of the 90th and 95th precipitation percentiles is shown at the end of this section.

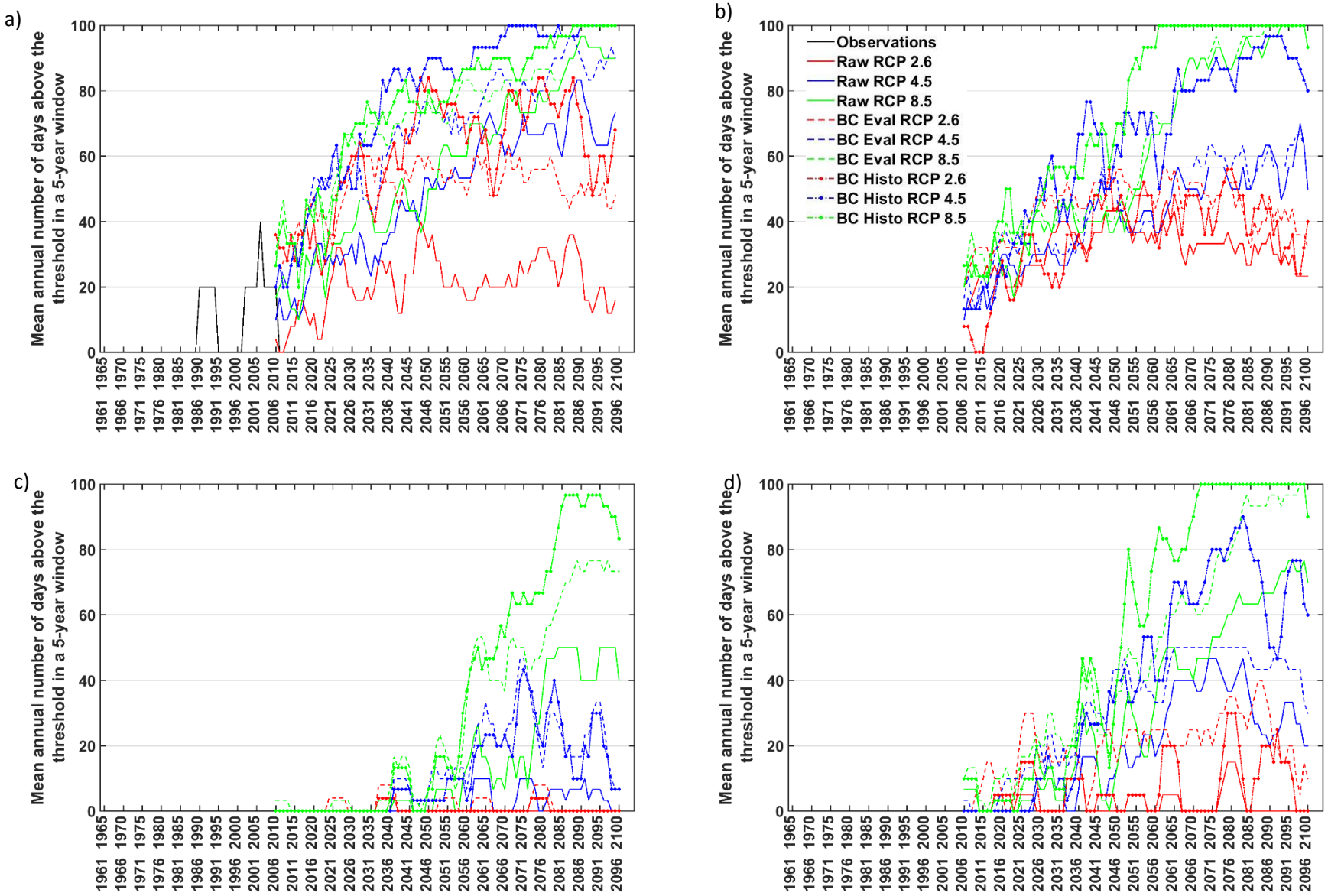

Figure 5. 13 Number of years in a 5-year moving window when the temperature threshold is exceeded for each catchment shown for the uncorrected and bias corrected RCP projections for: a) upper Thames, b) Glaslyn, c) Calder and d) Coquet catchments, note that observations are equal to zero for b), c) and d)

5.3.2.1. Mean annual precipitation

Initially, the analysis of the annual accumulated precipitation time series shows that all uncorrected RCP projections are biased compared to the observed precipitation in all of the catchments (Fig. 5.14). The annual precipitation is overestimated in the upper Thames (~200mm/yr), Calder (~400 mm/yr) and Coquet (~200 mm/yr) catchments, whereas it is underestimated for the Glaslyn catchment (~600 mm/yr). After bias correction, both approaches reduce the biases in the time series. The time series from both correction approaches are similar in all catchments except for the Glaslyn catchment where BC-Histo constantly simulates slightly lower annual precipitation volumes compared to BC-Eval. A large annual variability is observed among all projections for each of the study catchments. The linear regression analysis of the trends from 2006 to 2100 indicates that only the trends in the Coquet catchment statistically significant for BC-Eval driven by RCP 4.5 and for the uncorrected and bias-corrected projections for RCP 8.5 (t-test, p-values < 0.05) (Table B1). There is no difference in the climate change signal direction from the uncorrected and bias-corrected projections, except for cases driven by RCP 8.5 for the upper Thames and Glaslyn catchments. However, in both cases trends close to zero make this finding negligible.

In order to obtain a better understanding of any difference in the mean annual precipitation, an analysis of the changes in three future 30-year time slices (2011-2040, 2041-2070, 2071-2100) compared to a 30-year reference period (1976-2005) is performed. As stated above, the uncorrected RCP projections simulate annual precipitation increases for the upper Thames, Calder and Coquet catchments, and decreases for the Glaslyn catchment (Fig. 5.15). However, as explained above, the RCP projections are biased. Now, considering the changes from the bias-corrected projections, there are cases when the projection from the different correction approaches contradict each other. Specifically, for the upper Thames catchment the projections from RCP 2.6 for all time slices have a different direction of change (Fig. 5.15a). This is also the case for all RCPs and time slices from the Glaslyn catchment (Fig. 5.15b). For the Calder catchment, this happens for the 2011-2040 time slice when using the RCP 4.5 and 8.5 projections and for the 2041-2070 period driven by RCPs 2.6 and 8.5 (Fig. 5.15c). The relevance of this issue increases for the cases where the standard deviation of the bias–corrected simulations doesn't overlap. Thus, even if this only happens for the Glaslyn catchment driven by RCP 2.6, this highlights the possible implications of the bias correction approaches for the projection of future precipitation. This could be an effect of the biases in the uncorrected RCM simulations (Fig. A8) which are not fully corrected by the bias correction approaches. For the remaining catchments and RCP projections, the standard deviation from both correction approaches overlaps (in a smaller proportion for RCP 4.5 and 8.5 projections in the Glaslyn catchment). For the Coquet catchment all projections have an increase in precipitation (Fig. 5.15d).

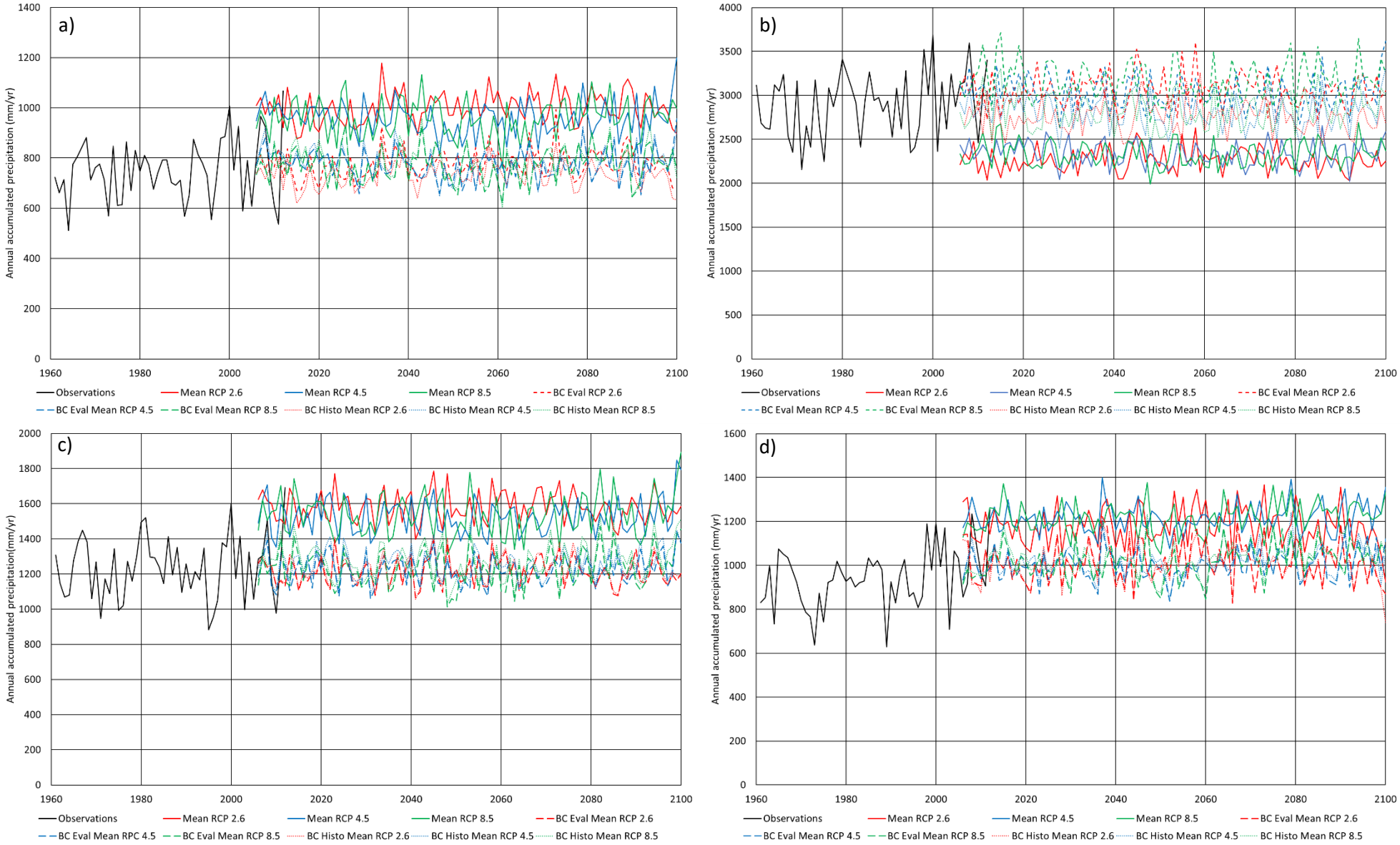

Figure 5. 14 Annual accumulated precipitation time series for the uncorrected and bias corrected RCP projections for: a) upper Thames, b) Glaslyn, c) Calder and d) Coquet catchments (please note the differences in the y-axis)

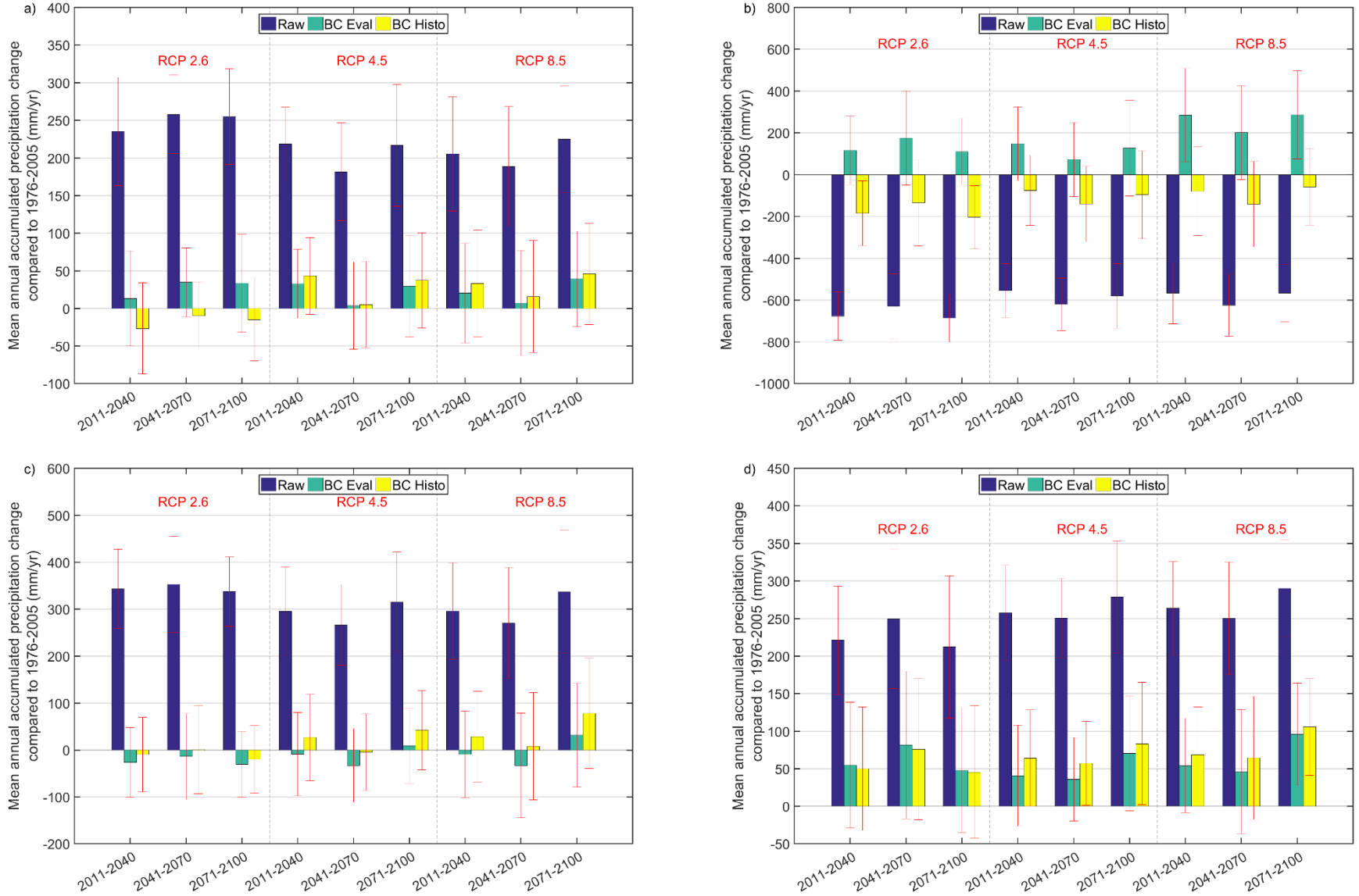

Figure 5. 15 Precipitation change compared to 1976-2005 under RCP 2.6, 4.5 and 8.5 emission scenarios using uncorrected and bias corrected outputs for the a) Upper Thames, b) Glaslyn, c) Calder and d) Coquet catchments

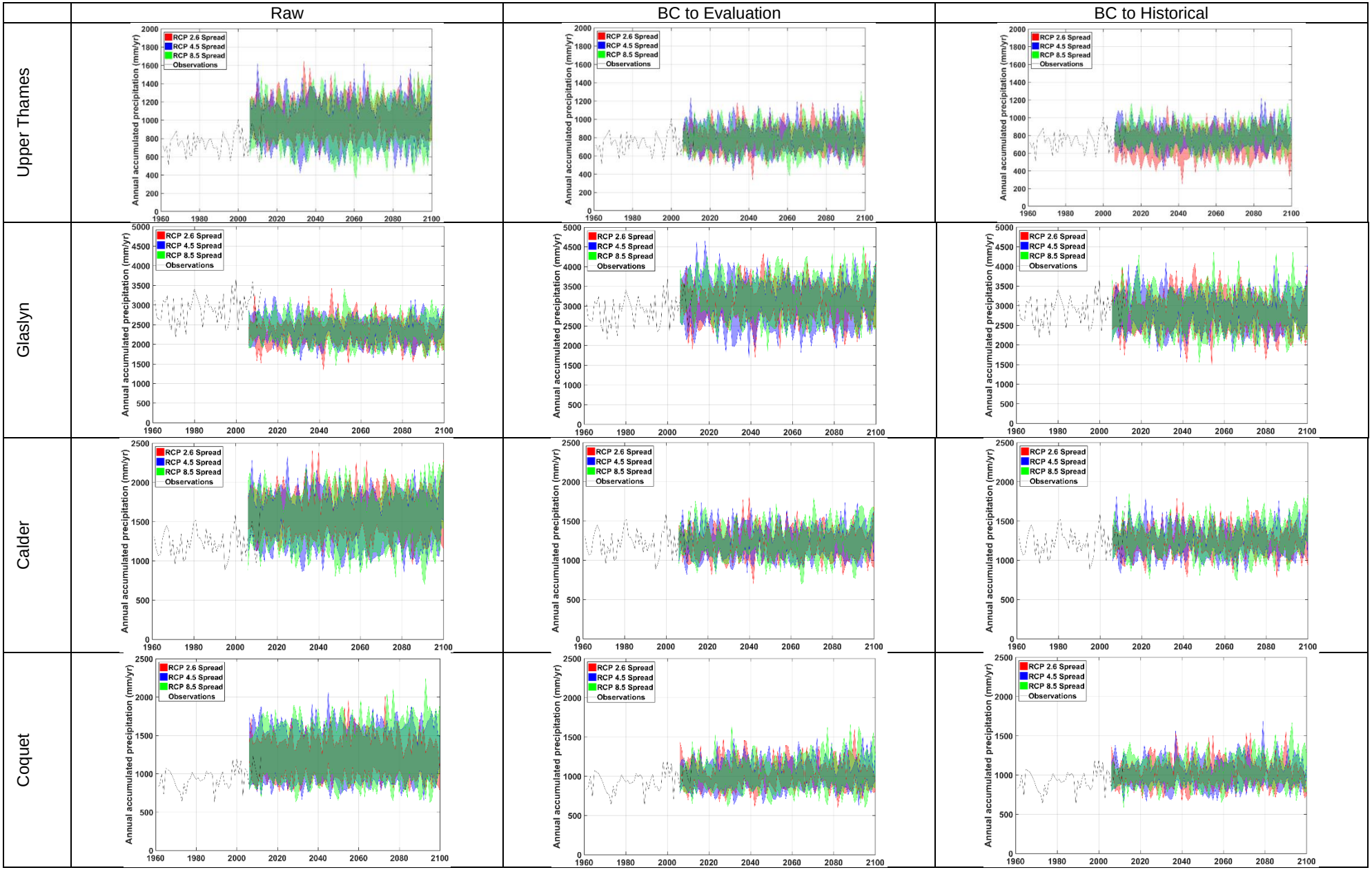

Figure 5. 16. Spread in the mean annual accumulated precipitation for each RCP using uncorrected and bias corrected projections for all catchments

The statistical significance of the changes is evaluated by comparing the standard deviation of the models' ensemble with the mean of the reference period. Significant changes are observed in the Glaslyn catchment for the BC-Histo projections driven by RCP 2.6 during 2011-2040 and 2041-2100. In the same catchment, the BC-Eval projections dirven by RCP 8.5 during 2011-2040 and 2041-2100 are also statistically significant. In the Coquet catchment, statistically significant changes are observed for the BC-Histo projections driven by RCP 4.5 during 2041-2070 and 2071-2100 and driven by RCP 8.5 during 2071-2100.

Annual precipitation changes by the end of the century using BC-Eval range from 4% to 5% for the upper Thames, from 4% to 10% for the Glaslyn, from -2% to 3% for the Calder and from 5% to 10% for the Coquet catchment (Table B4). In contrast, BC-Histo projects changes ranging from -2% to 6% for the upper Thames, from -7% to -2% for the Glaslyn, from -2% to 6% for the Calder and from 5% to 11% for the Coquet catchment.

This chapter looks into the robustness of the climate change signal after applying the both bias correction approaches. Therefore, the cases in which the directions of change of the bias correction approaches are opposite are mentioned next. In terms of percentage, for the upper Thames catchment BC-Eval projects changes ranging from 2% to 5% for RCP 2.6 whereas BC-Histo projects changes ranging from -1% to -4% (Table B4). For the Glaslyn catchment, BC-Eval projects changes from 4% to 6% for RCP 2.6, from 3% to 5% for RCP 4.5 and from 7% to 10% for RCP 8.5. For the same catchment, BC-Histo projects changes varying from -5% to -7% for RCP 2.6, from -3% to -5% for RCP 4.5 and from -2% to -5% for RCP 8.5. The BC-Eval projections for the Calder range from -3% to 1% for RCP 4.5 and from -3% to 3% for RCP 8.5. In contrast, the BC-Histo method projects changes varying from 0% to 3% for RCP 4.5 and from 1% to 6% for RCP 8.5.

Another relevant factor from the precipitation projections is the simulation spread as it involves the uncertainty from using an ensemble of models. For all catchments, the spread from the uncorrected RCPs is slightly deviated from the observations (Fig. 5.16). This is more noticeable for the Glaslyn catchment, for which the observations are at the upper end of the spread. For the rest of the catchments, the observations lie within the spread but are slightly deviated towards the lower section. After bias correction, the observations from all of the catchments lie within the simulation spread. Evaluating the simulation variability and spread statistics (shown in Table B4), the standard deviation from the bias-corrected projections (using both approaches) varies slightly for all catchments except for the Glaslyn. Also, the range of the projections is reduced after applying both bias correction approaches. Again, this is the case for all catchments except for the Glaslyn catchment. For the three other catchments, the spread reduction in relation to the uncorrected projection is similar for each of the bias correction approaches. In other words, the range of the uncorrected projections is reduced by a similar extent by both bias correction approaches. The range difference between both bias corrected projections is small compared to the reduction they both produce to the uncorrected projection. This is explained by the fact that RCMs have more influence on simulating precipitation than the GCMs. Therefore, by correcting the RCM biases (using BC-Eval), most of the precipitation simulation biases are reduced. As it was explained above, the Glaslyn catchment is a special case in which the range and standard deviation

from the uncorrected RCMs increase after bias correction. This potentially is a result from the incapacity of the climate projections to simulate the actual standard deviation of the observations (Table B4). For this specific catchment the standard deviation from the uncorrected RCMs is lower than the observed standard deviation and, therefore the bias correction methods increase the standard deviation and spread of the projections in an effort to match the variability from the observations.

5.3.2.2. Mean monthly precipitation

Considering now the uncorrected mean monthly projected precipitation, time series tend to be biased from the observations. For the upper Thames (Fig. A21), Calder (Fig. A23) and Coquet (Fig. A24) catchments the projections overestimate the observations whereas for the Glaslyn catchment the opposite happens (Fig. A22). The biases are reduced after bias correction.

The changes in the monthly precipitation compared to the reference period (1976 to 2005) provide a different picture for each catchment. It has been shown above that the uncorrected projections have biases from the observations. Therefore, only results from the bias-corrected projections are included in the following analysis. In the upper Thames, the projections indicate a decrease in the monthly precipitation for summer, and an overall increase for the rest of the seasons (Fig. A25). However, for RCP 2.6 the results are more diverse. Also, there are cases where the result is not robust (e.g. the climate change signal from the bias correction approaches have opposite directions). This is more common for RCP 2.6., for example, in February, May, September and December. From the cases that are not robust, the larger difference between the projections with opposite directions can reach up to 10 mm. Compared to the reference period, changes in the monthly precipitation can reach volumes up to +/-15 mm for RCP 2.6, +/- 18 mm for RCP 4.5 and +/- 20 mm for RCP 8.5.

For the Glaslyn catchment, the simulations project decreases in the monthly precipitation for autumn and summer and increases for winter and spring (Fig. A26). This pattern is more evident for RCPs 4.5 and 8.5. However, there are some cases when the climate change from both bias correction approaches has an opposite direction, for example, December for all RCPs and in different months from RCP 2.6. For these cases, the differences between the projected changes from each bias correction approach can be as large as 70 mm (December, RCP 8.5). Compared to the reference period, changes in the precipitation volumes can reach up to +/- 50 mm for RCP 2.6, +/- 60 mm for RCP 4.5 and +/- 90 mm for RCP 8.5

In the Calder catchment, decreases in precipitation are generally projected for summer and increases for winter (Fig. A27). For the rest of the seasons the projection trend is not so well defined. For this catchment, the precipitation changes range from +/-50mm for all RCPs, with the largest change observed in February and March. Similar to the rest of the catchments, there are cases where the climate change signal is not in the same direction, with differences as large as 20 mm between the different approaches (October, RCP 8.5).

Finally, for the Coquet catchment all RCP projections expect an increase in the precipitation for all of the months (Fig. A28). For all RCPs, the projections for all months have the same direction except for August and September. The largest difference between non-robust projections is 15 mm (August, RCP

2.6). In comparison to the reference period, the projections largest increases are 25 mm for RCP 2.6 and 4.5, and almost 40 mm for RCP 8.5.

5.3.2.3. Threshold exceedance

The exceedance thresholds analysed for precipitation are the 90th and 95th precipitation percentiles as they evaluate the frequency in the projected extreme and very extreme precipitation. For this analysis, the average number of days in a year when the threshold is exceeded is assessed. For the exceedance of the 90th precipitation percentile, a linear regression analysis indicates that there is a statistically significant trend (t-test, p-value < 0.05) for the raw and BC-Histo RCP 8.5 projections in the Glaslyn catchment (Table B3). Also, there are significant trends for RCP 8.5 in the Calder and Coquet catchments (both for the uncorrected and bias-corrected projections), for the bias-corrected RCP 4.5 in the Calder catchment and for BC-Histo RCP 4.5 in the Coquet catchment. Nevertheless, in comparison to the available observations, for the 90th precipitation percentile the uncorrected projections overestimate the frequency of days above the threshold for the upper Thames, Calder and Coquet catchments and underestimates the frequency for the Glaslyn catchment (Fig.5.17). The bias-corrected projections reduce the gap between the observations and simulations. However, for the upper Thames and Glaslyn catchments the bias correction reduces but does not entirely remove the bias. This could be an effect of the application of the double Gamma bias-correction technique, which has biases simulating the 90th precipitation percentile compared to the rest of the distribution (Section 4.3.5, Fig 4.27 bottom row). The number of days per year above the 90th precipitation percentile is projected to range between 40 and 50 for the upper Thames and Glaslyn, and between 35 and 45 for the Calder and Coquet for most of the period (Fig. 5.17).

It is also important to assess the monthly variation in the frequency of threshold exceedance compared to the reference period (1976-2005). For each catchment, the projected monthly variation is different. Only considering the bias-corrected projections, for the upper Thames catchment, increases in the frequency of days above the 90th precipitation percentile are projected in all months (Fig. A29). However, there are some months where one of the bias-corrected projections decrease (e.g. March). Nevertheless, reductions in the projections are commonly not robust as the bias correction approaches give outputs with opposite direction. Largest differences between the projections and observations indicate an increase in the frequency of almost two days per month, generally for April.

In the Glaslyn catchment, the bias-corrected projections also indicate an increase in the number of days above the 90th precipitation percentile (Fig. A30). This increase is larger in winter when it can reach up to five days per month compared to the reference period. The changes in the frequency are projected to be smaller during summer. Also, there are a few cases when the models project a decrease in the frequency of exceedance. Nevertheless, these have different change direction for each bias correction approach.

All RCP projections for the Calder catchment generally simulate an increase of the number of days above the 90th precipitation percentile for all months except for January, March, August and September (Fig. A31). The largest changes are projected in February and November with increases in the

frequency of events of almost two days per month. In contrast with the other catchments, all the bias-corrected results from this catchment have the same change direction for both of the bias correction approaches.

In the Coquet catchment, the number of days above the 90th precipitation percentile is also projected to increase overall (Fig. A32). There are months for which the projections simulate a slight decrease in the frequency (March and August), but increases are expected for the rest of the year with higher increases in winter. The largest increment is almost of two days above the 90th percentile per month (February).

Now, considering a more intense precipitation threshold, for the 95th precipitation threshold, the bias correction methods give results in line with the observations for all of the catchments. A linear regression analysis indicated that the annual trend is statistically significant for all projections driven by RCP 8.5 in all catchments and for RCP 4.5 for the Calder and Coquet catchments (Table B3).

Graphically, trends are easier to observe using a 5-year moving window of the mean annual number of days exceeding the 95th precipitation percentile (Fig. 5.18). It is also noticeable that the bias from the uncorrected projections is smaller for all catchments compared to the bias from the 90th precipitation percentile threshold. The projected monthly number of days above the 95th precipitation percentile is different for each catchment. Nevertheless, for all catchments the largest change between the projections and the reference period (1976-2005) is not more than +/- 1 day per month. For the upper Thames, most of the RCPs project increases in the frequency of days above the 95th percentile throughout the year (Fig. A33). Few cases project a robust decrease in the frequency for August and December. For the Glaslyn catchment, frequency increases are projected for December and February for all RCPs (Fig. A34). For late spring and summer early summer there is no large difference from the reference period. Finally, for late summer and autumn the models project a decrease in the frequency for most RCPs and bias correction approaches. Additionally, there are cases where the direction of the change simulated by the bias correction methods has opposite direction, for instance March, September and October driven by RCP 8.5. The projections for the Calder catchment indicate a decrease in the frequency in January, March, April and from August to October (Fig. A35). Also, the months with larger frequency increases are February and November. This pattern is observed in all of the RCP scenarios only varying the magnitude of the change. There are few cases where the direction of change is not robust for both bias correction approaches, but in such cases the difference between the output from each method is small compared to the largest projected change. For the Coquet catchment, the projections simulate an increase in the monthly frequency of days above the 95th precipitation percentile throughout most of the year (Fig. A36). Cases when the frequency decreases for August through November are mostly for RCP 2.6, with fewer reductions for the remaining RCP scenarios. Most changes are robust, but there are few cases when this is different (e.g. September driven by RCP 2.6, June driven by RCP 4.5 and August driven by RCP 8.5).

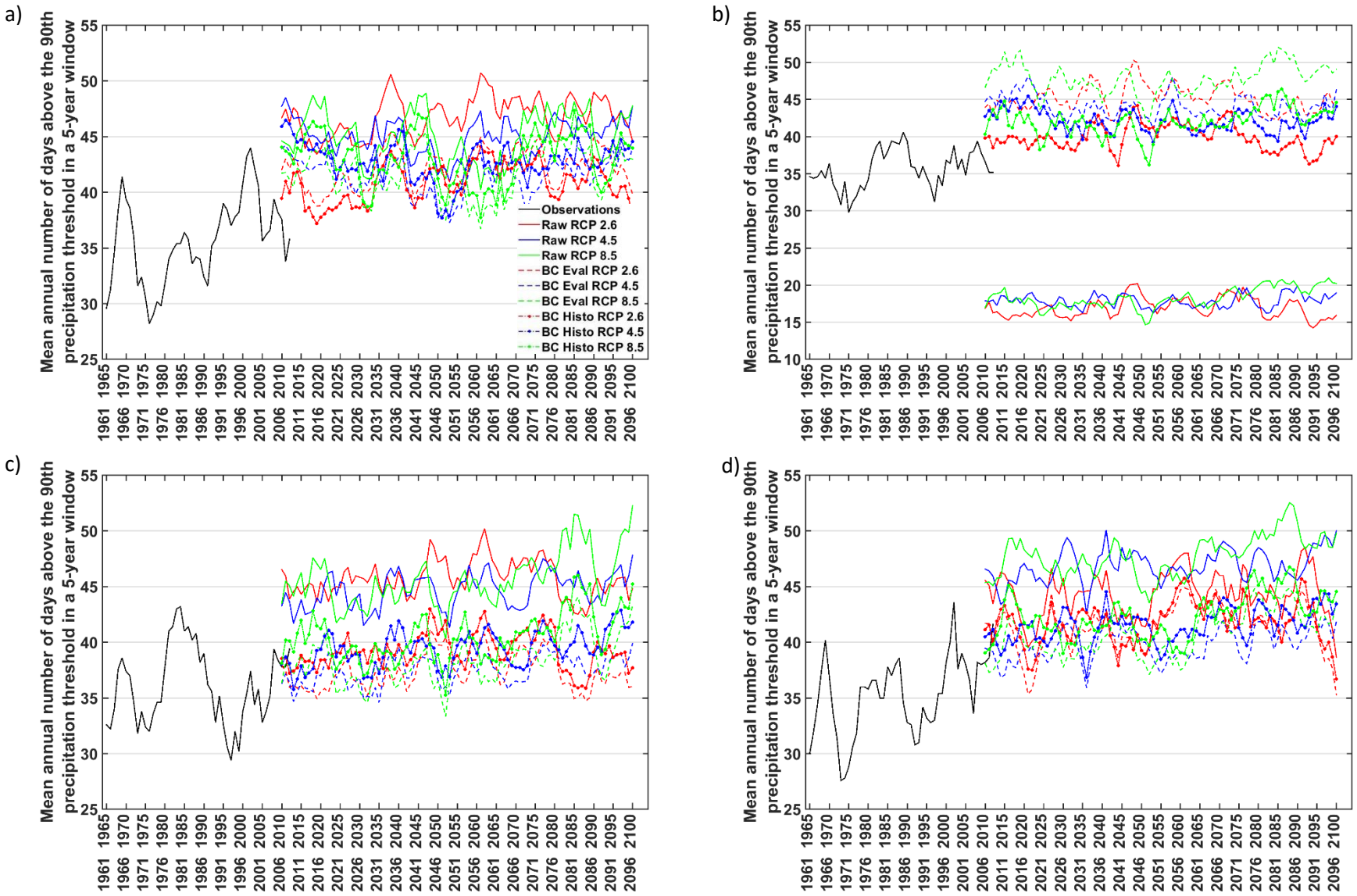

Figure 5. 17 Mean annual number of days in a 5-year moving window when the 90th precipitation percentile is exceeded for each catchment shown for the uncorrected and bias corrected RCP projections for: a) upper Thames, b) Glaslyn, c) Calder and d) Coquet catchments

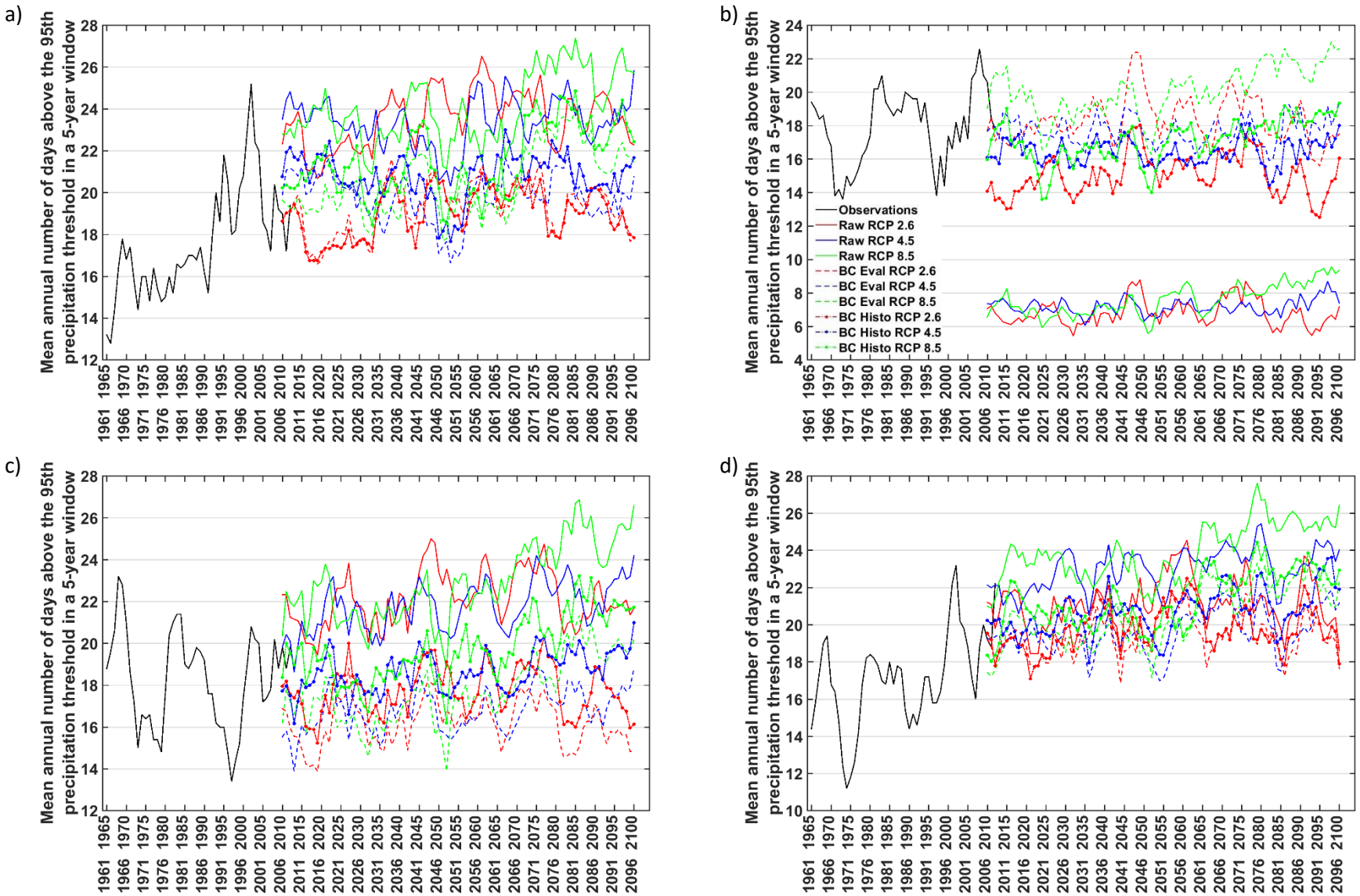

Figure 5. 18 Mean annual number of days in a 5-year moving window when the 95th precipitation percentile is exceeded for each catchment shown for the uncorrected and bias corrected RCP projections for: a) upper Thames, b) Glaslyn, c) Calder and d) Coquet catchments

5.4. Summary and discussion

This chapter assesses the temperature and precipitation projections driven by RCPs 2.6, 4.5 and 8.5 for the four study catchments. Projections from six GCM-RCM combinations are used to simulate the future scenarios in each catchment. The selected projections are a subset of the thirteen available combinations from the Euro-CORDEX project and are chosen following defined criteria. The criteria evaluate the skill of the GCM-RCM simulations to reproduce the observed distribution parameters for precipitation (scale and shape) and temperature (mean and standard deviation). Furthermore, the similarity between the distribution parameters of the historical and evaluation GCM-RCM simulations is also evaluated. The six combinations are selected based on their skill considering both criteria. The selection is performed for each catchment; thus the selected combinations differ between the catchments (Table 5.1). The six selected combinations are expected to give a reliable and comprehensive range of projections that are suitable for the analysis of climate change impacts. A different approach could select only the combinations with simulation skill above a set threshold. However, such approach does not guarantee the inclusion of a minimum number of combinations. As a consequence, such method might not include a comprehensive range of projections that consider different simulation approaches.

Additionally, two different bias correction approaches are used, namely BC-Eval and BC-Histo. The BC-Eval approach uses the evaluation runs (which are driven by perfect boundary conditions using the Era-Interim reanalysis) to train the bias correction technique. In contrast, the BC-Histo approach uses the historical runs (driven by GCMs) to train the correction technique. In theory, the BC-Eval approach only corrects RCM biases, whereas the BC-Histo approach corrects the GCM-RCM combination biases. BC-Eval is often used by the climate community to evaluate the skill of RCM bias correction (e.g. Kotlarski et al., 2014; Prein et al., 2015; Casanueva et al., 2016). In contrast, the impact communities often employ the BC-Histo method as it reduces biases from both the GCM and RCMs, providing projections with a reduced simulation spread.

Considering the above, the chapter answers the research question:

iii) to what extent are the projected changes in climate robust, considering both bias correction approaches?

Here, robustness means that the direction of change is the same for both bias correction approaches considering the multi-model ensemble mean (MEM). Furthermore, the chapter gives information about the variations in the future precipitation and temperature projections compared to the 1976-2005 reference period. The analysis includes the assessment of annual and monthly means as well as the occurrence of extreme events.

In the reference period has a gap when compared to the uncorrected projections. Biases are larger for precipitation than for temperature. This highlights the need for bias correcting the climate simulations. Mean annual temperature increases are projected for all catchments, and are statistically significant from 2006 to

2100 for all RCPs in all catchments. Knutti and Sedlacek (2013) also found that the temperature change was statistically significant in the UK, but they only analysed RCP 8.5. Precipitation mainly increases in winter and decreases in summer in all catchments, similar to findings from Schneider et al. (2013) and Knutti and Sedlacek (2013) for the UK. The mean annual precipitation change projected for the catchments is similar to the projections obtained by Giorgi et al. (2014) which ranges from no change to an increase of 75 mm/year. The occurrence of days above the 90th precipitation percentile increases all year and the 95th precipitation percentile frequency varies from catchment to catchment. Overall, the projected mean annual temperature increase is similar for all catchments as well as the frequency of extreme precipitation events.

There are differences in the projected change of temperature for each RCP. Whereas RCP 2.6 projects the same change magnitude through 2006-2100, the other RCPs project an increasing temperature though the century. The projected temperature change for 2071 to 2100 driven by RCP 4.5 has similar magnitude than the change projected for 2041 to 2070 for RCP 8.5. Nevertheless, results are similar to Schneider et al. (2013), who projected temperature increases of at least 2°C for the UK by 2100. For precipitation, the projected changes are not so different between the RCP projections for each 30-year time slices. In the case of the trend of the frequency of occurrence of extreme precipitation from 2006 to 2100, all cases driven by RCP 8.5 and half of the cases driven by RCP 4.5 are statistically significant. It can be concluded that the main difference between the RCP projections is the difference in the projected annual mean temperature, whereas for precipitation differences between the RCPs exist for the extremes and are not evident for the mean changes.

The bias correction approaches reduce the simulation spread from each variable differently. Whereas BC-Eval and BC-Histo reduce the precipitation spread to a similar extent, for temperature BC-Histo reduces the spread further than BC-Eval. Nevertheless, the most relevant result is to assess whether there are contrasting climate change signals by applying each of the approaches. Considering the MEM, for the case of temperature there is no difference in the climate change signal direction, therefore projecting a robust change. However, BC-Histo gives the largest changes for all cases. Considering the precipitation changes, there are cases when the climate change signal has different directions for each of the bias correction approaches, for example in the Glaslyn catchment. Therefore, in contrast to Mbaye et al. (2016) who evaluated the impact of bias correction to the projected change in temperature and precipitation, here the climate change signal direction changes after quantile mapping bias correction depending on the used approach. Additionally, there is no evidence suggesting that bias correction improves the climate change trend (Maraun 2016). Furthermore, the standard deviation of the MEM change simulated by both approaches do not overlap for the bias corrected precipitation in the Glaslyn catchment, implying completely different projections. In this catchment, the uncorrected models have a gap in their simulation of future projections when compared to the reference period time series. This represents the largest contrasting result from the use of both approaches. For the remaining catchments there are also cases where the MEM change direction from both approaches differs, but the difference is small and their standard deviation

overlap. The trends of the bias-corrected projections from 2006 to 2100 are not largely different between each approach. The MEM of the bias-corrected approaches gave results with different change direction. Nevertheless, most differences were small and only for the Glaslyn catchment there were cases when the change directions where completely different as the standard deviation from both approached did not overlap. Therefore, it is important to examine the simulation spread in impact assessments to consider the range of possible changes. If only the MEM projections are considered, then the result might differ for each of the bias correction methods. Nevertheless, if the standard deviation of the result is also assessed, then there is no large difference in the projections, except for the Glaslyn catchment, for which the uncorrected RCMs have the largest biases.

Summarizing the above information, considering the MEM projections, it can be concluded that the temperature changes are robust and statistically significant. Nevertheless, for precipitation there are cases when results are not robust, especially for the Glaslyn catchment as the bias-correction approaches give contradictory change signals. This can be an effect of the large biases from the uncorrected RCMs that don't give an appropriate input for bias-correction to be robust. For the remaining cases, the difference between the projections is small and if the deviation is considered then it can be concluded that there is no significant difference between the bias-corrected projections. Nevertheless, if only the MEM is considered, then opposite signals are obtained.

In this chapter, the results from the BC-Eval and BC-Histo approaches are analysed. However, it is acknowledged that for an analysis of the impacts of climate change, the end user requires a decrease in the overall projection biases in order to increase the confidence in decision-making based on the bias-corrected projections. Thus, in an assessment of the impacts of climate change, BC-Histo represents the best approach. For consistency, the remainder of this study presents results from the uncorrected, BC-Eval and BC-Histo projections.

Finally, climate model biases are time dependent and therefore a change in the reference period would imply a change in the bias and the bias correction parameters (Huang et al., 2014; Maraun, 2016). When comparing results from different studies, this might be problematic as there is no standard reference period to use in the analysis of impacts. Reference periods from previous studies vary from 1961-1990 (Arnell & Lloyd-Hughes, 2014), 1970-1999 (Van Vliet et al., 2015), 1972-2005 (Giuntoli et al., 2015), 1971-2000 (Schneider et al., 2013; Mbaye et al., 2016) and 1986-2005 (Stocker et al., 2013), just to mention a few. Here, the reference period is selected based on the availability of observed climate and river flow data, which turned to be a 30-year period ranging from 1976 to 2005. The same reference period has been used in previous studies (e.g. Giorgi et al., 2014; Prudhomme et al., 2013). Considering this, there might be cases when the selected reference period plays an important role in the interpretation of results (mainly when large fluctuations in the climate occur). However, this is not analysed as it is beyond the scope of this research.

6. Climate change impacts to hydrology and hydropower

6.1. Introduction

This chapter continues with the analysis by including an assessment of the climate change impact on flow regimes of the study catchments and the impacts on run-of-the-river (RoR) hydropower schemes. Similar to chapter 5, this chapter focuses on the climate change impact change direction after applying two bias correction approaches (BC-Eval and BC-Histo, section 5.2.1) to the six GCM-RCM simulations. Results are considered robust when the change direction is similar for the simulations corrected by both approaches. This procedure addresses the second part of research question **iii) …to what extent are the projected climate change impacts on flow regimes and hydropower generation robust, considering both bias correction approaches.** Furthermore, the chapter analyses the projected changes in hydropower due to climate change, therefore addressing the main objective of the thesis: **assessing the climate change impacts on the efficiency and feasibility of RoR hydropower schemes in the UK.**

Hydropower can play a relevant role if included in the optimal renewable energy share (Francois et al., 2016). This is mainly due to the influence of weather in the variation of wind and solar energy generation (von Bremen et al., 2010). Hydropower is an alternative to complement the energy demand when the solar and wind sources are not productive. If integrated, the hydropower share in an optimal generation mix could reach 65% in England (Francois et al., 2016). This has attracted the attention of the government and groups of individuals interested in participating in the generation of hydropower through RoR schemes within the UK (e.g. EA, 2010; EA. 2011). Nevertheless, preliminary RoR hydropower analyses often lack an assessment of climate change impacts, and just recently this area is started to being analysed (e.g. Tamm et al., 2016).

The chapter presents an analysis of the annual and monthly mean river flow and hydropower generation projections along with their future change compared with the reference period (1976-2005). Additionally, the projected exceedance frequency of relevant river flow and hydropower operational thresholds is analysed. These results are shown for both the BC-Eval and BC-Histo bias correction approaches to evaluate whether differences arise from the choice of the approach. The river flow results are shown first followed by the hydropower results. Through the chapter, the results are shown based on multi-model ensemble mean (MEM) unless the contrary is stated.

6.2. Projected river flow simulation

The methodology for river flow simulation is similar to the one employed in chapter 4, with slight variations. In summary, the uncorrected and bias-corrected temperature and precipitation (using the double Gamma distribution correction) GCM-RCM outputs are used to simulate each catchment's climate from 2006 to 2100. This permits the evaluation of the uncertainty in the projections and also evaluates the role of the bias correction method. PET is estimated using the simulated temperature as input for the Oudin formula (Oudin et al., 2005) as this is a required input for the hydrological model. Finally, for each catchment, the precipitation and PET simulations (both uncorrected and bias-corrected) are used to drive the HEC-HMS hydrological model in order to simulate the future river flow from 2006 to 2100. Similar to chapter 5 where the climate variables are analysed, here the mean annual

and monthly river flow projections are analysed along with changes in the high (Q10) and low (Q95) flows frequencies. These extreme flow measures are used as they are important measurements influencing the river regime.

A common reference data is defined with the objective of being independent from the bias correction approaches. Consistent with chapter 5, the observed river flow is selected as reference data for the 1976-2005 period. In order to support this decision, for their overlapping period (1989-2005) a Mann-Whitney test of same equal means and variances is used to evaluate the similarity between the observed time series and the averaged bias corrected time series (from the BC-Eval and BC-Histo methods). The test results indicate that the time series have the same means and variances in all catchments (p-values > 0.05) (Table 6.1). Therefore, the observations are used as reference data for comparison of the projected changes. Results from the uncorrected and bias corrected projections using both approaches are shown in the following sections.

Table 6. 1 p-values from the difference in means and variances tests between the observations and the averaged (BC-Eval and BC-Histo) bias-corrected river flow time series, a p-value > 0.05 indicates that there is no difference between the means and variances from both time series.

	River flow
Upper Thames	0.68
Glaslyn	0.73
Calder	0.56
Coquet	0.65

6.2.1. Mean annual river flow

The mean annual river flow time series for the uncorrected projections are biased from the observations for all catchments (Fig. 6.1). These biases overestimate river flow for the upper Thames (~20 m^3/s), Calder (~5 m^3/s) and Coquet (~ 2 m^3/s) catchments and underestimate it for the Glaslyn catchment (~ 2 m^3/s). After using both bias correction approaches, the mean river flow biases decrease. A linear regression analysis from 2006 to 2100 indicates that trends in river flow in only two projections are statistically significant when using a t-test (p-value < 0.05). Such cases are the BC-Eval projection driven by RCP 2.6 for the upper Thames and the uncorrected projection driven by RCP 8.5 in the Glaslyn catchment (Table B5, first columns). There are no changes in the trend from the uncorrected projections after bias correction, except for RCP 8.5 in the upper Thames catchment. For this case, the uncorrected and statistically-significant trend projects a decrease in the mean annual river flow of 1 m^3/s by the end of the century, whereas the BC-Eval method projects an increase of 0.3 m^3/s.

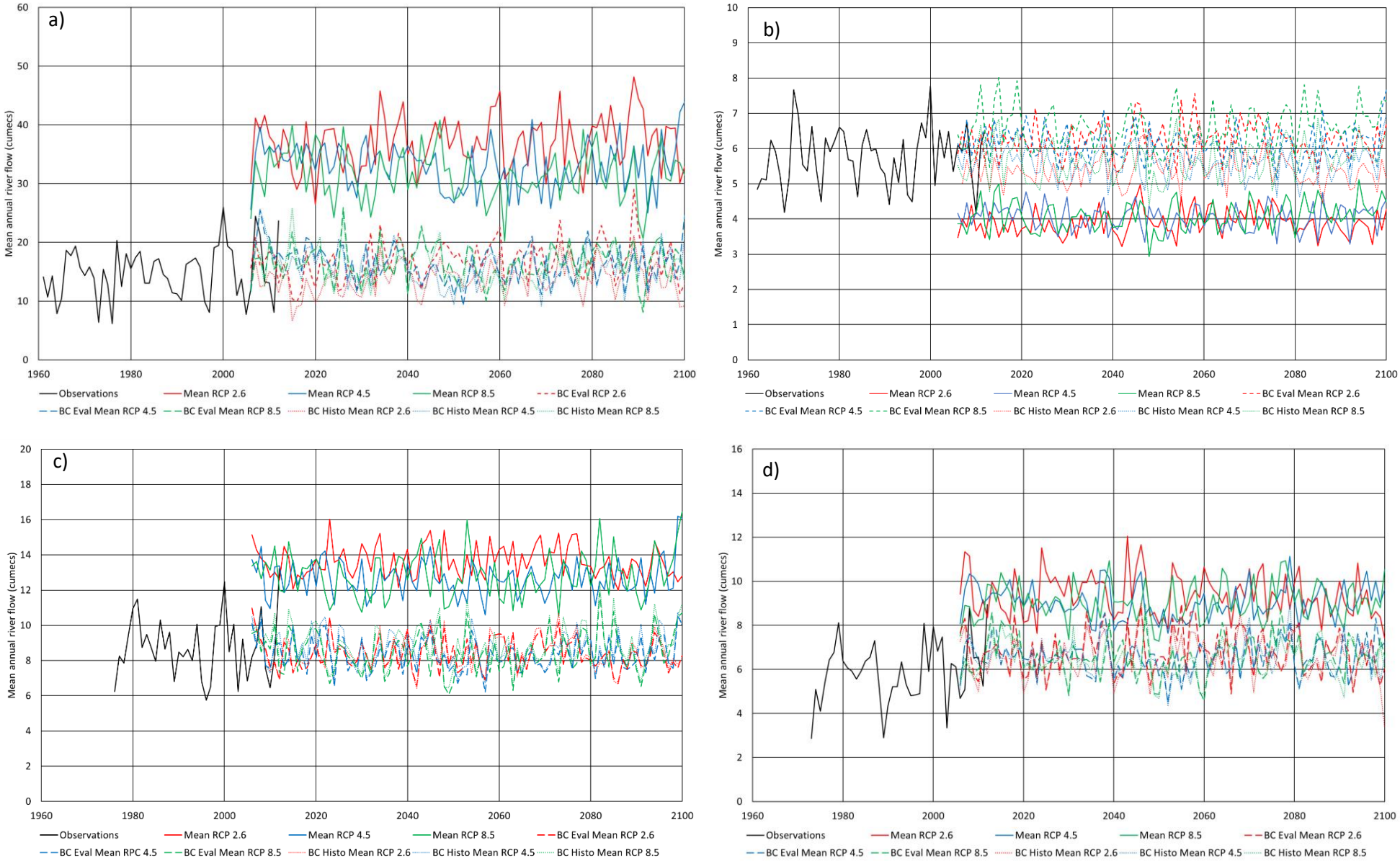

Figure 6. 1 Mean annual river flow time series for the uncorrected and bias corrected RCP projections for: a) upper Thames, b) Glaslyn, c) Calder and d) Coquet catchments

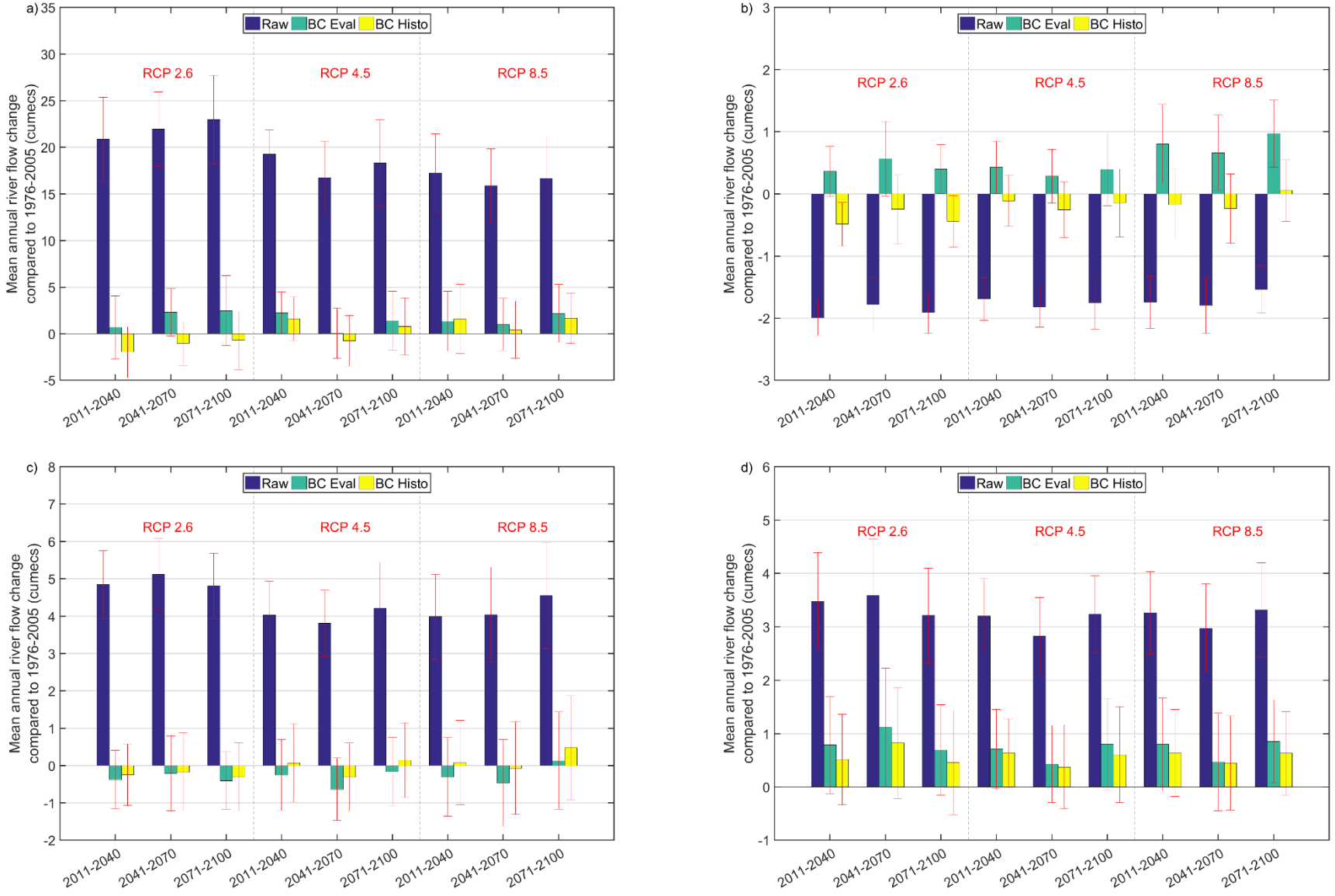

Figure 6. 2 Projected river flow change compared to 1976-2005 under RCPs 2.6, 4.5 and 8.5 using uncorrected and bias corrected outputs for the a) Upper Thames, b) Glaslyn, c) Calder and d) Coquet catchments. The standard deviation from the ensemble simulation is represented by the red bars

The projected changes in the mean annual river flow are evaluated at three different 30-year time periods in the future (2011-2040, 2041-2070 and 2071-2100) compared with the reference period (1976-2005) (Fig. 6.2). The following text only refers to the bias-corrected projections as the uncorrected projections have large biases (Fig. 6.1). For all catchments, except for the upper Thames, the projected river flow change is not larger than +/- 1 m^3/s for all time slices compared to the reference period. In contrast, for the upper Thames, changes in the future river flow range from 2.5 to -2 m^3/s. Nevertheless, this is the larger catchment included in the analysis, which also has the largest river flow. In terms of robustness in the direction of the projected change, the bias correction approaches give changes in opposite direction for the upper Thames driven by RCP 2.6, for the Calder catchment when simulating the RCP 4.5 scenario and for all scenarios and time slices for the Glaslyn catchment. From such cases, only the Glaslyn catchment has periods when the standard deviation from the different bias correction approaches don't overlap each other for RCP 2.6. Results are robust in the remaining cases as the direction of change is the same for both bias correction approaches.

Considering the projected changes in each time slice (2011-2040, 2041-2070 and 2071-2100) as a percentage of change compared to the reference period (1976-2005) gives an idea of the magnitude of the change and allows the comparison between the results from both bias correction methods. Results can be contrasting in terms of their climate change signal direction and extent according to the bias correction approach used (Table B6, last columns). The cases when this occurs are described next. For the upper Thames, BC-Eval outputs range from 5% to 17% for RCP 2.6, whereas BC-Histo projects changes ranging from -5% to -13%. In the Glaslyn catchment the BC-Eval method projects changes varying from 6% to 10% for RCP 2.6, from 5% to 7% for RCP 4.5 and from 11% to 17% for RCP 8.5, whereas BC-Histo gives changes varying from -4% to -8% for RCP 2.6, from -2% to -4% for RCP 4.5 and from -4% to 1% for RCP 8.5. For the Coquet and Calder catchments there are no cases of this type. Cases when the climate change signal from both bias correction approaches has the same direction for the three time slices are also observed. In the upper Thames, the RCP 8.5 projection estimates river flow changes ranging between 3% and 15%. For the Calder catchment the projected changes vary between -5% and -2% when driven by RCP 2.6. Finally, for the Coquet catchment all RCPs indicate a robust increase in river flow throughout the century. The increase ranges between 9% and 19% when driven by RCP 2.6, between 6% and 14% when driven by RCP 4.5 and between 8 and 14% when driven by RCP 8.5.

The statistical significance of the projected changes is evaluated by comparing the simulation standard deviation from the model ensemble with the mean of the reference period. Changes projected by BC-Histo in the Glaslyn catchment are statistically significant when driven by RCP 2.6 during 2011 to 2040 and 2071 to 2100. For this catchment, the BC-Eval projected changes are statistically significant when driven by RCP 8.5 during 2011 to 2040 and 2071 to 2100. For the Coquet catchment the BC-Eval bias-corrected projected change driven by RCP 8.5 during 2071 to 2100 is statistically significant. There are no other cases were the changes are statistically significant.

The variability of the different climate projections is important for the analysis of future river flow as it serves as basis for determining strategies for climate change adaptation considering the different

possible scenarios (e.g. flood response, water availability, etc.). Both the ensemble spread and standard deviation of the ensemble mean are considered. The simulation range is defined as the difference between the minimum and maximum simulations considering the six GCM-RCM simulations that are used for the analysis. As for precipitation, the observed river flow time series is included in the lower extreme of the range of the uncorrected projections for the upper Thames, Calder and Coquet catchments (Fig. 6.3). For the Glaslyn catchment, the observed river flow time series is slightly underestimated by the spread of the range of the uncorrected projections. After bias correction, the standard deviation of the uncorrected projection generally remains unchanged or reduced (Table B6). Also, the bias correction approaches decrease the range from the projections and fit the observations in the centre of the simulation range. Only for the Glaslyn catchment, the range of the bias-corrected projections remains as large as the range of the uncorrected projections. The ensemble spread of the uncorrected projections is reduced by both bias correction approaches for the remaining catchments. For the Glaslyn catchment this relates to the inability of the climate models to accurately simulate the standard deviation from the observed precipitation (section 5.3.2.1), consequently impacting the river flow simulation. Finally, as for the precipitation results, the ensemble spread of the uncorrected river flow projections is reduced by both bias correction approaches to a similar extent. This demonstrates that for these catchments, precipitation has more influence than temperature when simulating river flow. Nevertheless, for RCPs 4.5 and 8.5 in the upper Thames catchment, compared to BC-Eval, BC-Histo further reduces the projection range, decreasing it by 5 m^3/s. This indicates that for this specific catchment, temperature has an important effect in the river flow simulation.

6.2.2.Mean monthly river flow

In order to assess the projected changes in the flow regime, the mean monthly river flow is analysed. This is important as changes in the seasonality of the flow regime might impact the activities and sectors that depend on the availability of water such as hydropower generation. Furthermore, the flow regime is also critical for river ecology (Poff et al., 1997). As the uncorrected climate simulations result in biased projected river flow simulations (Fig. 6.1), only the bias-corrected projections will be described.

For the upper Thames, compared to the reference period from 1976-2005, projections indicate an increase in the mean monthly river flow for all the year, except from October and November (Fig. 6.4). Most of the projections for each month and time slice are robust with only few cases when the direction of change from the bias correction approaches differs. The largest changes are increases of 8 m^3/s for February and March under RCP 8.5. Compared to the reference period, the projected changes would potentially modify the actual river flow regime as the difference between wet and dry seasons would increase.

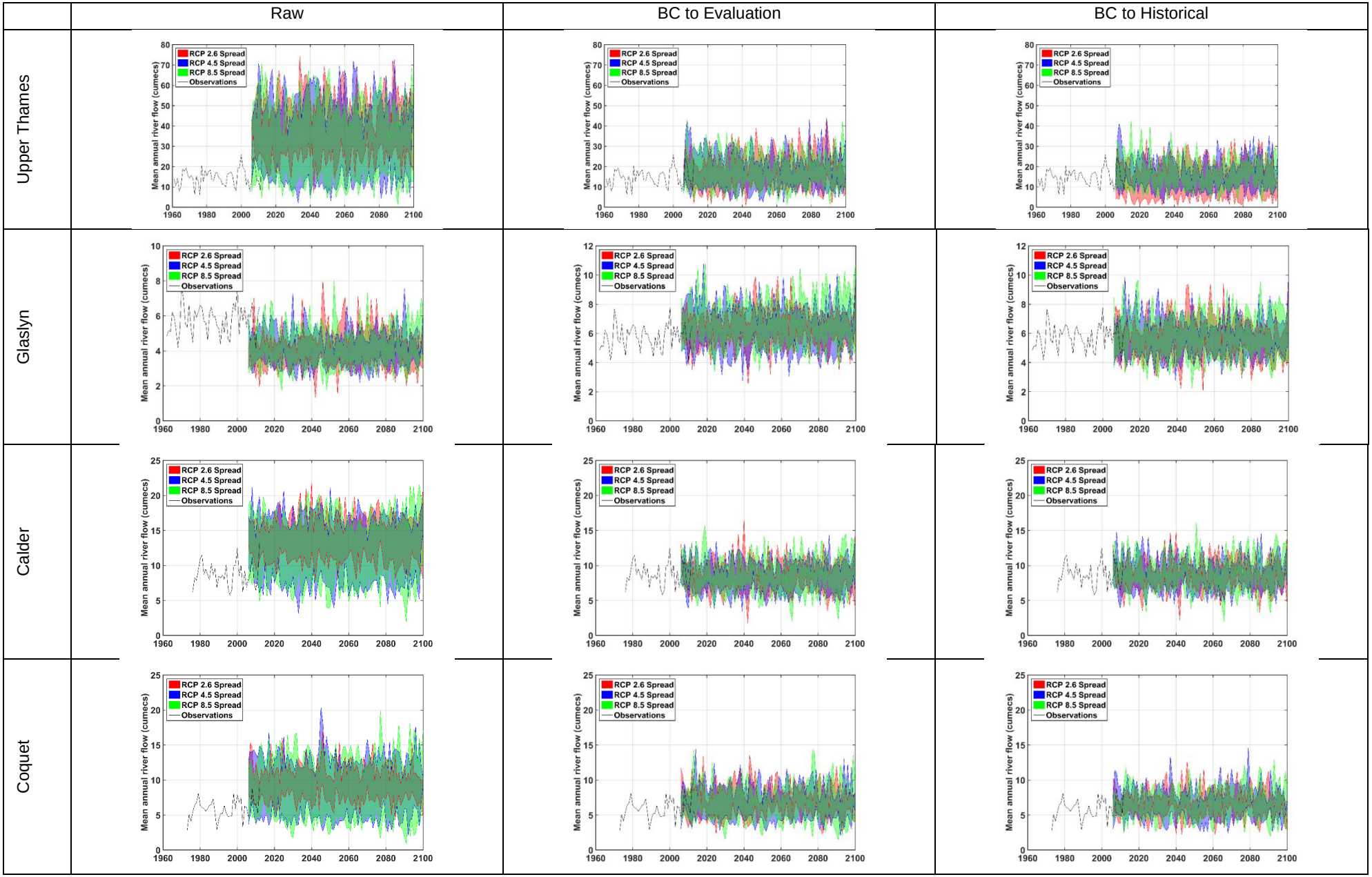

Figure 6. 3 Mean annual river flow simulation spread for each RCP using uncorrected and bias corrected projections for all catchments

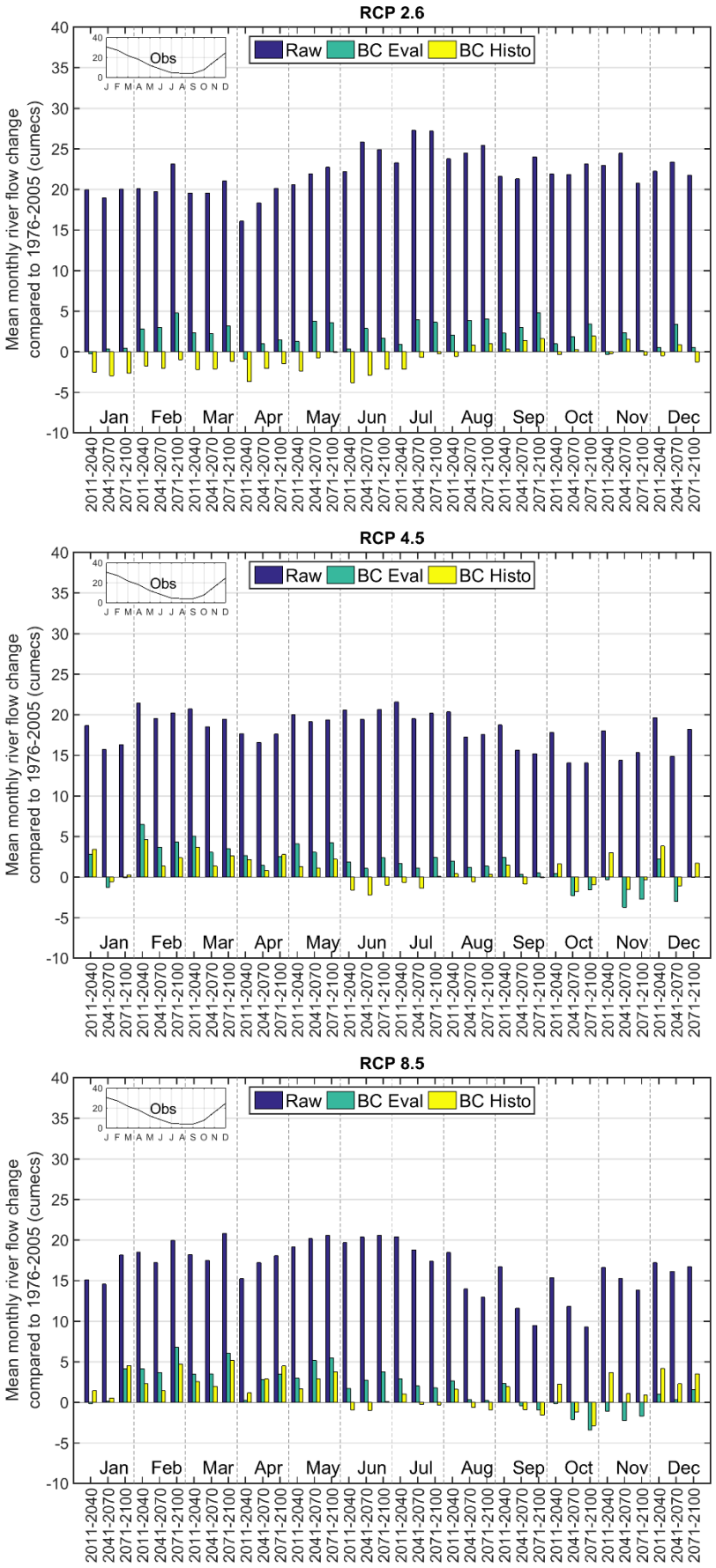

Figure 6. 4 Mean monthly change in the river flow compared to 1976-2005 for the upper Thames catchment for the 2.6, 4.5 and 8.5 RCP scenarios for the uncorrected and bias-corrected simulations

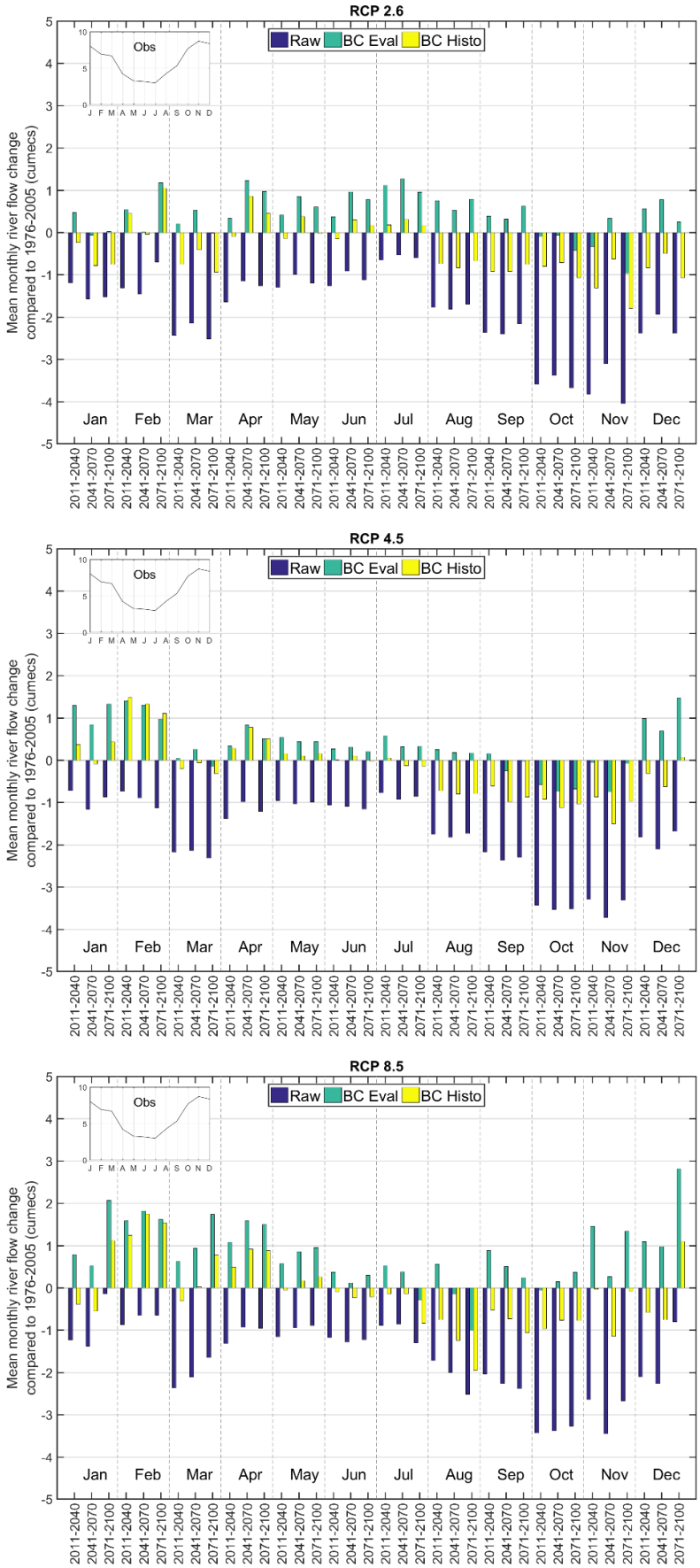

Figure 6. 5 Mean monthly change in the river flow compared to 1976-2005 for the Glaslyn catchment for the 2.6, 4.5 and 8.5 RCP scenarios for the uncorrected and bias-corrected simulations

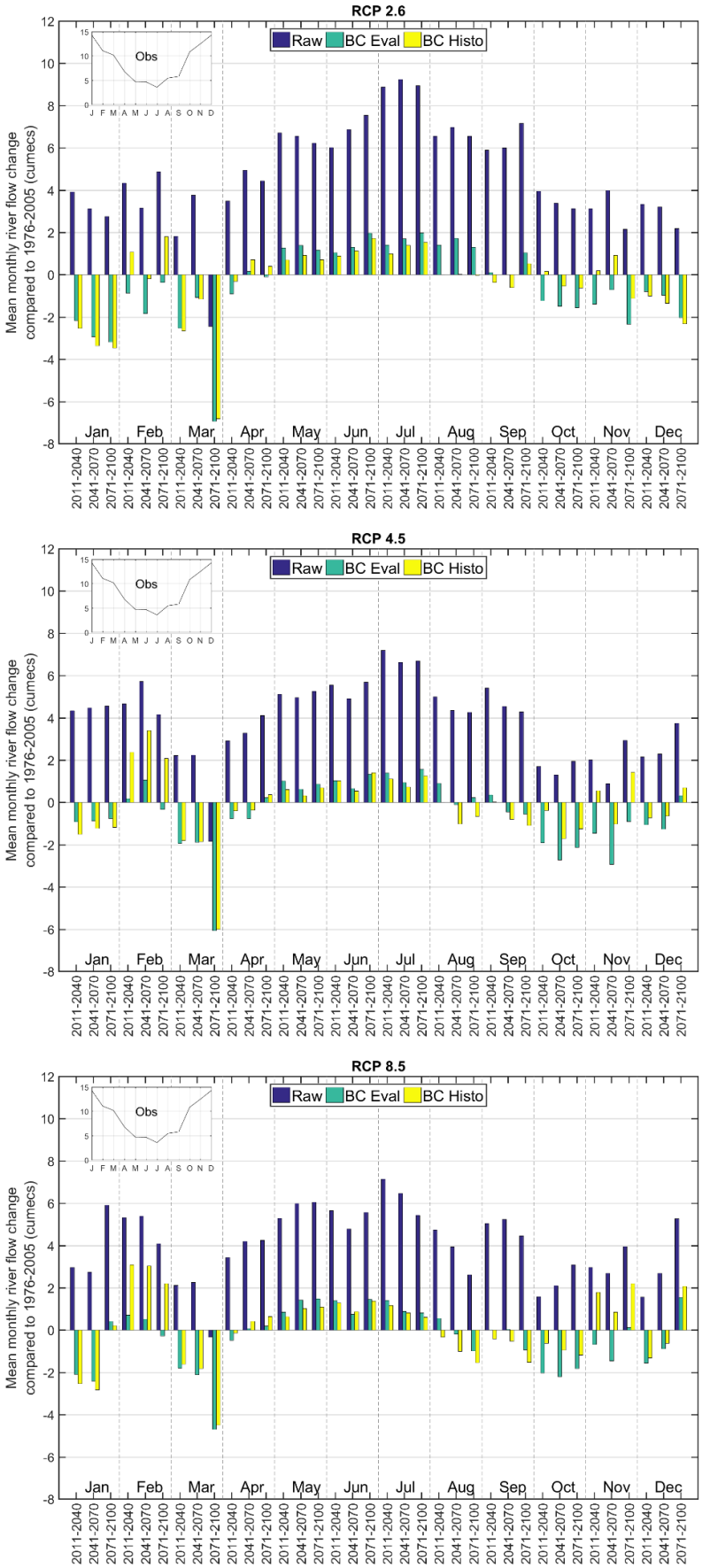

Figure 6. 6 Mean monthly change in the river flow compared to 1976-2005 for the Calder catchment for the 2.6, 4.5 and 8.5 RCP scenarios for the uncorrected and bias-corrected simulations

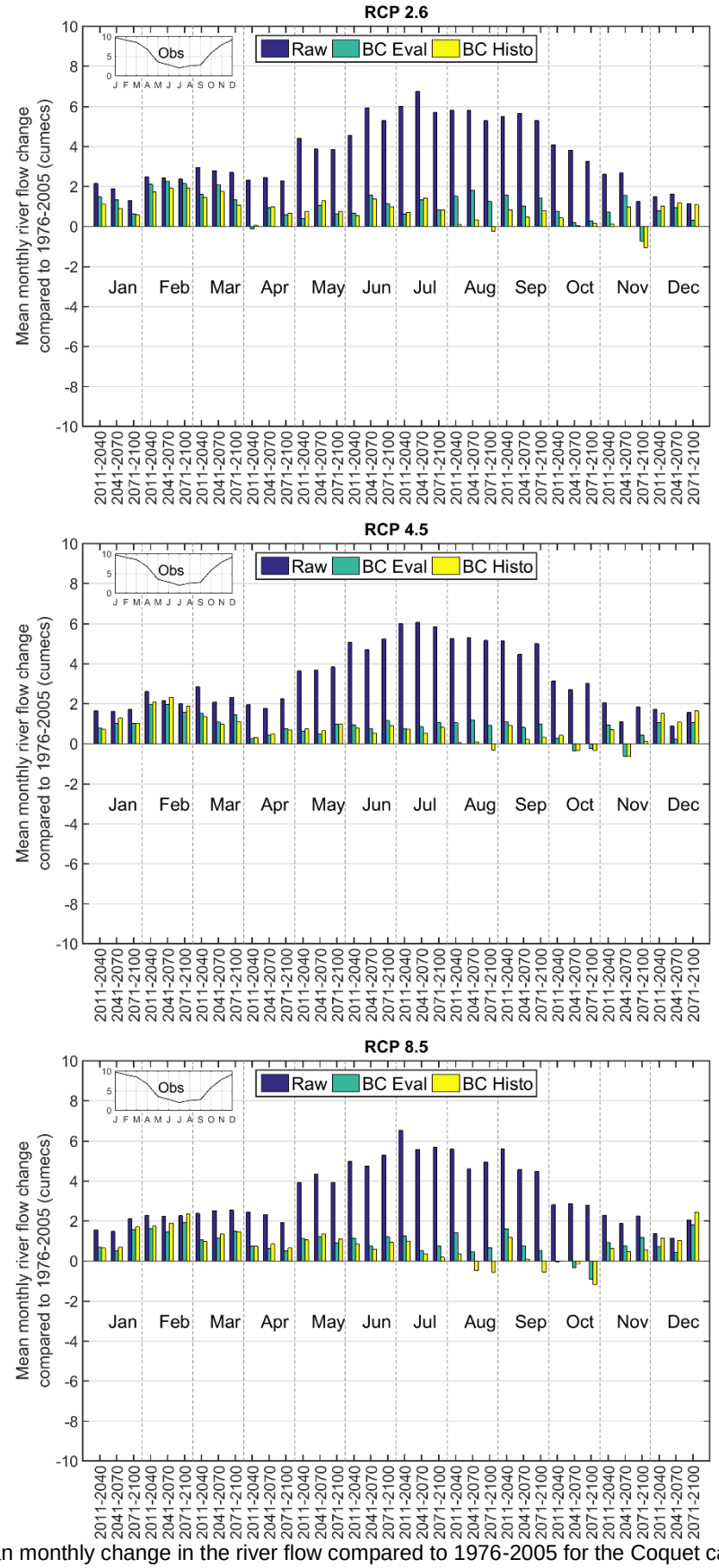

Figure 6. 7 Mean monthly change in the river flow compared to 1976-2005 for the Coquet catchment for the 2.6, 4.5 and 8.5 RCP scenarios for the uncorrected and bias-corrected simulations

For the Glaslyn catchment, the projections generally simulate an increase in the mean monthly river flow from January to July and a decrease in the remaining months (Fig. 6.5). With such changes, the current river regime would be slightly modified by increasing the river flow volume from its current wettest season, winter. Results are consistent with the changes in the monthly precipitation (Section 5.3.2.2). The largest changes are projected for models driven by RCP 8.5 with increases in January and February between 2 and 3 m^3/s. There are cases where the change signal is different for both bias correction approaches (e.g. January, September, October and December for RCP 8.5; August and December for RCP 4.5; March, August, September and December for RCP 2.6).

For the Calder catchment, slight increases are simulated from May to July and decreases for the remaining months, except for February when larger increases are projected (Fig. 6.6). The projected changes imply a modification of the river regime towards a river flow volume more equally distributed throughout the year. Results are consistent with the projected changes in the monthly precipitation (section 5.3.2.2). Largest changes are observed in March for all RCPs with decreases as large as 7 m^3/s (70% of the current mean monthly observed river flow). Most of the projected changes are robust, except for some cases mainly in November and February during 2071-2100.

For the Coquet catchment, the largest changes in the mean monthly river flow are projected to be increases in January, February, March and December (Fig. 6.7) with slight increases for the remaining months. These projections indicate an overall increase with the largest increase for winter. For this catchment, the projected monthly river flow closely follows the monthly variation in precipitation (sections 5.3.2.2). For all cases the projected change is robust.

6.2.3. Flow duration curves

The FDC gives an insight of the amount of the time that a certain river flow volume is reached or exceeded. It provides an estimation on the probability of occurrence of the whole river flow distribution. In other words, comparing the projected changes in the future FDC against the reference period (1976-2005) gives an approximation of any “drying-up” or “wetting-up” trends in the catchment. In all the study catchments the bias corrected methods decrease the simulation spread of the FDCs projected by the models (Figs. A37 to A40). Compared to the current FDC, for the upper Thames the bias correction methods and RCP scenarios project volume decreases from Q80 to Q100 (low flows) and increases from Q20 to Q50 (Fig. A37). For the high flows (Q10), the projections do not show a major change in this catchment, except for BC-Histo for 2011-2040 and 2071-2100 when the Q10 increases. For the Glaslyn catchment the BC-Histo approach projects decreases in the low flows region (Fig. A38). Additionally, BC-Eval projects increases in the high-flows region (Q5 to Q20) and decreases in the low flows for most RCP scenarios and time slices in this catchment. In the Calder catchment, the BC-Eval method projects increases in the high flow region from mid-century for RCP 8.5 (Fig. A39). No large changes are observed in the low flow zone. Similar results are obtained from BC-Histo. Finally, in the Coquet catchment, the BC-Eval projections indicate potential increases in the river flow volume for most of the FDC with slight changes in the low flows region (Fig. A40). BC-Histo gives similar results with the increase in the projected river flow being more evident for all RCPs in most of the FDC (from Q10 to Q80).

Considering the MEM and only the low (Q95) and high (Q10) flows metrics used through this research, the projected magnitude changes for the entire century vary per catchment, RCP and bias correction approach. For the upper Thames the high flows are projected to increase in all RCPs and bias correction approaches, except for BC-Histo RCP 2.6. The low flows are projected to decrease using both bias correction approaches for al RCPs. In the Glaslyn catchment BC-Eval project increases in the high flows for all RCPs, whereas BC-Histo project increases for RCP 4.5 and RCP 8.5. The low flows vary slightly but are projected to increase in all RCPs using BC-Eval and a decrease using BC-Histo. For the Calder catchment the magnitude of the high flows is projected to increase and the magnitude of low flows to decrease for all RCPs and both bias correction approaches. Finally, in the Coquet catchment, the magnitude of the high flow is projeced to increase in for all RCPs for both bias correction approaches, whereas the magnitude of low flows is projected to decrease except for RCP 4.5 and 8.5 when using the BC-Eval approach.

6.2.4. Threshold exceedance

As for the precipitation and temperature analysis, this section provides an assessment of the average number of times in a year that the Q10 is exceed or the Q95 is not reached. Both thresholds evaluate the number of times that low (Q95) and high (Q10) flows are projected to occur within the catchments. A linear regression analysis from 2006 to 2100 indicates that the trend in the projected frequency of the Q10 are only statistically significant in four cases (t-test, p-value < 0.05) (Table B7). In other words, the test evaluates the significance of the frequency of high flows in the projections. Specifically, only the trends from the uncorrected and BC-Eval RCP 2.6 projections for the upper Thames and from the uncorrected and BC-Histo RCP 8.5 projections for the Glaslyn.

The analysis of the annual frequency of high flows occurrence in a 5-year moving window is now considered to get a better insight of the trends by removing the annual variability. When compared to the observations, the uncorrected projections overestimate the frequency of occurrence of high flows for the upper Thames, Calder and Coquet catchments, and underestimate the occurrence for the Glaslyn catchment. The biases from the uncorrected projections are reduced by both bias correction methods to the same extent, except for the Glaslyn catchment (Fig. 6.8). For this catchment, the BC-Eval method results overestimate the observed occurrence whereas the BC-Histo method gives results that agree with the observations. The bias-corrected projections for the entire scenario are similar to the observed occurrence in most cases. For the upper Thames, the projected occurrence over the entire scenario ranges from 15 to 75 days per year above the Q10 with an average of 46 days per year above the Q10. Considering the difference between the different emission scenarios, there is an average 3 days per year increase in the average frequency between the different RCPs (43 days per year for RCP 2.6, 46 days per year for RCP 4.5 and 49 days per year for RCP 8.5) (Fig. 6.8a). For the Glaslyn catchment, the days above the Q10 range from 32 to 58 year per day with an overall average of 44 days per year. The difference in the projection average per RCP varies from 1 to 4 days per year (42 days per year for RCP 2.6, 43 days per year for RCP 4.5 and 46 days per year for RCP 8.5) (Fig. 6.8b). For the Calder catchment, the projected frequencies range from 28 to 57 days per year with an average of 40 days per year. The averaged frequency for RCP 2.6 is 39 days per year, for RCP 4.5 is 40 days

per year and for RCP 8.5 is 42 days per year (Fig. 6.8c). Finally, for the Coquet catchment the projected frequency of days above the Q10 ranges from 35 to 66 days per year with an average of 48 days per year, which is also the same averaged projection for each of the RCPs (Fig. 6.8d).

The projected monthly frequency of the high flows varies differently for each catchment. Considering the changes over the entire scenario, for the upper Thames, increases in the frequency are expected for all year except for January and February. The largest increases are projected to be in spring and the beginning of summer (Fig. A41). For the Glaslyn catchment increases are projected throughout most of the year with largest increases during winter (Fig. A42). For the Calder catchment, the projections indicate increases over all the year, mostly during winter. Decreases are expected in October and in January (Fig. A43). Finally, for the Coquet catchment increases are projected for all year with no big difference among the seasons (Fig. A44).

Now, considering the annual frequency of days with low flows (below the Q95), the uncorrected projections tend to underestimate the frequency compared to their bias-corrected outputs for all catchments except for the Glaslyn catchment, where the opposite happens (Fig. 6.9). For this threshold, only the trends driven by the RCP 8.5 projection are statistically significant in the upper Thames, Glaslyn and Coquet catchments (based on a linear regression analysis using a t-test with p-values < 0.05). The test evaluates how statistically significant are the projected frequency of low flows in the future. For the Coquet catchment all RCP 8.5 projections are statistically significant, whereas for the other two catchments only the bias-corrected projections are significant (Table B7).

The bias-corrected projections give similar results except for RCP 2.6 in the upper Thames, where BC-Histo gives a higher frequency than for the rest of the projections (Fig. 6.9a). Considering the bias-corrected projections for the upper Thames, the frequency of the annual number of days below Q95 varies from 22 to 102 with an average of 50 days per year. For this catchment, the frequency of days in a year below the Q95 decreases as the RCP projection increases. The number of days below the Q95 is 56 days per year for RCP 2.6, and 46 days per year for RCP 4.5 and RCP 8.5. For the Glaslyn catchment the projected frequency ranges from 7 to 41 days per year with an average of 21 days per year. In this catchment the annual frequency of days below the Q95 is 19 days per year for RCP 2.6, 20 days per year for RCP 4.5 and 23 days per year for RCP8.5. For the Calder catchment the projected frequency of low flows varies from 11 days per year to 66 days per year with an average of 34 days per year. For RCP 2.6 the average frequency is 32 days per year, whereas for RCP 4.5 frequency is 35 days per year and 34 days per year for RCP 8.5. Finally, for the Coquet catchment the range of the frequency of low flows varies from 5 to 48 days per year with an average frequency of 25 days per year. In this catchment, the average projection for RCP 2.6 is 20 days per year whereas for RCP 4.5 it is 26 days per year and 28 days per year for RCP 8.5. The average frequencies shown above are averages using the outputs from both of the bias correction methods.

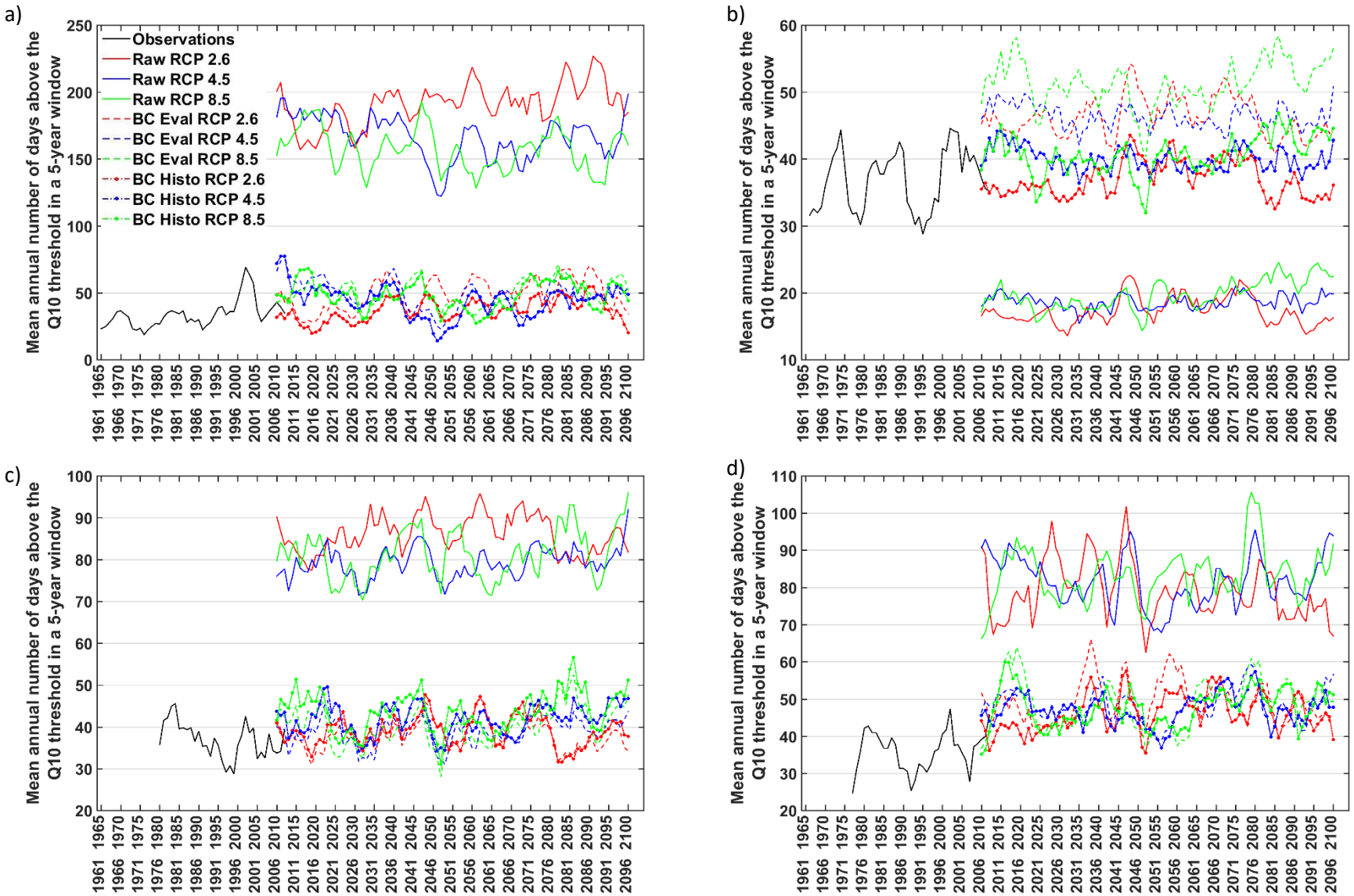

Figure 6. 8 Mean annual number of days in a year in a 5-year moving window when the Q10 is exceeded for the uncorrected and bias corrected RCP projections for: a) upper Thames, b) Glaslyn, c) Calder and d) Coquet catchments. Please note the differences in the y-axis

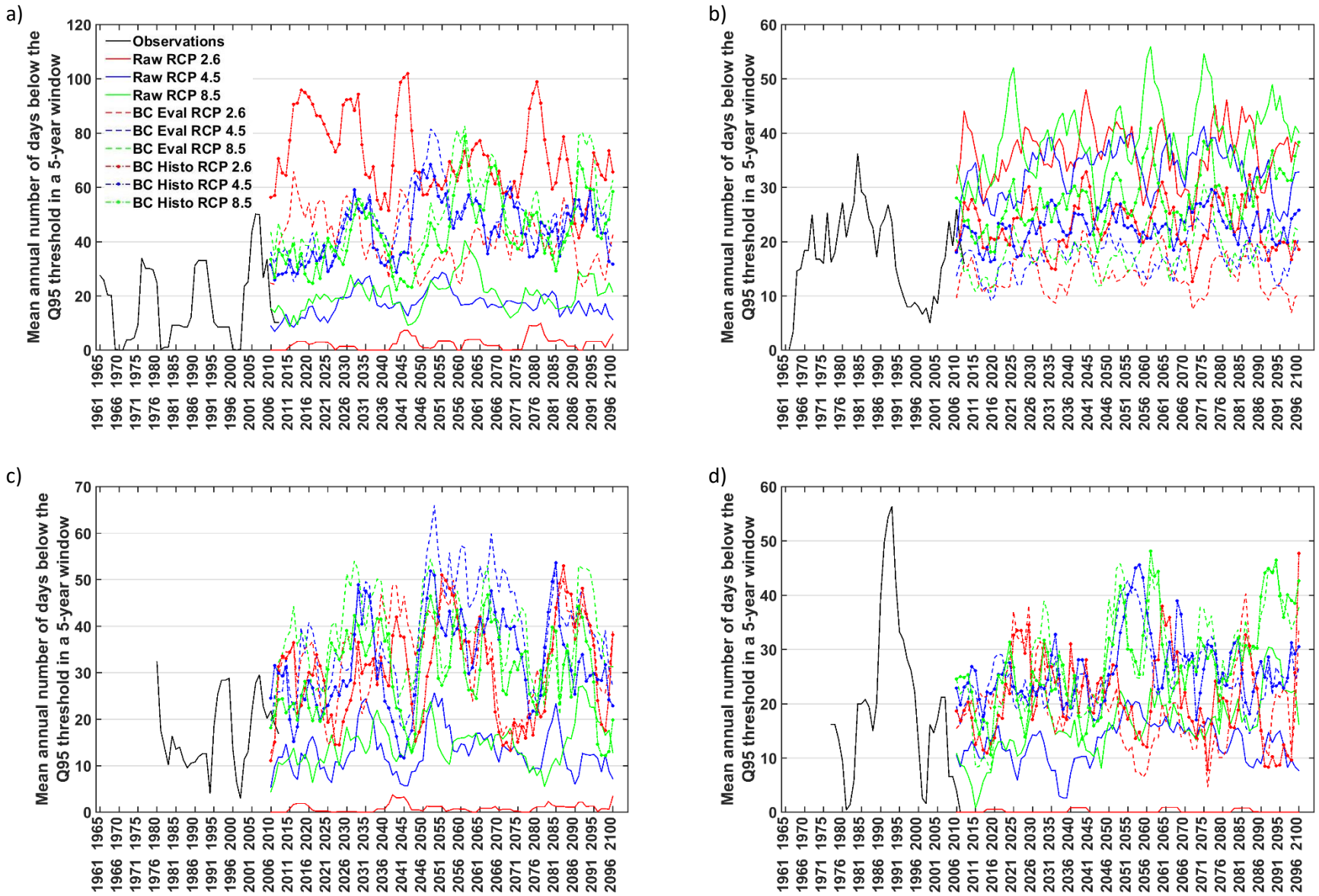

Figure 6. 9 Mean annual number of days in a year in a 5-year moving window when the river flow is below the Q95 for the uncorrected and bias corrected RCP projections for: a) upper Thames, b) Glaslyn, c) Calder and d) Coquet catchment. Please note the differences in the y-axis

The variation in the monthly frequency of low flows also varies according to the catchment, but with a tendency for an increase for the last part of the year in all catchments. Frequently, RCP 2.6 projects a more diverse range of changes than RCP 4.5 and 8.5. Nevertheless, all RCPs agree in the change direction for most cases. For the upper Thames catchment, the increases are expected for all year with largest increases from August to December (Fig. A45). The projections for the Glaslyn catchment show increases for summer and autumn with no definitive change in the remaining seasons (Fig. A46). For the Calder catchment, increases are projected for all year except for August when decreases are projected (Fig. A47). Finally, for the Coquet catchment the projections indicate increases in autumn and decreases in summer with no change in the remaining seasons (Fig. A48).

6.3. Projected hydropower

This section considers the estimated future hydropower generation based on the projected river flow using the precipitation and temperature outputs from the climate change models. The section covers the methodology used to estimate the hydropower generation in each catchment, the evaluation of the hydropower generation simulation against observed data and the projections of future hydropower generation for each catchment. Similar to temperature, precipitation and river flow, results are shown for both bias correction approaches (BC-Eval and BC-Histo). This procedure permits the evaluation of whether the projected changes are robust, with both approaches projecting the same change direction.

6.3.1. Estimation of the past and present hydropower generation

The estimation of hydropower generation is done by simulating the parameters from the general hydropower equation (section 1.8). Relevant flows used for the simulation of hydropower generation are explained next.

- Qd: maximum flow of water diverted to the hydropower scheme.
- Qmin: hands-off flow (below this flow the abstraction from the river stops).
- Qmax: high flow that represents flooding conditions in which the hydropower scheme is stopped to avoid damages to the turbine and facility.

The values of these flows vary for each scheme. Mainly for the schemes that are currently operating, the Qmin and Qmax values are defined based on their design and current operation. In contrast, for the proposed schemes the Qmin has not been defined as there is no design for the schemes yet. Thus, for these schemes a value equivalent to the Q95 flow is used as Qmin. Additionally, for the proposed schemes a Qd value is defined based on the scheme's head and maximum generation (estimated in EA, 2010) and the projected turbine efficiency. Finally, the Qmax for all schemes is defined using usual values for RoR schemes, equivalent to the catchment's Q2 flow (Hanggi and Weingartner, 2012). As described in section 2.7, two of the hydropower schemes are currently in operation (Glaslyn and Calder), whereas the remaining two (Upper Thames and Coquet) are proposed by the Environmental Agency (EA, 2010). For the simulation of hydropower generation, the design parameters for the currently operating schemes and the proposed parameters for the potential schemes are used. Such parameters are shown in Table 6.2. In the following sections, the simulation method for each RoR scheme is explained, including the calibration procedure to improve the simulation skill for the installed schemes

Table 6. 2 Characteristics of the hydropower schemes

	Upper Thames	Glaslyn	Calder	Coquet
Status	Feasible	In operation	In operation	Feasible
Turbine	Archimedes screw	Pelton	Archimedes screw	Archimedes screw
Head (m)	1.7	176.0	2.2	2.0
Maximum generation (kW)	225	640	100	118
Qmin (Hands off flow) (m^3/s)	1.90	0.09	1.28	0.84
Qd (Maximum extraction) (m^3/s)	17.52	0.45	7.31	7.81
Qmax (Extraction interrupted) (m^3/s)	62.6	28.2	42.3	29.9

6.3.1.1. Upper Thames

The upper Thames hydropower scheme is a potential site proposed by the UK Environment Agency (EA, 2010). Therefore, there is no generation data available. The simulation of the potential past and future generation is performed using the design parameters as estimated by the Environment Agency (Table 6.2) and the observed river flow data. As the scheme is proposed to be located near the river flow gauging station, the data from the gauge can be directly used as an estimation of the water volume available for the scheme. The proposed turbine for the site is an Archimedes screw. Therefore, the efficiency percentages estimated for the Calder scheme's turbine are used for the simulation of hydropower generation in this scheme (section 4.3.1.3). This is done because the Calder scheme is the only site using an Archimedes screw that has real output data that serves to compare with the simulated data. Therefore, its values are expected to represent reality better. However, these are only estimations and the coefficients could be different if the scheme is built due to the different flows and landscape characteristics, among other factors.

6.3.1.2. Glaslyn

The Glaslyn catchment hydropower scheme began operations in May 2014. Largest generation is normally observed during autumn and winter (Fig. 6.10). The arrangement of the scheme is different from the others included in this study as it has a large pipe diverting the inlet volume from the river using a Pelton turbine as generator (section 2.7.2). Also, the head of the scheme is the highest of all of the study sites included in this research. Another important characteristic of the scheme is that the inlet is not located near a gauging station. Therefore, for this site the available water for the inlet was simulated using the hydrological model parameters defined in the calibration of the hydrological model (Table 3.2), only varying the catchment's area and land cover. Then a relationship between the resulting simulations and the downstream gauge observations is used to simulate the future flow available at the inlet as a function of the flow through the gauge as this catchment follows mostly a natural regime. The generation simulation also considers the Qmin, Qmax and maximum capacity parameters. Considering the above, the hydropower generation is simulated for this scheme and compared to the available records (May 2014 to Dec 2015). The calibration of the model aims to decrease two objective functions, namely the annual mean percentage error and the monthly absolute mean percentage error, by changing the value of the scheme's efficiency. The calibration is performed manually, finding that an efficiency of 90% gives

the best fit between simulations and observations. The resulting monthly mean percentage error is below +/- 30 except for two months, with the largest error being for September (60%), which is a result of the low generation recorded in September 2014 (Fig. 6.11). This model is used for the simulation of future hydropower generation in this site.

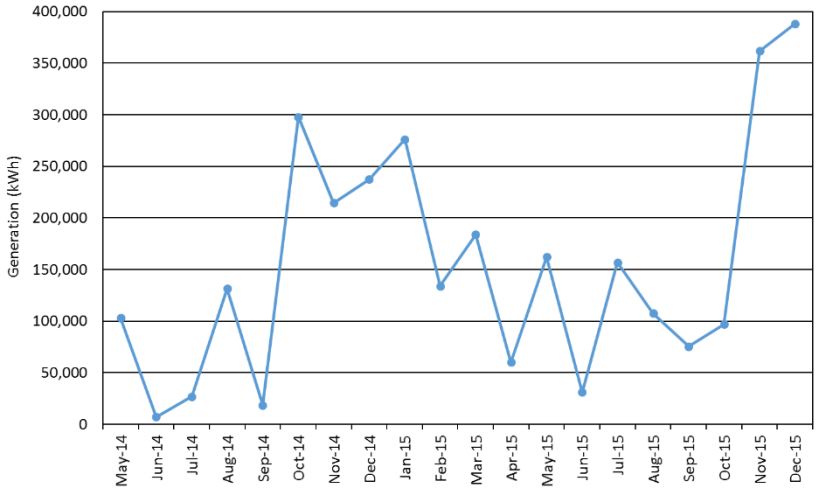

Figure 6. 10 Monthly hydropower generation of the Glaslyn catchment scheme, data for 2016 and 2017 is not available

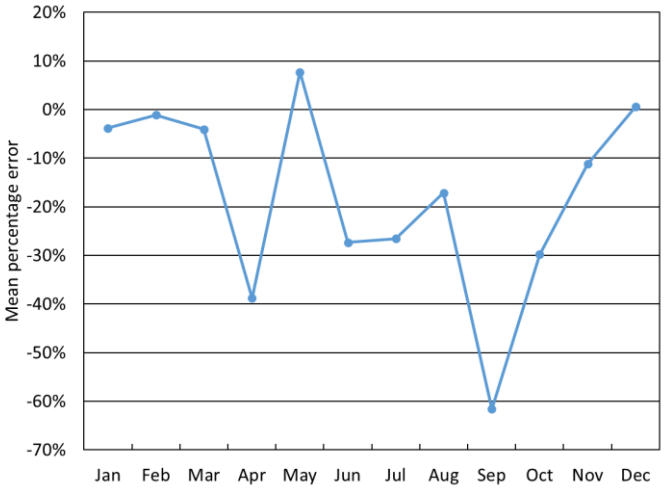

Figure 6. 11 Mean percentage error of the monthly generation simulation for the Glaslyn catchment hydropower scheme

6.3.1.3. Calder

The Calder catchment hydropower scheme is located at the catchment's outlet. Therefore, the volume of water available for the scheme is recorded by the catchment's river flow gauge (section 2.7.3). The scheme began operation in November 2014. Since then, the monthly generation has varied (Fig. 6.12). However, winter normally has the largest generation within a year, whereas generation decreases during summer. Available data of the scheme's generation (from 2015 and 2016) are used to calibrate the simulation of the hydropower output. The simulation considers that the generation will be stopped when the river flow is below the Qmin (or HOF) and above the Qmax (Table 6.3). Additionally, Qmin has to be flowing in the river at all times if such volume is available, therefore only volumes above this threshold can be diverted to the scheme. The scheme is not able to extract more water than the maximum extraction volume and it is not capable of producing more energy than the turbine's maximum

capacity. Finally, the estimation uses the design head as a fixed value throughout the simulation. Establishing the efficiency of the scheme based on the observed efficiency is complex as there are certain difficulties interpreting the observed data (discussed in section 6.5). Therefore, the scheme's efficiency is not fixed and it is used as calibration parameter. Thus, the generation model for this scheme is calibrated by modifying its efficiency considering two objective functions: decrease the annual mean percentage error and decrease the monthly absolute mean percentage error. The calibration is manual and compared to the calibration procedure from the Glaslyn scheme, it has a variation that is explained in the next paragraph.

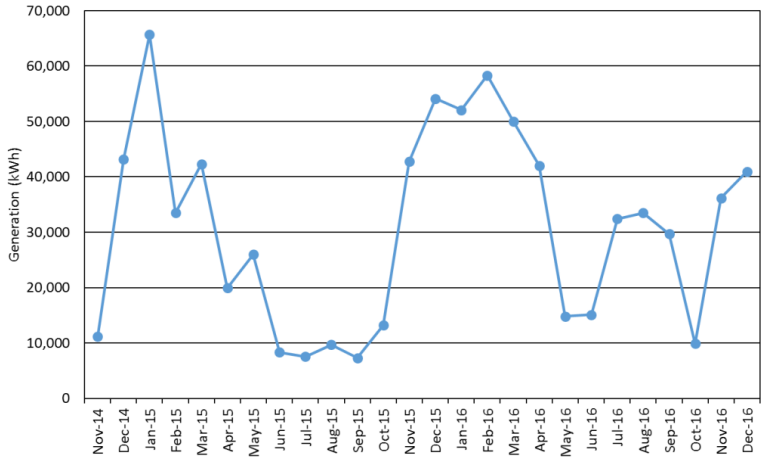

Figure 6. 12 Monthly hydropower generation of the Calder catchment scheme

After calibration, initial results show a good simulation skill (mean percentage error of 3% for 2015 and -2% for 2016). Nevertheless, the simulation of the monthly generation gave different results per season (Fig. 6.13). Specifically, the winter and spring generation have small biases, whereas the summer and autumn generation is overestimated. This is a clear seasonal behaviour. The efficiency of a scheme is a function of the flow rate (Tamm et al., 2016), therefore two different efficiencies are defined. One is used for the low flow seasons (summer and autumn) whereas the other is for the high flow seasons (winter and spring).

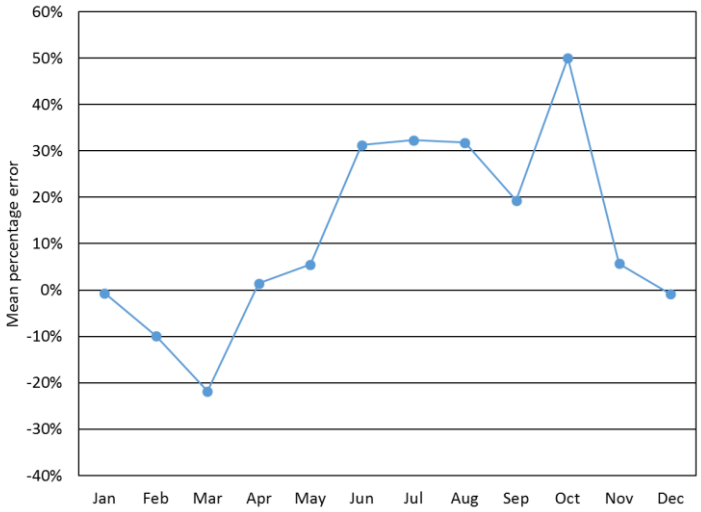

Figure 6. 13 Mean percentage error of the initial simulation of the monthly generation for the Calder catchment hydropower scheme

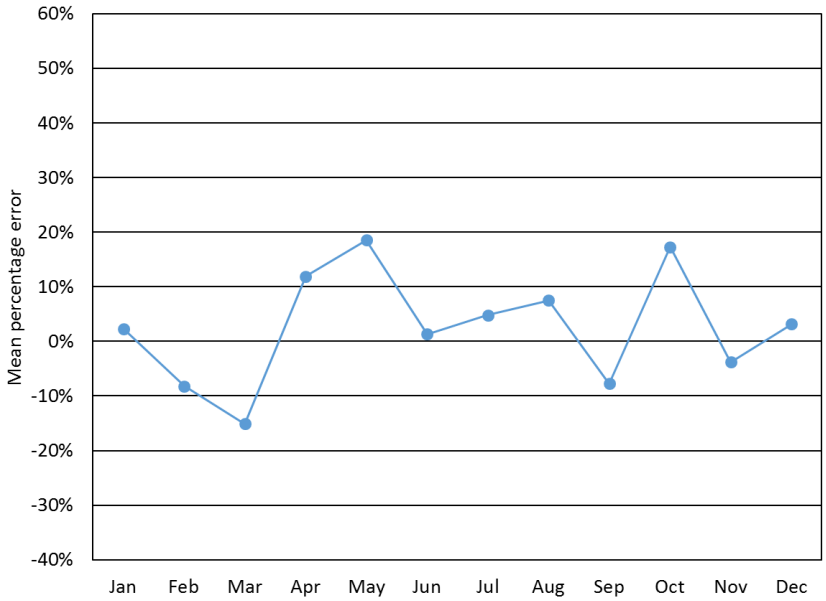

Figure 6. 14 Mean percentage error of the calibrated simulation of the monthly generation for the Calder catchment hydropower scheme

The use of two different efficiencies improved the simulation results. The calibrated efficiency values are 48% for winter and spring and 32% for summer and autumn. With these efficiencies, the simulation outputs have the highest agreement with the scheme's monthly generation records. The highest mean percentage error for the monthly generation does not exceed +/- 20% and is under +/-10% for eight of the months (Fig. 6.14). Regarding the annual generation, the simulation results provide a good estimation of the actual generation with simulation errors of 2% for 2015 and -6% for 2016. This model is used to estimate the scheme's potential past and future generation.

6.3.1.4. Coquet

The Coquet hydropower scheme has been proposed by the Environment Agency as a potential site (EA, 2010). Therefore, design data estimated by the Environment Agency (Table 6.3) is used to estimate the past and future generation of the scheme. Additionally, an Archimedes screw is proposed as turbine for the scheme. Thus, the efficiency percentages from the Calder hydropower scheme are used as it is a similar turbine (section 6.3.1.3). Therefore, the simulation of the hydropower output uses an efficiency of 48% for winter and spring and of 32% for summer and autumn. Since this is a proposed site, there is no generation data available for comparison against the simulated generation.

6.4. Projections of the future hydropower generation

This section shows the projections for the hydropower generation in each catchment. Initially, the mean annual hydropower time series will be explained along with the projected changes throughout the century, compared against the reference period (1976-2005) for which hydropower is simulated using the developed models and the observed river flow. Afterwards, the monthly hydropower generation changes are shown. At the end of the section, the projected frequency of exceedance of thresholds that are relevant for the operation of the hydropower schemes is described. Similar to the other results sections, these are based on the MEM, except when the contrary is stated.

6.4.1.Mean annual hydropower

The uncorrected projections simulate biased mean annual hydropower generation compared to the reference period for all catchments (e.g. there is a gap between the reference period time series and the projections time series) (Fig. 6.15). This is expected for the uncorrected projections as the same happens for the case of temperature (Fig. 5.9) and precipitation (Fig. 5.14). Long generation records for the hydropower schemes are not available as two of them are proposed sites and the remaining two have only been operating for a maximum of three years. Therefore, generation is estimated for the reference period (1976-2005) using the models and parameters described in section 6.3.1. As for the precipitation and river flow projections, the mean annual hydropower is overestimated for the upper Thames, Calder and Coquet catchments and underestimated in the Glaslyn catchment. After bias correction using both approaches, the gap between the projections and reference period is reduced. A linear regression analysis from 2006 to 2100 is applied to the annual hydropower time series to evaluate whether the generation trend is statistically significant (e.g. significant annual changes are projected). There is no statistically significant trend in hydropower generation in the bias corrected projections under any of the scenarios (Table B5, last column). Only the trends from the uncorrected RCP 4.5 and 8.5 projections in the upper Thames and the uncorrected RCP 8.5 in the Calder and Glaslyn catchments are statistically significant (t-test, p-value < 0.05). For RCP 2.6 in the upper Thames and Coquet catchments, the climate change signal direction changes from a negative to a positive trend. There is no change in the climate change signal direction after bias correction for the remaining cases. However, the magnitude of the trends from the uncorrected projections change after bias correction. This can be attributed to the fact that different factors affect the hydropower generation which are not directly linked to the mean annual river flow (e.g. maximum generation, maximum river flow extraction, Hands Off Flow).

The estimated projection from the reference period (1976-2005) is compared with the projected mean generation from three non-overlapping 30-year periods: (2011-2040, 2041-2070 and 2071-2100) (Fig. 6.16). The uncorrected projections are generally biased from the mean annual hydropower generation estimations. Therefore, the following analysis only considers the bias corrected projections which give robust results (projected changes with the same direction after using both bias correction approaches) for most of the catchments, time slices and RCPs. Opposite climate change signals are obtained for the beginning and middle of the century for the upper Thames (Fig. 6.16a) and for the end of the century for the Calder catchment when driven by RCP 2.6 (Fig. 6.16c). However, these changes are small and the standard deviation from both bias correction approaches overlap each other, indicating that these differences are not statistically significant. Results from the Glaslyn catchment show differences in the climate change signal direction from both bias correction approaches for all the century for RCP 2.6 and in the middle of the century for RCP 4.5 and 8.5 (Fig. 6.16b).

The statistical significance of the changes is evaluated by comparing the standard deviation of the model simulations with the mean of the reference period. It is observed that the BC-Eval bias-corrected projected changes for the upper Thames scheme are statistically significant during 2041-2070 and 2071-2100 when driven by RCP 2.6. For the same catchment, the projected changes from both bias correction approaches are significant during 2011-2040 when driven by RCP 4.5. In the Glaslyn

catchment, the BC-Eval projected changes are statistically significant for all RCPs and time periods. Finally, for the Coquet catchment, all the projected changes are statistically significant.

Also, there are cases when the standard deviation from the bias correction approaches do not overlap each other, giving completely different scenarios. Changes from the reference period considering the MEM range from -50 MWh to 150 MWh for the upper Thames, from -200 MWh to 190 MWh for the Glaslyn, from -15 MWh to 10 MWh for the Calder and from 40 MWh to 75 MWh for the Coquet catchment.

Different results are obtained for each catchment and when considering the change percentage of each future time slice (2006-2040, 2041-2070 and 2071-2100) compared to the 1976-2005 reference period (Table B8). Similar to river flow, there are cases when the climate change signal direction from the outputs of the bias correction approaches is contradictory. Such cases only occur for the Glaslyn catchment when driven by RCP 2.6, where, as stated above these changes are not statistically significant. For such projection, BC-Eval estimates changes ranging between 11% and 14% whereas BC-Histo estimates a variation between -3% and -7%. Cases where both climate change signals have the same direction for the considered time slices are more frequent. In the upper Thames catchment, the change in the hydropower generation is estimated to range between 3% and 21% when driven by RCP 4.5 and between 10% and 19% when driven by RCP 8.5. For the Coquet catchment, all RCPs project an increase in the hydropower generation when using either of the bias correction approaches. The changes vary between 18% and 28% for RCP 2.6, between 16% and 22% for RCP 4.5 and between 17% and 23% for RCP 8.5.

The variability in the projected generation is also important to evaluate if the bias correction approaches change the variability simulated by the uncorrected GCM-RCM simulations. An assessment of the variability of the projections indicates that the bias corrected approaches always change the range from the uncorrected projections to make it agree with the observed range (Table B8). This happens for both cases, when the uncorrected projections underestimate or overestimate the observed range. Thus, bias correction fits the projection to reproduce scenarios that are closer to the reference period variability. Nevertheless, this doesn't happen for the standard deviation. The bias correction approaches modify the projected standard deviation, but the bias-corrected standard deviation is not always closer to the observed standard deviation.

In general, throughout the century there is an increase in the projected changes in hydropower generation for the Coquet and upper Thames schemes, little change in the Calder scheme and an uncertain direction for the Glaslyn scheme. Certain projected changes are statistically significant in all the catchments, except for the Calder catchment. The most robust projection is obtained for the Coquet catchment compared to the rest of the catchments.

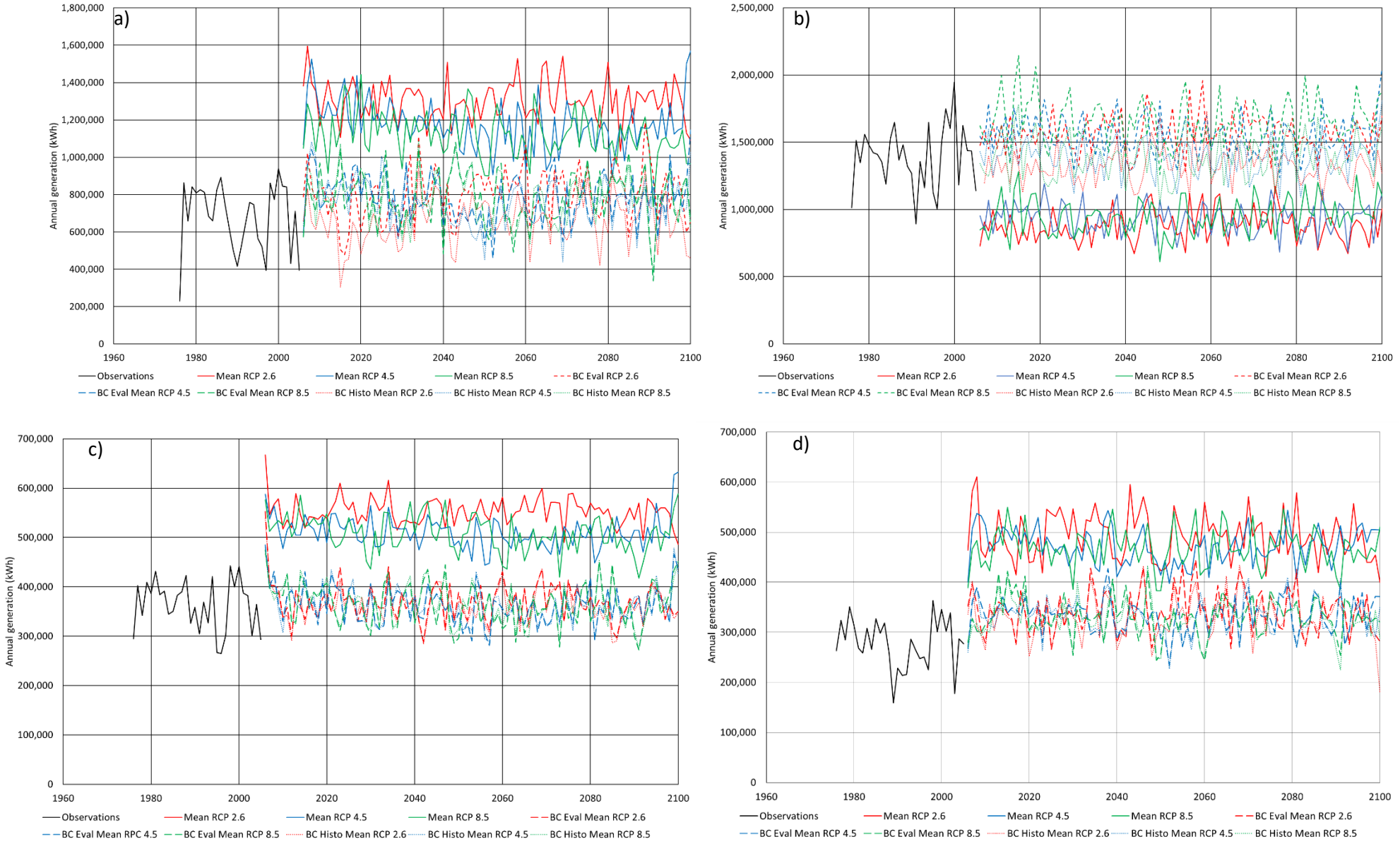

Figure 6. 15 Mean annual hydropower generation (kWh) time series for the uncorrected and bias corrected RCP projections for: a) upper Thames, b) Glaslyn, c) Calder and d) Coquet catchments

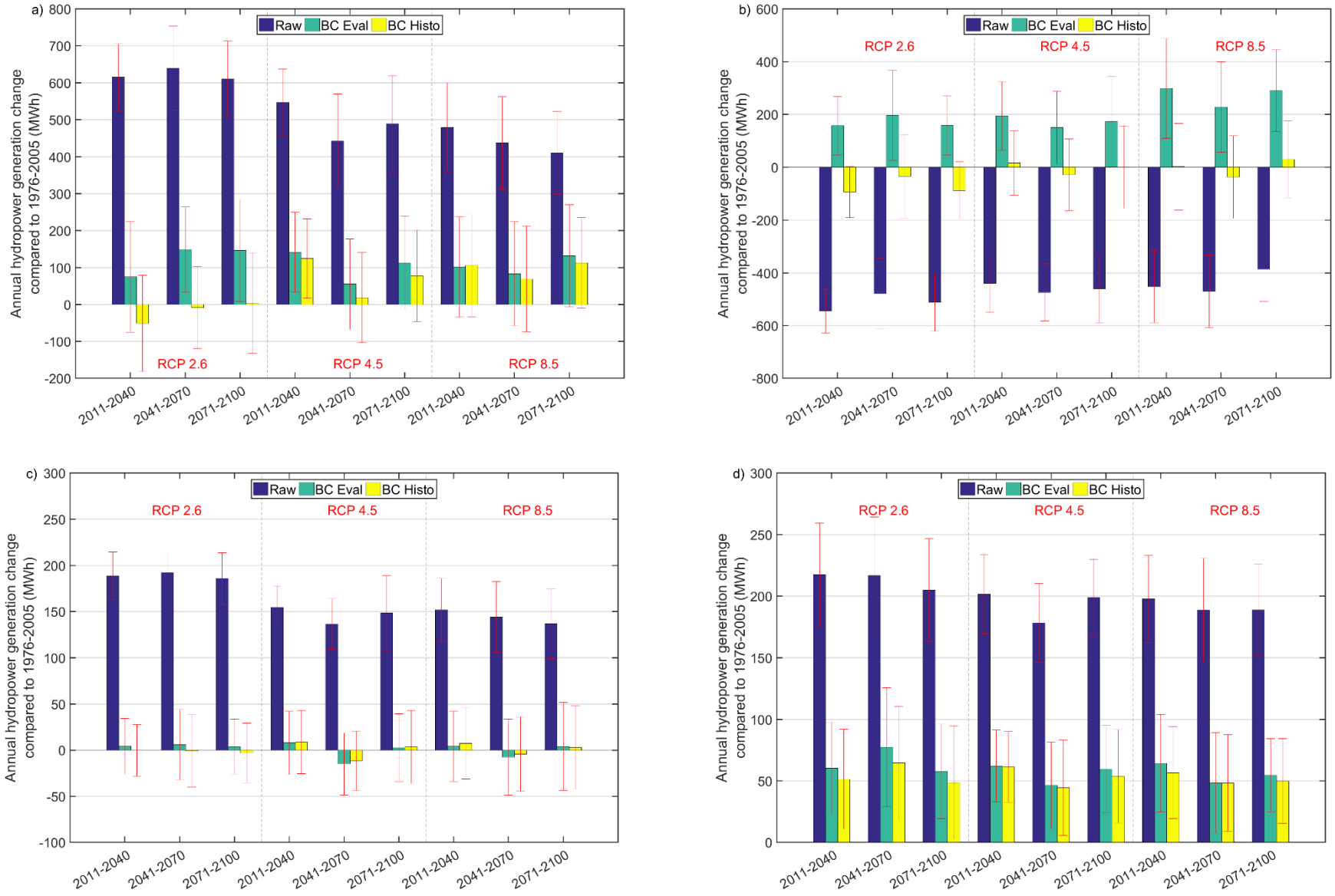

Figure 6. 16 Projected hydropower change compared to 1976-2005 under RCPs 2.6, 4.5 and 8.5 using uncorrected and bias corrected outputs for the a) Upper Thames, b) Glaslyn, c) Calder and d) Coquet catchment. Please note the differences in the y-axis. The standard deviation of the model simulations is represented by the red bars

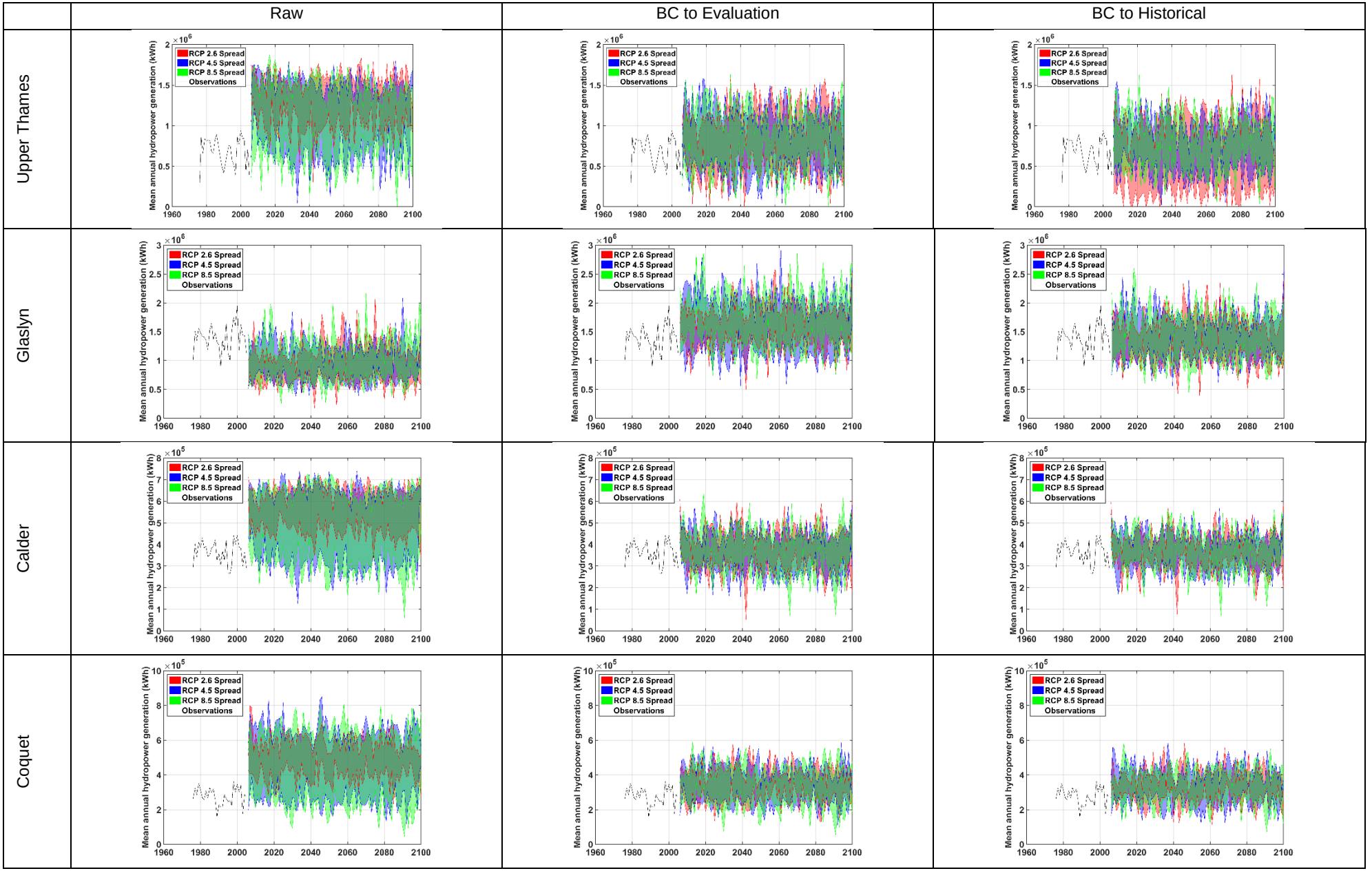

Figure 6. 17 Mean annual hydropower generation spread for each RCP using uncorrected and bias corrected projections for all catchments. Please note the differences in the y-axis

The effect of the bias correction approaches is observed by the reduction in the model simulation spread, here defined as the difference of the minimum and maximum of the ensemble simulations (Fig. 6.17). Compared to the uncorrected projections, the ensemble spread is reduced by both bias correction approaches to a similar extent. Furthermore, there is no evident difference between the ensemble simulations spread from the different RCPs.

6.4.2.Mean monthly hydropower

Commonly, the monthly hydropower generation projections from RCP 4.5 and 8.5 give similar results. In contrast, the monthly hydropower generation simulated by RCP 2.6 gives a more variable picture in each catchment. It has been shown that the uncorrected projections are biased from the hydropower generation of the reference period (Fig. 6.15). Thus, in the following lines only the bias corrected projections are described.

For the upper Thames catchment, RCP 4.5 and 8.5 project generation increases for all year except in January, October and November (Fig. 6.18). In contrast, RCP 2.6 simulates decreases in the mean hydropower generation from January to July when using the BC-Histo approach. However, most of these projected decreases are not robust. The greatest robust increases in hydropower generation are projected for February and the greatest decreases of October, both with magnitudes of change of 20 MWh compared to the reference period. Increases are projected for all months and are larger for winter and spring.

In the Glaslyn catchment, projections from RCP 2.6 have a larger monthly variation than the remaining RCPs (Fig. 6.19). However, the projections normally indicate decreases in the hydropower generation from June to November and increases in winter. For the remaining months the projections from each RCP are different and a consistent change cannot be identified. Winter results are not robust as the direction of change from each of the bias correction approaches is opposite. The largest changes do not exceed +/-60 kWh and are observed during January, August and December for the projections driven by RCP 8.5. As a consequence of the projections, the difference between the low and high generation seasons enlarges.

For the Calder catchment, hydropower is projected to vary slightly during all months (Fig. 6.20). this is linked with the small changes in river flow. All RCPs project a large decrease for March, reaching up to -30 MWh when driven by RCP 2.6. Besides this large decrease in the generation, for the rest of the months the changes in projections are not larger than +/-10 MWh. In general, increases are projected for February and from May to July with decreases for the remaining months. Most of the monthly projections for this catchment are in the same direction for both bias correction approaches. The projections indicate slight changes in the hydropower production that will lead to a more stable generation through the year.

Finally, for the Coquet catchment, increases in the hydropower generation are projected for most of the months (Fig. 6.21). All RCPs project decreases for October, November and December but increases for the remaining months. The largest increases are projected for February and May, with an approximate magnitude of 10 MWh. Most of the projections for this catchment are robust.

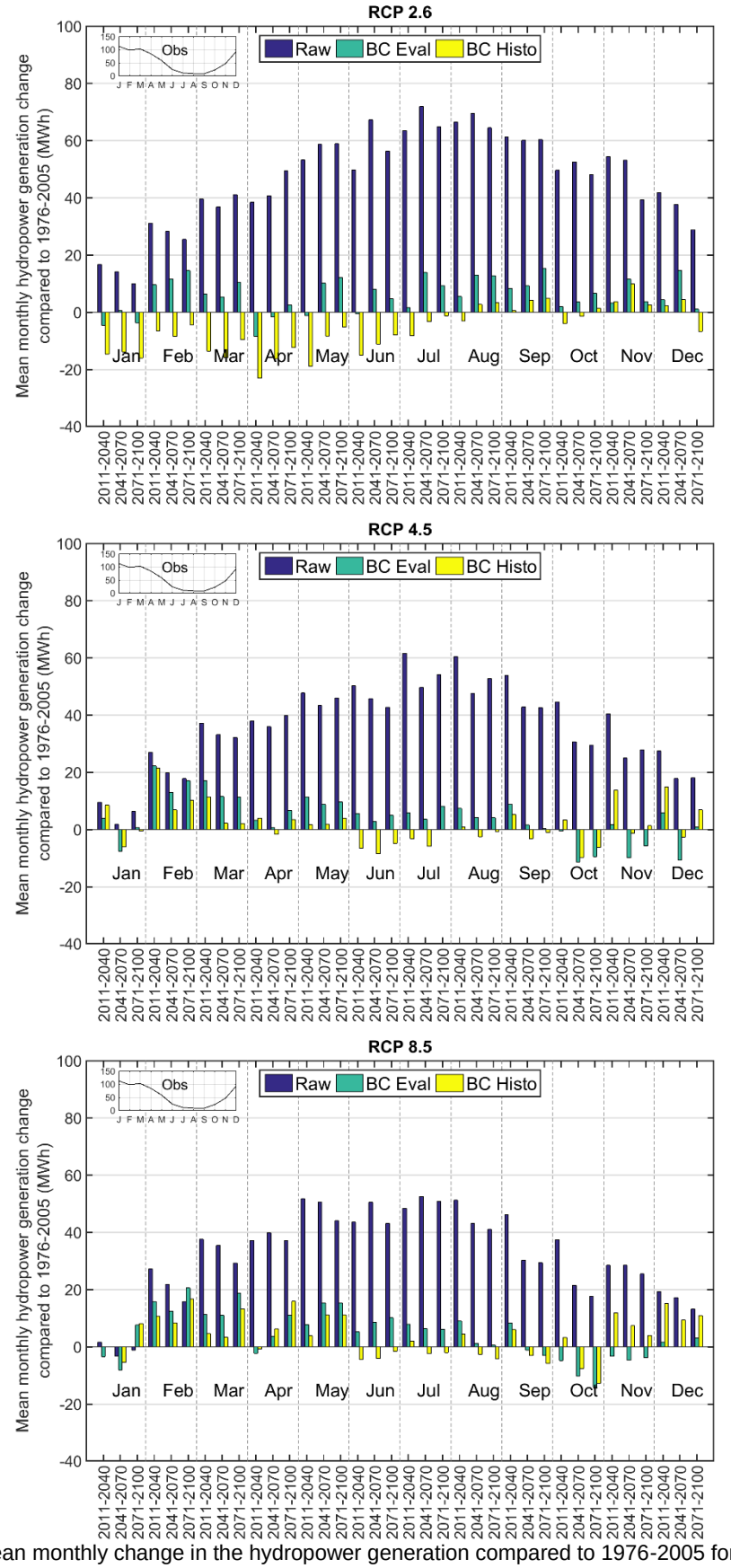

Figure 6. 18 Mean monthly change in the hydropower generation compared to 1976-2005 for the Upper Thames catchment for the uncorrected and bias-corrected 2.6, 4.5 and 8.5 RCP scenarios

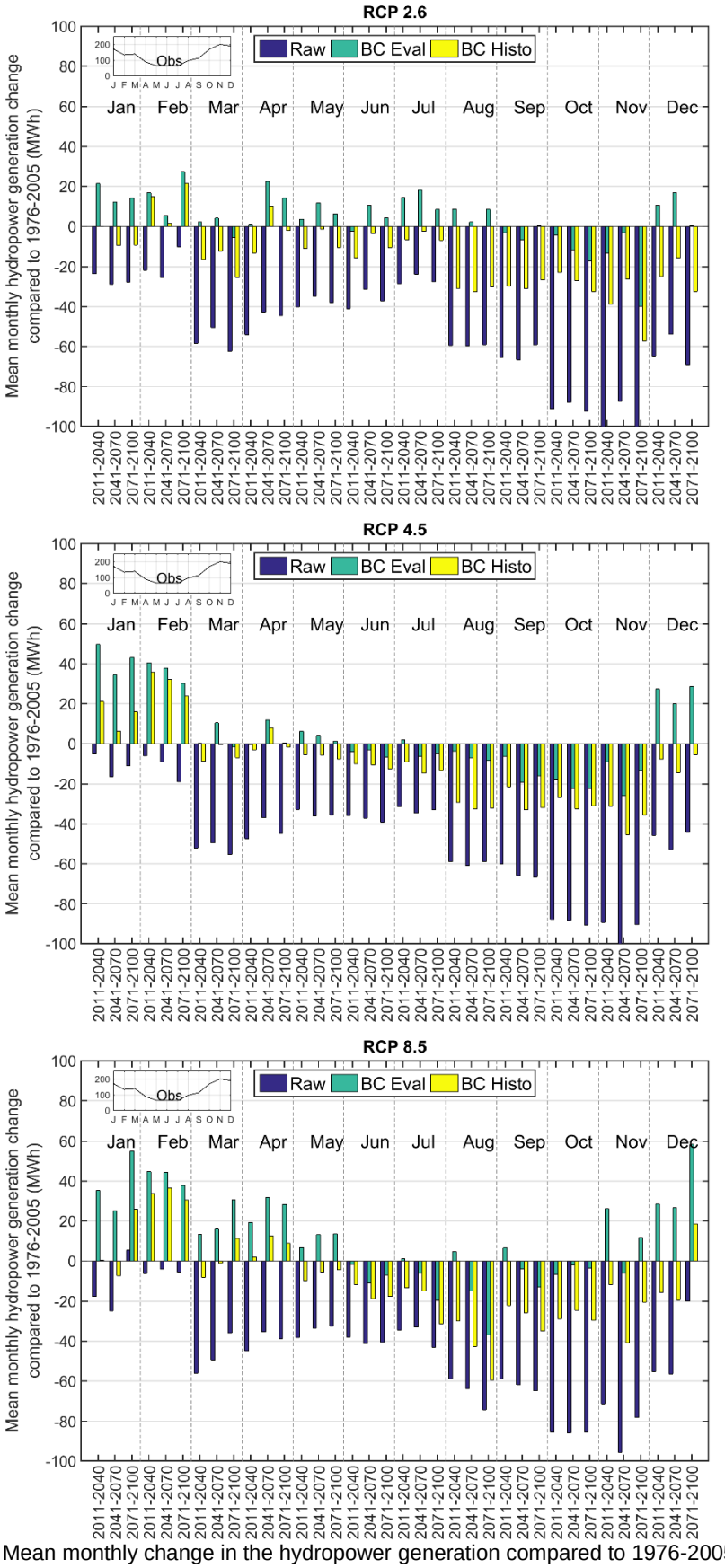

Figure 6. 19 Mean monthly change in the hydropower generation compared to 1976-2005 for the Glaslyn catchment for the uncorrected and bias-corrected 2.6, 4.5 and 8.5 RCP scenarios

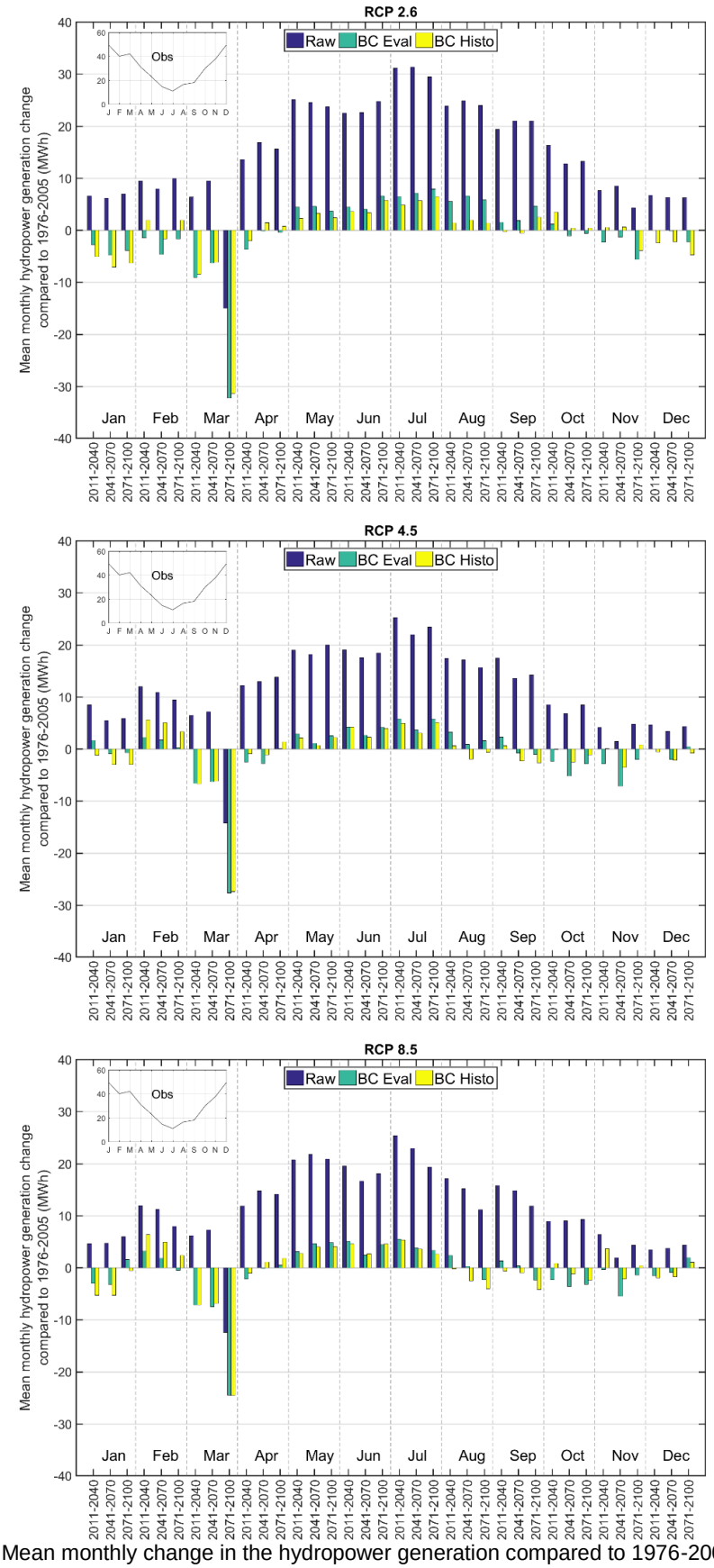

Figure 6. 20 Mean monthly change in the hydropower generation compared to 1976-2005 for the Calder catchment for the uncorrected and bias-corrected 2.6, 4.5 and 8.5 RCP scenarios

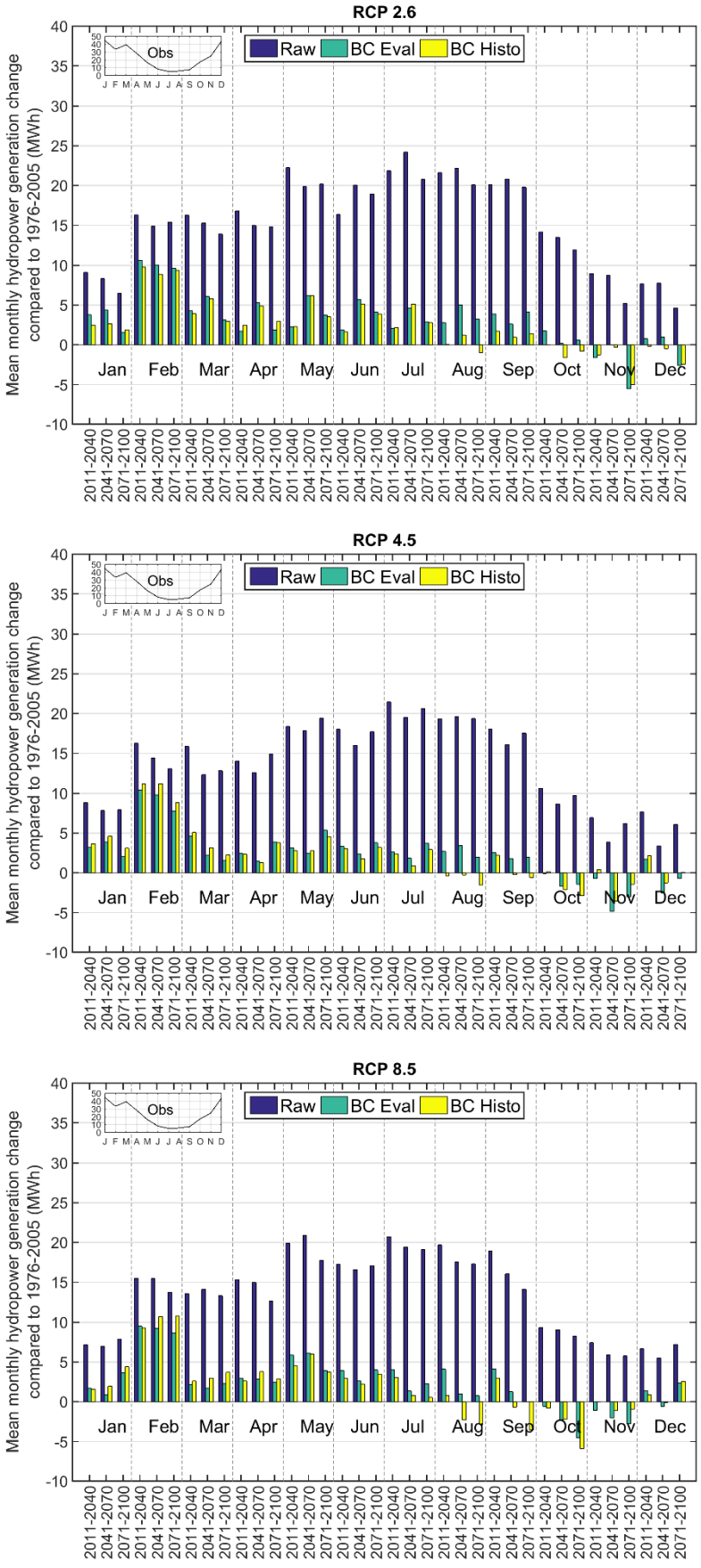

Figure 6. 21 Mean monthly change in the hydropower generation compared to 1976-2005 for the Coquet catchment for the uncorrected and bias-corrected 2.6, 4.5 and 8.5 RCP scenarios

The statistical significance of the monthly variation is evaluated by comparing the simulated monthly MEM and the standard deviation. For the upper Thames, the changes are statistically significant during summer for BC-Eval for all the century (Table B9). In the Glaslyn catchment the changes are statistically significant for August, September and October when bias corrected using BC-Histo (Table B10). For the Calder catchment, the statistically significant changes are projected in June and July for both bias correction approaches driven by RCP 2.6 and 4.5 (Table B11). Finally for the Coquet catchment, statistically significant changes occur in February for both bias correction approaches (Table B12).

6.4.3. Threshold exceedance

Two thresholds are relevant for the hydropower generation. Both of these thresholds impact on the hydropower generation by stopping the generation once the thresholds are reached. The first, Qmax, represents the extreme high flow threshold for which the scheme has to stop to avoid damages (Francois et al., 2016). The other threshold is the Qmin or Hands Off Flow. If river flow volumes below this threshold are reached, then the hydropower scheme is not able to extract water from the river and generation ceases. The exceedance frequency from both thresholds is analysed in the following lines.

A linear regression analysis is performed from 2006 to 2100 to identify the trends in the annual frequency of days above Qmax that are statistically significant (t-test, p-value < 0.05) (Table B7). For the upper Thames, only the trend from the uncorrected RCP 2.6 is statistically significant. For the Glaslyn catchment there are significant trends in Qmax for the uncorrected RCP 2.6 and for both bias-corrected RCP 8.5 projections. For the Calder catchment trends in all projections driven by RCP 8.5 are significant. Finally, Qmax trends in all RCP 8.5 projections and all RCP 4.5 projections except the uncorrected projection are statistically significant for the Coquet catchment. All of the statistically significant trends are positive, indicating an increase in the number of days when the Qmax is reached.

Considering the annual mean number of days above the Qmax in a 5-year moving window aids in the identification of trends and of variability throughout the century (Fig. 6.22). For most of the catchments the bias corrected projections give simulations that agree with the observations. For the upper Thames the observed annual frequency for the entire scenario ranges from 0 to 15 day per year whereas the bias-corrected projections vary from 0 to 10 days per year. In the Glaslyn catchment the observed annual frequency varies from 0.5 to 2.5 days per year. After bias correction, the projections simulate annual frequencies ranging from 0.3 to 1.5 days per year. In the Calder catchment the observed frequency ranges from 4 to 12 days per year and the bias-corrected projections estimate a variability ranging from 2 to 8 days per year. Finally, in the Coquet catchment the observed frequency varies from 5 to 10 days per year and the frequency of the projections ranges from 3 to 12 days per year. The multi decadal variability projects perceptible increases by the end of the century only for RCP 8.5

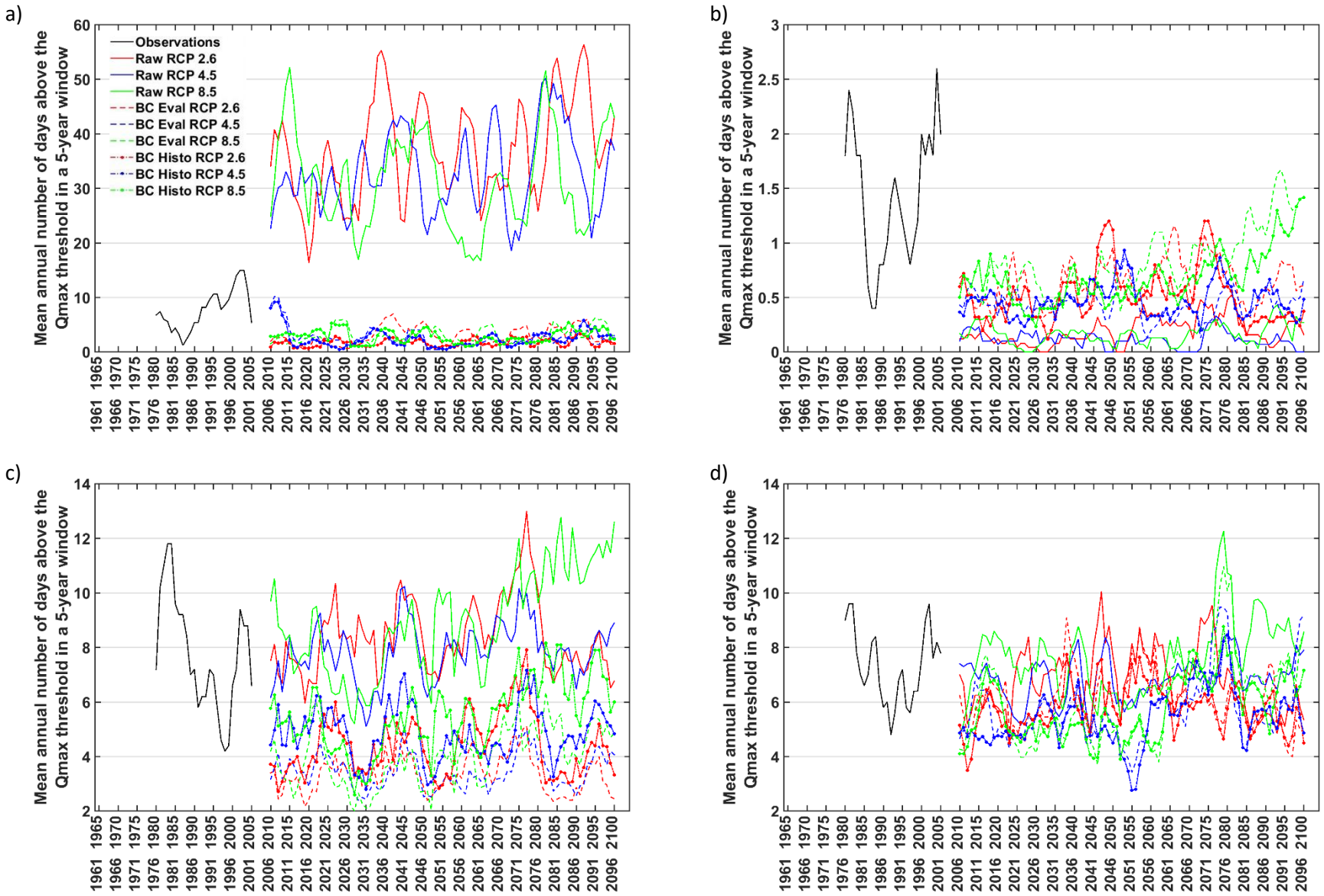

Figure 6. 22 Mean annual number of days in a year in a 5-year moving window when the inlet flow is above Qmax for the uncorrected and bias corrected RCP projections for: a) upper Thames, b) Glaslyn, c) Calder and d) Coquet catchments. Please note the differences in the y-axis

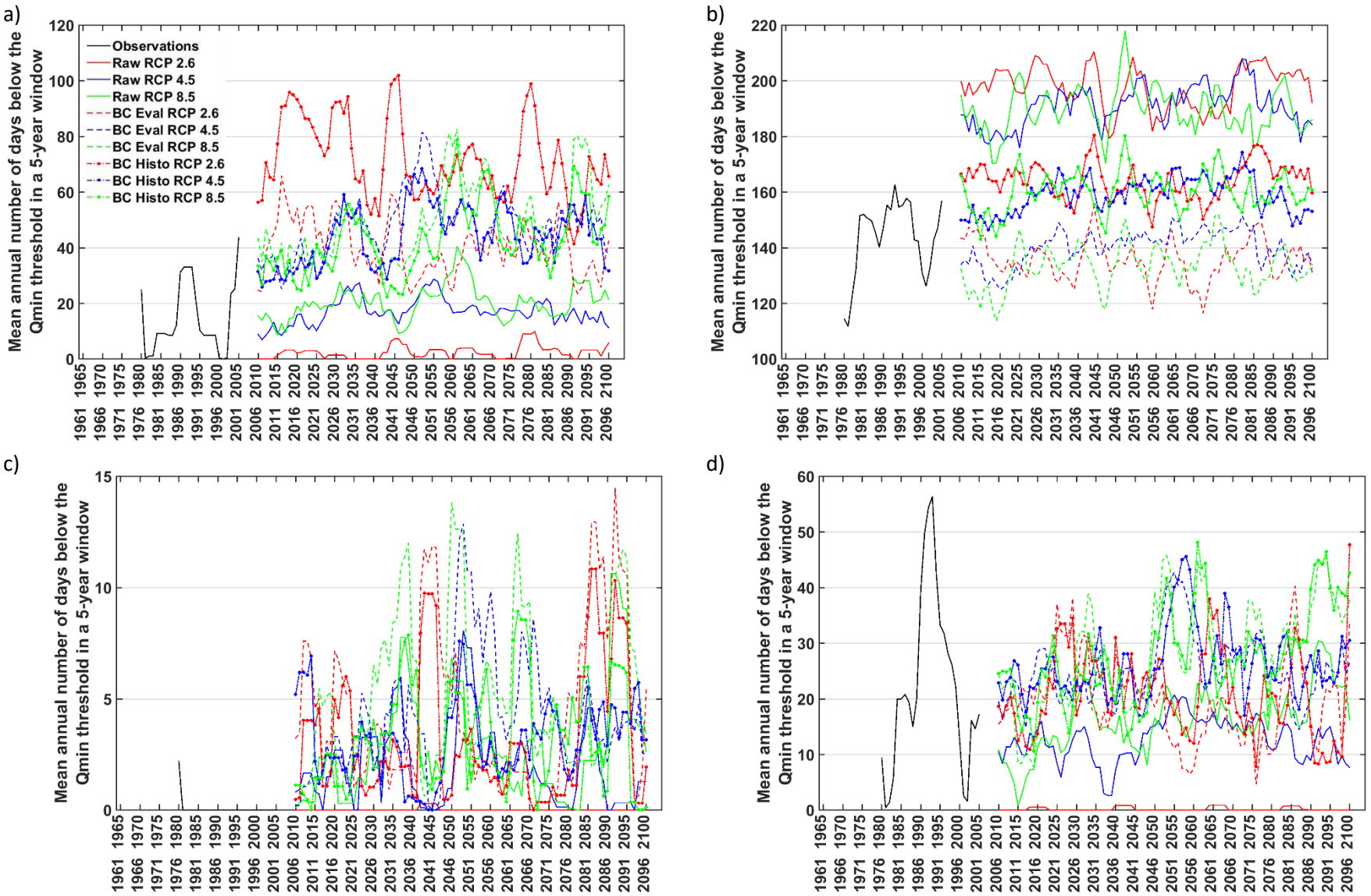

Figure 6. 23 Mean annual number of days in a year in a 5-year moving window when the inlet flow is below Qmin for the uncorrected and bias corrected RCP projections for: a) upper Thames, b) Glaslyn, c) Calder and d) Coquet catchments. Please note the differences in the y-axis

The monthly distribution of the cases when the threshold is reached can give an estimation of the periods of the year when the scheme may not be able to work. Considering only the bias-corrected projections, for the upper Thames decreases in the frequency compared to the reference period are projected for winter in all RCPs with no changes in the remaining months (Fig. A49). In the case of the Glaslyn catchment, decreases are projected from January to March and from October to December. The remaining months do not project any change (Fig. A50). Similar results are obtained for the Calder catchment, where the frequency is projected to decrease during autumn and winter with a slight variation for the remaining months (Fig. A51). For the Coquet catchment, decreases in the frequency are projected from January to March and from October to December. Slight increases are projected for the rest of the months (Fig. A52). The largest decrease by the end of the century are p for the upper Thames (2 day, followed by the Calder (1 day) and the Glaslyn and Coquet (0.5 days) catchments.

There are fewer cases when the trend in the frequency of days below the Qmin is statistically significant (Table B7). This impacts the operation of the scheme as it will not operate due to ecological restraints if the Qmin flow is not reached. The only cases are for both bias-corrected projections driven by 8.5 in the upper Thames and Coquet catchments. Most of the coefficients are positive, indicating an increase in the number of days when the flow at the scheme's inlet is below the Qmin.

Generally, for the average frequency in a 5-year moving average, the bias-corrected projections agree with the observations compared to the uncorrected projections (Fig. 6.23). For all catchments, a trend is not clear except for the projections driven by RCP 8.5 in the Coquet catchment. For the upper Thames, the frequency of the entire scenario varies from 0 to 40 days below Qmin per year, whereas the bias-corrected projections range from 25 to 100 days below Qmin per year (Fig. 6.23a). In the Glaslyn catchment, the observations range from 120 to 160 days below Qmin per year and the bias-corrected projections estimate a frequency ranging from 120 to 180 days below Qmin per year (Fig. 6.23b). In the Calder catchment, the frequency in the observed period is zero for all years but one. For the same catchment, the frequency from the bias-corrected projections range from 0 to 15 days below Qmin per year (Fig. 6.23c). Finally, for the Coquet catchment the frequency from the observations ranges from 0 to 55 days below Qmin per year. In contrast, the bias-corrected projections estimate a frequency varying from 5 to 50 days below Qmin per year (Fig. 6.23d).

The monthly distribution of the projected number of days below the Qmin is different for each catchment. For the upper Thames (Fig. A53) and Calder (Fig. A55) catchments, the projections show an increase in the frequency throughout the year. The main difference is that the largest increases for the upper Thames are expected to occur from September to December, whereas for the Calder catchment they are projected to occur from July to November. In the Glaslyn catchment decreases in the frequency are expected during winter and increases for the rest of the year (Fig. A54). Nevertheless, RCPs 2.6 and 8.5 bias corrected by BC-Eval project some decreases in the frequency for the non-winter months. Finally, in the Coquet catchment all RCPs project a similar picture (Fig. E28). Decreases in the frequency are expected for July

and August and increases from September to December with no large changes for the remaining months. The largest changes are projected for the upper Thames, Glaslyn and Coquet catchments. In the Calder catchment, changes are small in relation to the other catchments.

6.5. Limitations

There are limitations that complicate the simulation of the hydropower output. Initially, the available observation records are relatively short. For the sites included in this study the length of the available records range between 24 and 18 months. These records include the start-up period from the hydropower schemes. Thus, the observations include a period of inconsistency in the system until it stabilizes. Also, due to the length of the observations some of the inter-annual variability might be missed. Furthermore, some of the observational records have incoherency problems (e.g. actual output largely exceeding the theoretical output) and therefore a previous quality check proves to be beneficial.

In particular, for the Glaslyn catchment scheme, its location represents another source of uncertainty. This scheme is distant from the river flow gauging station. Thus, to estimate the future volume of water available for the scheme's inlet, a ratio between the present simulated inlet volume and the observed volume at the gauge is used (section 6.1.1.2). This is expected to give reasonable results as the hydrological model has a good skill in simulating the river flow at the catchments gauging station (sections 3.5 and 3.6) and due to the small area of the catchment, its parameters and properties are not expected to vary much within its extension.

6.6. Summary and discussion

This chapter assess the projected changes in future river flow from the four study catchments based in the uncorrected and bias-corrected climate simulations from six GCM-RCM combinations. Two bias correction approaches are used to evaluate the robustness of the results by 1) using the evaluation simulations to obtain the correction parameters (BC-Eval), and 2) using the historical simulations to train the bias-correction method (BC-Histo). Thus, the first research question that this chapter focusses on is:

iii) to what extent are the projected changes in river flow robust, considering both bias correction approaches?

Similar to chapter 5, robustness is evaluated using the climate change signal from the MEM of both bias correction approaches. The chapter also evaluates the changes in RoR hydropower generation based on the simulated river flow. This represents the final analysis from this research and aims to answer the main objective of the thesis:

To assess how climate change will affect RoR hydropower efficiency and feasibility within UK study catchments. Similar to the analysis of river flow, robustness in the climate change signal is evaluated by comparing the change direction using the MEM from both bias correction approaches.

The uncorrected river flow projections are biased compared to the reference period. This has also been identified previously for other catchments within the UK (Cloke et al., 2013; Wetterhall et al., 2012). Furthermore, for all catchments the frequency of days above the Q10 is projected to increase as well as the frequency of days below the Q95, which is consistent with the findings from (Giuntoli et al., 2015 and Kay and Jones, 2012). From these, only the low flow frequency from 2006 to 2100 driven by RCP 8.5 is statistically significant. The projected river flow changes are not very different between the RCP projections for each 30-year time period (2011-2040, 2041-2070 and 2071-2100). Considering the projected river flow changes for the Glaslyn catchment based on the bias-corrected MEM, each bias correction approach results in different climate change directions. This as a consequence of the precipitation bias correction. Increases in the magnitude of the extreme precipitation and dry spell lengths normally indicate an increase in the magnitude of high flows (similar to the findings from Dankers et al., 2014) and a decrease in the magnitude of low flows, nevertheless their significance was not assessed. Changes in the river flow regime show a large variability among the catchments. In general summer flow changes slightly (either increases or decreases depending on the catchment) and winter flow generally increases.

Considering the robustness of the river flow climate change signal, most cases project a robust signal. Only the Glaslyn catchment gives contradictory climate change signals which might be an effect of the poor simulation skill from the uncorrected GCM-RCM combination, not providing an adequate input for bias correction as stated by Maraun (2016). Therefore, it can be concluded that the robustness of the climate change signal after bias correction largely depends on the skill from the uncorrected RCMs and therefore the importance for their continuous development and improvement, and in the case of small complex catchments such as the Glaslyn, increasing the simulation resolution.

In this study, the observations are used as reference data to evaluate the changes in future projections. Whereas this is not a relevant issue for precipitation and temperature as the climate models are bias-corrected to the observations, for river flow this is not the case. River flow is not bias corrected but instead it is simulated using the bias-corrected precipitation and temperature outputs, therefore including the hydrological model biases in the simulation. In principle this can be problematic. However, from the results observed in this chapter and the statistical analysis of the means and variance from the observations and simulations (section 6.2) this is not a major issue for the results of this study.

The assessment of climate change impact to RoR hydropower schemes is relevant (Francois et al 2016; Kumar et al., 2011). Previous studies have assessed the impacts of climate change on hydropower feasibility (e.g. Lehner et al., 2005; Hamududu and Killingtveit, 2010). Nevertheless, such studies focused on the global change, mainly relating hydropower potential with the available river flow. However, a simple analysis of the future changes in the mean annual river flow is not enough to estimate the real potential or change in the efficiency of a hydropower scheme. As it is shown in section 6.3.1, the actual hydropower generation from a scheme depends on the water volume available, but it should also be within the scheme's operation thresholds (HOF and maximum extraction). Furthermore, the generation will largely depend on

the installed capacity of the scheme. In other words, the mean river flow might increase, but if the scheme is not capable to use such increased volume, then the generation will not increase linearly. Therefore, an analysis of climate change impacts should be performed specifically for each scheme considering its own operational parameters.

Recent studies have focused on the impacts of climate change on existing and proposed RoR hydropower schemes in Estonia (e.g. Tamm et al., 2016) and the UK (Carless and Whitehead, 2013). These studies represent the first approaches to analyse the potential changes in future generation in specific RoR schemes. In contrast to these studies, here the outputs from a larger ensemble of climate projections obtained from the Euro-CORDEX models are used. A larger ensemble provides a wider range of possible projections that gives a stronger climate change output as it is based in a larger number of models. Additionally, here the parametric quantile mapping bias-correction method is used as it has been proven to be more efficient than other methods (Teutschbein and Seibert, 2012; Lafon et al., 2013; Teng et al., 2015). Furthermore, an analysis of the changes in the frequency of the days when the scheme would not be operating is performed.

The river flow climate change impacts can be linked to the expected changes in the hydropower generation. Robust changes in river flow project increases for the upper Thames driven by RCP 8.5 and for the Coquet catchment driven by all RCPs during all the time periods analysed in this study (2011-2040, 2041-2070, 2071-2100). This cases are also robust for the hydropower generation. From the robust changes, hydropower generation is expected to increase in all of them. For the remaining cases, results vary according to the catchment, RCP and bias correction approach. The statistically significant trends from all catchments project an increase in both the high flows and low flows frequencies as well as the frequencies from the thresholds affecting hydropower operation (Qmax and Qmin). Furthermore, changes in the river flow regime and in the monthly hydropower generation are projected, increasing the differences between the wet and dry months for the Glaslyn catchment and decreasing the difference for the rest of the catchments.

One of the main limitations of the study is the lack of long-term data from the hydropower generation records. For the selected operating schemes, only two years of data were available to calibrate the hydropower generation model. Due to the length of the records, the interannual variation could be misinterpreted and biases might be present between the simulated and real potential generation.

Regarding the robustness of the climate change signal, an important result from the analysis is that the BC-Eval and the BC-Histo can provide opposite climate change signals when only considering the MEM. This could impact the follow-up and mitigation actions. However, the choice of BC approach depends on the end user needs. Normally, BC-Eval has been used in climate studies analysing the RCM skill, whereas BC-Histo is commonly used in impact assessments where the end user objective is to reduce the biases to the maximum. Nevertheless, BC-Eval removes only the RCM biases whereas BC-Histo removes both the GCM and RCM biases. However, BC-Histo might be risky for the analysis of climate change impacts as bias

correction is merely a statistical error that don't correct theoretical model errors (Maraun, 2016). This has been discussed in detail in the last paragraph of section 4.4.

Considering the above and briefly detailing the results, by the end of the century compared to the 1976-2005 reference period, hydropower generation for the upper Thames is projected to increase between 1% and 22%: For the Glaslyn catchment the projected changes by the end of the century range from between -6% and 21%. In the Calder catchment the projections indicate no real change by the end of the century (ranging between -1% and 1%). For the Coquet catchment the hydropower potential increases by the end of the century between 18% and 22%. Additionally, the projected trend simulates an annual increasing trend in the number of days that the generation is stopped due to flow volumes being above the maximum threshold. In a monthly analysis, projection generally increases for the winter months, with smaller increases or decreases in the summer generation. This happens for all catchments, except for the Calder catchment where there is variation throughout the months. Considering the robustness of the changes, the Glaslyn catchment change is uncertain due to the opposite direction of change after applying bias correction. Considering the results shown here, the relevance of analysing the individual schemes is highlighted as the projected changes cannot be generalized as each scheme has its own operational properties. Therefore, similar analysis to this one are required to assess the hydropower potential and efficiency.

7. Conclusions

Renewable energy represents an option to mitigate climate change by generating energy with lower CO_2 emissions compared to fossil fuel energy sources. The transition to renewable energy has attracted considerable interest in the last decade. Therefore, governments have set renewable energy generation targets. For the UK, the target expects that 15% of the total energy should come from renewable sources by 2020 (Act CC, 2008). From the renewable sources mix, expanding the installed hydropower capacity can play an important role towards achieving this target. However, all of the suitable sites for water-storage hydropower schemes in the UK are already installed. Therefore, the hydropower capacity is more likely to increase by installing new run-of-the-river (RoR) schemes. Climate change might affect the RoR hydropower generation considerably. Nevertheless, the impacts of climate change are seldom considered during the planning stages of RoR hydropower. This study addresses this knowledge gap by developing and presenting a methodology by which the effects of climate change on RoR schemes can be assessed.

The methodology shown in this study has the objective of assessing the impacts of climate change in RoR hydropower schemes located within study catchments with contrasting characteristics that are representative of the catchments found across the UK. The analysis comprises two installed and two potential hydropower schemes and employs state-of-the-art RCM simulations from the Euro-CORDEX initiative driven by GCMs from CMIP5 to project future changes in climate. Quantile mapping bias correction has been performed to the climate simulations to decrease their biases. The climate simulations are used to drive a HEC-HMS hydrological model for each catchment. The simulated river flow is used to estimate the current and future hydropower generation based on three RCP scenarios: RCP 2.6, 4.5 and 8.5.

Results show that compared to the reference period (1976-2005), the RoR hydropower generation is projected to increase (considering the BC-Histo approach) by the end of the century (2071-2100) for most RCPs and catchments. In most catchments, the generation increases with higher RCP scenarios. The generation changes range between 1% and 17% in the upper Thames site, between -6% and 2% in the Glaslyn site, between –1% and 1% in the Calder catchment, and between 18% and 19% for the Coquet catchment site. The projected change shows a clear generation increase for the upper Thames and the Coquet schemes. For the Glaslyn catchment, the projected change is smaller compared to the current generation. Finally, in the Coquet scheme, the generation is projected to vary slightly as a consequence of the scheme's installed capacity, which does not takes advantage of all the water available for generation.

The results indicate a general potential for increasing the UK's current hydropower generation in the future. Nevertheless, this will depend on the characteristics of each site (e.g. installed capacity). Therefore, it is important and essential to consider the impact of climate change on future generation when evaluating the feasibility of the schemes and to define the most appropriate capacity to install. The study sites that are used here represent a small sample from all potential sites within the UK. However, given their climate, hydrological and physical characteristics, these sites are considered to provide results that can be expanded to the wider hydropower potential within the UK. Furthermore, the study sites lie on the regions

where 85% of England and Wales' total potential capacity is located. Therefore, the results shown here are considered to be representative of the general hydropower potential in this region.

The methodology used in this study demonstrates that the assessment of future hydropower generation as an effect of climate change goes beyond the mere analysis of variations in the future mean annual runoff. Even if the mean annual runoff gives an initial approximation of the future potential generation, inclusion of the frequency of low and high flow events is required for a realistic assessment of future hydropower changes as the hydropower schemes have operation thresholds at both ends of the river flow distribution. Moreover, the generation capacity of currently installed schemes and the potential capacity of future schemes is also important to consider as the hydropower generation will be limited by this capacity. In other words, even if the river flow is largely increased, the actual hydropower generation will be bounded by the scheme's capacity. The study developed here includes the aspects mentioned above. The generation capacity, and the low and high flows threshold specifications of each scheme have been included in the analysis. Furthermore, the theoretical generation estimation has been calibrated using the actual generation from the currently operating schemes to give better estimations of the projected generation. Given the characteristics of the methodology that is developed in this research, it can be used in other geographical areas as it involves open source models and data that can be easily obtained for other regions of the world.

The results from this study are also supported by the use of a climate change multi-model approach. Using a set of climate models, both GCMs and RCMs increase the robustness of the projected change. Here, projections from six GCM-RCM combinations are used to evaluate the future changes in climate, river flow and hydropower generation from RoR schemes. This is in contrast to Tamm et al. (2016) who used two RCMs and Carless and White (2013) who used a single model.

Furthermore, the bias correction method used in this study corrects the entire distribution of the climate variables. The bias correction method used here is superior in reducing the biases compared to the methods used in the studies mentioned in the previous paragraph (Lafon et al., 2013; Teng et al., 2015; Teutschbein and Seibert, 2012). Therefore, more reliable results are expected.

Overall, the results from this research are supported by the developed methodology and assumed to provide a consistent and robust estimation of the future changes in RoR hydropower generation for the analyzed schemes. This research has also identified sources of uncertainty. The most important is the fact that the bias correction approach used can give different change signals, even with non-overlapping standard deviations. Therefore, different interpretation of the impacts can arise from the use of each of the bias correction approaches. Other results indicate the greater influence from the GCMs for the simulation of temperature compared to RCMs, and the greater influence of RCMs in the simulation of precipitation (sections 5.3.1.1 and 5.3.2.1).

Results answering the main objective of the research indicate a different picture for each of the analyzed study sites. This highlights the importance of developing an analysis of this type for each scheme as the results cannot be generalized because each scheme has its own operation characteristics. Overall, three of the study sites project a generation range that is more balanced towards an increase in the future hydropower generation by the end of the century compared to the reference period. In the upper Thames hydropower generation is projected to increase between 1% and 22%. In the Glaslyn catchment the projected changes range between -6% and 21% and between 18% and 22% for the Coquet catchment. Interestingly, for the Calder catchment the projections indicate range between -1% and 1.

In addition to the main objective of the research, during the development of this study three research questions were answered:

i) Is the relative performance of the 0.11° Euro-CORDEX RCMs better than their 0.44° version to simulate climate and river flow? (Chapter 4)

ii) Is the current skill of the Euro-CORDEX RCMs able to generate useful inputs for the analysis of climate change impacts to hydrology? (Chapter 4)

iii) To what extent are the projected changes in climate (Chapter 5), flow regime and hydropower generation (Chapter 6) robust when considering two different bias correction approaches (namely using RCMs driven by perfect boundary conditions or RCMs driven by GCMs to train the bias correction method)?

In summary, the high-resolution RCMs give a clear added value in the simulation of temperature in catchments (Coquet and Glaslyn) with complex orography where the low-resolution RCMs cannot reproduce the temperature changes related to the elevation differences. For the case of precipitation, the high-resolution RCM simulation biases are smaller than the low-resolution biases only for the Glaslyn catchment. Nevertheless, the biases from the high-resolution simulations are still large and are not reliable for being used as drivers of an impact analysis. As a consequence, the simulated river flow from the Glaslyn catchment is biased from the observations when using either the high or low resolution simulations. In contrast, for the rest of the study catchments there is no clear added value from using the high-resolution simulations for the simulation of river flow.

The second research question analyses the usefulness of the uncorrected RCMs to provide reliable river flow simulations. As stated in the previous paragraph, for the Glaslyn catchment the river flow simulations are largely biased. In contrast, for the rest of the catchments the simulation spread cover the observations when considering the flow duration curve (analogue to the river flow distribution). However, the simulation spread is large, giving several possible scenarios. A possibility to reduce the simulation spread and remove the bias is to bias-correct the RCM outputs. This approach gives a better simulation of the river flow by removing the biases and decreasing the simulation spread. However, bias-corrected simulations should be used with caution as they are not based in physical properties nor correct the fundamental errors of the

climate models (discussed in section 4.4, last paragraph). Furthermore, there are a range of bias correction methods and approaches that can contribute to the uncertainty of the climate and impact projections.

The final research question is related to the robustness of the bias correction approaches. Here, two approaches are analysed: 1) remove only the RCM bias, and 2) remove the GCM and RCM bias. A multi-model ensemble consisting of six GCM-RCM simulations is used and their mean (MEM) employed to evaluate the robustness of the correction. A robust result is expected to give climate change signals in the same direction for both methods, whereas if the resulting climate change signals have opposite direction (and these differences are significant) then the results are not robust. It is found that for temperature the bias correction approaches are robust as both project increases. In contrast, the precipitation projections have opposite change directions in some cases and as a consequence the simulated river flow also has opposite directions in some cases. Nevertheless, the differences in the MEMs from the non-robust cases is not large, except for the Glaslyn catchment. For this catchment, the bias correction approaches give very different results in which the multi-model standard deviation from each does not overlap. This is considered to be a problem related to the low skill from the uncorrected RCM to simulate the climate of this topographically-complex catchment. As a consequence of the poor simulation skill, the bias correction methods give opposite climate change signals. Therefore, the need for the continuous improvement and development of RCMs along with their resolution increase is important for the analysis of the impacts of climate change.

7.1. Limitations of the study

One of the limitations of the study is that it only considers the impacts of climate change in the analysis. Nevertheless, future changes in catchment hydrology will also be driven by water management and land use. Climate change is expected to be one of the main drivers of future changes in the water cycle, but also other anthropogenic factors will have an influence. For instance, potential changes in the land use and urbanization of the study catchments could lead to different results as the hydrology of the catchments would be modified. The same could happen by potential changes in the water management or from economic activities that rely on the availability of water, such as agriculture, industries or drinking water supply. Considering the study catchments that are included in this analysis, changes are more probable to happen in the upper Thames and Calder catchments because these are the most populated catchments and also include an important number of water users, such as agriculture (in the upper Thames), industries (in the Calder) and large urban settlements (in both catchments). In contrast, future land use changes for the Glaslyn and Coquet catchments are not very probable as these catchments have a natural river regime and there are no large human settlements nor industries because of their location, difficult access and physical characteristics (complex topography, upland catchments).

In this study, for each of the study catchments river flow is simulated using the HEC-HMS hydrological model. Although the simulation skill of the hydrological model is good for all the catchments (sections 3.5 and 3.6), previously it has been found that different hydrological models can give contrasting results due to

the different concepts, formulae and parameterizations they use (Prudhomme et al., 2014; Dankers et al., 2014). Furthermore, the hydrological model uncertainty can be as large as the GCM uncertainty (Prudhomme et al., 2014). Therefore, one of the limitations of this study is the use of only one hydrological model to simulate future river flow projections. As a consequence, the study does not consider the uncertainty of the hydrological model. Thus, the different projections arising from distinct conceptions of different hydrological models are not considered and could hide important and divergent results If a set of hydrological models is used in an analysis of this type, then the hydrological model uncertainty could be evaluated and compared with the other sources of uncertainty (GCM, RCM, RCP scenario, bias correction method, etc). In addition, the uncertainty of the hydrological model could be reduced if a standard evaluation of the hydrological models was applied for every catchment (discussed in detail in section 3.7). However, the definition of a standard evaluation is not easy as it should consider catchments with different characteristics (e.g. continuous and intermittent catchments) as well as performance measures that are related to the different aspects of the simulation (e.g. high and low flows, mean flow, etc.).

7.2. Areas of future research

There is a need to standardize concepts and methods for the analysis of climate change hydrological impacts. Currently, there is no a standardized approach for the evaluation of the simulation skill of hydrological models. Commonly the hydrological model simulation skill is based on the Nash-Sutcliffe Efficiency Index (NSE). However, this approach might be limited for certain regions. For instance, relying solely in the NSE for arid or semi-arid catchments where there might not be any river flow for most of the year might not be enough as the model might accurately simulate the days with no flow but have problems simulating the days with river flow. In this hypothetical case, as the days with river flow are less frequent the NSE would suffer small changes. Therefore, a standardized protocol to evaluate the hydrological simulation skill in a global context is required. The lack of a current protocol might be a cause of the large hydrological model uncertainty that has been observed before (e.g. Prudhomme et al., 2014). Besides the widely used NSE, metrics focusing on the FDC (e.g. Crookes et al., 2009; Kay et al., 2015) could be used or follow up the work from other initiatives trying to develop common means for the evaluation of simulations (e.g. Maraun et al., 2015).

Furthermore, the application of some of the basic hydrological concepts has not been consistent in the analysis of climate change hydrological impacts. For instance, the high (Q10) and low (Q95) flows estimate has not been used consistently in some publications (e.g. Giuntoli et al., 2015). Even if this might not be a major issue, it demonstrates the need to create a protocol that would benefit the research community by giving guidelines for the studies that assess the hydrological impacts of climate change.

Also, there are research gaps in the development of hydrological models related to the estimation and measurement of local parameters required by the models (Clark et al., 2016). The estimation of the local parameters represent a challenge and an opportunity to improve the skill of the hydrological models to simulate the river flow.

Regarding the simulation skill of the current state-of-the-art climate models (both GCMs and RCMs), the biases between observations and simulations indicate that there is still work to be done simulating the climate processes correctly. For instance, the GCMs should concentrate in getting the simulation of storm tracks better and RCMs focus on simulating orographic precipitation. In other words, research should focus on the accurate representation of key processes for the analysis of impacts. In this context, the impact community would benefit from evaluating the GCMs and RCMs based on such key processes, and therefore minimize the need for bias correction.

Finally, most adaptation measures are location-specific (Van Vliet et al., 2015), therefore there is a need to perform catchment scale analysis to evaluate the impacts of climate change. However, as the climate model outputs might be large for the scale required, uncertainties in the analysis will arise. Nevertheless, the uncertainties of the climate change impact analysis should not be a barrier for decision-making (Knutti and Sedlacek, 2013). Also, as shown above RCM development, improvement and resolution increase should continue in order to perform reliable analysis of climate change impacts. Although bias correction is an approach that can be used to reduce the RCM biases, a RCMs having a good simulation skill would always be the best option to use in an impacts assessment and certainly it would benefit the impact community. In contrast, due to resolution differences the application of uncorrected GCM simulations are not commonly used in catchment-scale analyses. Therefore, for these cases bias-correction represents an important step towards generating post-processed simulations applicable in the analysis of impacts. Nevertheless, as stated above, ideally there should not be the need for bias correction, but this is not accomplished with the current state-of-the-art RCMs.

8. Bibliography

Act, C. C. (2008). Elizabeth II. Chapter 27.

Ahmed, F. (2012). A hydrologic model of kemptville basin—calibration and extended validation. Water resources management, 26(9), 2583-2604.

Ahmed, K. F., Wang, G., Silander, J., Wilson, A. M., Allen, J. M., Horton, R., and Anyah, R. (2013). Statistical downscaling and bias correction of climate model outputs for climate change impact assessment in the US northeast. Global and Planetary Change, 100, 320-332.

Allen, M.R. and Ingram, W.J. (2002). Constraints on future changes in climate and the hydrologic cycle. Nature, 419(6903), 224-232.

Allen, R.G., Pereira, L.S., Raes, D., Smith, M. (1998). Crop evapotranspiration – Guidelines for computing crop water requirements – FAO irrigation and drainage paper 56. Food and Agriculture Organization of the United Nations, Rome. ISBN 92-5-104219-5.

Arnell, N. W. and Lloyd-Hughes, B. (2014). The global-scale impacts of climate change on water resources and flooding under new climate and socio-economic scenarios. Climatic change, 122(1-2), 127-140.

Arnell, N. W., and Gosling, S. N. (2013). The impacts of climate change on river flow regimes at the global scale. Journal of Hydrology, 486, 351-364. doi: DOI 10.1016/j.jhydrol.2013.02.010

Arnell, N.W. (2011). Uncertainty in the relationship between climate forcing and hydrological response in UK catchments. Hydrology and Earth System Sciences, 15(3), 897-912.

Azmat, M., Laio, F., and Poggi, D. (2015). Estimation of water resources availability and mini-hydro productivity in high-altitude scarcely-gauged watershed. Water resources management, 29(14), 5037-5054.

Babel, M. S., Bhusal, S. P., Wahid, S. M., and Agarwal, A. (2014). Climate change and water resources in the Bagmati River Basin, Nepal. Theoretical and applied climatology, 115(3-4), 639-654.

Bartholomeus, R.P., Stagge, J.H., Tallaksen, L.M. and Witte, J.P.M. (2015). Sensitivity of potential evaporation estimates to 100 years of climate variability. Hydrology and Earth System Sciences, 19(2), pp.997-1014

Bedient, P. B. & Huber, W. C. (1992). Hydrology and floodplain analysis. Addison-Wesley, New York, NY.

Bell, V. A. and Moore R. J. (1999). An elevation-dependent snowmelt model for upland Britain. Hydrol. Process., 13:1887-1903.

Bell, V. A., Kay, A. L., Cole, S. J., Jones, R. G., Moore, R. J., and Reynard, N. S. (2012). How might climate change affect river flows across the Thames Basin? An area-wide analysis using the UKCP09 Regional Climate Model ensemble. Journal of Hydrology, 442, 89-104.

Bell, V. A., Kay, A. L., Jones, R. G. and Moore, R. J. (2007). Development of a high resolution grid-based river flow model for use with regional climate model output. Hydrology and Earth System Sciences, 11(1), 532-549.

Benestad, R. E. (2007). Novel methods for inferring future changes in extreme rainfall over Northern Europe. Climate Research, 34(3), 195-210. doi: Doi 10.3354/Cr00693

Benestad, R. E. (2007). Novel methods for inferring future changes in extreme rainfall over Northern Europe. Climate Research, 34(3), 195-210. doi: Doi 10.3354/Cr00693

Beven, K. J. (2001): Rainfall-runoff Modelling, The Primer. John Wiley&Sons Ltd, 360.

Beven, K. J., Kirkby, M. J., Schofield, N. and Tagg, A. F. (1984). Testing a physically-based flood forecasting model (TOPMODEL) for three UK catchments. Journal of Hydrology, 69(1-4), 119-143.

Bindoff, N. L., Stott, P. A., AchutaRao, K. M., Allen, M. R., Gillett, N., Gutzler, D., Hansingo, K., Hegerl, G., Hu, Y., Jain, S. and Mokhov, I. I. (2013). Detection and attribution of climate change: from global to regional.

Block, P. J., Souza, F. A., Sun, L. Q., & Kwon, H. H. (2009). A Streamflow Forecasting Framework using Multiple Climate and Hydrological Models. Journal of the American Water Resources Association, 45(4), 828-843. doi: DOI 10.1111/j.1752-1688.2009.00327.

Bluesky, Landmap (2014): Bluesky 5m resolution Digital Terrain Model (DTM) for England and Wales. NERC Earth Observation Data Centre, April 30th, 2016.

Böhm, U., Kücken, M., Ahrens, W., Block, A., Hauffe, D., Keuler, K., Rockel, B., Will, A. (2006). CLM-the climate version of LM: Brief description and long-term applications. Tech. Rep., COSMO Newsletter.

Brands, S., Gutiérrez, J. M., Herrera, S. and Cofiño, A. S. (2012). On the use of reanalysis data for downscaling. Journal of Climate, 25(7), 2517-2526.

Brown, C., Meeks, R., Hunu, K., and Yu, W. (2011). Hydroclimate risk to economic growth in sub-Saharan Africa. Climatic Change, 106(4), 621-647. doi: DOI 10.1007/s10584-010-9956-9

Bulcock, H. H. and Jewitt, G. P. (2010). Spatial mapping of leaf area index using hyperspectral remote sensing for hydrological applications with a particular focus on canopy interception. Hydrol. Earth Sci., 14, 383-392.

Campbell, J. B. (2007). Introduction to remote sensing. 4th Edition, The Guilford Press, New York. ISBN-13: 978-1-59385-319-8.

Cannon, A.J., Sobie, S.R., Murdock, T.Q. (2015). Bias correction of GCM precipitation by quantile mapping: How well do methods preserve changes in quantiles and extremes? Journal of Climate, 28(17), 6938-6959.

Carless, D., and Whitehead, P. G. (2013). The potential impacts of climate change on hydropower generation in Mid Wales. Hydrology Research, 44(3), 495-505. doi: Doi 10.2166/Nh.2012.012

Casanueva, A., Kotlarski, S., Herrera, S., Fernández, J., Gutiérrez, J. M., Boberg, F., Colette, A., Christensen, O. B., Goergen, K., Jacob, D., Keuler, K., Nikulin, G., Teichmann, C., Vautard, R. (2015). Daily precipitation

statistics in a EURO-CORDEX RCM ensemble: added value of raw and bias-corrected high-resolution simulations. Clim. Dyn. 1-19. doi: 10.1007/s00382-015-2865-x
Cattiaux, J., Douville, H., and Peings, Y. (2013). European temperatures in CMIP5: origins of present-day biases and future uncertainties. Climate dynamics, 41(11-12), 2889-2907.
CEC (1998). Layman's guidebook on how to develop a small hydro site. European Small Hydropower Association. Comission of the European Communities
Chan, S.C., Kendon, E.J., Fowley, H.J., Blenkinsop, S., Ferro, C.A.T., Stephenson, D.B., (2013). Does increasing the spatial resolution of a regional climate model improve the simulated daily precipitation? Clim. Dyn. 41, 1475-1495. doi: 10.1007/s00382-012-1568-9.
Chang, E. K., Guo, Y., and Xia, X. (2012). CMIP5 multimodel ensemble projection of storm track change under global warming. Journal of Geophysical Research: Atmospheres, 117(D23).
Charlton, M. B., and Arnell, N. W. (2014). Assessing the impacts of climate change on river flows in England using the UKCP09 climate change projections. Journal of hydrology, 519, 1723-1738.
Chen, D. L., Achberger, C., Raisanen, J., & Hellstrom, C. (2006). Using statistical downscaling to quantify the GCM-related uncertainty in regional climate change scenarios: A case study of Swedish precipitation. Advances in Atmospheric Sciences, 23(1), 54-60. doi: DOI 10.1007/s00376-006-0006-5
Chen, J., Brissette, F. P., Chaumont, D., & Braun, M. (2013). Performance and uncertainty evaluation of empirical downscaling methods in quantifying the climate change impacts on hydrology over two North American river basins. Journal of Hydrology, 479, 200-214. doi: DOI 10.1016/j.jhydrol.2012.11.062
Chen, J., Brissette, F.P. and Lucas-Picher, P. (2015). Assessing the limits of bias-correcting climate model outputs for climate change impact studies. Journal of Geophysical Research: Atmospheres, 120(3), 1123-1136.
Christensen, J.H., Boberg, F., Christensen, O.B., Lucas-Picher, P. (2008). On the need for bias correction of regional climate change projections of temperature and precipitation. Geophys. Res. Lett. 35(20), L20709. doi: 10.1029/2008GL035694.
Christensen, O.B., Christensen, J.H., Machenhauer, B., Botzet, M. (1998). Very high-resolution regional climate simulations over Scandinavia-present climate. J. Clim. 11(12), 3204-3229.
Christierson, B.V., Vidal, J.P., Wade, S.D. (2012). Using UKCP09 probabilistic climate information for UK water resource planning. J. Hydrol. 424-425: 48-67. doi: 10.1016/j.hydrol.2011.12.020.
Clark, M. P., Wilby, R. L., Gutmann, E. D., Vano, J. A., Gangopadhyay, S., Wood, A. W., Fowler, H.J., Prudhomme, C., Arnold, J.R. and Brekke, L. D. (2016). Characterizing uncertainty of the hydrologic impacts of climate change. Current Climate Change Reports, 2(2), 55-64.
Cloke, H.L., Wetterhall, F., He, Y., Freer, J.E., Pappenberger, F. (2013). Modelling climate impact on floods with ensemble climate projections. Q. J. R. Meteorol. Soc. 139, 282-297. doi: 10.1002/qj.1998
Crawford, N. H., and Linsley, R. K. (1966). Digital Simulation in Hydrology'Stanford Watershed Model 4.
Crooks S. M., Kay, A. L., Reynard, N. S. (2009). Regionalised Impacts of Climate Change on Flood Flows: hydrological models, catchments and calibration. Defra, J.
Cubasch, U., D. Wuebbles, D. Chen, M.C. Facchini, D. Frame, N. Mahowald, and J.-G. Winther, (2013) Introduction. In: Climate Change 2013: The Physical Science Basis. Contribution of Working Group I to the Fifth Assessment Report of the Intergovernmental Panel on Climate Change [Stocker, T.F., D. Qin, G.-K. Plattner, M. Tignor, S.K. Allen, J. Boschung, A. Nauels, Y. Xia, V. Bex and P.M. Midgley (eds.)]. Cambridge University Press, Cambridge, United Kingdom and New York, NY, USA.
Dankers, R., Arnell, N. W., Clark, D. B., Falloon, P. D., Fekete, B. M., Gosling, S. N., Heinke, J., Kim, H., Masaki, Y., Satoh, Y. and Stacke, T. (2014). First look at changes in flood hazard in the Inter-Sectoral Impact Model Intercomparison Project ensemble. Proceedings of the National Academy of Sciences, 111(9), 3257-3261.
Dankers, r., Christensen, O.B., Feyen, L., Kalas, M., de Roo, A. (2007). Evaluation of very high-resolution climate model data for simulating flood hazards in the Upper Danude Basin. J. Hydrol., 347: 319-331. doi: 10.1016/j.hydrol.2007.09.055.
Danner, C. L., McKinney, D. C., Teasley, R. L. and Sandoval-Solis, S. (2006). Documentation and testing of the WEAP model for the Rio Grande/Bravo basin. Center for Research in Water Resources, University of Texas at Austin.
Dariane, A. B., Javadianzadeh, M. M. and James, L. D. (2016). Developing an efficient auto-calibration algorithm for HEC-HMS program. Water resources management, 30(6), 1923-1937.
Davie, T. (2008). Fundamentals of hydrology. Taylor & Francis.
De Leeuw, J., Methven, J., and Blackburn, M. (2015). Evaluation of ERA-Interim reanalysis precipitation products using England and Wales observations. Quarterly Journal of the Royal Meteorological Society, 141(688), 798-806.
De Roo, A. P. J., Wesseling, C. G. and Van Deursen, W. P. A. (2000). Physically based river basin modelling within a GIS: the LISFLOOD model. Hydrological Processes, 14(11-12), 1981-1992.
DECC (2017). Digest of United Kingdom Energy Statistics. Department of Energy and Climate Change. TSO, London.

Dee, D.P., Uppala, S.M., Simmons, A.J., Berrisford, P., Poli, P., Kobayashi, S., Andrae, U., Balmaseda, M.A., Balsamo, G., Bauer, P., Bechtold, P. (2011). The ERA-Interim reanalysis: Configuration and performance of the data assimilation system. Quarterly Journal of the royal meteorological society, 137(656), 553-597.
Defra (2011). Agriculture in the United Kingdom 2010. Department for Environment, Foor, Rural Affairs, Department of Agriculture and Rural Development, Welsh Assembly Government, The Department of Rural Affairs and Heritage, The Scottish Government, Rural and Environment Research and Analysis Directorate
Deque, M. (2007). Frequency of precipitation and temperature extremes over France in an anthropogenic scenario: Model results and statistical correction according to observed values. Global and Planetary Change, 57(1-2), 16-26. doi: DOI 10.1016/j.gloplacha.2006.11.030
Derdour, A., Bouanani, A., and Babahamed, K. (2017). Hydrological modeling in semi-arid region using HEC-HMS model. case study in Ain Sefra watershed, Ksour Mountains (SW-Algeria). Journal of Fundamental and Applied Sciences, 9(2), 1027-1049.
Dettinger, M. D., Cayan, D. R., Meyer, M., and Jeton, A. E. (2004). Simulated hydrologic responses to climate variations and change in the Merced, Carson, and American River basins, Sierra Nevada, California, 1900-2099. Climatic Change, 62(1-3), 283-317. doi: Doi 10.1023/B:Clim.0000013683.13346.4f
Di Luca, A., de Elía, R., Laprise, R. (2015). Challenges in the quest for added value of regional climate dynamical downscaling. Curr. Clim. Change Rep. 1, 10-21. doi: 10.1007/s40641-015-0003-9.
Diaz-Nieto, J., and Wilby, R. L. (2005). A comparison of statistical downscaling and climate change factor methods: Impacts on low flows in the River Thames, United Kingdom. Climatic Change, 69(2-3), 245-268. doi: DOI 10.1007/s10584-005-1157-6
Dibike, Y. B. and Coulibaly, P. (2005). Hydrologic impact of climate change in the Saguenay watershed: comparison of downscaling methods and hydrologic models. Journal of hydrology, 307(1), 145-163.
Donohue, R.J., McVicar, T.R., Roderick, M.L. (2010). Assessing the ability of potential evaporation formulations to capture the dynamics in evaporative demand within a changing climate. Journal of Hydrology, 386(1), 186-197.
EA (2009). Good practice guidelines to the environment agency hydropower handbook. The environmental assessment of proposed low head hydropower developments. Environment Agency. Bristol, UK.
EA (2010). Mapping hydropower opportunities and sensitivities in England and Wales. Technical report. Environment Agency. Bristol, UK.
EA (2011). Middle Severn catchment hydropower pre-feasibility study. Jeremy Benn Associates Limited, Telford and Wrekin Council & Environment Agency Midlands. UK.
Eden, J.M., Widmann, M., Maraun, D., Vrac, M. (2014). Comparison of GCM- and RCM-simulated precipitation following stochastic postprocessing. J. Geophys. Res. Atmos. 119, 11040-11053. doi:10.1002/2014JD021732.
Ehret, U., Zehe, E., Wulfmeyer, V., Warrach-Sagi, K., Liebert, J. (2012). Should we apply bias correction to global and regional climate model data? Hydrol. Earth Syst. Sci. 16, 3391-3404. doi: 10.5194/hess-16-3391-2012.
EIA (2010). International Energy Outlook. U.S. Energy Information Agency, US Department of Energy, Washington, DC, USA, 328 pp.
El Alfy, M. (2016). Assessing the impact of arid area urbanization on flash floods using GIS, remote sensing, and HEC-HMS rainfall–runoff modeling. Hydrology Research, 47(6), 1142-1160.
European Union (2014). European Union: Council of the European Union, Conclusions on 2030 Climate and Energy Policy framework. Brussels European Council, 23 October 2014.
European Union (2017). European Union: Council of the European Union, Outcome of the council meeting, Transport, Telecommunications and energy. Brussels European Council, 26 June 2017.
Feldman, A. D. (2000). Hydrologic modeling system HEC-HMS, technical reference manual. Hydrologic Engineering Center, US Army Corps of Engineers; 155pp. Davis, USA.
Fowler, H. J., Blenkinsop, S., & Tebaldi, C. (2007). Linking climate change modelling to impacts studies: recent advances in downscaling techniques for hydrological modelling. International Journal of Climatology, 27(12), 1547-1578. doi: Doi 10.1002/Joc.1556
Fowler, H. J., Ekstrom, M., Kilsby, C. G., and Jones, P. D. (2005). New estimates of future changes in extreme rainfall across the UK using regional climate model integrations. Assessment of control climate. Journal of Hydrology, 300(1-4), 212-233. doi: DOI 10.1016/j.jhydrol.2004.06.017
Fowler, H.J. and Kilsby, C.G. (2007). Using regional climate model data to simulate historical an future river flows in northwest England. Clim. Change. 80: 337-367.
François, B., Borga, M., Anquetin, S., Creutin, J.D., Engeland, K., Favre, A.C., Hingray, B., Ramos, M.H., Raynaud, D., Renard, B. and Sauquet, E. (2014). Integrating hydropower and intermittent climate-related renewable energies: a call for hydrology. Hydrol. Process, 28(21), pp.5465-5468.
François, B., Hingray, B., Raynaud, D., Borga, M.and & Creutin, J. D. (2016). Increasing climate-related-energy penetration by integrating run-of-the river hydropower to wind/solar mix. Renewable Energy, 87, 686-696.
Frei, C., Christensen, J. H., Deque, M., Jacob, D., Jones, R. G., & Vidale, P. L. (2003). Daily precipitation statistics in regional climate models: Evaluation and intercomparison for the European Alps. Journal of Geophysical Research-Atmospheres, 108(D3). doi: Artn 4124 Doi 10.1029/2002jd002287

Frias, M. D., Zorita, E., Fernandez, J., & Rodriguez-Puebla, C. (2006). Testing statistical downscaling methods in simulated climates. Geophysical Research Letters, 33(19). doi: Artn L19807 Doi 10.1029/2006gl027453
Giorgi, F., Coppola, E., and Raffaele, F. (2014). A consistent picture of the hydroclimatic response to global warming from multiple indices: Models and observations. Journal of Geophysical Research: Atmospheres, 119(20).
Giorgi, F., Jones, C., Asrar, G.R. (2009). Addressing climate information needs at the regional level: the CORDEX framework. World Meteorological Organization (WMO) Bulletin, 58(3), 175.
Giuntoli, I., Vidal, J. P., Prudhomme, C. and Hannah, D. M. (2015). Future hydrological extremes: the uncertainty from multiple global climate and global hydrological models. Earth System Dynamics, 6(1), 267.
Graham, P.L., Andréasson, J., Carlsson, B. (2007). Assessing climate change impacts on hydrology from an ensemble of regional climate models, model scales and linking methods – a case study on the Lule River basin. Climatic change 81: 293-307. doi: 10.1007/s10584-006-921-5-2.
Grillakis, M.G., Koutroulis, A.G., Tsanis, I.K. (2013). Multisegment statistical bias correction of daily GCM precipitation output. Journal of Geophysical Research: Atmospheres, 118(8), 3150-3162.
Gumindoga, W., Rwasoka, D. T., Nhapi, I. and Dube, T. (2016). Ungauged runoff simulation in Upper Manyame Catchment, Zimbabwe: Application of the HEC-HMS model. Physics and Chemistry of the Earth, Parts A/B/C.
Gustard, A., Bullock, A., Dixon, J. M. (1992). Low flow estimation in the United Kingdom. Wallingford, Institute of Hydrology, 88pp. (IH Report No.108).
Gutjahr, O. and Heinemann, G. (2013). Comparing precipitation bias correction methods for high-resolution regional climate simulations using COSMO-CLM. Theoretical and Applied Climatology, 114(3-4), 511-529.
Guyennon, N., Romano, E., Portoghese, I., Salerno, F., Calmanti, S., Petrangeli, A. B., Tartari, G., and Copetti, D. (2013). Benefits from using combined dynamical-statistical downscaling approaches-lessons from a case study in the Mediterranean region. Hydrology and Earth System Sciences, 17(2), 705.
Hamon, W.R. (1961). Estimating potential evapotranspiration. J. Hydr. Eng. Div. ASCE. 871, 107-120.
Hamududu, B. and Killingtveit, A. (2012). Assessing Climate Change Impacts on Global Hydropower. Energies, 5(2), 305-322. doi: Doi 10.3390/En5020305
Hänggi, P. and Weingartner, R. (2012). Variations in discharge volumes for hydropower generation in Switzerland. Water resources management, 26(5), 1231-1252.
Hannaford, J. (2015). Climate-driven changes in UK river flows: A review of the evidence. Progress in Physical Geography, 39(1), 29-48.
Hannaford, J. and Buys, G. (2012). Trends in seasonal river flow regimes in the UK. Journal of Hydrology, 475, pp.158-174.
Hannaford, J. and Marsh, T.J. (2008). High‐flow and flood trends in a network of undisturbed catchments in the UK. International Journal of Climatology, 28(10), pp.1325-1338.
Haylock, M. R., Cawley, G. C., Harpham, C., Wilby, R. L., & Goodess, C. M. (2006). Downscaling heavy precipitation over the United Kingdom: A comparison of dynamical and statistical methods and their future scenarios. International Journal of Climatology, 26(10), 1397-1415. doi: Doi 10.1002/Joc.1318
Herrera, S., Fita, L., Fernández, J., & Gutiérrez, J. M. (2010). Evaluation of the mean and extreme precipitation regimes from the ENSEMBLES regional climate multimodel simulations over Spain. Journal of Geophysical Research: Atmospheres, 115(D21).
Hough, M. N., and Jones, R. J. A.: The UnitedKingdom Meteorological Office rainfall and evaporation calculation system: MORECS version 2.0-an overview, Hydrology and Earth System Sciences, 1, 227-239, doi:10.5194/hess-1-227-1997, 1997.
Hrachowitz, M., Savenije, H. H. G., Blöschl, G., McDonnell, J. J., Sivapalan, M., Pomeroy, J. W., Arheimer, B., Blume, T., Clark, M.P., Ehret, U. and Fenicia, F. (2013). A decade of Predictions in Ungauged Basins (PUB)—a review. Hydrological sciences journal, 58(6), 1198-1255.
Huang, S., Krysanove, V., Hatterman, F. F. (2014). Does bias correction increase relibility of flood projections under climate change? A case study of large rivers in Germany. Int. J. Climatol. 34, 3780-3800. doi: 10.1002/joc.3945.
Ibrahim-Bathis, K., and Ahmed, S. A. (2016). Rainfall-runoff modelling of Doddahalla watershed—an application of HEC-HMS and SCN-CN in ungauged agricultural watershed. Arabian Journal of Geosciences, 9(3), 170.
IJHD (2010). World Atlas & Industry Guide. International Journal of Hydropower and Dams, Wallington, Surrey, UK, 405 pp.
Ines, A. V. M., and Hansen, J. W. (2006). Bias correction of daily GCM rainfall for crop simulation studies. Agricultural and Forest Meteorology, 138(1-4), 44-53. doi: DOI 10.1016/j.agrformet.2006.03.009
IPCC (2007): Climate Change 2007: Synthesis Report. Contribution of Working Groups I, II and III to the Fourth Assessment Report of the Intergovernmental Panel on Climate Change [Core Writing Team, Pachauri, R.K and Reisinger, A. (eds.)]. IPCC, Geneva, Switzerland, 104 pp
IPCC (2013). Climate Change 2013: The Physical Science Basis. Contribution of Woking Group I to the Fifth Assessment Report of the Intergovernmental Panel on Climate Change [Stocker, TF, Qin D, Plattner GK, Tignor M, Allen SK, Boschung J, Nauels A, Xia Y, Bex V and Midgley PM (eds.)]. Cambridge University Press, Cambridge, United Kingdom and New York, NY, USA, 1535pp.

IPCC, (2014): Climate Change 2014: Synthesis Report. Contribution of Working Groups I, II and III to the Fifth Assessment Report of the Intergovernmental Panel on Climate Change [Core Writing Team, R.K. Pachauri and L.A. Meyer (eds.)]. IPCC, Geneva, Switzerland, 151 pp.

Jacob, D., Petersen, J., Eggert, B., Alias, A., Christensen, O.B., Bouwer, L.M., Braun, A., Colette, A., Déqué, M., Georgievski, G., Georgopoulou, E., Gobiet, A., Menut, L., Nikulin, G., Haensler, A., Hempelmann, N., Jones, C., Keuler, K., Kovats, S., Kröner, N., Kotlarski, S., Kriegsmann, A., Martin, E., van Meijgaard, E., Moseley, C., Pfeifer, S., Preuschmann, S., Radermacher, C., Radtke, K., Rechid, D., Rounsevell, M., Samuelsson, P., Somot, S., Soussana, J.F., Teichmann, C., Valentini, R., Vautard, R., Weber, B., Yiou, P., (2014). EURO-CORDEX: new high-resolution climate change projections for European impact research. Reg. Environ. Change. 14,563-578. doi: 10.1007/s10113-013-0499-2.

Jiménez Cisneros, B.E., T. Oki, N.W. Arnell, G. Benito, J.G. Cogley, P. Döll, T. Jiang, S.S. Mwakalila, (2014). Freshwater resources. In: Climate Change 2014: Impacts,Adaptation, and Vulnerability. Part A: Global and Sectoral Aspects. Contribution of Working Group II to the Fifth Assessment Report of the Intergovernmental Panel on Climate Change [Field, C.B., V.R. Barros, D.J. Dokken, K.J. Mach, M.D. Mastrandrea, T.E. Bilir, M. Chatterjee, K.L. Ebi, Y.O. Estrada, R.C. Genova, B. Girma, E.S. Kissel, A.N. Levy, S. MacCracken, P.R. Mastrandrea, and L.L.White (eds.)]. Cambridge University Press, Cambridge, United Kingdom and New York, NY, USA, pp. 229-269.

Johnson, F. and Sharma, A. (2009). Measurement of GCM skill in predicting variables relevant for hydroclimatological assessments. Journal of Climate, 22(16), 4373-4382. doi: 10.1175/2009JCLI2681.1

Jones, M. R., Fowler, H. J., Kilsby, C. G., and Blenkinsop, S. (2012). An assessment of changes in seasonal and annual extreme rainfall in the UK between 1961 and 2009. International Journal of Climatology, 33(5), 1178-1194.

Jones, P., Harpham, C., Kilsby, C., Glenis, V., and Burton, A. (2010). UK Climate Projections science report: Projections of future daily climate for the UK from the Weather Generator. UK Climate Projections.

Jury, M. W., Prein, A. F., Truhetz, H. and Gobiet, A. (2015). Evaluation of CMIP5 models in the context of dynamical downscaling over Europe. Journal of Climate, 28(14), 5575-5582.

Kay, A.L. and Davies, H.N. (2008). Calculating potential evaporation from climate model data: A source of uncertainty for hydrological climate change impacts. Journal of Hydrology, 358(3), 221-239

Kay, A.L., Bell, V.A., Blyth, E. M., Crooks, S. M., Davies, H.N., Reynards, N. S. (2013). A hydrological perspective on evaporation: historical trends and future projections in Britain. Journal of Water and Climate Change, 4(3) 193-208. doi: 10.2166/wcc.2013.014.

Kay, A.L., Davies, H.N., Bell, V.A., Jones, R.G. (2009). Comparison of uncertainty for climate change impacts: flood frequency in England. Clim. Change. 92: 41-63. doi: 10.1007/s10584-008-9471-4.

Kay, A.L., Jones, D.A. (2012). Transient changes in flood frequency and timing in Britain under potential projections of climate change. Int. J. Climatol. 32: 489-502. doi: 10.1002/joc.2288.

Kay, A.L., Rudd, A.C., Davies, H.N., Kendon, E.J., Jones, R.G. (2015). Use of very high resolution climate model data for hydrological modelling: baseline performance and future flood changes. Clim. Change. 133:193-208. doi: 10.1007/s10584-015-1455-6.

Keller, V. D. J., Tanguy, M., Prosdocimi, I., Terry, J. A., Hitt, O., Cole, S. J., Fry, M., Morris, D.G. and Dixon, H. (2015). CEH-GEAR: 1 km resolution daily and monthly areal rainfall estimates for the UK for hydrological and other applications. Earth System Science Data, 7(1), 143-155.

Kendon, E.J., Roberts, N.M., Senior, C.A., Roberts, M.J. (2012). Realism of rainfall in a very high-resolution regional climate model. J. Climate. 25(17): 5791-5806. doi: 10.1175/JCLI-D-11-00562.1

Kim, K.B., Kwon, H.H., Han, D. (2016). Precipitation ensembles conforming to natural variations derived from a regional climate model using a new bias correction scheme. Hydrology and Earth System Sciences,20(5), 2019-2034.

Kingston, D.G., Todd, M.C., Taylor, R.G., Thompson, J.R., Arnell, N.W. (2009). Uncertainty in the estimation of potential evapotranspiration under climate change. Geophysical Research Letters, 36(20).

Kleinn, J., Frei, C., Gurtz, J., Luthi, D., Vidale, P. L., and Schar, C. (2005). Hydrologic simulations in the Rhine basin driven by a regional climate model. Journal of Geophysical Research-Atmospheres, 110(D4). doi: Artn D04102 Doi 10.1029/2004jd005143

Knutti, R. and Sedláček, J. (2013). Robustness and uncertainties in the new CMIP5 climate model projections. Nature Climate Change, 3(4), 369-373.

Kotlarski, S., Keuler, K., Christensen, O.B., Colette, A., Déqué, M., Gobiet, A., Goergen, K., Jacob, D., Lüthi, D., van Meijgaard, E., Nikulin, G., Schär, C., Teichutard, R., Warrach-Sagi, K., Wulfmeyer, V., (2014). Regional climate modeling on European scales: a joint standard evaluation of the EURO-CORDEX RCM ensemble. Geosci. Model Dev. 7, 1297-1333. doi: 10.5194/gmd-7-1297-2014.

Koutroulis, A.G., Grillakis, M.G., Tsanis, I.K. and Papadimitriou, L. (2016). Evaluation of precipitation and temperature simulation performance of the CMIP3 and CMIP5 historical experiments. Climate Dynamics, 47(5-6), pp.1881-1898.

Kozak, J. A., Ahuja, L. R., Green T. R. and Ma, L. (2007). Modelling crop canopy and residue rainfall interception effects on soil hydrological components for semi-arid agriculture. Hydrol. Process., 21, 229-241.

Kumar, A., Schei, T., Ahenkorah, A., Caceres Rodriguez, R., Devernay, J.M., Freitas, M., Hall, D., Killingtveit, A., & Liu, Z. (2011). Hydropower. In IPCC Special Report on Renewable Energy Sources and Climate Change Mitigation edited by Edenhofer, O., Pichs-Madruga, R., Sokona, Y., Seyboth, K., Matschoss, P., Kadner, S., Zwickel, T., Eickemeier, P., Hansen, G., Schlomer, S., von Stechow, C. Cambridge University Press, Cambridge, United Kingdom and New York, NY, USA.

Lafon, T., Dadson, S., Buys, G., Prudhomme, C. (2013). Bias correction of daily precipitation simulated by a regional climate model: a comparison of methods. Int. J. Climatol. 33:1367-1381. doi:10.1002/joc.3518.

Lawley, R. and Garcia-Bajo, M. (2010). The national superficial deposit thickness model (version 5). British Geological Survey Internal Report, OR/09/049; 18pp. Nottingham, UK.

Ledbetter, R., Prudhomme, C. and Arnell, N. (2012). A method for incorporating climate variability in climate change impact assessments: Sensitivity of river flows in the Eden catchment to precipitation scenarios. Climatic Change, 113(3-4), pp.803-823.

Lehner, B., Czisch, G., & Vassolo, S. (2005). The impact of global change on the hydropower potential of Europe: a model-based analysis. Energy Policy, 33(7), 839-855. doi: DOI 10.1016/j.enpol.2003.10.018

Leung, L. R., Mearns, L. O., Giorgi, F., & Wilby, R. L. (2003). Regional climate research - Needs and opportunities. Bulletin of the American Meteorological Society, 84(1), 89-95. doi: Doi 10.1175/Bams-84-1-89

Lindström, G., Johansson, B., Persson, M., Gardelin, M. and Bergström, S. (1997). Development and test of the distributed HBV-96 hydrological model. Journal of hydrology, 201(1-4), 272-288.

Lindström, G., Pers, C., Rosberg, J., Strömqvist, J. and Arheimer, B. (2010). Development and testing of the HYPE (Hydrological Predictions for the Environment) water quality model for different spatial scales. Hydrology research, 41(3-4), 295-319.

Madani, K. (2011). Hydropower licensing and climate change: Insights from cooperative game theory. Advances in Water Resources, 34(2), 174-183. doi: DOI 10.1016/j.advwatres.2010.10.003

Maraun, D. (2013). Bias correction, quantile mapping, and downscaling: revisiting the inflation issue. J. Climate. 26, 2137-2143. doi: 10.1175/JCLI-D-12-00821.1.

Maraun, D. (2016). Bias correcting climate change simulations-a critical review. Current Climate Change Reports, 2(4), 211-220.

Maraun, D. and Widmann, M. (2015). The representation of location by a regional climate model in complex terrain. Hydrol. Earth Syst. Sci. 19, 3449-3456. doi: 10.5194/hess-19-3449-2015.

Maraun, D., Wetterhall., F., Ireson, A.M., Chandler, R.E., Kendon, E.J., Widmann, M., Brienen, S., Rust, H.W., Sauter, T., Themeβl, M., Venema, V.K.C., Chun, K.P., Goodess, C.M., Jones, R.G., Onof, C., Vrac, M., Thiele-Eich. (2010). Precipitation downscaling under climate change: recent developments to bridge the gap between dynamical models and the end user. Rev. Geophys. 48, RG3003. doi:10.1029/2009RG000314.

Maraun, D., Widmann, M. (2015). The representation of location by a regional climate model in complex terrain. Hydrol. Earth Syst. Sci. 19, 3449-3456. doi: 10.5194/hess-19-3449-2015.

Maraun, D., Widmann, M., Gutiérrez, J.M., Kotlarski, S., Chandler, E., Hertig, E., Wibig, J., Huth, R., Wilcke, R.A.I., (2015). VALUE: A framework to validate dowsncaling approaches for climate change studies. Earth's Future. 3, 1-14. doi: 10.1002/2014EF000259.

Marsh, T. J. and Hannaford, J. (Eds.) (2008). UK Hydrometric Register. Hydrological data UK series. Centre for Ecology & Hydrology. 210 pp.

Maurer, E. P., Adam, J. C., and Wood, A. W. (2009). Climate model based consensus on the hydrologic impacts of climate change to the Rio Lempa basin of Central America. Hydrology and Earth System Sciences, 13(2), 183-194.

Mbaye, M. L., Haensler, A., Hagemann, S., Gaye, A. T., Moseley, C., and Afouda, A. (2016). Impact of statistical bias correction on the projected climate change signals of the regional climate model REMO over the Senegal River Basin. International Journal of Climatology, 36(4), 2035-2049.

McVicar, T.R., Roderick, M.L., Donohue, R.J., Li, L.T., Van Niel, T.G., Thomas, A., Grieser, J., Jhajharia, D., Himri, Y., Mahowald, N.M., Mescherskaya, A.V. (2012). Global review and synthesis of trends in observed terrestrial near-surface wind speeds: Implications for evaporation. Journal of Hydrology, 416, 182-205.

Mehran, A., AghaKouchak, A., and Phillips, T. J. (2014). Evaluation of CMIP5 continental precipitation simulations relative to satellite-based gauge-adjusted observations. Journal of Geophysical Research: Atmospheres, 119(4), 1695-1707.

Minns, A. W. and Hall, M. J. (1996). Artificial neural networks as rainfall-runoff models. Hydrological sciences journal, 41(3), 399-417.

Moore, R. J. (2007). The PDM rainfall-runoff model. Hydrology and Earth System Sciences Discussions, 11(1), 483-499.

Moriasi, D. N., Arnold, J. G., Van Liew, M. W., Bingner, R. L., Harmel, R. D. and Veith, T. L. (2007). Model evaluation guidelines for systematic quantification of accuracy in watershed simulation. American Society of Agricultural and Biological Engineers, Vol. 50, 3; 885-900.

Morris D. G. and Flavin R. W. (1990). A digital terrain model for hydrology. Proc 4th International Symposium on Spatial Data Handling. Vol. 1, Jul 23-27; pp 250-262. Zurich.

Morris D. G. and Flavin R. W. (1994). Sub-set of UK 50m y 50m hydrological digital terrain model grids. NERC, Institute of Hydrology, Wallingford.
Morris, D. G., and Flavin, R. W.: A digital terrain model for hydrology., Proceedings of the 4th International Symposium on Spatial Data Handling, 1, 250-262, 1990.
Morton, D., Rowland, C., Wood, C., Meek, L., Marston, C., Smith, G., Wadsworth, R. and Simpson, I. (2011). Final Report for LCM2007-the new UK land cover map. Countryside Survey Technical Report No 11/07.
Moss, R. H., Edmonds, J. A., Hibbard, K. A., Manning, M. R., Rose, S. K., Van Vuuren, D. P., Carter, T.R., Emori, S., Kainuma, M., Kram, T. and Meehl, G. A. (2010). The next generation of scenarios for climate change research and assessment. Nature, 463(7282), 747.
Muerth, M., Gauvin St-Denis, B., Ricard, S., Velázquez, J. A., Schmid, J., Minville, M., Caya, D., Chaumont, D., Ludwig, R. and Turcotte, R. (2013). On the need for bias correction in regional climate scenarios to assess climate change impacts on river runoff. Hydrology and Earth System Sciences Discussions, 10205-10243.
Murphy, J. M., Sexton, D. M., Jenkins, G. J., Booth, B. B., Brown, C. C., Clark, R. T., Collins, M., Harris, G.R., Kendon, E.J., Betts, R.A.and Brown, S. J. (2009). UK climate projections science report: climate change projections.
Nash, J.E. and Suttcliffe, J.V. (1970). River flow forecasting through conceptual models. Part I: a discussion of principles. J. Hydrol. 10, 282-290.
Noreña, J. E. O., Garcia, C. G., Conde, A. C., Magana, V., and Esqueda, G. S. T. (2009). Vulnerability of water resources in the face of potential climate change: generation of hydroelectric power in Colombia. Atmosfera, 22(3), 229-252.
Onöl, B. (2012). Effects of coastal topography on climate: High-resolution simulation with a regional climate model. Clim. Res. 52: 159-174. doi: 10.3354/cr01077.
Oudin, L., Hervieu, F., Michel, C., Perrin, C., Andréassian, V., Anctil, F., Loumagne, C. (2005). Which potential evapotranspiration input for a lumped rainfall-runoff model? Part 2 – Towards a simple and efficient potential evapotranspiration model for rainfall-runoff modelling. J. Hydrol. 303, 290-306. doi: 10.1016/j.jhydrol.2004.08.026.
Pappenberger, F., & Beven, K. J. (2006). Ignorance is bliss: Or seven reasons not to use uncertainty analysis. Water resources research, 42(5).
Parry, M. L., Canziani, O. F., Palutikof, J. P., van der Linden, P. J., and Hanson, C. E. (2007). Climate Change 2007: Impacts, Adaptation and Vulnerability, Contribution of Working Group II to the Fourth Assessment Report of the Intergovernmental Panel on Climate Change, Cambridge University Press, Cambridge, UK
Pechlivanidis, I.G., Jackson, B.M., McIntyre, N.R. and Wheater, H.S., 2011. Catchment scale hydrological modelling: a review of model types, calibration approaches and uncertainty analysis methods in the context of recent developments in technology and applications. Global NEST Journal, 13(3), pp.193-214.
Perrin, C., Michel, C., and Andréassian, V. (2003). Improvement of a parsimonious model for streamflow simulation. Journal of hydrology, 279(1), 275-289.
Piani, C., Haerter, J. O., & Coppola, E. (2010). Statistical bias correction for daily precipitation in regional climate models over Europe. Theoretical and Applied Climatology, 99(1-2), 187-192. doi: 10.1007/s00704-009-0134-9
Poff, N. L., Allan, J. D., Bain, M. B., Karr, J. R., Prestegaard, K. L., Richter, B. D., Sparks, R.E. and Stromberg, J. C. (1997). The natural flow regime. BioScience, 47(11), 769-784.
Prein, A.F., Gobiet, A., Truhetz, H., Keuler, K., Goergen, K., Teichmann, C., Fox Maule, C., van Meijgaard, E., Déqué, M., Nikulin, G., Vautard, R., Colette, A., Kjellström, E., Jacob, D. (2015). Precipitation in the EURO-CORDEX 0.11° and 0.44° simulations: high resolution, high benefits? Clim. Dyn. doi: 10.1007/s00382-015-2589-y.
Prudhomme, C. and Davies, H. (2009). Assessing uncertainties in climate change impact analyses on the river flow regimes in the UK. Part 1: baseline climate. Climatic Change, 93(1-2), 177-195. doi: DOI 10.1007/s10584-008-9464-3
Prudhomme, C., Giuntoli, I., Robinson, E. L., Clark, D. B., Arnell, N. W., Dankers, R., Fekete, B.M., Franssen, W., Gerten, D., Gosling, S.N. and Hagemann, S. (2014). Hydrological droughts in the 21st century, hotspots and uncertainties from a global multimodel ensemble experiment. Proceedings of the National Academy of Sciences, 111(9), 3262-3267.
Prudhomme, C., Haxon, T., Crooks, S., Jackson, C., Barkwith, A., Williamson, J., Kelvin, J., Mackay, J., Wang, L., Young, A., Watts, G. (2013). Future flows hydrology: an ensemble of daily river flow and monthly groundwater levels for use for climate change impact assessment across Great Britain. Earth Syst. Sci. Data 5: 101-107. doi:10-5194/essd-5-101-2013.
Prudhomme, C., Jakob, D., Svensson, C. (2003). Uncertainty and climate change impact on the flood regime of small UK catchments. J. Hydrol. 227: 1-23. doi: 10.1016/S0022-1694(03)00065-9.
Prudhomme, C., Young, A., Watts, G., Haxton, T., Crooks, S., Williamson, J., Davies, H., Dadson, S. and Allen, S. (2012). The drying up of Britain? A national estimate of changes in seasonal river flows from 11 Regional Climate Model simulations. Hydrological Processes, 26(7), 1115-1118.

Prudhomme, C., Parry, S., Hannaford, J., Clark, D.B., Hagemann, S. and Voss, F. (2011). How well do large-scale models reproduce regional hydrological extremes in Europe? Journal of Hydrometeorology, 12(6), pp.1181-1204.
Raghunath, H. M. (2006). Hydrology: principles, analysis and design. New Age International.
Ramesh, K. V. and Goswami, P. (2014). Assessing reliability of regional climate projections: the case of Indian monsoon. Scientific reports, 4.
Rawls, W. J. and Brakensiek, D. L. (1982). Estimating soil water retention from soil properties. Journal of Irrigation and Drainage Division, ASCE, 108 (IR2), 166-171.
Robinson, E. L., Blyth, E. M., Clark, D. B., Finch, J., & Rudd, A. C. (2017). Trends in atmospheric evaporative demand in Great Britain using high-resolution meteorological data. Hydrology and Earth System Sciences, 21(2), 1189.
Robinson, E. L., Blyth, E., Clark, D. B., Finch, J., Rudd, A. C. (2015). Climate hydrology and ecology research support system meteorological dataset (1961-2012) [CHESS-met] . NERC-Environmental Information Data Centre doi:10.5285/80887755-1426-4dab-a4a6-250919d5020c
Rockel, B. (2015). The regional dowsncaling approach: a brief history and recent advances. Curr. Clim. Change Rep. 1:22-29. doi: 10.1007/s40641-014-0001-3.
Rockel, B., Will, A., Hense, A. (2008). Special issue on regional climate modelling with COSMO-CLM (CCLM). Meteorol. Z. 17, 477-485.
Rojas, R., Feyen, L., Dosio, A., Bavera, D. (2011). Improving pan-European hydrological simulation of extreme events through statistical bias correction of RCM-driven climate simulations. Hydrol. Earth Syst. Sci. 15, 2599-2620. doi: 10.5194/hess-15-2599-2011.
Rudd, A.C. and Kay, A.L. (2016). Use of very high resolution climate model data for hydrological modelling: estimation of potential evaporation. Hydrology Research, 47(3), 660-670.
Rummukainen, M. (2010). State-of-the-art with regional climate models. Wiley Interdisciplinary Reviews-Climate Change, 1(1), 82-96. doi: Doi 10.1002/Wcc.008
Rummukainen, M. B. (2016). Added value in regional climate modeling. WIREs Clim. Change 7:145-159. doi: 10.1002/wcc.378
Samuelsson, P., Jones, C.G., Willén, U., Ullerstig, A., Gollvik, S., Hansson, U., Jansson, C., Kjellström, E., Nikulin, G., Wyser, K. (2011). The Rossby Centre Regional Climate Model RCA3: model description and performance. Tellus 63A:4-23. doi: 10.1111/j.1600-0870.2010.00478.x.
Savenije, H. H. G. (2004). The importance of interception and why we should delete the term evapotranspiration from our vocabulary. Hydrol. Process., 18, 1507-1511.
Schaefli, B., and Gupta, H. V. (2007). Do Nash values have value?. Hydrological Processes, 21(15), 2075-2080.
Schär, C., Ban, N., Fischer, E.M., Rajczak, J., Schmidli, J., Frei, C., Giorgi, F., Karl, T.R., Kendon, E.J., Tank, A.M.K., O'Gorman, P.A. (2016). Percentile indices for assessing changes in heavy precipitation events.Climatic Change, 137(1-2), 201-216.
Scharffenberg, W. A. and Fleming, M. J. (2013). HEC-HMS User's Manual. Washington, DC.
Scharffenberg, W. A., Fleming, M. J. and Feldman, A. D. (2003). The Hydrologic Modeling System (HEC-HMS): Toward a Complete Framework for Hydrologic Engineering. In World Water & Environmental Resources Congress 2003 (pp. 1-8).
Schneider, C., Laizé, C. L. R., Acreman, M. C., and Florke, M. (2013). How will climate change modify river flow regimes in Europe?. Hydrology and Earth System Sciences, 17(1), 325-339.
Schwartz, F., Pegallapati, R. and Shahidehpour, M. (2005, June). Small hydro as green power. In Power Engineering Society General Meeting, 2005. IEEE (pp. 2050-2057). IEEE.
Seiller, G. and Anctil, F. (2016). How do potential evapotranspiration formulae influence hydrological projections?. Hydrological Sciences Journal, 61(12), 2249-2266.
Shaw, E. M., Beven, K. J., Chappell, N. A., & Lamb, R. (2010). Hydrology in practice. CRC Press.
Shaw, S. B. And Riha, S., J. (2011). Assessing temperature-based PET equations under a changing climate in temperate, deciduous forests. Hydrol. Process. 25, 1466-1478.
Sillmann, J., Kharin, V.V., Zhang, X., Zwiers, F.W. and Bronaugh, D. (2013). Climate extremes indices in the CMIP5 multimodel ensemble: Part 1. Model evaluation in the present climate. Journal of Geophysical Research: Atmospheres, 118(4), pp.1716-1733.
Singh, V. P. and Frevert, D. K. (Eds.). (2006). Watershed models. Taylor & Francis.
Skamarock, W.C., Klemp, J., Dudhia, J., Gill, D., Barker, D., Wang, W., Powers, J. (2008). A description of the advanced research wrf version 3, Tech. Rep., NCAR Technical Note 475, 113pp.
Smith, A., Bates, P., Freer, J., and Wetterhall, F. (2014). Investigating the application of climate models in flood projection across the UK. Hydrological Processes, 28(5), 2810-2823. doi: 10.1002/hyp.9815
Solomon, S., Qin, D., Manning, M., Chen, Z., Marquis, M., Averyt, K.B., Tignor, M. and Miller, H.L. (eds.) (2007) Contribution of Working Group I to the Fourth Assessment Report of the Intergovernmental Panel on Climate Change. Cambridge University Press, Cambridge, United Kingdom and New York, NY, USA.
Sorooshian, S. and Gupta, V. K. (1995). Model calibration. Computer models of watershed hydrology, 23-68.

Spackman, E. (1993). Calculation and mapping of rainfall averages for 1961–90. University of Salford, Manchester, 15.

Stocker, T.F., D. Qin, G.-K. Plattner, L.V. Alexander, S.K. Allen, N.L. Bindoff, F.-M. Bréon, J.A. Church, U. Cubasch, S. Emori, P. Forster, P. Friedlingstein, N. Gillett, J.M. Gregory, D.L. Hartmann, E. Jansen, B. Kirtman, R. Knutti, K. Krishna Kumar, P. Lemke, J. Marotzke, V. Masson-Delmotte, G.A. Meehl, I.I. Mokhov, S. Piao, V. Ramaswamy, D.Randall, M. Rhein, M. Rojas, C. Sabine, D. Shindell, L.D. Talley, D.G. Vaughan and S.-P. Xie, (2013). Technical Summary. In: Climate Change 2013: The Physical Science Basis. Contribution of Working Group I to the Fifth Assessment Report of the Intergovernmental Panel on Climate Change [Stocker, T.F., D. Qin, G.-K. Plattner, M. Tignor, S.K. Allen, J. Boschung, A. Nauels, Y. Xia, V. Bex and P.M. Midgley (eds.)]. Cambridge University Press, Cambridge, United Kingdom and New York, NY, USA.

Tamm, O., Luhamaa, A., and Tamm, T. (2016). Modeling future changes in the North-Estonian hydropower production by using SWAT. Hydrology Research, 47(4), 835-846.

Tanguy, M., Dixon, H., Prosdocimi, I., Morris, D.G., Keller, V.D.J., 2014. Gridded estimates of daily and monthly areal rainfall for the UK (1890–2012) [CEH-GEAR]. NERC Environmental Information Data Centre. doi: 10.5285/5dc179dc-f692-49ba-9326-a6893a503f6e.

Taylor, A. B. and Schwartz, H. E. (1952). Unit-hydrograph lag and peak flow related to basin characteristics. Am. Geophys. Union Trans. 33(2), 235-246.

Taylor, K. E., Stouffer, R. J., Meehl, G. A. (2012). An overview of CMIP5 and the experiment design. American Meteorological Society. DOI:10.1175/BAMS-D-11-00094.1

Teng, J., Potter, N.J., Chiew, F.H.S., Zhang, L., Wang, B., Vaze, J., Evans, J.P. (2015). How does bias correction of regional climate model precipitation affect modeled runoff? Hydrol. Earth Syst. Sci. 19, 711-728. doi: 10.5194/hess-19-711-2015.

Teutschbein, C. and Seibert, J. (2012). Bias correction of regional climate model simulations for hydrological climate-change impact studies: Review and evaluation of different methods. Journal of Hydrology, 456, pp.12-29.

Thom, H.C.S. (1958). A note on the gamma distribution. Mon. Weather Rev. 86 (4), 117–122.

Todini, E. (1996). The ARNO rainfall—runoff model. Journal of hydrology, 175(1-4), 339-382.

Todini, E., and Ciarapica, L. (2002). The TOPKAPI model. Mathematical models of large watershed hydrology, 471-506.

Torma, C., Giorgi, F., Coppola, E. (2015). Added value of regional climate modeling over areas characterized by complex terrain – Precipitation over the Alps. J. Geophys. Res. Atmos. 120:3957-3972. doi: 10.1002/2014JD022781

US Department of Energy (1983). Microhydrpower handbook. Volume 1. Idaho Falls, USA.

van Meijgaard, E., van Ulft, L.H., Lenderink, G., de Roode, S.R., Wipfler, L., Boers, R., Timmermans, R.M.A. (2012). Refinement and application of a regional atmospheric model for climate scenario calculations of Western Europe. Climate changes Spatial Planning publication: KvR 054/12.

Van Steenbergen, N. and Willems, P. (2012). Method for testing the accuracy of rainfall–runoff models in predicting peak flow changes due to rainfall changes, in a climate changing context. Journal of hydrology, 414, 425-434.

van Vliet, M. T., Donnelly, C., Strömbäck, L., Capell, R. and Ludwig, F. (2015). European scale climate information services for water use sectors. Journal of Hydrology, 528, 503-513.

Van Vuuren, D. P., Edmonds, J., Kainuma, M., Riahi, K., Thomson, A., Hibbard, K., Hurtt, G.C., Kram, T., Krey, V., Lamarque, J.F. and Masui, T. (2011). The representative concentration pathways: an overview. Climatic change, 109(1-2), 5.

Velázquez, J.A., Troin, M., Caya, D., Brissette, F. (2015). Evaluating the time-invariance hypothesis of climate model bias correction: implications for hydrological impact studies. J. Hydrometeor. 16, 2013-2026. doi: 10.1175/JHM-D-14-0159-.1.

VijayaVenkataRaman, S., Iniyan, S., and Goic, R. (2012). A review of climate change, mitigation and adaptation. Renewable & Sustainable Energy Reviews, 16(1), 878-897. doi: DOI 10.1016/j.rser.2011.09.009

Von Bremen, L. (2010). Large-scale variability of weather dependent renewable energy sources. In Management of weather and climate risk in the energy industry (pp. 189-206). Springer, Dordrecht.

Von Hoyningen-Huene, J. (1981). Die interzeption des Niederschlages in landwirtschaftlichen Pflanzenbenstanden. Deutscher Verband fur Wasserwirtschaft und Kultubau, Verlag Paul Parey-Hamburg, Schirften, 57, 1 -66.

Vrac, M., Drobinski, P., Merlo, A., Herrmann, M., Lavaysse, C., Li, L., & Somot, S. (2012). Dynamical and statistical downscaling of the French Mediterranean climate: uncertainty assessment. Natural Hazards and Earth System Sciences, 12(9), 2769-2784. doi: DOI 10.5194/nhess-12-2769-2012

Walsh, C. L., Blenkinsop, S., Fowler, H. J., Burton, A., Dawson, R. J., Glenis, V., Manninga, L.J. and Kilsby, C. G. (2015). Adaptation of water resource systems to an uncertain future. Hydrology & Earth System Sciences Discussions, 12(9).

Wang, M., Zhang, L. and Baddoo, T. D. (2016). Hydrological Modeling in A Semi-Arid Region Using HEC-HMS. Journal of Water Resource and Hydraulic Engineering Sept, 5(3), 105-115.

Watts, G., Battarbee, R.W., Bloomfield, J.P., Crossman, J., Daccache, A., Durance, I., Elliott, J.A., Garner, G., Hannaford, J., Hannah, D.M., Hess, T. (2015). Climate change and water in the UK–past changes and future prospects. Progress in Physical Geography, 39(1), 6-28.
Wetterhall, F. (2014). Uncertainties in downscaling of climate model output for impact studies. Presentation at the CWC Workshop "NWP/Hydrological model coupling", London, UK.
Wetterhall, F., He, Y., Cloke, H., & Pappenberger, F. (2011). Effects of temporal resolution of input precipitation on the performance of hydrological forecasting. Adv. Geosci., 29, 21-25. doi: 10.5194/adgeo-29-21-2011
Wetterhall, F., Pappenberger, F., He, Y., Freer, J., Cloke, H.L. (2012). Conditioning model output statistics of regional climate model precipitation on circulation patterns. Nonlin. Processes Geophys. 19, 623-633. doi: 10.5194/npg-19-623-2012.
Wilby, R. L. (2005). Uncertainty in water resource model parameters used for climate change impact assessment. Hydrological Processes, 19(16), 3201-3219.
Wilby, R. L., and Harris, I. (2006). A framework for assessing uncertainties in climate change impacts: Low-flow scenarios for the River Thames, UK. Water Resources Research, 42(2).
Wilby, R. L., and Wigley, T. M. L. (1997). Downscaling general circulation model output: a review of methods and limitations. Progress in Physical Geography, 21(4), 530-548.
Wilby, R. L., Whitehead, P. G., Wade, A. J., Butterfield, D., Davis, R. J., & Watts, G. (2006). Integrated modelling of climate change impacts on water resources and quality in a lowland catchment: River Kennet, UK. Journal of Hydrology, 330(1-2), 204-220.
Wilcke, R.A.I., Mendlik, T., Gobiet, A. (2013). Multi-variable error correction of regional climate models. Climatic Change. 120, 871-887. doi: 10.1007/s10584-013-0845-x.
Wójcik, R. (2015). Reliability of CMIP5 GCM simulations in reproducing atmospheric circulation over Europe and the North Atlantic: a statistical downscaling perspective. International Journal of Climatology, 35(5), 714-732.
Wong, G., Maraun, D., Vrac, M., Widmann, M., Eden, J.M., Kent, T. (2014). Stochastic model output statistics for bias correcting and downscaling precipitation including extremes. Journal of Climate, 27(18), 6940-6959.
Woods, G., Tickle, A., Chandler, A. and Beardmore J. (2010). Peak power: developing micro hydro power in the Peak District. Friends of the Peak District. Sheffield, UK.
Xu, C.Y., Singh, V.P. (2001). Evaluation and generalization of temperature-based methods for calculating evaporation. Hydrol. Process. 15, 305-319.
Yang, W., Andréasson, J., Graham, L.P., Olsson, J., Rosberg, J., Wetterhall, F. (2010). Distribution-based scaling to improve usability of regional climate model projections for hydrological climate change impacts studies. Hydrology Research, 41(3-4), 211-229.
Yoon, J. H., Leung, L. R. and Correia, J. (2012). Comparison of dynamically and statistically downscaled seasonal climate forecasts for the cold season over the United States. Journal of Geophysical Research-Atmospheres, 117.
Zappa, G., Shaffrey, L. C. and Hodges, K. I. (2013). The ability of CMIP5 models to simulate North Atlantic extratropical cyclones. Journal of Climate, 26(15), 5379-5396.
Zema, D. A., Labate, A., Martino, D. and Zimbone, S. M. (2017). Comparing Different Infiltration Methods of the HEC-HMS Model: The Case Study of the Mésima Torrent (Southern Italy). Land Degradation & Development, 28(1), 294-308.
Zhang, X., Alexander, L., Hegerl, G.C., Jones, P., Tank, A.K., Peterson, T.C., Trewin, B., Zwiers, F.W. (2011). Indices for monitoring changes in extremes based on daily temperature and precipitation data. Wiley Interdisciplinary Reviews: Climate Change, 2(6),851-870

Annex A

This annex includes the supplementary figures for all the chapters.

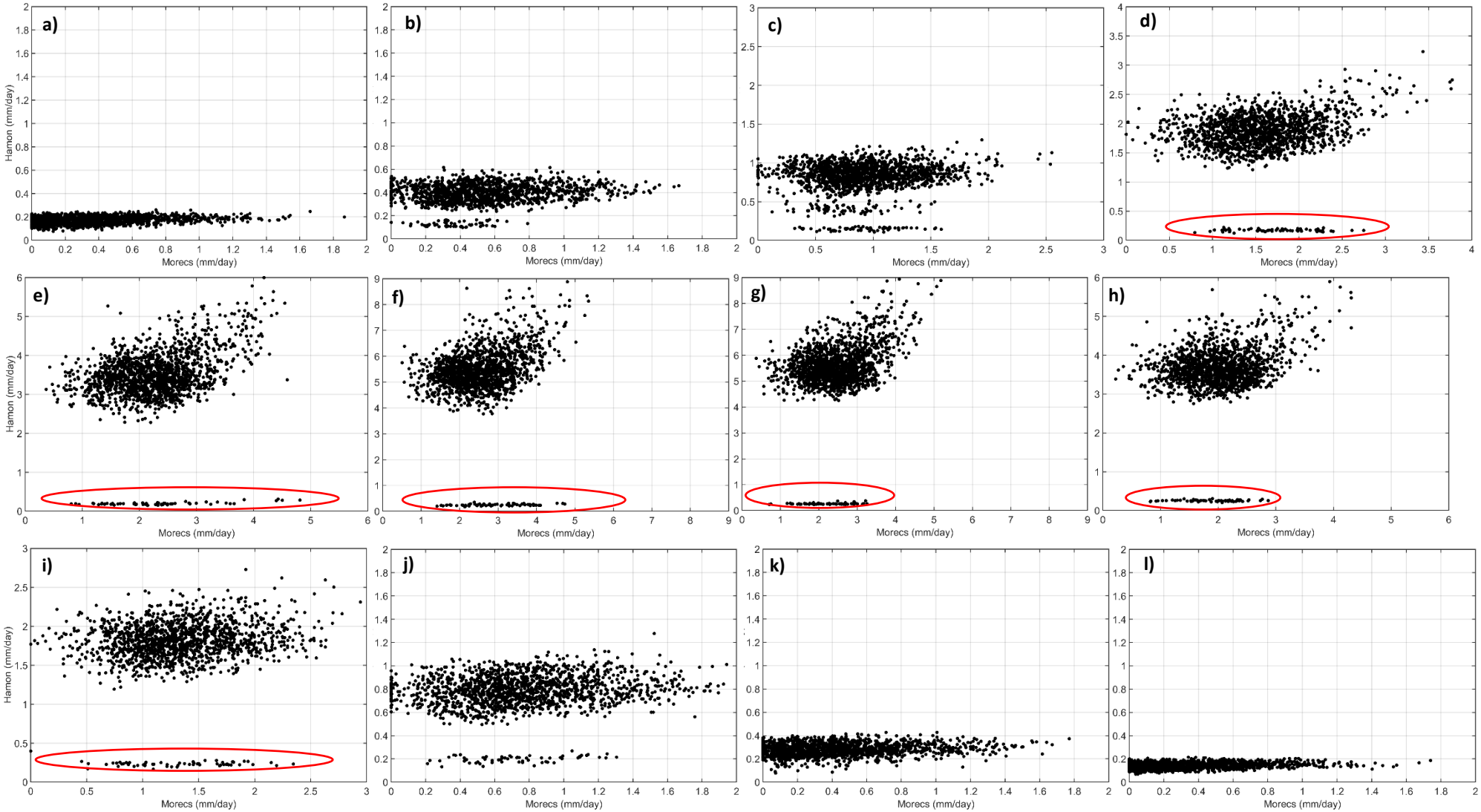

Figure A 1 Scatter plots between daily observed (Morecs) and simulated PET using the Hamon formula for the Glaslyn catchment: a) January, b) February, c) March, d) April, e) May, f) June, g) July, h) August, i) September, j) October, k) November, and l) December. Please note the difference in the axis. Frequent underestimated days are circled in red

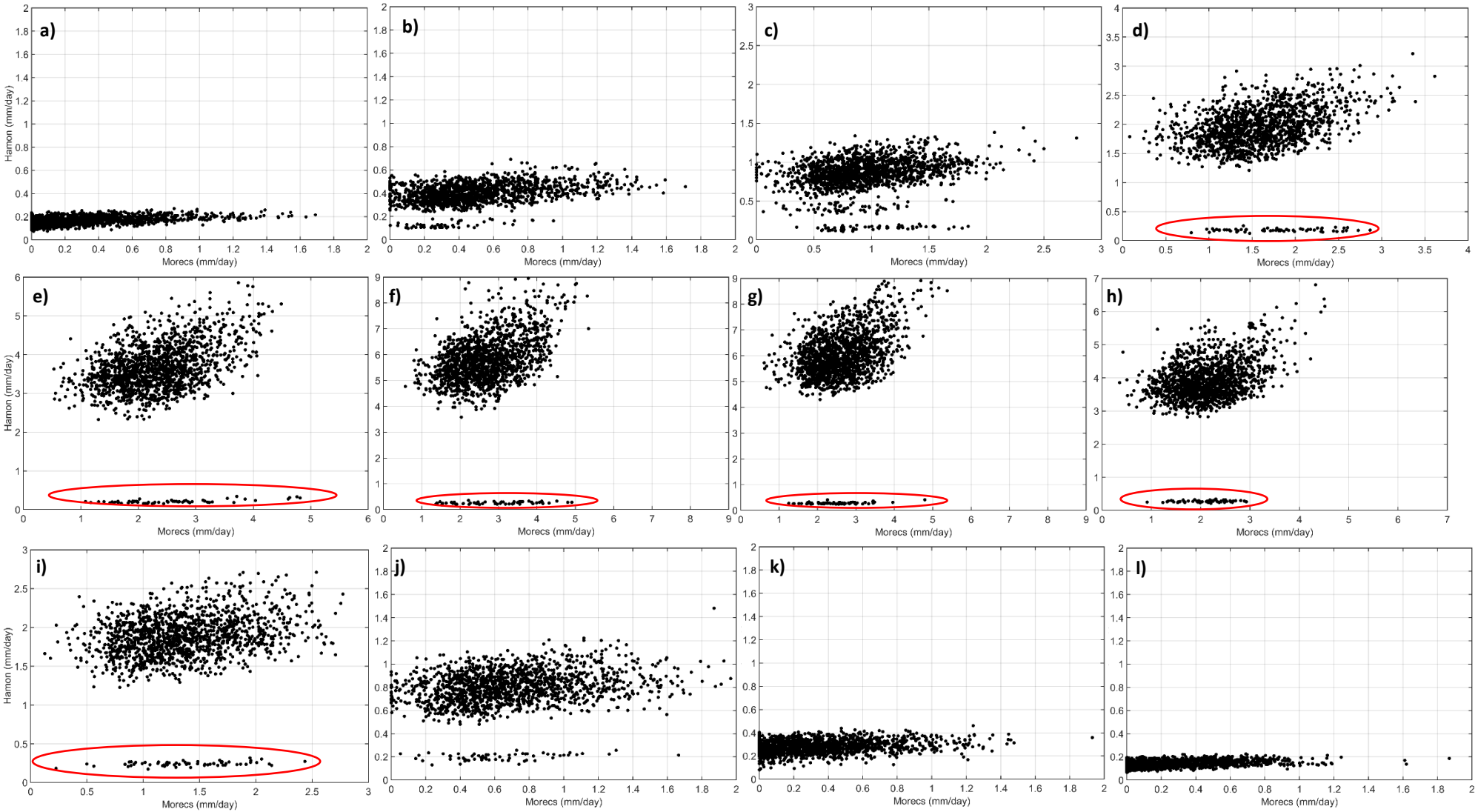

Figure A 2 Scatter plots between daily observed (Morecs) and simulated PET using the Hamon formula for the Calder catchment: a) January, b) February, c) March, d) April, e) May, f) June, g) July, h) August, i) September, j) October, k) November, and l) December. Please note the difference in the axis. Frequent underestimated days are circled in red

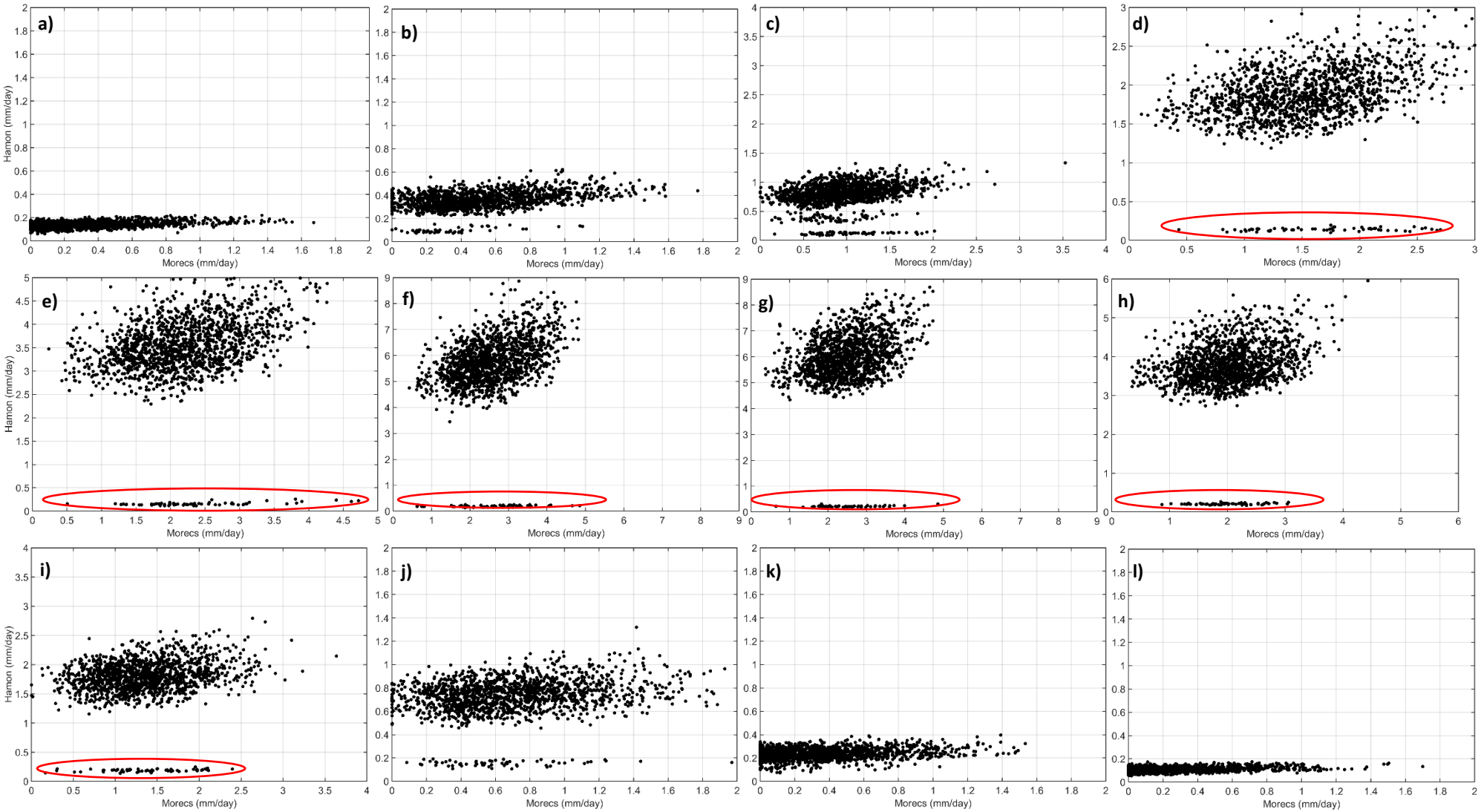

Figure A 3 Scatter plots between daily observed (Morecs) and simulated PET using the Hamon formula for the Coquet catchment: a) January, b) February, c) March, d) April, e) May, f) June, g) July, h) August, i) September, j) October, k) November, and l) December. Please note the difference in the axis. Frequent underestimated days are circled in red

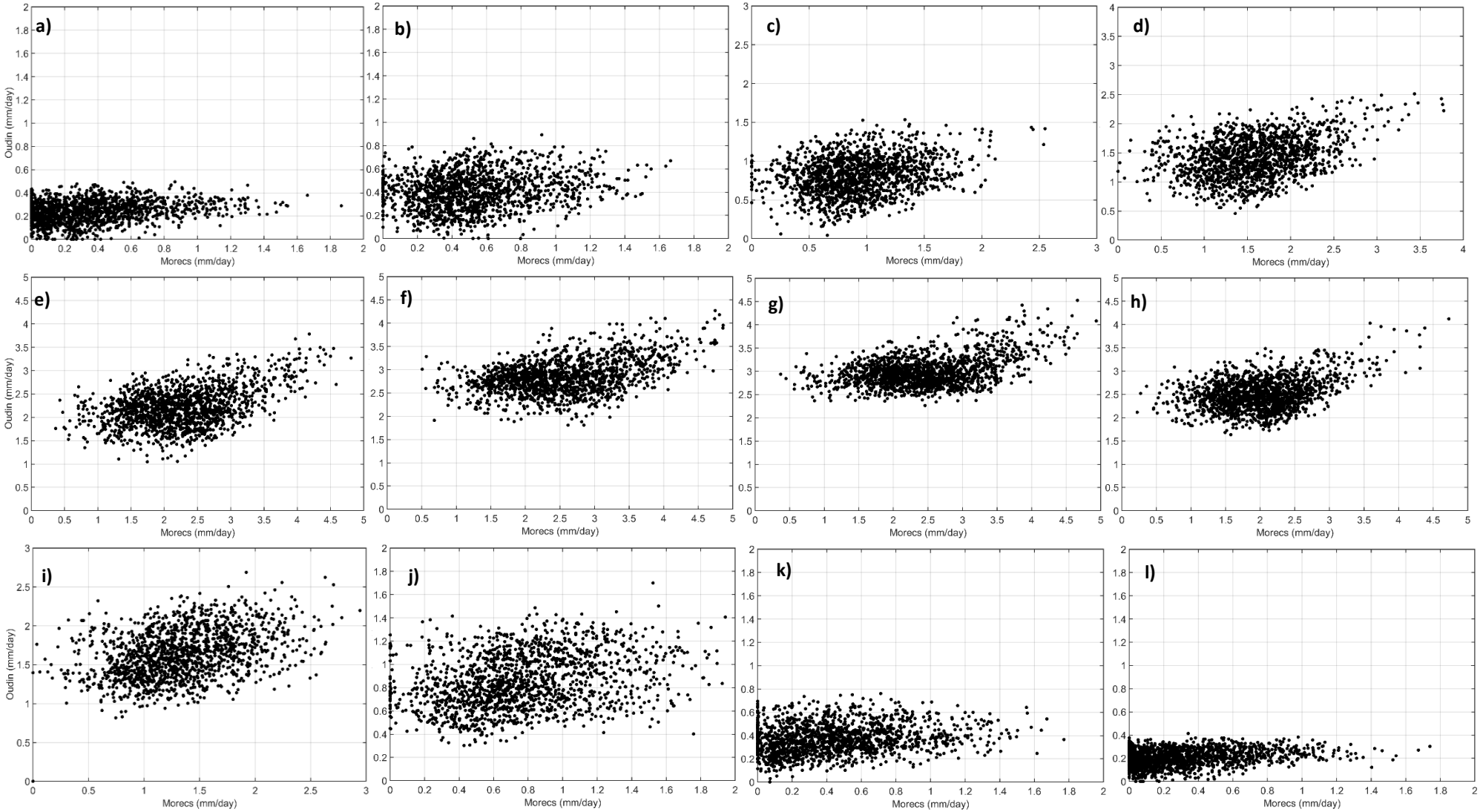

Figure A 4 Scatter plots between daily observed (Morecs) and simulated PET using the Oudin formula for the Glaslyn catchment: a) January, b) February, c) March, d) April, e) May, f) June, g) July, h) August, i) September, j) October, k) November, and l) December. Please note the difference in the axis

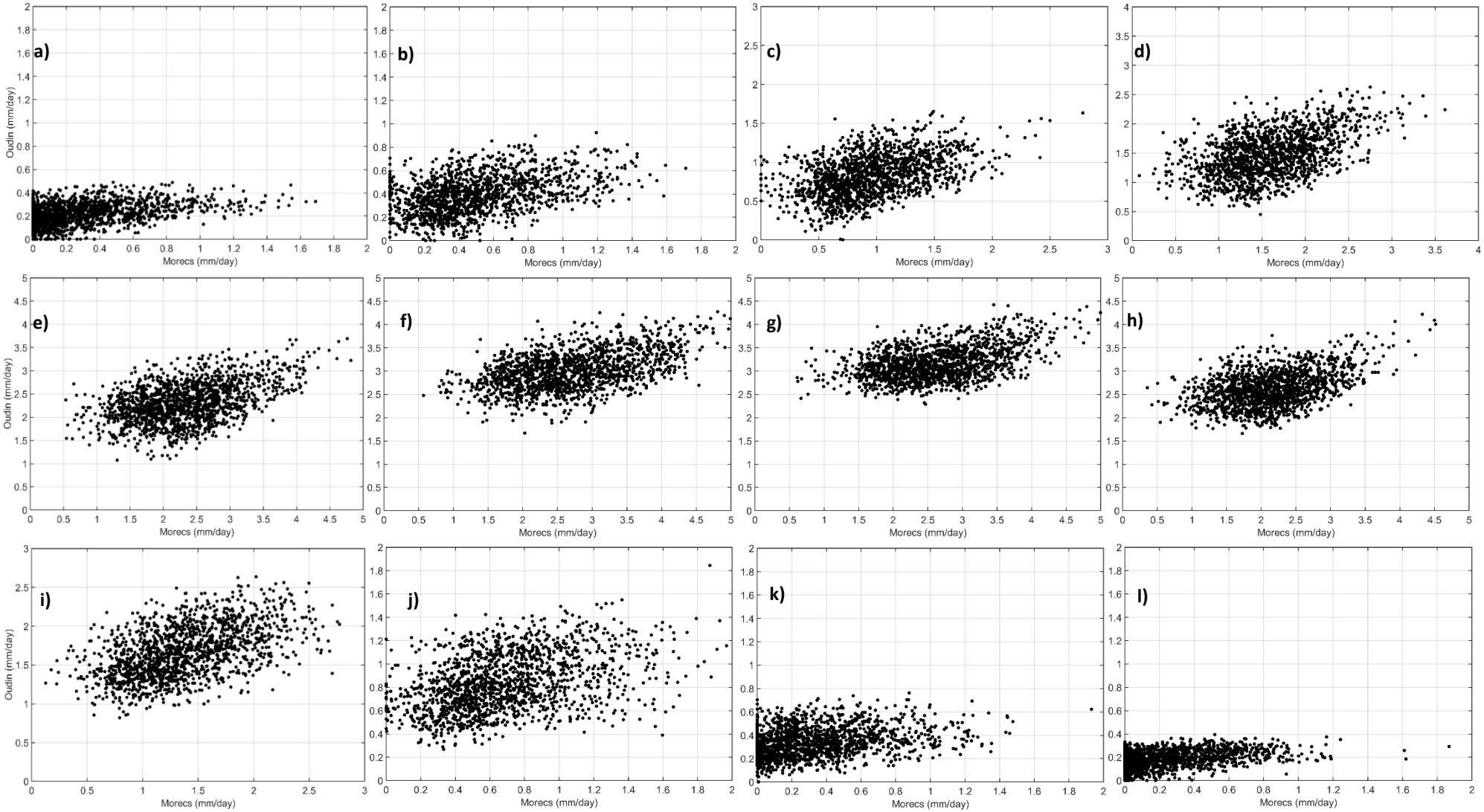

Figure A 5 Scatter plots between daily observed (Morecs) and simulated PET using the Oudin formula for the Calder catchment: a) January, b) February, c) March, d) April, e) May, f) June, g) July, h) August, i) September, j) October, k) November, and l) December. Please note the difference in the axis

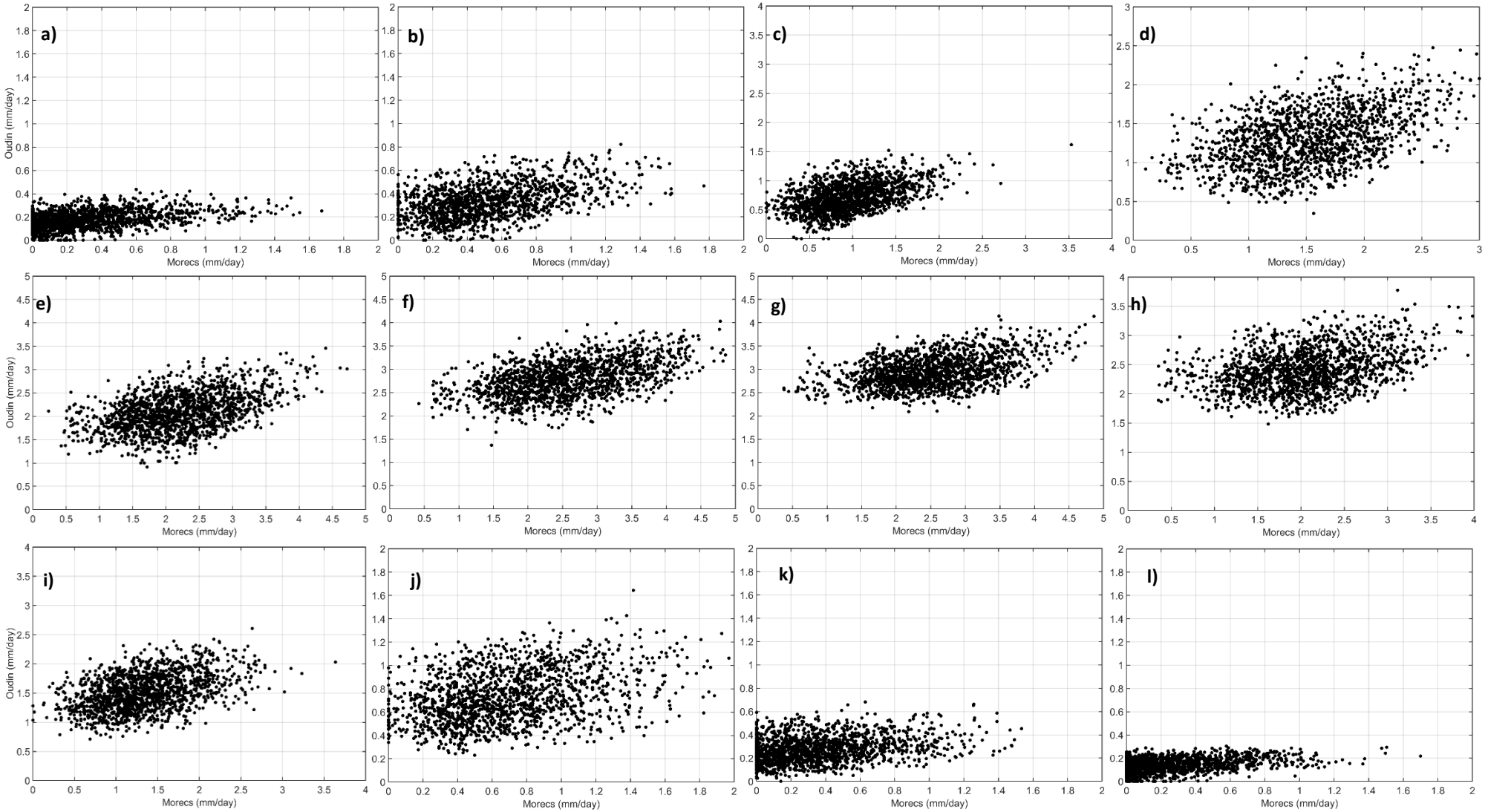

Figure A 6 Scatter plots between daily observed (Morecs) and simulated PET using the Oudin formula for the Coquet catchment: a) January, b) February, c) March, d) April, e) May, f) June, g) July, h) August, i) September, j) October, k) November, and l) December. Please note the difference in the axis

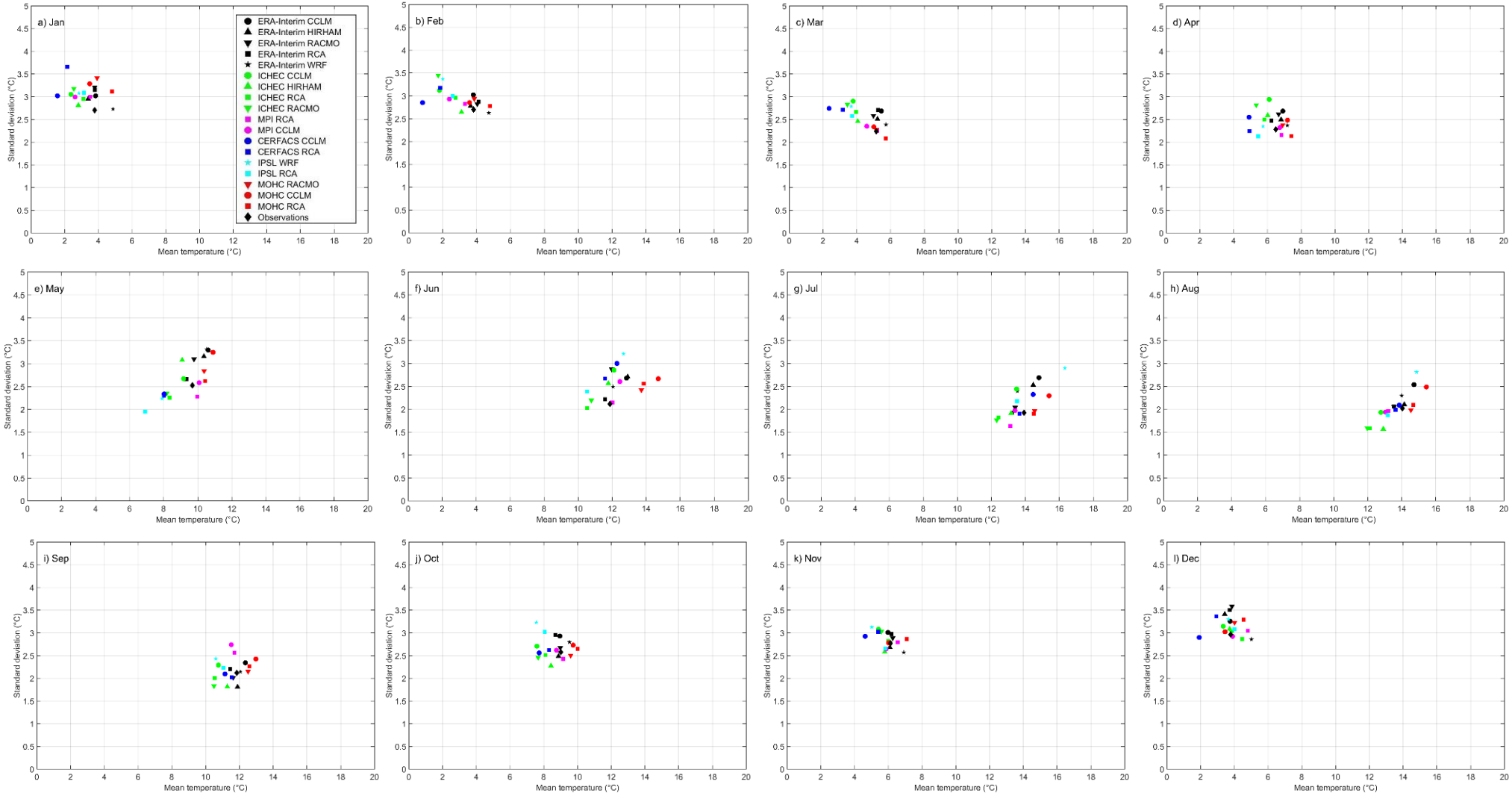

Figure A 7 Temperature distribution parameters for the observations, evaluation and historical simulations for the Glaslyn catchment

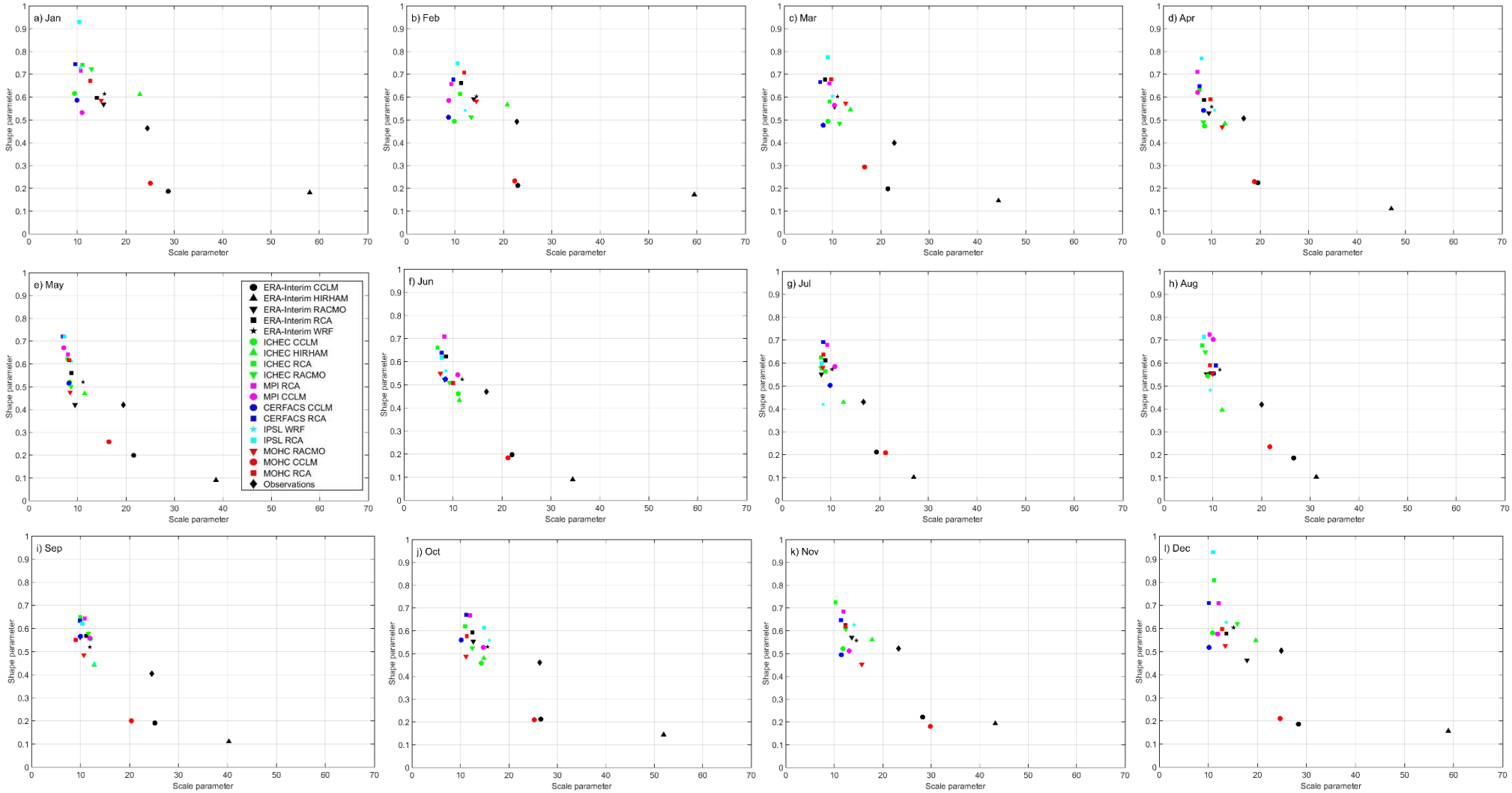

Figure A 8 Precipitation distribution parameters for the observations, evaluation and historical simulations for the Glaslyn catchment

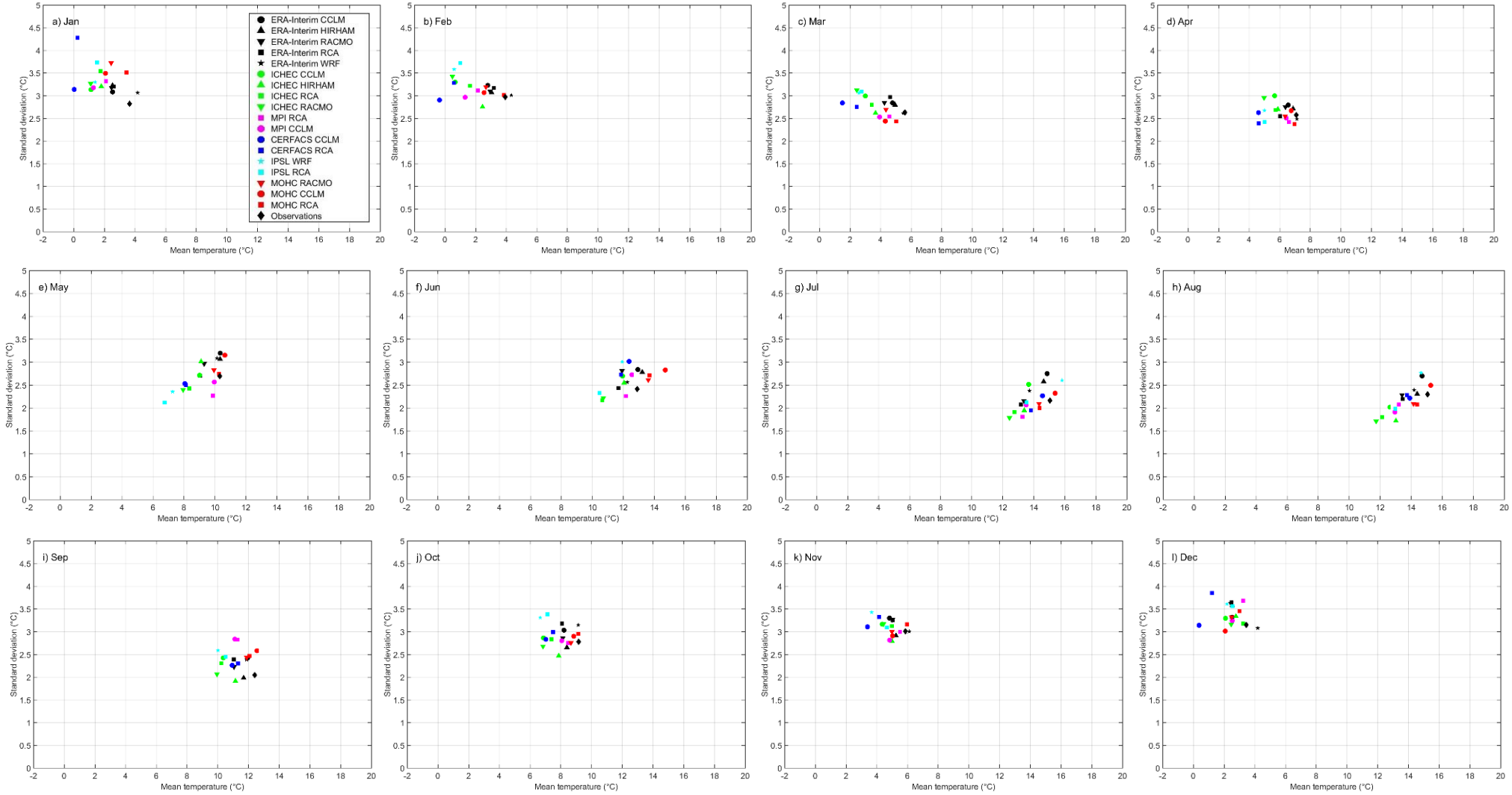

Figure A 9 Temperature distribution parameters for the observations, evaluation and historical simulations for the Calder catchment

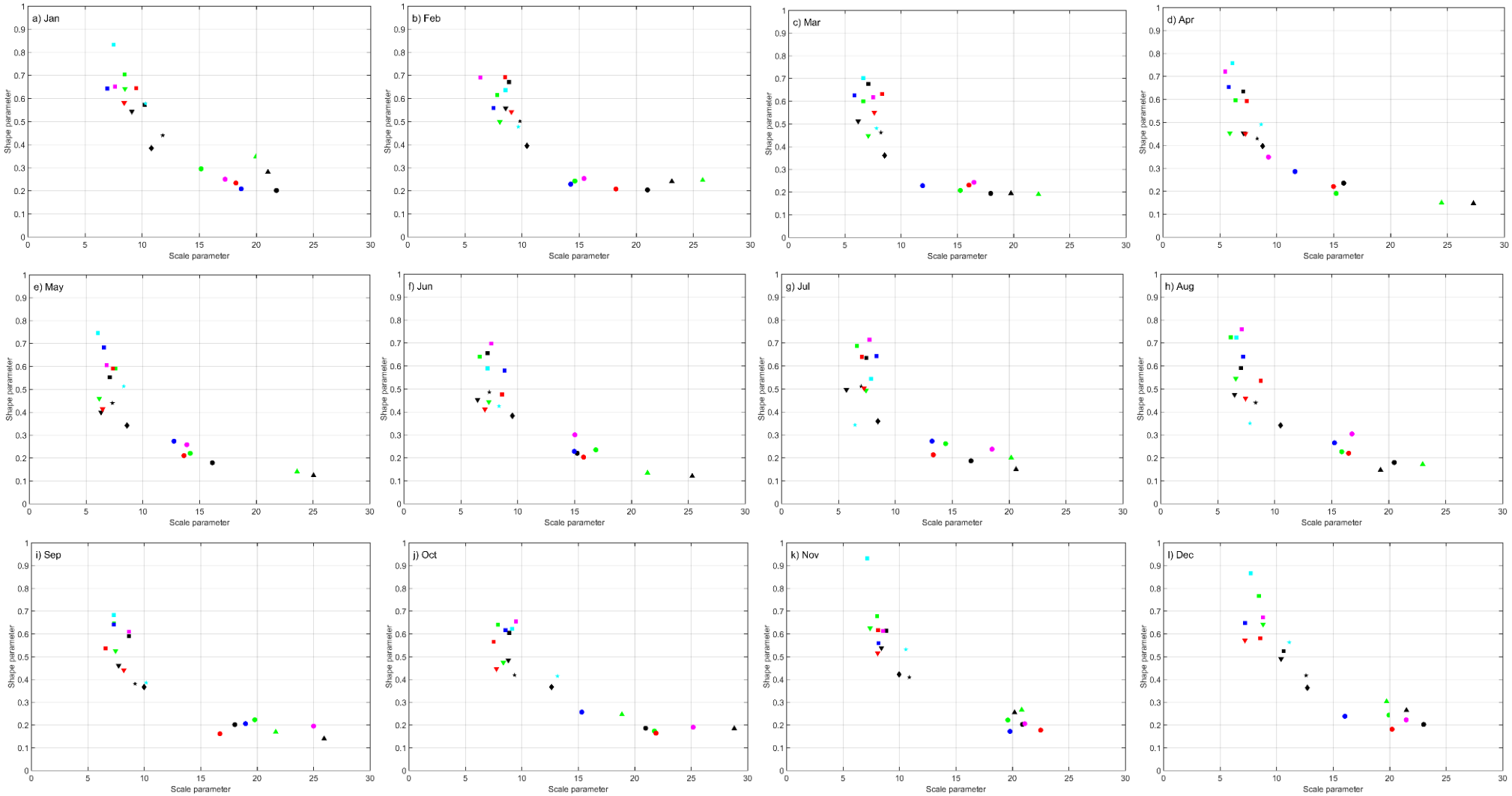

Figure A 10 Precipitation distribution parameters for the observations, evaluation and historical simulations for the Calder catchment

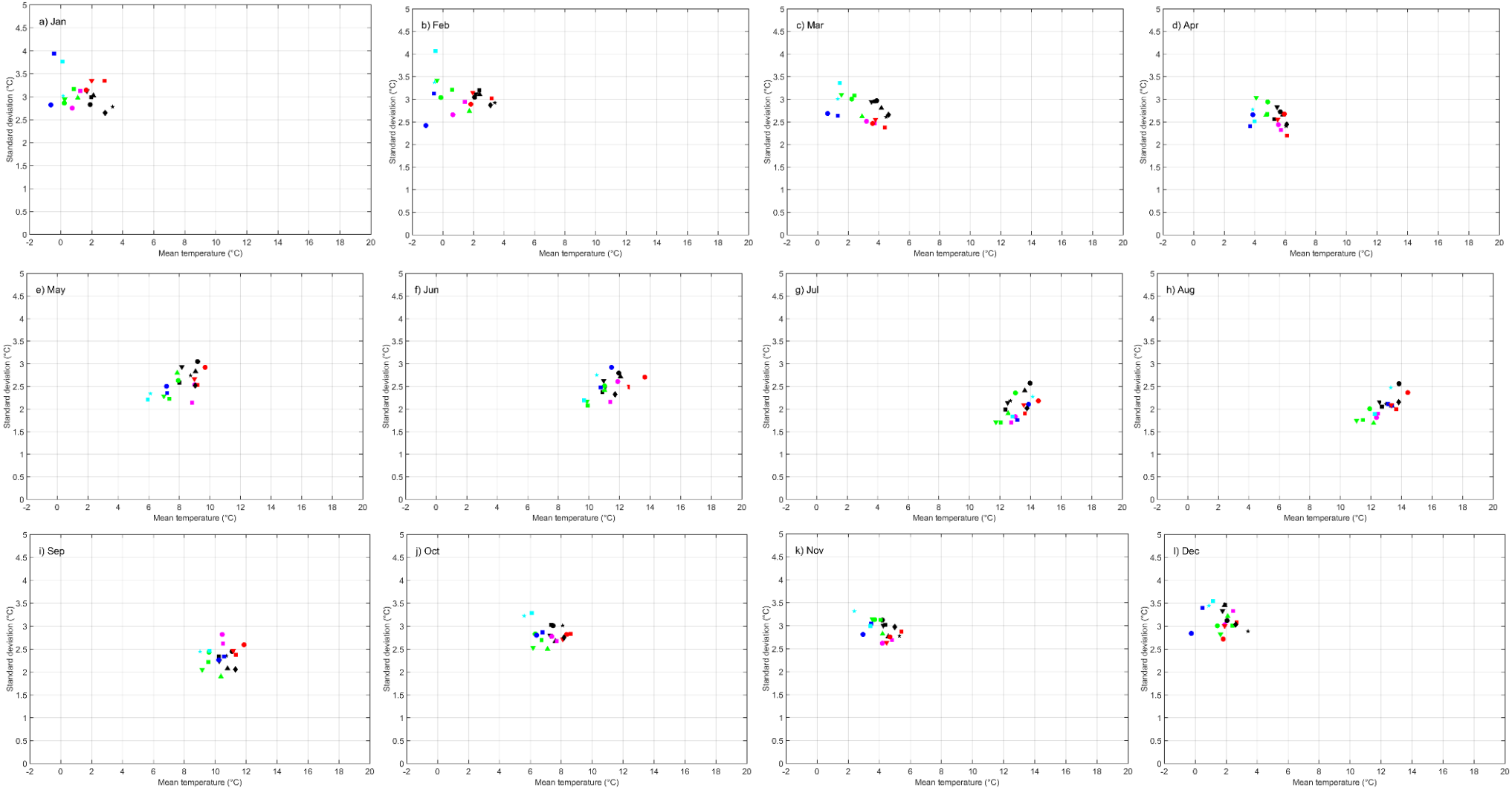

Figure A 11 Temperature distribution parameters for the observations, evaluation and historical simulations for the Coquet catchment

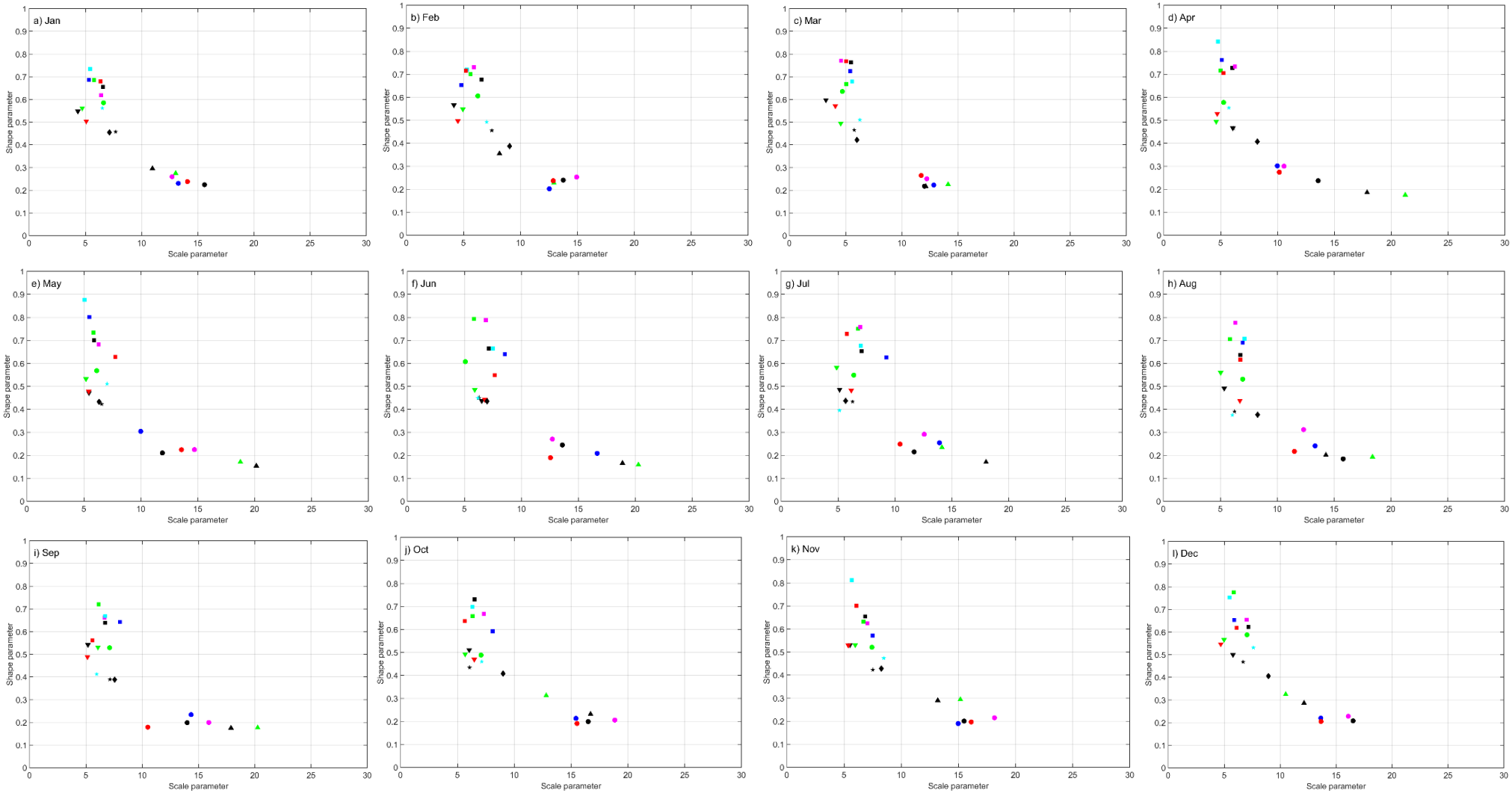

Figure A 12 Precipitation distribution parameters for the observations, evaluation and historical simulations for the Coquet catchment

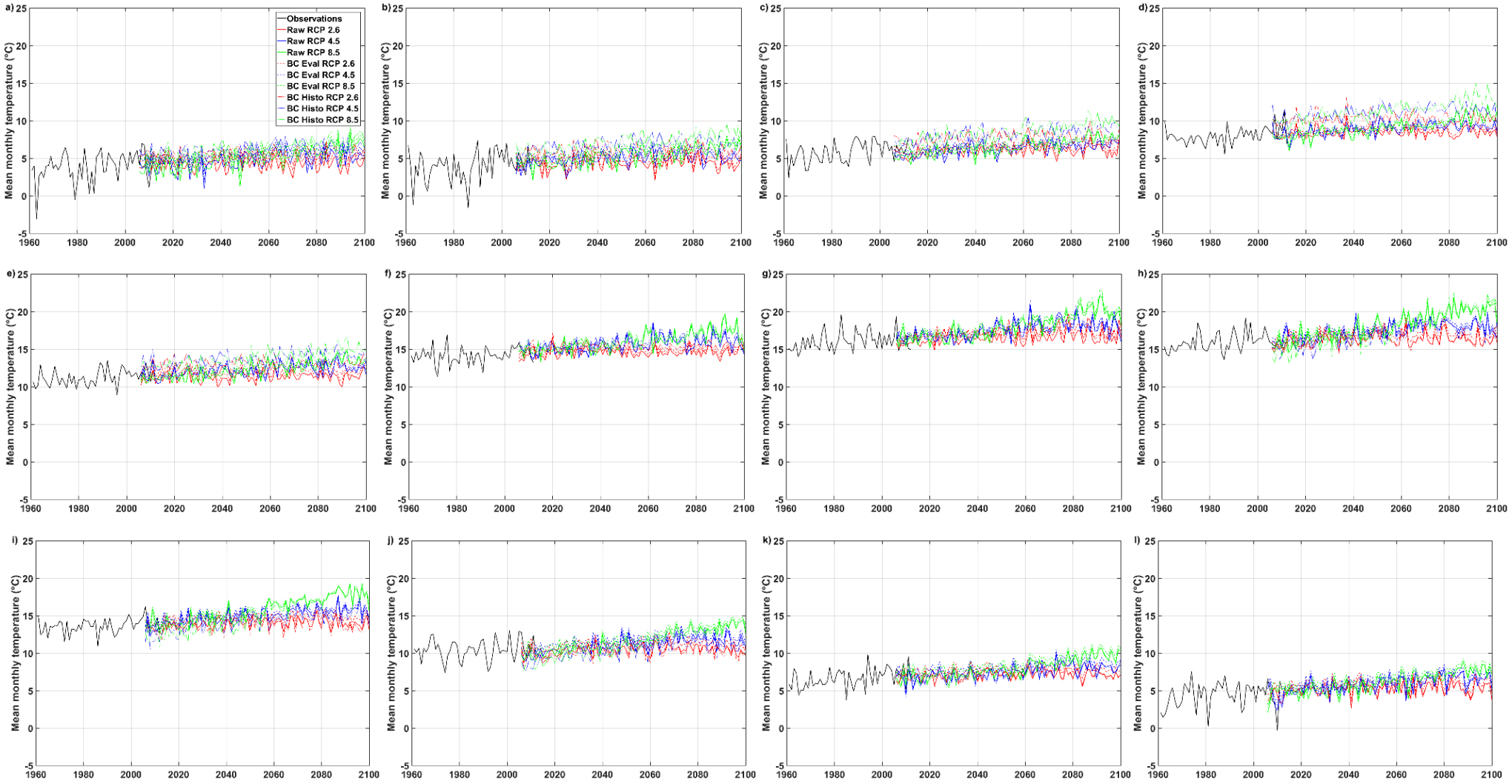

Figure A 13 Mean monthly temperature projections time series for the raw and uncorrected 2.6, 4.5 and 8.5 RCP scenarios in the upper Thames catchment: a) January, b) February, c) March, d) April, e) May, f) June, g) July, h) August, i) September, j) October, k) November and l) December

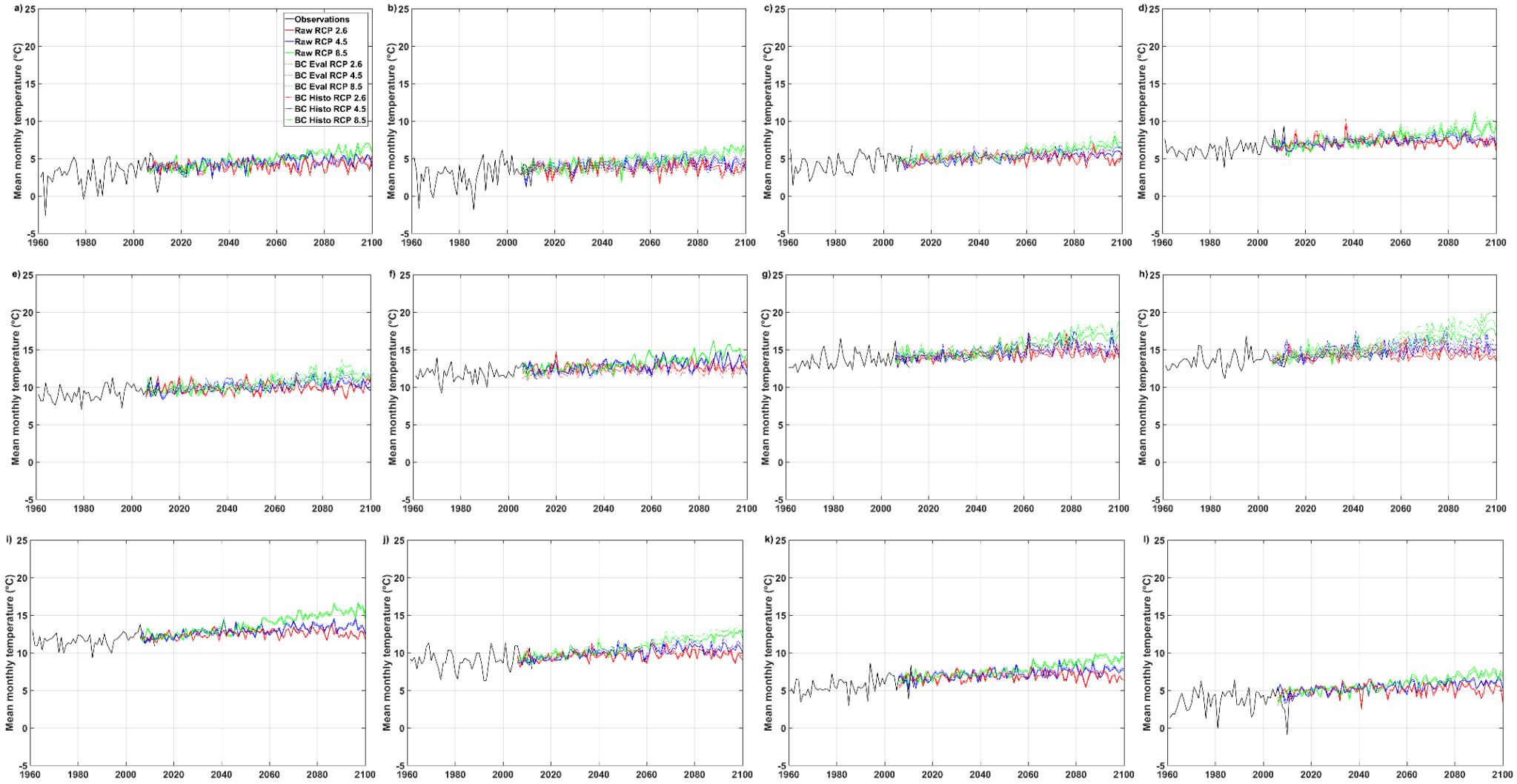

Figure A 14 Mean monthly temperature projections time series for the raw and uncorrected 2.6, 4.5 and 8.5 RCP scenarios in the Glaslyn catchment: a) January, b) February, c) March, d) April, e) May, f) June, g) July, h) August, i) September, j) October, k) November and l) December

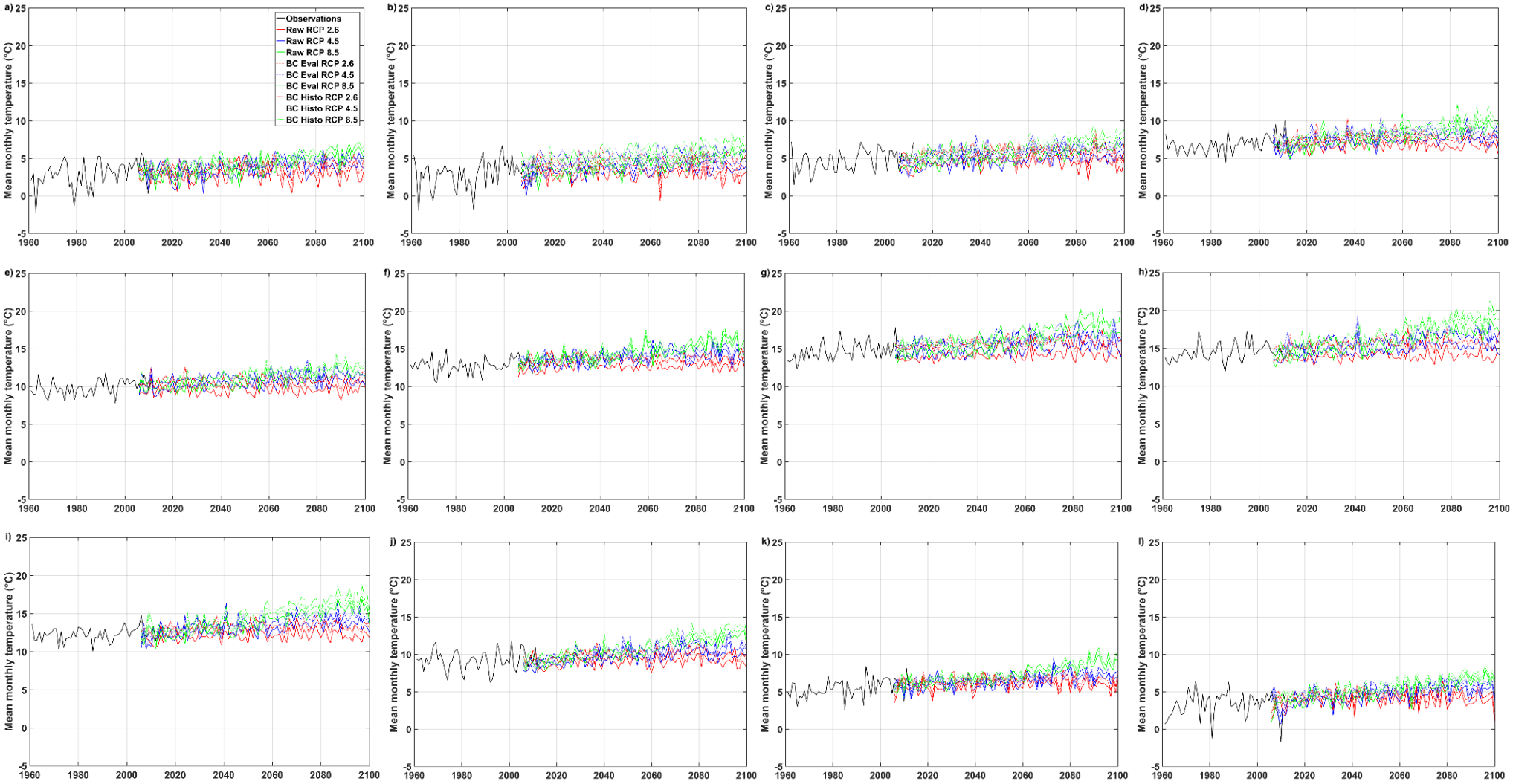

Figure A 15 Mean monthly temperature projections time series for the raw and uncorrected 2.6, 4.5 and 8.5 RCP scenarios in the Calder catchment: a) January, b) February, c) March, d) April, e) May, f) June, g) July, h) August, i) September, j) October, k) November and l) December

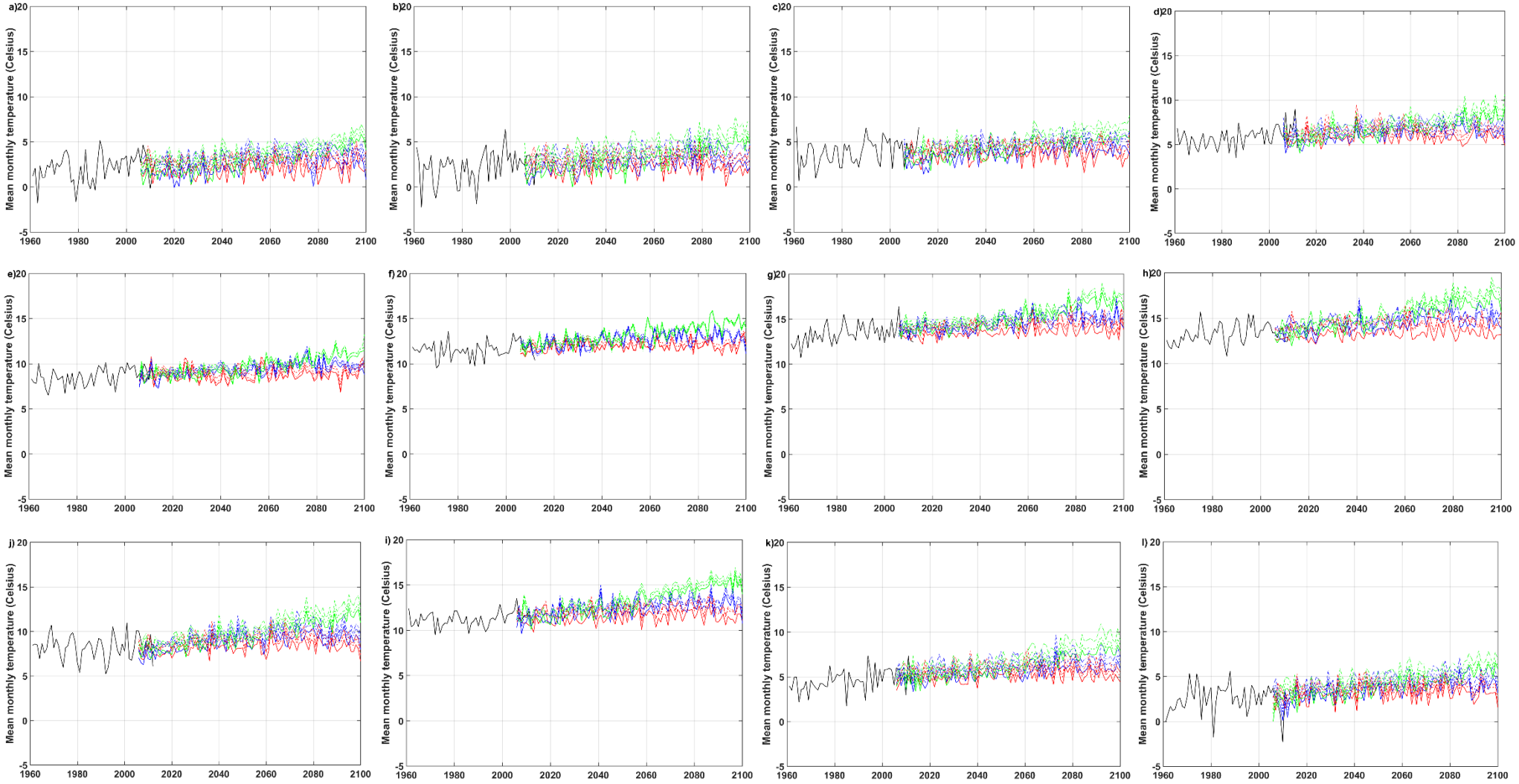

Figure A 16 Mean monthly temperature projections time series for the raw and uncorrected 2.6, 4.5 and 8.5 RCP scenarios in the Coquet catchment: a) January, b) February, c) March, d) April, e) May, f) June, g) July, h) August, i) September, j) October, k) November and l) December

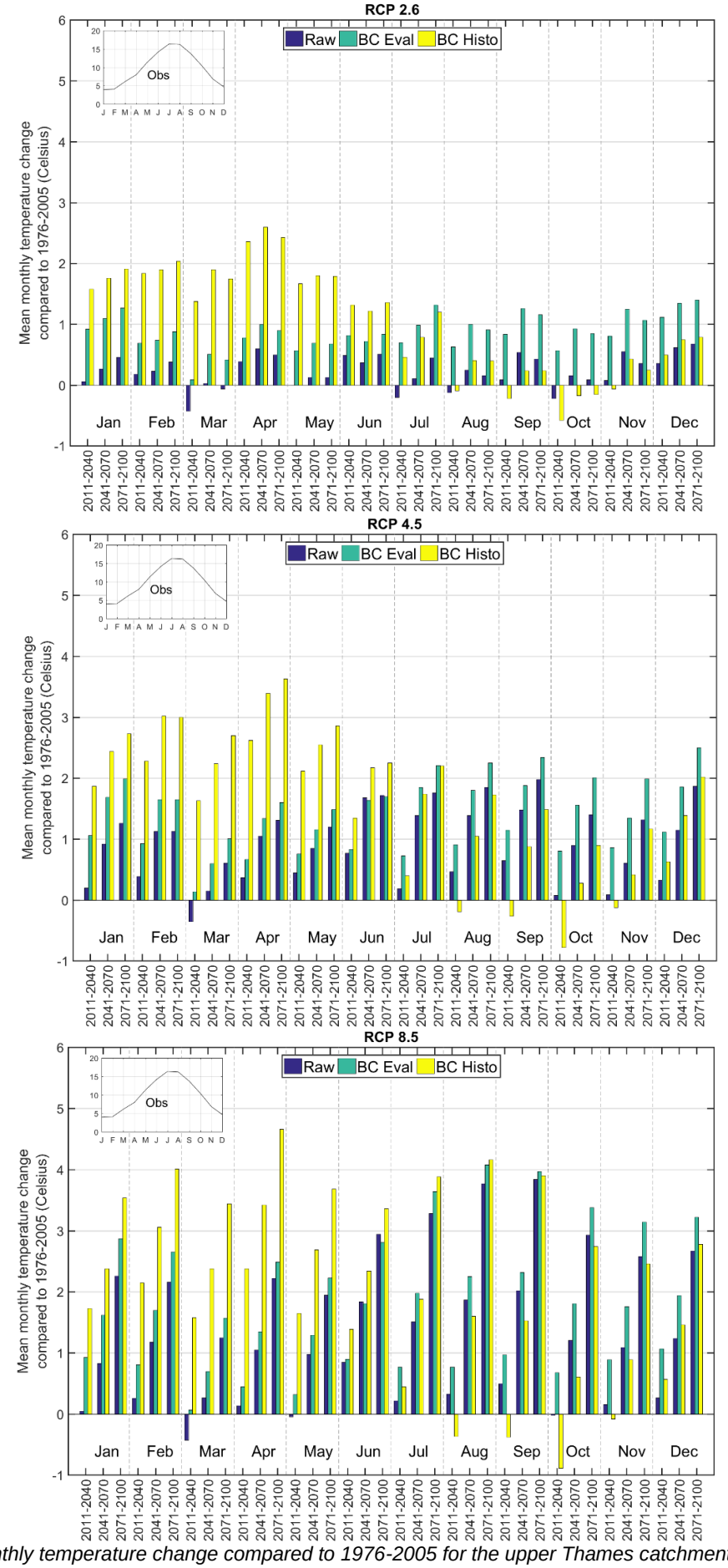

Figure A 17 Mean monthly temperature change compared to 1976-2005 for the upper Thames catchment for the 2.6, 4.5 and 8.5 RCP scenarios for the uncorrected and bias-corrected simulations

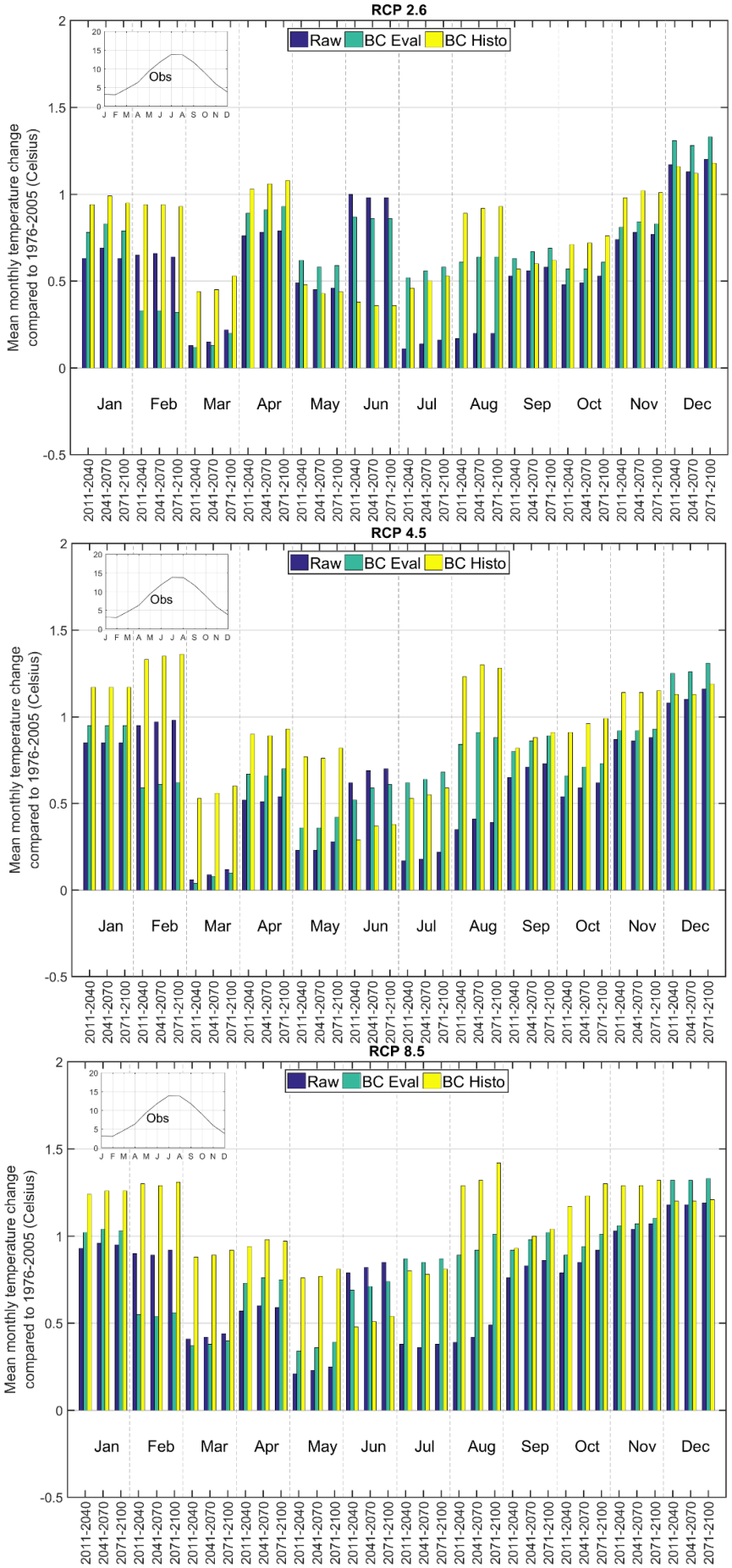

Figure A 18 Mean monthly temperature change compared to 1976-2005 for the Glaslyn catchment for the 2.6, 4.5 and 8.5 RCP scenarios for the uncorrected and bias-corrected simulations

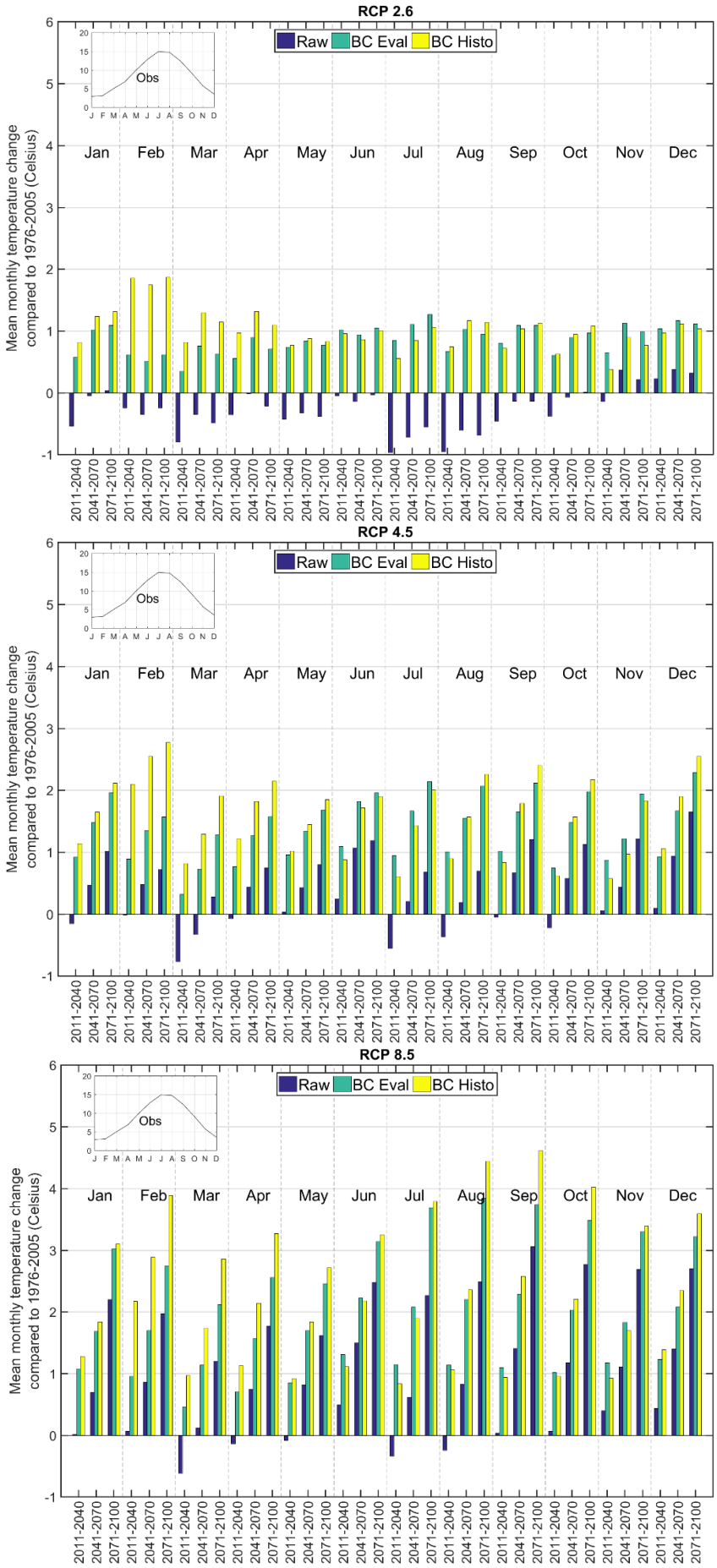

Figure A 19 Mean monthly temperature change compared to 1976-2005 for the Calder catchment for the 2.6, 4.5 and 8.5 RCP scenarios for the uncorrected and bias-corrected simulations

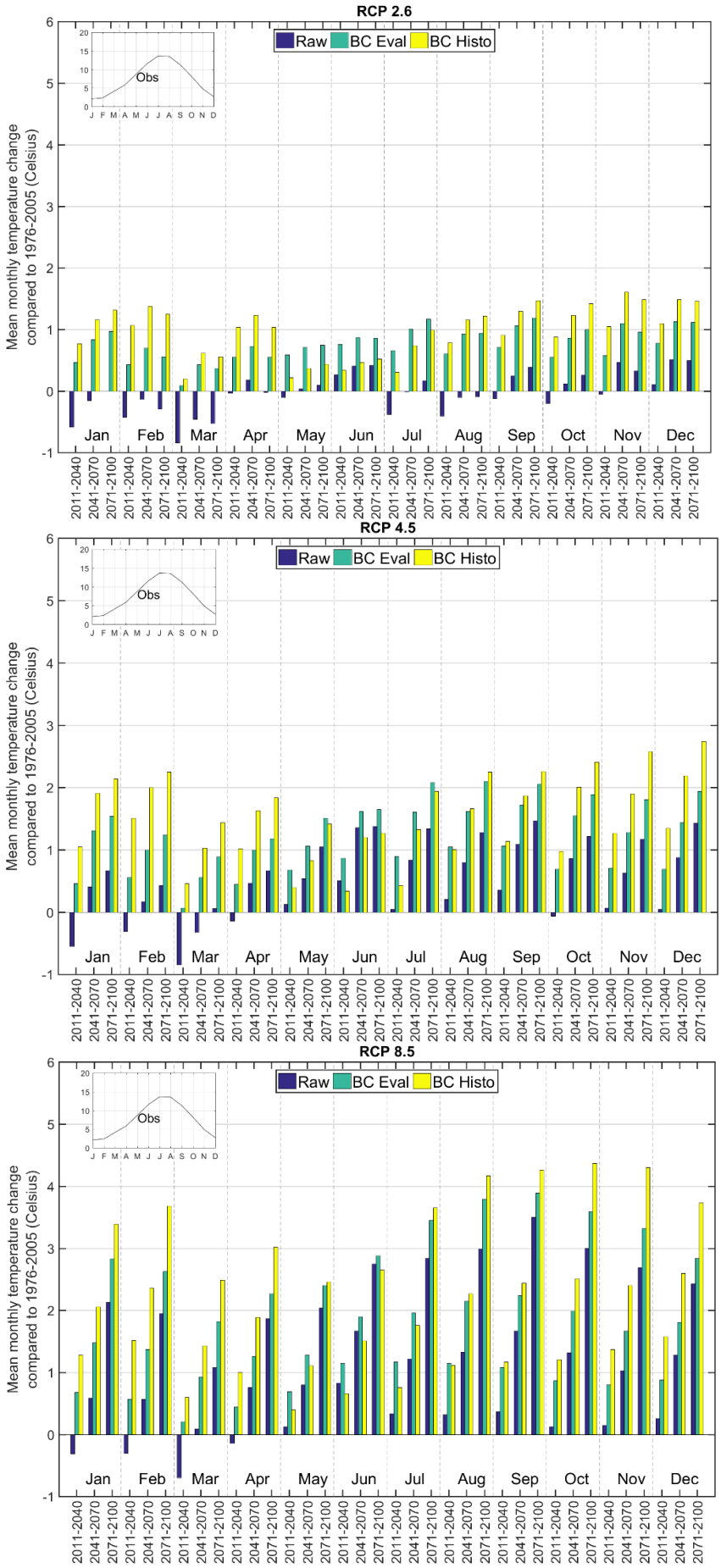

Figure A 20 Mean monthly temperature change compared to 1976-2005 for the Coquet catchment for the 2.6, 4.5 and 8.5 RCP scenarios for the uncorrected and bias-corrected simulations

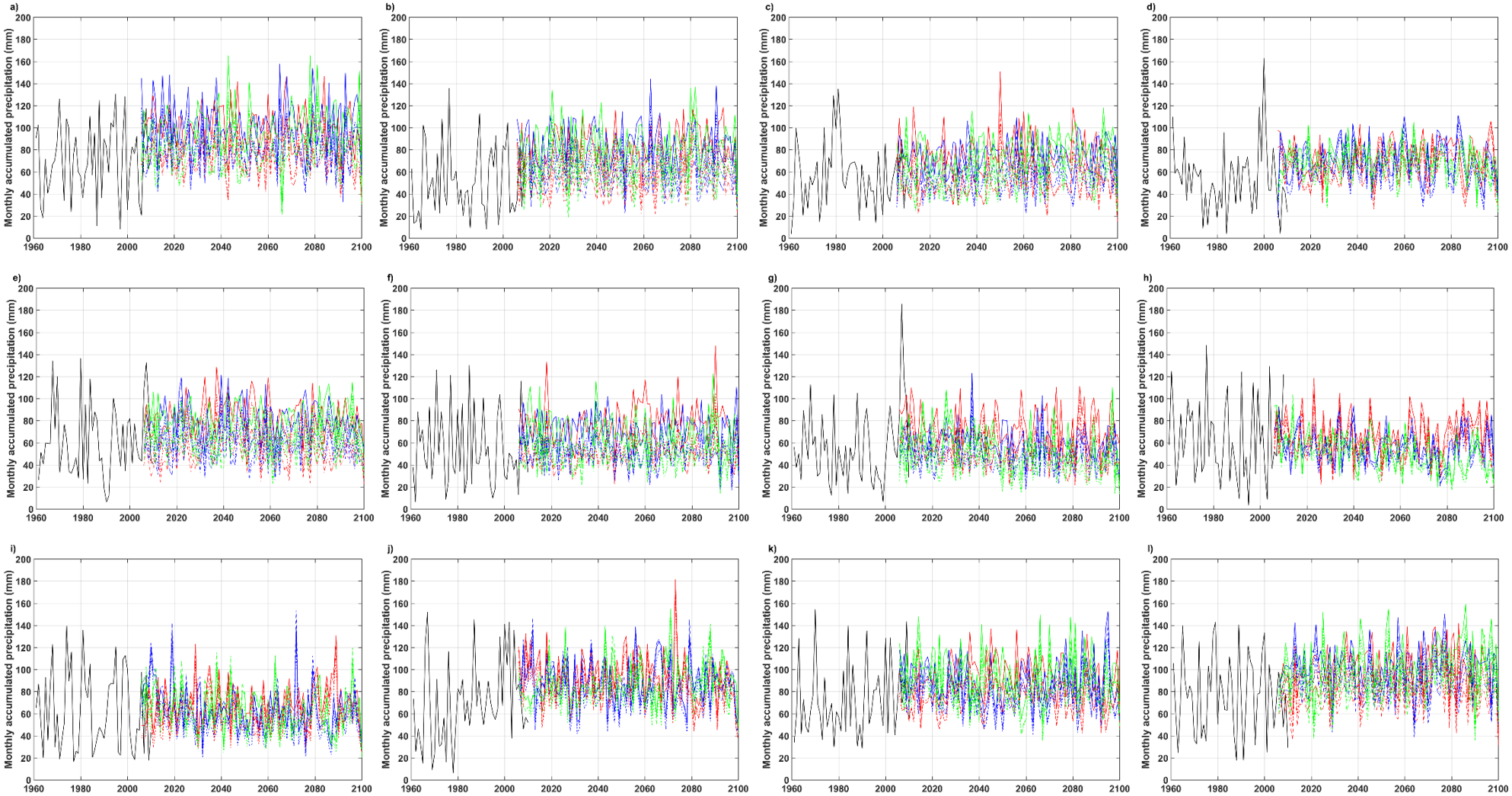

Figure A 21 Mean monthly precipitation projections time series for the raw and uncorrected 2.6, 4.5 and 8.5 RCP scenarios in the upper Thames catchment: a) January, b) February, c) March, d) April, e) May, f) June, g) July, h) August, i) September, j) October, k) November and l) December

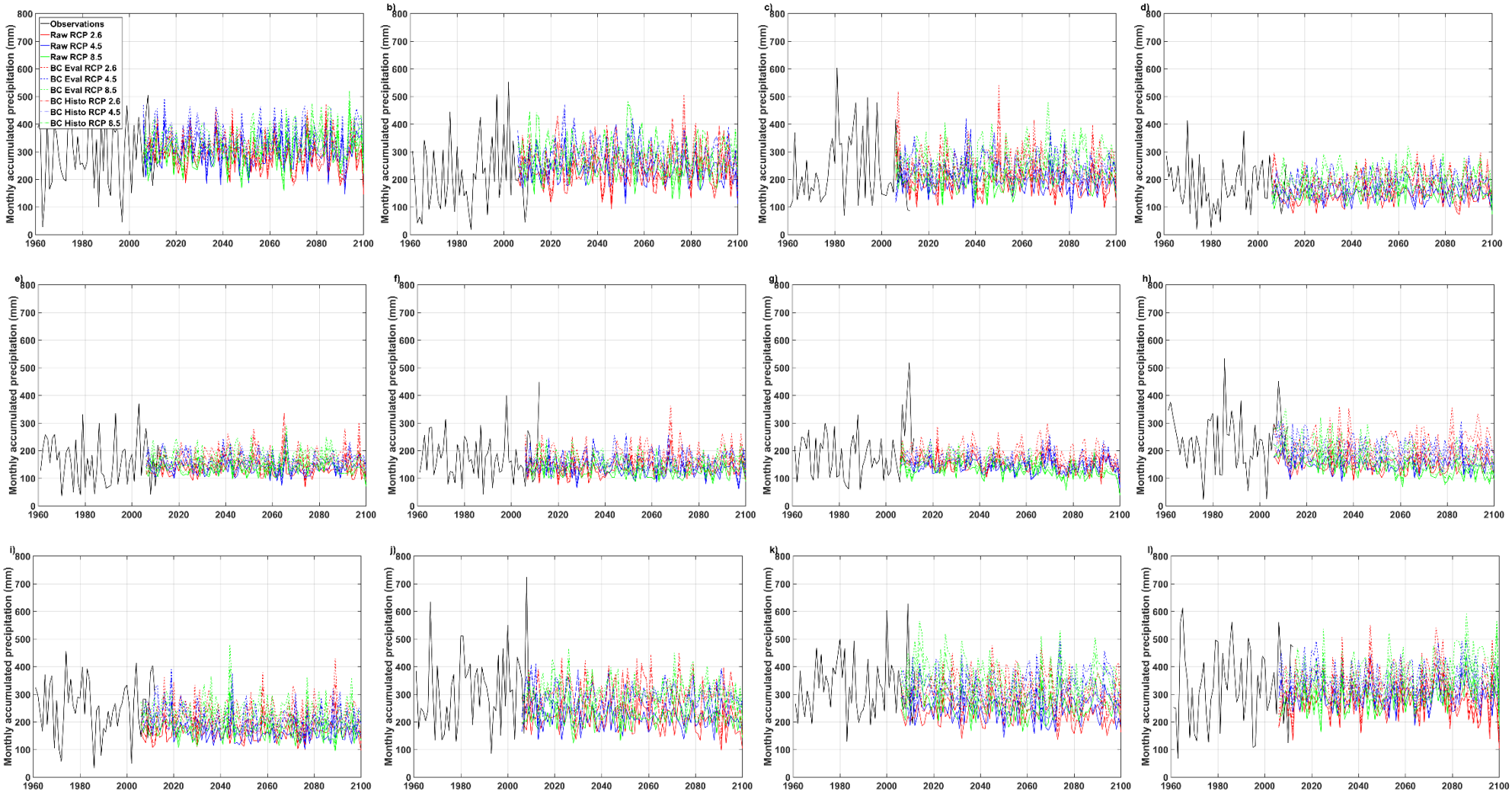

Figure A 22 Mean monthly precipitation projections time series for the raw and uncorrected 2.6, 4.5 and 8.5 RCP scenarios in the Glaslyn catchment: a) January, b) February, c) March, d) April, e) May, f) June, g) July, h) August, i) September, j) October, k) November and l) December

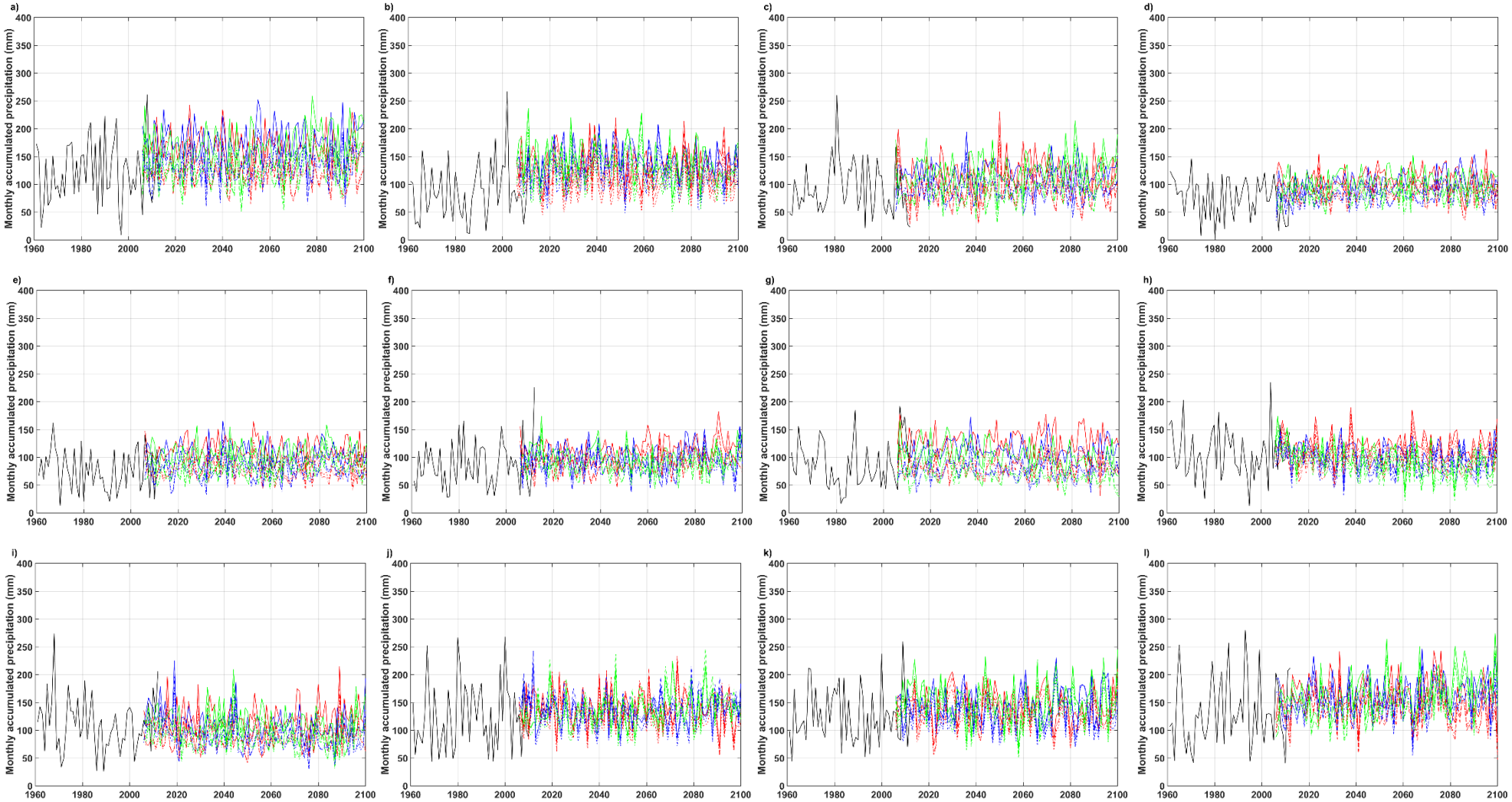

Figure A 23 Mean monthly precipitation projections time series for the raw and uncorrected 2.6, 4.5 and 8.5 RCP scenarios in the Calder catchment: a) January, b) February, c) March, d) April, e) May, f) June, g) July, h) August, i) September, j) October, k) November and l) December

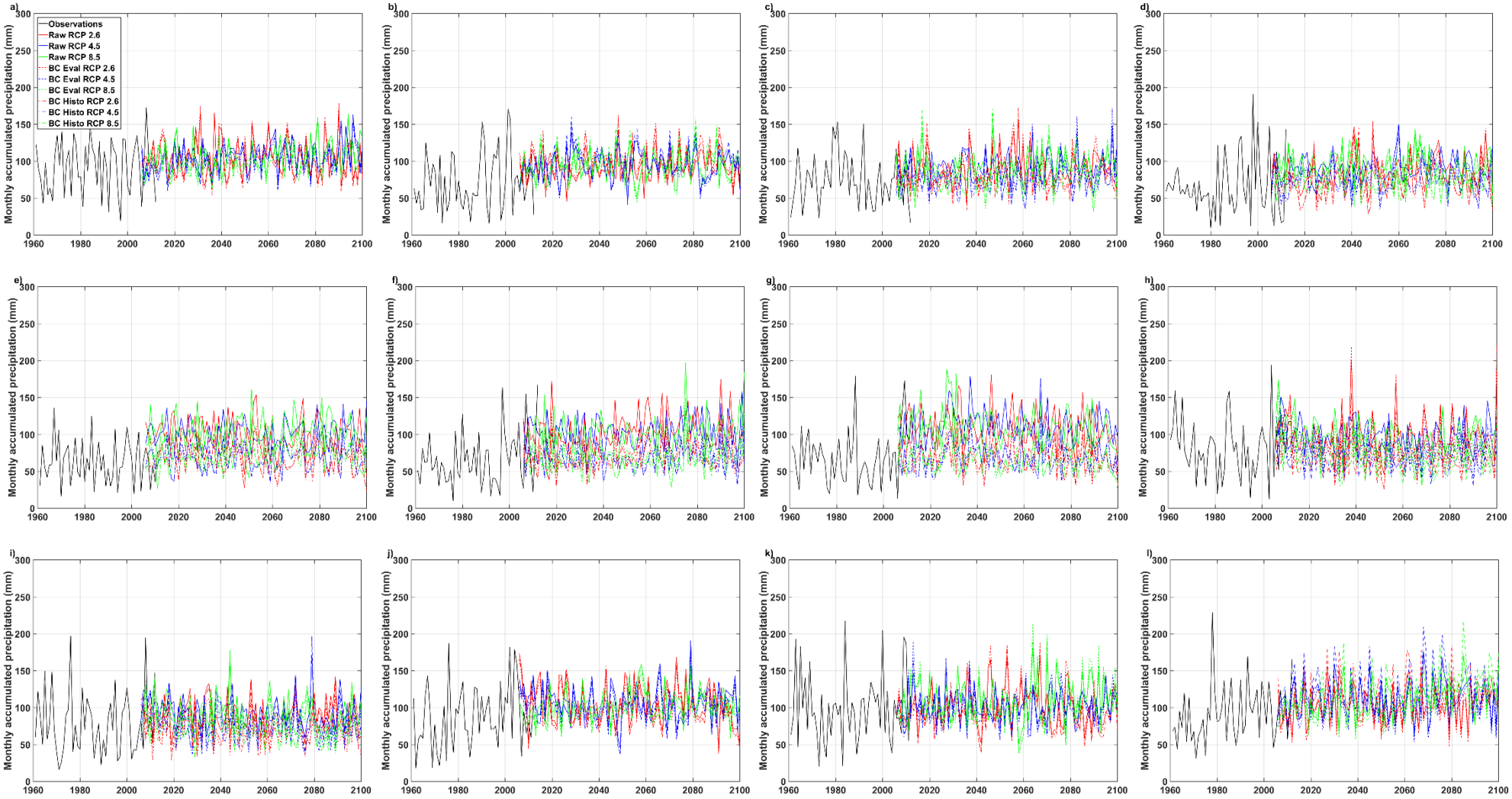

Figure A 24 Mean monthly precipitation projections time series for the raw and uncorrected 2.6, 4.5 and 8.5 RCP scenarios in the Coquet catchment: a) January, b) February, c) March, d) April, e) May, f) June, g) July, h) August, i) September, j) October, k) November and l) December

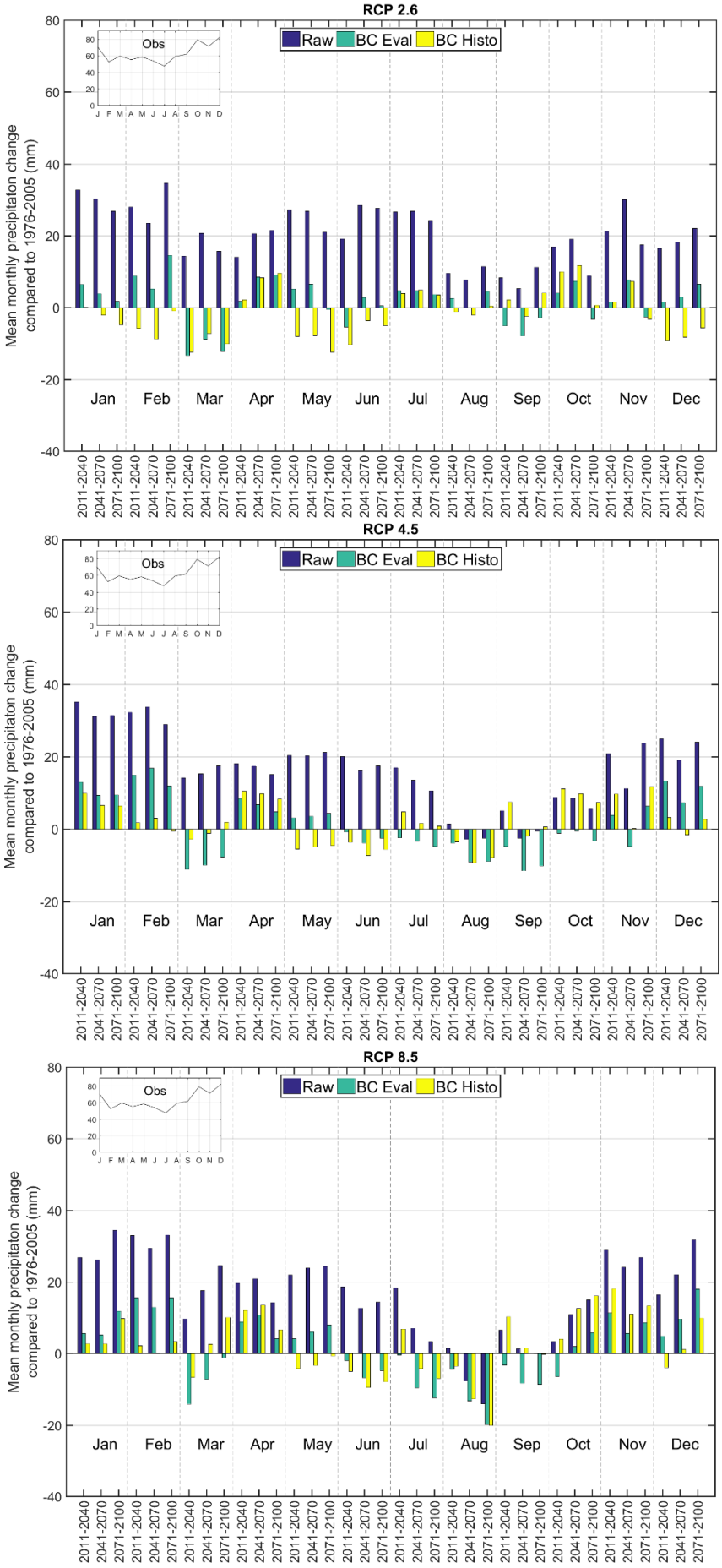

Figure A 25 Mean monthly precipitation change compared to 1976-2005 for the upper Thames catchment for the 2.6, 4.5 and 8.5 RCP scenarios for the uncorrected and bias-corrected simulations

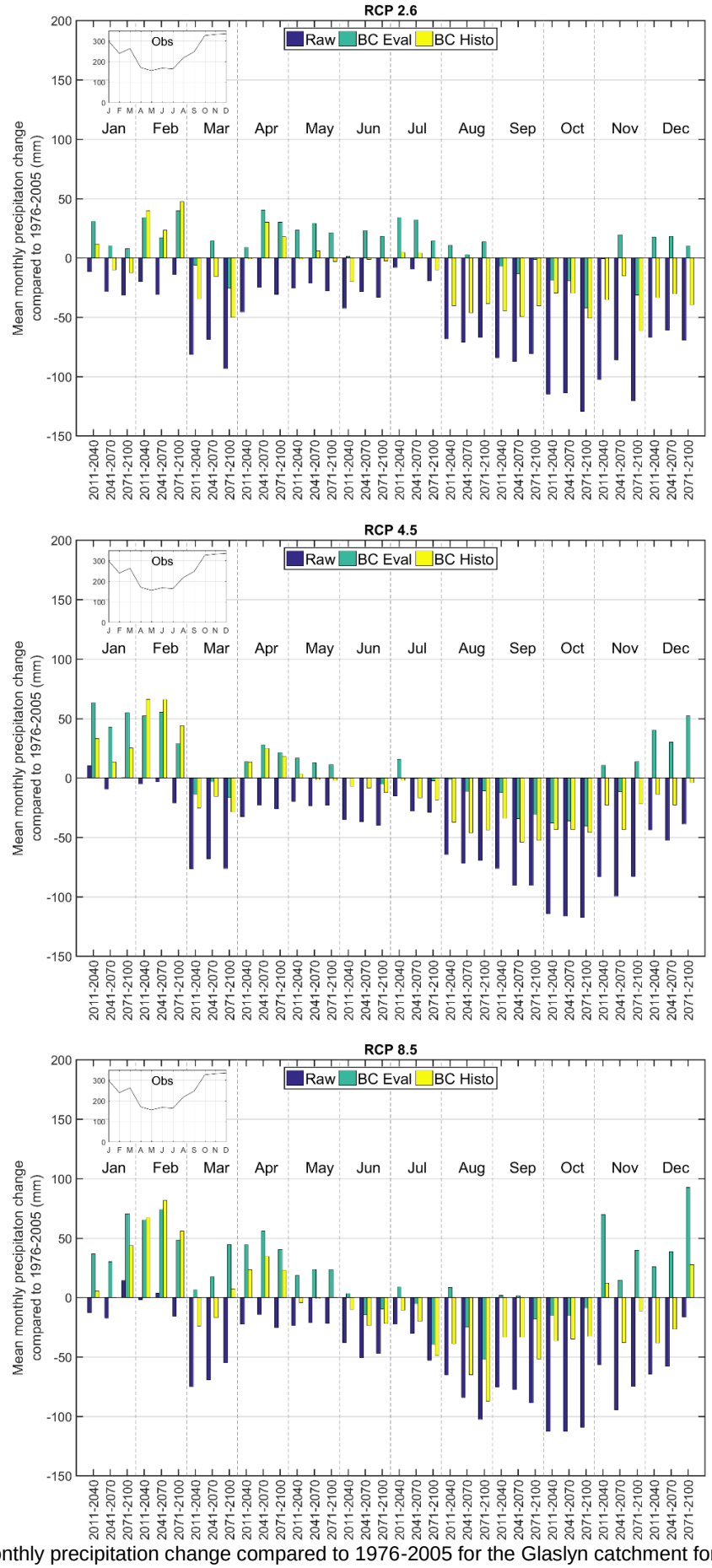

Figure A 26 Mean monthly precipitation change compared to 1976-2005 for the Glaslyn catchment for the 2.6, 4.5 and 8.5 RCP scenarios for the uncorrected and bias-corrected simulations

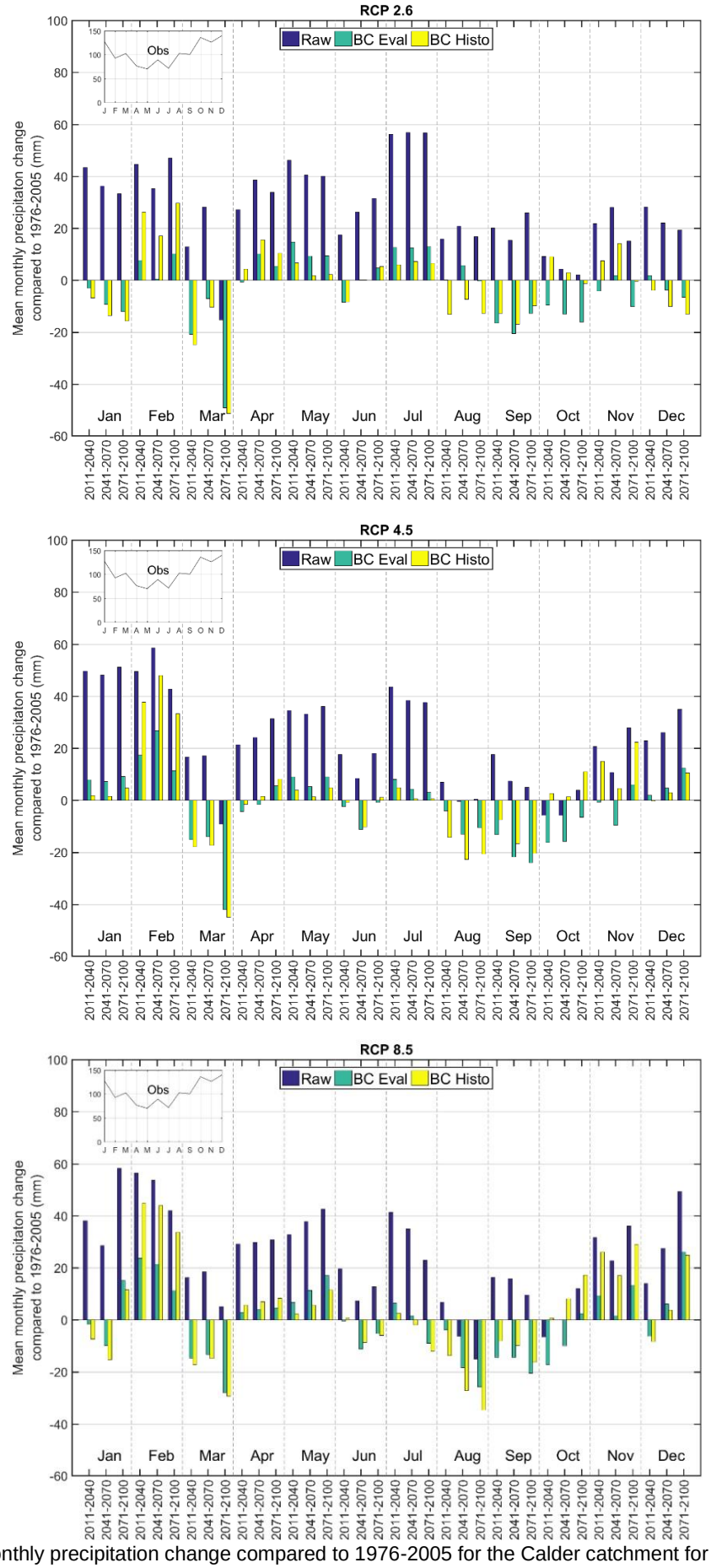

Figure A 27 Mean monthly precipitation change compared to 1976-2005 for the Calder catchment for the 2.6, 4.5 and 8.5 RCP scenarios for the uncorrected and bias-corrected simulations

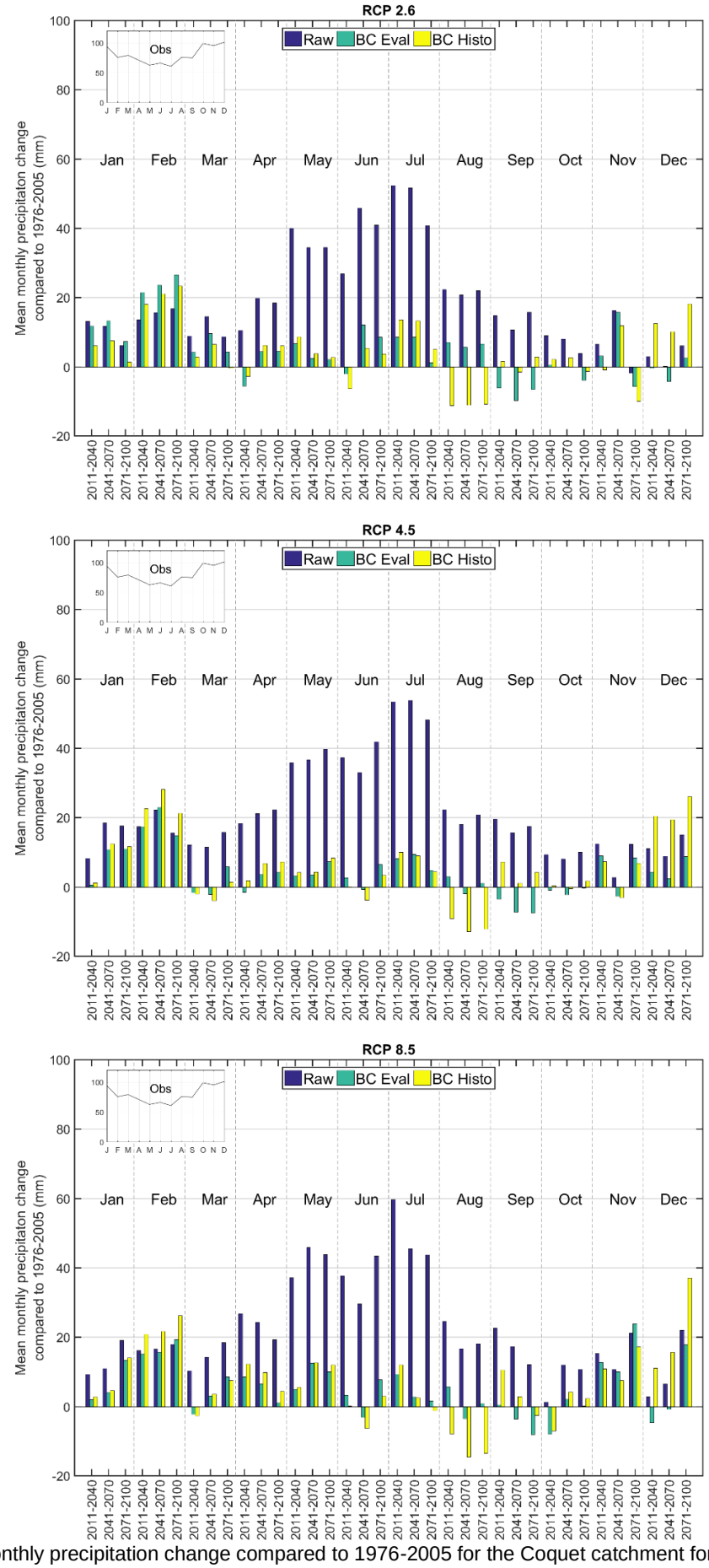

Figure A 28 Mean monthly precipitation change compared to 1976-2005 for the Coquet catchment for the 2.6, 4.5 and 8.5 RCP scenarios for the uncorrected and bias-corrected simulations

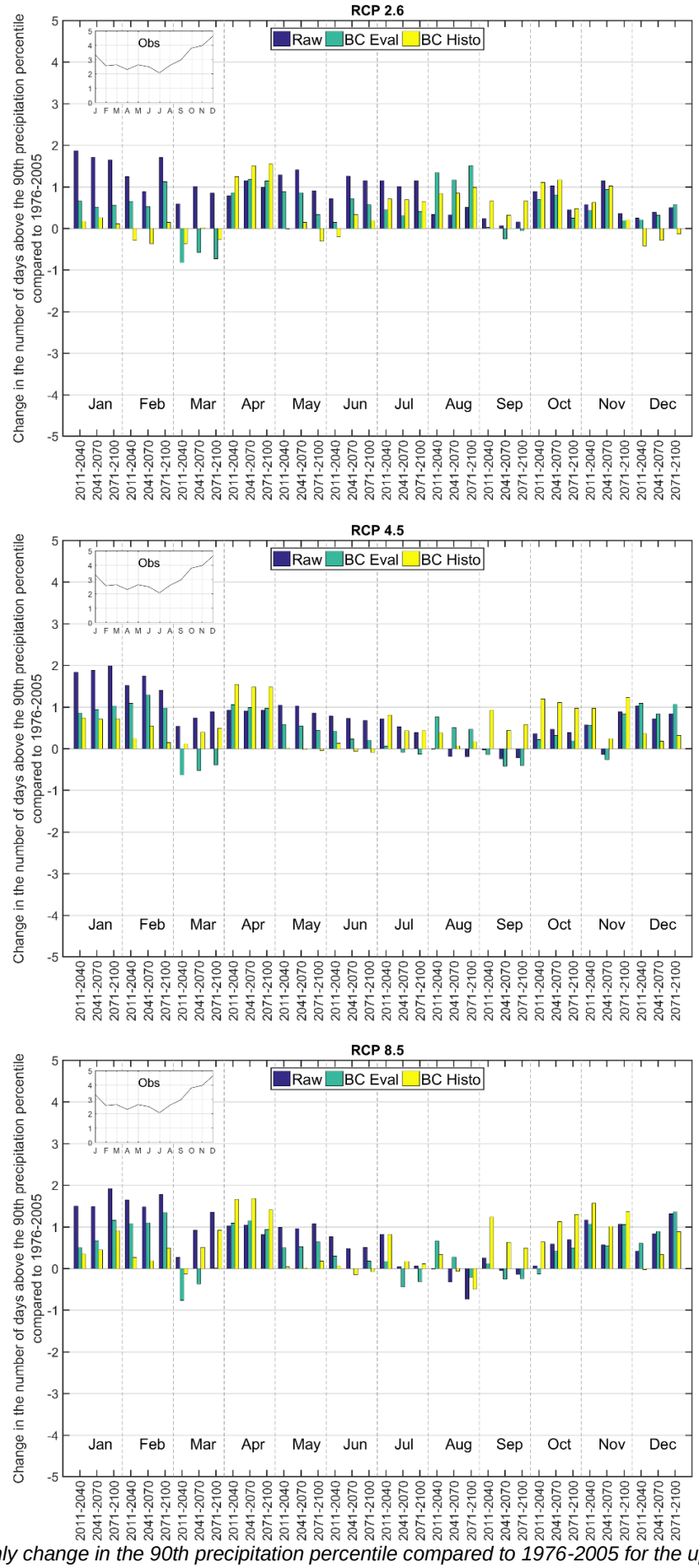

Figure A 29 Mean monthly change in the 90th precipitation percentile compared to 1976-2005 for the upper Thames catchment for the 2.6, 4.5 and 8.5 RCP scenarios for the uncorrected and bias-corrected simulations

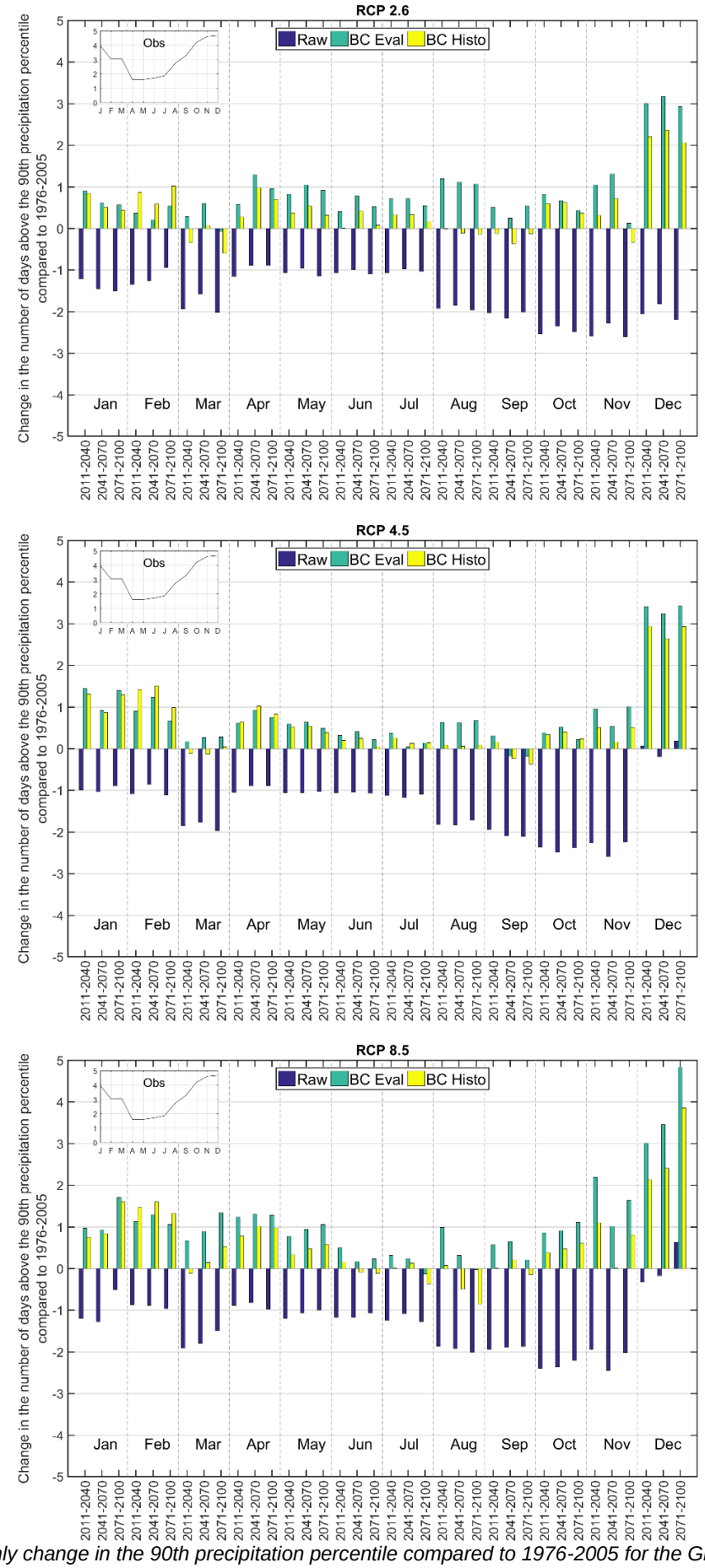

Figure A 30 Mean monthly change in the 90th precipitation percentile compared to 1976-2005 for the Glaslyn catchment for the 2.6, 4.5 and 8.5 RCP scenarios for the uncorrected and bias-corrected simulations

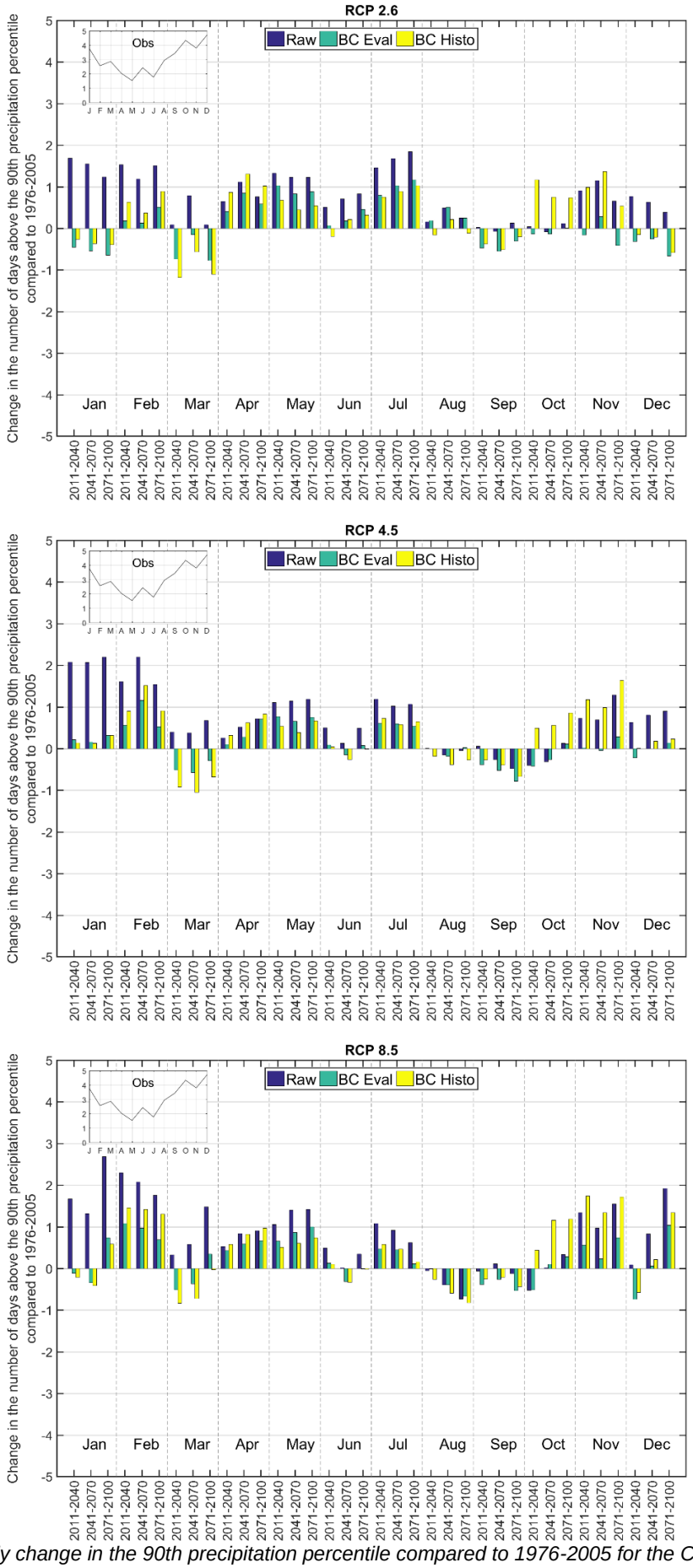

Figure A 31 Mean monthly change in the 90th precipitation percentile compared to 1976-2005 for the Calder catchment for the 2.6, 4.5 and 8.5 RCP scenarios for the uncorrected and bias-corrected simulations

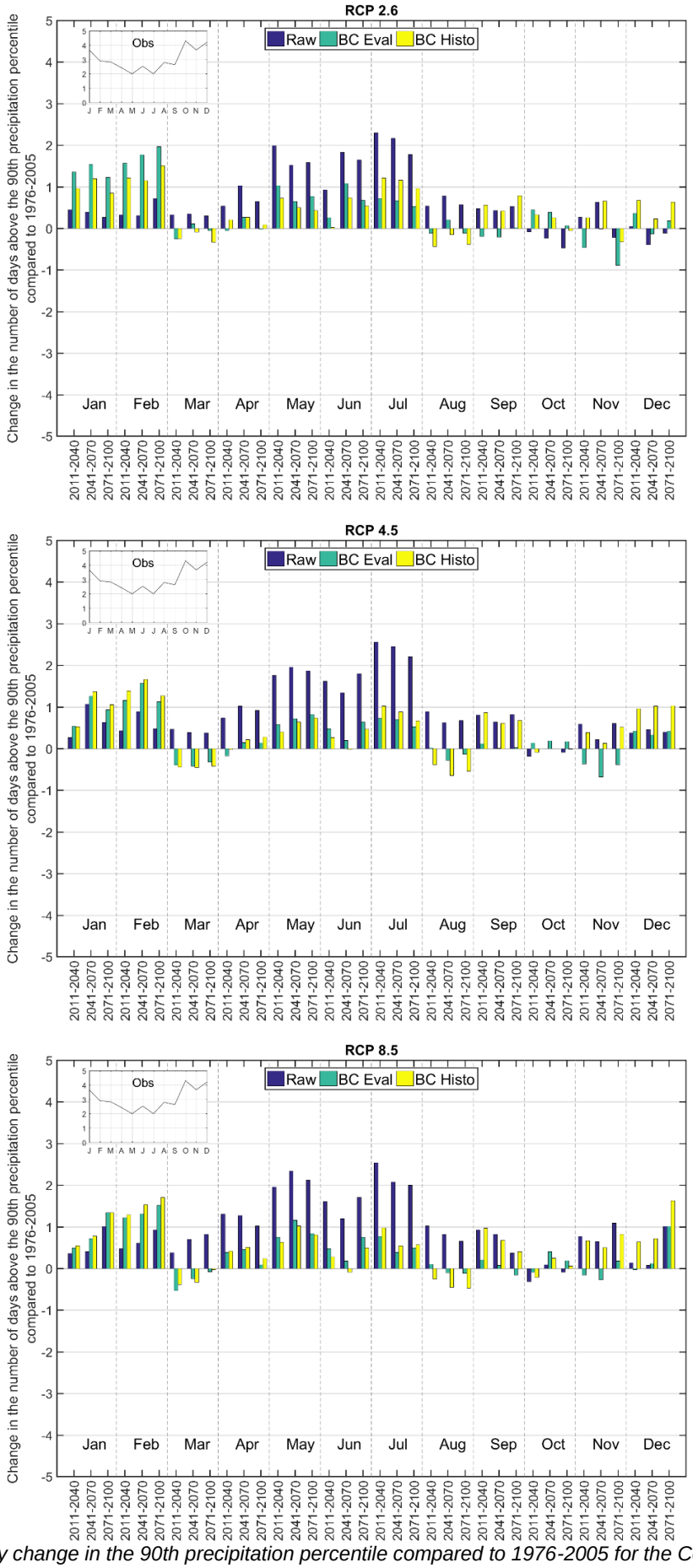

Figure A 32 Mean monthly change in the 90th precipitation percentile compared to 1976-2005 for the Coquet catchment for the 2.6, 4.5 and 8.5 RCP scenarios for the uncorrected and bias-corrected simulations

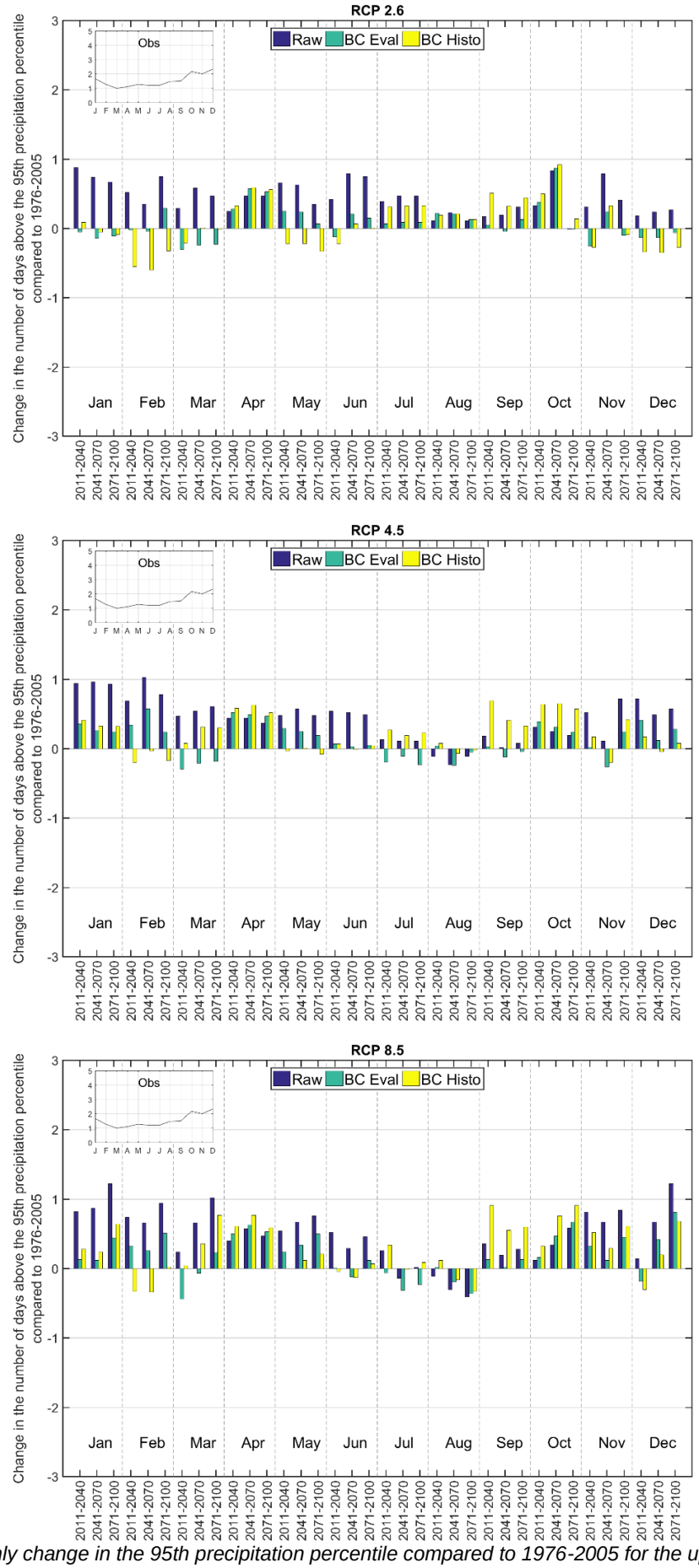

Figure A 33 Mean monthly change in the 95th precipitation percentile compared to 1976-2005 for the upper Thames catchment for the 2.6, 4.5 and 8.5 RCP scenarios for the uncorrected and bias-corrected simulations

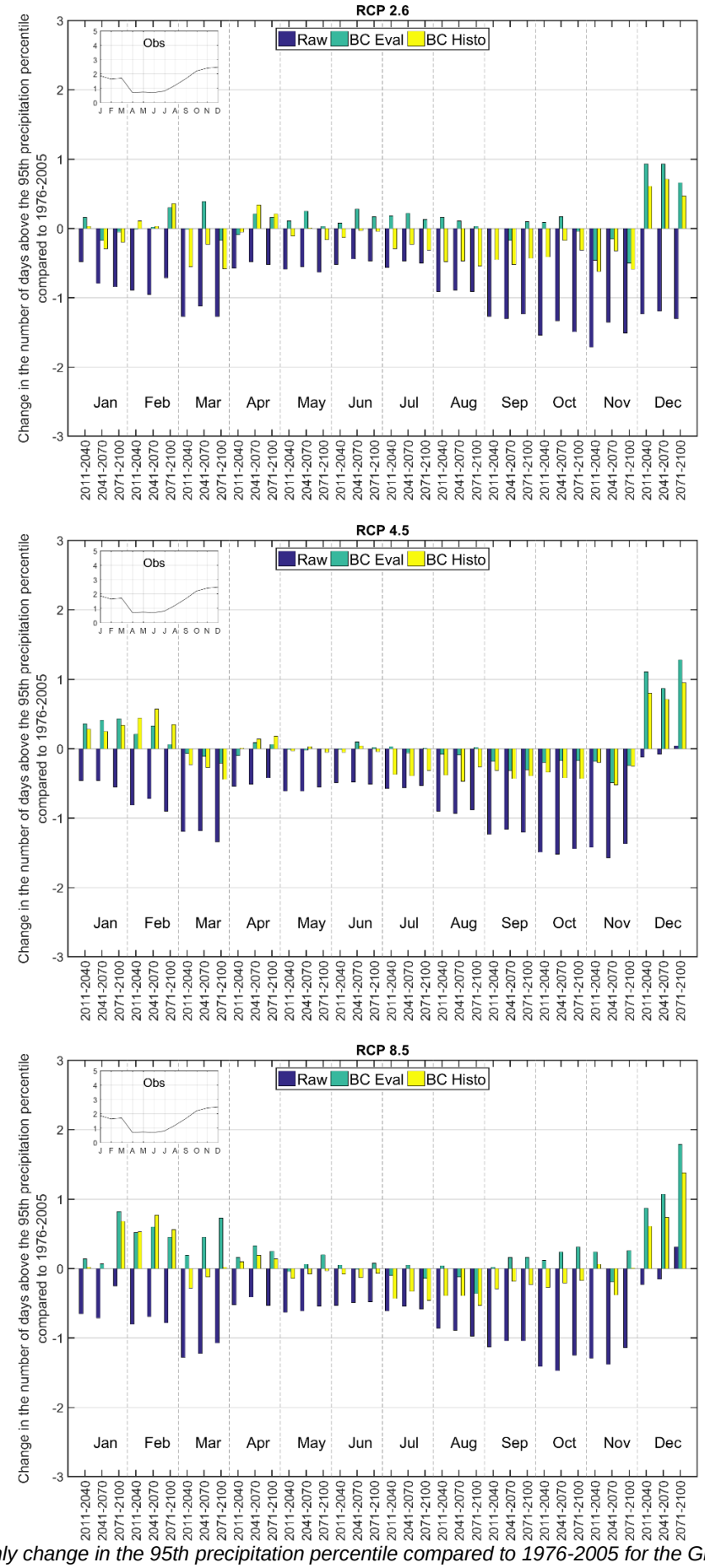

Figure A 34 Mean monthly change in the 95th precipitation percentile compared to 1976-2005 for the Glaslyn catchment for the 2.6, 4.5 and 8.5 RCP scenarios for the uncorrected and bias-corrected simulations

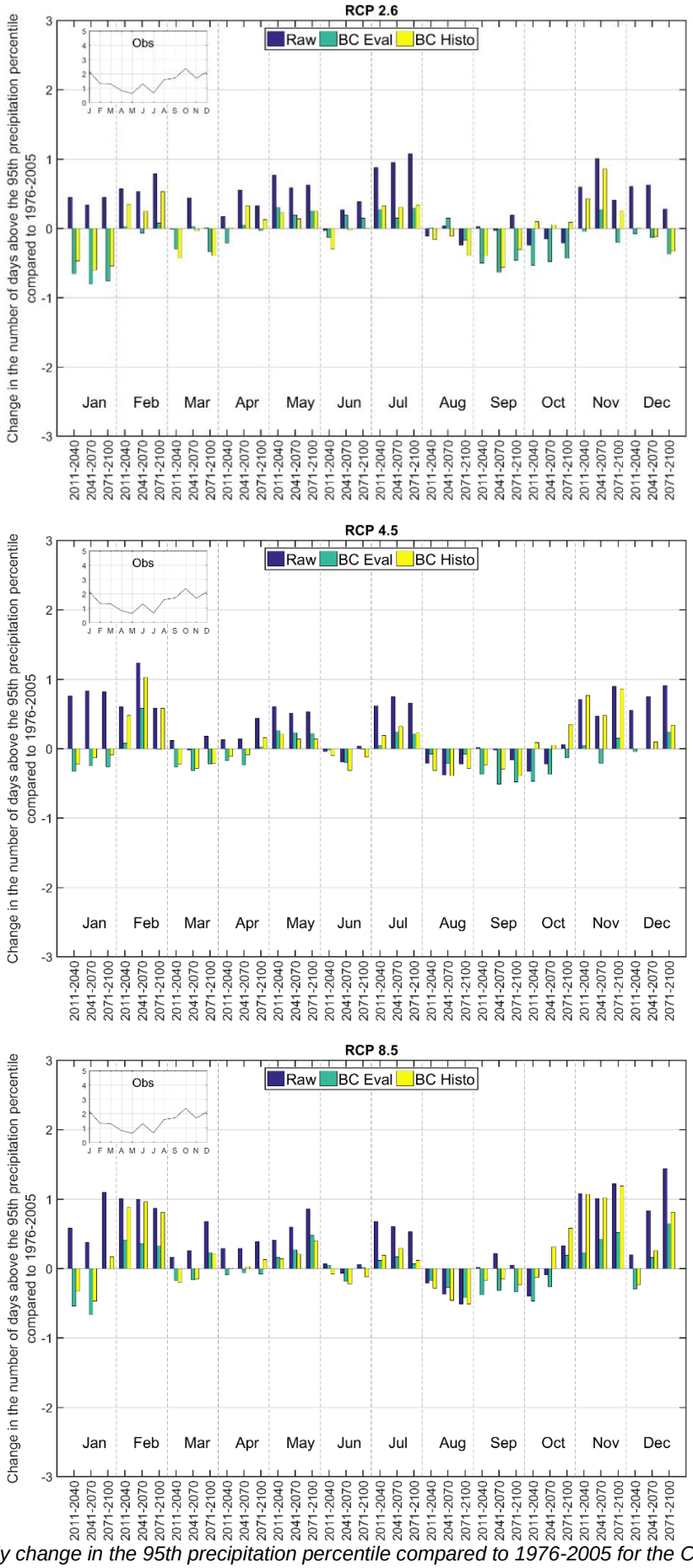

Figure A 35 Mean monthly change in the 95th precipitation percentile compared to 1976-2005 for the Calder catchment for the 2.6, 4.5 and 8.5 RCP scenarios for the uncorrected and bias-corrected simulations

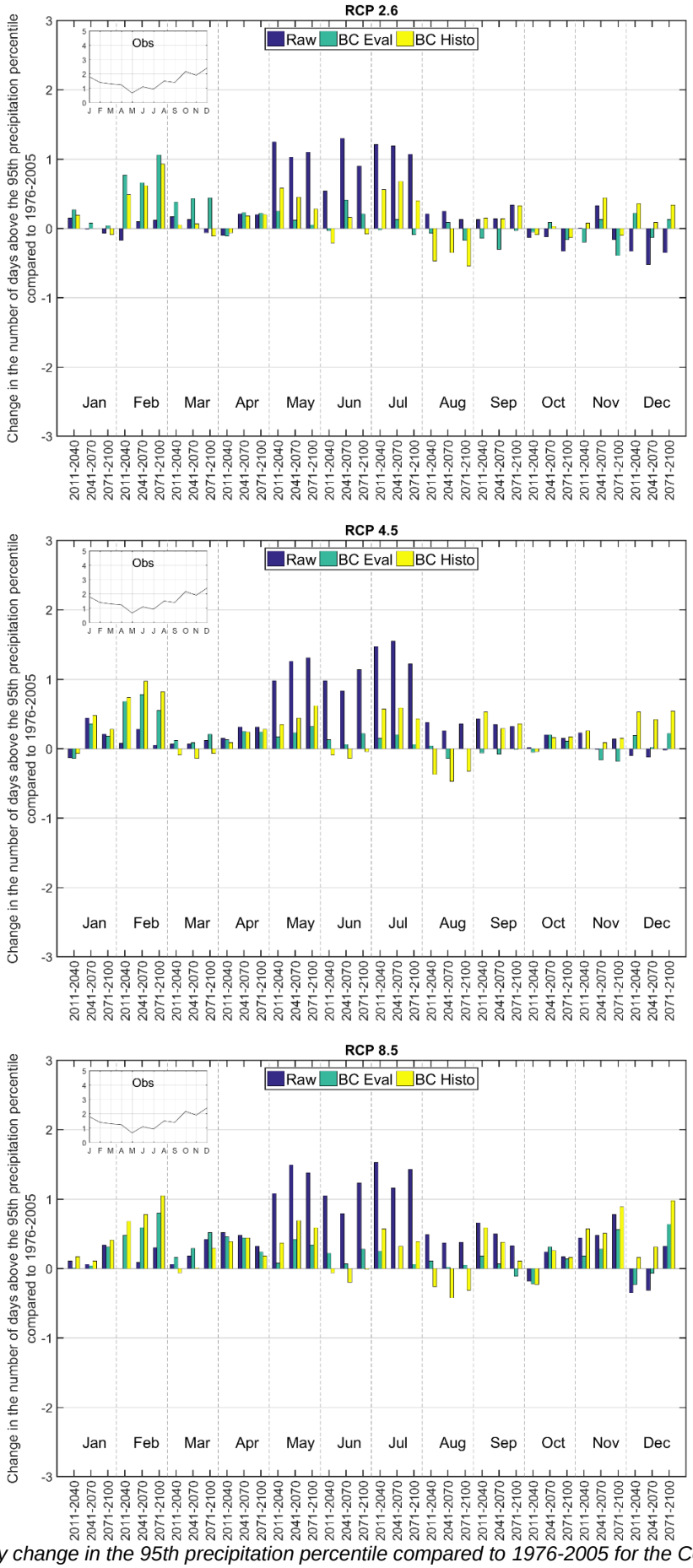

Figure A 36 Mean monthly change in the 95th precipitation percentile compared to 1976-2005 for the Coquet catchment for the 2.6, 4.5 and 8.5 RCP scenarios for the uncorrected and bias-corrected simulation

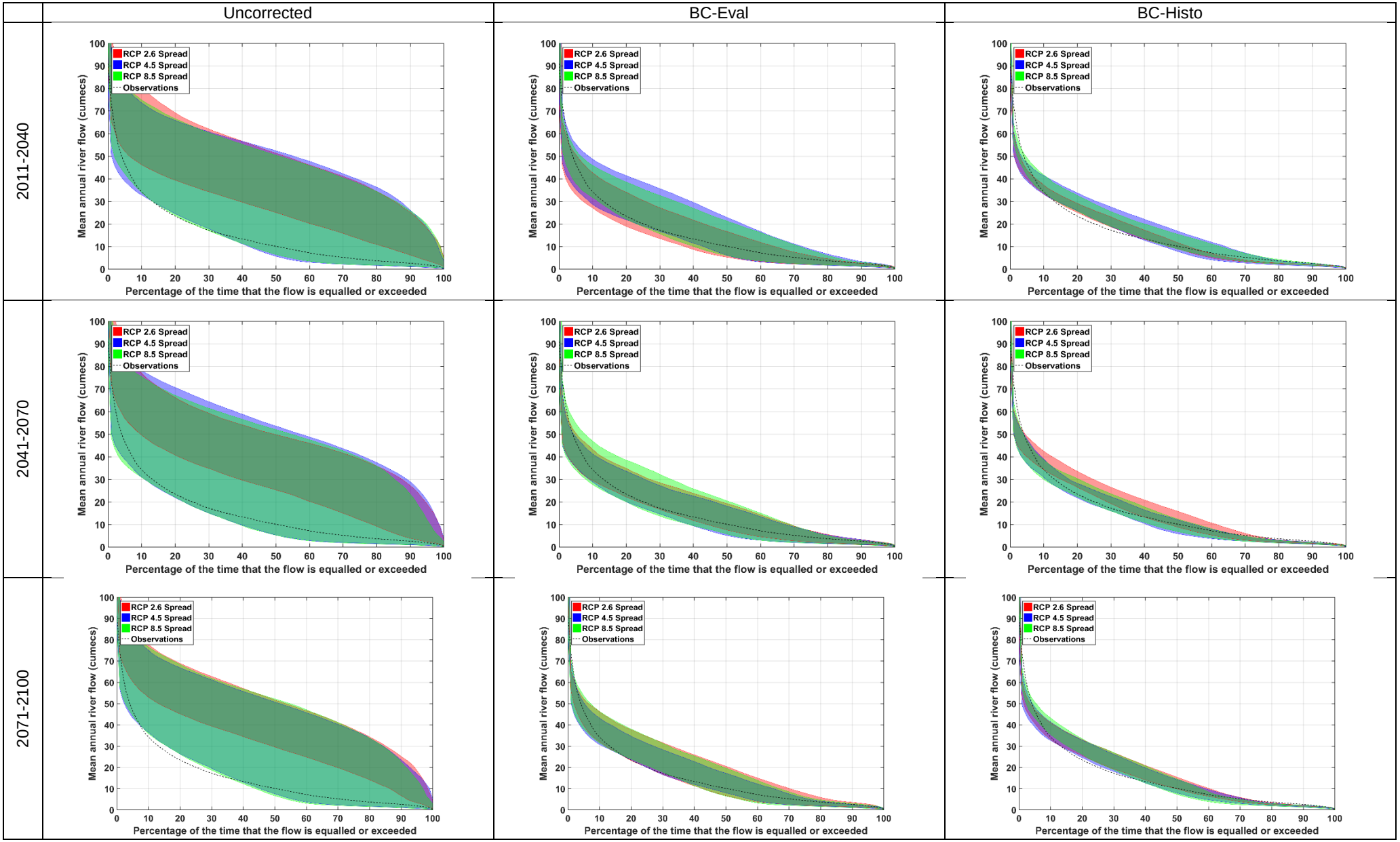

Figure A 37 Flow duration curves for the uncorrected and bias-corrected projected RCPs for the different time slices in the upper Thames catchment

	Uncorrected	BC-Eval	BC-Histo
2011-2040	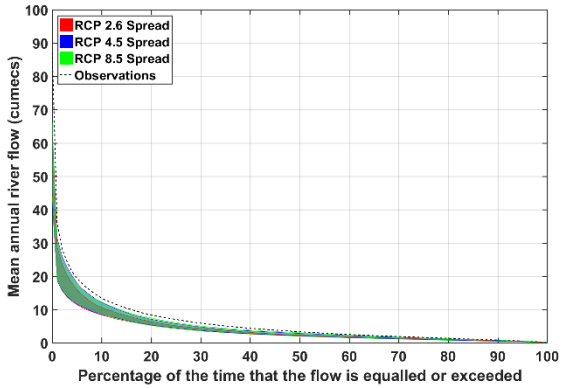	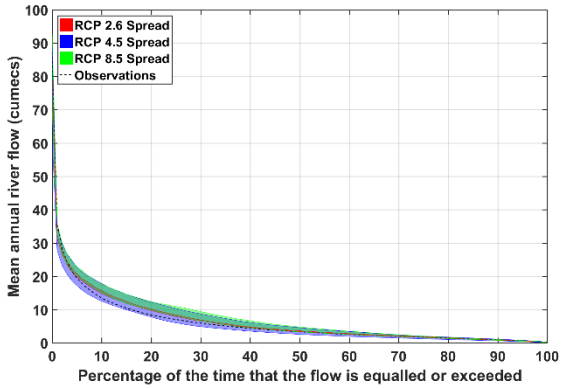	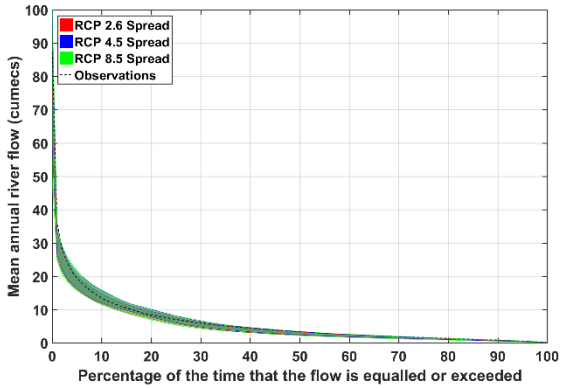
2041-2070	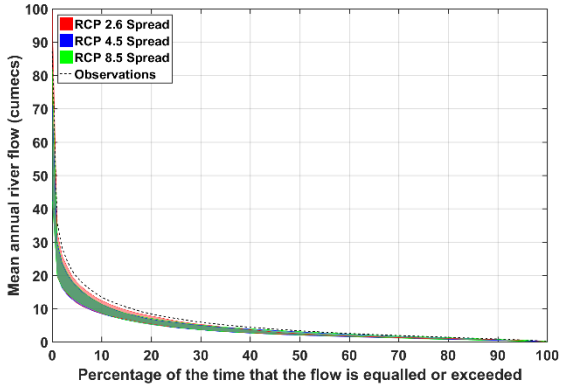	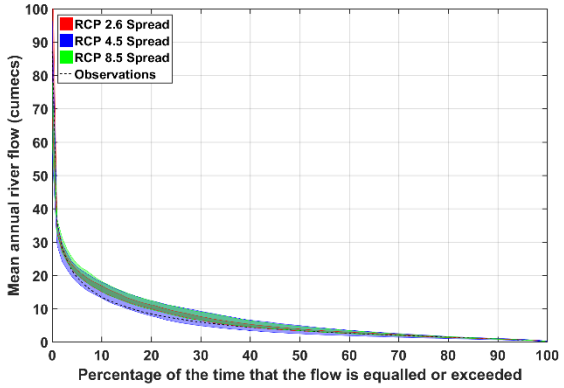	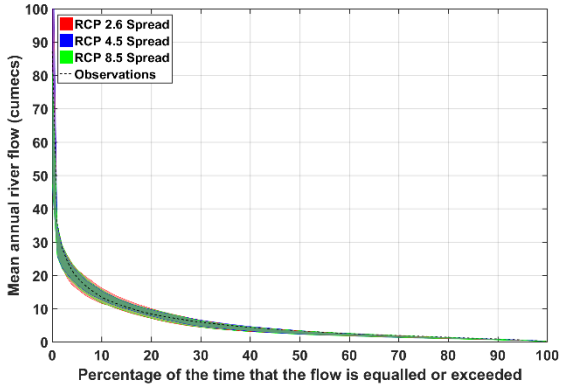
2071-2100	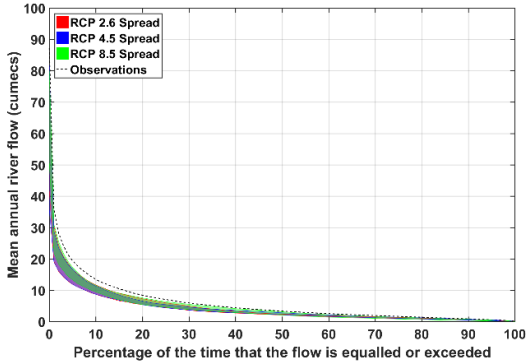	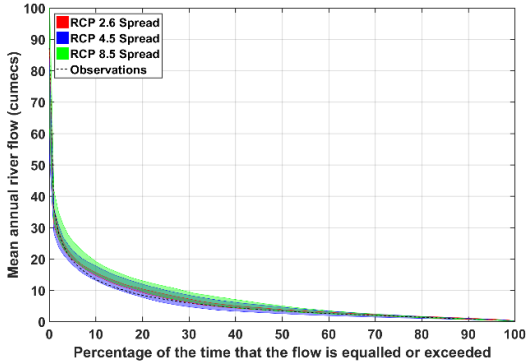	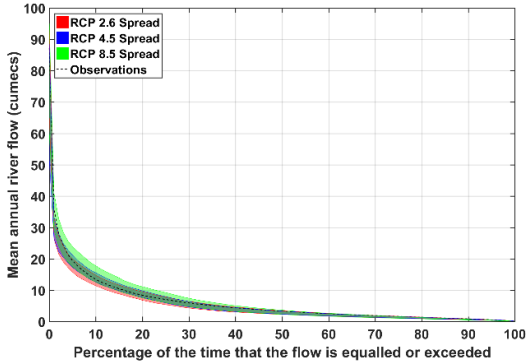

*F*igure A 38 Flow duration curves for the uncorrected and bias-corrected projected RCPs for the different time slices in the Glaslyn catchment

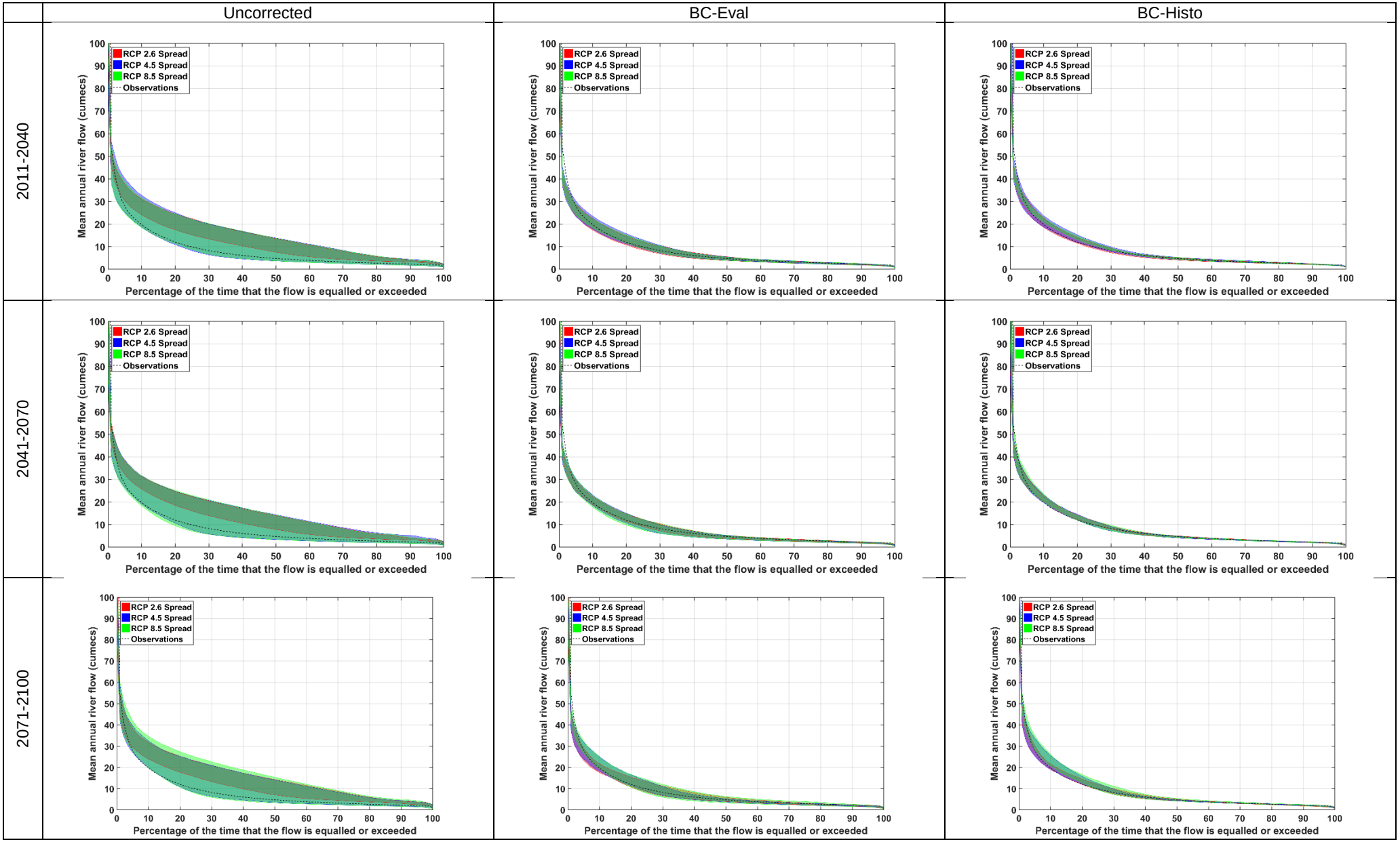

Figure A 39 Flow duration curves for the uncorrected and bias-corrected projected RCPs for the different time slices in the Calder catchment

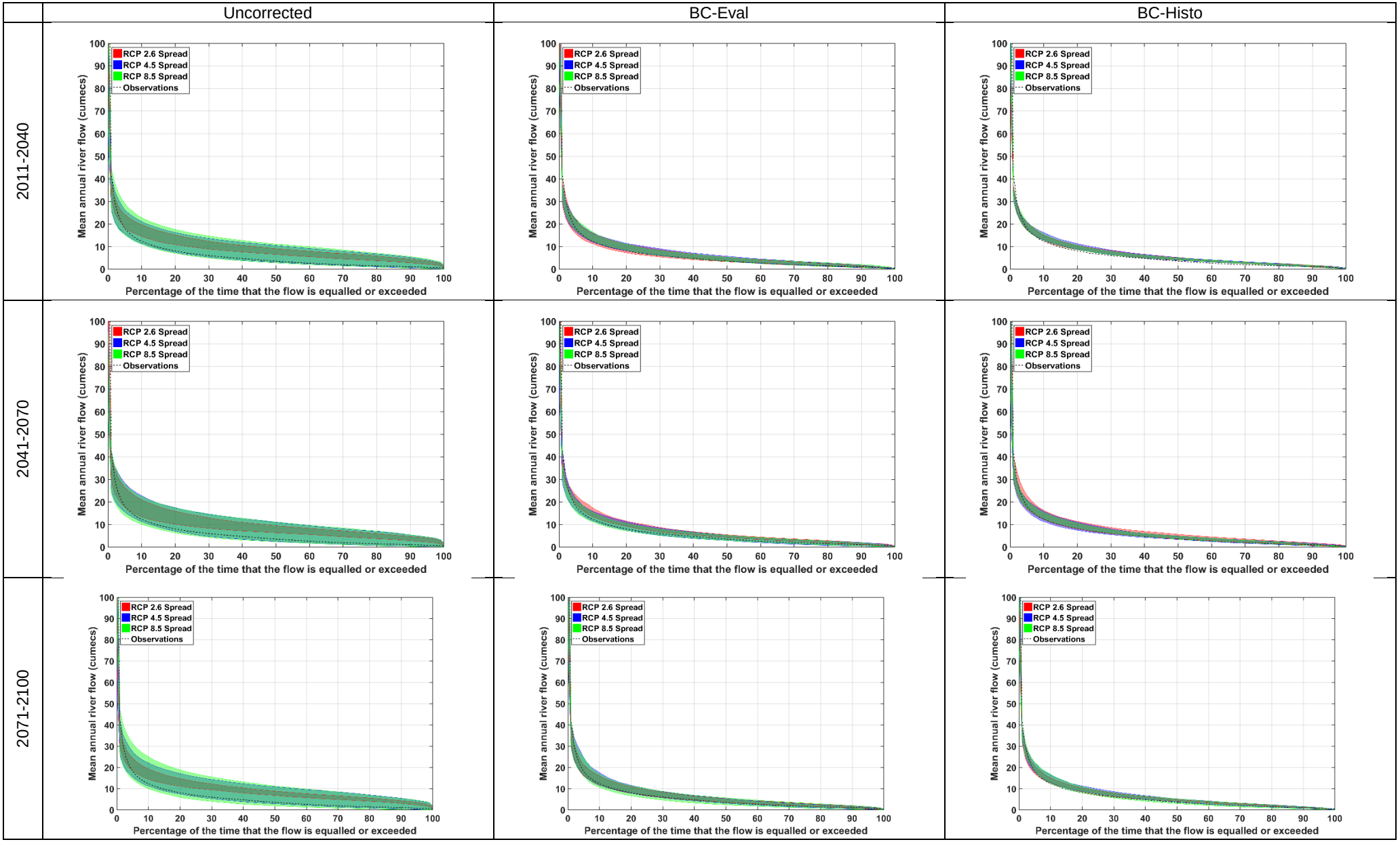

Figure A 40 Flow duration curves for the uncorrected and bias-corrected projected RCPs for the different time slices in the Coquet catchment

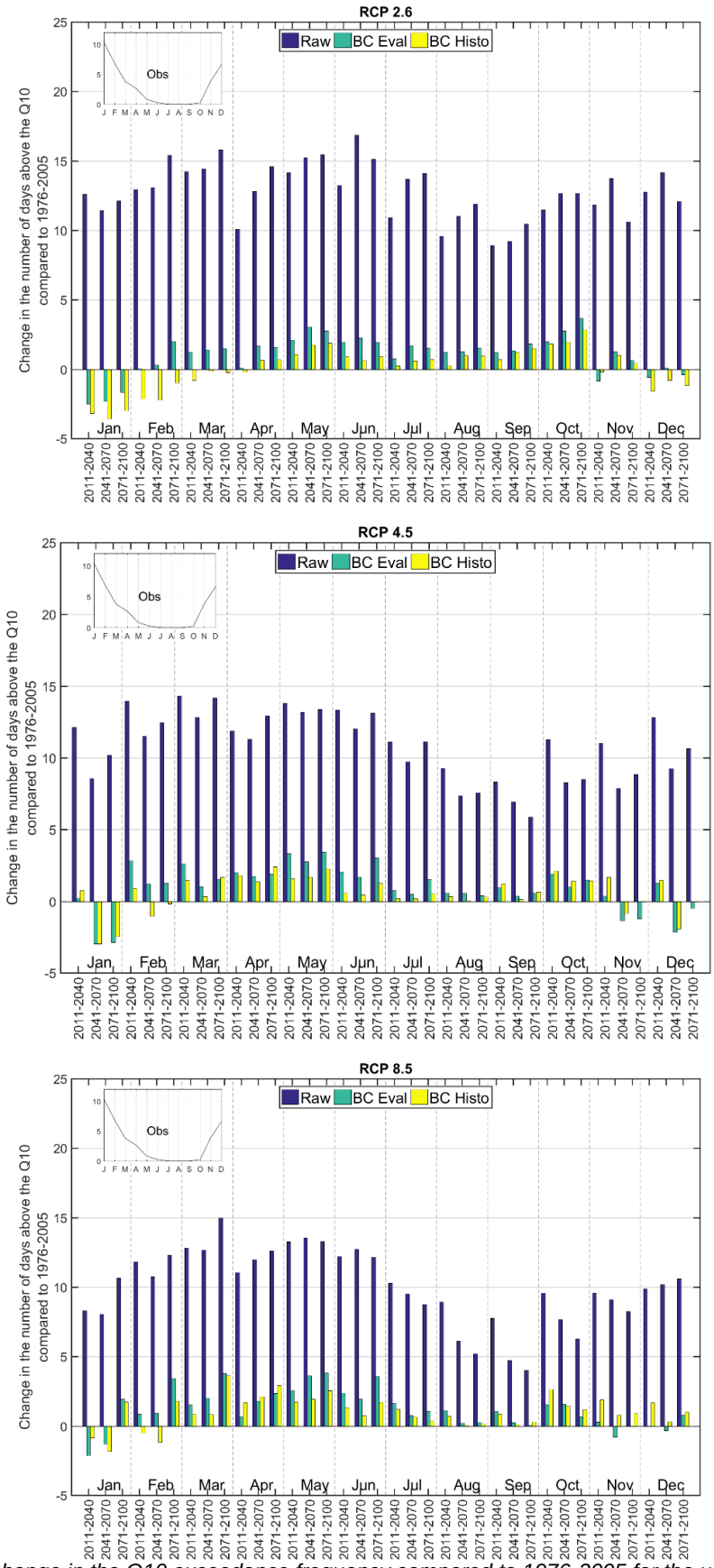

Figure A 41 Mean monthly change in the Q10 exceedance frequency compared to 1976-2005 for the upper Thames catchment for the uncorrected and bias-corrected 2.6, 4.5 and 8.5 RCP scenarios

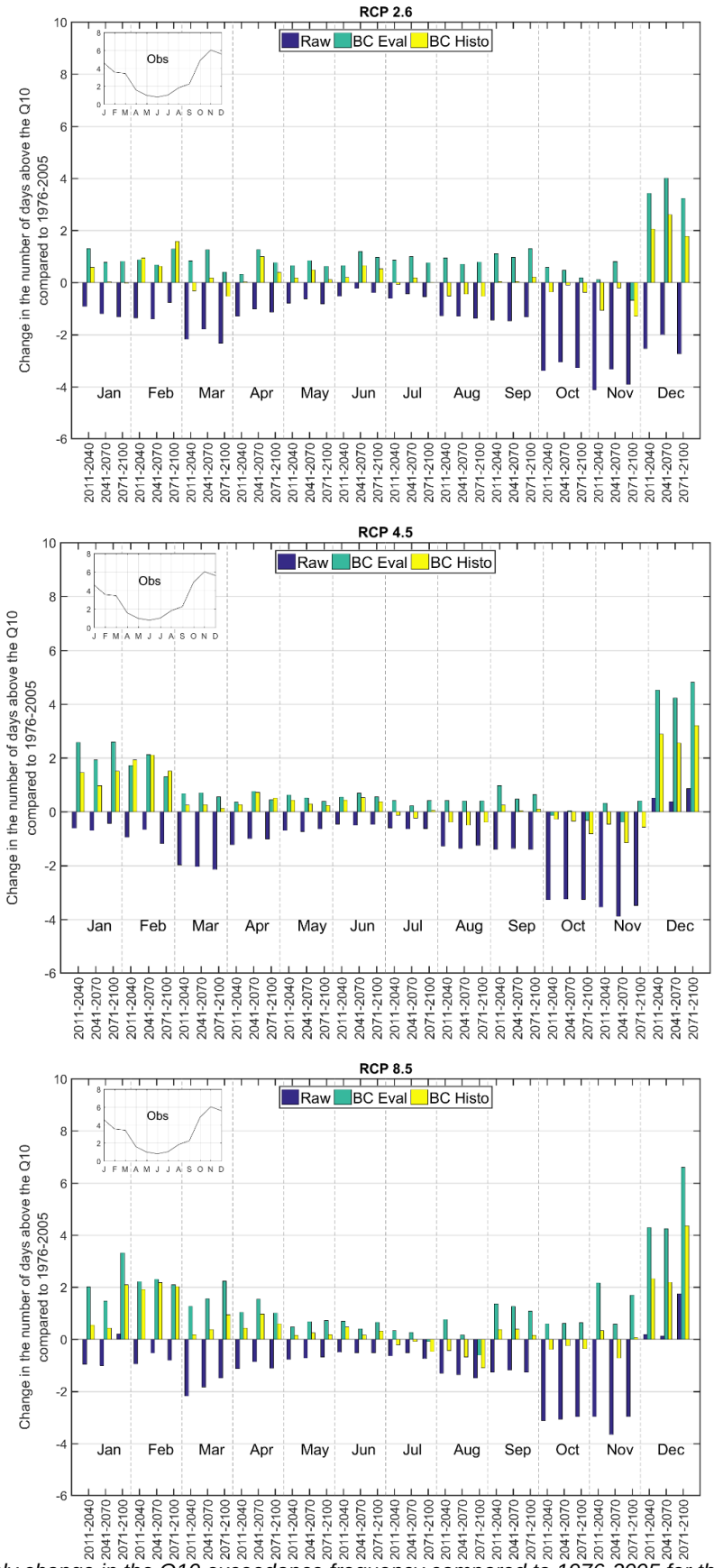

Figure A 42 Mean monthly change in the Q10 exceedance frequency compared to 1976-2005 for the Glaslyn catchment for the uncorrected and bias-corrected 2.6, 4.5 and 8.5 RCP scenarios

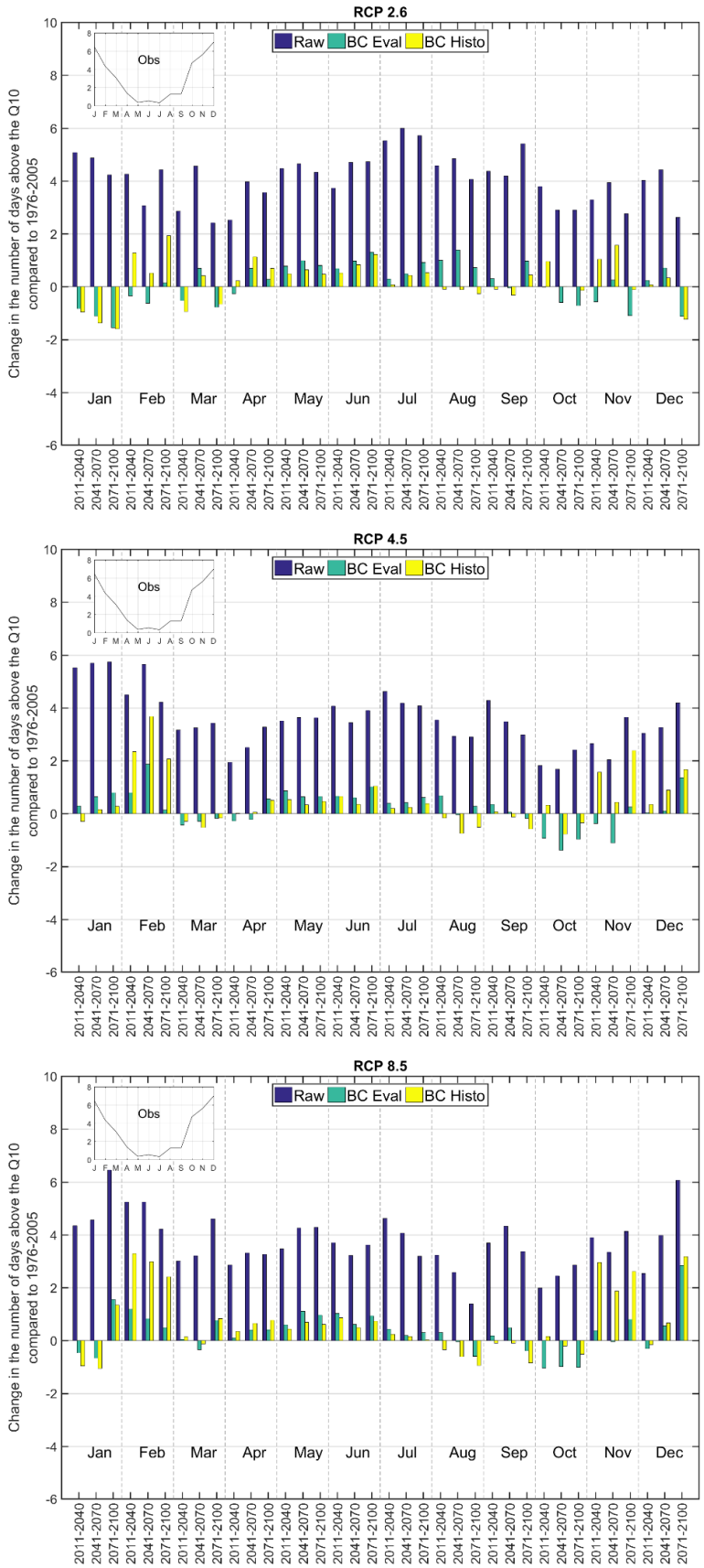

Figure A 43 Mean monthly change in the Q10 exceedance frequency compared to 1976-2005 for the Calder catchment for the uncorrected and bias-corrected 2.6, 4.5 and 8.5 RCP scenarios

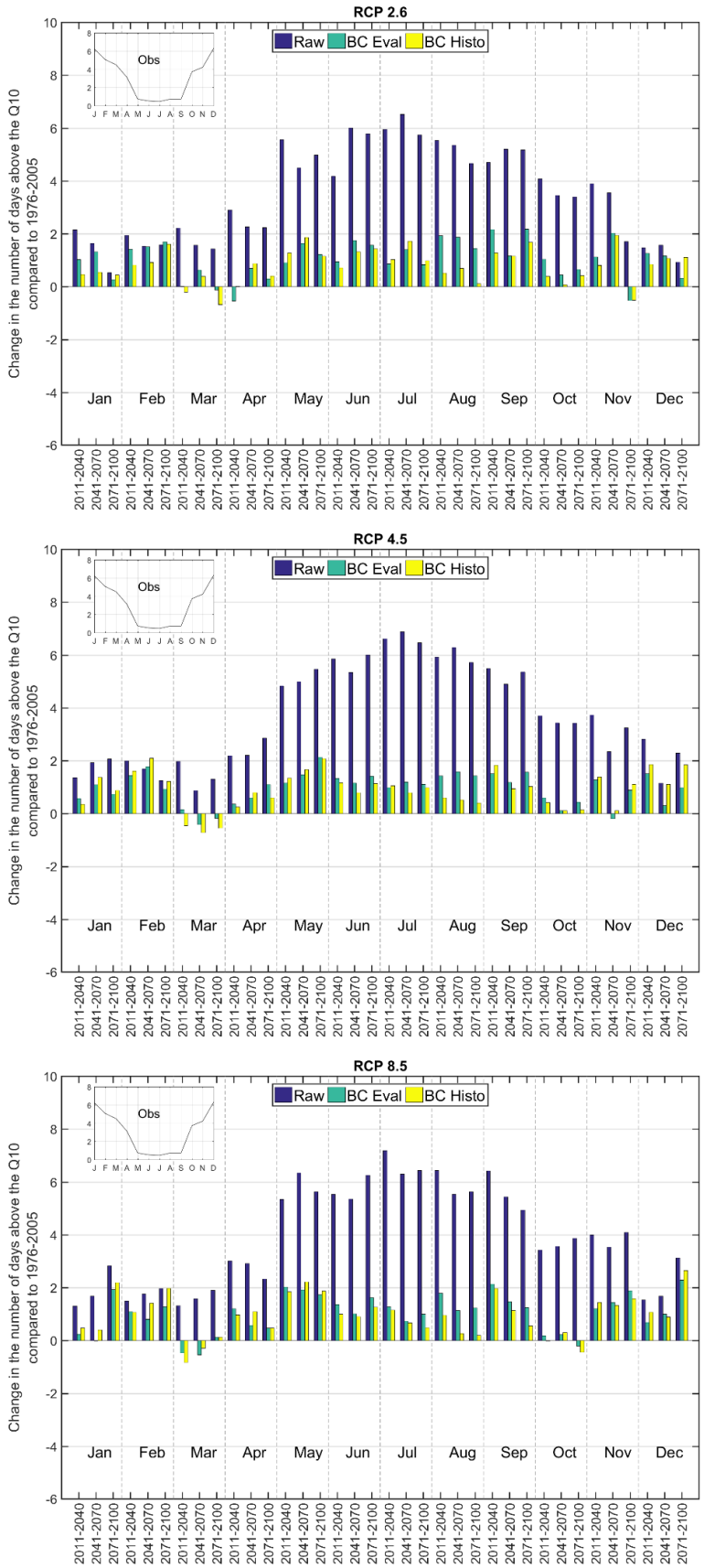

Figure A 44 Mean monthly change in the Q10 exceedance frequency compared to 1976-2005 for the Coquet catchment for the uncorrected and bias-corrected 2.6, 4.5 and 8.5 RCP scenarios

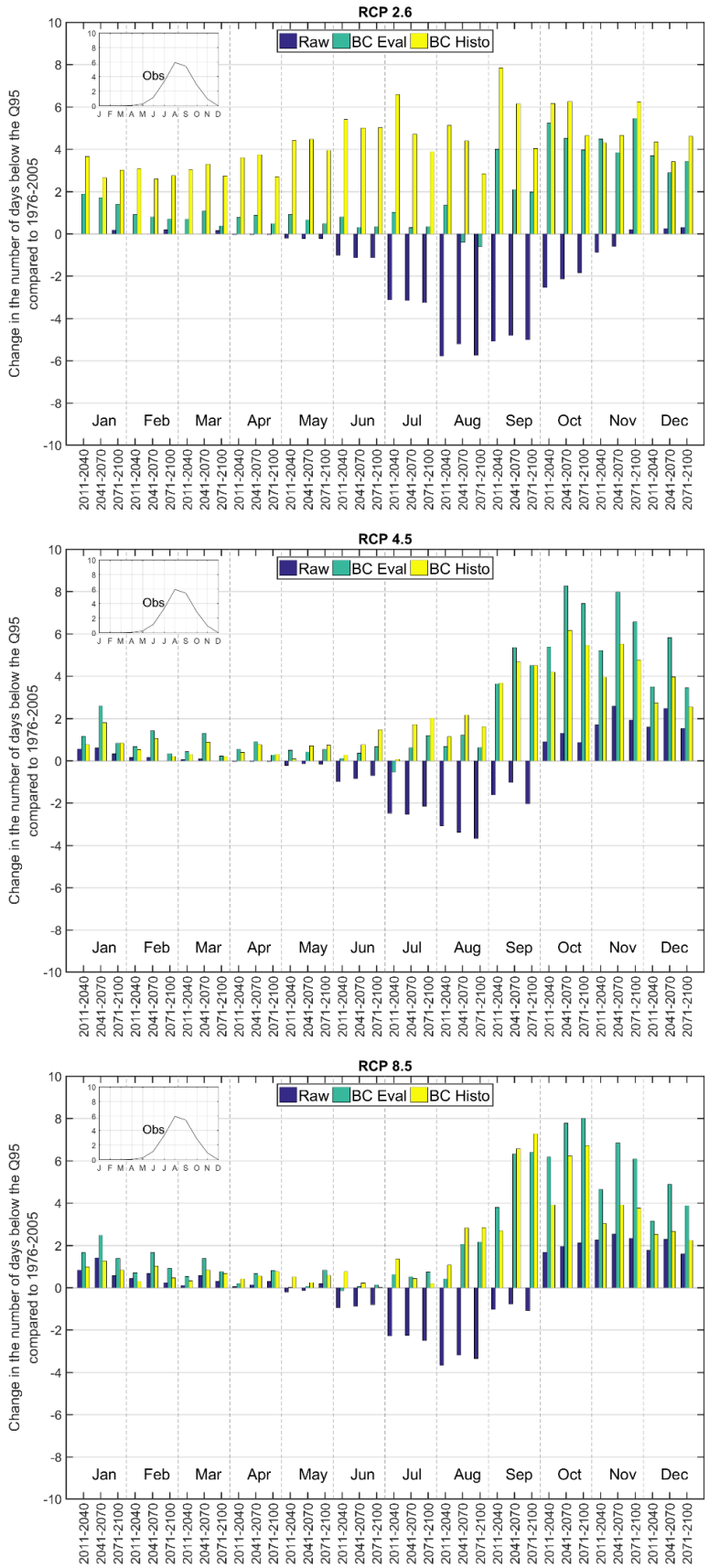

Figure A 45 Mean monthly change in the frequency of flows below the Q95 compared to 1976-2005 for the upper Thames catchment for the uncorrected and bias-corrected 2.6, 4.5 and 8.5 RCP scenarios

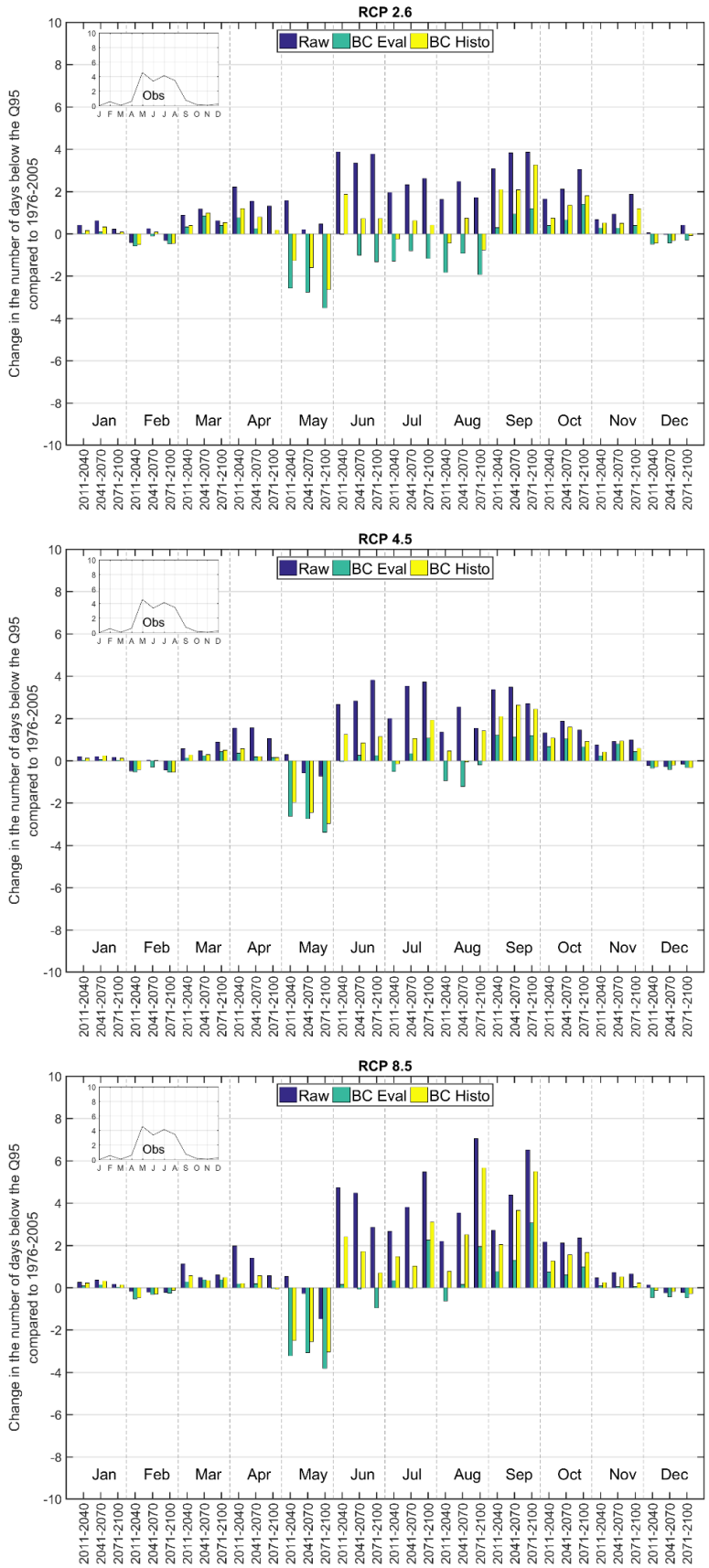

Figure A 46 Mean monthly change in the frequency of flows below the Q95 compared to 1976-2005 for the Glaslyn catchment for the uncorrected and bias-corrected 2.6, 4.5 and 8.5 RCP scenarios

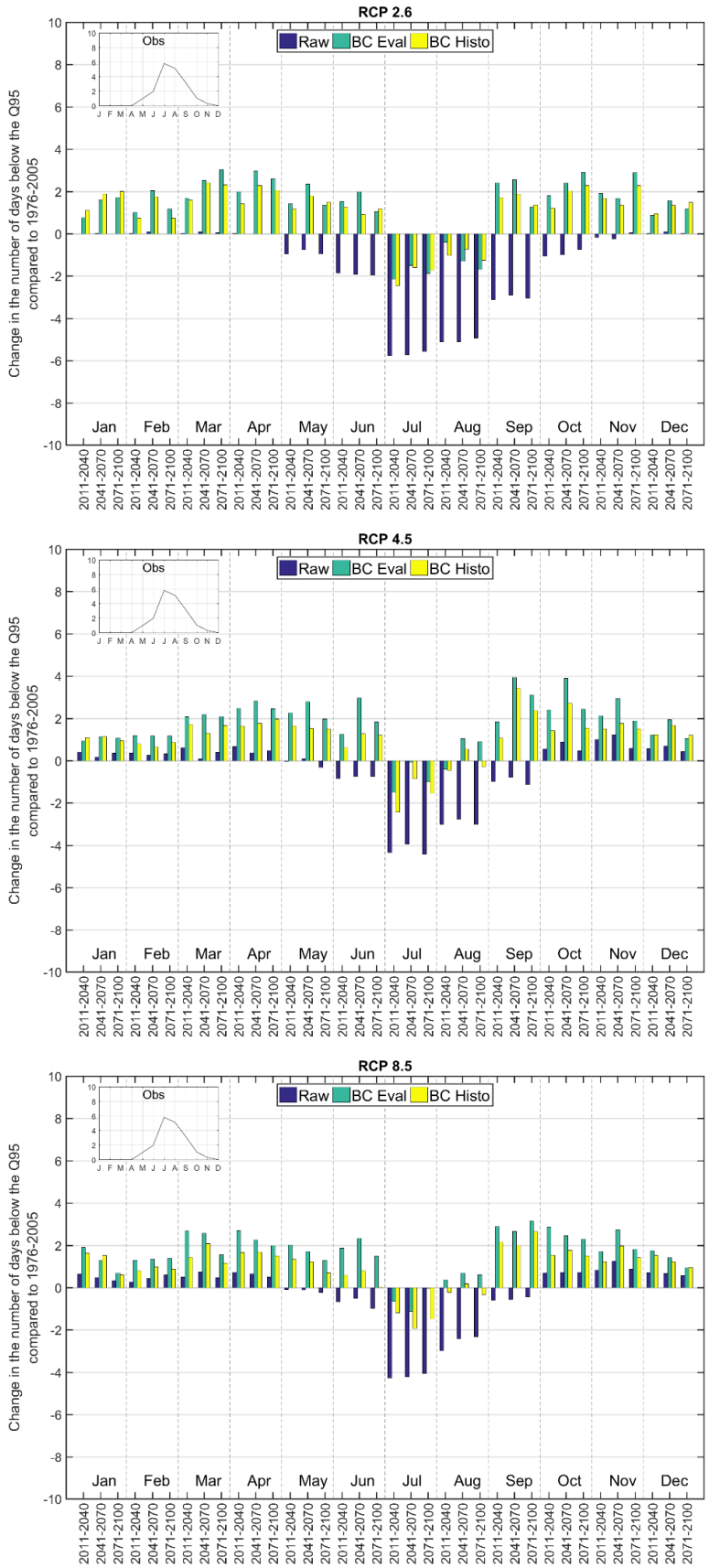

Figure A 47 Mean monthly change in the frequency of flows below the Q95 compared to 1976-2005 for the Calder catchment for the uncorrected and bias-corrected 2.6, 4.5 and 8.5 RCP scenarios

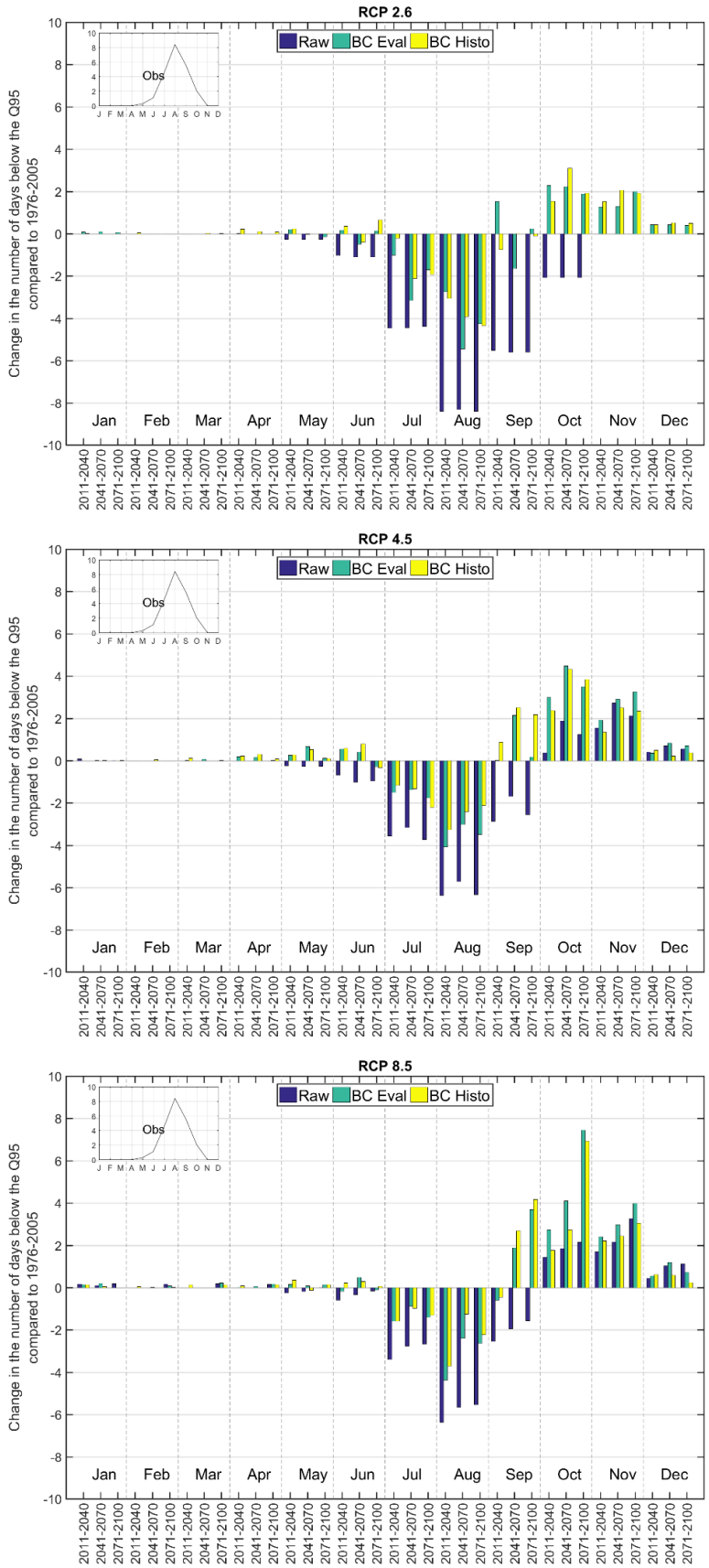

Figure A 48 Mean monthly change in the frequency of flows below the Q95 compared to 1976-2005 for the Coquet catchment for the uncorrected and bias-corrected 2.6, 4.5 and 8.5 RCP scenarios

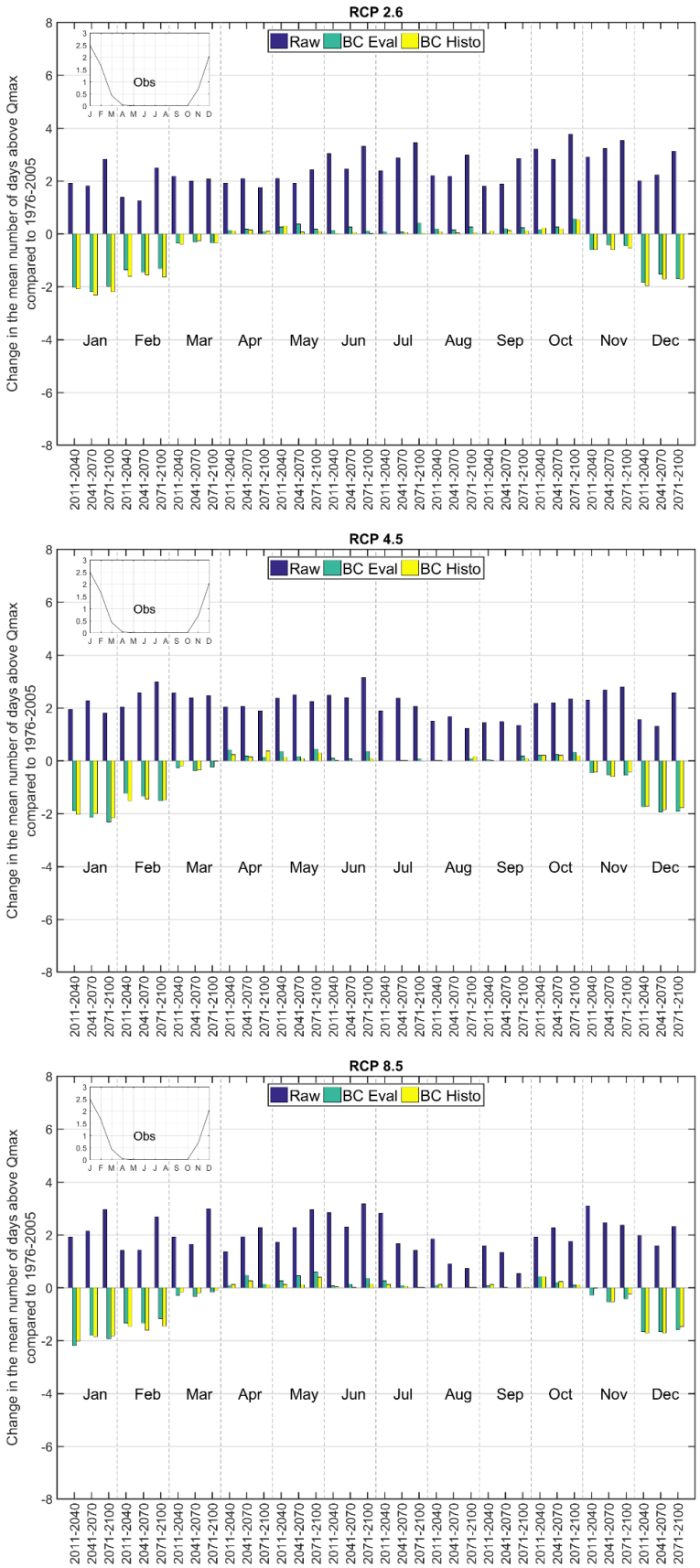

Figure A 49 Change in the monthly mean number of days above Qmax compared to 1976-2005 for the upper Thames catchment for the uncorrected and bias-corrected 2.6, 4.5 and 8.5 RCP scenarios

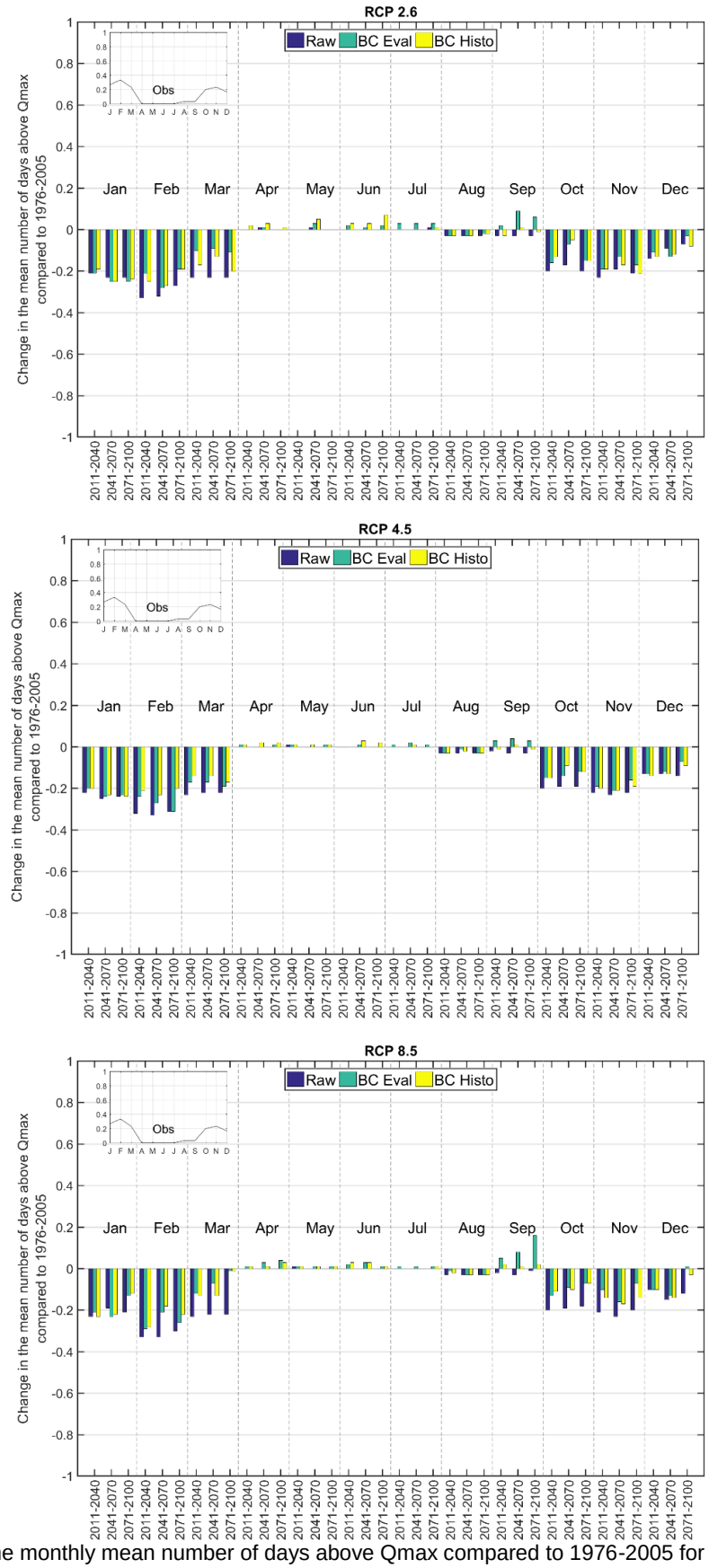

a

Figure A 50 Change in the monthly mean number of days above Qmax compared to 1976-2005 for the Glaslyn catchment for the uncorrected and bias-corrected 2.6, 4.5 and 8.5 RCP scenarios

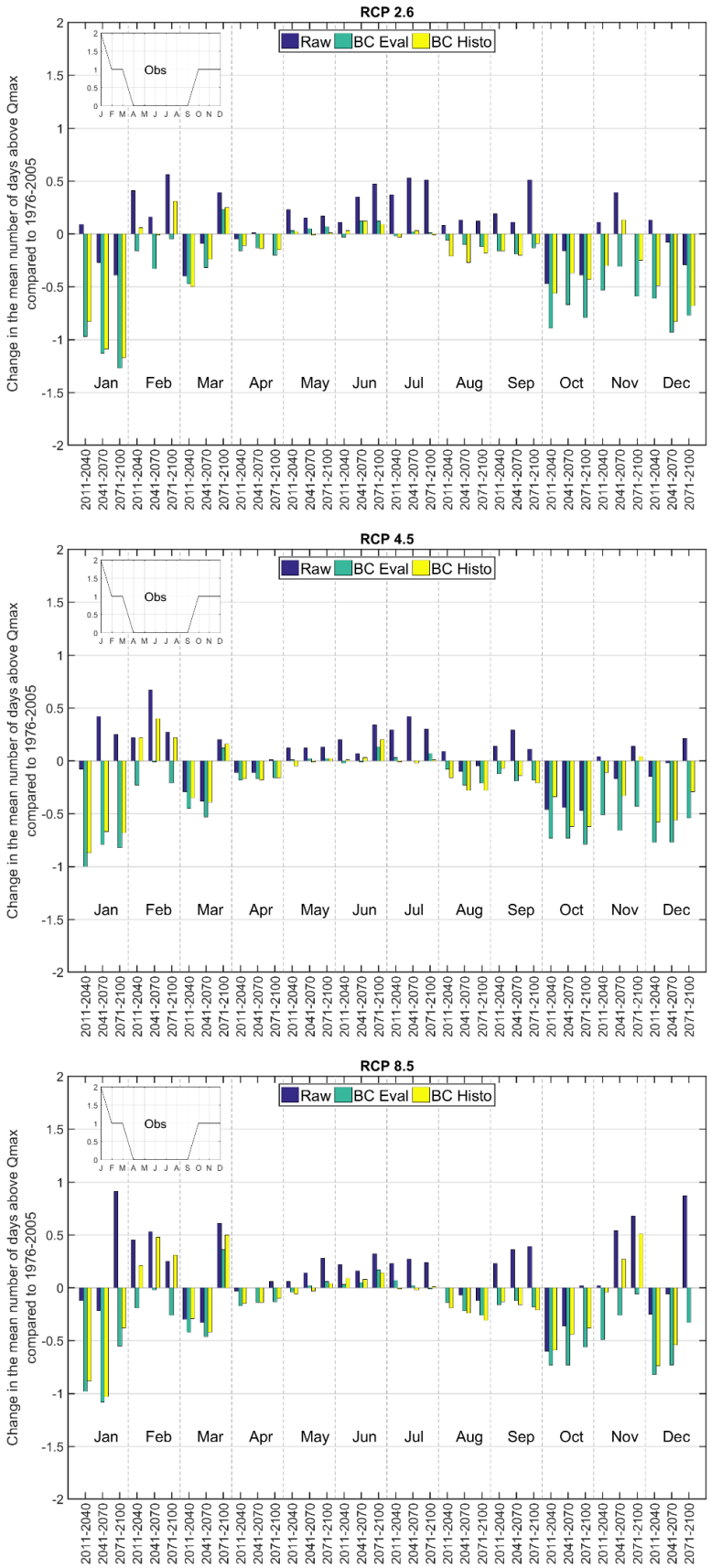

Figure A 51 Change in the monthly mean number of days above Qmax compared to 1976-2005 for the Calder catchment for the uncorrected and bias-corrected 2.6, 4.5 and 8.5 RCP scenarios

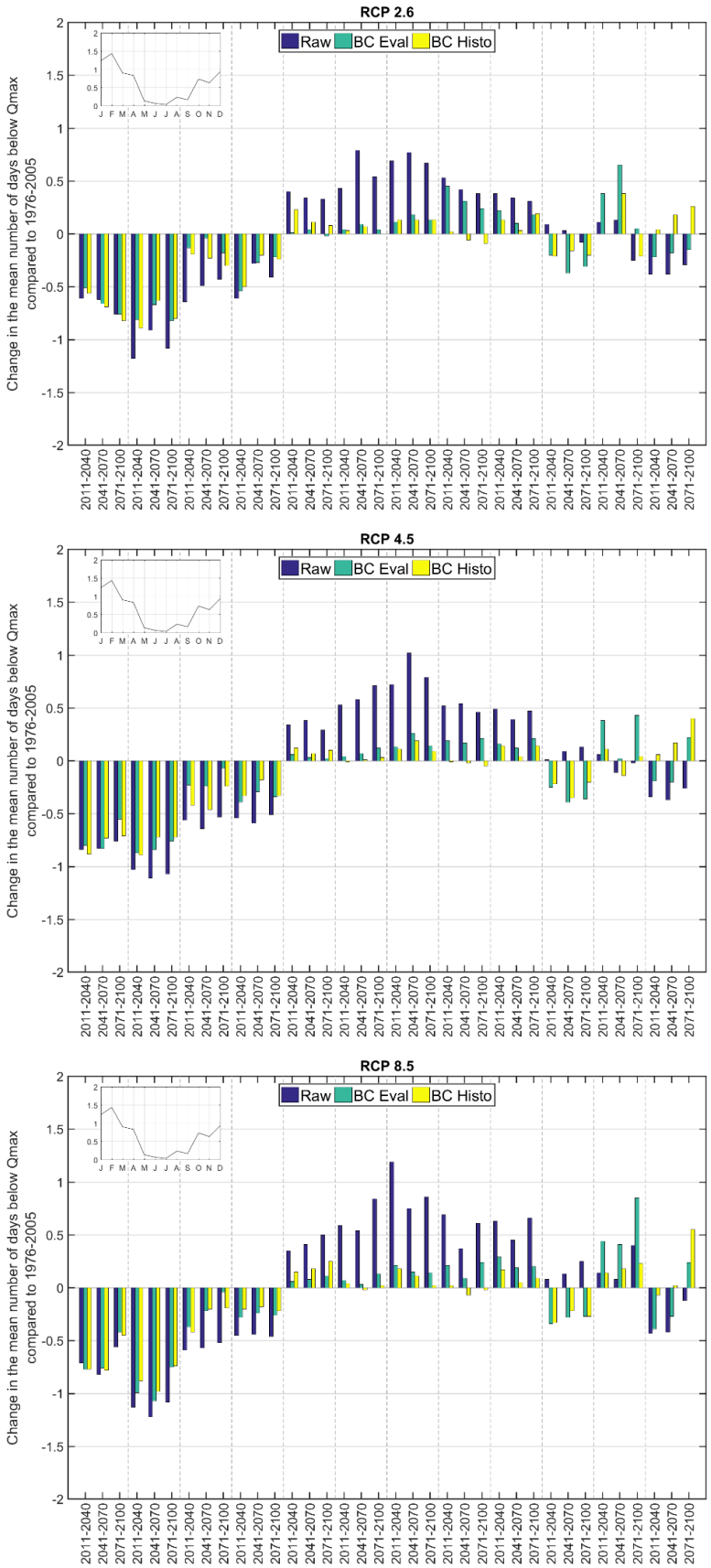

Figure A 52 Change in the monthly mean number of days above Qmax compared to 1976-2005 for the Coquet catchment for the uncorrected and bias-corrected 2.6, 4.5 and 8.5 RCP scenarios

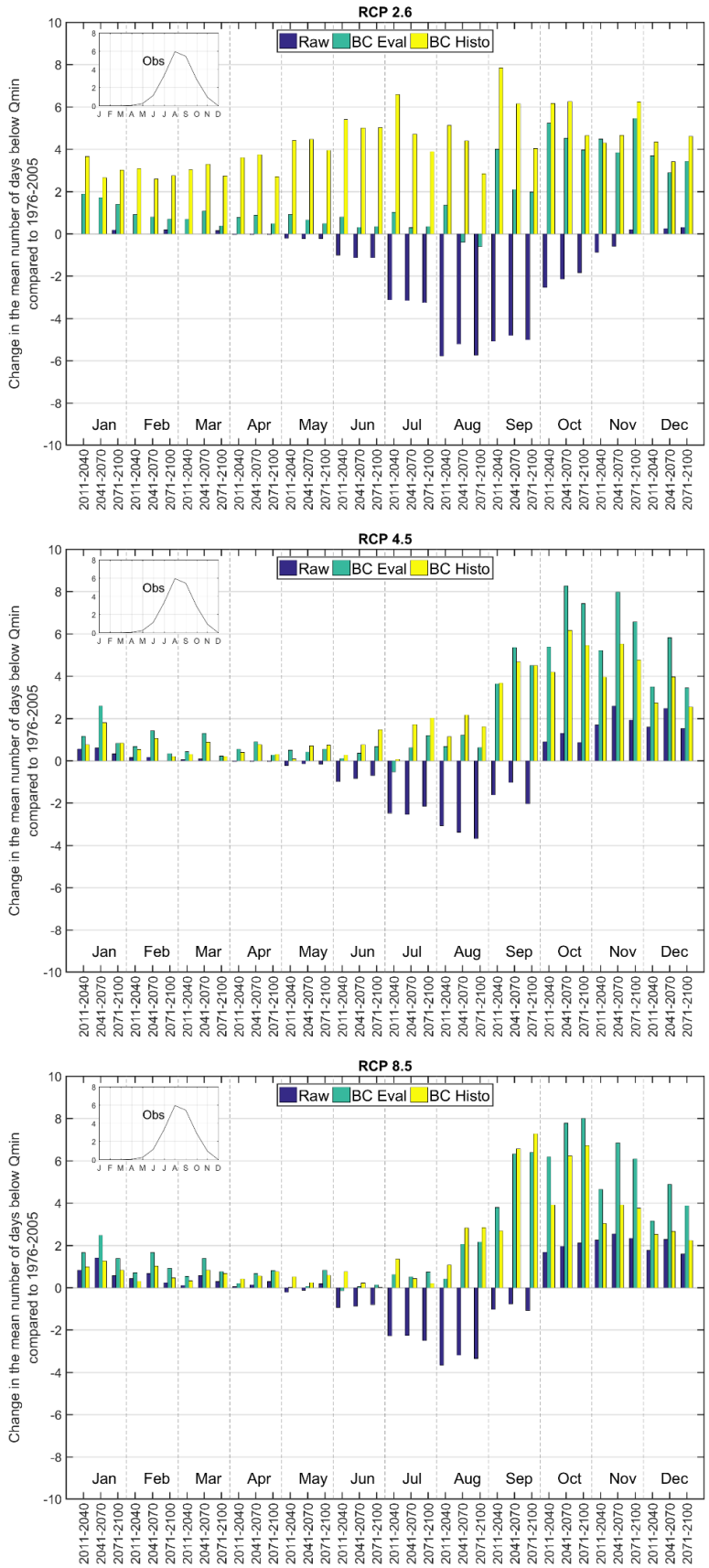

Figure A 53 Change in the monthly mean number of days below Qmin compared to 1976-2005 for the upper Thames catchment for the uncorrected and bias-corrected 2.6, 4.5 and 8.5 RCP scenarios

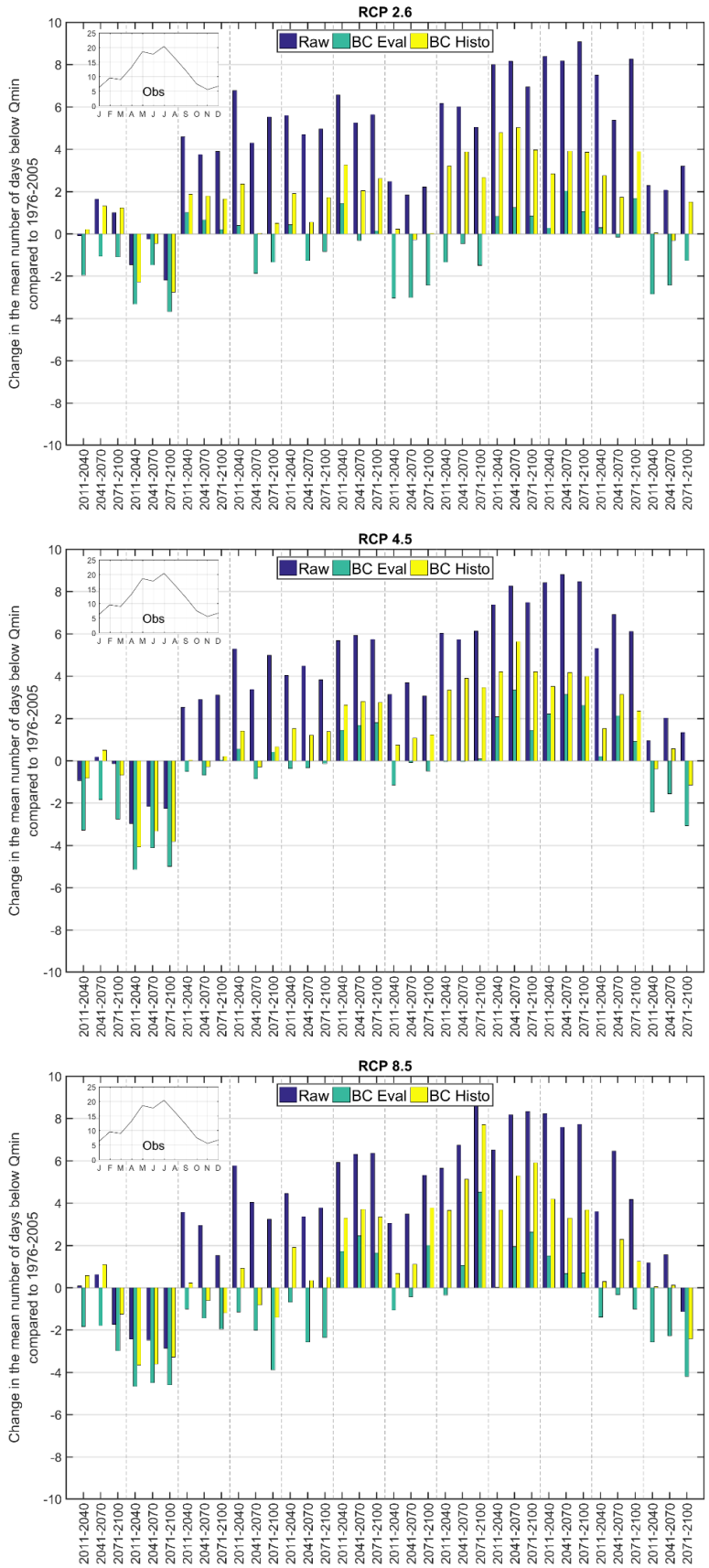

Figure A 54 Change in the monthly mean number of days below Qmin compared to 1976-2005 for the Glaslyn catchment for the uncorrected and bias-corrected 2.6, 4.5 and 8.5 RCP scenarios

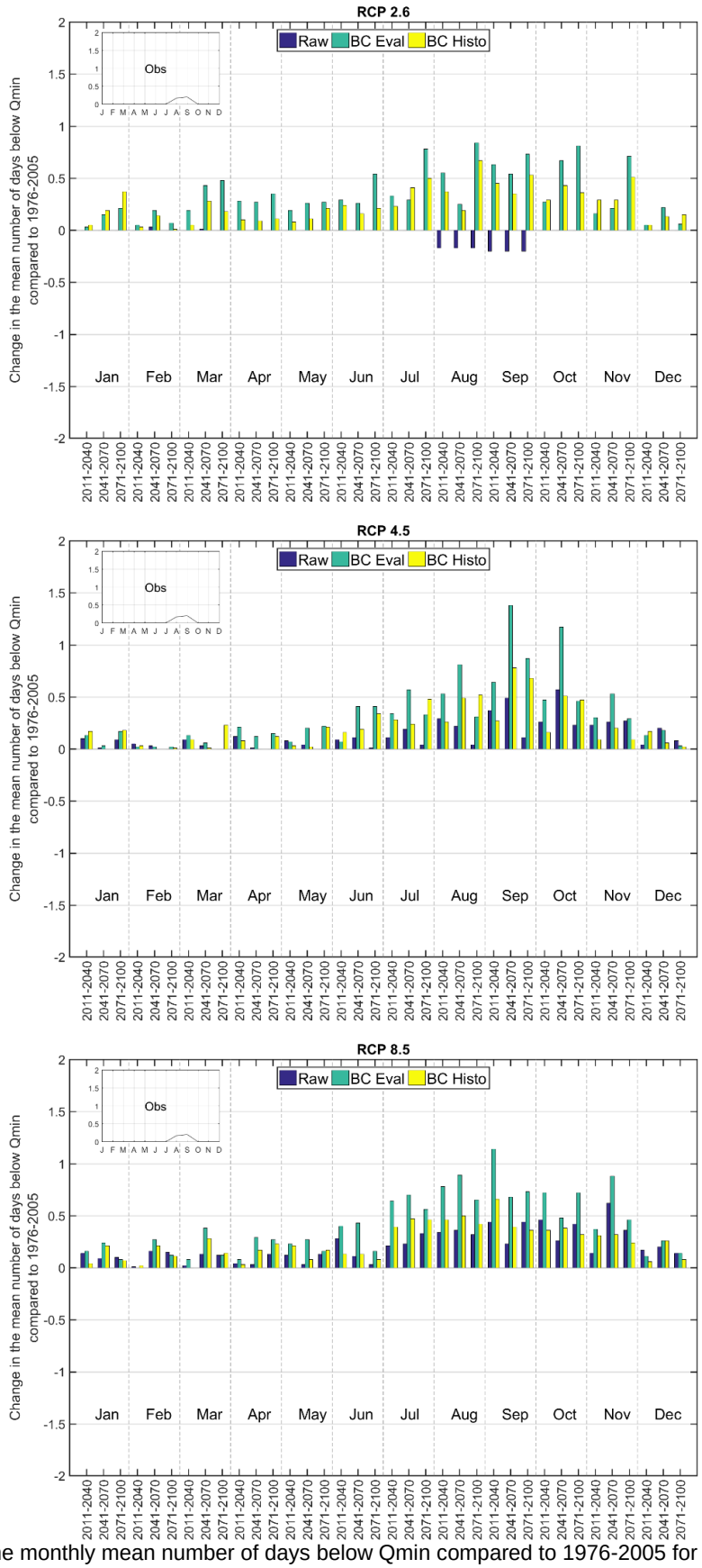

Figure A 55 Change in the monthly mean number of days below Qmin compared to 1976-2005 for the Calder catchment for the uncorrected and bias-corrected 2.6, 4.5 and 8.5 RCP scenarios

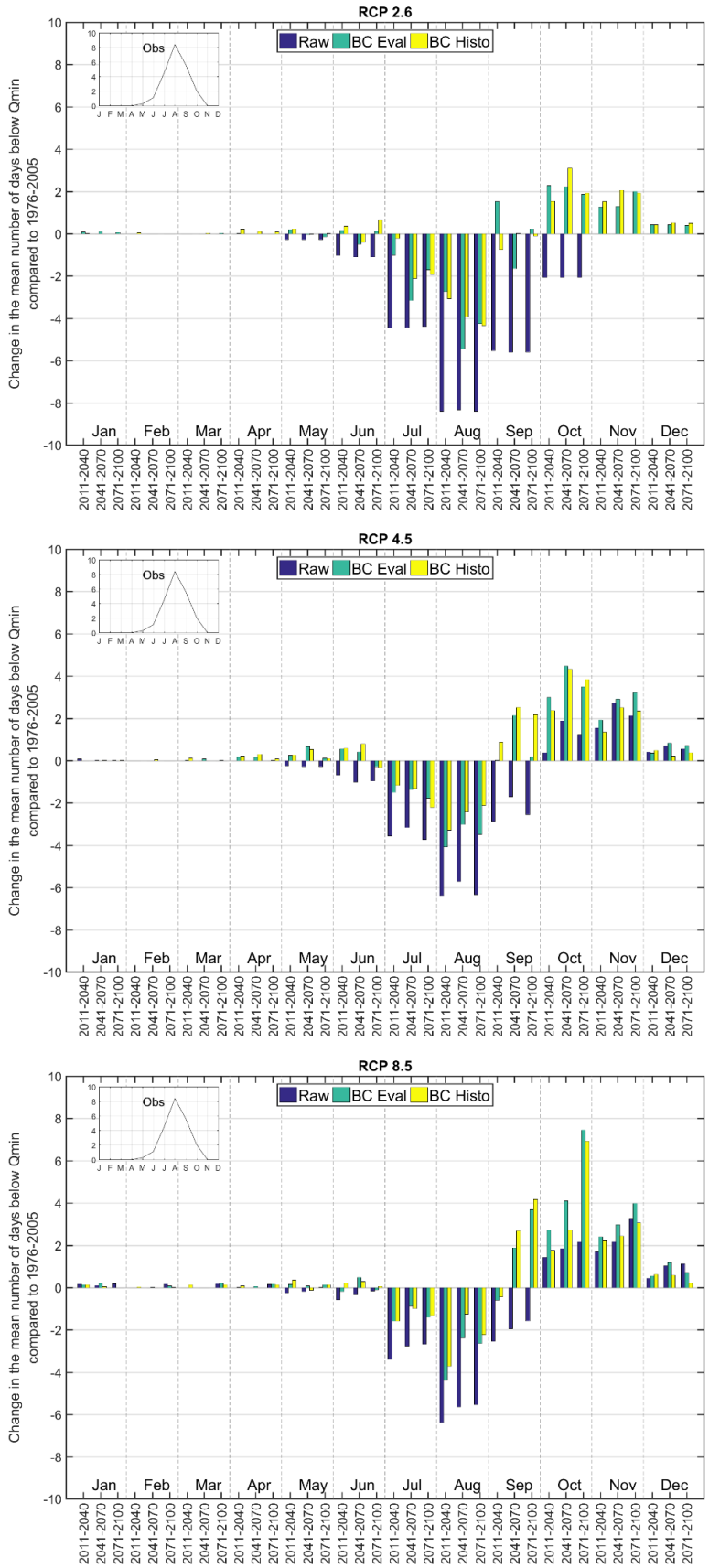

Figure A 56 Change in the monthly mean number of days below Qmin compared to 1976-2005 for the Coquet catchment for the uncorrected and bias-corrected 2.6, 4.5 and 8.5 RCP scenarios

Annex B

This annex includes the supplementary tables for all chapters

Table B 1 Regression coefficients for the trends of the uncorrected and bias corrected temperature and precipitation projections

		Temperature (°C/yr)									Precipitation (mm/yr)								
		RCP 2.6			RCP 4.5			RCP 8.5			RCP 2.6			RCP 4.5			RCP 8.5		
		Raw	BC-Eval	BC-Histo	Raw	BC-Eval	BC-Histo	Raw	BC-Eval	BC-Histo	Raw	BC-Eval	BC-Histo	Raw	BC-Eval	BC-Histo	Raw	BC-Eval	BC-Histo
Upper Thames	1976-2005	**0.05**									1.09								
	2006-2100	**0.01**	**0.01**	**0.01**	**0.02**	**0.02**	**0.02**	**0.04**	**0.04**	**0.04**	0.29	0.28	0.18	0.00	-0.08	-0.14	0.11	0.13	-0.01
Glaslyn	1976-2005	**0.04**									0.39								
	2006-2100	**0.01**	**0.00**	**0.01**	**0.02**	**0.01**	**0.02**	**0.03**	**0.03**	**0.04**	-0.13	0.00	-0.31	-0.54	-0.37	-0.46	-0.01	0.00	0.39
Calder	1976-2005	**0.04**									-2.47								
	2006-2100	**0.01**	**0.00**	**0.01**	**0.02**	**0.02**	**0.02**	**0.04**	**0.03**	**0.04**	-0.12	-0.09	-0.15	0.35	0.27	0.22	0.46	0.48	0.59
Coquet	1976-2005	**0.04**									2.35								
	2006-2100	**0.01**	**0.01**	**0.01**	**0.02**	**0.02**	**0.02**	**0.04**	**0.04**	**0.04**	-0.15	0.00	0.00	0.33	**0.50**	0.34	**0.52**	**0.80**	**0.72**

* Regression constants that are statistically significant are shown in bold (t-test, p-value < 0.05)

Table B 2 Temperature range, standard deviation and change percentage for the uncorrected and bias-corrected RCP projections

		Range (°C)									St. Dev. (°C)									Change (%)								
		RCP 2.6			RCP 4.5			RCP 8.5			RCP 2.6			RCP 4.5			RCP 8.5			RCP 2.6			RCP 4.5			RCP 8.5		
		Raw	BC-Eval	BC-Histo	Raw	BC-Eval	BC-Histo	Raw	BC-Eval	BC-Histo	Raw	BC-Eval	BC-Histo	Raw	BC-Eval	BC-Histo	Raw	BC-Eval	BC-Histo	Raw	BC-Eval	BC-Histo	Raw	BC-Eval	BC-Histo	Raw	BC-Eval	BC-Histo
Upper Thames	1976-2005	2.0									0.6																	
	2011-2040	2.0	2.3	1.3	2.1	2.0	1.4	3.2	3.5	2.6	0.3	0.3	0.4	0.3	0.3	0.3	0.4	0.4	0.4	0	7	8	2	8	9	1	7	8
	2041-2070	1.7	2.0	1.1	2.7	2.3	1.8	3.5	3.6	3.0	0.3	0.3	0.3	0.4	0.4	0.5	0.6	0.5	0.6	3	9	11	10	15	18	12	17	20
	2071-2100	1.9	2.1	1.3	2.5	2.3	1.7	4.0	3.9	3.5	0.3	0.3	0.4	0.4	0.3	0.3	0.6	0.5	0.6	3	9	11	14	19	22	27	30	36
Glaslyn	1976-2005	1.8									0.5																	
	2011-2040	2.4	2.6	1.2	2.2	2.3	1.3	2.2	2.3	1.2	0.3	0.3	0.3	0.3	0.3	0.3	0.3	0.2	0.3	6	7	8	5	7	9	7	9	11
	2041-2070	2.2	2.5	1.0	2.7	2.8	1.4	2.6	2.7	1.4	0.3	0.3	0.3	0.3	0.3	0.3	0.5	0.5	0.5	10	11	13	14	15	18	19	20	24
	2071-2100	2.1	2.4	1.1	2.6	2.7	1.5	2.8	2.9	1.8	0.3	0.3	0.3	0.3	0.3	0.3	0.4	0.4	0.4	10	11	13	18	19	24	34	35	40
Calder	1976-2005	1.9									0.6																	
	2011-2040	2.3	2.2	0.9	2.1	1.8	1.1	2.2	1.9	1.1	0.4	0.3	0.4	0.3	0.3	0.3	0.4	0.4	0.4	-5	8	10	-2	10	11	0	12	13
	2041-2070	2.0	1.9	0.9	2.9	2.4	1.4	2.6	2.2	1.5	0.3	0.3	0.3	0.4	0.3	0.4	0.5	0.5	0.6	-2	11	13	5	17	19	11	22	25
	2071-2100	2.1	2.0	0.9	2.6	2.2	1.5	2.9	2.4	1.9	0.3	0.3	0.4	0.3	0.3	0.3	0.5	0.5	0.5	-2	11	13	11	22	25	27	37	42
Coquet	1976-2005	1.8									0.5																	
	2011-2040	2.4	2.3	0.9	2.2	2.1	1.1	2.4	2.1	1.1	0.3	0.3	0.3	0.3	0.3	0.3	0.3	0.3	0.3	-3	7	10	-1	9	12	1	11	14
	2041-2070	2.1	2.0	0.7	2.9	2.5	1.2	2.7	2.3	1.2	0.3	0.2	0.3	0.3	0.3	0.4	0.5	0.5	0.6	1	11	14	9	18	22	14	22	27
	2071-2100	2.1	2.0	0.8	2.6	2.3	1.3	2.8	2.4	1.4	0.3	0.3	0.3	0.4	0.3	0.3	0.5	0.4	0.5	1	12	15	13	22	27	33	40	47

Table B 3 Coefficients of the linear regression analysis of the average annual frequency of years above the temperature threshold and number of days above the 90th and 95th precipitation percentile (statistically significant coefficients based on a t-test are shown in bold)

			Upper Thames		Glaslyn		Calder		Coquet	
	RCP	Output	1976-2005	2006-2100	1976-2005	2006-2100	1976-2005	2006-2100	1976-2005	2006-2100
Annual temperature threshold	RCP 2.6	Raw	0.003	0.001	N/A	0.001	N/A	0.000	N/A	0.000
		BC-Eval		**0.007**		**0.005**		**0.001**		**0.004**
		BC-Histo		**0.008**		**0.010**		**0.006**		**0.013**
	RCP 4.5	Raw		0.001		**0.001**		0.000		0.000
		BC-Eval		**0.006**		**0.005**		**0.003**		**0.005**
		BC-Histo		**0.006**		**0.009**		**0.010**		**0.012**
	RCP 8.5	Raw		**0.004**		**0.004**		0.000		0.001
		BC-Eval		**0.008**		**0.009**		**0.003**		**0.010**
		BC-Histo		**0.007**		**0.010**		**0.013**		**0.014**
90th Precip. Percentile	RCP 2.6	Raw	0.23	0.02	-0.03	0.00	**-0.30**	0.00	0.07	-0.01
		BC-Eval		0.02		-0.01		0.01		0.00
		BC-Histo		0.02		-0.01		0.00		0.00
	RCP 4.5	Raw		0.01		0.00		0.03		0.02
		BC-Eval		0.00		-0.01		**0.03**		0.03
		BC-Histo		0.00		-0.01		**0.03**		**0.03**
	RCP 8.5	Raw		0.01		**0.03**		**0.06**		**0.04**
		BC-Eval		0.01		0.02		**0.05**		**0.05**
		BC-Histo		0.00		**0.03**		**0.05**		**0.04**
95th Precip. Percentile	RCP 2.6	Raw	0.21	0.02	-0.03	0.00	-0.07	0.01	0.06	0.00
		BC-Eval		0.01		0.00		0.00		0.00
		BC-Histo		0.01		0.01		0.00		0.00
	RCP 4.5	Raw		0.01		0.00		**0.03**		**0.02**
		BC-Eval		0.00		0.00		**0.02**		**0.02**
		BC-Histo		0.00		0.00		**0.02**		**0.02**
	RCP 8.5	Raw		**0.04**		**0.03**		**0.06**		**0.04**
		BC-Eval		**0.04**		**0.04**		**0.05**		**0.05**
		BC-Histo		**0.03**		**0.03**		**0.04**		**0.04**

Table B 4 Precipitation range, standard deviation and change percentage for the uncorrected and bias-corrected RCP projections

		Range (mm/yr)									St. Dev. (mm/yr)									Change (%)								
		RCP 2.6			RCP 4.5			RCP 8.5			RCP 2.6			RCP 4.5			RCP 8.5			RCP 2.6			RCP 4.5			RCP 8.5		
		Raw	BC-Eval	BC-Histo	Raw	BC-Eval	BC-Histo	Raw	BC-Eval	BC-Histo	Raw	BC-Eval	BC-Histo	Raw	BC-Eval	BC-Histo	Raw	BC-Eval	BC-Histo	Raw	BC-Eval	BC-Histo	Raw	BC-Eval	BC-Histo	Raw	BC-Eval	BC-Histo
Upper Thames	1976-2005	453									110																	
	2011-2040	450	303	371	578	350	281	546	314	273	72	63	61	49	46	51	76	66	71	31	2	-4	29	4	6	27	3	4
	2041-2070	455	305	369	577	311	245	629	364	284	52	46	45	65	58	58	80	70	75	34	5	-1	24	1	1	25	1	2
	2071-2100	408	317	347	544	319	299	622	353	300	64	65	55	81	67	63	71	63	67	34	4	-2	29	4	5	30	5	6
Glaslyn	1976-2005	1441									365																	
	2011-2040	608	877	957	759	1358	1084	748	1058	1097	119	172	165	139	185	177	151	231	219	-23	4	-6	-19	5	-3	-19	10	-3
	2041-2070	736	1032	1117	688	1211	905	839	1252	1239	155	225	207	126	177	180	148	225	204	-22	6	-5	-21	3	-5	-21	7	-5
	2071-2100	646	924	950	669	1159	972	817	1254	1170	115	160	151	155	229	209	137	211	183	-23	4	-7	-20	4	-3	-19	10	-2
Calder	1976-2005	717									172																	
	2011-2040	609	378	357	773	441	446	736	377	374	84	74	79	94	89	92	103	92	97	28	-2	-1	24	-1	2	24	-1	2
	2041-2070	594	361	332	763	423	379	832	435	427	102	92	94	86	79	81	118	112	114	29	-1	0	22	-3	0	22	-3	1
	2071-2100	675	372	331	755	418	387	868	498	501	74	70	72	106	79	84	131	111	118	27	-2	-2	25	1	3	27	3	6
Coquet	1976-2005	563									123																	
	2011-2040	547	366	302	789	412	359	814	389	369	72	84	82	63	67	64	62	63	63	23	6	5	27	4	7	28	6	7
	2041-2070	581	310	321	809	400	382	823	414	385	92	98	94	53	56	56	75	83	82	26	9	8	26	4	6	26	5	7
	2071-2100	526	341	300	766	377	335	925	509	427	95	83	88	75	77	82	64	68	64	22	5	5	29	7	9	30	10	11

Table B 5 Regression coefficients for the trends of the uncorrected and bias corrected river flow an hydropower generation projections

		River flow (cumecs/yr)									Hydropower generation (MWh/yr)								
		RCP 2.6			RCP 4.5			RCP 8.5			RCP 2.6			RCP 4.5			RCP 8.5		
		Raw	BC-Eval	BC-Histo	Raw	BC-Eval	BC-Histo	Raw	BC-Eval	BC-Histo	Raw	BC-Eval	BC-Histo	Raw	BC-Eval	BC-Histo	Raw	BC-Eval	BC-Histo
Upper Thames	1976-2005	0.020									-1.933								
	2006-2100	0.029	**0.025**	0.017	-0.010	-0.018	-0.018	-0.016	0.003	-0.011	-0.290	0.975	0.705	**-1.101**	-0.432	-0.758	**-1.286**	-0.103	-0.440
Glaslyn	1976-2005	0.006									2.660								
	2006-2100	0.001	0.001	0.001	-0.001	-0.001	-0.001	**0.003**	0.003	0.004	0.392	0.172	0.124	-0.425	-0.329	-0.312	**1.029**	0.006	0.450
Calder	1976-2005	-0.014									-0.936								
	2006-2100	-0.002	-0.003	-0.003	0.002	-0.001	-0.001	0.005	0.002	0.002	-0.135	-0.148	-0.180	-0.138	-0.205	-0.167	**-0.347**	-0.174	-0.237
Coquet	1976-2005	-0.011									-0.603								
	2006-2100	-0.005	-0.001	0.000	0.000	0.001	0.000	0.003	0.002	0.001	-0.233	0.011	0.023	-0.061	-0.025	-0.078	-0.044	-0.086	-0.036

Table B 6 River flow range, standard deviation and change percentage for the uncorrected and bias-corrected RCP projections

		Range (cumecs)									St. Dev. (cumecs)									Change (%)								
		RCP 2.6			RCP 4.5			RCP 8.5			RCP 2.6			RCP 4.5			RCP 8.5			RCP 2.6			RCP 4.5			RCP 8.5		
		Raw	BC-Eval	BC-Histo	Raw	BC-Eval	BC-Histo	Raw	BC-Eval	BC-Histo	Raw	BC-Eval	BC-Histo	Raw	BC-Eval	BC-Histo	Raw	BC-Eval	BC-Histo	Raw	BC-Eval	BC-Histo	Raw	BC-Eval	BC-Histo	Raw	BC-Eval	BC-Histo
Upper Thames	1976-2005					19.8									4.4													
	2011-2040	30.2	16.4	17.4	40.8	19.9	14.7	40.6	19.1	15.8	4.5	3.4	2.8	2.6	2.2	2.4	4.2	3.2	3.7	139	5	-13	129	15	11	115	9	11
	2041-2070	31.2	17.2	18.7	43.5	16.4	13.0	41.0	17.6	13.2	4.0	2.5	2.4	3.9	2.7	2.7	3.9	2.8	3.1	147	15	-7	112	0	-5	106	7	3
	2071-2100	28.0	18.1	19.2	36.7	17.1	15.0	38.1	17.1	13.7	4.7	3.8	3.2	4.7	3.2	3.1	4.3	3.1	2.7	153	17	-5	122	9	5	111	15	11
Glaslyn	1976-2005					3.4									0.8													
	2011-2040	1.7	2.2	2.4	2.3	3.5	3.1	2.3	3.0	3.2	0.3	0.4	0.4	0.4	0.4	0.5	0.4	0.7	0.6	-34	6	-8	-29	7	-2	-30	14	-3
	2041-2070	2.4	2.8	3.1	1.9	3.1	2.4	2.3	3.2	3.3	0.4	0.6	0.6	0.3	0.4	0.4	0.4	0.6	0.6	-31	10	-4	-31	5	-4	-31	11	-4
	2071-2100	2.2	2.2	2.5	2.0	3.0	2.6	2.4	3.6	3.2	0.3	0.4	0.4	0.4	0.6	0.5	0.4	0.5	0.5	-33	7	-8	-30	7	-2	-27	17	1
Calder	1976-2005					6.7									1.6													
	2011-2040	6.3	4.4	4.1	10.4	5.0	5.3	9.9	4.7	4.3	0.9	0.8	0.8	0.9	1.0	1.1	1.1	1.1	1.1	56	-4	-3	47	-3	1	46	-3	1
	2041-2070	6.4	4.2	4.0	10.0	4.6	4.5	10.7	4.9	4.7	1.0	1.0	1.1	0.9	0.8	0.9	1.3	1.2	1.2	59	-2	-2	44	-7	-4	47	-5	-1
	2071-2100	6.9	4.5	4.0	9.3	4.6	4.4	10.9	5.5	5.4	0.9	0.8	0.9	1.2	0.9	1.0	1.4	1.3	1.4	55	-5	-4	49	-2	2	52	2	6
Coquet	1976-2005					5.2									1.2													
	2011-2040	4.7	4.5	3.3	8.3	5.1	4.4	9.4	5.0	4.2	0.9	0.9	0.9	0.7	0.7	0.6	0.8	0.9	0.8	59	13	9	54	12	11	55	13	11
	2041-2070	4.7	3.7	3.7	9.0	4.9	4.4	9.3	4.6	4.5	1.1	1.1	1.0	0.7	0.7	0.8	0.8	0.9	0.9	60	19	14	48	7	6	50	8	8
	2071-2100	4.4	3.9	3.5	8.5	4.8	4.2	10.3	6.1	5.0	0.9	0.8	1.0	0.7	0.9	0.9	0.9	0.8	0.8	54	12	8	55	14	10	56	14	11

Table B 7 Coefficients of the linear regression analysis of the average annual daily frequency of days above the Q10 and Qmax and days below the Q95 Qmin (statistically significant coefficients based on a t-test are shown in bold, p-value < 0.05)

			Upper Thames		Glaslyn		Calder		Coquet	
	RCP	Output	1976-2005	2006-2100	1976-2005	2006-2100	1976-2005	2006-2100	1976-2005	2006-2100
Q10 River Flow	RCP 2.6	Raw	0.59	**0.26**	0.18	0.01	-0.14	-0.01	-0.11	-0.11
		BC-Eval		**0.15**		0.00		-0.01		-0.02
		BC-Histo		0.11		0.01		-0.01		0.02
	RCP 4.5	Raw		-0.12		0.00		0.06		-0.02
		BC-Eval		-0.11		0.00		0.03		0.02
		BC-Histo		-0.10		-0.01		0.03		0.02
	RCP 8.5	Raw		-0.10		**0.06**		0.09		0.10
		BC-Eval		0.13		0.04		0.06		0.06
		BC-Histo		0.01		**0.05**		0.05		0.06
Q95 River Flow	RCP 2.6	Raw	0.39	0.04	-0.88	0.03	-0.22	0.01	0.13	0.00
		BC-Eval		-0.06		0.00		0.10		0.00
		BC-Histo		-0.14		0.00		0.14		0.06
	RCP 4.5	Raw		0.02		0.04		0.01		0.01
		BC-Eval		0.10		0.03		0.14		0.03
		BC-Histo		0.12		0.04		0.09		0.05
	RCP 8.5	Raw		0.06		0.09		0.06		**0.13**
		BC-Eval		**0.24**		**0.06**		0.03		**0.21**
		BC-Histo		**0.24**		**0.11**		0.03		**0.20**
Days above Qmax	RCP 2.6	Raw	0.155	**0.141**	-0.022	**0.002**	-0.059	0.006	-0.021	-0.009
		BC-Eval		0.017		0.002		-0.001		-0.006
		BC-Histo		0.006		0.000		0.004		-0.002
	RCP 4.5	Raw		0.083		-0.001		0.012		0.007
		BC-Eval		-0.023		0.000		0.003		**0.021**
		BC-Histo		-0.006		0.001		0.001		**0.014**
	RCP 8.5	Raw		0.009		0.001		**0.051**		**0.025**
		BC-Eval		0.015		**0.009**		**0.021**		**0.036**
		BC-Histo		0.001		**0.006**		**0.027**		**0.025**
Days below Qmin	RCP 2.6	Raw	0.388	0.035	0.500	-0.040	-0.071	0.000	0.134	0.000
		BC-Eval		-0.057		-0.042		0.033		0.004
		BC-Histo		-0.140		-0.016		0.022		0.064
	RCP 4.5	Raw		0.022		0.082		-0.006		0.015
		BC-Eval		0.099		0.061		0.021		0.030
		BC-Histo		0.116		0.057		0.012		0.049
	RCP 8.5	Raw		0.064		-0.016		0.023		**0.129**
		BC-Eval		**0.240**		0.064		0.022		**0.215**
		BC-Histo		**0.239**		0.032		0.014		**0.199**

Table B 8 Hydropower generation range, standard deviation and change percentage for the uncorrected and bias-corrected RCP projections

		Range (MWh)									St. Dev. (MWh)									Change (%)								
		RCP 2.6			RCP 4.5			RCP 8.5			RCP 2.6			RCP 4.5			RCP 8.5			RCP 2.6			RCP 4.5			RCP 8.5		
		Raw	BC-Eval	BC-Histo	Raw	BC-Eval	BC-Histo	Raw	BC-Eval	BC-Histo	Raw	BC-Eval	BC-Histo	Raw	BC-Eval	BC-Histo	Raw	BC-Eval	BC-Histo	Raw	BC-Eval	BC-Histo	Raw	BC-Eval	BC-Histo	Raw	BC-Eval	BC-Histo
Upper Thames	1976-2005	709									181																	
	2011-2040	528	731	849	968	825	652	990	817	672	90	150	131	90	108	107	121	136	138	91	11	-8	81	21	18	71	15	16
	2041-2070	650	740	919	936	754	607	962	707	565	113	115	112	128	122	122	125	141	143	94	22	-1	65	8	3	64	12	10
	2071-2100	540	775	921	821	722	659	829	704	589	102	138	136	130	127	123	111	138	123	90	22	1	72	17	11	61	19	17
Glaslyn	1976-2005	953									242																	
	2011-2040	491	628	679	688	1038	860	714	894	873	90	121	108	113	131	128	137	197	170	-39	11	-7	-32	14	1	-33	21	0
	2041-2070	697	784	828	612	979	681	729	958	889	133	171	157	108	138	136	138	172	157	-34	14	-3	-34	11	-2	-34	16	-3
	2071-2100	665	697	713	604	900	728	731	957	844	109	112	108	129	172	156	121	155	145	-37	11	-6	-33	12	0	-28	21	2
Calder	1976-2005	178									51																	
	2011-2040	179	180	152	355	194	176	349	192	164	26	30	28	23	34	34	34	38	39	52	1	0	43	2	2	42	1	2
	2041-2070	193	166	150	373	194	174	379	197	171	22	38	39	27	34	32	38	41	40	53	2	0	38	-4	-3	40	-2	-1
	2071-2100	219	191	158	331	184	156	359	202	166	28	30	32	41	37	40	38	48	45	51	1	-1	41	1	1	38	1	1
Coquet	1976-2005	204									50																	
	2011-2040	214	202	160	405	232	211	427	234	198	42	37	41	32	29	29	35	40	37	78	22	18	73	22	22	71	23	20
	2041-2070	199	165	170	404	214	205	443	210	200	48	48	46	32	35	39	42	41	39	78	28	23	64	17	16	68	17	17
	2071-2100	193	169	159	396	198	188	447	256	216	42	38	46	31	35	38	37	30	34	74	21	18	72	22	19	68	20	18

Table B 9 Projected mean changes in the hydropower generation for the upper Thames scheme (MWh). Statistically significant changes are shown in red based in an analysis of the average change and the standard deviation

		RCP 26 Mean			RCP 26 StDev			RCP 45 Mean			RCP 45 StDev			RCP 85 Mean			RCP 85 StDev		
		Raw	Eval	Histo	Raw	Eval	Histo	Raw	Eval	Histo	Raw	Eval	Histo	Raw	Eval	Histo	Raw	Eval	Histo
Jan	2011-2040	**21.6**	0.3	-9.7	19.6	22.6	21.8	14.4	8.8	13.4	18.7	22.9	20.7	6.6	1.5	4.9	16.4	31.8	28.1
	2041-2070	19.2	5.6	-9.0	20.1	26.3	24.9	6.8	-2.7	-1.2	17.2	25.7	23.4	1.7	-3.2	-0.5	24.1	27.5	24.7
	2071-2100	14.9	1.2	-11.2	20.6	19.5	20.7	11.3	5.6	4.3	23.0	19.9	18.6	3.7	12.6	13.0	22.9	25.5	23.8
Feb	2011-2040	**33.0**	11.5	-4.5	13.0	20.0	16.6	**29.0**	**24.1**	**23.4**	14.7	17.9	19.2	**29.1**	17.7	12.6	18.9	24.0	24.5
	2041-2070	**30.1**	13.5	-6.5	18.5	25.6	25.3	**21.8**	14.8	8.7	19.2	26.9	25.1	**23.8**	14.3	10.3	22.3	24.7	24.2
	2071-2100	**27.4**	16.4	-2.6	17.3	20.4	20.1	**19.8**	**19.0**	12.2	18.8	19.5	20.8	17.8	22.5	18.6	24.3	26.2	26.6
Mar	2011-2040	**32.6**	-0.5	-20.5	17.7	24.4	20.7	**30.3**	10.2	4.5	16.1	20.4	23.7	**30.6**	4.3	-2.3	17.0	25.2	27.2
	2041-2070	**29.9**	-1.6	-22.8	23.9	26.2	24.3	**26.3**	4.7	-4.7	19.0	25.2	25.8	**28.5**	4.2	-3.6	17.9	23.7	23.3
	2071-2100	**34.3**	3.5	-16.6	16.6	23.0	20.8	**25.2**	4.3	-4.9	18.8	23.0	23.3	22.4	11.8	6.3	23.1	29.4	30.2
Apr	2011-2040	**39.9**	-7.0	-21.6	20.9	25.2	26.0	**39.4**	4.6	5.4	15.8	15.0	19.1	**38.7**	-0.9	0.6	17.0	22.8	26.8
	2041-2070	**42.2**	-0.3	-14.8	19.3	25.9	26.2	**37.4**	2.1	-0.3	22.8	23.7	25.7	**41.3**	5.1	7.7	15.9	23.9	29.2
	2071-2100	**50.8**	3.9	-10.9	18.3	23.3	21.3	**41.3**	8.0	4.9	20.7	20.2	21.5	**38.7**	12.5	17.4	25.1	24.2	26.4
May	2011-2040	**63.5**	9.1	-8.6	19.4	21.2	21.7	**58.0**	**21.7**	11.9	17.3	17.5	20.0	**62.1**	17.9	14.1	16.4	19.9	21.5
	2041-2070	**68.9**	20.4	1.9	17.2	22.0	22.6	**53.7**	19.0	12.2	23.9	22.7	25.7	**60.9**	25.5	21.4	23.8	25.5	26.7
	2071-2100	**69.2**	22.4	5.1	22.8	28.4	23.2	**56.3**	19.9	14.3	20.7	26.0	26.6	**54.3**	**25.6**	**21.3**	29.1	24.7	20.1
Jun	2011-2040	**64.8**	14.5	0.1	22.2	18.0	15.8	**65.3**	**20.7**	8.5	16.9	19.8	15.2	**58.7**	**20.3**	10.6	17.7	17.8	17.4
	2041-2070	**82.3**	**23.1**	3.9	19.7	16.3	13.3	**60.8**	17.9	6.6	19.9	19.2	14.7	**65.5**	**23.7**	11.0	20.3	14.9	14.4
	2071-2100	**71.3**	**19.8**	7.1	22.9	17.1	12.3	**57.8**	**20.0**	10.3	19.5	16.5	17.0	**58.1**	**25.2**	13.5	19.0	18.7	15.5
Jul	2011-2040	**74.6**	12.8	3.0	18.6	14.2	11.1	**72.8**	**17.0**	8.0	16.0	14.0	10.9	**59.6**	**19.1**	13.2	21.6	14.5	14.4
	2041-2070	**83.1**	**25.1**	7.9	19.4	17.7	11.9	**60.8**	**14.7**	5.3	22.3	12.3	10.3	**63.7**	**17.5**	8.9	17.7	13.1	11.9
	2071-2100	**76.1**	**20.5**	9.8	22.0	18.4	12.5	**65.4**	**19.2**	11.1	19.8	16.2	13.1	**62.0**	**17.3**	9.1	17.5	16.0	12.1
Aug	2011-2040	**71.2**	10.1	1.6	14.4	17.3	10.8	**65.1**	12.0	5.5	15.9	12.2	12.0	**55.9**	13.7	9.1	21.8	13.7	12.5
	2041-2070	**74.1**	**17.7**	7.3	11.9	16.3	12.3	**52.3**	8.9	2.1	21.6	11.4	9.1	**47.8**	5.8	2.0	20.0	9.6	9.1
	2071-2100	**69.1**	17.5	8.0	12.1	18.7	12.8	**57.4**	8.8	4.0	18.6	8.9	7.6	**45.7**	5.2	0.5	20.0	11.8	9.1
Sep	2011-2040	**65.0**	12.0	4.3	22.6	18.0	12.3	**57.7**	**12.5**	9.0	16.4	11.9	14.3	**49.9**	12.0	9.7	18.6	13.4	13.8
	2041-2070	**63.8**	13.0	8.0	24.5	13.3	11.4	**46.6**	5.3	0.6	20.2	11.8	8.9	**34.0**	2.5	0.6	19.3	8.9	7.7
	2071-2100	**64.0**	**19.0**	8.6	24.6	16.8	14.1	**46.4**	4.0	2.7	18.6	8.4	9.0	**33.1**	0.7	-2.1	19.9	8.4	9.1
Oct	2011-2040	**56.7**	9.0	3.1	20.3	18.4	17.1	**51.7**	6.4	10.4	18.7	16.2	19.1	**44.5**	2.2	10.3	20.9	14.0	19.4
	2041-2070	**59.6**	10.7	5.7	21.1	19.1	15.9	**37.7**	-4.3	-2.7	15.8	14.3	15.8	**28.6**	-3.1	-0.6	21.7	15.5	18.5
	2071-2100	**55.1**	13.6	8.4	21.2	17.6	16.9	**36.5**	-2.4	0.8	19.8	13.4	18.0	**24.7**	-7.0	-5.7	16.3	10.5	13.0
Nov	2011-2040	**52.6**	1.4	1.9	18.1	20.6	18.0	**38.6**	-0.1	12.0	18.9	23.5	28.6	**26.8**	-5.1	10.1	21.9	19.5	21.6
	2041-2070	**51.4**	9.7	8.1	19.3	21.6	20.8	**23.2**	-11.7	-3.2	17.5	18.0	22.9	**26.7**	-6.5	5.5	22.8	22.7	30.2
	2071-2100	**37.5**	1.9	0.7	25.7	18.7	20.3	**26.0**	-7.6	-0.5	17.7	18.2	24.1	**23.7**	-5.7	2.1	19.9	22.4	23.5
Dec	2011-2040	**39.3**	1.7	-0.3	16.7	25.5	22.6	**24.9**	3.2	12.3	20.1	26.6	23.7	16.8	-1.0	12.5	20.7	33.5	31.5
	2041-2070	**35.1**	12.0	1.9	18.1	25.3	22.3	15.2	-13.4	-5.3	19.8	22.7	27.4	14.6	-2.7	6.8	20.9	29.0	30.9
	2071-2100	**26.3**	-1.5	-9.3	24.6	22.1	24.6	15.4	-1.8	4.3	21.9	28.5	27.6	10.5	0.5	8.3	26.2	27.9	24.2

Table B 10 Projected mean changes in the hydropower generation for the Glaslyn scheme (MWh). Statistically significant changes are shown in red based in an analysis of the average change and the standard deviation

		RCP 26 Mean			RCP 26 StDev			RCP 45 Mean			RCP 45 StDev			RCP 85 Mean			RCP 85 StDev		
		Raw	Eval	Histo	Raw	Eval	Histo	Raw	Eval	Histo	Raw	Eval	Histo	Raw	Eval	Histo	Raw	Eval	Histo
Jan	2011-2040	-23.7	21.4	0.0	27.4	28.5	30.8	-5.1	**49.8**	21.2	35.8	42.7	44.6	-17.6	35.4	0.5	33.0	43.4	40.1
	2041-2070	-28.9	12.4	-9.5	40.4	45.0	43.0	-16.5	34.4	6.3	34.5	41.0	42.0	-24.9	25.3	-7.2	42.8	44.6	47.6
	2071-2100	-27.7	14.3	-9.2	49.7	53.8	50.7	-11.1	43.0	16.0	45.7	48.4	48.1	5.6	**54.9**	26.0	36.4	41.0	41.2
Feb	2011-2040	-21.8	16.7	15.1	36.6	41.5	41.9	-6.1	**40.6**	35.9	34.2	39.4	37.3	-6.2	44.7	33.9	37.5	47.7	44.5
	2041-2070	-25.4	5.4	1.7	37.9	45.1	46.2	-8.9	37.9	32.3	32.4	40.5	41.1	-4.1	**44.3**	36.6	33.9	39.3	38.3
	2071-2100	-10.2	27.4	21.5	44.8	49.7	50.4	-19.0	30.3	23.8	32.7	36.4	32.9	-5.5	37.9	30.5	36.9	44.4	43.6
Mar	2011-2040	**-58.4**	2.2	-16.5	26.9	36.9	34.1	**-52.0**	0.2	-8.6	29.7	36.1	35.2	**-56.0**	13.3	-8.2	30.6	44.4	40.0
	2041-2070	**-50.5**	4.1	-12.4	34.2	49.9	44.4	**-49.5**	10.5	-0.5	20.3	32.1	33.8	**-49.3**	16.4	-1.0	34.5	46.4	42.4
	2071-2100	**-62.3**	-5.5	-25.4	27.7	39.0	35.6	**-55.2**	-1.6	-6.9	34.0	44.7	43.4	**-35.9**	30.7	11.3	31.1	37.2	36.1
Apr	2011-2040	**-54.0**	1.2	-13.2	14.5	29.3	23.1	**-47.3**	-0.5	-2.9	21.3	31.8	29.6	**-44.8**	19.4	2.0	16.7	31.8	28.0
	2041-2070	**-42.6**	22.6	10.3	18.6	35.4	30.3	**-36.9**	12.0	8.0	17.9	26.1	27.0	**-35.3**	31.6	12.6	22.9	38.2	32.8
	2071-2100	**-44.4**	14.3	-2.2	21.3	32.8	32.1	**-44.8**	0.4	-1.7	22.0	29.9	28.3	**-38.7**	**28.3**	8.8	19.1	24.7	23.5
May	2011-2040	**-40.1**	3.7	-11.1	10.3	18.0	16.8	**-32.7**	6.2	-5.5	13.4	23.4	20.5	**-38.1**	6.8	-9.8	11.0	25.1	18.9
	2041-2070	**-34.8**	11.7	-1.4	20.2	29.6	29.1	**-36.0**	4.2	-5.7	13.5	25.0	24.4	**-33.4**	13.3	-5.5	16.0	25.9	21.8
	2071-2100	**-38.1**	6.4	-10.6	15.5	26.7	22.5	**-35.5**	1.3	-7.7	12.2	18.8	17.2	**-32.5**	13.5	-4.5	12.1	19.3	16.0
Jun	2011-2040	**-41.2**	-2.3	-15.8	13.2	29.9	25.0	**-35.9**	-3.9	-9.9	15.2	22.3	21.0	**-38.1**	-1.8	-11.8	11.2	23.7	20.7
	2041-2070	**-31.3**	10.7	-3.6	20.2	32.6	29.1	**-37.1**	-2.9	-10.5	13.5	22.4	22.1	**-41.3**	-10.9	**-18.7**	10.9	19.1	18.4
	2071-2100	**-37.2**	4.5	-10.6	12.6	23.6	18.6	**-39.1**	-6.6	-12.5	12.3	23.2	21.1	**-40.6**	-6.9	-17.7	10.9	21.7	17.8
Jul	2011-2040	**-28.5**	14.5	-6.5	14.9	24.4	19.4	**-31.3**	2.0	-9.2	10.2	17.9	15.8	**-34.4**	1.2	-13.5	12.1	23.5	18.2
	2041-2070	**-23.9**	18.2	-2.3	22.3	33.3	30.2	**-34.6**	-6.1	-14.6	15.9	24.7	22.8	**-33.0**	-6.1	-14.9	14.5	19.6	19.8
	2071-2100	**-27.6**	8.5	-6.9	17.9	28.6	24.0	**-32.9**	-5.0	-13.2	11.8	19.1	18.8	**-43.1**	-19.7	**-31.3**	12.1	20.4	17.7
Aug	2011-2040	**-59.3**	8.6	**-30.8**	18.2	37.2	28.2	**-58.9**	-3.8	**-29.2**	15.8	26.7	23.4	**-58.9**	4.8	**-29.9**	16.2	29.7	23.9
	2041-2070	**-59.6**	2.2	**-32.6**	19.8	28.6	21.8	**-60.8**	-6.9	**-32.6**	12.1	23.2	17.9	**-63.8**	-14.9	**-42.6**	15.0	30.7	21.8
	2071-2100	**-59.0**	8.6	**-30.1**	17.7	30.1	24.3	**-58.9**	-8.5	**-32.2**	13.6	22.9	20.2	**-74.3**	-37.0	**-59.3**	10.4	19.9	13.2
Sep	2011-2040	**-65.3**	-2.9	**-29.8**	19.1	32.0	26.1	**-60.0**	-6.3	-21.5	22.1	33.5	31.7	**-58.8**	6.5	-22.3	17.9	33.9	26.0
	2041-2070	**-66.6**	-6.7	**-31.0**	20.1	29.5	26.6	**-65.9**	-19.2	**-33.0**	20.2	29.0	27.0	**-61.7**	-3.9	-25.8	20.7	35.0	29.6
	2071-2100	**-59.0**	0.4	-26.7	21.8	33.7	27.5	**-66.6**	-15.9	**-32.0**	17.4	29.3	26.3	**-64.7**	-13.1	**-34.9**	18.4	31.1	26.1
Oct	2011-2040	**-91.1**	-4.2	-22.9	23.8	41.7	32.2	**-87.8**	-17.6	-26.8	29.4	36.3	37.2	**-85.5**	-6.6	-28.9	28.8	41.4	40.4
	2041-2070	**-87.9**	-11.6	-27.1	34.0	49.4	42.3	**-88.4**	-22.5	**-32.5**	25.0	33.6	31.3	**-85.8**	-2.1	-24.6	25.3	36.0	32.7
	2071-2100	**-92.4**	-17.1	-32.4	28.1	41.2	39.3	**-90.6**	-22.3	**-31.0**	23.1	30.9	30.2	**-85.5**	-3.5	-29.6	21.8	36.6	33.0
Nov	2011-2040	**-103.8**	-13.3	**-38.8**	22.6	35.5	32.3	**-89.5**	-9.0	-31.3	27.4	32.7	33.2	**-71.2**	26.2	-11.7	34.1	45.7	42.2
	2041-2070	**-87.3**	-3.2	-26.3	31.2	39.4	36.7	**-100.6**	-26.0	**-45.4**	26.9	34.3	34.4	**-95.7**	-6.0	-40.8	30.7	44.4	42.1
	2071-2100	**-112.9**	**-39.8**	**-57.2**	21.0	30.1	23.3	**-90.4**	-13.4	**-35.5**	30.9	39.2	37.7	**-78.0**	11.8	-20.5	24.4	34.3	31.0
Dec	2011-2040	**-64.7**	10.6	-25.0	33.3	38.7	35.7	**-45.7**	27.3	-7.6	31.3	34.1	35.9	**-55.2**	28.4	-15.8	35.4	43.6	43.1
	2041-2070	**-53.9**	17.1	-15.6	41.0	47.4	42.1	**-52.7**	20.0	-14.5	28.4	33.2	34.8	**-56.3**	26.6	-19.5	29.8	34.1	34.3
	2071-2100	**-69.0**	0.4	-32.5	44.8	53.1	50.1	**-44.1**	28.6	-5.5	30.3	35.4	34.4	-20.1	58.3	18.7	34.3	40.5	39.5

Table B 11 Projected mean changes in the hydropower generation for the Calder scheme (MWh). Statistically significant changes are shown in red based in an analysis of the average change and the standard deviation

		RCP 26 Mean			RCP 26 StDev			RCP 45 Mean			RCP 45 StDev			RCP 85 Mean			RCP 85 StDev		
		Raw	Eval	Histo	Raw	Eval	Histo	Raw	Eval	Histo	Raw	Eval	Histo	Raw	Eval	Histo	Raw	Eval	Histo
Jan	2011-2040	**6.6**	-2.8	-5.1	6.4	7.6	7.8	**8.5**	1.6	-1.2	7.2	10.1	9.6	4.6	-3.0	-5.2	6.9	8.3	8.3
	2041-2070	6.2	-4.8	-7.0	7.2	10.5	10.8	5.5	-0.9	-3.0	5.9	6.9	7.1	4.7	-3.2	-5.2	6.7	9.5	9.9
	2071-2100	**7.0**	-3.9	-6.3	5.4	8.6	8.6	5.9	-0.7	-3.0	7.0	9.1	8.8	6.0	1.6	-0.5	7.1	9.4	9.0
Feb	2011-2040	**9.5**	-1.4	1.9	7.9	9.3	8.3	**12.0**	2.2	5.6	6.2	7.5	7.2	**11.9**	3.2	6.4	6.3	9.2	8.8
	2041-2070	**8.0**	-4.6	-1.6	7.5	9.4	9.5	**10.9**	1.7	5.1	6.1	7.4	7.1	**11.2**	1.8	4.9	6.2	8.0	7.0
	2071-2100	**9.9**	-1.6	1.9	5.8	7.3	7.0	**9.4**	0.2	3.3	6.7	8.0	7.2	8.0	-0.5	2.4	8.0	10.0	9.3
Mar	2011-2040	6.4	-9.1	-8.5	9.2	8.9	9.4	**6.5**	-6.6	-6.7	6.4	7.3	6.7	6.1	-7.2	-7.1	7.5	9.1	8.8
	2041-2070	**9.5**	-6.3	-6.1	7.9	10.4	10.0	**7.2**	-6.3	-6.2	7.1	7.6	7.2	7.3	-7.5	-6.9	7.5	9.1	9.0
	2071-2100	**-15.0**	**-32.2**	**-31.4**	8.0	8.2	8.5	**-14.2**	**-27.7**	**-27.4**	8.1	8.3	8.6	**-12.4**	**-24.5**	**-24.5**	7.3	9.8	8.9
Apr	2011-2040	**13.6**	-3.7	-2.0	7.8	8.0	7.9	**12.2**	-2.5	-0.9	6.3	6.3	5.5	**11.8**	-2.1	-1.1	6.6	7.2	6.4
	2041-2070	**16.8**	-0.1	1.4	6.3	7.9	8.4	**12.9**	-2.7	-1.1	5.1	5.6	4.9	**14.8**	-0.1	1.1	7.7	8.5	8.5
	2071-2100	**15.6**	-0.4	0.7	9.3	9.2	9.3	**13.8**	0.1	1.4	7.6	7.9	7.9	**14.1**	0.5	1.8	6.6	7.5	7.3
May	2011-2040	**25.1**	4.4	2.3	6.4	7.8	7.0	**19.0**	2.9	2.2	7.7	8.4	7.8	**20.7**	3.1	2.8	7.1	7.5	7.6
	2041-2070	**24.5**	4.6	3.3	7.3	7.7	6.9	**18.2**	1.1	0.7	8.0	7.9	6.8	**21.8**	4.6	4.0	7.5	7.8	7.7
	2071-2100	**23.7**	3.7	2.4	7.7	7.3	7.1	**20.0**	2.6	2.2	5.7	6.1	6.0	**20.9**	4.8	4.1	5.6	6.3	6.0
Jun	2011-2040	**22.5**	4.4	3.6	6.8	5.5	5.2	**19.1**	4.2	4.2	6.4	6.2	6.2	**19.5**	**5.1**	4.6	6.1	4.9	5.3
	2041-2070	**22.6**	4.1	3.4	5.4	5.7	5.3	**17.6**	2.6	2.3	6.1	5.0	4.7	**16.7**	2.4	2.7	5.9	5.4	5.2
	2071-2100	**24.8**	**6.6**	**5.7**	6.5	4.9	5.2	**18.4**	4.2	4.0	7.4	6.0	5.8	**18.1**	4.4	4.6	6.5	5.5	5.6
Jul	2011-2040	**31.2**	**6.5**	**4.8**	6.1	5.3	4.4	**25.2**	**5.8**	**4.9**	6.0	4.8	4.2	**25.3**	**5.5**	5.3	6.9	5.0	5.5
	2041-2070	**31.4**	**7.1**	5.6	7.2	6.4	6.4	**22.0**	3.7	3.0	7.0	5.7	5.8	**22.9**	3.8	3.6	5.7	4.4	4.5
	2071-2100	**29.5**	**7.9**	**6.5**	8.4	6.0	5.8	**23.4**	**5.7**	5.1	6.3	5.6	6.1	**19.3**	3.3	2.6	5.5	4.5	4.6
Aug	2011-2040	**23.8**	5.6	1.4	5.5	8.3	7.3	**17.4**	3.2	0.6	6.4	5.9	6.1	**17.1**	2.4	-0.2	5.6	4.7	4.5
	2041-2070	**24.9**	6.6	2.0	4.5	7.0	5.5	**17.1**	0.9	-2.0	7.0	6.0	4.9	**15.1**	0.3	-2.5	7.9	6.7	5.9
	2071-2100	**24.0**	5.8	1.4	4.6	6.1	5.3	**15.7**	1.6	-0.6	6.2	6.2	5.6	**11.1**	-2.3	-4.0	6.5	4.6	3.9
Sep	2011-2040	**19.4**	1.5	-0.3	9.1	7.8	8.0	**17.5**	2.3	0.6	6.6	7.1	6.8	**15.8**	1.3	-0.6	6.6	5.7	5.8
	2041-2070	**21.0**	1.8	-0.5	6.2	4.5	4.3	**13.6**	-0.8	-2.3	5.1	5.2	6.0	**14.8**	0.4	-1.0	6.3	6.1	5.8
	2071-2100	**21.0**	4.7	2.5	9.2	8.9	8.6	**14.2**	-1.1	-2.6	8.0	6.1	5.9	**11.8**	-2.4	-4.2	6.2	5.3	4.7
Oct	2011-2040	**16.3**	1.2	3.5	8.6	11.0	10.0	**8.5**	-2.4	-0.1	5.9	7.3	7.5	**8.9**	-2.3	0.8	6.6	6.7	7.4
	2041-2070	**12.8**	-1.1	0.4	6.4	6.3	7.4	**6.8**	-5.2	-2.5	6.0	7.0	7.6	**9.0**	-3.6	-1.2	6.8	8.2	8.9
	2071-2100	**13.2**	-0.6	0.4	7.9	7.4	7.5	**8.5**	-2.9	-1.1	6.8	6.5	7.2	**9.3**	-3.2	-2.4	6.5	6.9	7.4
Nov	2011-2040	7.7	-2.3	0.6	7.7	7.6	8.6	4.1	-2.9	0.1	6.6	8.1	7.6	6.4	-0.4	3.7	7.8	9.2	8.6
	2041-2070	8.5	-1.3	0.6	6.2	7.5	7.6	1.5	-7.1	-3.5	7.2	9.4	9.3	1.9	-5.5	-2.1	8.0	9.5	9.4
	2071-2100	4.3	-5.6	-3.9	5.6	5.9	5.7	4.8	-2.0	0.8	9.2	10.2	9.5	4.4	-1.4	0.4	7.9	9.6	9.5
Dec	2011-2040	**6.7**	0.0	-2.4	5.2	6.8	6.8	4.7	0.0	-0.6	5.6	7.2	5.5	3.5	-1.5	-2.0	7.8	10.0	9.1
	2041-2070	6.3	-0.1	-2.2	7.6	9.8	9.6	3.4	-2.0	-2.1	7.8	9.0	8.6	3.7	-0.9	-1.8	7.4	9.5	8.6
	2071-2100	**6.3**	-2.2	-4.7	5.6	7.6	8.3	4.3	0.4	-0.8	5.7	6.7	6.4	4.4	2.0	1.1	6.5	7.9	7.7

Table B 12 Projected mean changes in the hydropower generation for the Coquet scheme (MWh). Statistically significant changes are shown in red based in an analysis of the average change and the standard deviation

		RCP 26 Mean			RCP 26 StDev			RCP 45 Mean			RCP 45 StDev			RCP 85 Mean			RCP 85 StDev		
		Raw	Eval	Histo	Raw	Eval	Histo	Raw	Eval	Histo	Raw	Eval	Histo	Raw	Eval	Histo	Raw	Eval	Histo
Jan	2011-2040	**9.1**	3.8	2.5	8.0	7.4	9.1	**8.8**	3.2	3.7	6.3	6.0	6.0	7.1	1.7	1.6	7.1	7.6	7.1
	2041-2070	**8.3**	4.4	2.7	7.6	9.4	8.5	**7.8**	3.9	4.6	6.7	6.7	7.5	7.0	0.9	1.9	7.4	7.2	6.3
	2071-2100	6.5	1.6	1.9	8.0	9.3	9.9	**7.9**	2.0	3.1	7.8	7.3	7.9	7.9	3.6	4.4	9.7	10.6	10.4
Feb	2011-2040	**16.3**	**10.6**	**9.7**	7.6	8.3	8.7	**16.3**	**10.4**	**11.2**	5.8	7.3	7.7	**15.5**	**9.5**	**9.3**	5.7	6.1	5.8
	2041-2070	**14.9**	**10.0**	**8.8**	7.2	6.5	6.1	**14.4**	**9.8**	**11.2**	7.3	7.1	7.5	**15.5**	**9.2**	**10.7**	7.8	7.5	7.2
	2071-2100	**15.4**	**9.6**	9.4	9.8	8.6	9.2	**13.1**	7.8	**8.8**	8.8	9.6	9.5	**13.8**	8.6	**10.7**	8.5	9.2	10.0
Mar	2011-2040	**16.3**	4.3	3.9	8.6	8.2	8.8	**15.9**	4.6	5.1	5.6	7.4	6.6	**13.6**	2.2	2.6	7.4	5.8	6.3
	2041-2070	**15.3**	6.1	5.8	8.4	9.4	9.4	**12.3**	2.2	3.2	7.0	7.2	8.0	**14.1**	1.7	3.0	7.7	7.5	7.4
	2071-2100	**13.9**	3.2	2.9	9.8	7.7	8.5	**12.8**	1.5	2.2	8.7	6.8	7.1	**13.3**	2.3	3.7	9.0	7.9	8.7
Apr	2011-2040	**16.8**	1.7	2.5	8.9	8.5	9.4	**14.0**	2.4	2.4	6.3	6.8	6.7	**15.3**	3.0	2.6	6.0	7.6	7.7
	2041-2070	**15.0**	5.3	4.9	7.9	8.9	9.1	**12.6**	1.5	1.3	5.7	7.6	7.8	**15.0**	2.9	3.8	7.9	7.7	8.6
	2071-2100	**14.9**	1.9	3.0	9.0	9.5	10.4	**14.9**	3.9	3.8	7.8	6.9	7.3	**12.6**	2.5	2.9	7.7	7.9	8.3
May	2011-2040	**22.2**	2.2	2.3	7.9	7.7	8.1	**18.4**	3.1	2.8	6.0	6.4	6.2	**19.9**	5.8	4.5	7.6	9.9	9.7
	2041-2070	**19.9**	6.2	6.2	8.5	10.5	11.4	**17.9**	2.5	2.8	5.9	7.6	8.2	**20.9**	6.1	6.0	8.8	10.3	10.1
	2071-2100	**20.2**	3.7	3.5	8.2	10.2	10.0	**19.4**	5.4	4.6	5.8	8.1	8.4	**17.8**	3.9	3.7	7.4	7.6	7.7
Jun	2011-2040	**16.4**	1.9	1.6	5.0	5.0	5.3	**18.0**	3.4	3.1	4.5	4.2	4.3	**17.3**	3.9	3.0	5.6	5.5	5.9
	2041-2070	**20.0**	5.7	5.1	4.8	6.4	7.0	**16.0**	2.4	1.8	5.0	4.4	4.7	**16.6**	2.6	2.2	5.1	4.6	5.2
	2071-2100	**18.9**	4.1	3.9	6.0	6.2	6.1	**17.7**	3.8	3.2	6.2	6.4	5.7	**17.1**	4.0	3.5	5.3	4.8	5.1
Jul	2011-2040	**21.8**	2.1	2.2	4.8	4.5	5.2	**21.4**	2.6	2.4	4.2	5.8	4.9	**20.7**	4.0	3.0	4.4	4.9	5.2
	2041-2070	**24.2**	4.6	5.1	5.9	7.2	7.7	**19.5**	1.8	0.9	5.2	3.6	4.1	**19.4**	1.4	0.8	4.0	3.7	4.2
	2071-2100	**20.7**	2.9	2.8	7.8	6.0	6.1	**20.6**	3.7	2.9	5.5	5.5	5.8	**19.1**	2.2	0.6	5.3	4.7	4.5
Aug	2011-2040	**21.6**	2.8	0.1	5.2	6.8	6.1	**19.3**	2.7	-0.3	4.9	5.5	4.7	**19.7**	4.1	0.8	5.1	5.5	4.9
	2041-2070	**22.2**	5.0	1.2	4.2	6.8	5.3	**19.6**	3.5	-0.3	5.6	5.0	4.7	**17.5**	1.0	-2.3	5.2	5.0	4.7
	2071-2100	**20.1**	3.3	-1.0	4.5	5.2	4.8	**19.4**	2.0	-1.5	4.4	4.6	4.2	**17.3**	0.8	-2.8	5.4	4.2	3.3
Sep	2011-2040	**20.1**	3.9	1.7	5.8	7.7	6.5	**18.0**	2.5	2.2	4.2	5.6	6.1	**18.9**	4.1	3.0	5.1	5.9	6.8
	2041-2070	**20.8**	2.6	0.9	7.1	8.3	7.1	**16.1**	1.8	-0.2	5.0	5.1	6.1	**16.1**	1.3	-0.7	4.5	5.8	5.8
	2071-2100	**19.8**	4.1	1.4	7.9	7.3	7.5	**17.5**	2.0	-0.6	2.9	5.6	5.7	**14.1**	0.0	-3.5	4.9	5.3	5.4
Oct	2011-2040	**14.2**	1.8	0.0	5.8	8.1	8.0	**10.6**	-0.1	0.1	4.7	6.0	6.2	**9.3**	-0.6	-0.8	5.3	5.8	6.4
	2041-2070	**13.5**	0.2	-1.6	7.0	8.5	7.2	**8.6**	-1.7	-2.1	4.7	5.2	6.3	**9.0**	-2.3	-2.2	4.8	6.1	6.8
	2071-2100	**11.9**	0.6	-0.8	8.2	7.8	8.4	**9.7**	-1.4	-2.9	5.2	7.0	7.8	**8.3**	-4.5	-5.9	5.5	6.3	6.3
Nov	2011-2040	**8.9**	-1.6	-1.3	6.5	6.3	6.3	**6.9**	-0.7	0.4	6.3	6.8	6.8	**7.4**	-1.1	0.0	5.0	5.9	5.9
	2041-2070	**8.8**	0.0	-0.3	6.2	8.5	7.4	3.9	-4.9	-3.5	4.8	5.5	5.4	5.9	-2.0	-1.1	6.3	7.2	7.2
	2071-2100	5.2	**-5.5**	-5.0	6.2	5.4	6.3	**6.2**	-3.0	-1.4	6.0	6.6	7.4	**5.8**	-2.8	-0.9	4.4	6.2	6.3
Dec	2011-2040	7.6	0.8	-0.2	7.7	8.6	8.8	**7.6**	1.7	2.2	7.5	8.7	8.3	6.7	1.4	0.9	6.8	9.0	7.7
	2041-2070	**7.8**	1.0	-0.5	7.5	11.0	8.7	3.4	-2.5	-1.3	7.7	8.4	7.6	5.5	-0.6	-0.1	6.5	8.8	6.6
	2071-2100	4.6	-2.6	-2.4	7.2	10.2	10.1	6.1	-0.7	0.1	8.3	8.0	7.6	7.2	2.4	2.6	7.7	9.5	7.9